MEANING, MEASUREMENT, AND FIELD APPLICATION OF FULLY SOFTENED SHEAR STRENGTH OF STIFF CLAYS AND CLAY SHALES

BY

CAI WANG

DISSERTATION

Submitted in partial fulfillment of the requirements
for the degree of Doctor of Philosophy in Civil Engineering
in the Graduate College of the
University of Illinois at Urbana-Champaign, 2019

Urbana, Illinois

Doctoral Committee:

Professor Gholamreza Mesri, Chair
Professor Timothy D. Stark
Professor Emeritus James H. Long
Professor Emeritus Stephen Marshak

ABSTRACT

The mobilized shear strength in the failure of natural and cut slopes is important for design and stability evaluation. The intact shear strength is rarely available at the time of first-time slope failures. It is generally accepted that only residual shear strength is available for the reactivated landslides. Although fully softened shear strength mobilized in first-time slope failures has been recognized for decades, a comprehensive investigation on fully softened shear strength has not been made, which consists of its meaning, measurement, and field application. This study aims to clarify the meaning of fully softened shear strength, to examine the best procedure for its measurement in laboratory tests, and to generalize its field application.

In this study, an empirical correlation for secant fully softened secant friction angle has been developed at 7 effective normal stresses, for a wide range of clay compositions characterized in terms of plasticity index from 10% to 250%, based on consolidated triaxial compression tests on remolded, normally consolidated specimens of 15 stiff clay and clay shale compositions.

The fully softened shear strength data interpreted from laboratory tests reported in the literature on reconstituted, normally consolidated specimens prepared from 55 materials, including soft to stiff clays, clay shales, mudstones, and clay minerals, were also collected and compared to the empirical correlation for fully softened shear strength developed in the present study. An examination was made for the potential dependence of laboratory measurements for fully softened shear strength on specimen preparation procedure and drainage condition during shear.

Fully softened shear strength mobilized in full-scale situations was also estimated by means of back-analyses of 63 first-time slope failures, in geologic materials including soft to stiff clays, clay shales, mudstones, marls, clayey silt, and glacial clays, using the observed slip surface or possible slip surface determined based on adequate field observations, together with the observed or assumed groundwater pressure conditions reported in the original references.

In summary, fully softened shear strength is defined at a random, predominantly edge to face arrangement and interaction of clay particles in a destructured stiff clay or clay shale composition.

In the field, though geological weakening may bring stiff clays and clay shales to the fully softened condition, it is not a prerequisite as fully softened condition results from progressive deformation along a global slip surface. In triaxial compression of normally consolidated specimens, reconstituted at a liquidity index near unity, a random arrangement of clay particles is mobilized at failure. For first-time slope failures in stratified deposits including stiff clays, clay shales, and mudstones, fully softened shear strength is mobilized on the back-scarp of the slip surface, while residual shear strength is available on the horizontal or subhorizontal segments. For first-time slope failures in unstratified deposits including 1) soft to firm clays of low to medium plasticity excluding soft clays of Eastern Canada, 2) stiff clays or clay shales with significant amount of calcium carbonate and quartz content, 3) clayey silts including loess, and 4) glacial clays, the mobilized shear strength on the entire slip surface is equal or greater than the fully softened shear strength.

ACKNOWLEDGEMENTS

This thesis is based on laboratory investigations and theoretical studies conducted at the University of Illinois at Urbana-Champaign. During the study, financial aid was provided by Civil and Environmental Department Fellowship, and Geotechnical Engineering Fellowship.

This thesis has been carried out under the direct supervisor of Professor Gholamreza Mesri. I am indebted to Professore Mesri for his patient guidance and encouragement in Geotechnical Engineering and in life.

I also wish to thank to my doctoral thesis committee members, Professor Timothy D. Stark, Professor Emeritus James H. Long, and Professor Emeritus Stephen Marshak for their contributions. Professor Stark has made available the GEO-SLOPE 7.23 slope stability analysis package.

I wish to thank CEE Machine Shop staff Tim Prunkard, and Darold F. Marrow for their help in the construction of laboratory apparatus components. I would like to also thank to our former geotechnical division staff Joyce Snider for her help and friendless.

My colleague and friend, Ozgun A. Numanoglu, has been like my family in Champaign, who has been always available in having technical discussions and giving suggestions in research, work and life. I deeply thank him for his love and support.

I am grateful to my colleagues, Thierno Kane and Vashish Taukoor, for the collaboration and help in laboratory work. Finally, I gratefully appreciate the love and support from my parents, Herong Wang and Shuping Chen.

TABLE OF CONTENTS

CHAPTER 1: INTRODUCTION

1.1. Background and motivation

The mobilized shear strength in slope failures of overconsolidated stiff clays and clay shales attracted early attention because back-calculated shear strength for slope failures was significantly lower than the peak or intact strength of undisturbed specimens measured in the laboratory tests. Residual shear strength was introduced by Skempton (1964) to explain the behavior of reactivated landslides. Terzaghi (1936) and Skempton (1948) had explained the geological weakening of stiff fissured clays in terms of erosional removal of overburden and lateral support, opening of fissures, infiltration of water into fissures, and swelling including breaking of diagenetic bonds. Geological shear strength deterioration may also result from mechanical and chemical weathering by repeated cycles of drying and wetting, or freezing and thawing.

Skempton (1970) proposed fully softened shear strength as the lower bound of mobilized strength for first-time slope failures in stiff fissured clays. Skempton (1970) equated the fully softened shear strength to peak shear strength of stiff clay composition in a normally consolidated state. Skempton (1977) examined the slope failures in London Clay in terms of a constant friction angle, and concluded that the back-calculated friction angle of 20° corresponds to the fully softened friction angle measured in the laboratory on reconstituted, normally consolidated London Clay. A definition was given by Mesri and Shahien (2003) that fully softened shear strength corresponds to a relatively random arrangement of clay particles with predominant edge to face interaction and interference. Mesri and Shahien (2003), also by means of back-analyses of slope failures, illustrated that for a majority of first-time slope failures, part of the global slip surface -horizontal or subhorizontal segment - may be at residual condition, with back-scarp mobilizing the fully softened shear strength, with a friction angle dependent on effective normal stress.

Although fully softened shear strength mobilized in first-time slope failures has been recognized for decades, a comprehensive investigation on fully softened shear strength has not been made, which consists of its meaning, measurement, and field application. This study aims to clarify the

meaning of fully softened shear strength, to examine the best procedure for its measurement in laboratory tests, and to generalize its field application.

1.2. Objective of the study

In the present study, fully softened shear strength is defined at a random, predominantly edge to face arrangement and interaction of clay particles in a destructured stiff clay or clay shale composition. In the field, though geological weakening may bring stiff clays and clay shales to the fully softened condition, it is not a prerequisite as fully softened condition results from progressive deformation along a global slip surface. In triaxial compression of normally consolidated specimens, reconstituted at a liquidity index near unity, a random arrangement of clay particles is mobilized at failure. Based on these hypotheses, the main objectives of this study are to

(1) develop an empirical correlation of fully softened shear strength for a wide range of clay compositions, characterized in terms of plasticity index, based on consolidated triaxial compression tests on remolded, normally consolidated specimens of stiff clay and clay shale compositions, at a wide range of effective normal stress, subjected to undrained shear with porewater pressure measurement,

(2) compare fully softened shear strength data from the laboratory tests reported in the literature to the proposed empirical correlation for secant fully softened friction angle,

(3) examine potential dependence of laboratory measurements for fully softened shear strength on specimen preparation procedure and drainage condition during shear,

(4) propose the best laboratory testing procedure to measure fully softened shear strength,

(5) estimate by back-analyses the fully softened shear strength mobilized on full-scale slip surfaces in the first-time slope failures,

(6) Generalize the field application of fully softened shear strength.

1.3. Scope

In this thesis, previous studies in relation to fully softened shear strength are reviewed in Chapters 2 to 5, and the present study of fully softened shear strength is presented in Chapters 6 to 8.

In Chapter 2, a literature review is made on laboratory measurement of fully softened shear strength, with respect to, 1) different procedures to prepare reconstituted specimens, and 2) two testing procedures in terms of mode of shear, namely, triaxial compression and ring shear.

In Chapter 3, a literature review is made on the estimation of fully softened shear strength mobilized in full-scale situations, by means of back-analysis of first-time slope failures.

In Chapter 4, case histories are reviewed, where fully softened shear strength was mobilized on part of, or on the entire slip surface in first-time slope failures, suggested by back-analyses in the original references.

In Chapter 5, a review is presented on empirical correlations of fully softened shear strength as a function of liquid limit or plasticity index.

In Chapter 6, the triaxial compression testing program in the present study is described, which includes consolidated triaxial compression tests on reconstituted specimens prepared from 15 stiff clay and clay shale compositions, consolidated under equal all-round pressure, and subjected to undrained shear with porewater pressure measurement, as well as drained shear tests. Test results are presented and evaluated. Based on the data from the triaxial compression tests, an empirical correlation for secant fully softened friction angle is developed for a wide range of clay compositions, characterized in terms of plasticity index, from 10% to 250%, at effective normal stress from 10 kPa to 700 kPa.

In Chapter 7, fully softened shear strength data interpreted from laboratory tests reported in the literature, on reconstituted specimens prepared from 55 materials, are compared to the empirical correlation for fully softened shear strength developed in the present study. An examination is made of the potential dependence of laboratory measurements for fully softened shear strength on specimen preparation procedure and drainage condition during shear.

In Chapter 8, fully softened shear strength mobilized in full-scale situations is estimated by means of back-analyses of 63 first-time slope failures using the observed slip surface or possible slip

surface determined based on adequate field observations, together with the observed or assumed groundwater pressure conditions reported in the original references. An examination is also included, in relation to the mobilized shear strength of first-time slides in soft clays of Eastern Canada.

Finally, in Chapter 9, summaries and conclusions are presented.

CHAPTER 2: LABORATORY MEASUREMENT OF FULLY SOFTENED SHEAR STRENGTH

Because normally consolidated state of an undisturbed stiff clay or clay shale specimen is reached at effective stresses exceeding the pre-consolidation pressure, fully softened shear strength, at all effective normal stresses, has been determined using reconstituted, normally consolidated specimens of random fabric as fully softened shear strength corresponds to a random, more or less edge to face arrangement of clay particles (Skempton 1970, Mesri and Shahien 2003). Skempton (1977) recommended that fully softened strength can be measured on remolded, normally consolidated clay, and gave an approximation of a constant fully softened friction angle (20 degree) of London Clay, based on drained direct shear tests by Gibson (1953) on remolded specimens, undrained triaxial compression tests with porewater pressure measurement by Bishop et al (1965) on specimens consolidated from slurry, and drained direct shear tests by Petley (1966) using specimens consolidated from slurry. However, the nonlinearity of the relationship between fully softened shear strength and effective normal stress is significant, which is mainly related to the degree of soil particle face to face interaction. In general, face to face interaction of platy particles is promoted as effective normal stress increases, even for a random arrangement of particles and subjected to equal all around pressure. Figure 2.1. is an example showing the pronounced curvature of the fully softened shear strength envelope determined from drained triaxial compression tests and undrained triaxial compression tests with porewater pressure measurement, on remolded Brenna, clay specimens consolidated under equal all around pressure, performed in the present research, in which the shear stress to effective normal stress ratio and secant fully softened friction angle of Brenna are plotted against the effective normal stress. In this chapter, the interpretation of shear strength of clays and shales from data in the literature are interpreted using non-linear failure envelope. The data for reconstituted specimens and two laboratory testing procedures to determine fully softened shear strength; namely, triaxial compression, and ring shear, are reviewed in this chapter.

2.1. Preparation of reconstituted specimens

The use of reconstituted, normally consolidated clay specimens to determine fully softened shear strength, as suggested by Skempton (1977), is widely accepted. However, Skempton (1977) did not specify the procedure for preparing the specimen and testing procedure. Terzaghi et al (1996) suggested that the most suitable method to determine the friction angle corresponding to a more or less random arrangement of particles would be reconstituted specimen either remolded at a water content higher than the liquid limit or consolidated from slurry, normally consolidated under an equal all-around pressure in triaxial cell, and then subjected to compression either under drained condition or undrained condition with porewater pressure measurement.

2.1.1. Mechanical Remolding

Mechanically remolded specimens have been used for the fully softened strength measurement. In order to measure the shear strength corresponding to the fully softened condition for the fissured, overconsolidated Lugagnano Clay in Italy, Cancelli (1981) performed triaxial compression tests on remolded specimens prepared at a water content close to the liquid limit, but did not include details of the remolding process.

Green and Wright (1986) carried out 2 series of undrained triaxial compression tests with porewater measurements on Beaumont Clay from Texas, to compare their fully softened shear strength parameters. The 2 series of tests were on specimens consolidated from slurry (discussed in the subsection 2.1.2), and on “packed” specimens. The packed specimens were made from the air-dried sample, which was crushed and passed through No. 40 U. S. standard sieve. Water was added to the processed clay to reach a water content close to the liquid limit and the sample was hydrated for 1 day in a moisture room. A spatula was then used to spread the clay paste into an acrylic tubing mold to fabricate the specimens.

Stark and Eid (1997), determined the fully softened shear strengths of 24 soils, including clays, shales, till, loess, and a silt deposit using a modified Bromhead ring shear device. Shales and mudstones were air-dried, ball-milled, and passed through No.200 U.S. standard sieve, to minimize the aggregation resulting from diagenetic bonding (Mesri and Cepeda-Diaz 1986). The

ball-milling procedure was not applied to the rest of the soils, which were crushed by motor and pestle, and then passed through No.40 U. S. standard sieve. Distilled water was added to the processed soils to obtain a liquidity index of 1.5 before they were allowed to hydrate in the moisture room for at least one week. Then, the hydrated remolded soil paste was packed with a spatula into the specimen container in the ring shear apparatus. Same procedures were used by Stark et al (2005), Gamez and Stark (2014), Eid and Rabie (2017), expect that a liquidity index of 1 was obtained for the remolded soils by Gamez and Stark (2014).

The fully softened shear strength of Gault Clay with different weathering classification was measured by Cooper et al (1998) on samples remolded at a water content of approximately 1.5 times of the plastic limit (liquidity index of 0.2) in both drained triaxial compression, and undrained triaxial compression tests with porewater measurement.

Castellanos and Brandon (2013), and Castellanos (2014), performed undrained triaxial compression tests with porewater measurement on 14 clays and 1 silt covering several geographic locations in United States. Soil samples were first soaked in either distilled water or site-specific water for at least two days. The soaked samples were pushed or washed through No.40 sieve, and mixed with water at liquidity index ranging from 0.6 and 2.0. Before the test specimen fabrication, these samples were air-dried in funnels or bowls with filter paper. Two types of reconstituted specimens were prepared for undrained triaxial compression tests with porewater pressure measurement. The first type of reconstituted clays were air-dried to liquidity index of 1, consolidated in a batch consolidometer and then specimens were trimmed for the shear stage. In the second type, clay specimens were packed with a spatula at lower liquidity index between 0.5 and 0.8 using a Harvard miniature compactor mold.

2.1.2. Consolidation of slurry

In University of Illinois, specimens of pure clay minerals for triaxial compression tests were prepared by sedimentation from a suspension water content (Olson 1962, 1963; Mesri and Olson 1970). The constant fully softened friction angle of Brown London Clay reported by Skempton (1977) was based on triaxial compression tests on specimens consolidated from slurry (Petley 1966)

and specimens consolidated from slurry as well as by compaction (Bishop et al 1965). Possibly for this reason, subsequent studies of fully softened shear strength have used specimens consolidated from slurry, or at water contents higher than the liquid limit, instead of remolding specimens at lower water contents.

The first series of consolidated undrained triaxial compression tests performed by Green and Wright (1986), were on specimens consolidated from slurry, prepared from air-dried Beaumont Clay passing No. 200 sieve, instead of No. 40 sieve, as was used for packed specimens. The fraction of samples passing No. 200 sieve was used to avoid binding between the piston and the tube during consolidation, and segregation of coarser material to the bottom of specimens. A liquidity index close to 5 was obtained for the slurry (suspension), which was hydrated overnight and vacuumed to remove the trapped air bubbles. Then the slurry was poured into a cylindrical tube and consolidated to a final pressure of 9.8 psi (68kPa). The center 3 inches of the consolidated specimen was trimmed for the triaxial compression tests. The water content of the consolidated specimens was near the liquid limit, similar to the water content at which the packed specimens were remolded.

Kayyal and Wright (1991) carried out consolidated undrained triaxial compression tests with porewater pressure measurement on reconstituted Paris and Beaumont Clays from Texas. The clays passing No. 40 sieve were mixed with water to liquidity index about 2.5. The slurry was consolidated to 2 psi (14kPa) in 1.5 in diameter Lucite cylinders, and the consolidated specimens were extruded and tested. The water content at the end of consolidation was close to the liquid limit.

Other measurements of fully softened shear strength using specimens consolidated from slurry include less details in relation to the specimen preparation. Crabb and Atkinson (1991) studied the fully softened shear strength of London Clay in triaxial compression tests on reconstituted specimens by oven-drying, pulverizing, mixing to a slurry water content (water content not specified), and reconsolidation. Nakano (2012) prepared specimens of 3 clays from 3 Japanese landslides for drained triaxial compression tests and direct shear tests, by consolidation of slurry to natural water content of clay. The sub-425 μm soil fractions of Japanese mudstone and loess

(Kimura 2015) were mixed with water to a slurry water content twice the liquid limit, which corresponds to liquidity index of 2.4 to 3.1, for the undrained triaxial compression tests, first consolidated in an acrylic cylinder, then trimming; and for ring shear tests consolidated in the specimen container of the ring shear device.

2.2. Triaxial compression tests

Triaxial compression test is the most wildly used testing procedure for determining fully softened shear strength. Cancelli (1981) reported data on the fully softened shear strength of fissured, overconsolidated Lugagnano Clay in Italy, in terms of a friction angle range and a negligible cohesion intercept, measured in triaxial compression tests on remolded specimens. The fully softened shear strength of Gault Clay was determined by Cooper et al (1998) on remolded specimens in both drained triaxial compression and undrained triaxial compression tests with porewater pressure measurement, and presented by a linear failure envelope with a single set of cohesion intercept and friction angle. Castellanos and Brandon (2013) and Castellanos (2014), recognizing that triaxial compression tests have been used successfully for fully softened measurement, carried out undrained triaxial compression tests with porewater measurement on 14 clays and 1 silt, covering several geographic locations in United States.

Crabb and Atkinson (1991), equating fully softened condition to the critical state, explained that the fully softened friction angle of remolded specimens is lower than that of specimens consolidated from slurry because a clearly defined critical state is not available due to the formation of well-defined shear planes at low strain levels for remolded specimens. The fully softened shear strength of specimens consolidated from slurry determined in triaxial compression tests have been reported by a linear shear strength envelope (Crabb and Atkinson 1991, Nakano 2012, Kimura et al 2015), by both linear and non-linear shear strength envelope (Green and Wright 1986), and by non-linear relationship between fully softened shear strength and effective normal stress (Kayyal and Wright 1991).

Green and Wright (1986) made comparisons between the fully softened shear strength obtained from specimens consolidated from slurry and specimens remolded at a water content close to the

liquid limit in undrained triaxial compression tests with porewater measurements. Green and Wright (1986) concluded that the differences were minimal in shear strength expressed in terms of a cohesion intercept and friction angle, as well as in terms of non-linear failure envelope. The data by Green and Wright (1986) are reproduced in Fig.2.2. As introduced previously, the remolding water content was similar to the water content of the specimens consolidated from slurry. It should be noted that these tests were carried out under relatively low consolidation pressures not higher than 20 psi (140 kPa), and the effective normal stress at failure is less than 100 kPa.

2.2.1. Methods of reconstituting specimens

According to the preceding review, the random fabric of clays and shales corresponding to the fully softened shear strength could be obtained using specimens prepared by consolidation of slurry at water content higher than the liquid limit, and by mechanically remolding at water content near the liquid limit. It is possible to have a difference in the degree of randomness in the arrangement of clay particles in the specimens prepared by different methods. The wildly used procedures to prepare reconstituted specimens in geotechnical engineering include sedimentation from suspension, consolidation from slurry, mechanical remolding at water content close to liquid limit, and compaction at lower water content, with water content at the beginning of consolidation being one of the major differences. The most random fabric and least aggregation of clay particles could be achieved in specimens sedimented from a suspension starting with very high water content, for example, at liquidity index of 5. For specimens prepared by consolidation of a slurry (for example, liquidity index of 2), edge to face interactions of clay particles are still promoted, but probably less predominant than those in specimens sedimented from a suspension. Some face to face interactions of clay particles might take place in the remolded specimens due to the shearing action imposed by the mechanical remolding process at water content near liquid limit. For specimens prepared by compaction at low water contents, sometimes close to the plastic limit, particle aggregations become significant.

In terms of shear strength parameters of clays, the results of triaxial compression tests on specimens consolidated from slurry and those remolded near liquidity index of one, are similar. Bishop et al (1965) obtained comparable failure envelopes for London Clay, in effective normal

stress range up to 2000 kPa, for specimens prepared from slurry water content and subjected to undrained triaxial compression tests with porewater pressure measurement, and specimens compacted at natural water content and tested in drained and undrained triaxial compression.

Sivakumar et al (2002) examined the particle orientation of reconstituted kaolin specimens (Series 1) produced by consolidation stating at a water content 1.5 times the liquid limit, under equal all around pressure of 500 kPa in a triaxial cell. For comparison, another series of specimens (Series 2) were first consolidated in the same way as Series 1 to a pressure of 50 kPa, then remolded in the membrane by hand to a cylindrical shape, and consolidated to 500 kPa. SEM images were taken after the specimen preparation, which show the pronounced particle orientation perpendicular to vertical direction in Series 1 specimens, and more random particle orientation with respect to vertical direction in Series 2 specimens. Some specimens were overconsolidated in the triaxial cell to various OCRs, and then sheared under undrained condition with porewater pressure measurement. The secant friction angles of Series 1 and Series 2 specimens at different effective normal stresses turned out to be similar, both for normally consolidated and overconsolidated specimens.

Suzuki and Dyvik (2017) studied two methods of reconstituting specimens using kaolinite, 1) slurry-based consolidation in a large consolidation box (CB specimens), and 2) mixing and extrusion of specimens in a pug mill under vacuum (PM specimens). The stress paths of the 2 types of specimens first consolidated under equal all around pressure, and then subjected to undrained triaxial compression with porewater pressure measurement, are reproduced in Fig.2.3, resulting to a single non-linear failure envelope. However, as suggested by Suzuki and Dyvik (2017), the behavior of CB specimens with water content near liquid limit after consolidation in the consolidation box, is more contractive, whereas PM specimens prepared in the pug mill at liquidity index of 0.6 to 0.7, display a more dilative behavior, at initial shear and at the stress state approaching failure.

In summary, because drained shear strength parameters determined on remolded specimens and specimens consolidated from slurry are comparable, remolded specimens, which require less preparation time, are preferred. The water content at which the triaxial specimen is prepared by

mechanical remolding needs to be high enough to produce random arrangement of clay particles, and at the same time, low enough to allow handling of the soft specimens. In the present research program, a liquidity index in the range 0.8 to 1.0 for clay composition in plasticity index range between 13% and 205%, satisfied both requirements.

2.2.2. Consolidated drained triaxial compression tests and undrained triaxial compression tests with porewater pressure measurement

For stability analysis of a drained slope failure, consolidated drained triaxial compression test may produce the most representative shear strength in terms of secant friction angle, as it resembles the drainage condition in the slope. However, the duration of a drained test, is relatively long to ensure porewater pressure dissipation, compared to that required for porewater pressure equalization in an undrained test. It is, therefore, necessary to compare the strength parameters obtained from drained tests and those from undrained tests, as it would be a great advantage to apply the shear strength parameters interpreted from undrained tests to the drained slope stability analyses. Bjerrum and Simons (1960) collected friction angles of remolded and undisturbed clays from literature, determined in drained and undrained triaxial compression tests with porewater pressure measurement, and concluded that friction angles for both remolded and undisturbed clays measured in drained triaxial compression tests are in reasonably close agreement with those in the undrained tests, if maximum effective stress ratio criterion, $(\sigma'_1/\sigma'_3)_{max}$ is used to define failure. One possible reason for slightly higher friction angle measured in undrained triaxial compression tests with porewater pressure measurement, as suggested by Casagrande and Wilson (1953), is prestress developing in undrained tests, which imposes a shear induced preconsolidation effect. To be more specific, for normally consolidated clays, the effective normal stress on the failure plane in undrained tests, decreases with the shear induced porewater pressure increase, while the effective normal stress on the failure plane in drained tests increases in the shearing process (Bjerrum and Simons 1960). However, prestress turned out to have little effect on the shear strength parameters according to Henkel (1956), Bjerrum and Simons (1960), because the shear strength of a clay is mainly controlled by the overconsolidation ratio prior to shear.

The triaxial compression tests on specimens prepared by consolidation of 0.01 N calcium montmorillonite suspension (starting from liquidity index of 5) by Mesri (1969), are a good example showing comparable drained shear strength parameters determined from drained shear and undrained shear with porewater pressure measurement. The plasticity index of the 0.01 N calcium montmorillonite is 167% at PH=5, and 170% at PH=7. The stress strain curves of the sedimented calcium montmorillonite, together with volume change and porewater pressure response, are reproduced in Fig.2.4 and Fig.2.5, and the drained and undrained stress paths, based on these data, are plotted in Fig.2.6. The drained and undrained stress paths yield a single, significantly curved failure envelope.

Same conclusions are reached for the drained and undrained triaxial compression tests with porewater measurement on reconstituted clay and clay shales with low to medium plasticity index. The stress paths and failure envelops are defined in Fig.2.7 and Fig.2.8, respectively using the original data, for reconstituted Bringelly Shale consolidated from a "slurry" at water content close to the liquid limit (William 2004 and 2005), and for 2 marine clays reconstituted by consolidation of slurry at a water content about twice the liquid limit (Sun et al 2014). Bringelly Shale is the major geological sequence in the Sydney Basin, with low plasticity index ranging from 7 to 12%. The two marine clays, Pujiang Clay, and Suzhou Clay, collected from the Yangtze River Delta, China, have plasticity index of 22% and 19%, respectively.

Because the failure envelope by stress path utilizes maximum stress ratio criterion, (σ'_1/σ'_3)max, it could be concluded that the drained shear strength parameters of reconstituted, normally consolidated clays and shales, measured in undrained triaxial compression tests with porewater pressure measurement defined at maximum stress ratio criterion, (σ'_1/σ'_3)max, are in close agreement with the ones in the drained tests. Therefore, the consolidated undrained triaxial compression tests with porewater pressure measurement on normally consolidated remolded specimens, which requires less duration for porewater pressure equalization than porewater pressure dissipation in drained tests, are preferred for the measurement of fully softened shear strength.

2.3. Ring Shear Tests

The ring shear device provides reliable measurement of drained residual strength of stiff clays and clay shales (Skempton 1985, Bromhead and Curtris 1983, Bromhead and Dixon 1986, Stark and Eid 1992). Stark and Eid (1997) used the Bromhead ring shear device to determine the fully softened strength parameters by dividing the fully softened friction angle data into three groups based on clay size fraction and presenting the data as a function of liquid limit, for three effective normal stresses (50, 100 and 400kPa). In the ring shear apparatus developed by Bromhead (1979), a 5 mm thick reconstituted specimen with an inside diameter of 70mm and an outside diameter of 100mm, is radially confined by the specimen container. To minimize friction between the loading platen and the specimen container, Stark and Vettel (1992) proposed a flush test procedure which includes the addition and reconsolidation of the specimen to limit to less than 1 mm the settlement of the top porous stone into the specimen container. However, the modified Bromhead ring shear tests on remolded specimens with the flush procedure still tended to underestimate the fully softened strength, partially due to the mode of shear represented in the ring shear test (Stark and Eid 1997), and possibly because in the Bromhead device almost immediately after the test begins, the failure surface may jump to the interface between the loading platen and the specimen, promoting soil particle reorientation, which no longer corresponds to a random arrangement of particles. Therefore, the mode of shear in the Bromhead ring shear device may not approximate the shear mode in the backscarp of first-time slides, where the fully softened shear strength is mobilized (discussed in Chapter 4). For this reason, from the ring shear data, the secant fully softened friction angle corresponding to triaxial compression mode of shear, were obtained by Stark and Eid (1997) by increasing of 2.5° of friction angle measured in the drained ring shear tests. This increase was decided based on the average difference between the measured friction angles in drained triaxial compression tests and those in the ring shear tests for reconstituted specimens of 4 shales and a glacial till composition (plasticity index ranging from 8% to 145%) at the effective normal stresses of 100 and 400 kPa. Further updates of the fully softened shear strength data, of other clays and data at lower effective normal stress, are reported in Stark et al. (2005), Gamez and Stark (2014), using the modified Bromhead ring shear device.

The modified Bromhead ring shear device was also used by Eid and Rabie (2017) on 40 clay, silt, mudstone, and shale samples, including those tested previously by Stark and Eid (1997), for determining fully softened shear strength at 6 effective normal stresses (10, 25, 50, 100, 200 and 400 kPa) , as a function of plasticity index up to 250%. However, a correction of 2.5° to the data was again applied to obtain the secant fully softened friction angle.

Kimura (2015) performed fully softened shear strength measurements on mudstones and loess from two landslides in Japan using a ring shear device designed by Gibo (1994), and compared them to those obtained from undrained triaxial compression tests with porewater pressure measurement. The annular specimen container in the ring shear apparatus developed by Gibo (1994) has an inside diameter of 60mm, and an outside diameter of 100mm. Kimura (2015) reported the average height of specimen after consolidation to be 20mm, which is much larger than that of specimens tested in the modified Bromhead ring shear device. The fully softened shear strengths of mudstone and loess are plotted in Fig.2.9 based on the reported test data by Kimura (2015). At effective normal stress range where data from undrained triaxial compression tests with porewater measurement are available, the fully softened shear strength parameters determined from ring shear tests and triaxial compression tests are comparable.

FIGURES

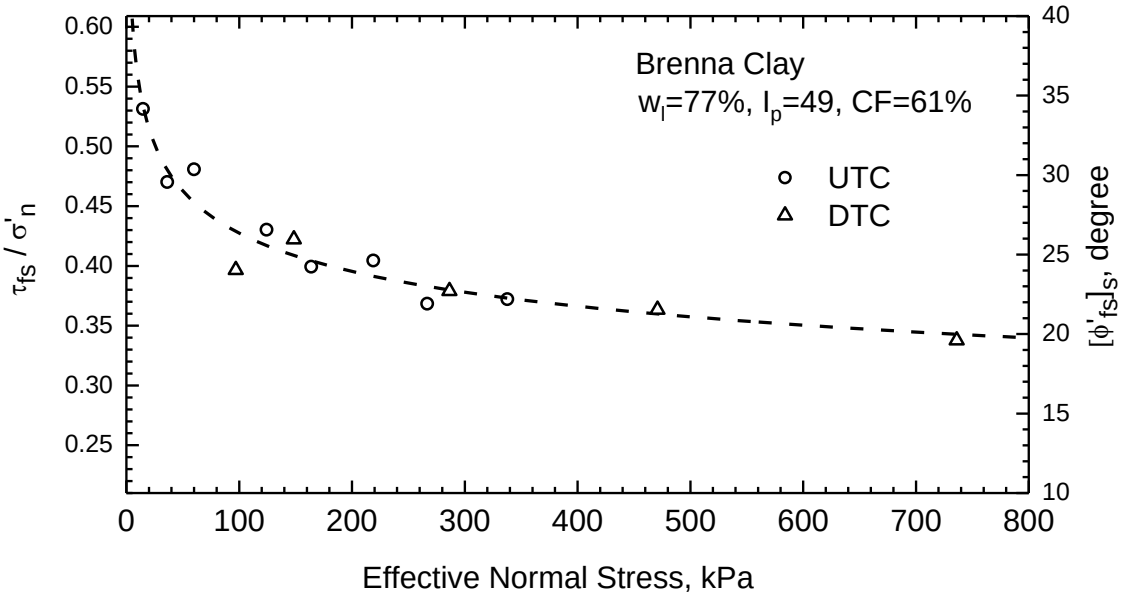

Figure 2.1. Drained triaxial compression tests and undrained triaxial compression tests with porewater measurement on Brenna Clay conducted at different effective normal stresses, showing the nonlinear shape of the fully softened shear strength envelope, and relationship of secant fully softened friction angle to effective normal stress

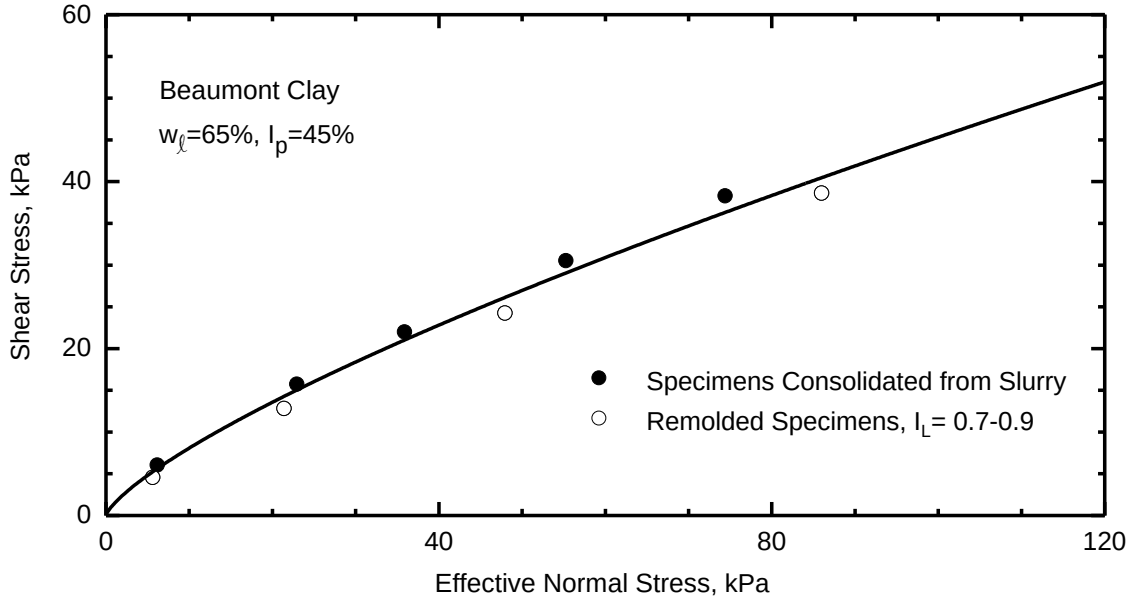

Figure 2.2. Fully softened shear strength of Beaumont Clay determined from undrained triaxial compression tests with porewater pressure measurement on specimens consolidated from slurry and remolded specimens (Data from Green and Wright 1986)

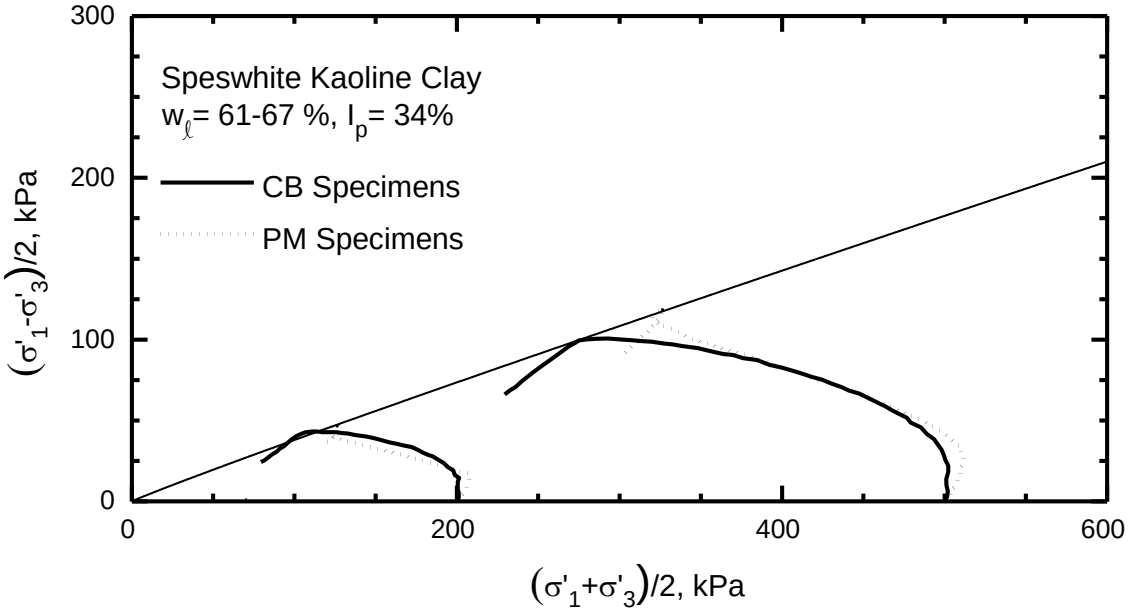

Figure 2.3. Stress path of Speswhite Kaoline Clay, prepared by consolidation from slurry (CB), and by mixing and extrusion in pug mill (PM) (Suzuki and Dyvik 2017)

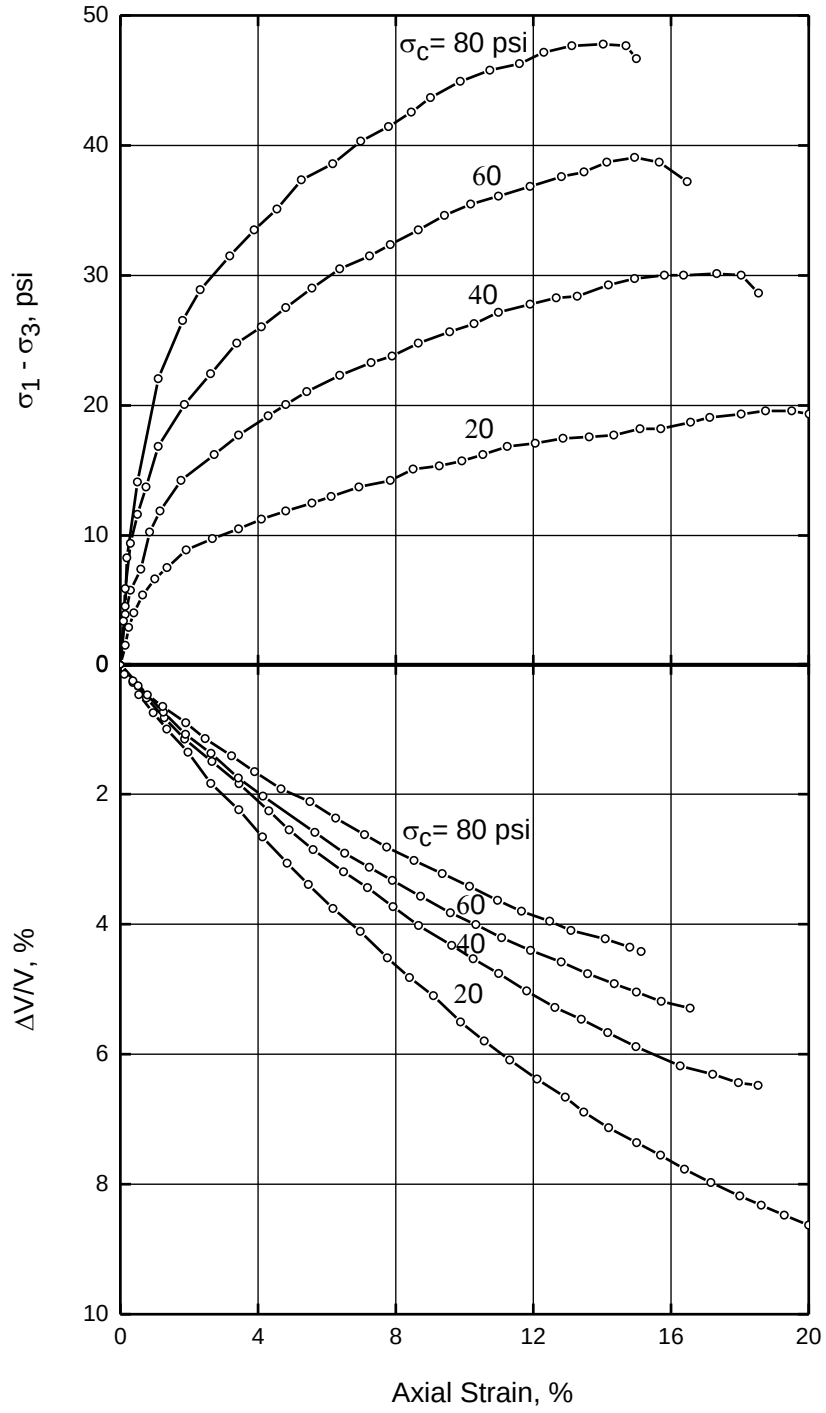

Figure 2.4. Drained Stress-strain curves of 0.01 N calcium montmorillonite (Mesri 1969)

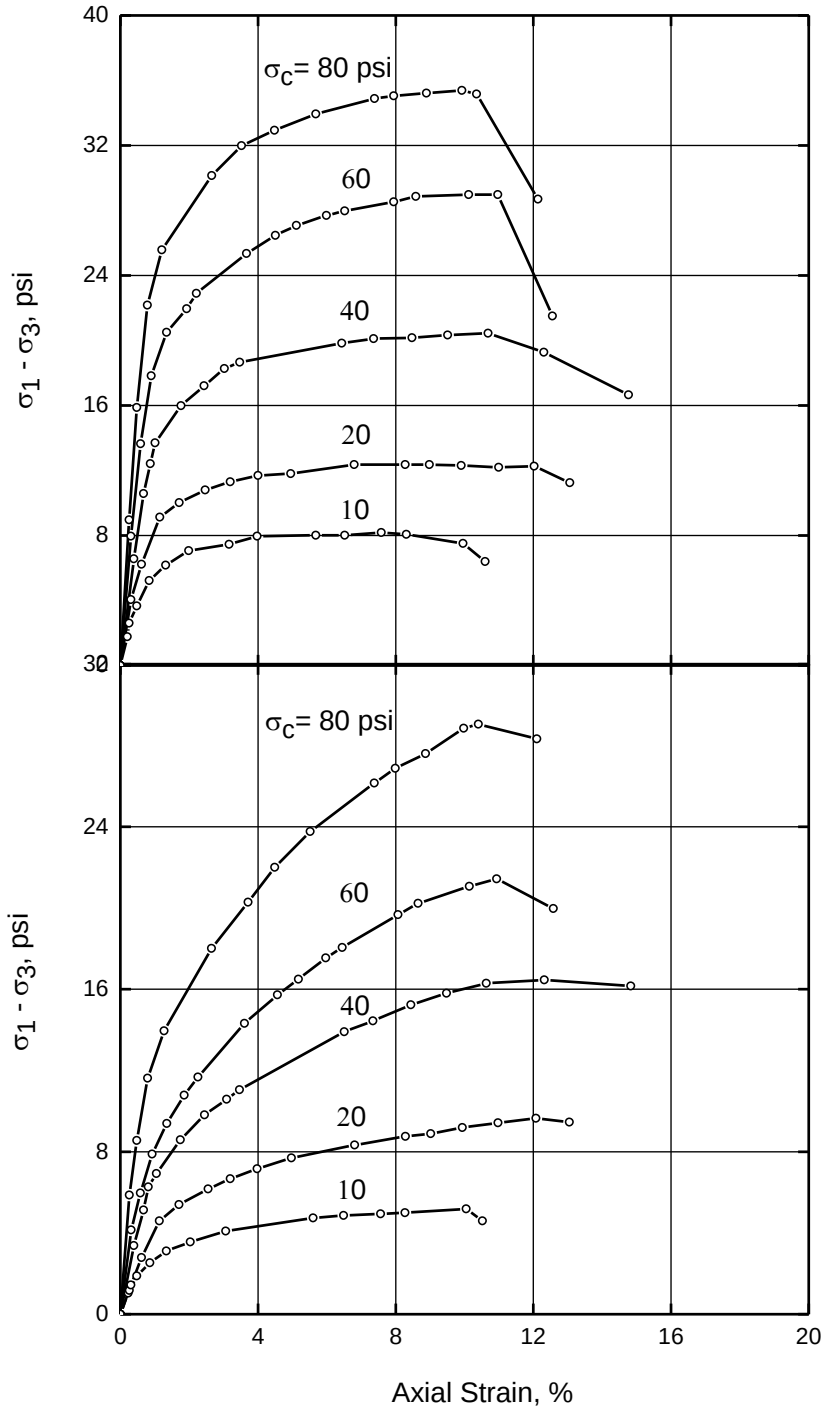

Figure 2.5. Undrained Stress-strain curves of 0.01 N calcium montmorillonite (Mesri 1969)

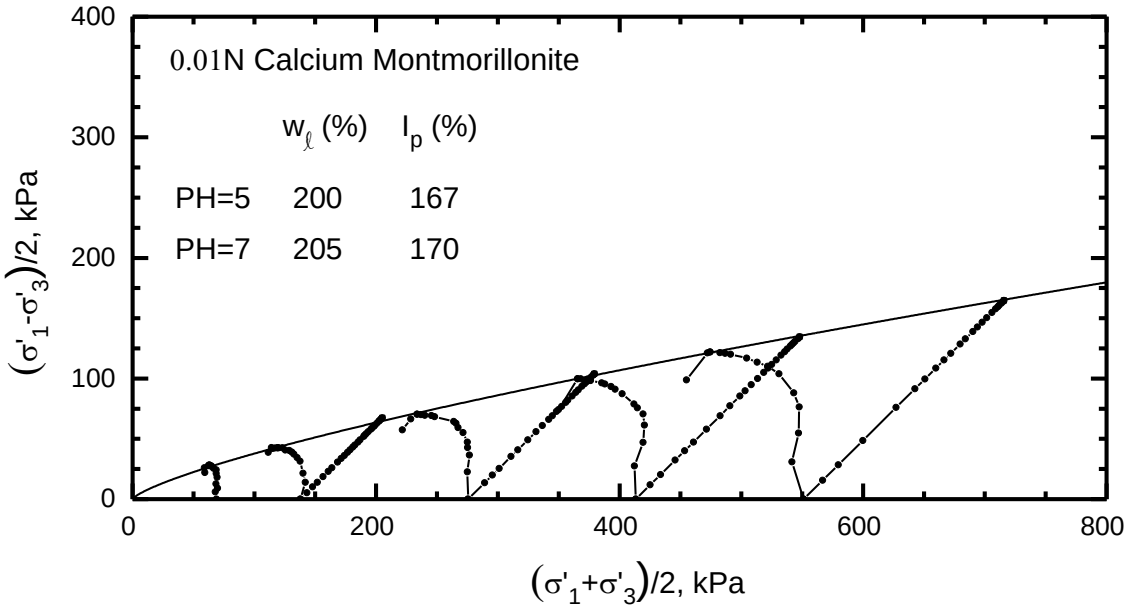

Figure 2.6. Shear Strength of calcium montmorillonite specimens prepared by consolidation starting from suspension, and subjected to drained, and undrained triaxial compression with porewater pressure measurement (Data from Mesri 1969)

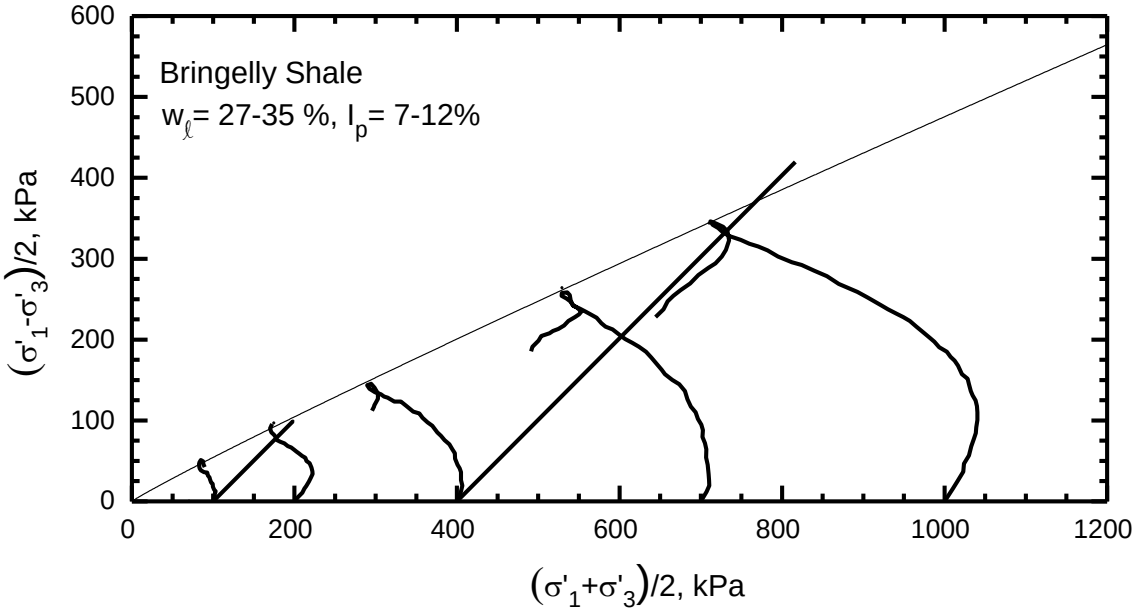

Figure 2.7. Shear Strength of Bringelly Shale prepared by consolidation starting from a mixture at water content close to liquid limit, and subjected to drained, and undrained triaxial compression with porewater pressure measurement (Data from William 2004)

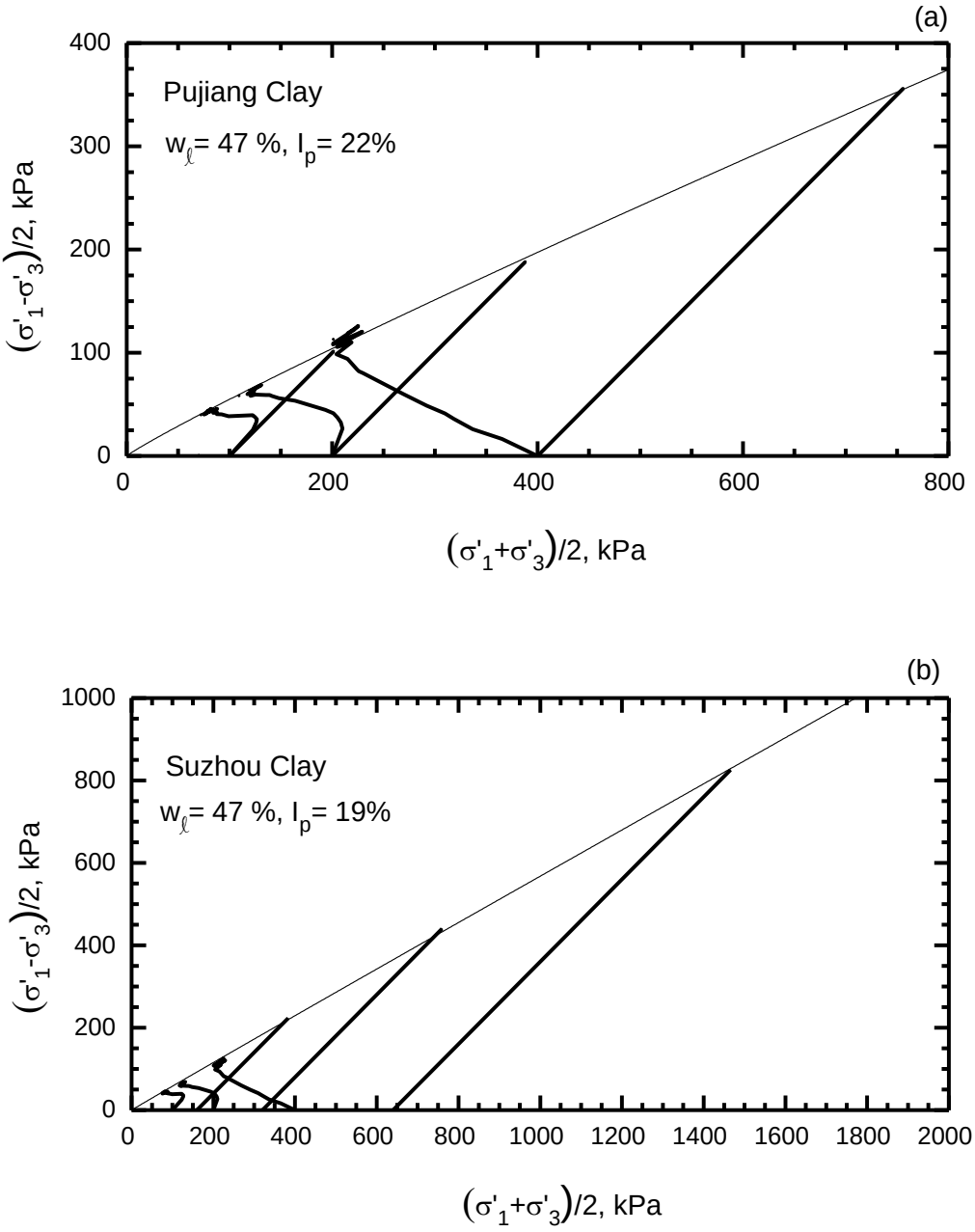

Figure 2.8. Shear Strength of two reconstituted marine clays consolidated from slurry at water content twice the liquid limit, measured in consolidated drained and undrained triaxial compression tests with porewater measurement a) Pujiang Clay b) Suzhou Clay (Data from Sun et al 2014)

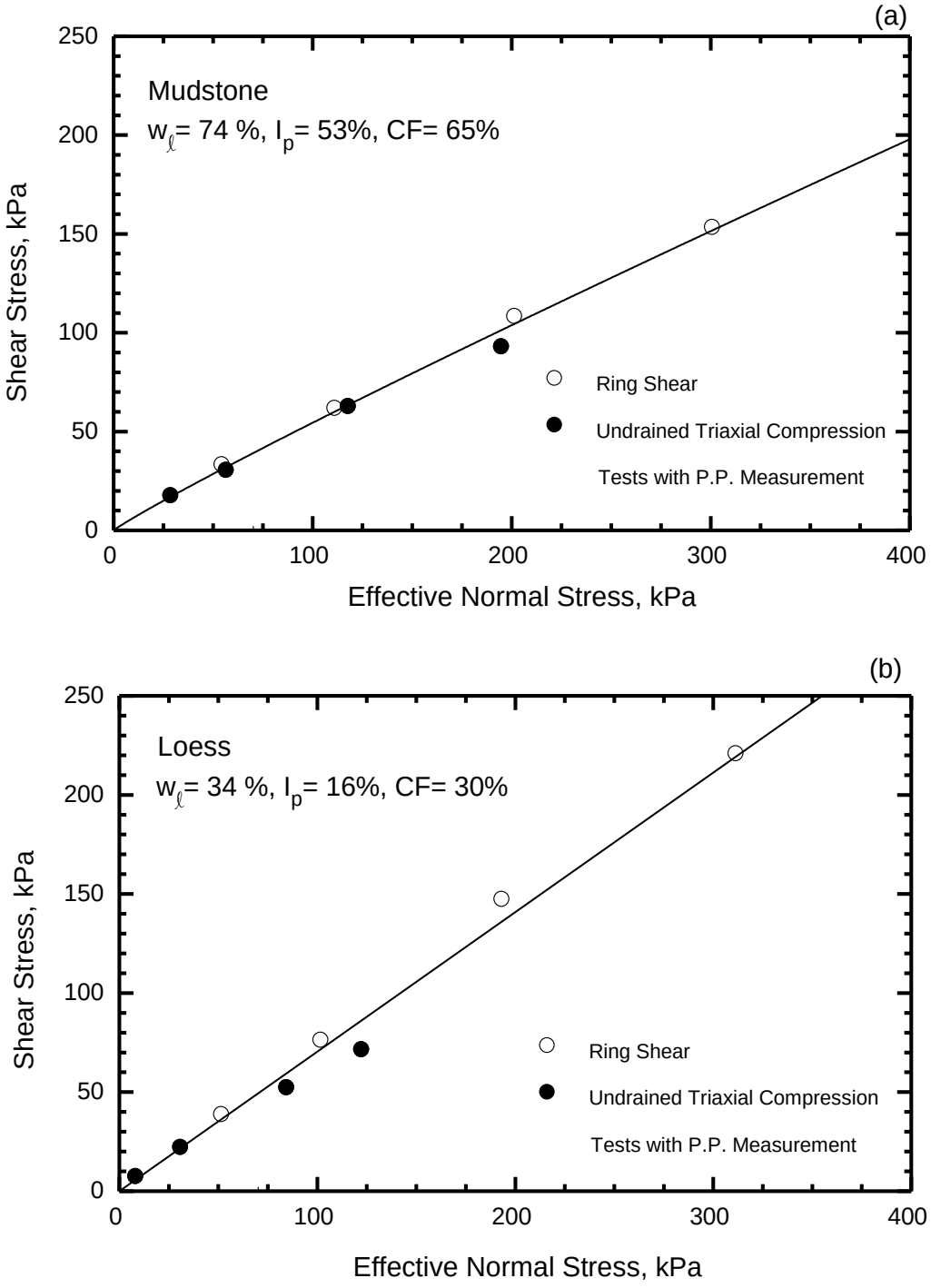

Figure 2.9. Fully softened shear strength of mudstone and loess determined from ring shear tests and from undrained triaxial compression tests with porewater pressure measurement on specimens consolidated from slurry (Data from Kimura 2015)

CHAPTER 3: FULLY SOFTENED SHEAR STRENGTH FROM BACK-ANALYSES OF SLOPE FAILURES

The shear strength measured in laboratory tests may or may not represent the mobilized shear strength on a full-scale slip surface in the field. The best estimate of shear strength mobilized in a full scale situation is obtained by back-analysis of slope failures, which has been previously used, for example, by James (1970), Skempton (1977), Sotiropoulos and Cavounidis (1980), Cancelli (1981), Chandler (1984b), Mesri and Abdel-Ghaffar (1993), Mesri and Shahien (2003). However, the back-analysis requires correct understanding of the stress and strain condition on the global slip surface.

It was concluded by Skempton (1970, 1977) that a first-time slide in stiff fissured clays only caused a relatively small displacement, which is not sufficient to reduce the mobilized shear strength on the slip failure to residual condition. Skempton (1977) examined the slope failures in London Clay in terms of a constant friction angle on the entire slip surface, and concluded that the back-calculated friction angle of 20° corresponds to the fully softened friction angle measured in the laboratory on remolded, normally consolidated London Clay. A similar approach, i.e., back-calculation with a constant friction angle, on the entire slip surface, was also adopted by James (1970) for first time slides in British stiff clays including London Clay, by Chandler (1984a, 1984b) for first time slope failures in London Clay and Upper Lias Clay, who concluded that the field strengths in first time slides in stiff clays agree with the fully softened shear strength.

D'Elia et al (1991) reported first-time coastal slope failures in Capo Spulico, Italy, triggered by the excessive rainfall which significantly increased the porewater pressure in the slopes in this semi-arid area. The slope consists of "Argille Varicolori", which is a structurally complex clay shale formation, with slickensides in some areas. D'Elia et al (1991) suggested that the back-calculated in-situ shear strength, expressed in terms of an average friction angle of 20 to 22 °, which is as high as those determined from drained direct shear tests on partially weathered clayshale, corresponds to fully softened shear strength.

Cancelli (1981) studied a first-time slide in 1978 at the source of a small stream tributary of River Albedosa, near S. Cristoforo, Italy, induced by the slope angle increase as a result of continuous erosion at the head of the valley by the stream source. The slope consists of surficial colluvial cover and Lugagnano Clay which is a fissured, overconsolidated clay. The back-analysis was carried out assuming fully softened condition because the failure could not be justified by the measured peak shear strength parameters. The back-calculated mean friction angle on the entire slip surface was 24°, lower than the measured fully softened friction angle (26° to 29°) in the triaxial compression tests on remolded Lugagnano Clay.

The limitations of some of the previous back-analyses are that 1) assumption of uniform shear strength condition, independent of shear strain distribution, is unrealistic due to the progressive nature of failure and shear strain distribution on the global slip surface, and 2) a single value of friction angle does not take into account the influence of effective normal stress on the friction angle. For these two reasons, the early studies on fully softened shear strength back-calculated from the first-time slope failures, do not provide information on the fully softened friction angle.

Mesri and Shahien (2003) systematically analyzed 99 case histories of slope failures (reactivated and first-time) in 36 soft clays to stiff clays and clay shales using a strain and stress-dependent approach. For the first-time slope failures in 14 homogenous soft to stiff clays, the back-calculated mobilized shear strength on the entire slip surface were equal to or slightly larger than the fully softened strength. Back-analyses of first-time slope failures in stiff clays and clay shales with a horizontal or subhorizontal segment of slip surface assumed at residual condition, with residual strength determined from empirical correlation of residual friction angle and effective normal stress and plasticity index, yielded back-calculated strength on the back-scarp of the slip surface in close agreement with the empirical data on fully softened shear strength (discussed in Chapter 4) based on laboratory tests of Eid (1996), and Stark and Eid (1997).

CHAPTER 4: MOBILIZED SHEAR STRENGTH IN FIRST-TIME SLOPE FAILURES

As introduced in Chapter 3, Skempton (1977) studied the slope failures in London Clay in terms of the constant friction angle of 20 degree, independent of effective normal stress, and concluded that the back-calculated friction angle of 20° corresponds to the fully softened friction angle measured in the laboratory on reconstituted, normally consolidated London Clay. Subsequent back-analyses assuming a uniform shear strength condition on the entire slip surface by James (1970), Chandler (1984a), Mesri and Abdel-Ghaffar (1993), Potts et al. (1997), Stark and Eid (1997) found that the mobilized shear strength for some slope failures in stiff fissured clays might be in between fully softened shear strength and residual shear strength. The assumption of uniform shear strength condition is unrealistic due to the progressive nature of failure. Stress concentration tends to start shear strain from the toe of a slope and propagate toward the crest of the slope, thus reducing the shear strength on the basal more or less horizontal segment of a slip surface to a lower value of shearing resistance.

4.1. Fully softened shear strength mobilized on part of the slip surface

Eigenbrod and Morgenstern (1971) reported a landslide in 1965 in the highway cut at the North wall of the valley of the North Saskatchewan River near the townsite of Devon, about 12 miles upstream of Edmonton, Alberta. The back-scarp of the slip surface (Fig.4.1a) cut through the upper 5 to 6m till overlying a thin coal seam underlain by the bedrock consisting of carbonaceous claystone, bentonite, fissured siltstone and clay stone, and bentonitic sandstone. The horizontal segment of the slip surface was at the boundary of the bentonitic clay and the coal. Eigenbrod and Morgenstern (1971) suggested that most of the back-slope material appeared softened and the slip surface was unlikely to cut through the intact bedrock. As a result, the measured shear strength from consolidated drained triaxial compression tests on “softened material” was used in the back-analysis. The back-calculated friction angle of 8° on the horizontal part within in the measured residual friction angle range from 5° to 10° determined from 3 drained triaxial compression tests under confining pressure of 30 psi (210 kPa) on samples obtained by pushing thin-walled tubes obliquely in the same pit, across the horizontal segment of the slip surface. According to Eigenbrod

and Morgenstern (1971), this first-time landslide formed within a significantly larger pre-existing slide block; and the bentonitic clay layer was sheared prior to the slope failure, and therefore, was at residual strength.

Dixon and Bromhead (1991) questioned as unrealistic the Skempton (1970) assumption of uniform strength condition on the entire slip surface in London Clay and concluded that residual condition had been reached on part of the global slip surface by the time of failure for the London Clay coastal slopes of the Isle of Sheppey (Fig.4.1b), by back-analysis using a fully softened friction angle only on the back-scarp. Dixon and Bromhead (1991) assigned an average friction angle of 20° on the back scarp, which is equal to the fully softened friction angle of London Clay defined by Skempton (1977). It was explained by Dixon and Bromhead (1991) that the basal part of the slip surface follows the bedding related plane of weakness and only small amount of displacement is required to bring the shear strength to residual condition.

The failure of a cut slope in Gault Clay at Selborne (Cooper 1998) taking place in a field experiment was found to be a result of progressive failure, with displacement initiating at the toe and extending into the slope. Field investigation revealed that the basal portion of the slip formed as a single, thin, highly polished, strongly striated slickensides, while the upper part of the slip across the bedding displayed a 20mm zone of shearing with much rougher surface (Fig.4.1c). A factor of safety of 1 was obtained by the time of recorded accelerating displacement in all inclinometers and extensometers, in the analysis by Cooper (1998), assuming a residual strength condition near the toe due to the appreciable shearing on the basal part of the slip surface, and assigning “first-time” shear strength parameters to the rest of the slip which, according to Cooper (1998), is a combination of the peak friction angle measured in the laboratory and a zero or near zero cohesion. This slope failure was also studied by Mesri and Shahien (2003) with the same assumption of residual shear strength measured by Cooper (1998) on the basal slip surface, which yields the mobilized shear strength on the rest of the slip surface similar to the empirical fully softened shear strength proposed by Mesri and Shahien (2003), and in the fully softened shear strength range of Gault Clay measured in triaxial compression tests (Cooper 1998).

The presence of a segment at residual condition in the first-time slope failures has been recognized (James 1970, Skempton 1970, Wilson 1970, Thomson 1971a,b, Parry 1972, Morgenstern 1977;1990; Imrie 1991; Brooker and Peck 1993) and intensively reviewed by Mesri and Shahien (2003). To sum up, in stiff clays and clay shales, either the residual condition already exists along bedding planes, laminations, or other stratigraphic or structural discontinuities before a cut is made or it develops as a result of progressive deformation along horizontal or subhorizontal portion of the slip surface. Relatively small displacements are sufficient to cause the clay to reach residual condition when shearing strain is localized in thin weak bands, and the clay particle orientation is substantially parallel to the direction of shearing (Mesri and Shahien 2003).

The limitation of some of the previous back-analyses is that, a constant friction angle does not take into account the influence of effective normal stress on the friction angle. Mesri and Shahien (2003) systematically analyzed 40 first-time slope failures in stiff clays and clay shales using a stress-dependent approach, with the assumption of residual shear strength mobilized on the horizontal or sub-horizontal basal segment of the slip surface. The mobilized shear strength on the back-scarp of the slides back-calculate by Mesri and Shahien (2003) agrees well with the empirical fully softened shear strength data (discussed in subsection 5.2.2) based on laboratory data from Eid (1996), and Stark and Eid (1997).

4.2. Fully softened shear strength mobilized on entire slip surface

Cases in which the mobilized shear strength on the entire slip surface is close to fully softened strength do exist. Skempton (1970) pointed out that the stability analyses of some European slides at Lodalen, Norway (Sevaldon 1956), Selset, UK (Skempton and Brown 1961) and Kimola, Finland (Kankare 1969a, 1969b), using the fully softened shear strength, lead to an underestimation of factor of safety by 30%. One common feature of these unstratified soft clays is the absence of fissures, which is responsible for a progressive failure in the field. Therefore, the appreciable softening is not available. It is also generally accepted that in unstratified clays with plasticity index smaller than 20% (Chandler 1984a, Mesri and Abdel-Ghaffar 1993), or clay content less than 20% (Skempton 1985), the mobilized shear strength in first-time slide is equal or greater than the fully softened shear strength.

One case with mobilized shear strength greater than the fully softened shear strength, and close to the peak strength, based on both the original reported and the analysis by others (e.g. Mesri and Shehien 2003), is the slide in heavily overconsolidated intact boulder clay in Selset, UK (Skempton and Brown 1961). In lightly overconsolidated soft to firm clays, the shear strength available at a first-time global failure, is indeed, not significantly higher, and in many cases equal to the fully softened shear strength (Kenney 1969, Janbu 1977, Mesri and Shahien 2003). It is therefore, at a first attempt, to generalize that in first-time failures in unstratified, lightly overconsolidated soft to firm clays with a low plasticity (generally smaller than 20%), the mobilized shear strength on the entire slip surface is equal to fully softened shear strength.

FIGURES

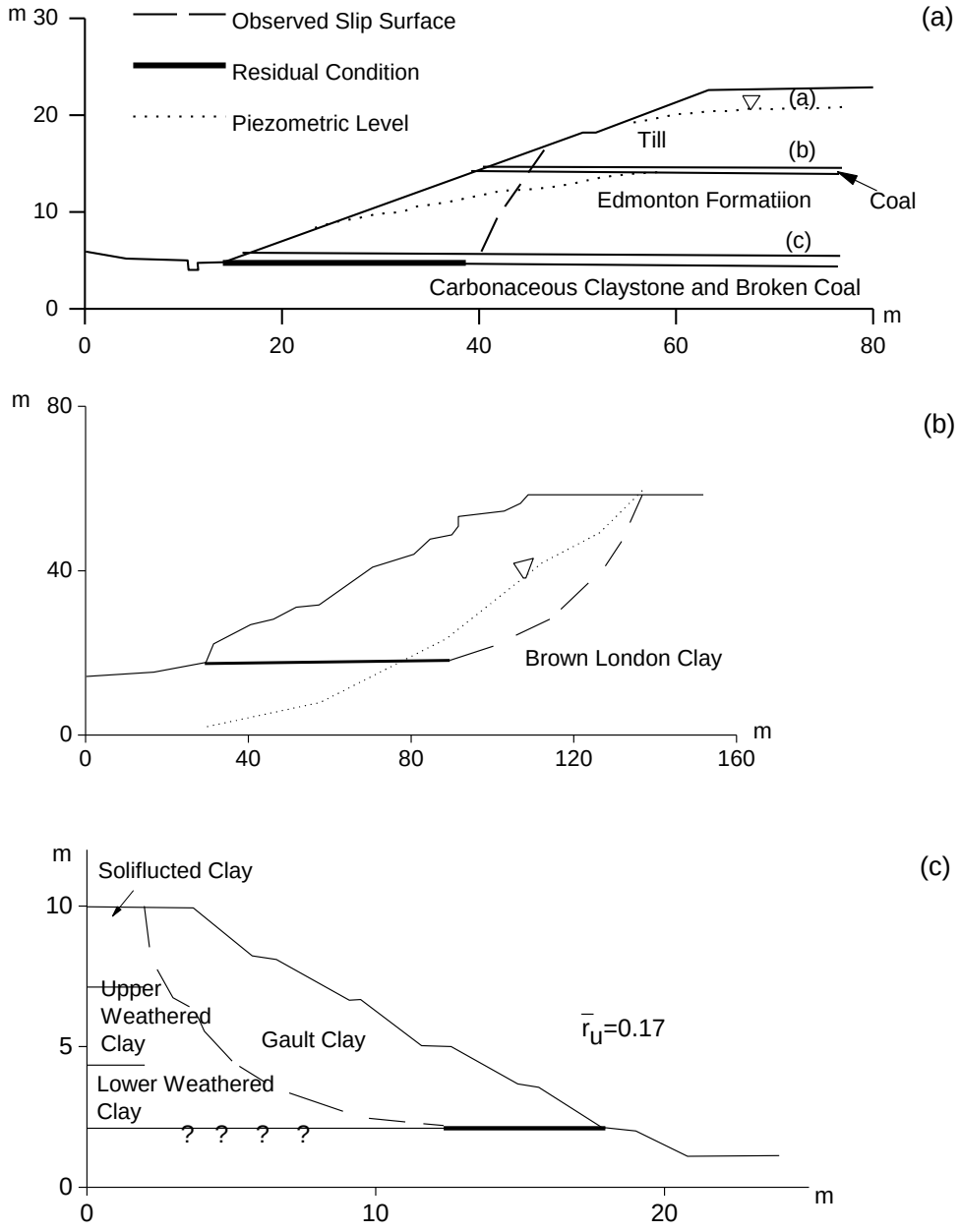

Figure 4.1. First-time slope failures with fully softened shear strength mobilized on part of the slip surface a) Edmonton, Canada, 1965 (Eigenbrod and Morgenstern 1971), b) Isle of Sheppey, England (Dixon and Bromhead 1991), and c) Selborne, UK (Cooper 1998, Mesri and Shahien 2003)

CHAPTER 5: EMPIRICAL CORRELATIONS OF FULLY SOFTENED SHEAR STRENGTH

A correlation should exist between the fully softened friction angle (also residual friction angle) and index properties such as the liquid limit or plasticity index for soil compositions, like stiff clays and clay shales, containing plate shaped clay minerals, as these index properties reflecting the water-holding ability of the particles, are directly or indirectly related to particle size and plateyness (Mesri and Cepeda-Diaz 1986). To be more specific, the liquid limit and plasticity index increase with the decrease of particle size (increase of particle surface area per unit weight) which is at the same time, an indication of increase in plateyness of common clay minerals

5.1. Fully softened shear strength data without the consideration of effective normal stress

Most empirical fully softened friction angle data available are presented as a function of plasticity index, though in some cases they were not documented as fully softened strength. Bjerrum and Simons (1960) collected the friction angle of undisturbed normally consolidated clays including mainly Scandinavian clays and a smaller number of clays from other countries, tested in consolidated drained triaxial compression and in undrained triaxial compression tests with porewater measurement, in which the maximum stress ratio, $(\sigma'_1/\sigma'_3)_{max}$, was used as the failure criterion. The smooth mean curve for these data provides a rough correlation between the friction angle and the plasticity index up to 100%, indicating a decrease of friction angle with the increase in plasticity index.

Values of the friction angle corresponding to a more or less random arrangement of soil particles for the full range of clay compositions (soft clays, soft and stiff clays, shales and clay minerals) were compiled by Terzaghi et al. (1996) and reflected in plasticity index up to 1000%. The majority of the data correspond to plasticity index ranging from 0 to 200%. The mean curve exhibiting the decrease of friction angle with the increase of plasticity index, consists of 2 smooth segments, first for Ip from 0 to 100%, and second for Ip from 100 to 1000%.

For both sets of friction angle data from Bjerrum and Simons (1960) and Terzaghi et al. (1996), the effective normal stress level at which the friction angle was determined, is not specified. The difference in effective normal stress is one reason for the wide range in friction angle at each plasticity index. Terzaghi et al (1996) explained that the high values of friction angle correspond to soils under low effective normal stresses while the lower ones correspond to soils under high effective normal stresses. Another factor resulting to the wide range is the difference in clay size fraction of soils as suggested by Terzaghi et al (1996) that the higher friction angles are determined for soils with clay size fraction of less than 20% whereas the lower ones for soils with clay size fraction of greater than 50%. These two reasons also attribute to 2 smooth segments of the mean curve, instead of a single curve for all the data. First, soils with a plasticity index greater than 100% usually contain a clay-size friction larger than 50% (Stark and Eid, 1997). Second, clay minerals with plasticity index greater than 100% were tested under high confining pressure up to 550 kPa in triaxial compression tests (Mesri 1969). The third possible explanation for the scatters included in the previous empirical correlation between the friction angle and index properties, as suggested by Mesri and Shahien (2003), is the effect of variable sample preparation, i.e., aggregation and disaggregation, on measurement of the index properties.

5.2. Fully softened shear strength data with the consideration of effective normal stress

The previous empirical correlations do not take into consideration the influence of effective normal stress on fully softened friction angle. The nonlinearity of the relationship between shear strength and effective normal stress is nevertheless significant, for intact, fully softened and residual strength (Chandler 1969, Hutchinson 1969, Bishop et al. 1971, Marsland 1972, Morgenstern 1977, Chandler 1982, Lambe 1985, Stark and Eid 1994, Eid 1996, Terzaghi et al. 1996, Stark and Eid 1997, Mesri and Shahien 2003). The pronounced curvature of the fully softened shear strength envelope is mainly related to the soil particle orientation. Face to face interaction of platy particles is promoted at high effective stresses, even for a random arrangement of particles. One convenient way for expressing a nonlinear relationship between shear strength and effective normal stress, is the use of secant friction angle.

5.2.1. Empirical correlation by Stark and Eid (1997)

Stark and Eid (1997) reported the data on the fully softened friction angle as a function of liquid limit with less scatter, in the form of secant friction angle, partly as a result of taking the influence of clay size fraction and effective normal stress into consideration, by dividing the fully softened friction angle data into three groups based on clay size fraction and presenting the data as a function of liquid limit, for three effective normal stresses (50, 100 and 400kPa). Another reason for less scatter is the third influence in the forgoing discussion in terms of sample preparation, as the samples for the index test and the friction angle measurement, were prepared in a consistent manner following the procedure developed by Mesri and Cepeda-Diaz (1986). These data of secant fully softened friction angle by Stark and Eid (1997) corresponding to triaxial compression mode of shear, were obtained by increasing 2.5° of the values measured in the ring shear tests. This increase was decided based on the average difference between the measured friction angles in drained triaxial compression tests and the values in the ring shear tests for reconstituted specimens of 4 shales and a glacial till composition (plasticity index ranging from 8% to 145%) at the effective normal stresses of 100 and 400 kPa. The 2.5° was also reasoned through comparison of friction angle data for sands and silts from literature, between the measured triaxial compression values and data from other laboratory modes of shear. Further updates of this correlation, which inludes the addition of data for other clays and data at lower effective normal stress, are reported in Stark et al. (2005), Stark and Hussain (2013), Gamez and Stark (2014). In all the revisions, the measured data and mean curves are presented as a function of liquid limit.

5.2.2. Empirical correlation by Mesri and Shahien (2003)

The data from Stark and Eid (1997) was utilized by Mesri and Shahien (2003) to develop correlations between secant fully softened friction angle and plasticity index. According to Mesri and Shahien (2003), for many clay and shale composition, plasticity index, to some extent, implies information on both liquid limit and clay size fraction. As this correlation serves as a basis and reference for this research, it is illuminated here in detail. Mesri and Shahien (2003) expressed intact, fully softened, and residual strength by

$$s(i) = \sigma'_n \tan\left[\phi'_i\right]_s^{\sigma'_n} \tag{5.1}$$

$$s(fs) = \sigma'_n \tan\left[\phi'_{fs}\right]_s^{\sigma'_n} \quad (5.2)$$

$$s(r) = \sigma'_n \tan\left[\phi'_r\right]_s^{\sigma'_n} \quad (5.3)$$

Where the secant friction angles $\left[\phi'_i\right]_s^{\sigma'_n}$, $\left[\phi'_{fs}\right]_s^{\sigma'_n}$, and $\left[\phi'_r\right]_s^{\sigma'_n}$ are functions of the effective normal stress.

The empirical equation for the intact strength envelope was proposed by Mesri and Abdel-Ghaffar (1993), derived from an empirical inter-relationship among shear strength, consolidation pressure, and water content, and rewritten by Mesri and Shahien (2003) as

$$s(i) = \sigma'_n \tan\left[\phi'_{fs}\right]_s^{p} \left[\frac{\sigma'_p}{\sigma'_n}\right]^{1-m} \quad (5.4)$$

Where $\left[\phi'_{fs}\right]_s^{p}$ is the secant fully softened friction angle at $\sigma'_n = \sigma'_p$, and σ'_p the preconsolidation pressure.

Similar empirical equations (Mesri and Shahien 2003) are used to define the nonlinear fully softened shear strength and residual shear strength envelopes.

$$s(fs) = \sigma'_n \tan\left[\phi'_{fs}\right]_s^{100} \left[\frac{100}{\sigma'_n}\right]^{1-m_{fs}} \quad (5.5)$$

$$s(r) = \sigma'_n \tan\left[\phi'_r\right]_s^{100} \left[\frac{100}{\sigma'_n}\right]^{1-m_r} \quad (5.6)$$

Where $\left[\phi'_{fs}\right]_s^{100}$ and $\left[\phi'_r\right]_s^{100}$ are, respectively, the secant fully softened and secant residual friction angles at $\sigma'_n = 100$ kPa, $(1 - m_{fs})$is the slope of $\log(\tan\left[\phi'_{fs}\right]_s / \tan\left[\phi'_{fs}\right]_s^{100})$ versus $\log(100/\sigma'_n)$, and $(1 - m_r)$is the slope of $\log(\tan\left[\phi'_r\right]_s / \tan\left[\phi'_r\right]_s^{100})$ versus $\log(100/\sigma'_n)$, for a given plasticity index. The empirical correlations between secant friction angle and plasticity index under three effective normal stresses, 50, 100 and 400 kPa, respectively, were presented by Mesri and Shahien (2003) as the mean curves, based on test data from Stark and Eid (1994), Eid (1996), and Stark and Eid (1997). The mean $\left[\phi'_{fs}\right]_s$ and $\left[\phi'_r\right]_s$ versus plasticity index I_p curve from Mesri and Shahien (2003) are reproduced in Fig.5.1 with I_p from 10% to 250%.

Mesri and Shahien (2003) reanalyzed 99 case histories of slope failures in 36 soft clays to stiff clays and clay shales using the observed slip surfaces and reported ground water pressures. Among

these cases, the back-analysis of 42 reactivated landslide sections was made in 11 stiff clays. These back-calculated strengths corresponding to a factor of safety of unity, are in good agreement with the empirical correlation curves for the residual strength. Therefore, the empirical data based on the laboratory tests on residual strength are assumed to reliably represent the mobilized values in the field (Mesri and Huvaj-Sarihan 2012), and are used for back-analyses of first time slope failures in the present research. Another two categories of slope failures analyzed by Mesri and Shahien (2003) were 1) first-time slope failures in 14 homogenous soft to stiff clays, in which the mobilized shear strength was equal to or larger than the fully softened strength, and 2) first-time slope failures with fully softened shear strength mobilized on part of the slip surface. For the second category of first-time landslides, the use of the empirical residual strength on the horizontal and subhorizontal segments of the slip surfaces yielded back-calculated strength on the back-scarps close to the empirical fully softened strength.

5.2.3. Empirical correlation by Eid and Rabie (2017)

In order to obtain fully softened shear strength at possible effective normal stress levels encountered in landslides, including low (10 and 25 kPa) and intermediate effective normal stress (200kPa), additional fully softened strength data as a function of plasticity index were presented by Eid and Rabie (2017) using the same sample preparation procedure and testing method in Stark and Eid (1997). In addition to the same soils used in Stark and Eid (1997), Eid and Rabie (2017) also performed ring shear tests on other clays and shales, mainly from Egypt. For the same soils used in Stark and Eid (1997), ring shear tests were only performed under 10, 25 and 200 kPa as a supplement. Other soils were tested in ring shear at all six effective normal stresses, i.e., 10, 25, 50, 100, 200 and 400 kPa. The shear strength under low effective normal stresses applies to shallow slope failures or zones with high pore-water pressure, for example, in London Clay and Lias Clay where the average effective normal stress is less than 50 kPa in most cases (James 1970, Chandler 1974, Chandler and Skempton 1974, Skempton 1977). This extension to low effective normal stress is very helpful as the fully softened shear strength envelope displays more significant curvature at low effective normal stresses. Similarly, an increase of 2.5° was applied by Eid and Rabie (2017) to the measured secant fully softened angles from ring shear tests to represent the mode of shear in the triaxial compression test. Eid and Rabie (2017) reported the empirical curves

at 6 effective normal stresses and an equation to estimate the secant friction angle at any combination of plasticity index and effective normal stress, which is essentially, a transformation of Eq.5.5 proposed by Mesri and Shahien (2003). In Fig.5.2 only the fully softened friction angle data of Eid and Rabie (2017) are replotted, together with the empirical curves developed using Eq.5.5 together with the values of average secant fully softened angle at 100kPa from Eid and Rabie (2017), which yields a satisfactory agreement with the measured fully softened friction angle. The mean $\left[\phi'_{fs}\right]_s$ versus plasticity index I_p at 50, 100, 400kPa proposed by Mesri and Shahien (2003) are shown for comparison.

FIGURES

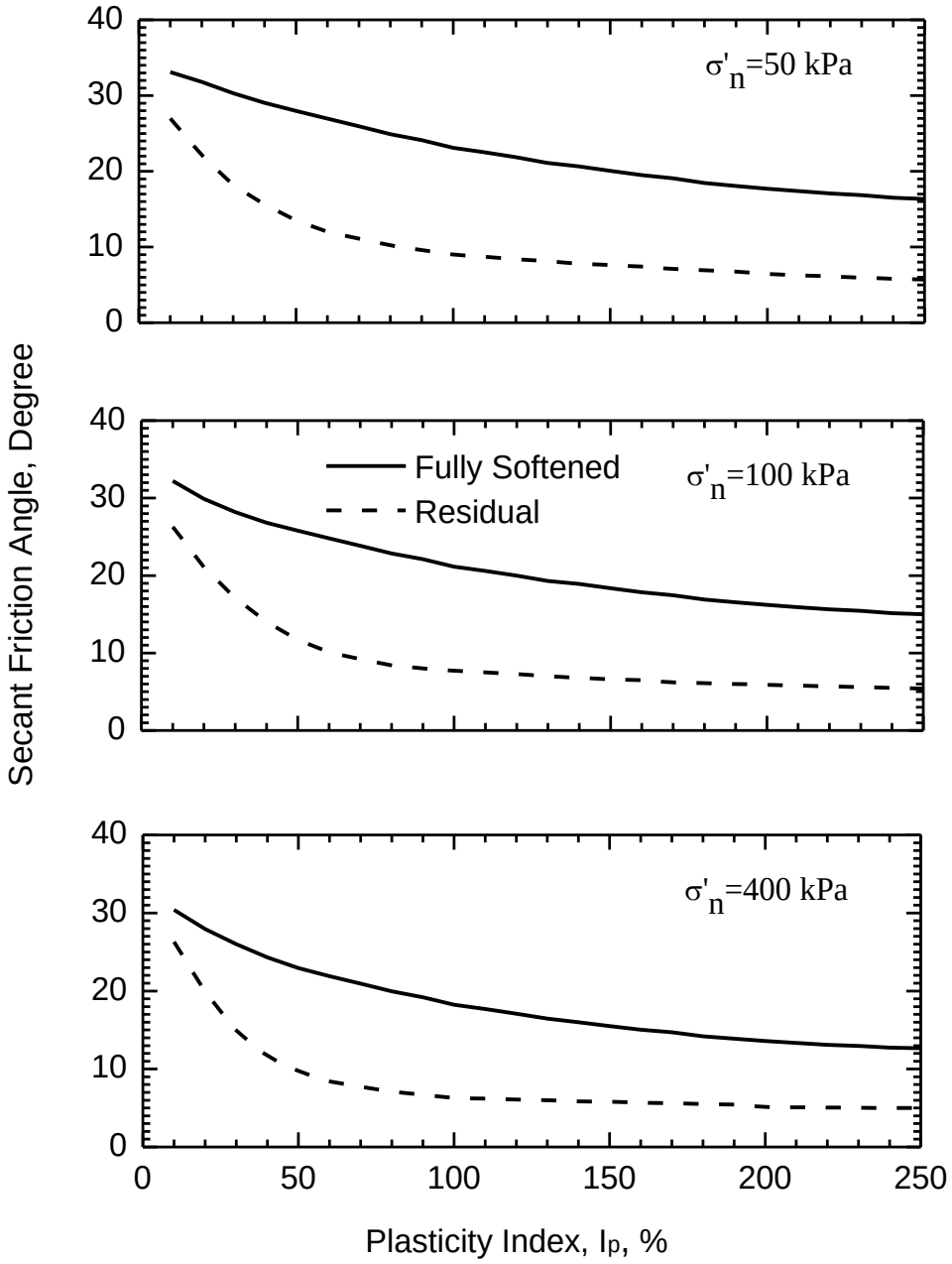

Figure 5.1. Mean empirical relationship for fully softened and residual strength, reproduced from Mesri and Shahien (2003)

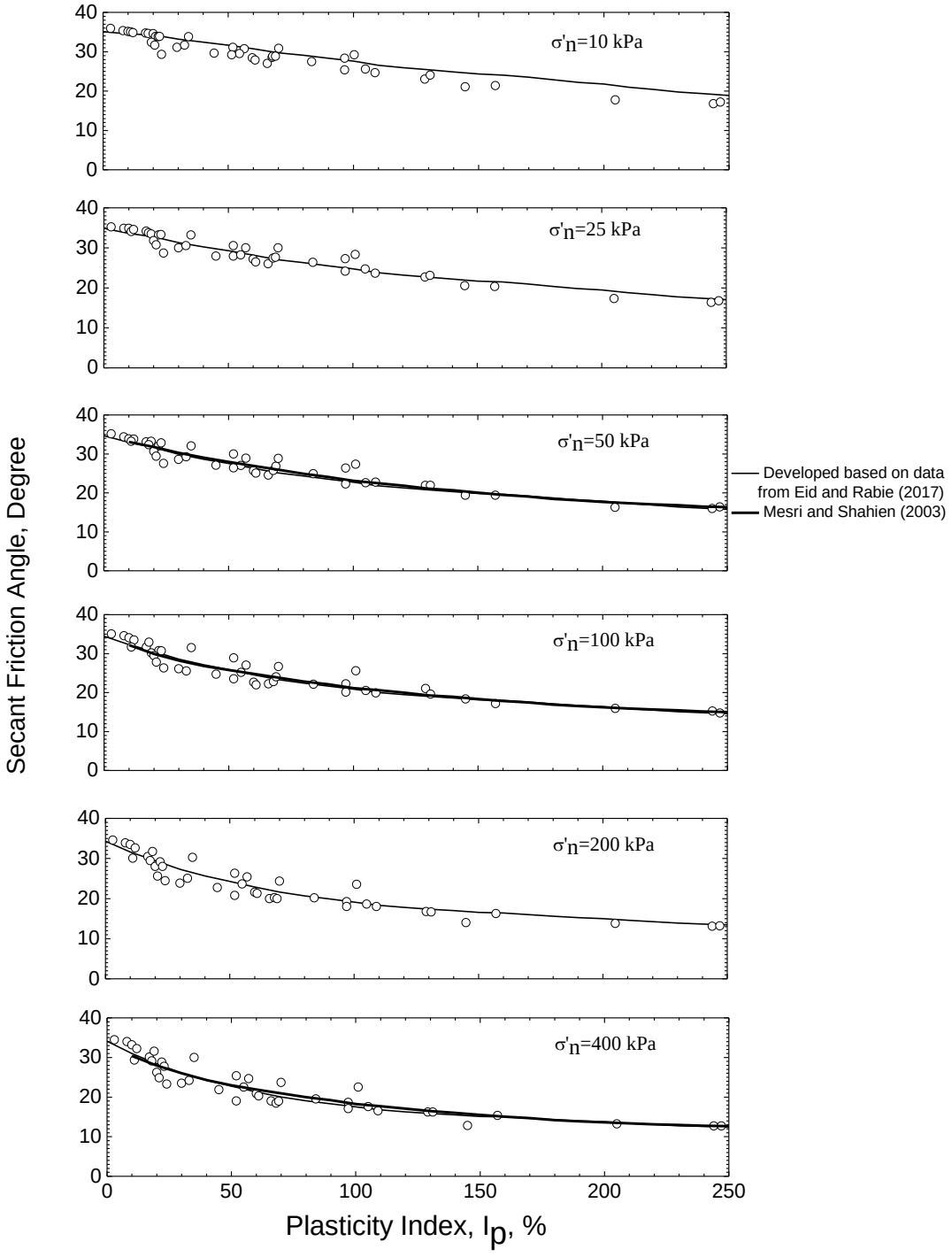

Figure 5.2. Corrected fully softened data measured in modified Bromhead ring tortional tests (data from Eid and Rabie 2017)

CHAPTER 6: TRIAXIAL COMPRESSION TESTING PROGRAM AND TEST RESULTS

In triaxial compression of normally consolidated specimens, reconstituted at a liquidity index near unity, a random arrangement of clay particles is mobilized at failure. This research aims to provide the fully softened shear strength for a wide range of clay compositions, characterized in terms of plasticity index, from 10% to 250%, measured in triaxial compression tests at effective normal stress from 10 to 700 kPa. The laboratory tests in this research include strain-controlled consolidated triaxial compression tests on reconstituted specimens prepared from 15 stiff clay and shale compositions, consolidated under equal all-round pressure, and subjected to undrained shear with porewater pressure measurement. For comparison, a limited number of drained tests were performed. Natural stiff clay and clay shales with very high plasticity (more than 100%) are rarely accessible; therefore, 3 highly plastic samples were obtained by mixing montmorillonitic stiff clays or shales, such as Brenna, with sodium montmorillonite (Mesri and Olson 1970). The laboratory work includes 51 consolidated undrained triaxial compression tests, together with 28 drained compression tests.

6. 1. Description of the clay and shale compositions

The 15 clay and shale compositions include 1) natural stiff clay and shales previously studied by Mesri and Cepeda-Diaz (1986), and Stark and Eid (1997) in the University of Illinois at Urbana-Champaign, 2) clays retrieved from 3 recent projects, which are Fargo Flood Control Project in North Dakota, Newmont Golden Quarry in Nevada, and Harris County Flood Control Project in Texas, and 3) clay and shale compositions reconstituted with montmorillonitic stiff clays or clay shales and sodium montmorillonite.

The index properties of clay and shale compositions are listed in Table 6.1. The plasticity index ranges from 13% to 217%, and clay size fraction from 20% to 78%. All the clay and clay shale compositions lie above A-line and below U-line in the Cassagrande Chart in Fig 6.1. Three of the clays, Glen Forest, South Richey, and Kuykendahl Clay, from the flood control project in Harris County, Texas, are classified as lean clay, CL, and the rest of the clay and shale compositions are

CH, highly plastic clay. The index properties are obtained from air dried samples, because clays and shales used in this investigation do not contain organic matter, or minerals that experience irreversible dehydration upon drying. Liquid limits were measured using a Casagrande cup, plastic limits were determined by hand rolling procedure (ASTM D4318), and clay size fractions were determined by sedimentation analysis in hydrometer tests.

Atterberg limit measurements were not performed on the 5 stiff clays and shales previously studied by Mesri and Cepeda-Diaz (1986), Stark and Eid (1997), because of the limited amount of samples. The index properties of these stiff clays and shales, marked with a and b in Table 6.1, are values reported by Mesri and Cepeda-Diaz (1986), and Stark and Eid (1997), respectively. The index properties of these clay and shales were obtained on ball-milled samples passing No. 200 U. S. standard sieve, to minimize the aggregation resulting from diagenetic bonding (Mesri and Cepeda-Diaz 1986). The remaining 10 materials, including the 7 natural stiff clays and 3 highly plastic mixtures, were also processed using ball-milling techniques. To examine the influence of disaggregation on the Atterberg limit, 6 natural stiff clays were also processed using the ASTM standard procedure - pulverized in the automatic grinder (further pulverized using the pestle and mortar if necessary), and passed through No. 40 U. S. standard sieve (ASTM D4318). The comparison of the plasticity indices obtained from samples processed using ball-milling techniques and those obtained from samples processed using ASTM D4318 standard procedures, is shown in Fig.6.2, together with the data (solid circles) for 22 shales reported by Eid (2001).

The Brenna Clay samples were taken at a depth from 30.5 to 32.5 ft (9.3 to 9.9m) below ground level in a Fargo Flood Control Project site in North Dakota. The Brenna Formation was sedimented in Lake Agassiz basin which formed in north-central US and extended into southern Canada. The lake existed from 13,000 to 8,000 years before present in Pleistocene Epoch (Quigley 1980). Clays of Brenna Formation are grayish brown to dark gray, soft to firm, generally unbedded, but with slickensides in places (Arndt 1977, Mesri and Huvaj 2004). The Brenna Formation is subdivided into Lower Brenna and Upper Brenna members, which have, respectively, liquid limit ranging from 62 to 103%, and 107 to 154% (Arndt 1977, Mesri and Huvaj 2004). The dark gray Brenna samples in the present research, with liquid limit of 77% and plasticity index of 49%, belong to Lower Brenna Formation, and are classified as highly plastic clay on the Casagrande Chart

(Terzaghi et al 1996). Direct shear test data for reconstituted Brenna are also included, which are from a separate investigation on remediation of stiff clay and clay shale slopes (Moridzadeh 2019).

The Newmont Golden Quarry Clay was taken at elevation 325 to 327.5 ft (99.0 to 99.8 m) from the North Dump in Newmont Gold Quarry, Neveda. This yellowish, gravelly clay has a clay size fraction of 56%, liquid limit of 115%, and plasticity index of 73%, and is classified as CH, highly plastic clay.

Brown London Clay was obtained from Bradwell, UK. London Clay Formation is a marine deposit of Eocene age, which crops out in the southeast of England (Skempton et al 1969, Skempton 1977). It was overconsolidated by the erosion of at least 150m of sediments. The upper 5 to 15 m of London Clay is oxidized to a brown color, which overlies the massive blue-gray clay (Skempton et al 1969, Skempton 1977). The main mineralogy of the clay fraction is illite and montmorillonite (Burnett and Fookes 1974). This intensively investigated clay is described as a stiff, fissued clay (Bishop et al 1965, Skempton and Petley 1967, Skempton et al 1969, Skempton and Chandler 1974, Skempton 1977). The Brown London Clay tested in the present research is brownish, with clay size fraction of 66%, liquid limit of 101%, and plasticity index of 66% (Stark and Eid 1997), which is higher than the typical value of 52% reported by Skempton (1977).

Beaumont Formation was the youngest Pleistocene epoch deposit laid down by rivers as levees and deltas in the early Wisconsin glacial age, in the southeast Texas parallel to the Gulf of Mexico coastline (Focht and Sullivan 1969, Al-Layla 1970). The overconsolidated clay is fissured resulting from multiple cycles of drying and wetting when it was exposed at the surface (Al-Layla 1970. The overconlidation ratio, caused by desiccation, is between 4 and 6 (Focht and Sullivan 1969, Al-Layla 1970). Beaumont Formation consists of tan and brownish-red clay interbedded with silt and sand layers, with clay size fraction ranging from 40 to 77% (Focht and Sullivan 1969, Al-Layla 1970). The main clay minerals of Beaumont Clay are montmorillonite (23 to 47%) and illite (28 to 55%), with some kaolinite and quartz (Al-Layla 1970, Huvaj-Sarihan 2009). Al-Layla (1970) reported typical liquid limit of Beaumont Clay in the range between 60 and 100%, plasticity index between 33 and 65%. The Beaumont Clay sample in the present research, is brownish red, with liquid limit of 67%, plasticity index of 44%, and clay size fraction of 66%.

Glen Forest, South Richey, Kuykendahl, and Mud Gully Clay were provided by Harris County flood control project, Texas, and are named after the project sites. The clays in Harris County region, reported by the flood control project, display a wide range of plasticity index, approximately from 10 to 80%.The color of these clay samples varies from tan /yellowish brown for clays with lower plasticity index, to reddish brown /red for clays with higher plasticity index. Glen Forest Clay samples retrieved from approximately 5 ft (1.5m) depth below ground level in the Glen Forest Regional Detention Basin, have a tan color, with liquid limit of 31% and plasticity index of 16% (CL). The brown clay samples from the South Richey Stormwater Detention Basin, display a liquid limit of 43% and plasticity index of 25% (CL). The yellowish brown clays from Kuykendahl Stormwater Detention Basin were obtained at 1 ft (0.3m) depth below ground level at the project site, and have a liquid limit of 31% and plasticity index of 13% (CL). Clay size fractions of Glen Forest, South Richey, Kuykendahl Clay, are, 20, 38, and 24%, respectively. Mud Gully Clay from depth 15 to 18ft (4.6 to 5.5 m) in the detention basin, is reddish brown, which displays a clay size fraction of 71%, liquid limit of 96% and plasticity index of 68%, and is classified as highly plastic clay.

Taylor Shale obtained from depths of 35 to 50m at the San Antonio Channel Improvement Project in San Antonio, Texas, is a massive-bedded, soft to moderately hard, blue-grey marine formation of Cretaceous age, a montmorillonitic clay with variable carbonate content (Green and Wallace 1993, Mesri et al 1994). The Taylor Shale samples used in present investigation have a liquid limit of 170%, plasticity index of 131%, and clay size fraction of 72% (Mesri and Cepeda-Diaz 1986).

Oahe Firm Shale samples were retrieved from Oahe Dam in South Dakota. The bedrock in Oahe dam site is the montmorillonitic Pierre Shale, which was derived from clays and silts in the late Cretaceous Age, compressed by the weight of overlying material into thinly bedded, dark gray to black shales and marls (Johns et al 1963, Knight 1963). Bentonite layers are present throughout the formation, and Oahe Firm Shale refers to the firm Pierre Shale free of weathering, without significant occurrence of bentonite layers, in comparison to Oahe bentonitic Shale studied by Stark and Eid (1997). The reported clay size fraction, liquid limit, plasticity index, of Oahe Firm Shale samples, are, 78, 138, and 97%, respectively (Stark and Eid 1997).

Lea Park Shale belongs to the Upper Craterous bedrock in Saskatchewan, and lies above Upper Colorado Group (Meijer Drees and Myhr 1981, Christiansen 1982). This highly plastic dark gray

montmorillonitic shale mainly consists of noncalcareous, marine silt and clay, with discontinuous bentonite seams in places (Insley et al 1977, Christiansen 1982, Nichol et al 2016). The reported liquid limit of Lea Park Shale is up to more than 90%, and plasticity index up to 72% (Larsen 2011, Nichol et al 2016). The clay size fraction, liquid limit, and plasticity index, of the Lea Park Shale samples tested in the present research, were reported to be 65, 253, and 205%, respectively (Stark and Eid 1997). One possible reason for significant lower plasticity index of Lea Park Shale reported by Larsen (2011) and Nichol et al (2016) is the sample preparation procedures for Atterberg limit measurements, which were not specified. It is possible that these Lea Park Shale samples were not ball-milled; therefore, significant aggregation survived after the sample preparation process. According to the triaxial compression tests in the present research, the plasticity index of 205% for Lea Park Shale is reasonable, because of the measured secant fully softened friction angle ranging from 9.7° at effective normal stress of 700 kPa, to 20.9° at effective normal stress of 10 kPa. A major influence of disaggregation was observed in the increase of liquid limit of highly aggregated Cucaracha Shale from the Panama Canal, from 49% to 156% by crushing the samples for 6 min in a disc mill (La Gatta 1970), and by ball-milling from 88% to 250% (Mesri et al 1978).

Patapsco Formation, which crops out between Washington, D.C., Baltimore, Maryland, and Annapolis, Maryland (Schluger and Roberson 1975), is a red and drab-colored sediment of the Lower Cretaceous Potomac Group (Glaser 1971, Schluger and Roberson 1975). The colors of Patapsco are related to the iron oxides. The main clay minerals in the Patapsco Formation are kaolinite and illite (Glaser 1971, Schluger and Roberson 1975). Mesri and Cepeda-Diaz (1986) reported a liquid limit of 77%, plasticity index of 52%, and clay size fraction of 59%, for Patapsco Shale sample.

The sodium montmorillonite used to obtain highly plastic samples by mixing with montmorillonitic clays and shales, has a liquid limit of 469%, and plastic index of 415%. The index properties together with the details of reconstituting highly plastic sample mixtures, are described in subsection 6.2.1.

6. 2. Triaxial Compression Testing Program

The triaxial testing system includes three parts, i.e., the triaxial cell, the cell pressure and back-pressure sources, and the loading apparatus. The all-stainless steel triaxial cells (Fig.6.3) used in the research were especially designed and constructed in the University of Illinois. These triaxial cells were designed to minimize compressibility of the drainage connections and minimize piston friction.

The transparent Plexiglas cylinder for 1 ½ inch (3.8 cm) diameter specimens has an outer diameter of 4 inch (10.1cm) and inter diameter of 3 ½ inch (8.9cm), which can withstand a cell pressure of up to 150 psi (1034 kPa). In this research, the confining pressure applied to the samples ranged from 4.5psi (30kPa) to, 80psi (550kPa) for undrained tests, and 115psi (790kPa) for drained tests, and the maximum back-pressure in consolidated undrained triaxial compression tests was 40psi (276 kPa), resulting in a maximum cell pressure of 120psi (827 kPa) in undrained tests.

The stainless steel cell top has a ball bushing and a bleed valve. Stationary ball bushing with an X-ring seal of 4 percent diametral compression is used because this combination was proved to be satisfactory in terms of piston friction (Olson and Campbell 1967). A wiper seal is fitted at the top to prevent dust from entering the assembly, and an X-ring (Minnesota Rubber Co.) seals off the cell pressure fluid (Choi 1982). A ½ cm layer of silicon oil is floated on the top of cell pressure fluid to minimize leakage and lubricate the piston.

The loading cap is a plain Perspex disc with a stainless steel tubular projection above the cap, serving as a guide for the loading piston during consolidation and axial loading, and a 1/2in (1.3 cm) diameter stainless steel ball seats within the guide. The stainless-steel loading piston for the triaxial cell, slides inside the stainless steel guide, which avoids misalignment of samples due to large volume changes during the consolidation stage.

The triaxial cell has one cell fluid/ cell pressure inlet, and two drainage connections for each of the top and bottom of the specimen. However, only the bottom drainage connections were used in the present investigation. The cell base described in detail by Adachi (1974) includes drainage lines made of continuous stainless tubing with inner diameter of 0.073 inch (0.19 cm) with no sharp bends or any intermediate connections, which minimizes the compressibility of the pore-pressure measuring system and eliminates the possibility of trapping air bubbles in the pore pressure lines.

O-ring grooves have been designed to minimize compressibility of the cell and prevent cell fluid leakage. The volume change in the consolidation stage and shearing stage of the drained tests, was measured by a burette connected to one of the bottom drainage lines.

Whatman No.1 slotted filter paper is used for the radial drain (Bishop and Henkel 1957), and Tekto polyester screen HD 7-6 is used for top and bottom drains. The specimen, sitting on a porous stone, is enclosed in a 0.070mm thick Trojan rubber membrane, and sealed at the loading cap and at the base pedestal by two 218 N70 Buna-N Nitrile 70 O-rings, which have an inside diameter of 1.25inch (3.18cm), outside diameter of 1.50inch (3.81cm), and cross-sectional diameter of 1/8inch (0.32cm). Figure 6.4 is a photograph of a specimen in the triaxial cell.

For the pressure-saturation and shearing stage, the triaxial cell is inside a Plexiglas tank filled with demineralized water, and the water temperature is maintained at 22°C by YSI Model 72 Proportional Temperature Controller and an electrical mixer to eliminate temperature fluctuations during the shear test. The triaxial cell sits between the axial loading press, which consists of a top screw jack in contact with the loading piston, and a bottom input shaft with a platen on its top. The platen is able to move up and down by means of the stepping motor which is connected to the electronic control unit (Olson et al 1971); and one revolution of the input shaft causes the platen to move 0.0025 inch (0.06 mm). The stepping motor shaft rotates 1.8 degree upon receipt of one command and stops. The shaft speed is dependent on the pulse commands from the electronic control unit designed and assembled in the University of Illinois at Urbana-Champaign (Olson et al 1971), which can accommodate time to failure in a triaxial specimen ranging from 15 minutes to nearly 1 yr. In the compression tests in this research, the loading piston stays stationary while the platen moves upward. The axial load during shearing and the axial deformation are measured by a high quality Wykeham-Farrance proving ring and a Baty dial gauge, respectively.

The constant cell pressure is provided by the Self-Compensating Mercury Control, Fig.6.5 (Bishop and Henkel 1957). This system is a reliable method for maintaining constant cell pressure as the head of the mercury column is kept constant with the help of the calibrated spring holding the mercury pot, which is able to retract to compensate for the mercury height change due to the volumetric change of the specimen or cell fluid in the triaxial cell.

Figure 6.6 is a photograph of the triaxial compression test system, including the triaxial cell, the loading system, the cell pressure and back-pressure source, and the temperature controller – one specimen is being consolidated under equal all around pressure, and the other specimen is being sheared.

The consolidated undrained triaxial compression tests performed in this research included 4 major steps, reconstituted specimen fabrication, consolidation under equal all around pressure, back pressure saturation, and shearing. The description of each stage is described here.

6.2.1. Specimen Fabrication

All natural clays, clay shales, and sodium montmorillonite were first air dried. Twelve natural clays and shales were pulverized in the automatic grinder (further pulverized using the pestle and mortar if necessary), and passed through No. 40 U. S. standard sieve (0.425mm). The sieved samples were thoroughly mixed in a container using a spatula, with distilled and deaired water to a liquidity index, IL, near 1.5, then allowed to temper in the moisture room with moisture and temperature control, for at least 2 weeks, before fabrication of triaxial specimen.

The preparation of highly plastic samples reconstituted with montmorillonitic clays and shales, and sodium montmorillonite, is summarized in the following paragraphs. The dry montmorillonite was crushed using a pestle and mortar, and the entire sample was mixed with deaired and distilled water to reach a liquidity index of 2. The montmorillonite slurry was hydrated in the moisture room for 1 month before Atterberg limit measurement and sample preparation (mixing). The highly plastic mixtures were reconstituted using hydrated clay and clay shales and sodium montmorillonite slurry.

In order to obtain clay compositions with a plasticity index higher than those for the natural stiff and clay shale compositions, a number of specimens were prepared and tested by adding sodium montmorillonite slurry (I_p = 415%) to one stiff clay and one clay shale. For Brenna-Montmorillonite Mixture 1, every 100 g dry Brenna Clay (I_p = 49%) was mixed with 5.9g of dry sodium montmorillonite. The liquid limit, plasticity index, and clay size fraction of Brenna-Montmorillonite Mixture 1, are 122%, 91%, and 69%, respectively. Every 100 g dry Brenna was mixed with 53.5 g sodium montmorillonite to obtain Brenna-Montmorillonite Mixture 2, which

displays the liquid limit, plasticity index, and clay size fraction, of, 174%, 140%, and 75%, respectively. For Taylor Shale-Montmorillonite Mixture, every 100g dry Taylor Shale (I_p = 131%) was mixed with 36.2 g dry montmorillonite. Taylor Shale-Montmorillonite Mixture has a liquid limit, plasticity index, and clay size fraction, of, 278%, 217%, and 78%.

The triaxial specimens were fabricated by "kneading", which includes the following steps. After being hydrated in the moisture room for at least 2 weeks, the water content of saturated sample was reduced on a large clean glass, by means of repeatedly mixing using a spatula, to a uniform consistency and an intended liquidity index in the range of 0.8-1.0 as described in Chapter 2. The actual liquidity index of 12 clay and clay shale compositions at time of kneading, as listed in Table 6.1, is in this recommended range or slightly higher. Three highly plastic clay and clay shale compositions, Newmont Clay (I_p = 73%), Brown London Clay (I_p = 66%) and Lea Park Shale (I_p = 205%), were kneaded at lower water content, corresponding to liquidity index of 0.45 to 0.55, 0.51 to 0.74, and 0.52 to 0.60, respectively, to ensure handling of soft specimens, and avoid significant compression and decrease in specimen diameter during consolidation under equal all around pressure before shear.

The 3.00 inch (7.6 cm) high specimens were produced by packing reconstituted soil using a spatula, layer by layer into a Plexiglas mold (Fig.6.7) without trapping air pockets. The term kneading, or kneaded soil was also explained by Lau (1998) in relation to similar process to prepare remolded Cowden Hill and London Clay specimens. The mold used to prepare the specimens, consists of a cylindrical tube, a disk, and a piston attached to a brass rod. The Plexiglas tube has an inside diameter of 1.50 inch (3.80 cm), and a length to produce a 3.0 inch (7.60 cm) long specimen.

6.2.2. Consolidation

The base drainage system of the triaxial cell was flushed with deaired and distilled water after the specimen setup to remove any air entrapped between the membrane and the sample or in the lines. The flushing was generally repeated 3 times with at least a 30 minute interval in between. The equal all around consolidation pressure was applied in increments using a pressure increment ratio of 1.0, allowing end-of-primary compression under each increment, expect the last pressure where half log cycle of secondary compression was allowed. The Casagrande construction (Casagrande

and Fadum 1940) was used to determine the end of primary consolidation. After primary consolidation plus half log cycle of secondary, the height of the soil specimen was measured using a cathodometer. Depending on the permeability of the specimen, which is related to the plasticity index/liquid limit, remolding water content, and consolidation pressure, the duration of end of primary consolidation of the last increment for the tests in this study, ranged from 4 hrs (Kuykendahl Clay consolidated at 85 kPa) to 14 days (Lea Park Shale consolidated at 100 kPa).

6.2.3. Pressure-saturation

Pressure-saturation was made for undrained triaxial compression tests after consolidation and before the shearing stage. Before pressure-saturation, the base drainage system of the triaxial cell was again flushed, 3 times with at least a 30 minute interval in between, with de-aired water to remove any air entrapped between the membrane and the sample or in the lines. A total back pressure of 40 psi (276 kPa) was applied to the system in four increment. At each increment of cell pressure (10psi, or 69 kPa), the porewater pressure response was measured by a Dynisco transducer and the Digital Strain Indicator by Vishay Micro-Measurements. If the B coefficient, $\Delta u / \Delta p$, did not reach 0.98 in four minutes after each cell pressure increment, a back pressure of 10 psi (69 kPa) was applied to bottom drainage system, and left on the sample for a duration of 2 to 24 hours depending on time available and the porewater pressure response before the application of back pressure. The process was repeated until a back pressure of 40 psi (276 kPa) was reached; back pressure line was turned off, and shearing was begun, and shear-induced porewater pressure was measured. For the consolidated drained triaxial compression tests, the system was not back-pressured after consolidation. However, before shear, the system was repeatedly flushed for a longer duration (24 hours or longer).

6.2.4. Shearing

For the consolidated drained triaxial compression tests, the strain rate should be slow enough so there is no buildup of shear-induced pore water pressure. In the undrained tests, appropriate strain rate should be selected to achieve porewater pressure equalization throughout the specimen,

especially because porewater pressure is commonly measured at the bottom of the specimen. The rate of axial deformation is expressed by

$$\dot{\delta} = \varepsilon_f \cdot L/t_f \tag{6.1}$$

Where $\dot{\delta}$ is the axial deformation rate, ε_f is the axial strain at failure, L is the height of the specimen after consolidation, and t_f the time to failure.

For drained tests, time to failure can is calculated using the following approach introduced by Gibson and Henkel (1954),

$$t_f = \frac{(L/2)^2}{\eta c_t (1-\bar{U}_f)} \tag{6.2}$$

Where L/2 is half of the specimen height; η is a numerical factor depending upon the extent and location of the drainage surfaces which are assumed to be fully draining. For the drainage from ends and radial boundary η is 35; c_t is the coefficient of consolidation in triaxial compression in the shearing stage; $\bar{U}_f$ is the degree of consolidation at failure, which is taken to be 95%.

The coefficient of consolidation in triaxial compression, c_t, is taken to be equal to c_a, which is the coefficient of consolidation in the consolidation stage under the last all around pressure in a triaxial cell. The values of c_a was calculated by Gibson and Henkel (1954) using a procedure by Silveira (1953) and Gibson and Lumb (1953), according to

$$T = \frac{c_a t}{a^2} \tag{6.3}$$

Where T and t are assumed to correspond to a degree of consolidation at "100 percent", and a is the radius of the specimen (This approach is not used in the present study).

For undrained tests, time to failure can be computed using the equation by Blight (1963) for tests with all-round drains,

$$t_f = 0.07 \frac{H^2}{c_t} \tag{6.4}$$

Where 0.07 is the time factor corresponding to 95% porewater pressure equalization in tests with all-around drains.

Based on the approaches developed by Gibson and Henkel (1954), and Blight (1963), alternative procedures have been suggested for estimating time to failure (Mesri and Ali 1987),

$$[\,t_f]_{DTC} = 50\,t_{50} \tag{6.5}$$

$$[\,t_f]_{UTC} = 8\,t_{50} \tag{6.6}$$

The t_{50} corresponds to 50% primary consolidation in the last pressure increment, and is computed using the Casagrande method (Casagrande and Fadum 1940) in the present study. If two specimens of the same clay or clay shale composition, are kneaded at the same water content, consolidated under the same equal all around pressure, but subjected to drained and undrained shear, respectively, the computed time to failure for the undrained test will be 1/6 of that for the drained test.

For the drained tests, the axial strain at failure, ε_f, is usually 15 to 20% for reconstituted normally consolidated or slightly overconsolidated clay, while it is usually in the range of 5 to 15% in the undrained tests. In the present study to determine the shear rate, values of ε_f equal to 16% was used for the drained tests, and 8% for undrained tests. The deformation rate is computed using Eq.6.1, together with Eq.6.5 and Eq.6.6, for drained and undrained tests, respectively. However, in order to accommodate test data recording in the undrained tests with porewater pressure measurement, the deformation rate used in the undrained tests, was actually around 1/5 to 1/3 of the computed values. The triaxial compression tests were stopped at an axial strain of approximately 20%. The duration of shearing, in undrained tests, ranged from 3 days (Kuykendahl Clay) to 60 days (Lea Park Shale), and the drained tests, lasted for 4 days (Kuykendahl Clay) to 70 days (Lea Park Shale). On average, for the same stiff clay and shale composition, the shearing duration of an undrained tests was half of that of the drained tests.

6.2.5. Dismantling the triaxial cell

After the shearing was completed, the loading piston was clamped in place, the proving ring was removed, and the cell pressure source was disconnected. After the cell fluid was emptied, the

specimens was removed from the pedestal. The specimen with filters removed, was cut into 5 disks along the specimen height, to obtain the water content distributions in the specimen.

6.3 Triaxial Compression Test Results

The photographs of the specimens were taken after each test, and the water content distribution in the specimen was determined. This section describes the stress-strain behaviors of the reconstituted normally consolidated clay and clay shale compositions, and stress paths together with the failure criteria. The stress-strain curves and stress paths presented in the present research, were corrected for the effects of rubber membrane and lateral filter paper drain, because they may contribute to the measured compressive strength of the specimen. Secant friction angles and axial strain at failure in drained triaxial compression tests are compared with those in undrained tests with porewater pressure measurement. Then, brief summaries are presented, in relation to ratios of undrained shear strength to consolidation pressure, and A-coefficient at failure. Finally, the correlation of secant fully softened friction angle is presented, as a function of plasticity index, at 7 effective normal stresses.

6.3.1 Shape of specimens at the end of tests

Example photos of the specimens at the end of undrained tests and drained tests are shown in Fig.6.8 and Fig.6. 9, respectively. A simple generalization could not be made about the shape of specimens at the end of the tests, in relation to, for example, plasticity index, consolidation pressure and drainage condition during the shearing process.

For the clays (Glen Forest, South Richey, and Kuykendahl) with lower plasticity index (13 to 25%), and Brenna-Sodium Montmorillonite Mixture 2 (I_p = 140 %), no shear planes were observed at the end of tests, either undrained or drained. The specimens bulged in the mid-height, which indicates that the stress distribution is not uniform along the specimen height as a result of end friction.

Remolded specimens of Brown London Clay (I_p = 66 %), Beaumont Clay (I_p = 44 %), Mud Gully Clay (I_p = 68 %), and Taylor Shale (I_p = 131%), displayed well defined single shear surfaces in

both drained and undrained tests. For Lea Park Shale (I_p = 205 %), Oahe Firm Shale (I_p = 97 %), and Patapsco Shale (I_p = 52%), a single shear plane was observed in the undrained tests, and specimens subjected to drained shear bulged in the mid-height of the specimen by the end of tests.

For Brenna clay (I_p = 49 %) subjected to consolidated undrained compression tests, a single shear surface developed in specimens with consolidation pressure in the range of 4.5 to 50 psi (31 to 345 kPa). For specimens consolidated at 60 and 80 psi (413 and 551 kPa), the specimens bulged nonuniformly. All the specimens at the end of drained tests remained cylindrical, which indicates that end effect was insignificant in these drained tests.

No shear planes were observed in drained tests on Newmont Gold Quarry Clay (I_p = 73%) consolidated at an equal all around pressure smaller than 80 psi (551 kPa), and the specimens slightly bulged by the end of tests. The specimens consolidated at 80 psi (551 kPa), and subjected to drained shear displayed a single shear plane at the end of test. Shear surfaces formed in Newmont Gold Quarry Clay in all the undrained tests. Two shear surfaces, making an angle of approximately 60 degrees with the horizontal direction, were present in the specimens consolidated at an intermediate pressure of 50 psi (345 kPa). However, only a single plane developed in all other specimens in the undrained tests.

For Brenna-Sodium Montmorillonite Mixture 1 (I_p = 91%), a single shear plane formed in all specimens in undrained tests with porewater pressure measurement, and in the specimen consolidated at 80 psi (551 kPa), and subjected to drained shear. The specimen consolidated at 30 psi (207 kPa), and subjected to drained shear, bulged in the mid-height.

Shear plane was not observed in the drained test on Taylor Shale-Sodium Montmorillonite Mixture (I_p = 217%), with more compression in the mid-height of the specimen. The same shape was observed in the specimen consolidated at 60 psi (413 kPa), and subjected to undrained shear with porewater pressure measurement. For the remaining two undrained tests, two shear planes formed in the specimen consolidated at 30 psi (207 kPa); the specimen consolidated at 10 psi 69 kPa remained cylindrical.

Shear planes are more likely to develope in undrained triaxial compression tests with porewater pressure measurement. For normally consolidated clays, the effective normal stress on the failure plane continues to increase in a drained test, so the specimen is in a normally consolidated state. However, the effective normal stress on the failure plane in an undrained test, decreases with increase of shear induced porewater pressure, and the specimen behaves like an overconsolidated clays, in which a shear plane is more likely to develop.

6.3.2 Water content distribution in the specimen at the end of tests

After the triaxial cell was dismantled, the specimen was cut into 5 disks along the height, and the water content of the 5 pieces was measured. For the 15 reconstituted normally consolidated clay and clay shale compositions, the water content distribution along the specimen height is quite uniform, with an average difference smaller than 1% among the 5 pieces. Figure 6. 10 and Fig.6.11 are examples of uniform water content distribution, in a Brown London Clay specimen subjected to undrained compression, and in a Newmont Clay specimen subjected to drained compression, respectively. It should be noticed that in some specimens, the water content at both ends, i.e., the top and bottom disks of the specimen, is 1 to 2% larger than that in the middle sections (Fig.6.12). It is possible that the specimen absorbed water from the porous disks in the process of dismantling.

In undrained triaxial compression tests on normally consolidated clays, the positive shear induced porewater pressure results to a decrease in effective normal stress on the failure plane, therefore, it is possible to observe a higher water content near the shear plane due to the redistribution of porewater. Henkel (1757) and Skempton (1977) reported higher water content near slip surfaces in London Clay in Mill Lane, Uxbridge, and Northolt, by 7%, as compared to in the main body of stratum. In the present study, a higher water content, by more than 1%, near the shear plane, was measured in undrained tests on 4 specimens, out of 51 tests. These specimens are Brenna Clay (Fig.6.13), consolidated at 15 psi (103 kPa), Brenna-Sodium Montmorillonite Mixture 1 (Fig.6.14) consolidated at 30 psi (207 kPa), Taylor shale consolidated at 40 psi (276 kPa), and Lea Park Shale consolidated at 5 psi (35kPa).

6.3.3 Stress-strain behavior

Brenna Clay and Beaumont Clay are described here as examples, and their undrained and drained test measurements are presented in Fig.6.15 to Fig.6.18. It can be seen from the stress-stain curves of consolidated undrained triaxial compression tests with porewater pressure measurement in Fig.6.15 and Fig.6.18 that, reconstituted Brenna Clay and Beaumont Clay compositions, kneaded at liquidity index of 0.7 to 1.0, display the typical behavior of remolded, normally consolidated clays. After maximum stress difference is reached, either a minor decrease takes place, or the axial stress levels off. Consistent behavior is also observed in the porewater pressure response; that is, the positive shear-induced porewater pressure increases till the failure strain and remains more or less constant afterwards. Similarly, drained tests display distinct ductile stress-strain relationship and contractive volumetric response, where the stress difference levels off after reaching a maximum, or undergoes a minor decrease. Except for slight differences observed in remolded specimens of Mud Gully Clay, and the three clays with lower plasticity, namely, Glen Forest, South Richey, and Kuykendahl Clay, the drained and undrained stress-strain behavior, together with the volume change and porewater pressure response, of the other 9 clay and clay shale compositions, including Newmont Clay, Brown London Clay and Lea Park Shale which were remolded at lower water content corresponding to I_L smaller than 0.7, are similar to those of Brenna and Beaumont Clays. The responses of the 15 reconstituted normally consolidated clay and clay shale compositions are contractive; positive shear induced porewater pressure was observed in all the undrained tests with A-coefficient at the point of stress path tangency generally less than 1.2, and positive volume change smaller than 10% was measured in all the drained tests.

The drop of axial stress after failure is related to the development of a shear plane, which promotes face to face interaction of clay particles. The decrease after reaching the maximum, is observed at consolidation pressures greater than 30 psi (207 kPa), while a constant stress is observed for most tests at lower consolidation pressures. The constant axial stress after the maximum, could possibly result from an increase in piston friction after the shear plane forms. More specifically, the specimen no longer deforms uniaxially after the shear plane develops, and the horizontal stress acting on the piston increases as the shear process continues. For specimens consolidated at lower pressures, this increase of horizontal stress is more significant, thus resulting in the increase of

axial load measured by the proving ring. When this load is divided by the corrected area which also increases in the shearing process, the axial stress remains more or less constant.

For Mud Gully Clay, as shown in Fig.6.19 and Fig.6.20, after reaching the maximum, a more significant drop in axial stress is observed at high consolidation pressures [specimen consolidated at 68 psi, or 469 kPa, subjected to undrained shear, and specimen consolidated at 80 psi, or 551 kPa, subjected to drained shear]. This behavior is consistent with the development of a shear plane in every Mud Gully Clay specimen, subjected to drained and undrained shear, which results in a distinct decrease of axial stress, due to enhanced face to face interaction of platy particles on the shear plane. A dilative response is observed in the volume change after the maximum axial stress for the specimen consolidated at 80 psi (551 kPa).

For the remolded specimens of three clays with lower plasticity index from 13 to 25% (see Glen Forest in Fig.6.21 and Fig.6.22), which bulged at mid-height of the specimen, axial stress did not decrease; indeed, it either remained constant after the maximum, or displayed a continuous small increase till the end of the test.

6.3.4 Stress path and failure criteria

For the drained triaxial compression tests, the stresses paths are straight lines in the 45-degree direction with respect to $(\sigma'_1 + \sigma'_3)/2$ axis (Fig.6.23 to Fig.6.27). The two failure criteria commonly used in engineering practice to determine drained shear strength parameters, namely, effective principal stress difference, $(\sigma'_1 - \sigma'_3)$, and effective principal stress ratio, σ'_1/σ'_3, maximize at the same axial strain.

However, in consolidated undrained tests with porewater pressure measurement, the maximum stress ratio might be reached at an axial strain before, the same, or after the maximum stress difference occurs, depending on the porewater pressure response. One significant observation for the tests in the present study, is that, for the majority of the undrained tests, the stress difference, $(\sigma'_1 - \sigma'_3)$, and stress ratio, σ'_1/σ'_3, maximized at a similar axial strain. The stress

ratio maximizes when the shear induced porewater pressure reaches a constant value. Therefore, the strains at maximum stress difference and strain at maximum stress ratio coincide. It should be noted that this observation is typical for normally consolidated destructured clays, particularly if the material is remolded (Kjaernsli and Simons 1962).

Figures 6.23 and 6.24 show the stress paths for both undrained and drained tests on Brenna Clay and Beaumont Clay, respectively. A curved failure envelope is fitted to the stress paths of each clay composition. The undrained stress paths for other 10 clay and clay shale compositions, with high plasticity index (I_p > 30%), and large clay size fraction (CF > 50%), display similar contractive response – the stress paths start first with a vertical segment, bend to the left, reaching a maximum ($\sigma'_1 - \sigma'_3$), and then drop off to the left. The contractive response was observed at all effective normal stresses in these reconstituted clay and clay shale compositions remolded at liquidity index range of 0.5 to 1.0; however, with average value of 0.8. A similar behavior for normally consolidated clay was also reported by Kimura et al (2015) for consolidated undrained triaxial compression tests with porewater measurements on reconstituted Neogene mudstone (I_p = 53%); consistent behavior of pure minerals with high plasticity index, is reviewed in Chapter 2 (reconstituted sodium montmorillonite by Mesri 1969, and reconstituted kaoline clay by Suzuki and Dyvik 2017). It can be seen from the stress paths of these clays that, limiting condition defined by the maximum stress difference, ($\sigma'_1 - \sigma'_3$), coincides with that by the maximum effective principle stress ratio, σ'_1/σ'_3, or by the stress path tangency,

$$\frac{(\sigma'_1-\sigma'_3)}{(\sigma'_1+\sigma'_3)} = \frac{\left(\frac{\sigma'_1}{\sigma'_3}-1\right)}{\left(\frac{\sigma'_1}{\sigma'_3}+1\right)} \tag{6.6}$$

Two clays, Glen Forest (Fig.6.25) and Kuykendahl (Fig.6.26), with low plasticity index (15% and 14%, respectively), and smaller clay size fraction (20% and 24%, respectively), also have stress paths starting initially bending to the left; however, then turn to right, behaving like a silt, with a distinct phase transformation point. This behavior is also observed in the two reconstituted marine clays (Sun et al 2014), namely, Pujiang Clay (I_p = 22%) and Suzhou Clay (I_p = 19%), in Fig.2.8. As the stress path beyond the phase transformation point is on the limiting failure envelope, the maximum stress difference and maximum stress ratio criteria still yield similar secant friction angles.

The South Richey Clay (Fig.6.27) with medium plasticity of 25% and a moderate clay size fraction of 38%, exhibits an intermediate behavior. After stress path reaches the maximum $(\sigma'_1 - \sigma'_3)$, no distinct bending to the left or right is present. Therefore, in this case, also drained shear strength parameters obtained from undrained tests, using stress difference and stress ratio criteria, are comparable.

For all the stiff clay and clay shale compositions, a single failure envelope could be determined from the stress paths of drained, and undrained triaxial compression tests with porewater pressure measurement, which indicates that the drained shear strength parameters obtained in undrained tests are in good agreement with the ones in the drained tests. A more detailed comparison of secant fully softened friction angle determined in the two types of tests are presented in subsection 6.3.5.

6.3.5 Comparison of secant fully softened friction angle determined in drained triaxial compression tests and those in undrained triaxial compression tests with porewater pressure measurement

Secant fully softened friction angles determined in drained triaxial compression tests and undrained tests with porewater pressure measurement, according to a procedure described in section 6.4, are computed at 7 effective normal stresses (10, 30, 50, 100, 200, 400, and 700 kPa) for each stiff clay and clay shale composition, and compared in Fig.6.28. For some stiff clay and clay shale compositions, because of the limited amount of available material, only one drained test was performed. Therefore, Figure 6.28 only includes secant friction angles determined in triaxial compression tests on 8 stiff clay and clay shale compositions (I_p = 13 to 91%), for which more than one drained test had been performed.

Figure 6. 28 shows a good agreement between the secant fully softened friction angle determined from drained triaxial compression tests and the friction angle determined from undrained tests with porewater pressure measurement, with an average difference of ± 1°. The maximum difference of

-3 degrees was observed in Mud Gully Clay at effective normal stress of 700 kPa; and for this clay, secant fully softened friction angle determined in drained tests is lower than the value in undrained tests, at all effective normal stresses. Mud Gully Clay specimens were kneaded at a liquidity index between 0.7 and 0.8, which is at the lower bound of the recommended liquidity index range. It is possible that, for Mud Gully Clay, at low water content, the pre-consolidation effect is more significant in undrained tests with porewater pressure measurement, thus resulting to higher secant friction angles (Casagrande and Wilson 1953). Furthermore, for Mud Gully Clay, the vertical strain at failure for the drained tests, was almost 3 times the vertical strain at failure for undrained tests.

6.3.6 Axial strain at failure

The axial strains at failure, ε_f, defined at maximum principle stress ratio, σ'_1/σ'_3, in drained triaxial compression tests and undrained triaxial compression tests with porewater pressure measurement, are compared in Fig.6.29. The range of axial strain at failure, for each stiff clay and clay shale composition, with more than one drained test, is presented by a box, and by a straight line for samples with one drained test. The axial strain at failure in drained tests, $[\varepsilon_f]_{DTC}$, on average, is twice the axial strain in undrained tests with porewater pressure measurement, $[\varepsilon_f]_{UTC}$.

Figure 6.30 shows the axial strains at failure for the 15 stiff clay and clay shale compositions, as a function of consolidation pressure. The red symbols represent axial strains at failure in drained triaxial compression tests, $[\varepsilon_f]_{DTC}$, and black symbols are those in undrained tests with porewater pressure measurement, $[\varepsilon_f]_{UTC}$. The axial strain at failure in drained tests, $[\varepsilon_f]_{DTC}$, ranges from 10 to 20%, with an average value of 16%, independent of consolidation pressure. For undrained tests with porewater pressure measurement, though with some scatter, average $[\varepsilon_f]_{UTC}$ increases with the consolidation pressure, from 5% at 30 kPa, to 10% at 600 kPa, with an average equal to 8%. The average axial strains at failure, $[\varepsilon_f]_{DTC}$ and $[\varepsilon_f]_{UTC}$, turn out to be similar to those assumed in subsection 6.2.4. in determining the imposed shear deformation rate.

It is possible that the difference in axial strain at failure in the two types of tests, results from the change of effective normal stress in the shearing stage. In a drained triaxial compression test, the

effective normal stress on the failure plane increases during the shearing process, which requires a larger axial strain to reach failure. In an undrained triaxial compression test with porewater pressure measurement on a normally consolidated clay, the effective normal stress on the failure plane decreases as a result of positive shear induced porewater pressure. Moreover, the development of shear plane, which is observed in most of the undrained triaxial compression tests with porewater pressure measurement, may contribute to failure by more face to face interaction of plate-shaped clay particles. The shear plane observed in both drained and undrained tests may also explain $[\varepsilon_f]_{DTC}$ and $[\varepsilon_f]_{UTC}$ values of Mud Gully Clay, at different consolidation pressures, being lower than the average in all the tests.

6.3.7 Undrained shear strength to consolidation pressure

The ratios of undrained shear strength to consolidation pressure, $s_u(TC)/\sigma'_{3c}$, for the 15 clay and shale compositions, as a function of plasticity index, are illustrated in Fig.6.31. For each stiff clay and clay shale, the range of values of $s_u(TC)/\sigma'_{3c}$, is shown for the consolidation pressure range used in the undrained triaxial compression tests on the reconstituted normally consolidated specimens.

The $s_u(TC)/\sigma'_{3c}$ values for compositions with plasticity index in the range of 50% to 130%, are smaller than the typical value of 0.32, for $s_u(TC)/\sigma'_{vc}$, or $s_{uo}(TC)/\sigma'_p$, reported by Terzaghi et al (1996), for undrained triaxial compression tests on soft clay and silt deposits with I_p in the range of 10% to 100%. However, the strain rates selected in the undrained tests in the present study, correspond to 2 to 20 times the time to failure for the $s_u(TC)/\sigma'_{vc}$, or $s_{uo}(TC)/\sigma'_p$ data reported by Terzaghi et al (1996) in the plasticity index range of 10% to 100%; and for Lea Park Shale, time to failure is 100 times the t_f for soft clay and silt data.

6.3.8 A-coefficient at failure

Figure 6.32 summarizes the range of values of A-coefficient at failure, $A_f = \Delta u'_f/(\sigma'_1 - \sigma'_3)_f$, for each of the 15 stiff clay and clay shale compositions, consolidated at all consolidation pressures in the undrained triaxial compression. The values of A-coefficient are in the range of 0.90 and 1.15 for the stiff clay and clay shale compositions with I_p less than 130%; for Lea Park Shale, Brenna-

Montmorillonite Mixture 2, Taylor Shale-Montmorillonite Mixture, A_f values are 1.44 to 1.56. For a given remolding water content, specimens subjected to low consolidation pressure tend to be less contractive during shear, and for each clay, smaller A_f is recorded; in most cases at the lowest consolidation pressure, 4.5 psi to 6 psi (31 kPa to 41 kPa). The difference in A_f could result from the difference in liquidity index at which the specimen is prepared, together with the magnitude of consolidation pressure.

6.4 Correlation of secant fully softened friction angle with plasticity index

With the failure envelop determined for each stiff clay and clay shale composition, the secant friction angle and effective normal stress at failure are given by

$$\sin\left[\phi'_{fs}\right]_s^{\sigma'_n} = \frac{(\sigma'_1/\sigma'_3)_f - 1}{(\sigma'_1+\sigma'_3)_f+1} \tag{6.7}$$

$$[\sigma'_n/\sigma'_3]_f = \frac{(\sigma'_1/\sigma'_3)_f+1}{2} - \frac{(\sigma'_1/\sigma'_3)_f-1}{2}\sin\left[\phi'_{fs}\right]_s^{\sigma'_n} \tag{6.8}$$

Where $[\sigma'_n/\sigma'_3]_f$ and $(\sigma'_3)_f$ correspond to the point of effective stress path tangency.

A relationship between secant fully softened friction angle and effective normal stress for each stiff clay and clay shale composition, was determined using Eqs.6.7 and 6.8, and then the secant fully softened friction angles at the 7 effective normal stresses (10, 30, 50, 100, 200, 400 and 700 kPa) was computed.

Figure 6.33 shows the secant fully softened friction angles of the 15 stiff clay and clay shale compositions, as a function of I_p. At effective normal stress of 100 kPa, the number next to each symbol is the clay size fraction in percent. A smooth mean curve is fitted to the data at effective normal stress of 100 kPa, which represents the $\left[\phi'_{fs}\right]_s^{100}$ as a function of plasticity index. The mean curves at other effective normal stresses were determined using Eq. 5.5, together with m_{fs}, which was determined by trial and error based on entire data at effective normal stress ranging from 10 kPa to 700 kPa. Figure 6. 34 illustrates the m_{fs} value as a function of plasticity index. The m_{fs} value decreases from 1.00 at I_p = 0%, to 0.840 at I_p range between 100 and 130%, and slightly increases afterward, to 0.878 at I_p = 250%. Figure 6. 34 indicates that, the relationship between fully softened shear strength and effective normal stress is linear at I_p = 0%, and it is most curved

at I_p = 100 to 130%. At low plasticity index, edge-to face interaction of clay particles is predominant even at high effective normal stresses. The fabric of stiff clay and clay shale compositions is most significantly influenced by the increase of effective normal stresses at an "intermediate" plasticity index, which promotes face to face interaction of clay particles. For stiff clay and clay shale compositions with very high plasticity index (I_p greater than 130%), some face to face interaction is already present at low effective normal stresses; therefore, the influence of effective normal stress increase is not as significant as that for stiff clay and clay shale compositions which display I_p = 100 to 130%. A similar conclusion was reached by Eid and Rabie (2017), based on the fully softened shear strength measurement in modified Bromhead ring shear device on 40 clay, silt, mudstone, and shale samples.

The preceding observations and interpolation of m_{fs} and the curvature of failure envelope, at various plasticity indices, agree with the decrease of secant fully softened friction angle, with the increase in effective normal stress, and with the increase of plasticity index, as was reported by Mesri and Shahien (2003).

The secant fully softened friction angles of 24 stiff clay and shale compositions, and 4 pure minerals determined from drained triaxial compression tests by Mesri and Cepeda-Diaz (1986), are superimposed in Fig.6.35, on the empirical correlation based on present study in Fig.6.33. The effective normal stresses at failure was near 200 kPa, for the tests on reconstituted normally consolidated specimens at an equal all around pressure of 207 kPa. Fig.6.35 shows a good agreement between the secant fully softened friction angles reported by Mesri and Cepeda-Diaz (1986), and the correlation developed based on data of the present study.

The secant fully softened friction angle data in Mesri and Shahien (2003), are compared in Fig.6.36 with the empirical correlation based on data from the present study; and again a good agreement is observed.

The mean curves (dashed lines), determined from corrected fully softened friction angle data from modified Bromhead ring shear device reported by Eid and Rabie (2017), are compared in Fig.6.37 with mean curves (solid lines) of the present study. As introduced in section 4.3, these dashed

empirical curves were also developed using Eq.5.5 together with the Eid and Rabie (2017) secant fully softened friction angle data at 100kPa. According to Fig.6.37, the mean curves based on the present study and those developed using the Eid and Rabie (2017) data, are quite comparable.

TABLES

Table 6.1. General information on clay and shale compositions tested in consolidated undrained and drained triaxial compression tests (all samples were ball-milled and passed through No. 200 U.S. standard sieve)

No.	Clay	Location	w_l(%)	w_p(%)	CF(%)	I_p(%)	I_L(%), c
1	Brenna	North Dakota, USA	77	28	61	49	0.71-1.00
2	Newmont	Nevada, USA	115	42	56	73	0.45-0.55
3	Brown London Clay, b	Bradwell, UK	101	35	66	66	0.51-0.74
4	Beaumont Clay	Texas, USA	67	23	59	44	0.81-1.03
5	Glen Forest	Texas, USA	31	15	20	16	0.81-1.03
6	Brenna-Na Montmorillonite Mixture 1	North Dakota, USA	122	31	69	91	0.70-0.82
7	South Richey	Texas, USA	44	19	38	25	0.84-1.05
8	Kuykendahl	Texas, USA	31	18	24	13	0.75-1.04
9	Mud Gully	Texas, USA	96	28	71	68	0.70-0.78
10	Taylor Shale, a	Texas, USA	170	39	72	131	0.73-0.85
11	Oahe Firm Shale, b	South Dakota, USA	138	41	78	97	1.10-1.36
12	Lea Park Shale, b	Saskatchewan, Canada	253	48	65	205	0.52-0.60
13	Patapsco Shale, a	Washington, D.C.	77	25	59	52	0.70-0.91
14	Brenna-Na Montmorillonite Mixture 2	North Dakota, USA	174	34	75	140	0.64-0.92
15	Taylor Shale-Na Montmorillonite Mixture	Texas, USA	278	61	78	217	0.74-0.91

a. Index properties from Mesri and Cepeda-Diaz (1986)

b. Index properties from Stark and Eid (1997)

c. Liquidity index refers to water content of reconstituted specimens

FIGURES

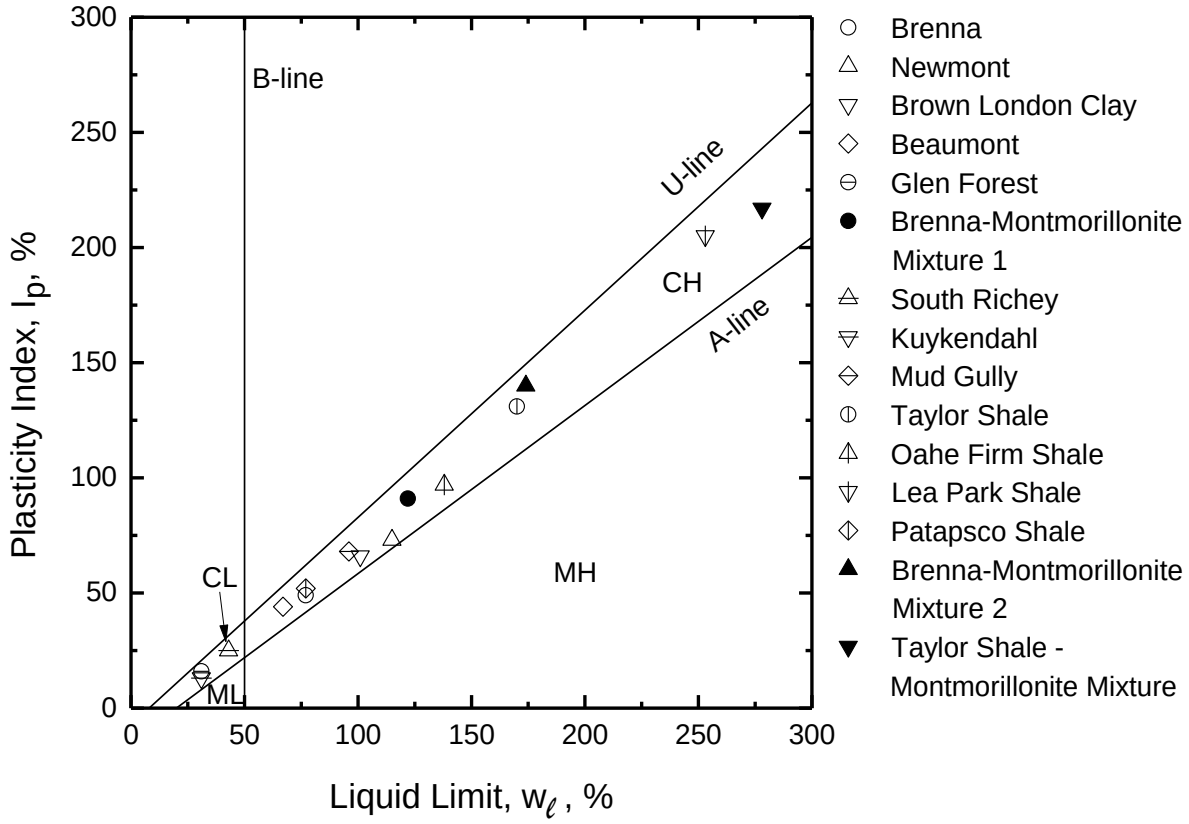

Figure 6.1. Casagrande chart of 16 clay and shale compositions tested in consolidated triaxial compression tests

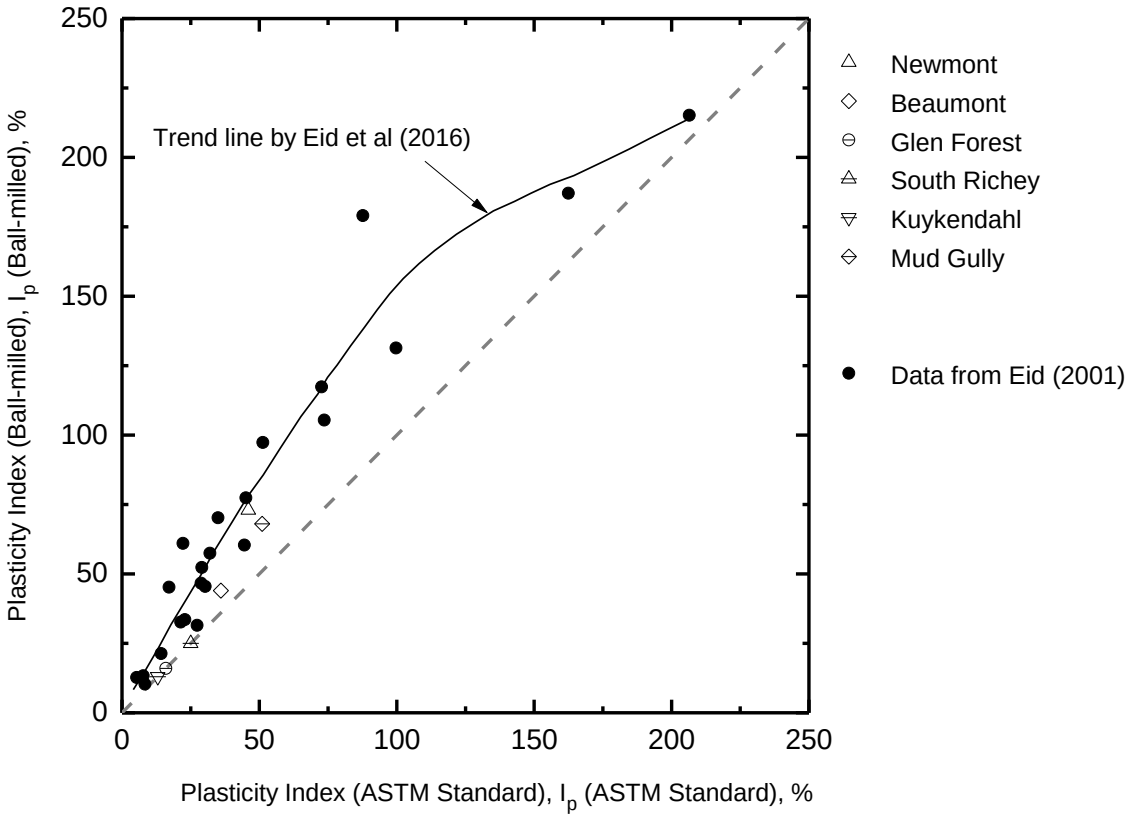

Figure 6.2. Comparison of the plasticity indices obtained from samples processed using ball-milling techniques and those obtained from samples processed using ASTM standard procedures

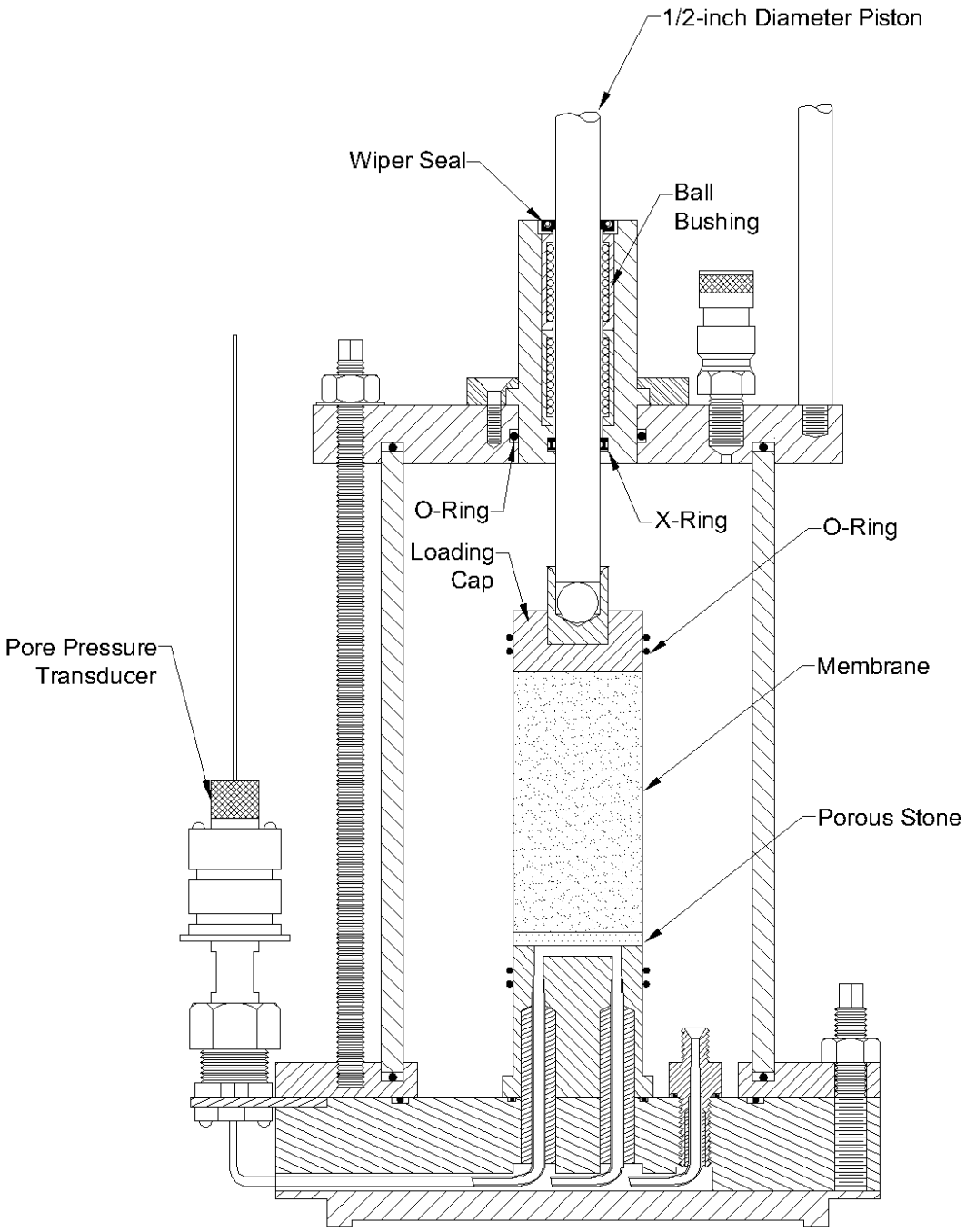

Figure 6.3. Triaxial cell in a consolidated undrained test with porewater pressure measurement

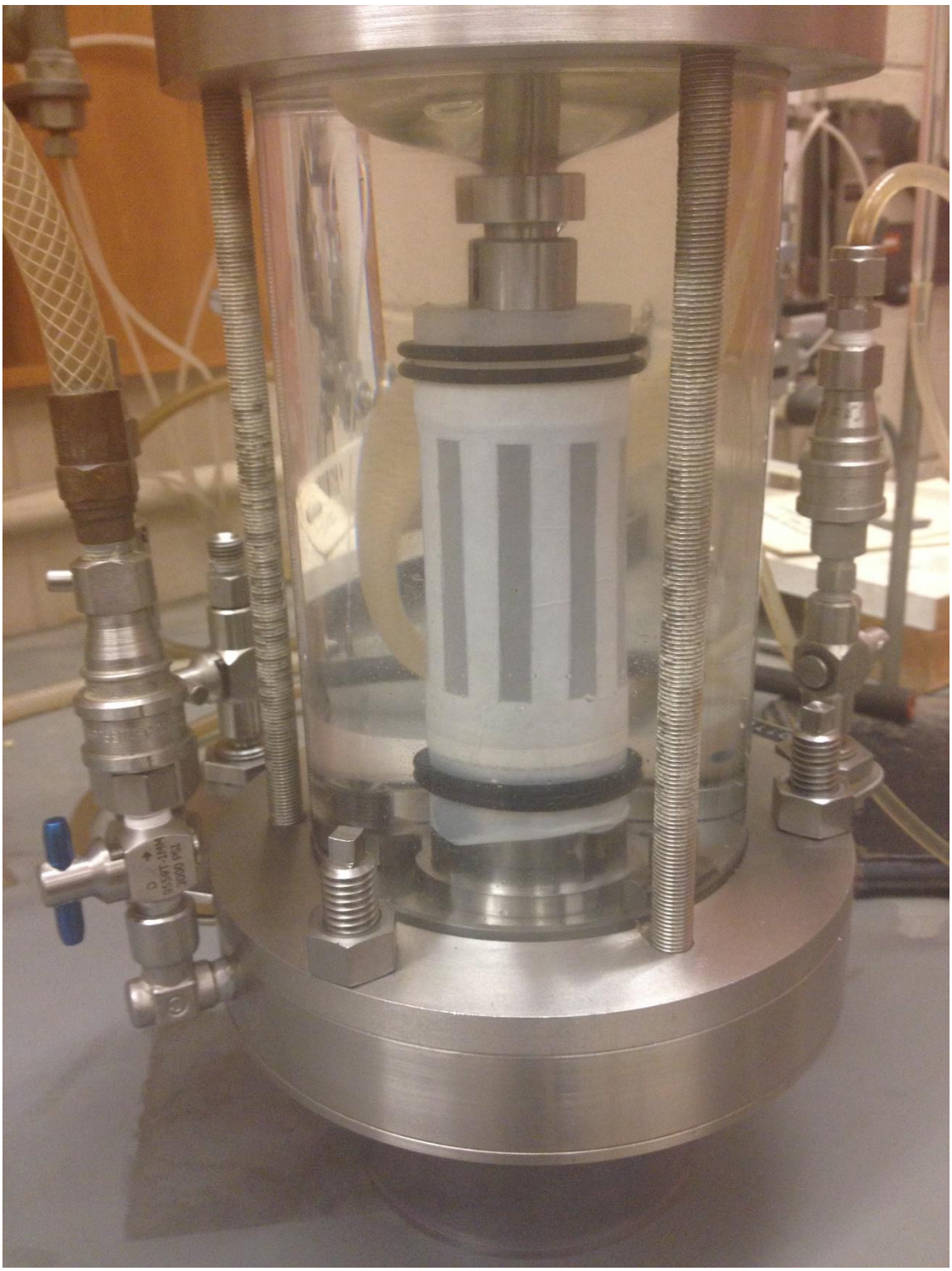

Figure 6.4. Photo of a specimen in the triaxial cell

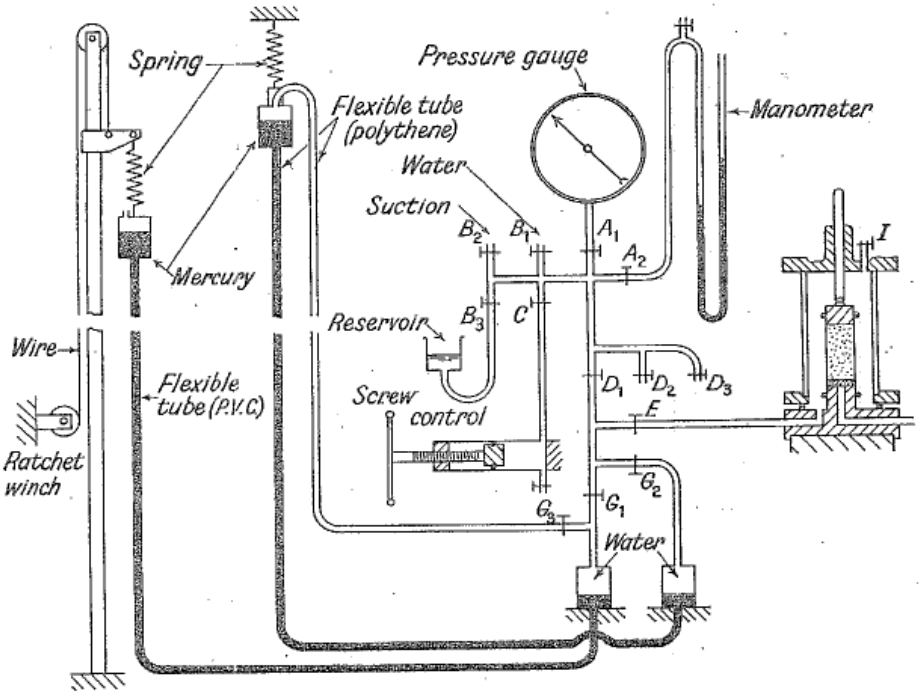

Figure 6.5. The layout of the self-compensating mercury control with extended pressure gauge (Bishop and Henkel 1957)

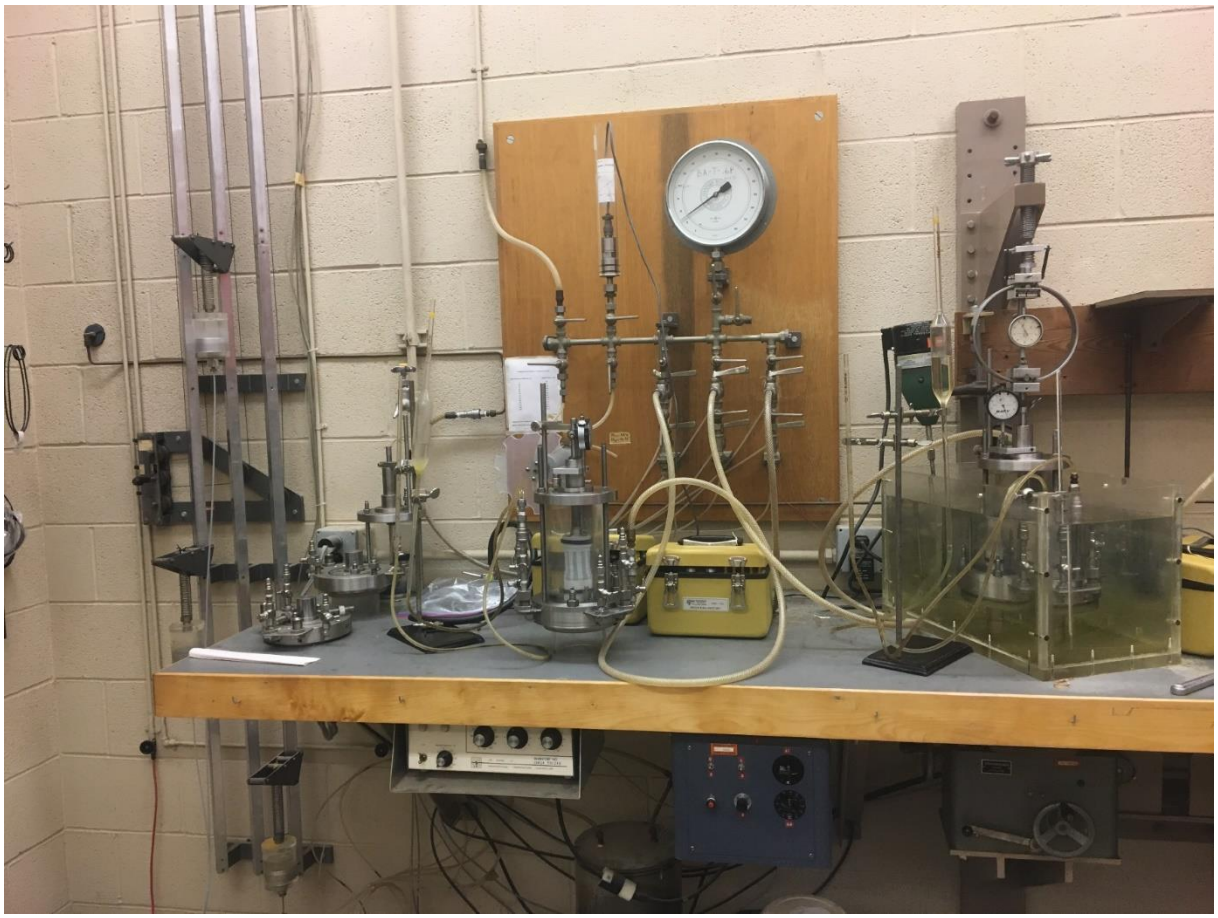

Figure 6.6. Photo of triaxial compression test system

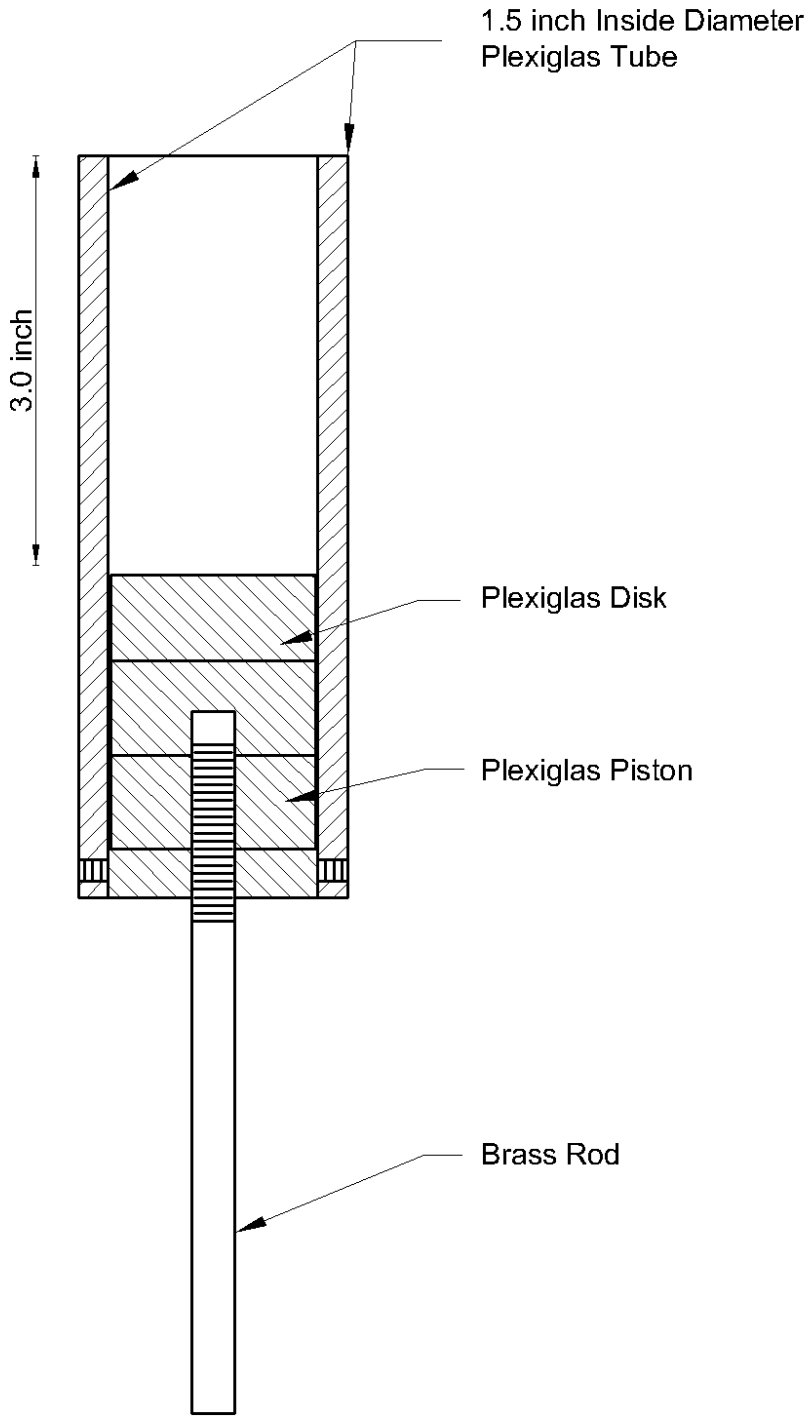

Figure 6.7. Plexiglas mold used to prepare the kneaded specimens

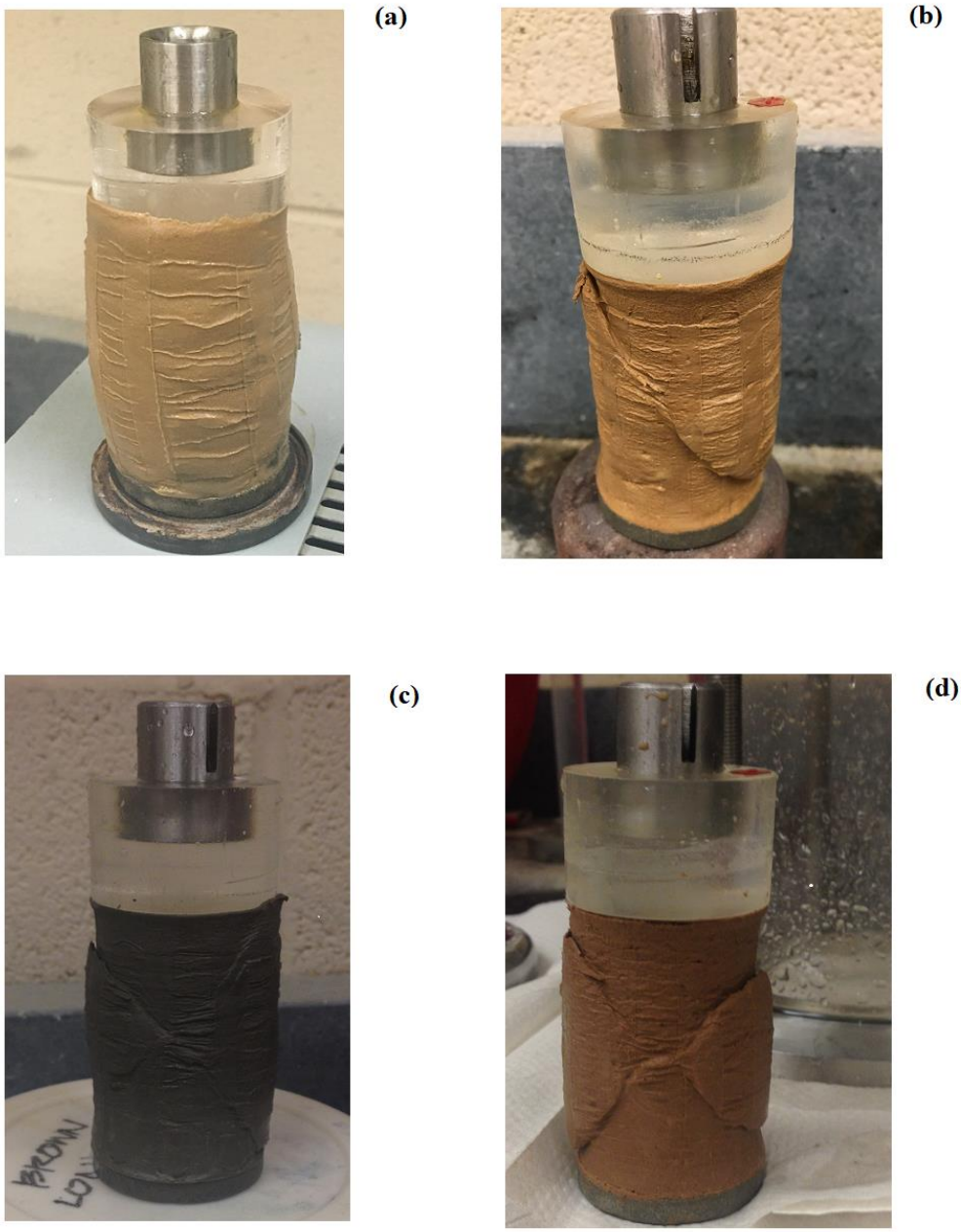

Figure 6.8. Photos of specimens at the end of consolidated undrained triaxial compression tests with porewater pressure measurement (a) budging in a Glen Forest Clay specimen consolidated at 5psi (b) single shear plane in a Beaumont Clay specimen consolidated at 80 psi (c) one distinct shear plane, and one shear plane not fully developed in a Brenna Clay specimen consolidated at 40 psi d) two intersecting shear planes in Newmont Gold Quarry Clay specimen consolidated at 50 psi (1 psi = 6.89 kPa)

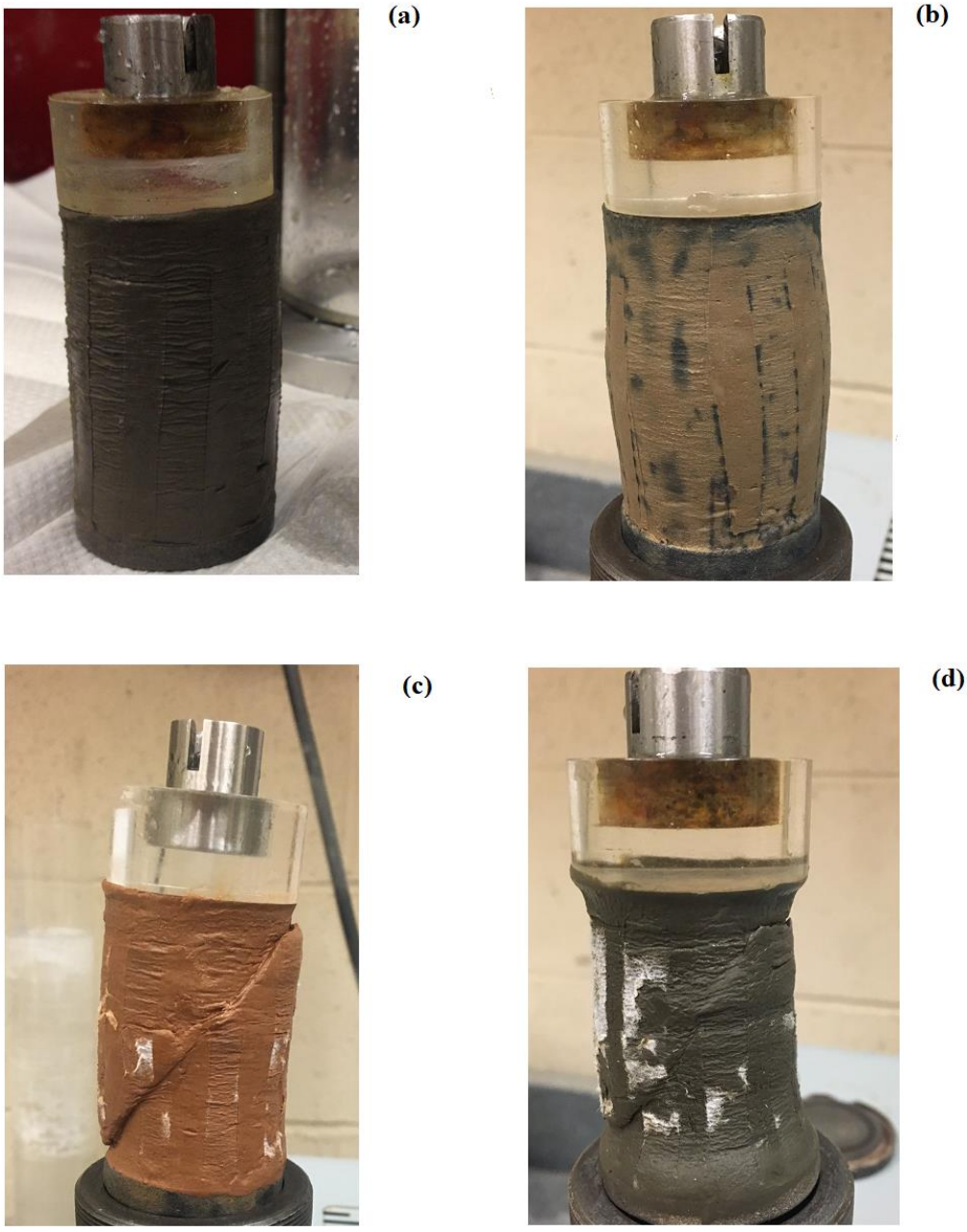

Figure 6.9. Photos of specimens at the end of consolidated drained triaxial compression tests (a) cylindrical shape of a Brenna Clay specimen consolidated at 10psi (b) budging in a Kuykendahl Clay specimen consolidated at 30 psi (c) single shear plane in a Mud Gully Clay specimen consolidated at 30 psi (d) single shear plane in a Brenna-Sodium Montmorillonite mixture 1 specimen consolidated at 80 psi (1 psi = 6.89 kPa)

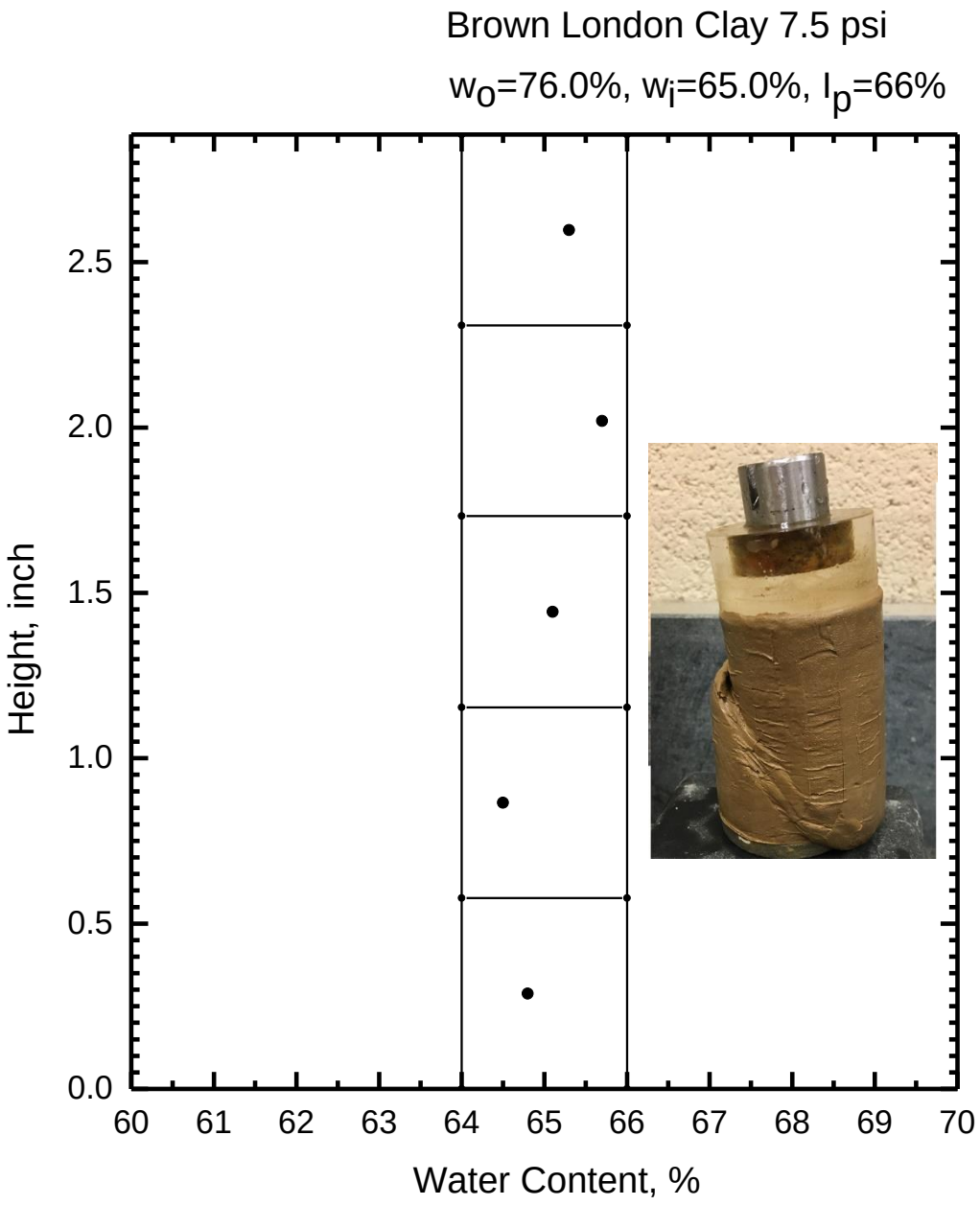

Figure 6.10. Water content at the end of an undrained triaxial compression test with porewater pressure on a Brown London Clay specimen consolidated at 7.5 psi

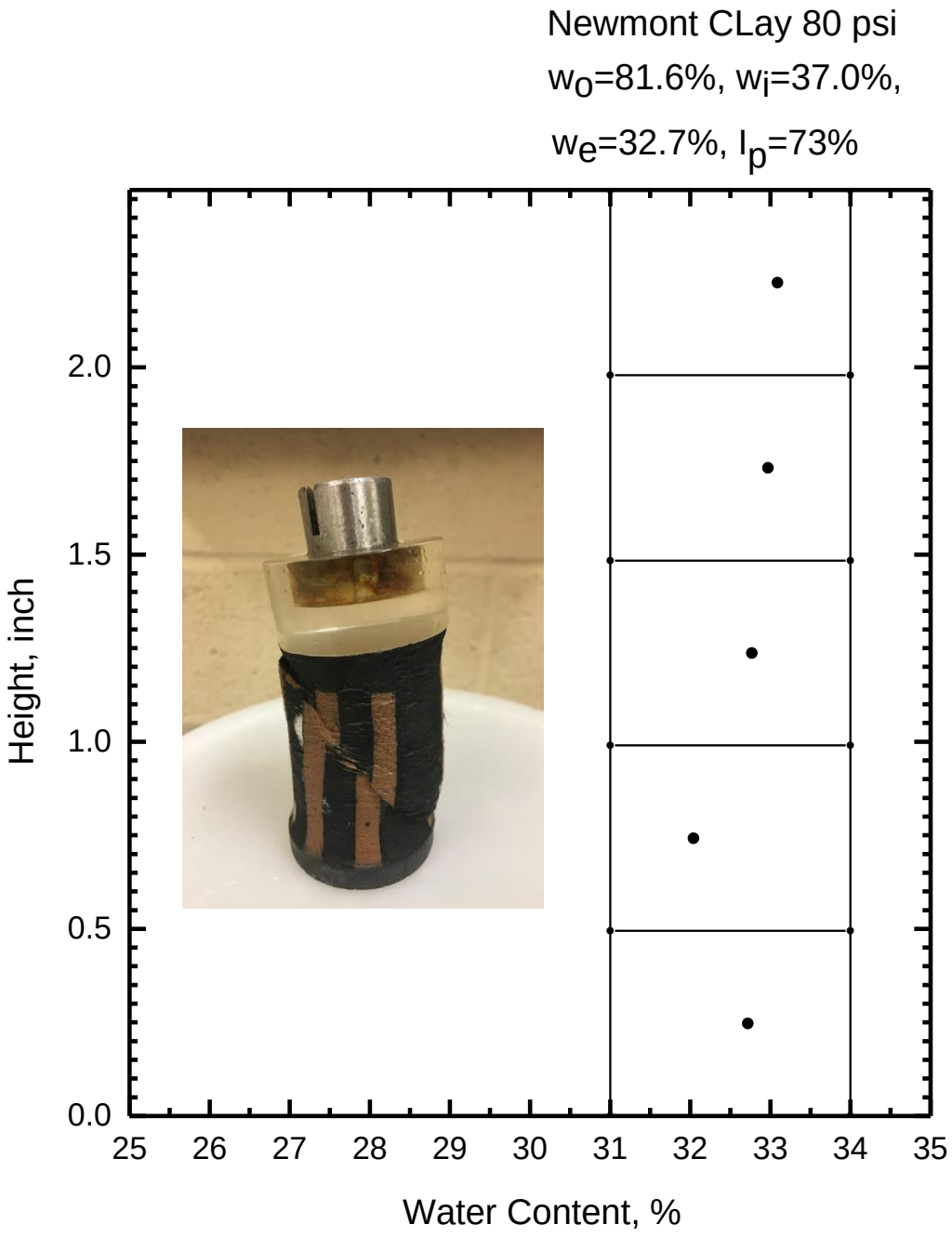

Figure 6.11. Water content at the end of a drained triaxial compression test on a Newmont Clay specimen consolidated at 80 psi

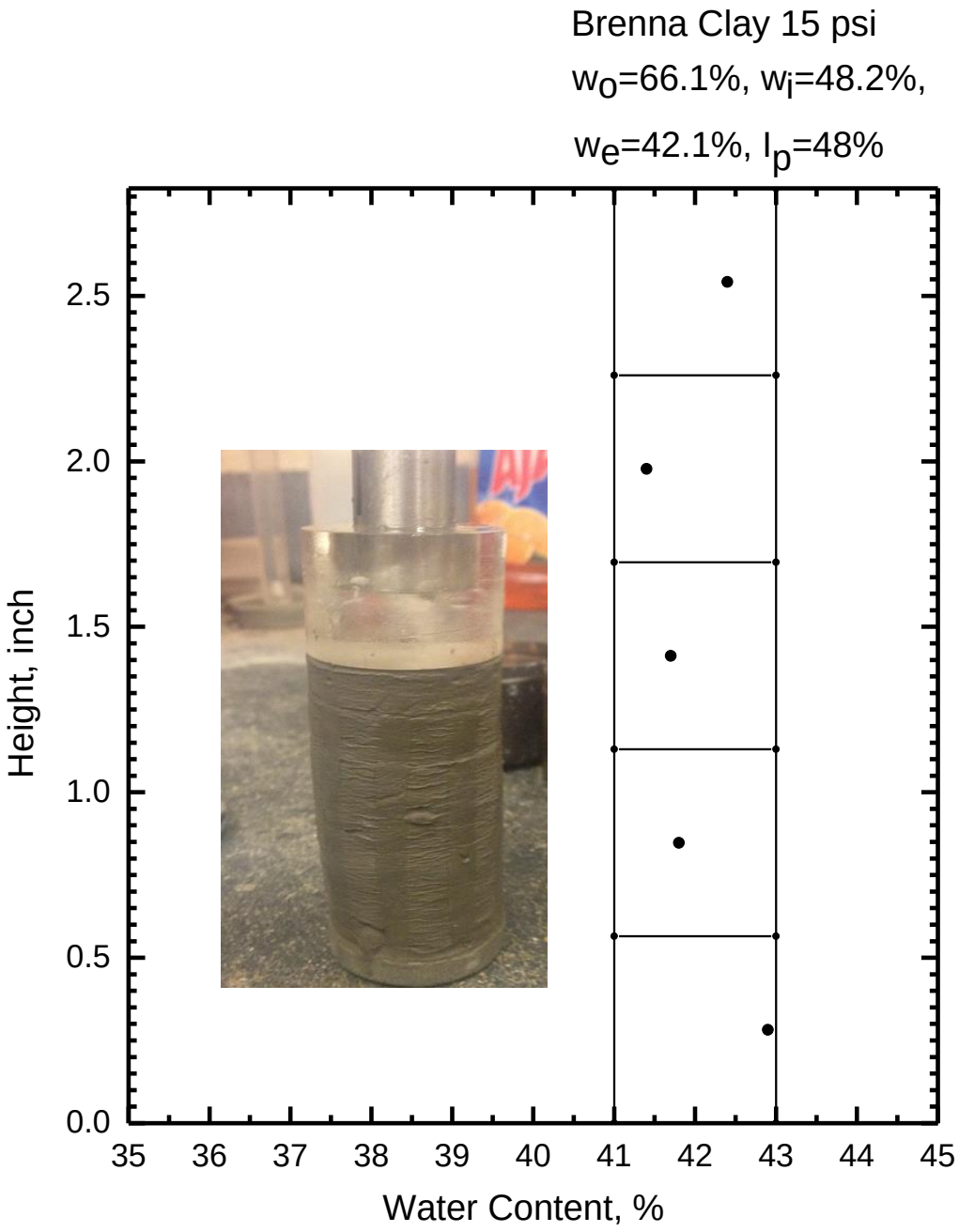

Figure 6.12. Water content at the end of a drained triaxial compression test on a Brenna Clay specimen consolidated at 15 psi

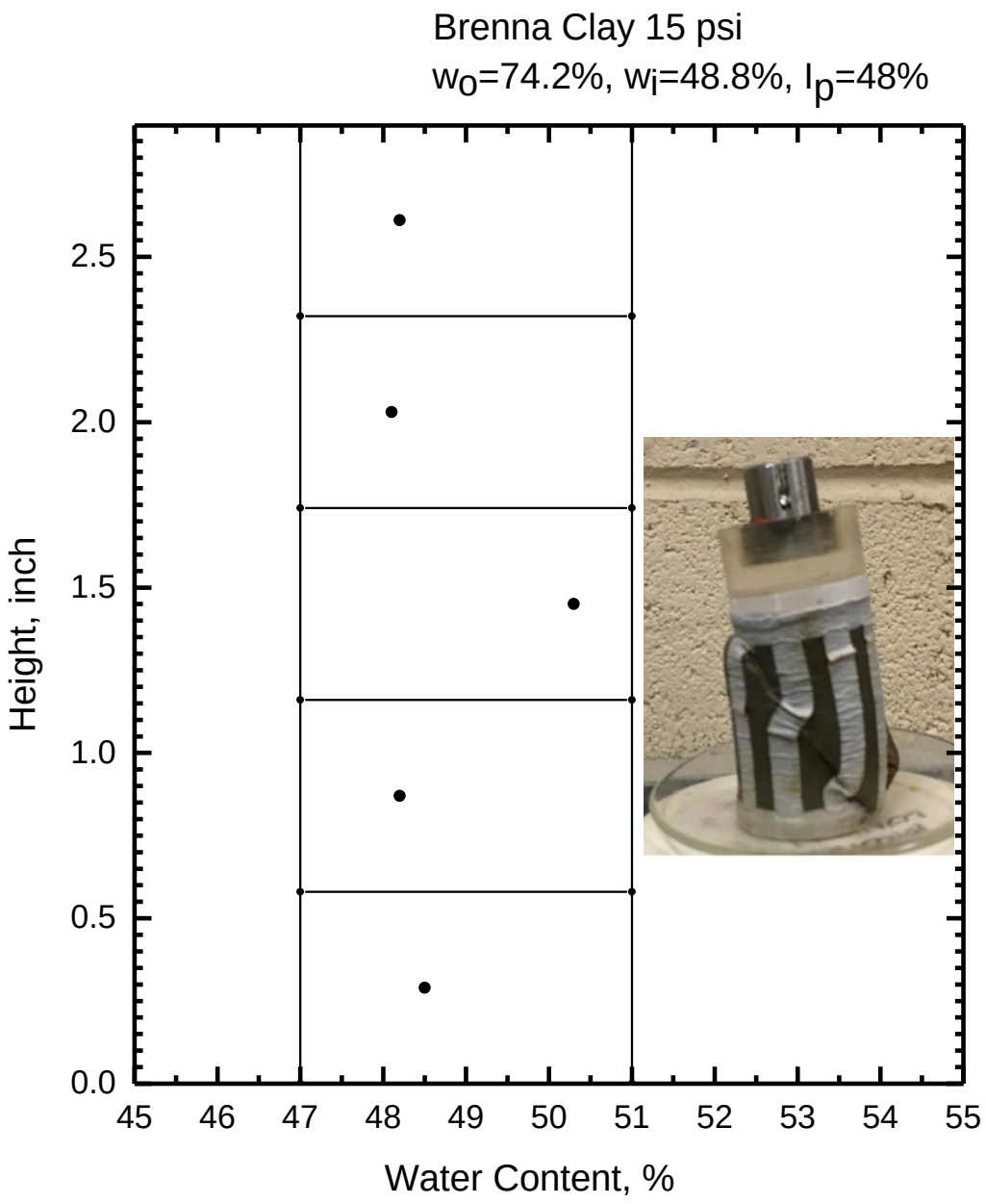

Figure 6.13. Water content at the end of an undrained triaxial compression test with porewater pressure on a Brenna Clay specimen consolidated at 15 psi

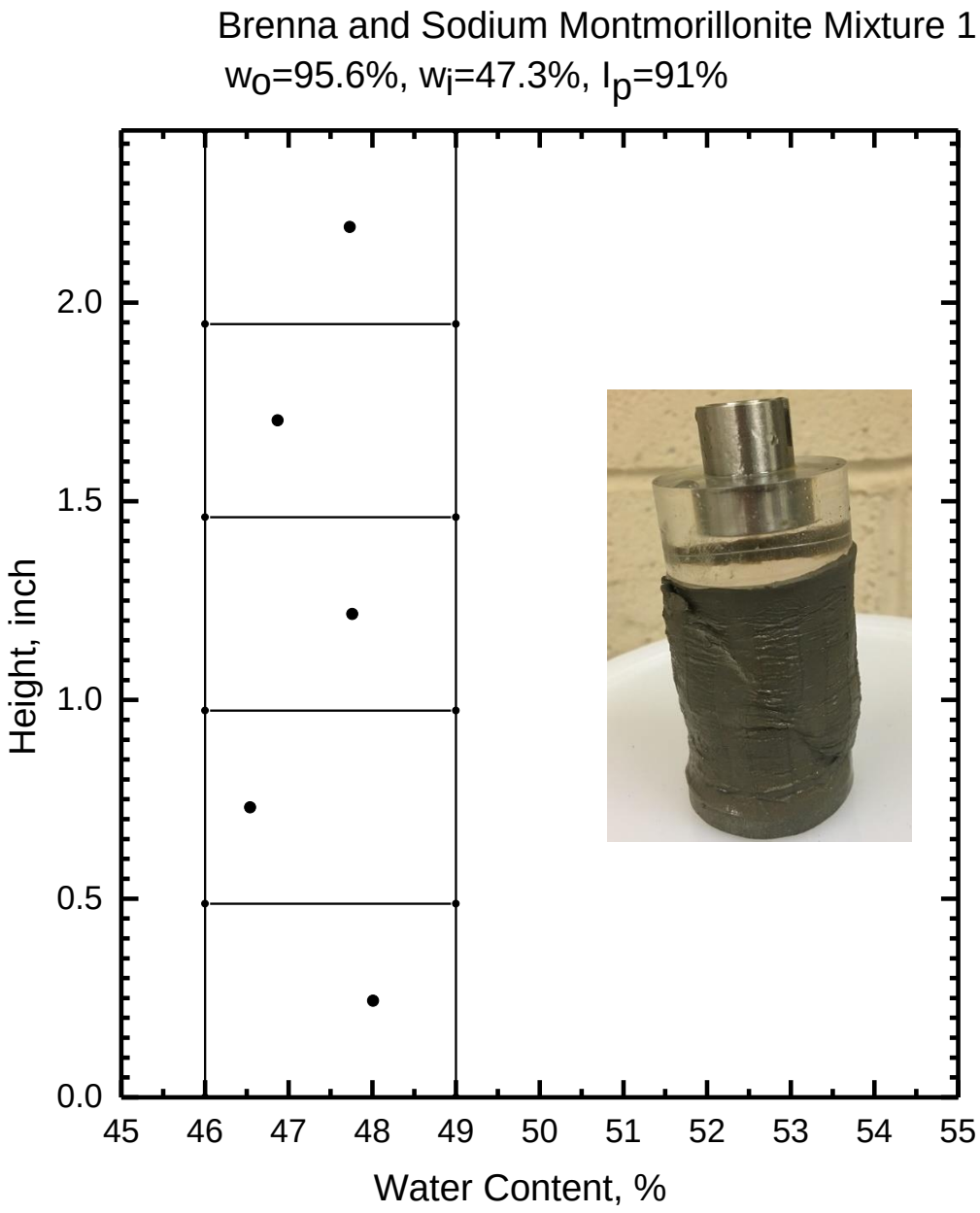

Figure 6.14. Water content at the end of an undrained triaxial compression test with porewater pressure on a Brenna and Sodium Montmorillonite Mixture 1 specimen consolidated at 30 psi

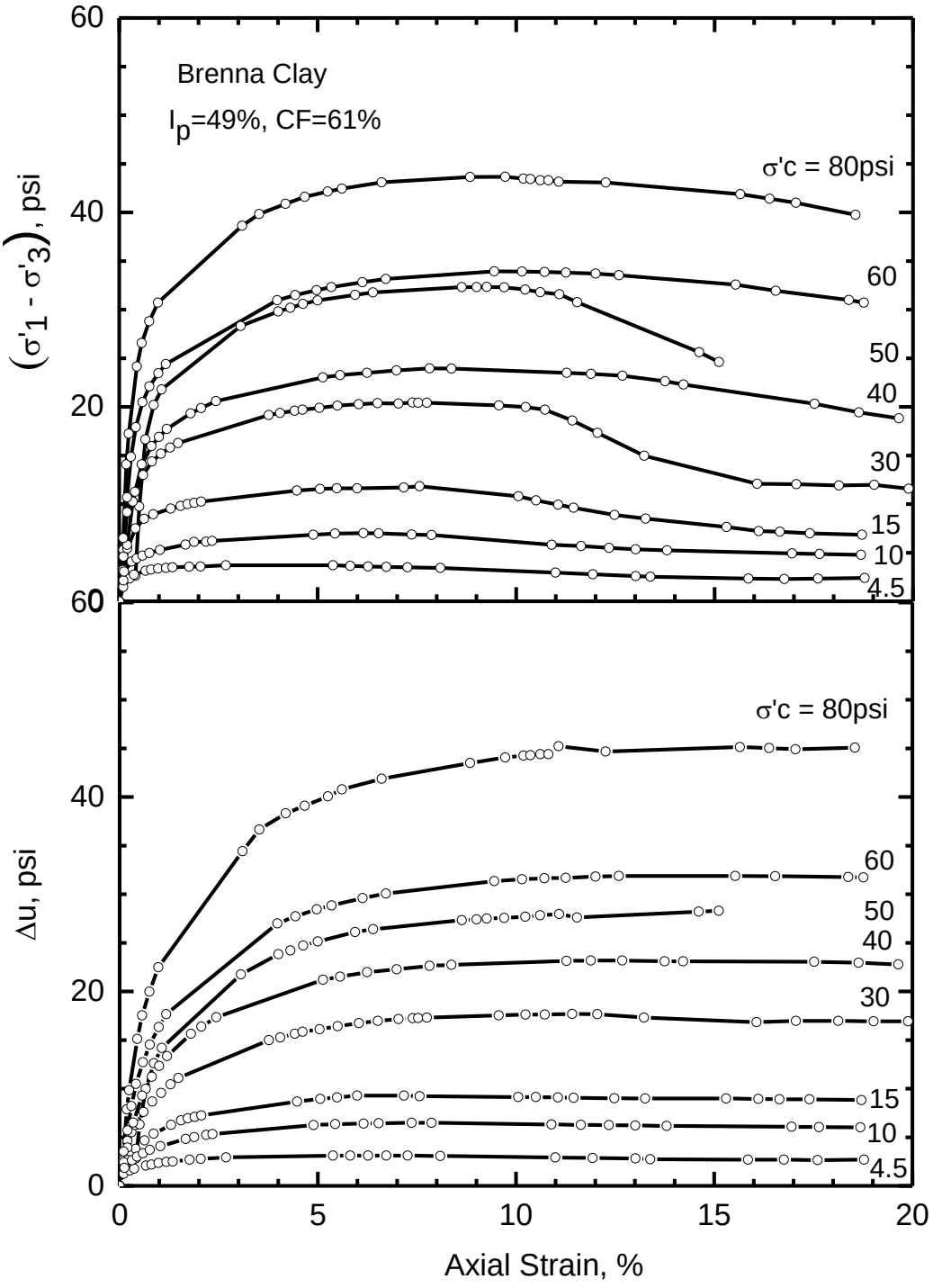

Figure 6.15. Stress-strain relationship and porewater pressure response of Brenna Clay in consolidated undrained triaxial compression tests

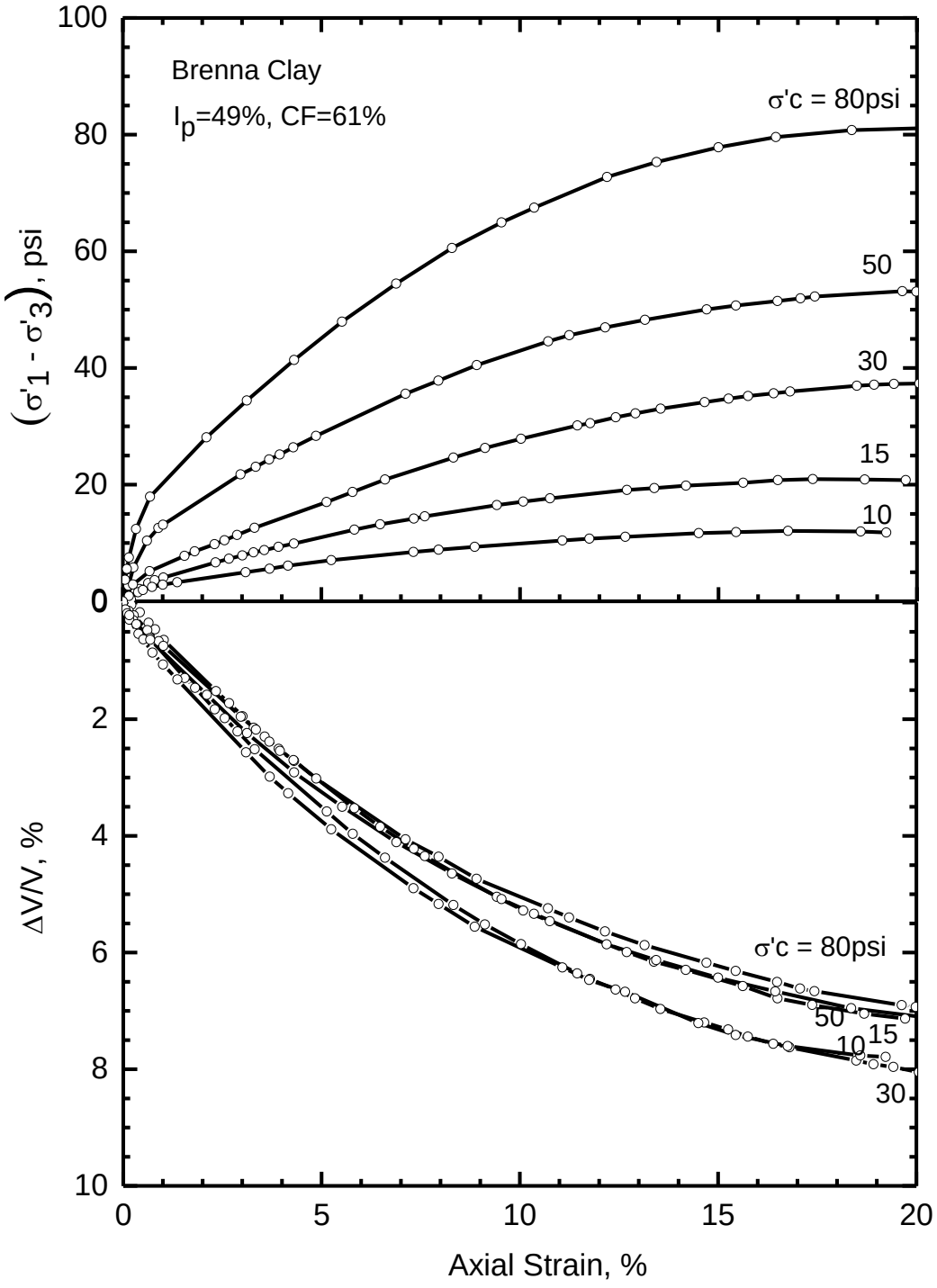

Figure 6.16. Stress-strain relationship and volume change of Brenna Clay in consolidated drained triaxial compression tests

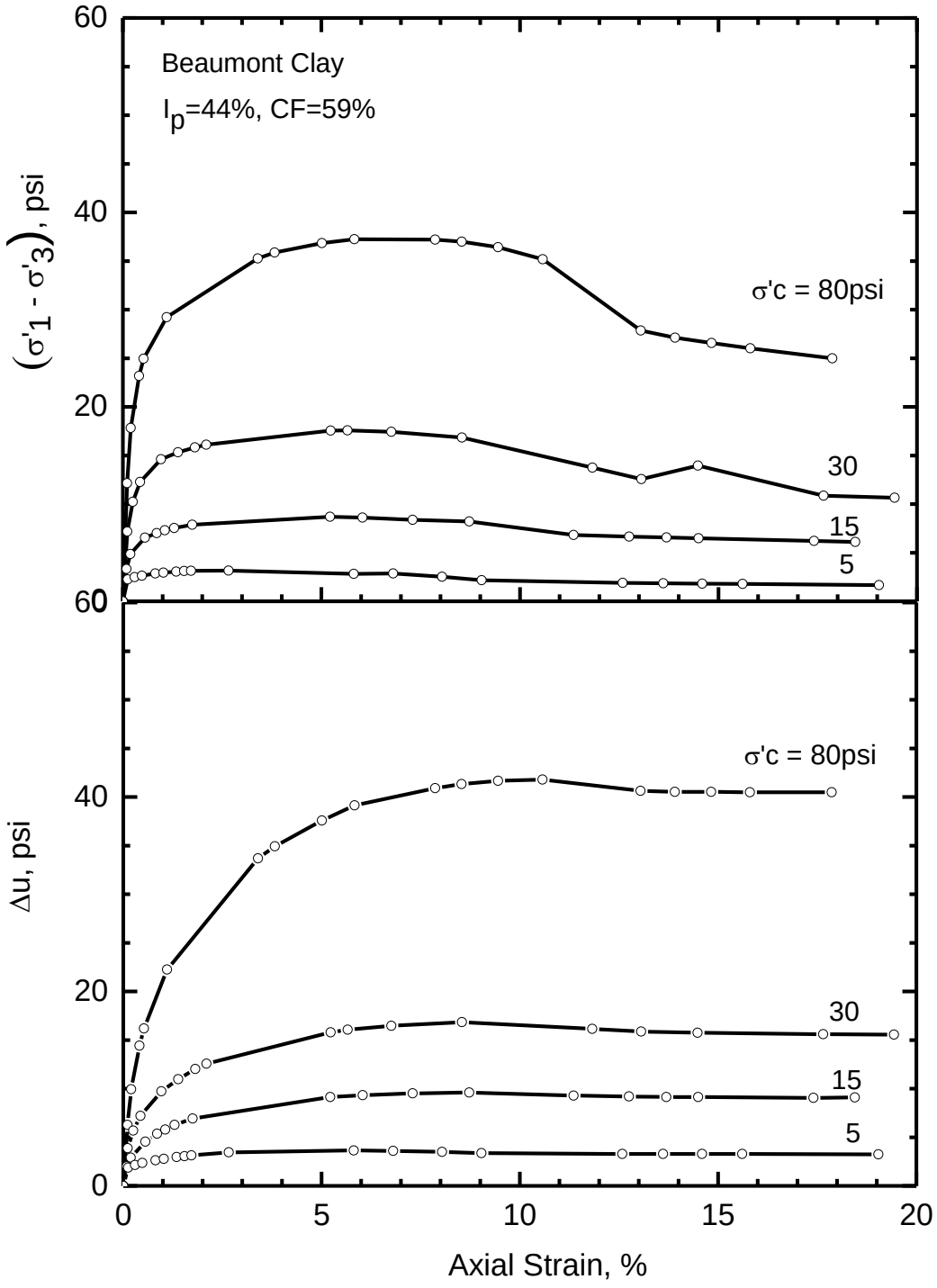

Figure 6.17. Stress-strain relationship and porewater pressure response of Beaumont Clay in consolidated undrained triaxial compression tests

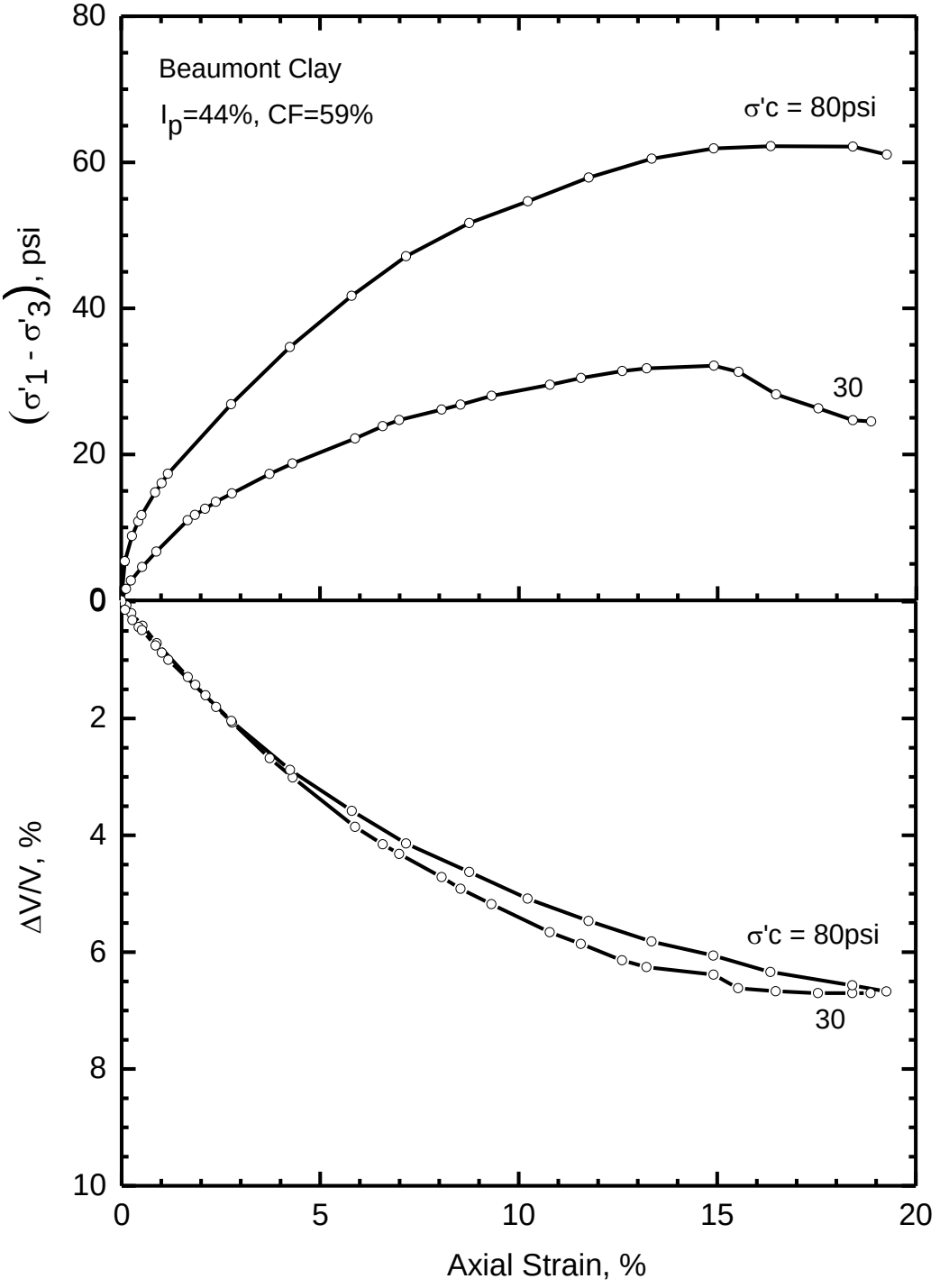

Figure 6.18. Stress-strain relationship and volume change of Beaumont Clay in consolidated drained triaxial compression tests

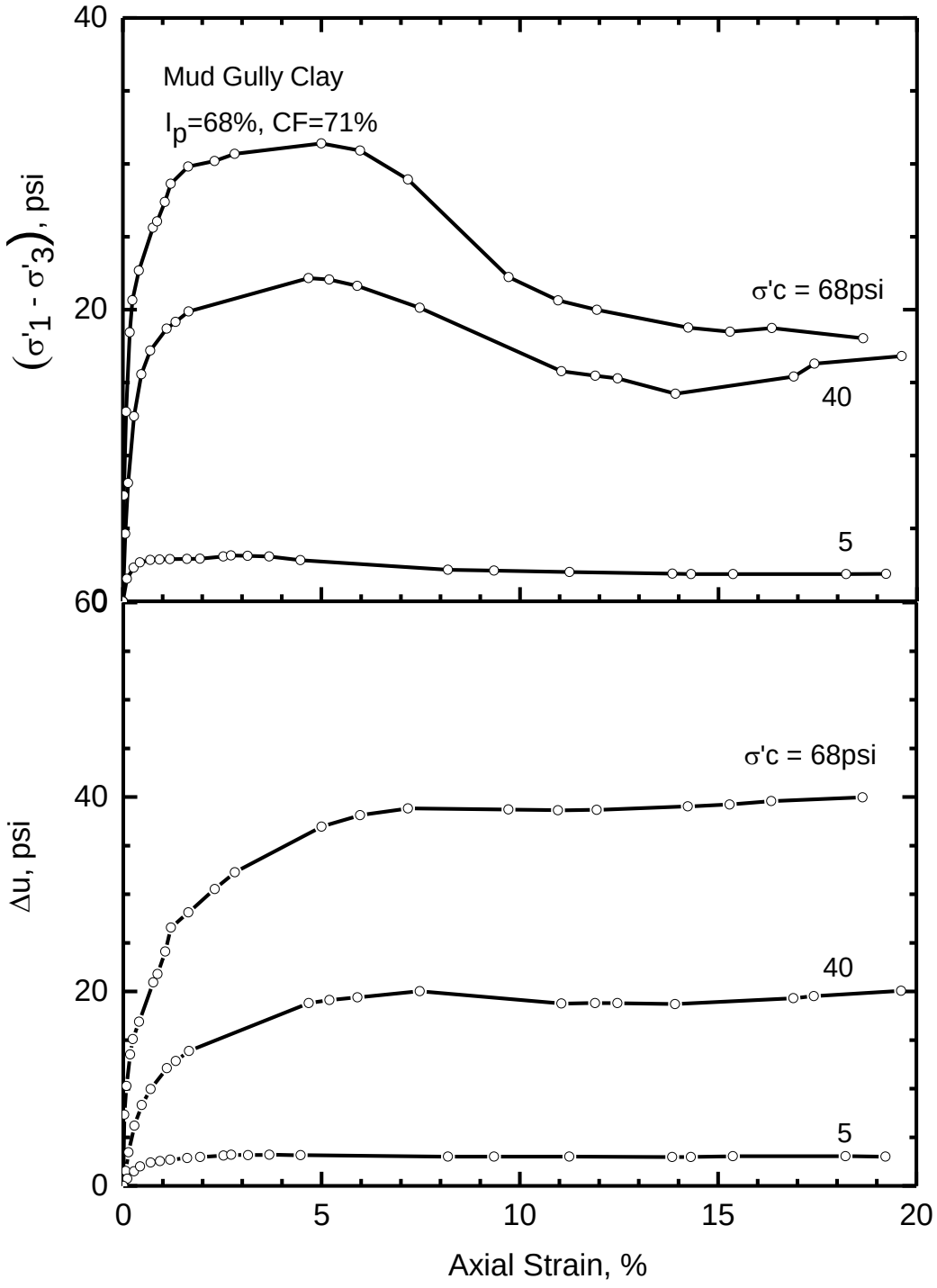

Figure 6.19. Stress-strain relationship and porewater pressure response of Mud Gully Clay in consolidated undrained triaxial compression tests

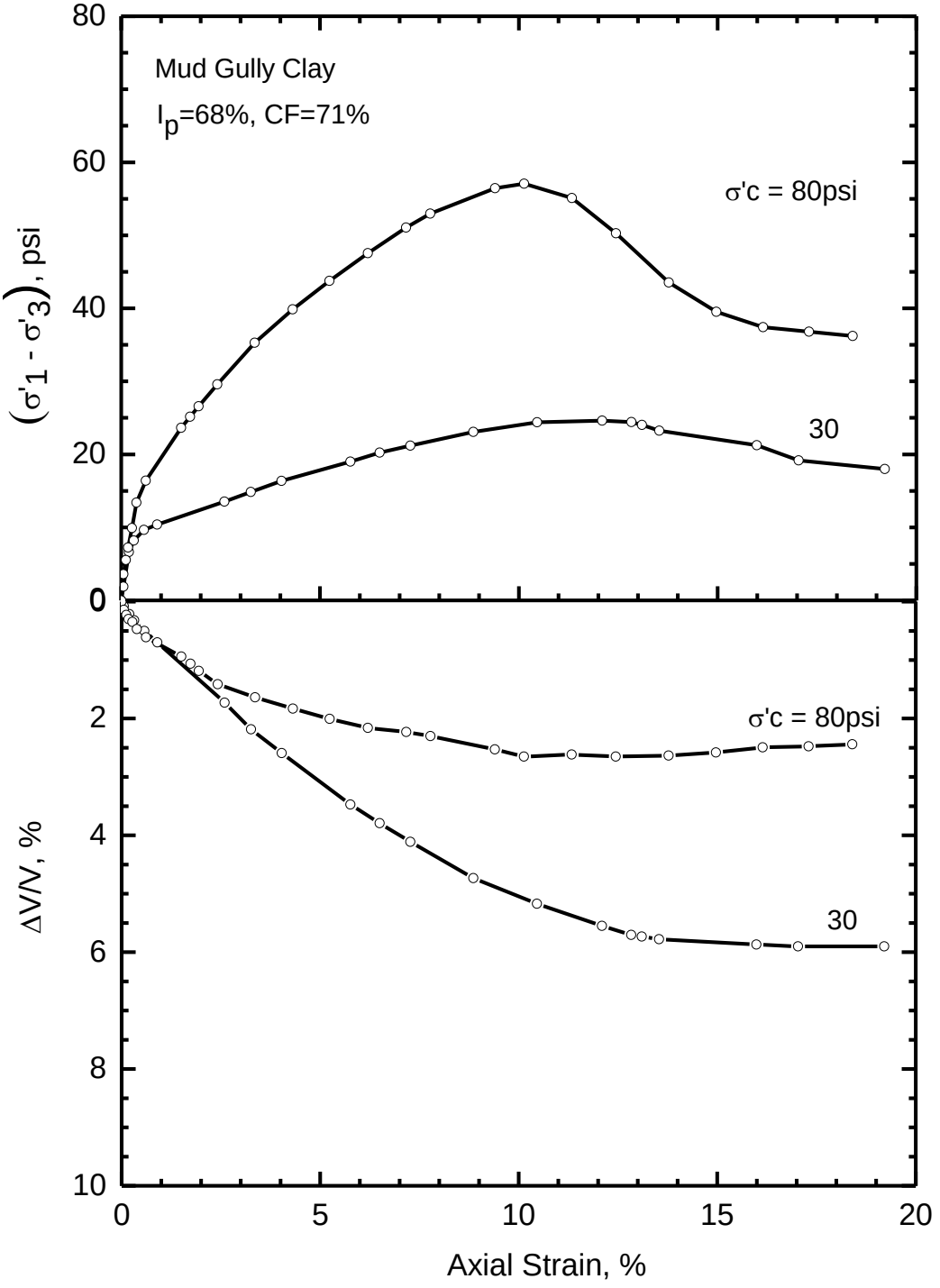

Figure 6.20. Stress-strain relationship and volume change of Mud Gully Clay in consolidated drained triaxial compression tests

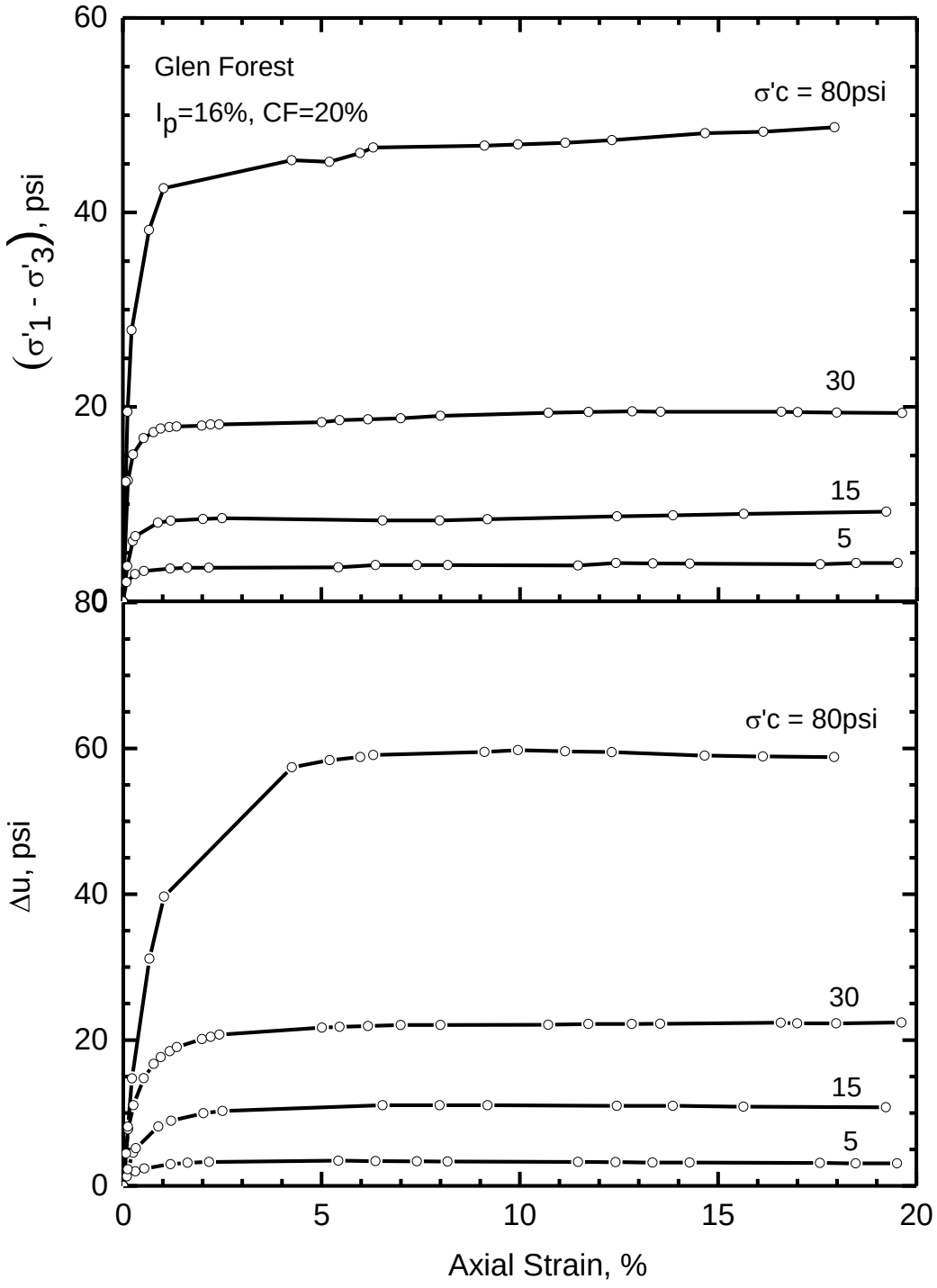

Figure 6.21. Stress-strain relationship and porewater pressure response Glen Forest Clay in consolidated undrained triaxial compression tests

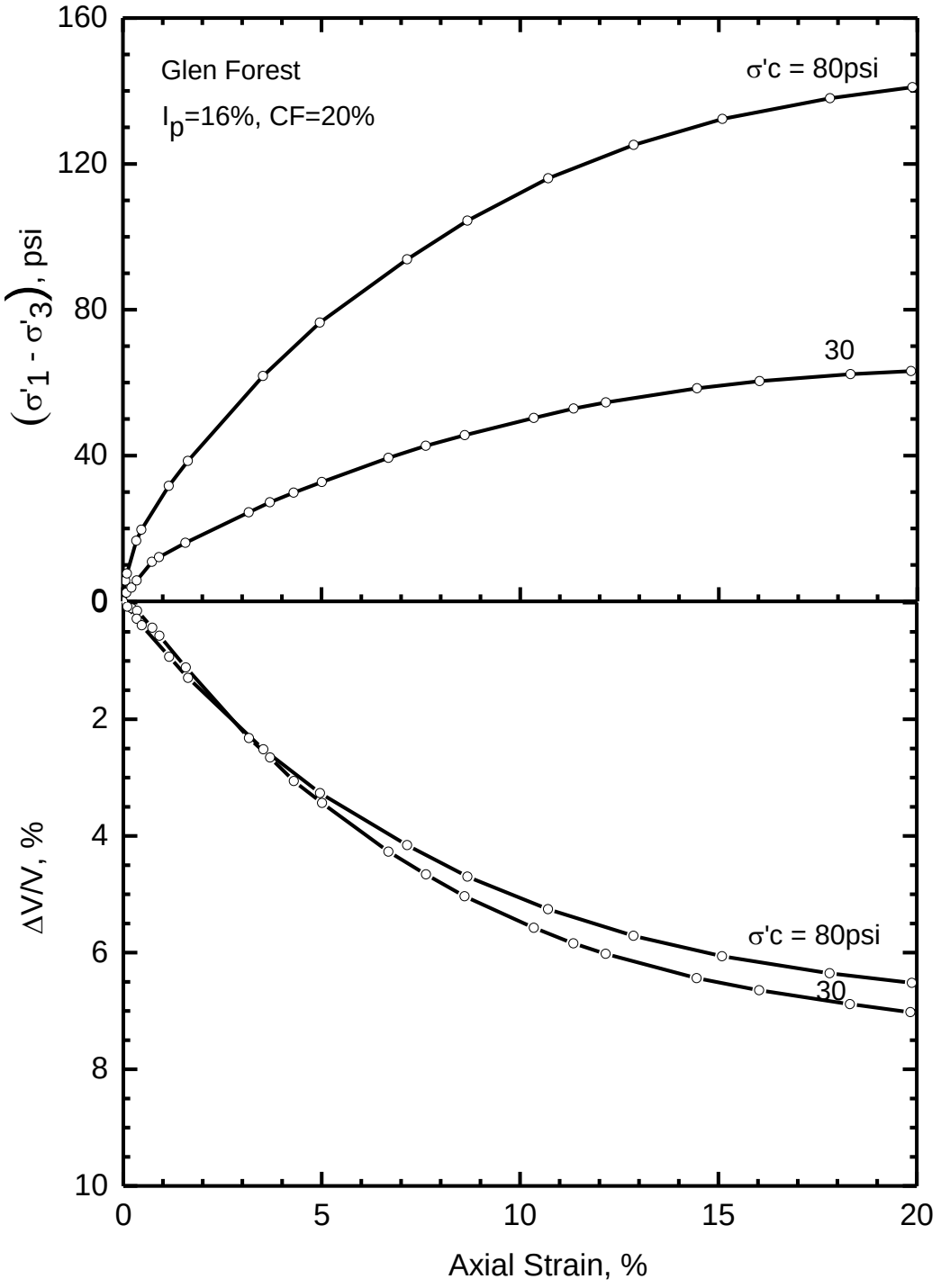

Figure 6.22. Stress-strain relationship and volume change of Glen Forest Clay in consolidated drained triaxial compression tests

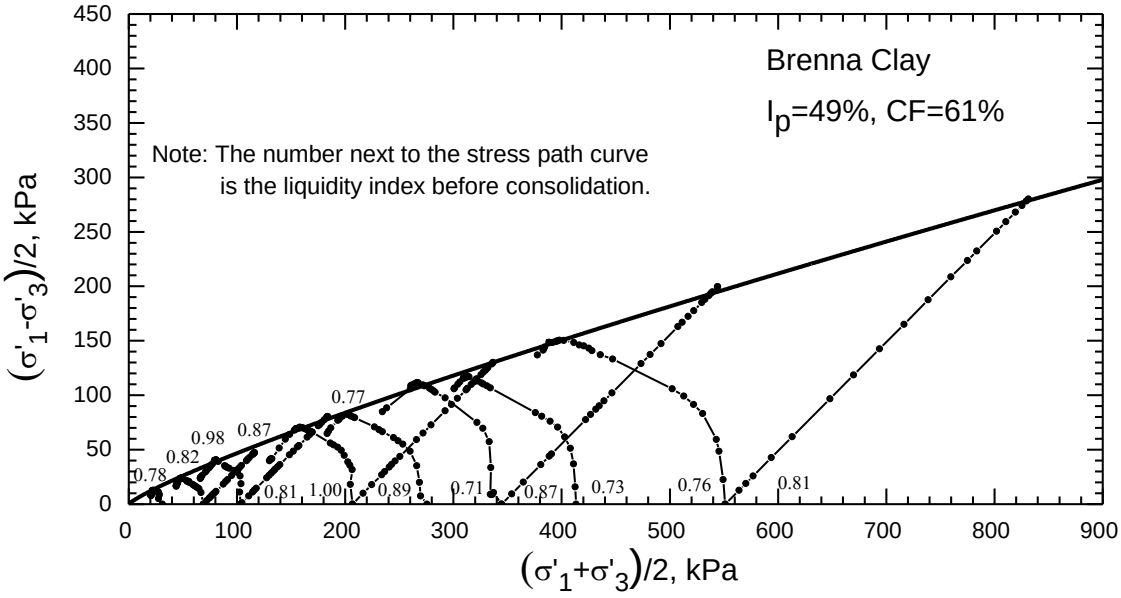

Figure 6.23. Stress path of Brenna Clay in consolidated drained and undrained triaxial compression tests

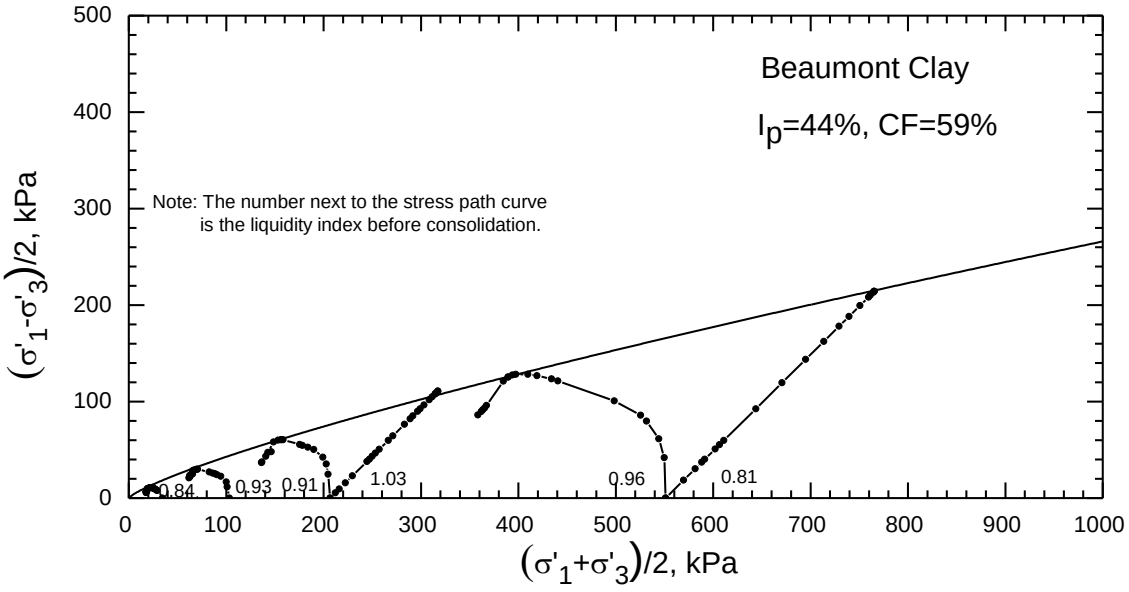

Figure 6.24. Stress path of Beaumont Clay in consolidated drained and undrained triaxial compression tests

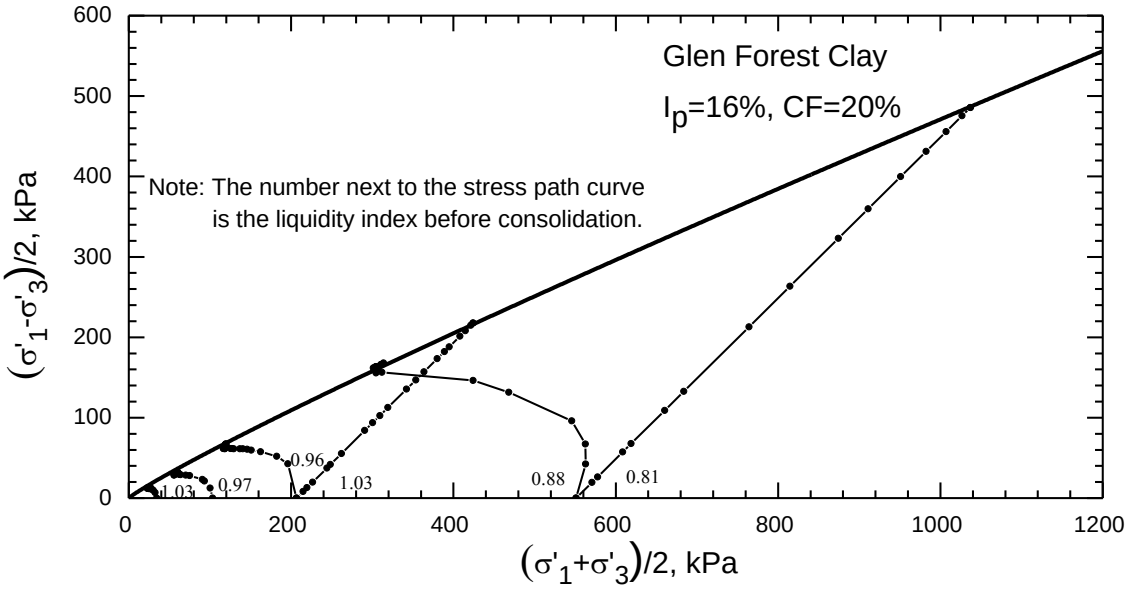

Figure 6.25. Stress path of Glen Forest Clay in consolidated drained and undrained triaxial compression tests

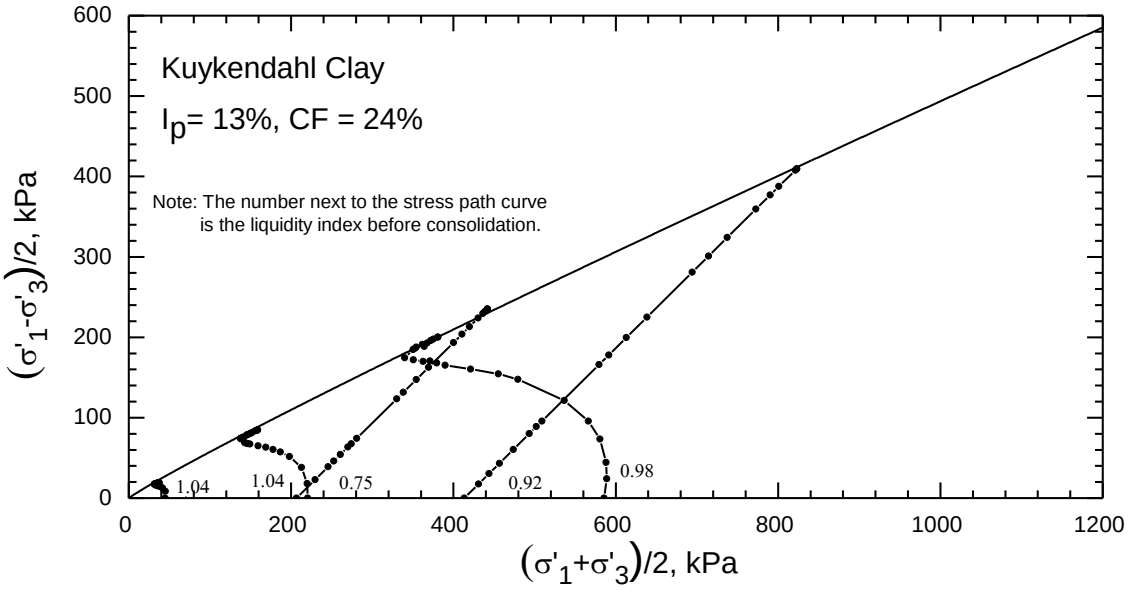

Figure 6.26. Stress path of Kuykendahl Clay in consolidated drained and undrained triaxial compression tests

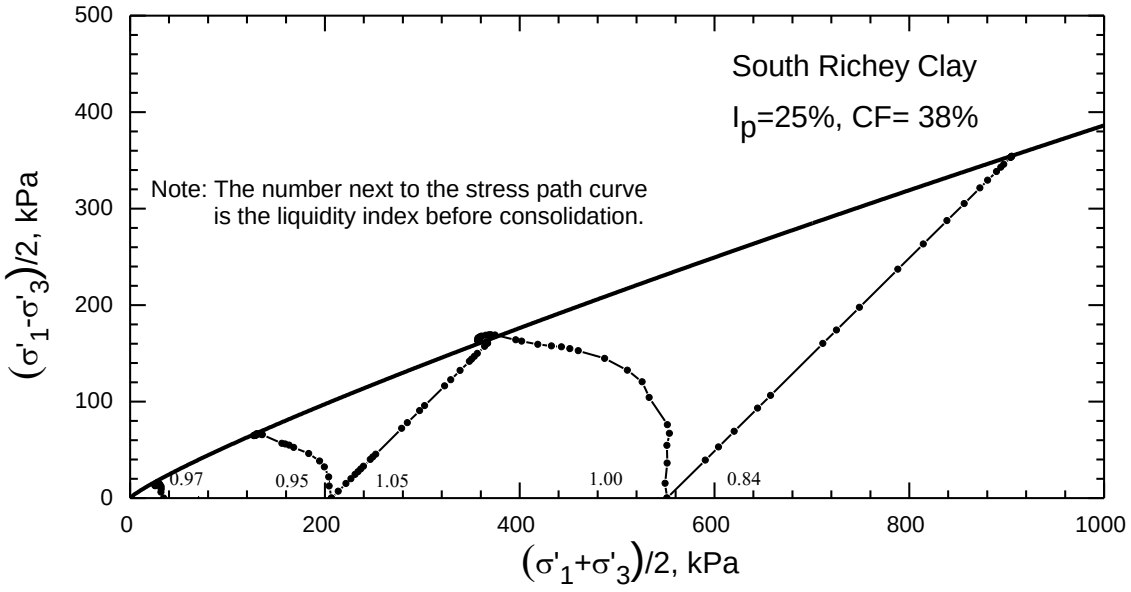

Figure 6.27. Stress path of South Richey Clay in consolidated drained and undrained triaxial compression tests

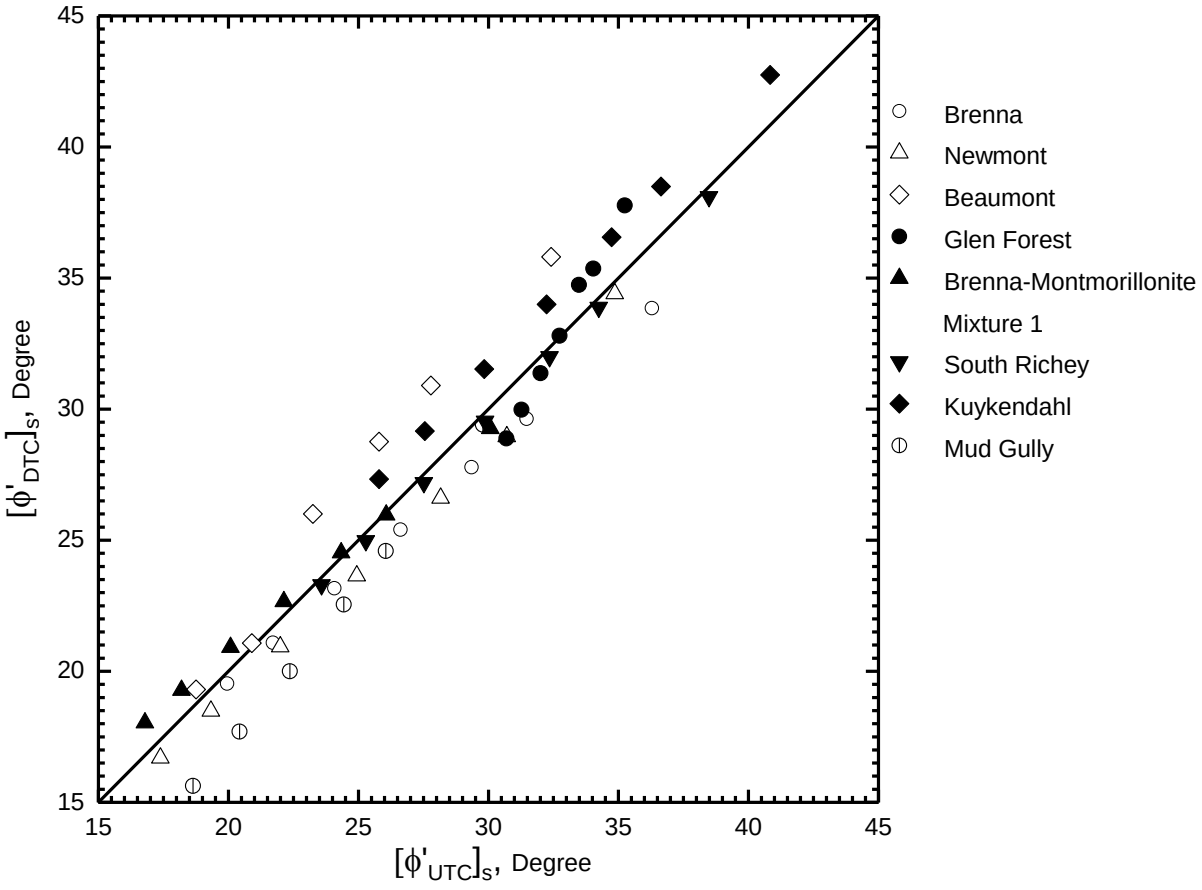

Figure 6.28. Comparison of secant fully softened friction angle determined in drained triaxial compression tests and those in undrained tests with porewater pressure measurement on 8 clay and shale compositions

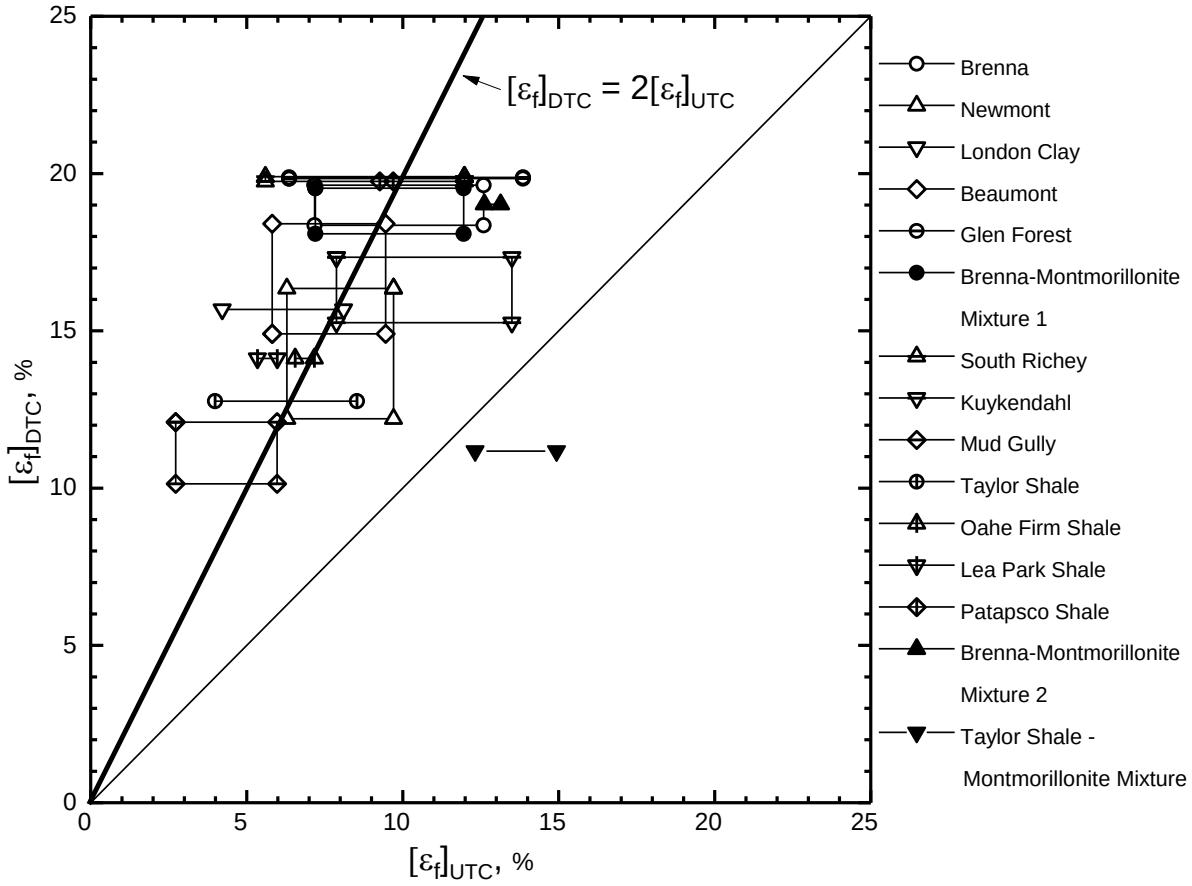

Figure 6.29. Comparison of axial strain at failure in drained triaxial compression tests and in undrained tests with porewater pressure measurement

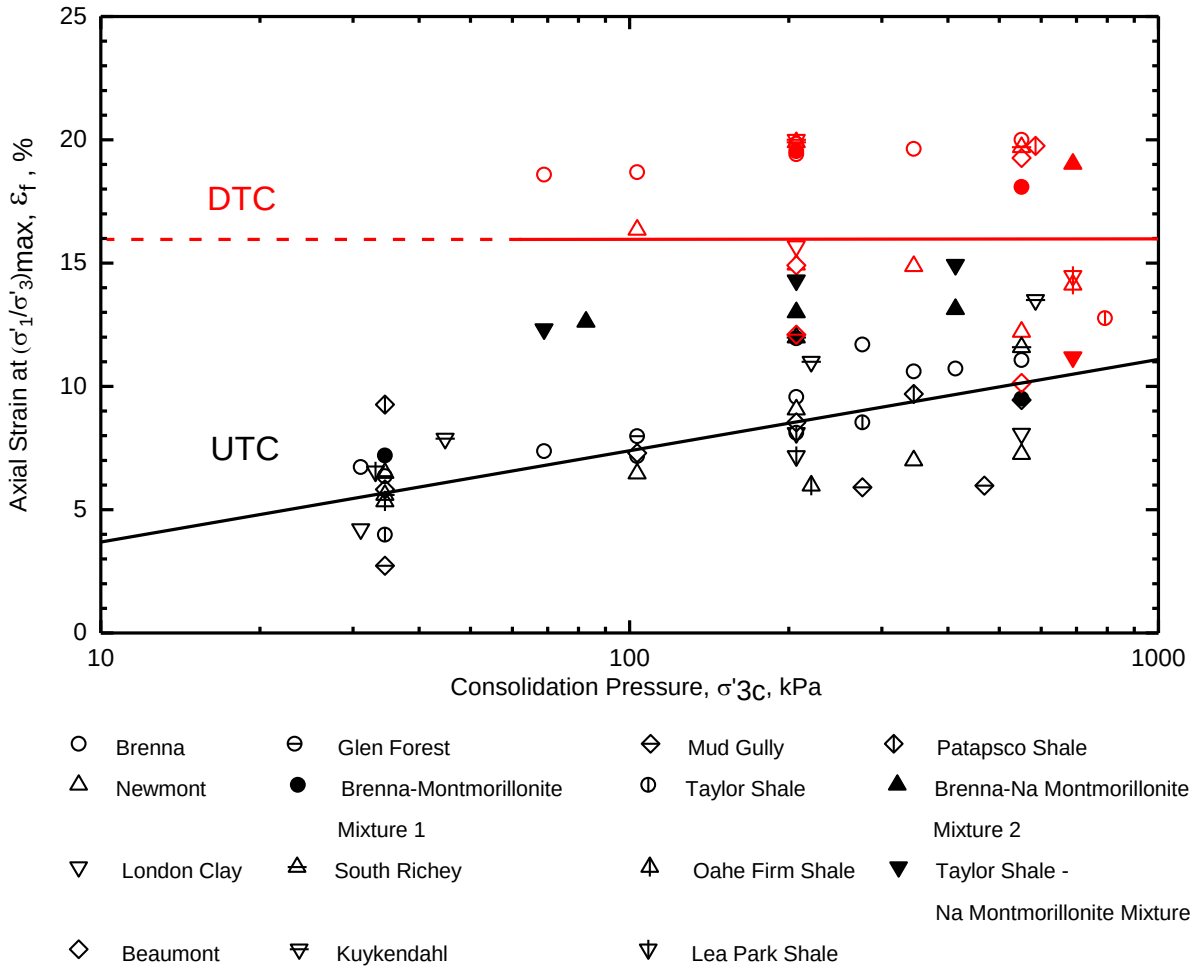

Figure 6.30. Axial strain at failure in drained triaxial compression tests and in undrained tests with porewater pressure measurement, as a function of consolidation pressure

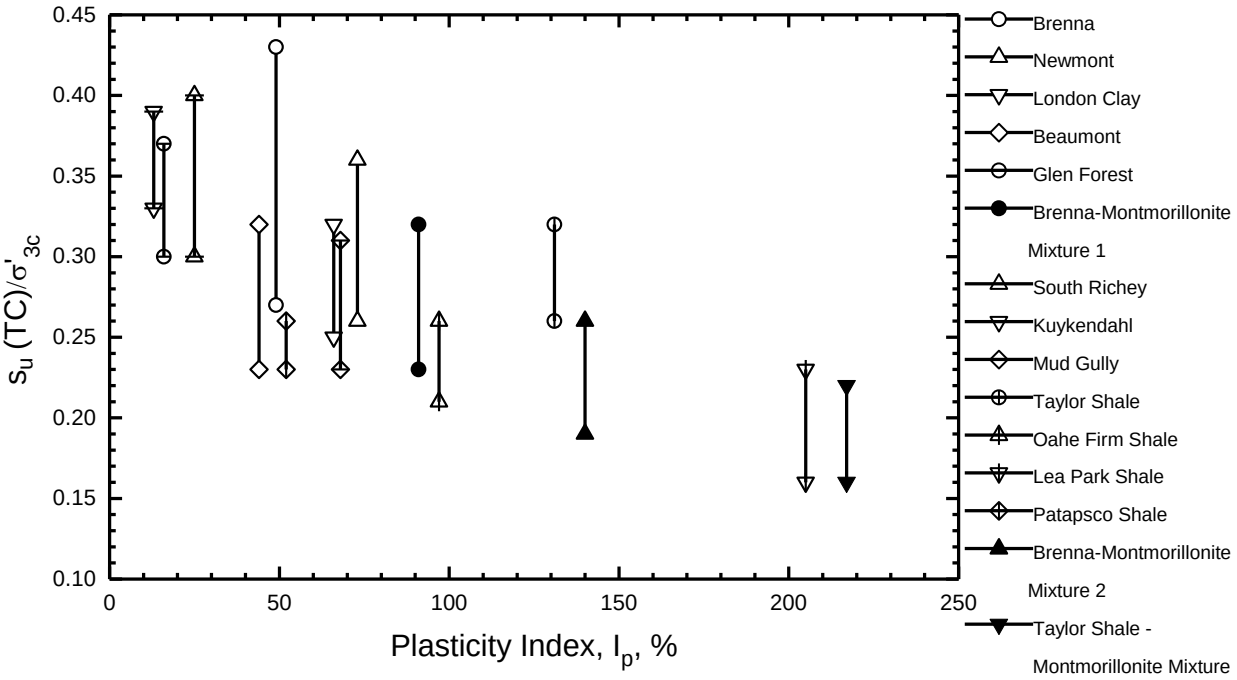

Figure 6.31. Ratios of undrained shear strength to consolidation pressure from consolidated undrained triaxial compression tests with porewater pressure measurement

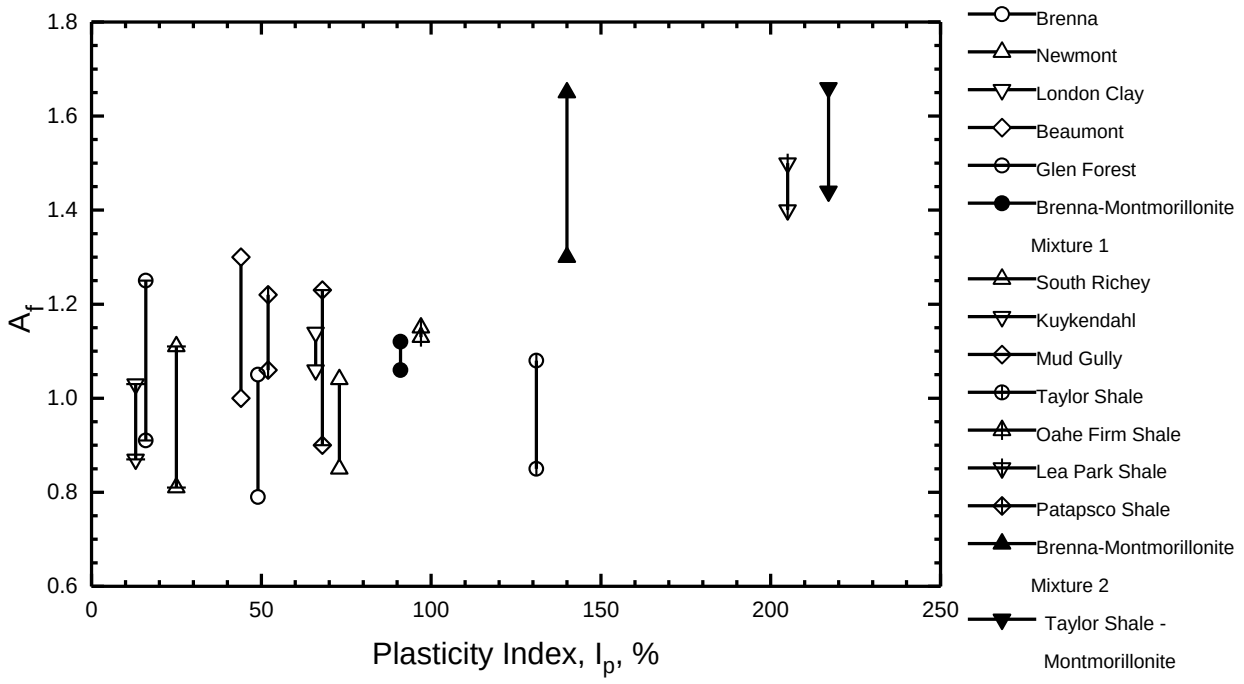

Figure 6.32. A-coefficient at failure in consolidated undrained triaxial compression tests with porewater pressure measurement

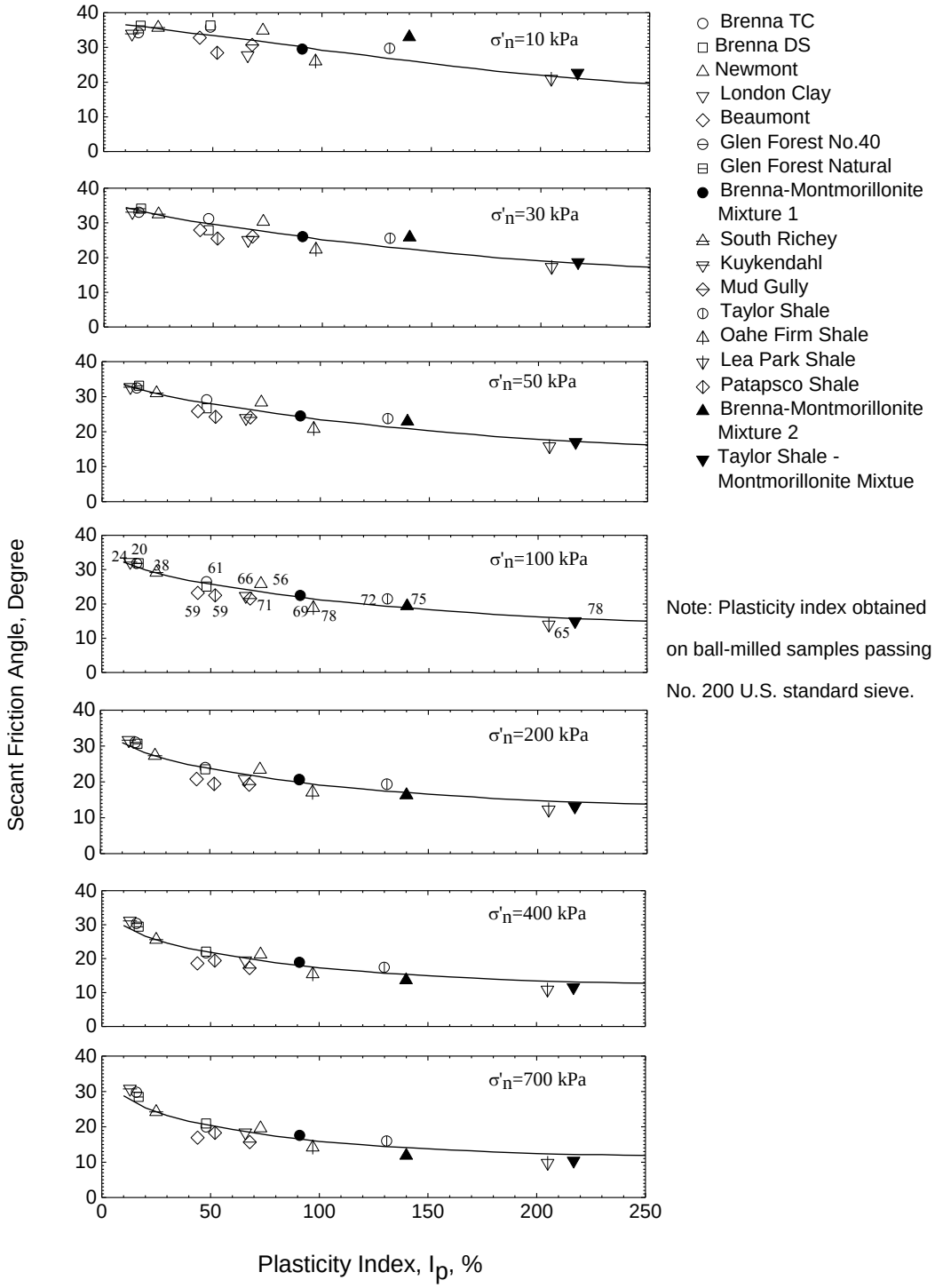

Figure 6.33. Fully softened shear strength data measured in consolidated drained and undrained triaxial compression tests (The number on each data point at $\sigma'_n = 100kPa$ is the clay size fraction in percent

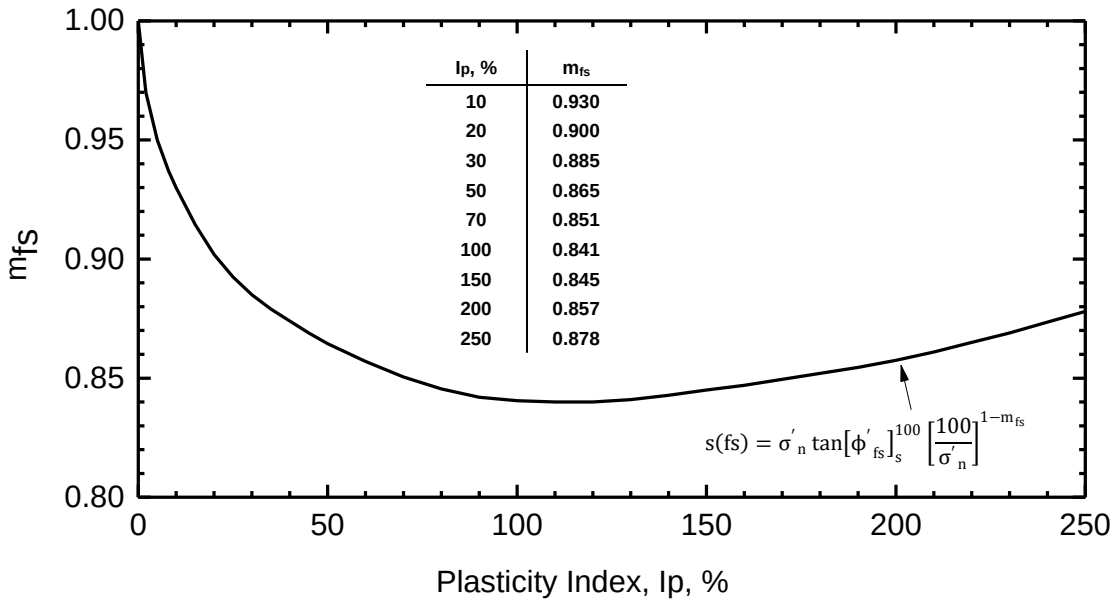

Figure 6.34. mfs as a function of plasticity index, determined from secant fully softened friction angles measured in consolidated drained and undrained triaxial compression tests

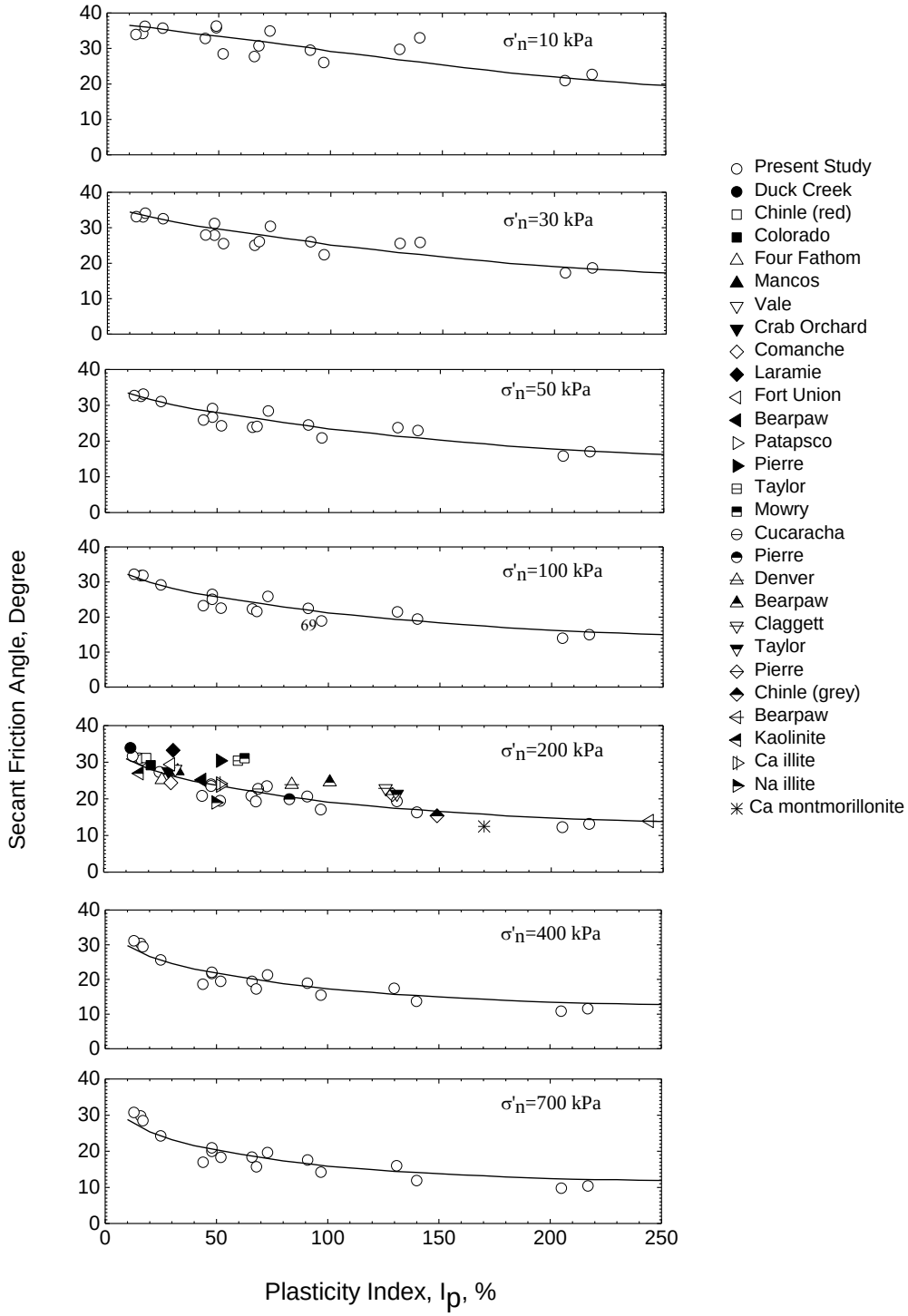

Figure 6.35. Secant fully softened friction angles of 24 clay and shale compositions, and 4 pure minerals measured in consolidated drained triaxial compression tests (Data from Mesri and Cepeda-Diaz 1986)

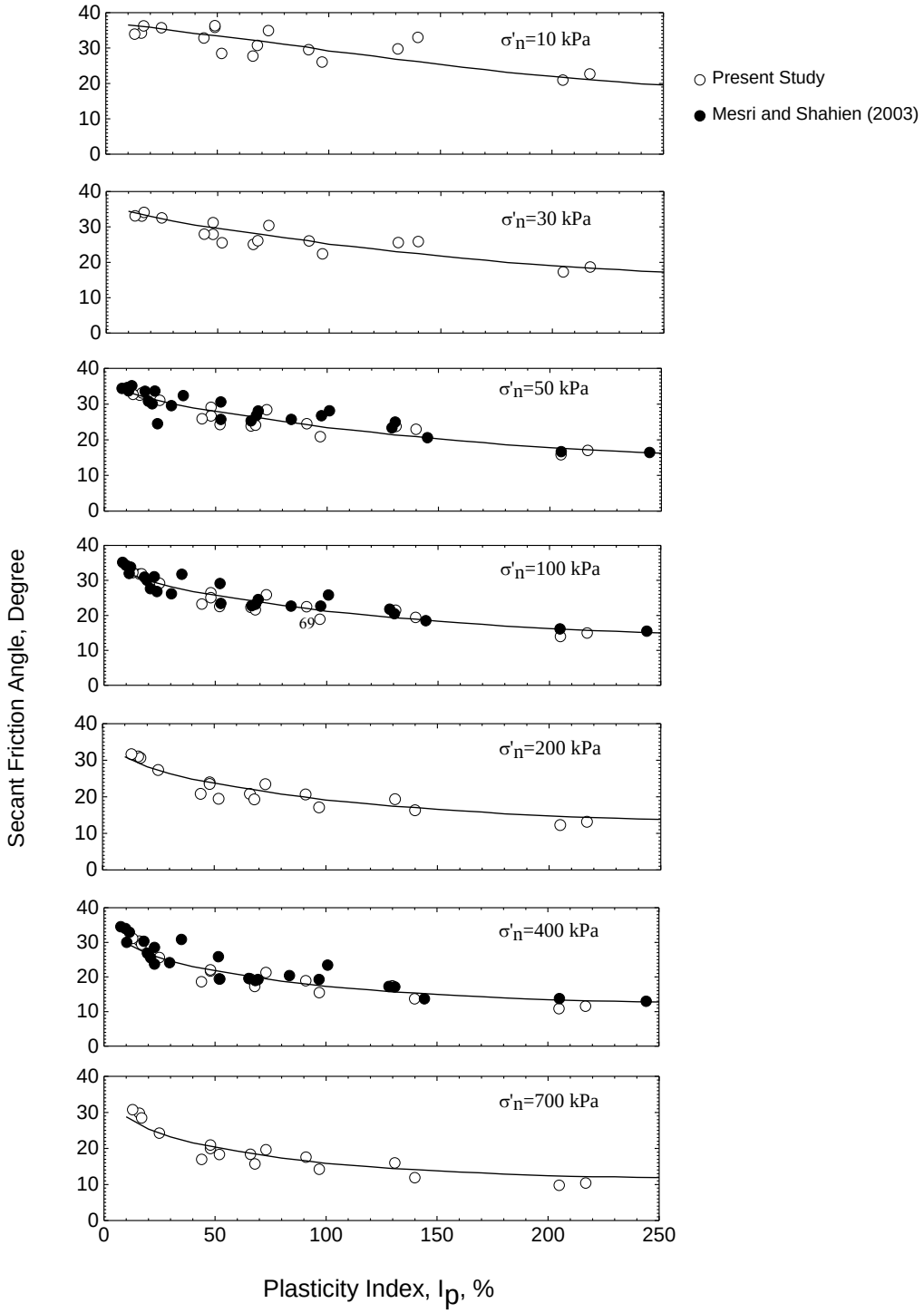

Figure 6.36. Secant fully softened friction angle data by Mesri and Shahien (2003) superimposed on the correlation developed in the present study

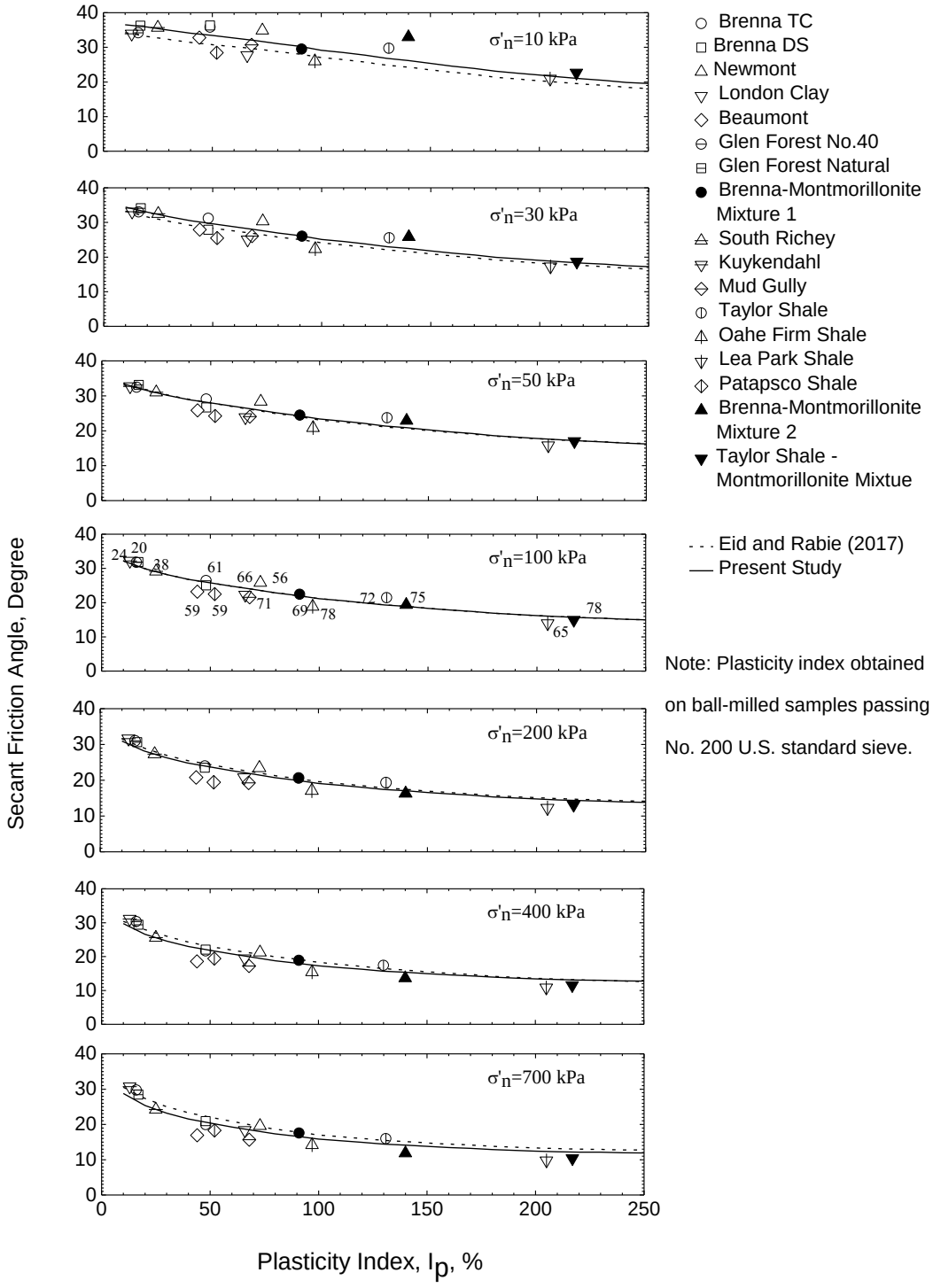

Figure 6.37. Fully softened friction angles measured in consolidated drained and undrained triaxial compression tests, superimposed on mean curves determined from corrected fully softened data in modified Bromhead ring shear device by Eid and Rabie (2017)

CHAPTER 7: FULLY SOFTENED SHEAR STRENGTH DATA INTERPRETED FROM LABORATORY TESTS IN THE LITERATURE

In this chapter, the fully softened shear strength data interpreted from laboratory triaxial compression tests reported in the literature, are compared to the empirical correlation for fully softened shear strength developed in Chapter 6. The data collection is based on the author's interpretation according to the definition of fully softened shear strength and specimen preparation procedures, even though in most cases these laboratory test results were not documented as fully softened strength measurements in the original references.

Different specimen types, and drainage conditions during the shearing process, are included, to study the potential dependence of shear strength measurements on specimen preparation procedure, and drainage condition during shear. In addition to the interpretation of data from triaxial compression tests, both drained, and undrained with porewater pressure measurement, an attempt was also made to examine a limited number of drained ring shear tests. As the materials reported in the literature were tested under various consolidation pressures, the secant fully softened friction angle is computed at effective normal stresses of 10, 30, 50, 100, 200, 400 and 700 kPa of the proposed empirical correlation.

7. 1. Reconstituted specimens used in laboratory tests reported in the literature

Because normally consolidated state of an undisturbed stiff clay or clay shale is reached at effective stresses exceeding the preconsolidation pressure, the fully softened shear strength, at all effective normal stresses, is interpreted from triaxial compression tests reported in the literature on reconstituted, normally consolidated specimens, likely with a random fabric (Skempton 1970, Mesri and Shahien 2003). The two types of reconstituted specimens used in the laboratory tests are 1) specimens prepared by mechanical remolding, or compaction, and 2) specimens consolidated from slurry or sedimented from suspension. For the triaxial compression tests, the secant friction angle is computed using maximum principal stress ratio failure criterion, $(\sigma'_1/\sigma'_3)_{\max}$, or from the stress paths tangency, if available.

The information on the reconstituted specimens of 55 compositions used in the triaxial compression tests reported in the literature, including soft clays, stiff clays, clay shales, mudstones, and clay minerals, is listed in Table 7.1, in terms of Atterberg limits, clay size fraction, specimen type/preparation procedure, water content of the specimen, and testing procedure/drainage condition during shear. Liquidity index is also computed, at which 1) the specimen was mechanically remolded, or compacted, and 2) the consolidation of slurry, or sedimentation of suspension started. Because some specimens for a particular material were prepared by more than one procedure, and/or subjected to more than one drainage condition during shear, Table 7.1 includes 68 series of tests, in terms of specimen preparation and testing procedures.

The plasticity index of the 55 compositions ranges from 9% (Saint-Jean-Vianney Clay by Saihi et al 2002) to 170% (0.01N Calcium Montmorillonite by Mesri 1969); and clay size fraction ranges from 12% (Shinano Clay by Nakano 2002) to 78% (Oahe Firm Shale by Stark and Eid 1997), as shown in the Cassagrande Chart in Fig.7.1; most of the compositions lie above the Casagrande A-line and below Casagrande U-line, and are classified as lean clay (CL) to highly plastic clay (CH). A small number of the materials are classified as high compressibility silt (MH).

Except for 4 compositions marked with “b” (Stark and Eid 1997), the index properties listed in Table 7.1, were determined on samples processed using the ASTM standard sample preparation procedure, or similar approaches, which include air drying and crushing of materials and sieving through No.40 U.S. standard sieve, or a similar sieve size for non-US standards. Materials marked with “b”, were processed by ball-milling, until the entire sample passed the No.200 U.S. standard sieve, to minimize the aggregation resulting from diagenetic bonding (Mesri and Cepeda-Diaz 1986).

7.1.1. Reconstituted specimens prepared by mechanical remolding, or compaction

The remolded specimens were prepared from 24 compositions. In the present study, reconstituted specimens prepared by mechanical remolding refer to those prepared at a water content, in general, near the liquid limit. The mechanical remolding procedure can be summarized as a process which

consists of, in sequence, 1) mixing samples with water and allowing it to hydrate for a sufficient period of time 2) uniformly drying the hydrated samples to the intended specimen water content, and 3) fabrication of the specimen, by kneading the soil paste into the triaxial specimen mold, avoiding trapping air.

The water content at which the materials were remolded was reported in various ways in the original references. In the present study a corresponding liquidity index is computed for each material and listed in Table 7.1. Specimens remolded at relatively low water content, for example, 0.3, are also included. The relatively low remolding water content, in some cases, was apparently necessary, to ensure the handling of remolded specimens (Lau 1988), or in other cases, possibly, a result of lack of control to obtain the intended higher water content. For the data collected from the literature, the liquidity index of remolded specimens subjected to triaxial compression, ranges from 0.3 to 1.0, with an average of 0.7.

7.1.2. Reconstituted specimens consolidated from slurry, or sedimented from suspension

The liquidity index values at which consolidation/sedimentation started, according to the information in the literature, was computed for the 38 compositions and are listed in Table 7.1. As reviewed in Chapter 2, compared to mechanically remolded specimens, this type of specimens were reconstituted starting with a higher water content. The specimens of this category were prepared by sedimentation from suspension, at liquidity index of 5 (Mesri 1969, Green and Wright 1986), or by consolidation of slurry, in general, with liquidity index of 2 to 3. For some of the specimens, consolidation started at a water content near the liquid limit. These specimens were still included in this category, and described as “consolidated in consolidometer” in Table 7.1, because they differ from the specimens prepared by mechanically remolding, which were not subjected to compression in the specimen preparation process.

7. 2. Undisturbed specimens

The friction angles were also interpreted for data from triaxial compression tests, both drained, and undrained with porewater pressure measurement, on 3 types of undisturbed specimens, as the mobilized shear strength on the entire or part of slip surface in first-time slope failures, in these

materials, approximates the fully softened shear strength (Mesri and Shahien 2003). These specimens listed in Table 7.2 and Table 7.3, are: (1) undisturbed soft clays of Eastern Canada, (2) undisturbed soft clays excluding soft clays of Eastern Canada, and (3) stiff clays with fissures or joints. According to the Casagrande chart in Fig.7.2, soft clays including those from Eastern Canada, are classified as lean clay (CL) to highly plastic clay (CH), and the stiff clays are highly plastic clay (CH). The secant friction angles of the undisturbed specimens are defined (details in sub-sections 7.2.1 to 7.2.3) to represent the mobilized shear strength in first-time slope failures

7.2.1. Undisturbed soft clays of Eastern Canada

The structured soft clays of Eastern Canada display a brittle response, with rapid shear strength decrease after the peak shear strength which is mobilized at small axial strain, about 1 %. This strain softening behavior of soft clays of Eastern Canada with natural water content, in general, larger than the liquid limit, is similar to that of an overconsolidated clay. However, the peak shear strength of soft clays of Eastern Canada, is partly produced by bonding or cementation between clay particles, which is not at equilibrium with the void ratio and effective stress condition in the specimen (Lefebvre and La Rochelle 1974, Lefebvre 1981, Terzaghi et al 1996). The mobilized shear strength in first-time slope failures in soft to firm clays in Eastern Canada, is close to the large-strain strength from triaxial compression tests, following the structural breakdown (Lefebvre and La Rochelle 1974, Lefebvre 1981, Mesri and Abdel-Ghaffar 1993, and Mesri and Shahien 2003). In the present study, the large-strain strength, defined at 8% of axial deformation (Lefebvre 1981), for 11 soft clays of Eastern Canada (Table 7.2), is in consolidated triaxial compression tests, both drained, and undrained with porewater pressure measurement.

7.2.2. Undisturbed soft clays excluding soft clays of Eastern Canada

Because the fully softened shear strength of a stiff clay or clay shale composition equals to the peak shear strength in its normally consolidated state (Skempton 1970), secant friction angles defined at peak shear strength are computed for triaxial compression tests on 5 undisturbed soft clays from Norway, Finland, and China. Specimens were consolidated prior to shearing, at pressures greater than the preconsolidation pressures, and then subjected to drained, or undrained triaxial compression with porewater pressure measurement.

7.2.3. Undisturbed stiff clays with fissures or joints

Skepmton (1977) considered shear strength from the peak strength measured along fissures or joints as being close to fully softened shear strength obtained from normally consolidated specimens prepared by consolidation starting from slurry. The fissured or jointed specimens in this category differ from the ones containing principle displacement/shear surfaces, and the discontinuities are characterized by Skempton and Petley (1967) as "a brittle-fracture type of surface along which the relative (shearing) movements, if not zero, must have been exceedingly small" and "joints or fissures usually in a more or less random arrangement, often with irregular, curved or conchoidal surfaces, and dimensions typically ranging from 1 to 10 or 20 cm, and exceptionally up to 40 or 50 cm." For the literature data interpreted for the present study, the tests were performed on undisturbed Blue London Clay specimens taken in such a manner that the test specimen could be set up with the discontinuity inclined at about 50° to the horizontal in the triaxial cell (Skempton and Petley 1967, and Skempton et al 1969). Secant friction angles, defined at peak shear strength, are computed at 7 effective normal stresses.

7. 3. Triaxial Compression Tests

An examination of drained ring shear tests on reconstituted specimens was attempted; however, the 5 series of ring shear tests performed on 4 materials from Japan, all using specimens with a thickness larger than 2 cm, consolidated from slurry (Okimi Clay by Ohtsuka and Isobe 2009, kaoline by Toyota et al 2009, and mudstones and loess by Kimura 2015), give larger secant fully softened friction angles than those of stiff clay and clay shale compositions with similar plasticity index. The larger friction angles for clays from Japan, might be explained by the minerology of some soils from Japan which include Kanto Loams (with water holding capacity not necessarily related to platyness). Therefore, because of limited data available in the literature, the interpretation of shear strength measurements from torsional ring shear tests is not presented in the present study.

The 68 series of triaxial compression tests on reconstituted specimens, consist of 24 series on mechanically remolded specimens, and 44 series on specimens consolidated from slurry, or sedimented from suspension. All specimens in the triaxial compression tests are cylindrical shaped.

For the cylindrical specimens, the height to diameter ratio is approximately 2.0, expect for reconstituted Tertiary Mudstone specimens (Nakamori 1996), and reconstituted specimens of Boom Clay (Bouazza et al 1996), which have, respectively, slightly larger ratios of, 2.3 and 2.4. Most specimens have a diameter ranging from 3.5 cm to 3.9cm, with an average diameter of 3.8 cm (1.5 inch). Specimens of larger size were also used. Yatabe et al (1991), Saihi et al (2002), Ghahremannejad (2003), Dev et al (2013), Li and Baudet (2016), performed triaxial compression tests on specimens with a diameter of 5 cm and a height of 10 cm. The diameter of the reconstituted East China Deep Clay specimens (Shang et al 2015) and the reconstituted Speswhite Kaolin (Suzuki and Dyvik 2017), are respectively, 6.2cm and 7.0cm.

Prior to shear, specimens were either consolidated under equal all around pressure, or consolidated under K_o condition. For undrained tests, a back-pressure (140 to 1380 kPa) was applied to the triaxial cell, therefore, it can be assumed that the measurement of porewater pressure, is reliable. A larger number of test data were interpreted from undrained tests with porewater pressure measurement, and only 14 series of tests were performed on reconstituted specimens subjected to drained shear. One reason for the small number of drained tests, is the longer testing period required for porewater pressure dissipation in drained tests, compared to that required for porewater pressure equalization in undrained tests.

The imposed axial deformation rates in triaxial compression tests on reconstituted, normally consolidated specimens reported in the literature, are listed in Table 7.4, and compared with the maximum allowable rates, estimated by Equations 6.1 to 6.6. It should be noticed that t_{50} values were not available in any tests. The maximum allowable rates of axial deformation, were computed as follows.

For the 14 series of drained tests, imposed axial deformation rates were reported in the original references only for 10 series of tests. Among the 10 series of tests, c_t was reported by Willam (2004, 2005), and t_f was computed using Eq.6.2. For the remaining 9 series of tests, time to failure was calculated by Eq.6.5, using a t_{50} value estimated from Fig.7.3. Figure 7.3 shows the range of t_{50} in the last load increment in the present research program, of the remolded specimens prepared from 15 stiff clay and clay shale compositions, with I_p in the range of 13% to 217%, prior to shear,

consolidated under equal all around pressure in the range of 4.5 psi (30 kPa) to 115 psi (790 kPa). For each composition, the higher bound of t_{50} corresponds to the largest consolidation pressure, and the lower bound corresponds to the smallest consolidation pressure. Therefore, t_{50} in the triaxial compression tests reported in the literature, could be estimated, according to the plasticity index of the material and the consolidation pressure level. When estimating $\dot{\delta}$ using Eq.6.2 and Eq.6.5, the axial strain at failure, ε_f , equal to 16%, was assumed, as it is the average value in the drained triaxial compression tests on remolded, normally consolidated specimens, performed in the present research program. According to Table 7.4, drained condition was achieved in these drained triaxial compression tests, as the reported imposed rates of axial deformation are slower than those computed using Equations 6.1, 6.2, and 6.5. For the remaining 4 series of drained triaxial compression tests (Cancelli 1981, Crabb and Atkinson 1991, Kawaguchi et al 2005, Mandaglio et al 2016) without reported imposed axial deformation rates, it is assumed that the tests were performed at rates to represent a drained shear condition.

For the 54 series of undrained triaxial compression tests with porewater pressure measurement, imposed rates of axial deformation were available in 27 series of tests. To calculate the maximum allowable deformation rates, time to failure was estimated by Eq.6.4 or 6.6. The c_t values were reported in 4 series of tests (Green and Wright 1986, William 2004, 2005, and Shang et al 2015), and t_f was computed using Eq.6.4. For the remaining 23 series of tests, t_f was computed by Eq.6.6, together with t_{50} estimated by the same procedure as described for the drained tests. For the undrained tests, ε_f was assumed to be 8%, which corresponds to the average of axial strain at failure, observed in the undrained triaxial compression tests with porewater pressure measurement on remolded, normally consolidated specimens, performed in the present research program. Table 7.4 indicates that porewater pressure equalization throughout the specimen was achieved in the 27 series of tests, because they were performed at rates slower than the computed maximum allowable rates of axial deformation. For the other 27 series of tests without reported imposed axial deformation rates, it is assumed that these tests were performed at a rate to achieve porewater pressure equalization throughout the specimen.

7. 4. Laboratory tests on reconstituted, normally consolidated specimens

The secant fully softened friction angles as a function of plasticity index, calculated from the laboratory tests on reconstituted, normally consolidated specimens reported in the literature, are summarized in Figures 7.4 and 7.5 at 7 effective normal stresses. The empirical correlation developed in the present study, is shown for comparison. Most of the data from the literature are at plasticity index range less than 70%. The relation of shear strength measurements on specimen preparation procedure and drainage condition during the shearing stage, are examined in the following sub-sections.

7. 4. 1. Specimen preparation

Figure 7.4 shows the secant fully softened friction angles computed from triaxial compression tests, both drained, and undrained with porewater pressure measurement, on reconstituted specimens prepared by two procedures. The secant friction angles calculated from laboratory tests on specimens remolded at liquidity index of 0.3 to 1.0, with an average of 0.7, are comparable to those obtained from tests on specimens consolidated from slurry, or sedimented from suspension. It is also illustrated in Fig.7.4 that, the fully softened shear strength interpreted from specimens prepared by the two procedures, at plasticity index between 9% and 170%, at all effective normal stresses, are in a good agreement with the empirical correlation developed in the present study. It can be concluded that for triaxial compression, the random arrangement and interaction of clay particles, is mobilized at failure on normally consolidated specimens, prepared by mechanical remolding at water content close to liquid limit, or by consolidation from a slurry/suspension water content.

7. 4. 2. Drainage condition in the shearing stage

As shown in Fig.7.5, for triaxial compression on reconstituted, normally consolidated specimens of plasticity index between 9% and 170%, the fully softened shear strength data interpreted from specimens subjected to undrained shear with porewater pressure measurement, at all effective normal stresses, are comparable to those from specimens subjected to drained shear. This observation indicates that prestress in undrained tests (Casagrande and Wilson 1953) does not have a noticeable effect on the drained shear strength parameters. Therefore, the consolidated undrained

triaxial compression tests with porewater pressure measurement on reconstituted normally consolidated specimens, which requires less duration for porewater pressure equalization in undrained tests, than porewater pressure dissipation in drained tests, are preferred for the measurement of fully softened friction angle.

7. 5. Shear strength interpreted from laboratory tests on undisturbed specimens

The secant friction angle data in Fig.7.6 include values for undisturbed specimen of stiff fissured clays, and soft clays, including those from Eastern Canada. The friction angles for the undrained triaxial compression tests on stiff fissured, or jointed clays, were defined at peak shear stress. The friction angle values for triaxial compression tests on soft clays of Eastern Canada, both drained, and undrained with porewater pressure measurement, were defined at 8% axial strain as suggested for the large strain strength by Lefebrve (1981). The friction angles for the drained and undrained triaxial compression tests on remaining soft clays were defined at peak shear stresses.

7. 5. 1. Secant friction angle defined at peak shear strength of undisturbed stiff clays with fissures or joints

The secant friction angles in Fig.7.6, defined at peak shear strength of undisturbed stiff clays with fissures or joints, subjected to undrained triaxial compression with porewater pressure measurement, at effective normal stresses equal or greater than 50 kPa, are similar to the fully softened friction angles from the empirical correlation. Because of joints and fissures, as well as other minor discontinuities in the undisturbed specimens, in the triaxial compression, the secant friction angles defined at peak shear strength, are most likely close to the secant friction angles mobilized on the back-scarp of the slip surface, in a first-time slope failure in stiff clay and clay shales.

7. 5. 2. Large-strain strength of soft clays of Eastern Canada

The triaxial compression tests on soft clays of Eastern Canada were performed at low effective normal stresses, to simulate the field condition of first-time shallow slope failures. As a result, the secant friction angles defined at 8% axial strain, are only available at effective normal stresses no larger than 100 kPa. As illustrated in Fig.7.6, at effective normal stresses equal or smaller than 50

kPa, large-strain friction angles of soft clays of Eastern Canada, are higher than fully softened friction angles from the empirical correlation. At effective normal stress of 100 kPa, large-strain friction angles, become similar to fully softened friction angles from the empirical correlation. Apparently, high consolidation pressures, in addition to shear strain, contribute to the breakdown of bonding between clay particles (Lefebvre and La Rochelle 1974, Lefebvre 1981, Mesri and Abdel-Ghaffar 1993).

7. 5. 3. Secant friction angle defined at peak shear strength of soft clays excluding clays of Eastern Canada

Because the 5 undisturbed soft clays from Norway, Finland and China, were consolidated prior to shear, at pressures equal or greater than the preconsolidation pressure, a condition close to the normally consolidated state could be assumed for these specimens. It can be seen from Fig.7.6 that, for the limited data at effective normal stress range of 30 kPa to 400 kPa, friction angles corresponding to the peak shear strength of these normally consolidated clays, are equal or greater than the fully softened friction angles from the empirical correlation. In the triaxial compression, the drained shear strength parameters defined at peak shear strength of the soft clays excluding soft clays of Eastern Canada, are close to those mobilized on the entire slip surfaces of first-time slope failures in these materials (Kenney 1967, Kenny and Drury 1973).

7. 6. Fully softened shear strength from reconstituted or undisturbed specimen

In engineering practice, undisturbed stiff clay and clay shale specimens may be preferred for determining fully softened shear strength, because specimen preparation is less time consuming, mainly consisting of trimming of the undisturbed specimens, compared to the procedures to reconstitute specimens.

The question arises in selecting the axial strain at which fully softened shear strength is defined. For an undisturbed overconsolidated clay subjected to drained triaxial compression, ideally, the fully softened condition is reached at the axial strain where volume increase levels off (Terzaghi et al 1996). However, for undisturbed stiff clay or clay shale specimens, a distinct shear plane is likely to develop at early stage of shearing, and stress concentration on the shear plane results in

some face to face interaction of clay particles, especially at high effective normal stresses. Therefore, the clay particle arrangement and interaction may not correspond to the random fabric of clay particles at which fully softened condition is defined. For this reason, the friction angle may be underestimated using a post-peak axial strain level such as, for example 15%.

In a personal experience with the Fargo Flood Control Project in South Dakota, the consolidated undrained triaxial compression tests with porewater pressure measurement on undisturbed Brenna and Sherack Clay, with I_p in the range of 28% and 90%, were examined by the author. It was found that the secant friction angles defined at 15% axial strain, especially at higher effective normal stresses, were lower than those interpolated from Mesri and Shahien (2003), which can be explained by the particle re-orientation on the shear plane. The maximum difference (5 degrees) was overserved for a Brenna Clay specimen with plasticity index of 90% that failed at effective normal stress of 197 kPa. This is consistent with the behavior explained by Mesri and Cepeda-Diaz (1986) that the decrease from fully softened friction angle to residual friction angle maximizes at intermediate mineralogical compositions, i.e., platy particles with predominantly edge to face interaction. Stark and Eid (1997) reported the difference between fully softened friction angle and residual angles for the same clay and clay shale compositions, as a function of liquid limit. The liquid limit, 116%, of this Brenna Clay, is in the range of liquid limit (110% to 170%) at which maximum difference between fully softened and residual strength was reported.

TABLES

Table 7.1. Materials used to prepare reconstituted specimens in the laboratory tests reported in literature

No.	Clay	Location	wl(%)	wp(%)	CF(%)	Ip	Specimen Type	w(%), c	Iu(%), d	Test	Reference
1	Panoche Shale, b	California, USA	53	29	50	24	Remolded	51	0.9	Drained Triaxial Compression	Stark and Eid (1997)
2	Oahe Firm Shale, b	South Dakota, USA	138	41	78	97	Remolded	106	0.7	Drained Triaxial Compression	Stark and Eid (1997)
3	Oahe Bentonitic Shale, b	South Dakota, USA	192	47	65	145	Remolded	137	0.6	Drained Triaxial Compression	Stark and Eid (1997)
4	Lugagnano Clay	Albedosa, Italy	40-60	20-25	-	20-28	Remolded	40-60	1.0	Drained Triaxial Compression	Cancelli (1981)
5	Gault Clay	Selborne, UK	60-75	20-22	38-48	40-50	Remolded	30-33	0.3	Undrained Triaxial Compression	Cooper (1998)
6	Beaumont Clay	Texas, USA	65	20	-	45	Remolded	51-61	0.7-0.9	Undrained Triaxial Compression	Green and Wright (1986)
7	Ringold Formation	Washington State, USA	39	13	-	26	Remolded	31	0.7	Undrained Triaxial Compression	Bareither et al (2015)
8	East China Deep Clay	China	52	24	48	28	Remolded	32	0.3	Undrained Triaxial Compression	Shang et al (2015)
9	Inuyose Clay	Inuyose, Japan	36	24	20	12	Remolded	-	-	Undrained Triaxial Compression	Yagi et al (1988)
10	Nuta Clay	Nuta, Japan	34	17	20	17	Remolded	-	-	Undrained Triaxial Compression	Yagi et al (1988)
11	Kawadotsurebi Clay	Kawadotsurebi, Japan	41	17	29	24	Remolded	-	-	Undrained Triaxial Compression	Yagi et al (1988)
12	Weald Clay	UK	46	22	38	24	Remolded	33	0.5	Undrained Triaxial Compression	Henkel and Sowa (1964)
13	Zhanjiang Clay	Zhanjiang, Japan	60	22	26	38	Remolded	-	-	Undrained Triaxial Compression	Kong et al (2015)
14	Red/Black Soil	Hubei, China	-	-	23	19	Remolded	-	-	Undrained Triaxial Compression	Liu et al. (2006)

Table 7.1. (Cont'd)

15	NOVA Clay	Northern Virginia, USA	66	28	17	38	Remolded	51-53	0.8	Undrained Triaxial Compression	Castellanos (2014)
16	Oak Harber	Ohio, USA	47	22	47	25	Remolded	36	0.6	Undrained Triaxial Compression	Castellanos (2014)
17	Todi Clay	Todi, Italy	43-54	23-26	33-43	20-28	Remolded	-	-	Undrained Triaxial Compression	Calabresi and Rampello (1987)
18	Montreal Silty Clay	Montreal, Canada	25	15	40	10	Remolded	23-25	1	Undrained Triaxial Compression	Selvadurai and Ghiabi (2007)
19	Younger Bay Mud	California, USA	51-59	19-25	-	32-34	Remolded	-	-	Undrained Triaxial Compression	Mitchell et al (1992)
20	Kaolinite Clay	India	54	29	60	25	Remolded	36	0.3	Undrained Triaxial Compression	Nagaraj and Somashekar (1979)
21	Champlain Fissured Clay	Quebec, Canada	50	28	-	22	Remolded	-	-	Undrained Triaxial Compression	Silvestri (1980)
22	Brno Clay	Brno, Czech Republic	75	32	50	43	Remolded	-	-	Undrained Triaxial Compression	Bohac et al (1995)
23	Speswhite Kaolin	Norway	61-67	28-32	-	34	Remolded	48-52	0.6	Undrained Triaxial Compression	Suzuki and Dyvik (2017)
24	Matsue Mudstone	Japan	94	26	36	68	Remolded	-	-	Undrained Triaxial Compression	Yatabe et al (1991)
25	Roccella Clay 2	Calabria, Italy	57	30	50-65	27	Consolidated from Slurry	-	2	Drained Triaxial Compression	Mandaglio et al (2016)
26	Shinano Clay	Shinano, Japan	35	20	12	15	Consolidated from Slurry	-	-	Drained Triaxial Compression	Nakano (2002)
27	Niiho Clay	Niiho, Japan	50	20	60	30	Consolidated from Slurry	-	-	Drained Triaxial Compression	Nakano (2002)
28	London Clay 1	London, UK	53	26	-	27	Consolidated from Slurry	-	-	Drained Triaxial Compression	Crabb and Atkinson (1991)
29	Pudong Clay	Shanghai, China	45	23	-	22	Consolidated from Slurry	-	-	Drained Triaxial Compression	Sun et al (2014)

Table 7.1. (Cont'd)

30	Pujiang Clay	Zhejiang, China	47	25	-	22	Consolidated from Slurry	-	-	Drained Triaxial Compression	Sun et al (2014)
31	Suzhou Clay	Jiangsu, China	36	17	-	19	Consolidated from Slurry	-	-	Drained Triaxial Compression	Sun et al (2014)
32	Bringelly Shale	Sydney, Australia	27-35	15-26	55	7-12	Consolidated in Consolidometer	-	1.0	Drained Triaxial Compression	William (2004, 2005)
33	NSF Clay	Japan	55	29	-	26	Consolidated from Slurry	-	3.1	Drained Triaxial Compression	Kawaguchi et al (2005)
34	0.01 N Calcium Montmorillonite	USA	200-205	33-35	35	167-170	Sedimented from Suspension	54-77	5.0	Undrained Triaxial Compression	Mesri (1969)
35	Tertiary Mudstone	Akitsu, Japan	76	16	46	60	Consolidated from Slurry	-	1.0	Undrained Triaxial Compression	Nakamori (1996)
36	Beaumont Clay	Texas, USA	65	20	-	45	Sedimented from Suspension	51-61	5.0	Undrained Triaxial Compression	Green and Wright (1986)
37	Paris Clay	Texas, USA	80	22	59	58	Consolidated from Slurry	40-67	2.5	Undrained Triaxial Compression	Kayyal and Wright (1991)
38	Beaumont Clay	Texas, USA	73	21	46	52	Consolidated from Slurry	29-53	2.5	Undrained Triaxial Compression	Kayyal and Wright (1991)
39	Colorado Clay	Colorado, USA	42	22	24	20	Consolidated in Consolidometer	33-34	1.0	Undrained Triaxial Compression	Castellanos and Brandon (2013), Castellanos
40	NOVA Clay	Northern Virginia, USA	66	28	17	38	Consolidated in Consolidometer	51-57	1	Undrained Triaxial Compression	Castellanos and Brandon (2013), Castellanos
41	Vicksburg Buckshot Clay	Virginia, USA	78	26	69	52	Consolidated in Consolidometer	61-63	1.0	Undrained Triaxial Compression	Castellanos and Brandon (2013), Castellanos
42	Alabama 1	Alabama, USA	42	23	33	19	Consolidated in Consolidometer	30-32	1.0	Undrained Triaxial Compression	Castellanos (2014)
43	Oak Harber	Ohio, USA	47	22	47	25	Consolidated in Consolidometer	36	1.0	Undrained Triaxial Compression	Castellanos (2014)
44	Boom Clay	Antwerp, Belgium	64	27	33	37	Consolidated from Slurry	-	1.4	Undrained Triaxial Compression	Bouazza et al (1996)

Table 7.1. (Cont'd)

45	Kaoline	India	52	24	34	28	Consolidated from Slurry	-	1.9	Undrained Triaxial Compression	Dev et al (2013)
46	IIT Lake Clay	Chennai, India	49	23	34	26	Consolidated from Slurry	-	1.9	Undrained Triaxial Compression	Dev et al (2013)
47	Cucaracha Shale	Panama Canal	74	30	63	44	Consolidated from Slurry	-	2.7	Undrained Triaxial Compression	Banks (1978)
48	Sienitic Residual Soil	Pocos de Caldas, Brazil	60	44	28	16	Consolidated from Slurry	-	1.0	Undrained Triaxial Compression	Carvalho et al (2011)
49	Mercia Mudstone	Leicestershire, UK	28	10	20	18	Consolidated from Slurry	-	1.7-2.8	Undrained Triaxial Compression	Stallebrass and Seward (2011)
50	Illite	USA	39	21	-	18	Consolidated in Consolidometer	-	1.1	Undrained Triaxial Compression	Yong and Vey (1963)
51	Kaolin	USA	70	41	-	29	Consolidated in Consolidometer	-	1.1	Undrained Triaxial Compression	Yong and Vey (1963)
52	Kaolin	Hong Kong, China	75	35	-	40	Consolidated from Slurry	-	1.6	Undrained Triaxial Compression	Li and Baudet (2016)
53	Hongqiao Clay	Shanghai, China	42	20	-	22	Consolidated from Slurry	-	3.0	Undrained Triaxial Compression	Sun et al (2014)
54	Pujiang Clay	Zhejiang, China	47	25	-	22	Consolidated from Slurry	-	2.9	Undrained Triaxial Compression	Sun et al (2014)
55	Suzhou Clay	Jiangsu, China	36	17	-	19	Consolidated from Slurry	-	3.1	Undrained Triaxial Compression	Sun et al (2014)
56	NSF Clay	Japan	55	29	-	26	Consolidated from Slurry	-	3.1	Undrained Triaxial Compression	Kawaguchi et al (2005)
57	Saint-Jean-Vianney clay	Quebec, Cananda	28	19	-	9	Consolidated from Slurry	-	-	Undrained Triaxial Compression	Saihi et al (2002)
58	M44 Clay	USA	60	25	50	35	Consolidated in Consolidometer	-	1.3	Undrained Triaxial Compression	Ghahremannejad (2003)
59	Blue London Clay 2	Brent, UK	71	26	59	45	Consolidated from Slurry	-	1.9	Undrained Triaxial Compression	Lau (1988)

Table 7.1. (Cont'd)

60	Speswhite Kaolin	Norway	61-67	28-32	-	34	Consolidated from Slurry	-	2.6-2.8	Undrained Triaxial Compression	Suzuki and Dyvik (2017)
61	Bringelly Shale	Sydney, Australia	27-35	15-26	55	7-12	Consolidated in Consolidometer	-	1.0	Undrained Triaxial Compression	William (2004, 2005)
62	Macau Marine Clay	Macau, China	40-60	20-40	75	30	Consolidated from Slurry	-	2.0-2.7	Undrained Triaxial Compression	Yan and Ma (2010)
63	Kaolin Clay	Japan	71	22	35	49	Consolidated from Slurry	-	2.4	Undrained Triaxial Compression	Toyota et al (2009)
64	0.01 N Calcium Montmorillonite	USA	200-205	33-35	35	167-170	Sedimented from Suspension	55-97	5.0	Undrained Triaxial Compression	Mesri (1969)
65	Oxford Clay	Bedford, UK	66	34	45	32	Consolidated in Consolidometer	-	1.3	Undrained Triaxial Compression	Kamal et al. (2014)
66	Kimmeridge Clay	Abingdon, UK	49	23	50	26	Consolidated in Consolidometer	-	1.3	Undrained Triaxial Compression	Kamal et al. (2014)
67	Gault Clay	Cambridge, UK	74	28	57	46	Consolidated in Consolidometer	-	1.3	Undrained Triaxial Compression	Kamal et al. (2014)
68	London Clay 2	London, UK	66	29	47	37	Consolidated in Consolidometer	-	1.3	Undrained Triaxial Compression	Kamal et al. (2014)

b. Samples ball milled and passed through No. 200 U.S. standard sieve.

c. Water content of the reconstituted specimens.

d. Liquidity index refers to water content at which 1) the specimen was mechanically remolded, or 2) the consolidation of slurry, or sedimentation of suspension started.

Table 7.2. Soft clays of Eastern Canada in the laboratory tests reported in literature

No.	Location	w_l(%)	w_p(%)	CF(%)	I_P	w_o(%)	I_l(%)	σ'_p (kPa)	Test	Reference
1	Lachute 1, Canada	55	23	-	32	80	1.8	130	Drained Triaxial Compression	Lefebvre (1981)
2	Lachute 2, Canada	60	21	-	39	60	1.0	185	Drained Triaxial Compression	Lefebvre (1981)
3	Batiscan, Canada	60	22	-	38	75	1.4	124	Drained Triaxial Compression	Lefebvre (1981)
4	St-Coeur-de Marie, Canada	40	22	-	18	50	1.6	260	Drained Triaxial Compression	Lefebvre (1981)
5	Rosemere, Canada	61	28	-	33	72	1.3	160	Drained Triaxial Compression	Lefebvre (1981)
6	St-Leon, Canada	53	26	-	27	57	1.1	230	Drained Triaxial Compression	Lefebvre (1981)
7	La Baie, Canada	30	18	-	12	45	2.3	360	Drained Triaxial Compression	Lefebvre (1981)
8	Chicoutimi, Canada	44	22	-	22	38	0.7	475	Drained Triaxial Compression	Lefebvre (1981)
9	Saint-Louis, Canada	50	25	80	25	65	1.6	193	Undrained Triaxial Compression	Lefebvre and LaRochelle (1974)
10	Rockcliffe, Canada	31-53	23-25	57-65	8-28	53-58	1.2-3.7	196-441	Drained Triaxial Compression	Crawford (1963), Eden and Mitchell (1971)
11	Range du Fleuve, Canada	70	20	-	50	80	1.2	50	Undrained Triaxial Compression	Tavenas et al (1978)

Table 7.3. Undisturbed soft clays excluding clays of Eastern Canada, and stiff clays with fissures or joints

No.	Clay	Location	w_l(%)	w_P(%)	CF(%)	I_P	σ'_p (kPa)	w_o(%)	Specimen Type	Test	Reference
1	Norwegian Quick Clay	Oslo, Norway	29-39	20-21	30-50	8-20	129-259	20-30	Undisturbed	Drained Triaxial Compression	Sevaldson (1956)
2	Norwegian Soft Silty Clay	Drammen River, Norway	27-37	17-20	30-42	10-17	106	34-40	Undisturbed	Drained Triaxial Compression	Kjaernsli and Simons (1962)
3	Finland Soft Glacial Clay	Kimola Canal, Finland	47-63	22-23	58	25-40	125-280	44-53	Undisturbed	Undrained Triaxial Compression	Kankare (1969a, b)
4	Norwegian Soft Silty Clay	Drammen River, Norway	27-37	17-20	30-42	10-17	106	34-40	Undisturbed	Undrained Triaxial Compression	Kjaernsli and Simons (1962)
5	Shanghai Soft Clay	Shanghai, China	44	22	-	22	50	52	Undisturbed	Undrained Triaxial Compression	Huang et al (2011)
6	Shanghai Clay	Shanghai, China	45-51	26-27	33	18-25	85-160	51-52	Undisturbed	Undrained Triaxial Compression	Li et al (2012)
8	Blue London Clay 1	Wraysbury, UK	62-76	30	55	32-46	-	-	Undisturbed with Joints	Undrained Triaxial Compression	Skempton and Petley (1967), Skempton et al (1969)
9	Blue London Clay 2	Wraysbury, UK	62-76	30	55	32-46	-	-	Undisturbed with Fissures	Undrained Triaxial Compression	Skempton and Petley (1967), Skempton et al (1969)

Table 7.4. Imposed deformation rates reported in triaxial compression tests in the literature

No.	Clay	$\dot{\delta}$ Imposed reported (mm/min)	$\dot{\delta}$ using Eq. 6.5 because t_{50} can be estimated (mm/min)	$\dot{\delta}$ using Eq. 6.2 because c_v was available (mm/min)	$\dot{\delta}$ using Eq. 6.6 because t_{50} can be estimated (mm/min)	$\dot{\delta}$ using Eq. 6.4 because c_v was available (mm/min)	Drainage condition
1	Panoche Shale, b	0.0010	0.0024	-	-	-	Drained Triaxial Compression
2	Oahe Firm Shale, b	0.0005	0.0007	-	-	-	Drained Triaxial Compression
3	Oahe Bentonitic Shale, b	0.0002	0.0003	-	-	-	Drained Triaxial Compression
4	Lugagnano Clay	-	-	-	-	-	Drained Triaxial Compression
5	Gault Clay	-	-	-	-	-	Undrained Triaxial Compression
6	Beaumont Clay	0.0007	-	-	-	0.0138	Undrained Triaxial Compression
7	Ringold Formation	0.0100	-	-	0.0109	-	Undrained Triaxial Compression
8	East China Deep Clay	0.0500	-	-	-	0.0512	Undrained Triaxial Compression
9	Inuyose Clay	-	-	-	-	-	Undrained Triaxial Compression
10	Nuta Clay	-	-	-	-	-	Undrained Triaxial Compression
11	Kawadotsurebi Clay	-	-	-	-	-	Undrained Triaxial Compression
12	Weald Clay						Undrained Triaxial Compression
13	Zhanjiang Clay	-	-	-	-	-	Undrained Triaxial Compression
14	Red/Black Soil	-	-	-	-	-	Undrained Triaxial Compression

Table 7.4. (Cont'd)

15	NOVA Clay	0.0033	-	-	0.0084	-	Undrained Triaxial Compression
16	Oak Harber	0.0052	-	-	0.0103	-	Undrained Triaxial Compression
17	Todi Clay	-	-	-	-	-	Undrained Triaxial Compression
18	Montreal Silty Clay	0.0230	-	-	0.0246	-	Undrained Triaxial Compression
19	Younger Bay Mud	-	-	-	-	-	Undrained Triaxial Compression
20	Kaolinite Clay	-	-	-	-	-	Undrained Triaxial Compression
21	Champlain Fissured Clay	-	-	-	-	-	Undrained Triaxial Compression
22	Brno Clay	-	-	-	-	-	Undrained Triaxial Compression
23	Speswhite Kaolin	0.0350	-	-	0.0368	-	Undrained Triaxial Compression
24	Matsue Mudstone	0.0125	-	-	0.0133	-	Undrained Triaxial Compression
25	Roccella Clay 2	-	-	-	-	-	Drained Triaxial Compression
26	Shinano Clay	0.0007	0.0025	-	-	-	Drained Triaxial Compression
27	Niiho Clay	0.0007	0.0018	-	-	-	Drained Triaxial Compression
28	London Clay 1	-	-	-	-	-	Drained Triaxial Compression
29	Pudong Clay	0.0021	0.0030	-	-	-	Drained Triaxial Compression
30	Pujiang Clay	0.0021	0.0030	-	-	-	Drained Triaxial Compression

Table 7.4. (Cont'd)

31	Suzhou Clay	0.0021	0.0035	-	-	-	Drained Triaxial Compression
32	Bringelly Shale	0.0030	-	0.0177	-	-	Drained Triaxial Compression
33	NSF Clay	-	-	-	-	-	Drained Triaxial Compression
34	0.01 N Calcium Montmorillonite	0.00004-0.004	0.0002	-	-	-	Drained Triaxial Compression
35	Tertiary Mudstone	-	-	-	-	-	Undrained Triaxial Compression
36	Beaumont Clay	0.0007	-	-		0.0046	Undrained Triaxial Compression
37	Paris Clay	-	-	-	-	-	Undrained Triaxial Compression
38	Beaumont Clay	-	-	-	-	-	Undrained Triaxial Compression
39	Colorado Clay	0.0091	-	-	0.0103	-	Undrained Triaxial Compression
40	NOVA Clay	0.0052	-	-	0.0089	-	Undrained Triaxial Compression
41	Vicksburg Buckshot Clay	0.0016	-	-	0.0069	-	Undrained Triaxial Compression
42	Alabama 1	0.0130	-	-	0.0152	-	Undrained Triaxial Compression
43	Oak Harber	0.0052	-	-	0.0080	-	Undrained Triaxial Compression
44	Boom Clay	-	-	-	-	-	Undrained Triaxial Compression
45	Kaoline	-	-	-	-	-	Undrained Triaxial Compression

Table 7.4. (Cont'd)

46	IIT Lake Clay	-	-	-	-	-	Undrained Triaxial Compression
47	Cucaracha Shale	0.0119	-	-	0.0127	-	Undrained Triaxial Compression
48	Sienitic Residual Soil	-	-	-	-	-	Undrained Triaxial Compression
49	Mercia Mudstone	-	-	-	-	-	Undrained Triaxial Compression
50	Illite	0.0254	-	-	0.0304	-	Undrained Triaxial Compression
51	Kaolin	0.0254	-	-	0.0271	-	Undrained Triaxial Compression
52	Kaolin	0.0025	-	-	0.0143	-	Undrained Triaxial Compression
53	Hongqiao Clay	0.0314	-	-	0.0345	-	Undrained Triaxial Compression
54	Pujiang Clay	0.0314	-	-	0.0345	-	Undrained Triaxial Compression
55	Suzhou Clay	0.0314	-	-	0.0345	-	Undrained Triaxial Compression
56	NSF Clay	-	-	-	-	-	Undrained Triaxial Compression
57	Saint-Jean-Vianney clay	0.0061	-	-	0.0500	-	Undrained Triaxial Compression
58	M44 Clay	0.0100	-	-	0.0143	-	Undrained Triaxial Compression
59	Blue London Clay 2	0.0063	-	-	0.0084	-	Undrained Triaxial Compression
60	Speswhite Kaolin	0.0350	-	-	0.0368	-	Undrained Triaxial Compression

Table 7.4. (Cont'd)

61	Bringelly Shale	0.1000	-	-	-	0.1203	Undrained Triaxial Compression
62	Macau Marine Clay	-	-	-	-	-	Undrained Triaxial Compression
63	Kaolin Clay	-	-	-	-	-	Undrained Triaxial Compression
64	0.01 N Calcium Montmorillonite	0.0004-0.04	-	-	0.0005	-	Undrained Triaxial Compression
65	Oxford Clay	-	-	-	-	-	Undrained Triaxial Compression
66	Kimmeridge Clay	-	-	-	-	-	Undrained Triaxial Compression
67	Gault Clay	-	-	-	-	-	Undrained Triaxial Compression
68	London Clay 2	-	-	-	-	-	Undrained Triaxial Compression

FIGURES

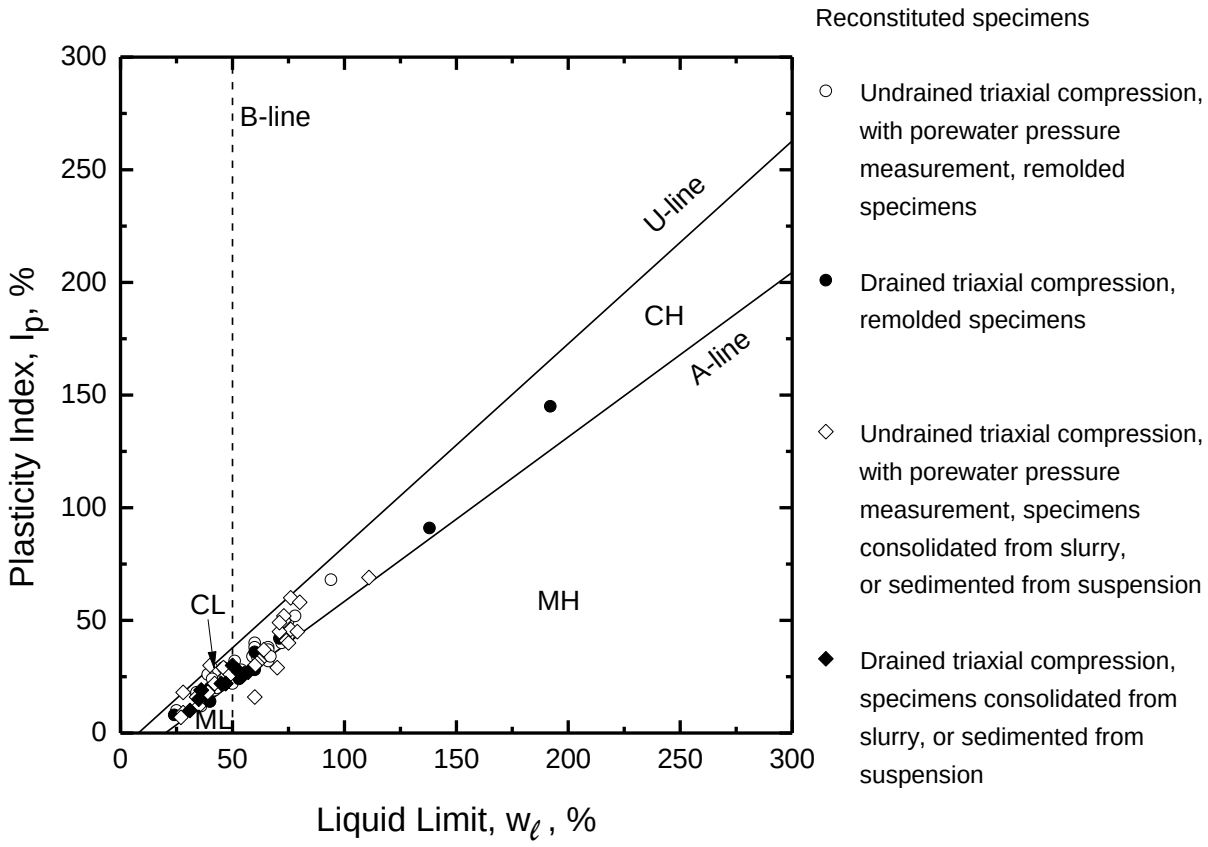

Figure 7.1. The Casagrande chart of 55 materials used to prepare reconstituted specimens in the laboratory triaxial compression tests reported in the literature

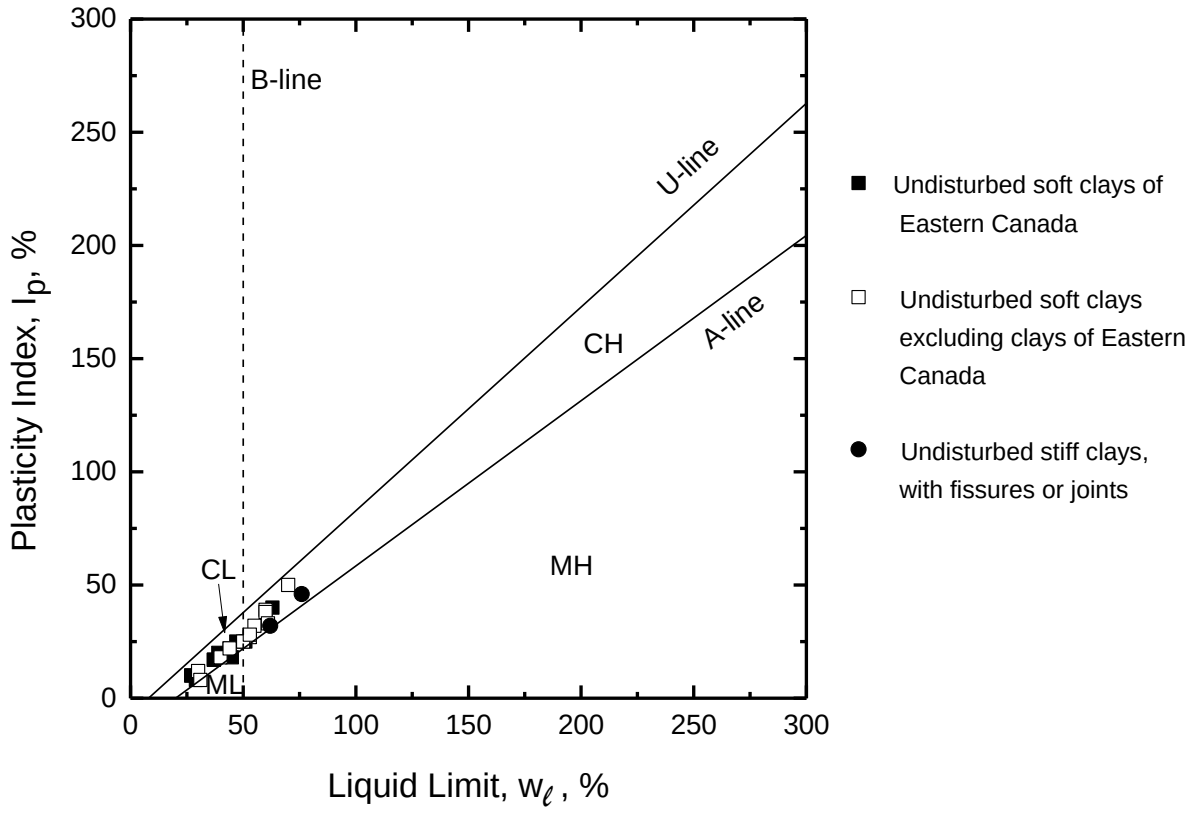

Figure 7.2. Casagrande chart of 11 soft clays of Eastern Canada, 5 soft clays from Norway, Finland and China, and Blue London Clays with fissures or joints

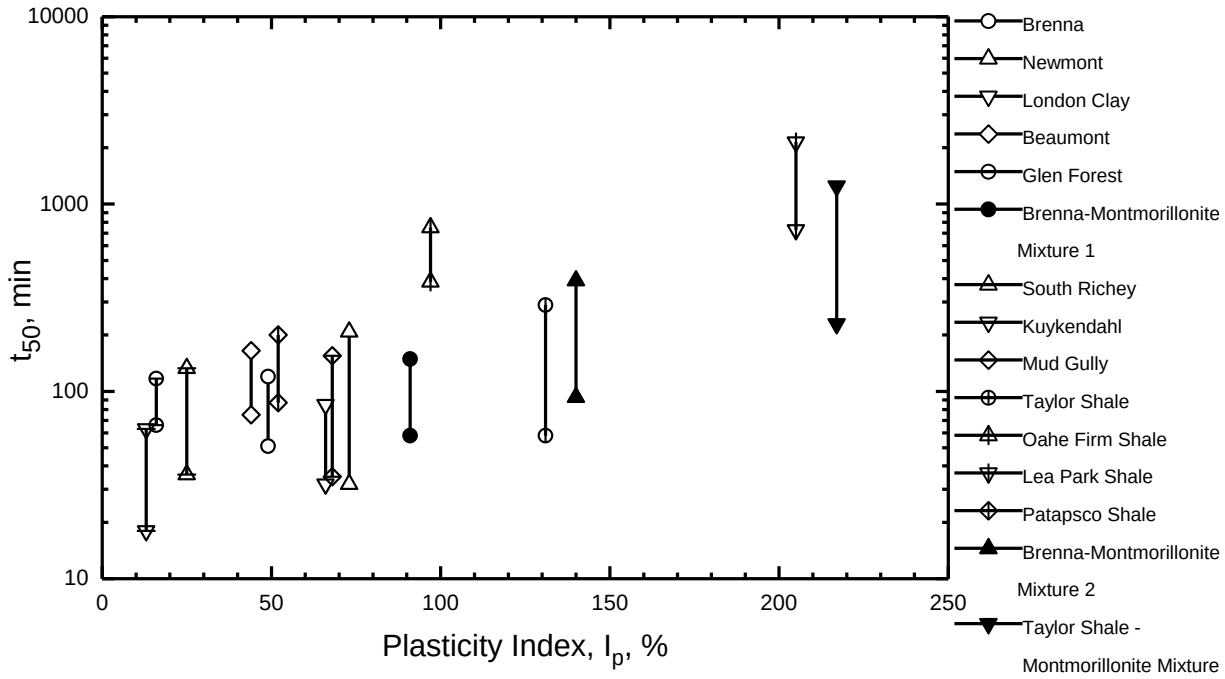

Figure 7.3. Range of t_{50} in the last load increment, of remolded specimens prepared from 15 stiff clay and clay shale compositions, prior to shear, consolidated under equal all around pressure in the range of 4.5 psi (30 kPa) to 115 psi (790 kPa)

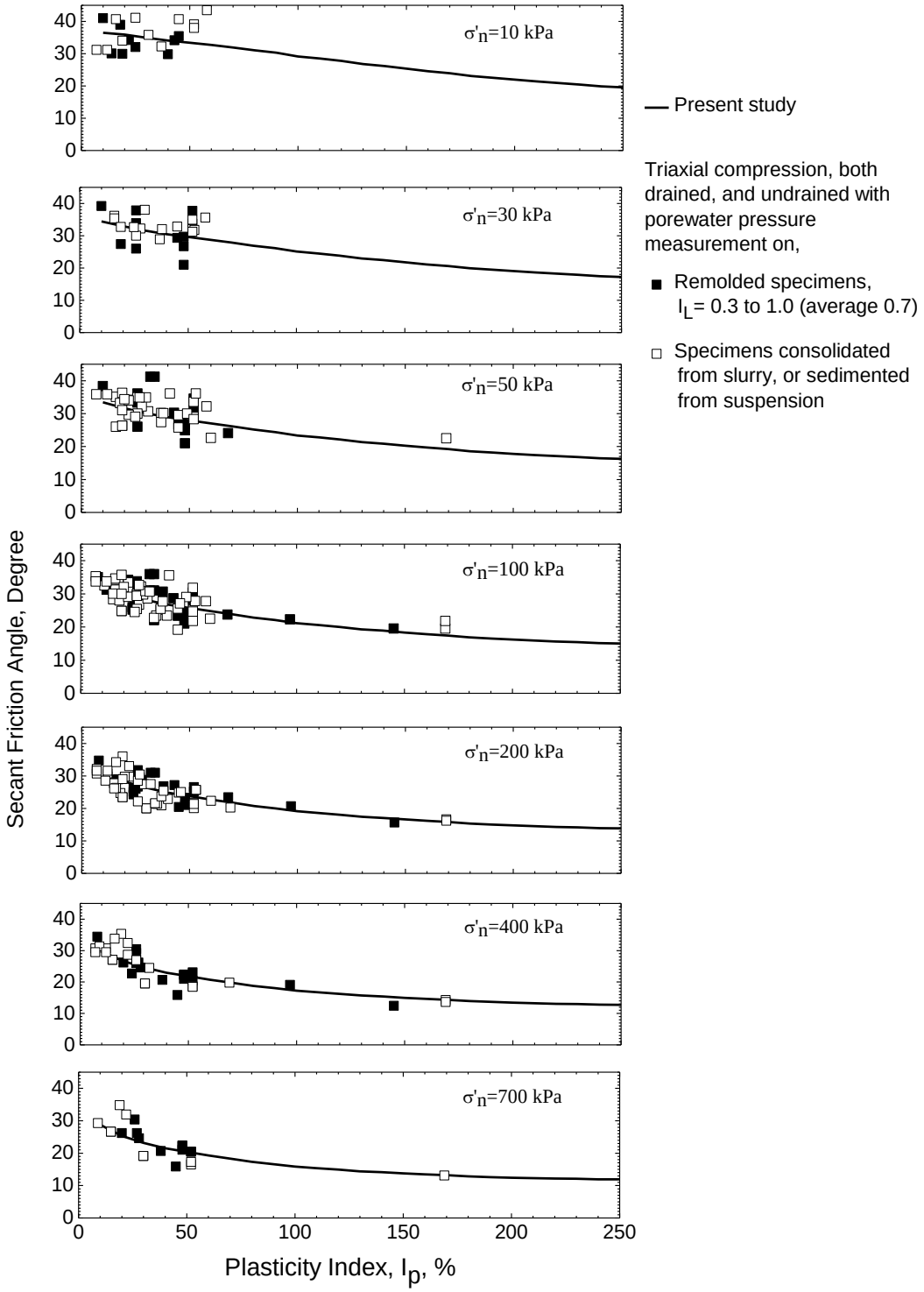

Figure 7.4. Secant fully softened friction angles interpreted from triaxial compression tests reported in literature, both drained, and undrained with porewater pressure measurement, on reconstituted, normally consolidated specimens prepared by two procedures

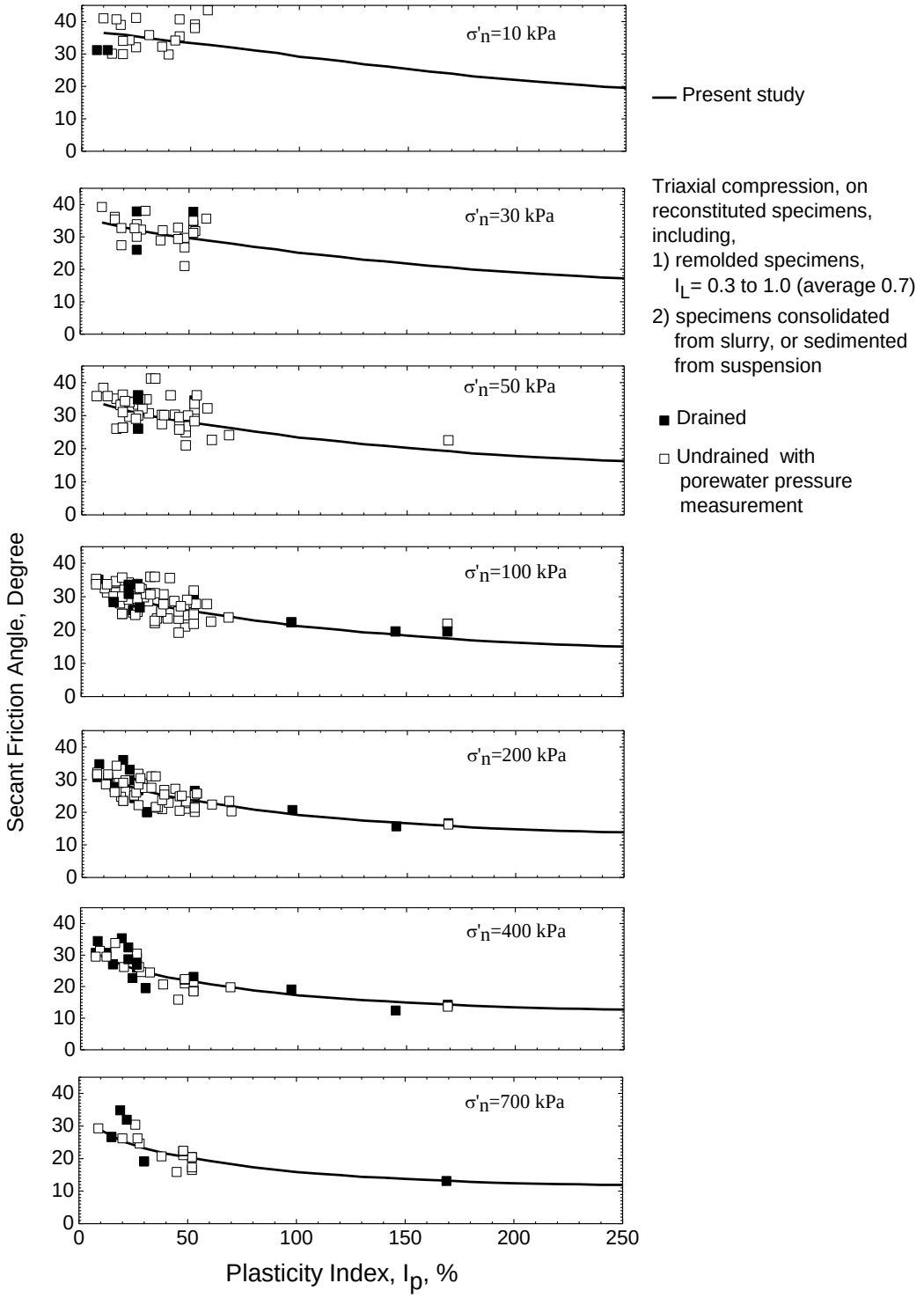

Figure 7.5. Secant fully softened friction angles interpreted from triaxial compression tests reported in literature, on reconstituted, normally consolidated specimens, subjected to drained, and undrained shear with porewater pressure measurement, respectively

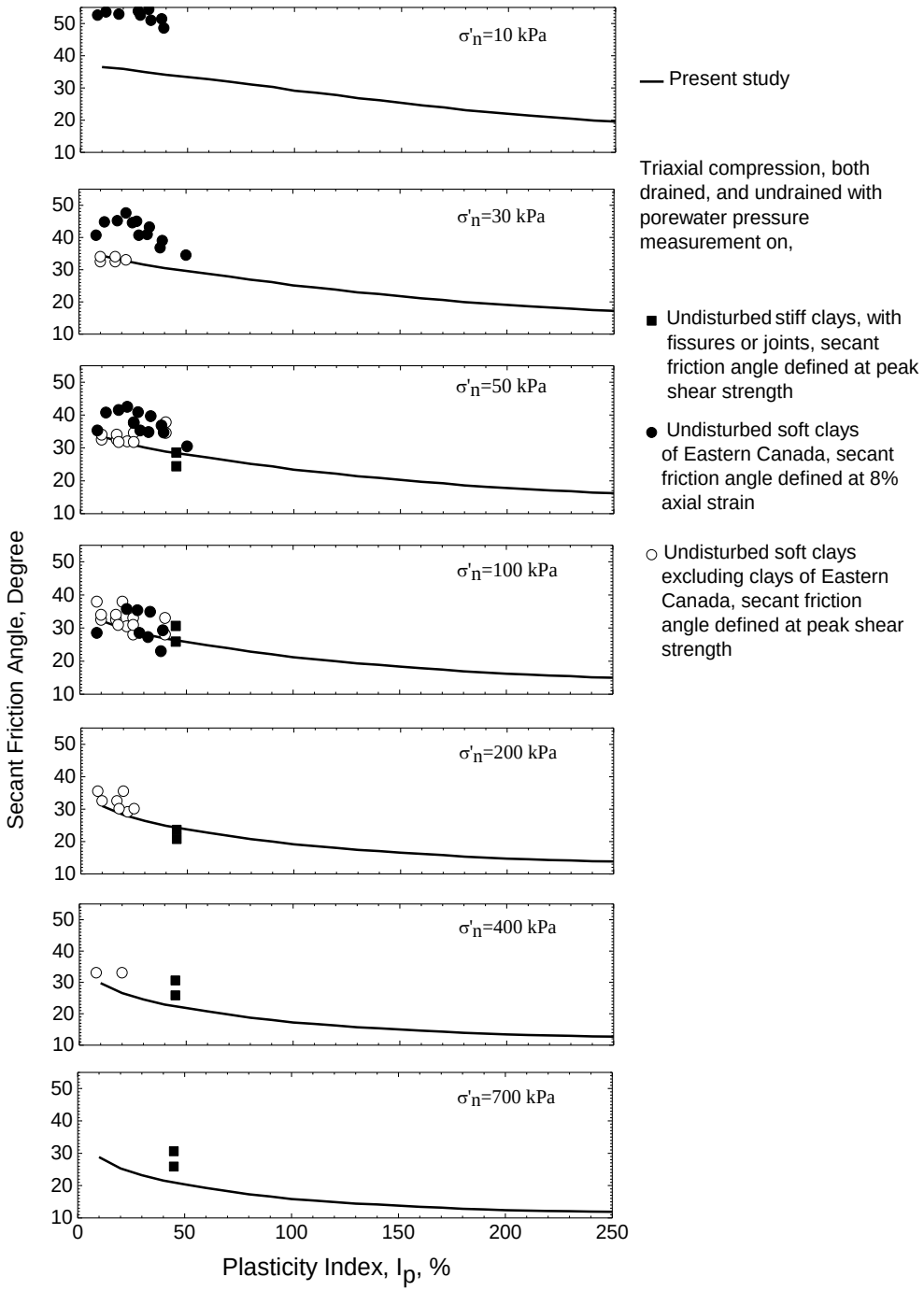

Figure 7.6. Secant friction angles defined at 8% axial deformation or at peak shear strength, from triaxial compression tests reported in literature, both drained, and undrained with porewater pressure measurement, on undisturbed soft clays of Eastern Canada, undisturbed soft clays excluding clays of Eastern Canada, and undisturbed stiff clays with fissures or joints

CHAPTER 8: FULLY SOFTENED SHEAR STRENGTH BACK-CALCULATED FROM FIRST-TIME SLOPE FAILURES

The shear strength measured in laboratory tests may or may not represent the mobilized shear strength on a full-scale slip surface in the field. The best estimate of shear strength mobilized in a full scale situation is obtained by back-analysis of slope failures. In this chapter, fully softened shear strength, expressed in terms of secant friction angles, back-calculated from first-time slope failures in stiff clays, clay shales, mudstone, soft to firm clays excluding soft clays of Eastern Canada, clayey silts, and loess, are compared in terms of plasticity index and effective normal stress with those from the empirical correlation in the present study, developed based on consolidated triaxial compression tests on normally consolidated, remolded specimens prepared from stiff clay and clay shale compositions. The back-analyses utilized the observed slip surface or possible slip surface determined based on adequate field observations, together with the observed or assumed groundwater conditions reported by the original references. An examination is also included, in relation to the mobilized shear strength of first-time slides in soft clays of Eastern Canada.

8.1. Back-analysis procedure

The 63 first-time failures of natural or cut slopes in 38 geologic materials, are summarized in Tables 8.1 and 8.2, in terms of plasticity index, clay size fraction, porewater pressure ratio ($\bar{r}_u = \frac{\gamma_w h}{\gamma z}$, where γ_w is the unit weight of water, γ the unit weight of clay, h piezometric height, z height of the slice), description of the basal part of slip surface, slope height, slope age, and ratio of slip surface segment assumed at fully softened shear strength condition to total slip surface length. For slope failures in Table 8.1, a basal portion of the slip surface at residual shear strength condition was assumed; for the slides in Table 8.2, the mobilized shear strength on the entire slip surface was close to fully softened shear strength. The two types of first-time slides are reviewed in detail in this chapter. Among the 63 first-time slope failures, 45 slides were in fissured stiff clays, clay shales, and mudstone, 6 were in stiff clay and clay shales with significant amount of calcium carbonate, the remaining 12 materials were in 1) glacial clay (boulder clay), 2) soft to firm clays (excluding soft clays of Eastern Canada), and 3) clayey silts, or loess.

The plasticity index of the geologic materials in Table 8.1, including fissured stiff clays, clay shales, and mudstone, ranges from 12% (slope failure in loam and blue clay at Wettern, Brussels, reported by Marivoet 1948) to 100% (slope failure in firm to stiff clay at Pendakomo, Cyprus, reported by Gostelow and Loucaides 1988). The plasticity index of the geologic materials in Table 8.2, including 1) soft to firm clays of low to medium plasticity excluding soft clays of Eastern Canada, 2) stiff clays or clay shales with significant amount of calcium carbonate content 3) clayey silt including loess, or 4) glacial clay, is in the range between 3% (slope failure in soft clay at Trondheim, Norway, reported by Janbu et al 1977) and 40% (slope failure in clayey marls at Aghios Konstantinos, Greece, reported by Alexandris et al 2011).

A reliable slope stability analysis requires three accurately reported information: slip surface geometry, ground water condition, and shear strength. The assumption of a factor of safety of unity for a slope failure, together with the other two reported components, makes it possible to back-calculate the shear strength mobilized on the actual slip surface. For this reason, only the observed slip surface or the possible slip surface determined based on adequate field observations, have been used in the present reanalyses. The ground water condition was available for most case histories; however, for the cases without the observed porewater pressures, the ground water conditions assumed in the original references were used. The groundwater condition in terms of porewater pressure ratio, $\bar{r}_u$, computed from the average value of porewater pressure along the slip surface is summarized in Tables 8.1 and 8.2. Back-analyses were carried out in terms of effective stress at failure using the Morgenstern and Price's method (1965) coded in the computer program GEO-SLOPE 7.23, together with non-linear relationship between shear strength and effective normal stress. The possible constraint from three dimensional effect was not considered in this research as it is not considered to be significant.

8.1.1. Assumption of shear strength condition

The existence of a slip surface segment at residual condition was determined based on the corresponding details of slip surface reported in the original reference. For the 45 first-time slope failures in fissured stiff clays, clay shales, and mudstone, listed in Table 8.1, either reported with a pre-existing discontinuity, or with a distinct horizontal or sub-horizontal slip surface segment, the residual condition (details explained in sub-section 8.1.2) was applied to pre-existing

discontinuity or to the horizontal or sub-horizontal basal portion of the slip surface. Then the back-calculation, assuming a factor of safety of unity, was carried out to determine mobilized shear strength on the back-scarp of the slip surface.

For the 18 first-time slope failures in geologic materials listed in Table 8.2, without a reported horizontal or sub-horizontal segment of observed slip surface, no segment was assumed to be at residual condition. The mobilized shear strength on the entire slip surface, was back-calculated assuming a factor of safety of unity.

8.1.2. Relationship between shear strength and effective normal stress

In the present study using the computer program GEO-SLOPE 7.23, a non-linear shear strength-effective normal stress relationship was selected as the shear strength input.

In the selection of the shear strength input, for slope failures with a segment of slip surface at residual shear strength condition, the empirical residual shear strength from Mesri and Shahien (2003) was assigned to the residual segment. The equation reformulated from Eq.5.6

$$\tan\left[\phi'_r\right]_s^{\sigma'_n} = \tan\left[\phi'_r\right]_s^{100}\left[\frac{100}{\sigma'_n}\right]^{1-m_r} \quad (8.1)$$

, together with $\left[\phi'_r\right]_s^{100}$ from Fig.5.1, and m_r versus I_p from Fig.8.1, were used to compute $\left[\phi'_r\right]_s^{\sigma'_n}$. Therefore, it is possible to determine the secant residual friction angles at any plasticity index as a function of effective normal stress on the slip surface.

For the back-scarp of first-time slope failures with a segment of slip surface at residual shear strength condition, and for the entire slip surface of first-time slides without a distinct horizontal or sub-horizontal basal part, the empirical fully softened shear strength from Mesri and Shahien (2003) served as an initial input [for the first trial the relationship between shear strength and effective normal stress, according to the plasticity index of the slope material, Eq.5.5, together with $\tan\left[\phi'_{fs}\right]_s^{100}$ and m_{fs} values from Mesri and Shahien (2003) was used]. The first combination of $\tan\left[\phi'_{fs}\right]_s^{100}$ and m_{fs}, may or may not give a factor of safety of 1, and then further adjustments were made until a factor of safety of unity was obtained.

8.2. First-time slope failures with a segment of slip surface at residual condition

In fissured stiff clays and clay shales, either the residual condition already exists along bedding planes, laminations, or other stratigraphic or structural discontinuities before a cut is made, or it develops as a result of progressive deformation along horizontal or subhorizontal portion of the slip surface. In the latter case, relatively small displacements are sufficient to take the clay to residual condition when shearing strain is localized near the toe or in thin weak bands, and the clay particle orientation is substantially parallel to the direction of shearing (Mesri and Shahien 2003).

In identifying a residual segment of the global slip surface in a first-time slope failure, the first step is to verify the existence of pre-existing discontinuities. The discontinuities include 1) stratigraphic discontinuities such as bedding planes, laminations, weak seams, and contact between soft and stiff layers, and 2) shear planes produced by old landslides buried beneath younger sediments, tectonic folding, glacial shearing, periglacial solifluction, valley rebound, or downslope creep of weathered colluvium on parent stiff clay or clay shales (Skempton and Petley 1967, Clarke et al 1970, Wilson 1970, Morgenstern 1977, Mesri and Shahien 2003). In the present study, segments of pre-existing discontinuities were reported in 13 slope failures, with 6 examples shown in Fig.8.2. Dixon and Bromhead (1991) suggested that the base of slip surface in first-time slides at Isle of Sheppey, England, followed the bedding plane of London Clay. Part of the failure was also found to be along the bedding plane in the cut at Grove Park, UK (James 1970). Part of the slip surfaces of first-time slope failures, were reported to be on the pre-existing shear planes of ancient landslides, at Devon, Canada (Eigenbrod and Morgenstern 1971), and at Grassano, Italy (Di Maio and Vassallo 2011). The basal parts of slip surfaces were on the contact between soft and stiff layers, of first-time slope failures in Brown London Clay at Northolt, Crews Hill, Whitstable, and New Cross (James 1970, Chandler and Skempton 1974, Skempton 1977); and in stiff clay at Wettern, Brussels (Marivoet 1948), stiff clay at Santa Barbara, Italy (Esu et al 1984), mudstone at Atistu, Japan (Nakamori et al 1996), and stiff clay at North to Central National Highway, Greece (Anagnostopoulos and Georgiadis 2004).

If bedding planes, laminations, or other stratigraphic or structural discontinuities are not reported in the slope failure in stiff clay and clay shales, the second step is to examine the geometry of the slip surface. For the slip surface in stiff clays and clay shales with a translational shape (Fig.8.3),

which consists of a curved back-scarp and a horizontal, or sub-horizontal basal portion, it is reasonable to assume that a residual condition was reached on the basal segment, due to the progressive nature of failure. Large stress concentration tends to start at the toe of a slope and propagate toward the top, thus reducing the shear strength on the basal more or less horizontal part of a slip surface to a lower value of shearing resistance. The propagation of straining was observed in the simulation of cut slopes in stiff fissured London clay, with swelling and strain softening, using the Imperical College Finite Element Program by Potts et al. (1991), where the shear strength near the toe dropped rapidly from peak to residual as the rupture zone developed. The progressive development of the failure was monitored by the displacement measurement in a cut slope, together with an observed slikensided base in Gault Clay, at Selborne, UK (Cooper et al. (1998). For this reason, in the present study, for the 33 first-time slope failures in stiff clays and clay shales with translational slip surfaces, where pre-existing discontinuities were not observed, at the time of failure residual condition was assumed to be on the horizontal or sub-horizontal base of the slip surface.

Two examples of first-time slope failures with segment of slip surface at residual condition, are described in detail in the following sub-sections. The details of the remaining 43 slope failures are available in Appendix A.

8.2.1. Slope failure at Santa Barbara, Italy

In the process of excavation of a 150m high cut, as part of the exploitation of the S. Barbara open-pit mine in the Arno Valley near Florence, Italy, a large slide took placed at 10pm on August 12th, 1983. Two rainstorms were reported a few days before the failure, while rainfall rates were below monthly averages during the three months before sliding. Between 1980 and 1983, the slope was gradually steepened from less than 10° to about 18°, with toe fixed due to the existence of nearby road and canal. The slide was a first-time failure as suggested by Esu et al (1984), because previous ground movements were not reported. The cross-section of the slope at the time of failure is reconstructed in Fig.8.4, in which the slide mass was about 510m long, with maximum depth of, approximately, 80m.

The excavation is in the Upper Valdarno Formation (Fig.8.4), which is a Pliocene lacustrine deposit, overlying the Tertiary sandstones interlayered with hard shales. The lacustrine deposits consist of Santa Barbara Clay, main coal seam, and basal sands, in a downward section. Santa Barbara Clay is an overconsolidated, jointed, fissured clay, layered with thin sand partings (Esu et al 1984), in the slide area, with natural water content of 43%, liquid limit of 80%, plasticity index of 35%, and clay size fraction of 30%. The observed slip surface cuts through Santa Barbara Clay, and passes through the contact between the clay and coal seam. Assuming steady state flow, Esu et al (1984), with the consideration of the high permeability of the in-situ clay, due to the sand partings and opening discontinuities, reported the ground water condition in Fig.8.4.

Because of the existence of a basal part of slip surface at the contact between the fissured clay and coal seam, residual condition was assumed for this segment, with residual shear strength at I_p = 35%, interpolated and extrapolated from Mesri and Shahien (2003). The input residual shear strength on each slice is presented as hollow squares, and the curved relationship between residual shear strength and effective normal stress of the slope material, defined by its plasticity index, is presented by a dash line. The residual shear strength (solid squares) from direct shear tests by Esu et al (1984) is slightly smaller the empirical residual shear strength determined from Mesri and Shahien (2003). The back-calculated shear strength on the back-scarp, hollow circles, is slightly lower than that from the empirical correlation in the present study (solid line), and is close to the lower bound of intact shear strength (solid circles) measured in direct shear tests and consolidated drained triaxial compression tests (Esu et al 1984). The same symbols are used for the back-analysis of all slope failures interpreted in the present study.

8.2.2. Slope failure at Selborne, UK

The failure of a 9m deep cut slope in Gault Clay described by Cooper et al. (1998), which was induced by controlled pore water pressure recharge, is an excellent example of progressive failure. This field experiment, intended to model a deep-seated failure in a slope experiencing natural pore water pressure recovery, was in the clay pit of Selborne Brick and Tile Company's Honey Lane works at Selborne, Hampshire, UK. The pore water pressure recharging commenced from January 1st, 1989 (referred as Day 0), following the slope excavation and instrument installation between August 1987 and August 1988. The engineered failure (Cooper et al 1998) indicated by the

recorded inclinometer displacements, took place in July 4th, 1989, and the final collapse occurred in mid-July.

The test site was heavily instrumented, with 62 piezometers, 12 inclinometer access tubes, 2 in place inclinometer strings and 10 surface wire extensometers. The study section of the slope was isolated at its sides by means of low friction panels to produce plane strain deformation. Feasibility study by piezometers suggested hydrostatic condition in the site before slope cutting. The feasibility study borings before the construction of the test site, and a later sampling at the early stage of the project revealed that the slope (Fig.8.5) consists of a top layer of soliflucted clay, weathered Gault Clay (upper and lower), unweathered Gault Clay, and a very thin layer of Lower Green Sand. The weathered Gault Clay is grey-brown, with iron staining, fine gypsum crystal, and some fossil fragments, while the unweathered stiff Gault Clay has a dark grey color, and is free of iron staining. Index properties such as Atterberg limits, are quite uniform throughout the clay deposit including the top soliflucted clay, with liquid limit ranging from 60% to 75%, and an average plastic limit of 22%, which, together give the plasticity index in the range of 40% and 50%. The clay size fraction varies between 38 and 48%.

The geometry and location of the slip surface was determined based on 2 post-mortem trenches excavated at the side panels immediately following the final collapse. The slip surface has a typical translational shape, including a horizontal base and curved back-scarp. Post-failure field investigation revealed that the basal portion of the slip, possibly at the interface between the weathered and unweathered Gault Clay, formed as a single, thin, highly polished, strongly striated slickenside, while the upper part of the slip across the bedding displayed a 20mm zone of shearing with much rougher surface. The displacement measurements after the pore pressure recharge, indicate a progressive development of the failure - immediate significant displacement near the toe, movement further into the slope in a similar pattern, and a very small amount of deflection only observed in the center and back of the slope. Appreciable displacement was finally recorded in the central part of the slope at the time of collapse. An average $\bar{r}_u$ of 0.17 was reported on Day 184, i.e., the day of engineered failure.

This failure was analyzed in detail by Mesri and Shahien (2003) assuming residual shear strength on the basal slip surface. In the present study, with the reported value of $\bar{r}_u$, and the observed slip surface, a back-analysis was made assigning residual strength (open squares) to the basal segment, interpreted from Mesri and Shahien (2003) corresponding to the plasticity index of Gault Clay. Reversal direct shear tests on precut specimens, ring shear tests and direct shear tests on slip surfaces recovered during post-failure excavation, were performed by Cooper et al (1988) to determine the residual shear strength. The measured residual strength data (solid squares) are within the empirical residual strength range from Mesri and Shahien (2003) for Ip between 40% and 50%. It is worth mentioning that in the slope failure analysis by Cooper et al (1998), the laboratory measured residual shear strength was used near the toe due to the appreciable shearing on the basal part of the slip surface.

This assumption of residual shear strength based on the highly polished nature of the base, yields the mobilized shear strength (open circles) on the back-scarp close to the lower bound of the fully softened shear strength from the empirical correlation in the present study of a clay with plasticity index of 40% to 50%. Drained and undrained triaxial compression tests and direct shear tests on undisturbed specimens provide the shear strength range of the undisturbed soliflucted clay and weathered Gault Clay. The fully softened shear strength of soliflucted clay and Gault Clay in triaxial compression tests was measured by Copper et al (1988) on samples reconstituted at a water content of approximately 1.5 times of the plastic limit. It can be seen from Fig.8.5 that the mobilized shear strength on the back-scarp lies at the lower bound of the intact strength range, and is slightly higher than the measured fully softened strength.

8.3. First-time slope failures with mobilized shear strength close to fully softened shear strength on the entire slip surface

It is generally accepted that in unstratified clays with plasticity index smaller than 20% (Chandler 1984a, Mesri and Abdel-Ghaffar 1993), or clay content less than 20% (Skempton 1985), the mobilized shear strength in first-time slope failures is equal or greater than the fully softened shear strength. Mesri and Shahien (2003) concluded that slopes where the mobilized shear strength is equal or greater than the fully softened shear strength, are generally either stiff clays of low plasticity such as glacial clays, or soft to firm clays of low to medium plasticity (Kenny 1967). Out

of the 18 geologic materials in Table 8.2, these generalizations apply to 12 of the materials involved in the first-time slope failures in the present study. The remaining 6 geologic materials (slopes 1 to 6 in Table 8.2), turn out to be stiff clays, clay shales, or marls, of low to high plasticity, however, which include significant amount of carbonate (calcareous clay) or quartz lenses.

Examples of cross-sections of first-time slope failures with mobilized shear strength close to fully softened on the entire slip surface, are shown in Fig.8.6. Compared to first-time slides with a segment of slip surface at residual shear strength condition, the slip surfaces in Fig.8.6, can be best described as rotational, without a distinct horizontal or sub-horizontal basal segment.

These first-time slides can be further divided into two categories based on different mechanisms leading to mobilized shear strength on the entire slip surface, similar to fully softened shear strength. The first category (slides 3, 5, and 7 in Fig.8.6) are slopes in glacial clays (boulder clays), or stiff clays or clay shales with significant calcium carbonate or quartz content. The inclusion of boulders, lenses of quartz, or calcium carbonate, contributes to the mobilized shear strength of the clay matrix, on entire slip surface, higher than the residual shear strength of a stiff clay and clay shale composition with similar I_p. The second category is geological materials, including soft to firm clays (excluding soft clays of Eastern Canada), clayey silts, and loess (slides 10, 16, and 17 in Fig.8.6), for which, the mobilized shear strength, close to the peak shear strength of undisturbed specimens in the triaxial compression (Kenney 1967, Kenny and Drury 1973), turns out to be similar to the fully softened shear strength of a stiff clay or clay shale composition with similar I_p.

In summary, for slope failures in unstratified geologic materials including 1) soft to firm clays of low to medium plasticity excluding soft clays of Eastern Canada, 2) stiff clays or clay shales with significant amount of calcium carbonate and quartz content, 3) clayey silts including loess, or 4) glacial clays, the mobilized shear strength on the entire slip surface, is expected to be greater than the residual strength of a stiff clay or clay shale composition, with similar I_p. The following sub-sections include two examples of first-time slope failures, with mobilized shear strength close to fully softened on the entire slip surface. The details of the remaining 16 slope failures are described in Appendix B.

8.3.1. Slope failure in clay shale with quartz and schistose lenses, at Voltaggio, Italy

A landside took place in November 1980 near the small town of Voltaggio, Italy, after a long rainy season. This site situates on the left-hand flank of River Lemme valley, and is part of the so-called "Sestri-Voltaggio zone", which is a great discontinuity line. The landslide area has a slope inclination of 7° to 15° uphill, and 30° to 35° near the toe (Fig.8.7). Significant toe erosion by the river meander was observed before the slip, and was regarded as one of the reasons for slope failure (Cancelli and Olcese 1984). The other two causes are, high ground water pressures, after the long rainy season, and softening of the clay shale, according to Cancelli and Olcese (1984). The first movement was a typical 65m long block slide along the toe to point B, including a formation of graben between A and B (Fig.8.7). Subsequent cracks enlarged the slide length to 70m.

The geotechnical investigations made in 3 borings after the slope failure revealed that the upper part of the slope, 0 to 10 m deep, consists of colluvial soils, formed by grey-brown, soft to firm silt with clay, which belongs to the Jurassic Torbi Formation. The underlying Lower Cretaceous Argille a Palombini del Passo della Bocchetta Formation, consists of black to dark grey, clay shales, including frequent, white lenses of quartz, schistose, folded, jointed and sheared by tectonic stresses. The liquid limits are 34% and 29%, and plastic limits are, 22% and 19%, respectively, for colluvial soils and clay shales, which give similar plasticity indices, 12% and 10% for the two soils. The inclinometer readings in the three boreholes showed that the slip surface was deeply penetrating into the shales, with maximum thickness of sliding mass of 14m. The piezometric levels were determined at the end of drilling operations, together with the observation of a spring in the lower part of the slope, pre-existing to the landslide.

The average $\bar{r}_u$ was 0.40 on this rotational slip surface, and the maximum effective normal stresses were about 180 kPa. The back-calculated shear strength for the entire slip surfaces agrees with that from the empirical correlation for fully softened shear strength in the present study, defined by Ip in the range of 10-12%. This result is consistent with the speculation by Cancelli and Olcese (1984) that the shear strength did not decrease to the residual values because the total displacement along the slip surface was restricted to a few decimeters.

8.3.2. Slope failure in soft clay, at Selnes, Norway

The initial slide of a retrogressive failure in quick clay at Selnes was examined here. Selnes is in the valley of the Namsen River, about 150 km north of Trondheim, Norway. Streams had eroded the valley significantly before a small landslide occurred in 1959, after which the banks were prone to surficial slides originating from stream erosion. At 3pm on April 18th, 1965, Selnes slide began, and some 200m long retrogression, completely destroyed the Selnes farm and killed many farm animals. Signs of instabilities prior to the failure and the development of sliding were observed by the locals.

The slide was in the soft quick clay of post-glacial marine origin, which has a natural water content of 34%, liquid limit between 22% and 35% (unweathered and weathered, respectively), plasticity index between 5% and 8%, and clay size fraction of 40%. Based on the contact between undisturbed clays and slide mass determined by soundings and vane borings, and the observed crack on the top of the slope, several rotational slip surfaces were assumed by Kenney (1967). In this research, the most possible slip surface for the initial side that started the retrogressive landsliding, according to the back-analysis by Kenney (1967), was selected and is shown in Fig.8.8, which is approximately 21m long and 10m deep. The ground water condition with overpressures at the toe of slope in Fig.8.8 corresponds to the more reasonable ground water condition suggested by Kenney (1967) based on 1) ground water level on the terrace being close to the ground surface, and 2) slope being wet all the time.

The back-calculated shear strength on the entire slip surface, at Ip = 8%, is comparable with that from the empirical correlation in the present study, and similar to the peak shear strength (solid circles) measured on the undisturbed weathered and unweathered quick clay in consolidated drained triaxial compression tests by Kenney (1967).

8.4. Summary of back-analyses

Figure 8.9 shows the back-calculated secant friction angles, at effective normal stress of 10, 30, 50, 100, 200, 400 and 700 kPa, over the back-scarp of observed slip surfaces for first-time slope failures with a segment of slip surface at residual condition (hollow circles), and over the entire

slip surfaces of first-time slope failures without distinct horizontal or sub-horizontal basal part of slip surface (solid circles) in soft clays, clays or marls with significant carbonate content, and clayey silts including loess. Figure 8.9 also includes input residual friction angles (hollow squares) from Mesri and Shahien (2003), on the horizontal or sub-horizontal basal portion of slip surfaces, for first-time slope failures with a segment of slip surface at residual condition. The dash lines at 50, 100, and 400 kPa were reproduced from the mean curves of residual friction angle data from Mesri and Shahien (2003), and the remaining dash lines were produced by interpolation or extrapolation, using Eq.5.6, together with $[\phi'_r]_s^{100}$ and m_r .The solid lines are empirical correlation developed in the present study for fully softened shear strength. Figure 8.10 compares the mobilized secant fully softened friction angle back-calculated in the present study with secant friction angles from the empirical correlation of fully softened shear strength at 7 effective normal stresses, developed in the present study.

The back-calculated secant friction angle data in Figures.8.9 suggest that fully softened shear strength condition have been commonly encountered in stiff clay and clay shales with plasticity index equal or smaller than 100% and at effective normal stresses less than about 200 kPa. The limited data at effective normal stress of 400 and 700 kPa, correspond to first-time slope failures (Appendix A) with a segment of slip surface at residual condition, in stiff Santa Barbara Clay, at Santa Barbara, Italy (Esu et al 1984), and in Brown London Clay, at Isle of Sheppey, England (Dixon and Bromhead 1991), and first-time slope failure (Appendix B) without a distinct horizontal or sub-horizontal basal part of slip surface, in Argille Scagliose Clay Shale, at Allori Coal Field, Italy (D'Elia et al 1988). The back-calculated mobilized secant friction angles are examined in the following sub-sections.

8.4.1. First-time slope failures with a segment of slip surface at residual condition

According to Figures.8.9 and 8.10, at all effective normal stresses, secant friction angles mobilized on the back-scarp of the overserved slip surfaces of 45 first-time slope failures, in fissured stiff clays, clay shales, and mudstone, where segment at residual condition was included, are comparable to those from the empirical correlation of fully softened shear strength developed in the present study, based on triaxial compression tests, with a typical difference of ± 2° (larger

differences explained in this sub-section). This observation justifies the assumption of residual shear strength condition on horizontal or sub-horizontal segment of slip surface and fully softened shear strength on the back-scarp on the global slip surfaces of first-time slope failures in stiff clay and clay shales. The agreement also indicates that the fully softened shear strength from the empirical correlation in the present study, developed based on the triaxial compression tests on remolded, normally consolidated specimens prepared from stiff clay and clay shale compositions, represents the mobilized shear strength on the back-scarp of full-scale slip surfaces of first-time slope failures in stiff clay and clay shales.

In Fig.8.10, the back-calculated secant friction angles in 4 cases, are approximately 5 degrees larger than those from the empirical correlation in the present study. Out of the 4 case histories, 3 were first-time slides in Oxford Clay, at Dauntsey, Hullavington, and Bincombe, UK (James 1970). On one hand, Oxford Clay is strongly laminated (Parry 1972), and its residual shear strength on the reported horizonal or sub-horizontal basal portion of the slip surface, is more likely controlled by layers with higher plasticity index. On the other hand, the mobilized shear strength on the back-scarp, cutting through various layers, is controlled by the entire slope material, which would be better characterized by a lower plasticity index, resulting from the inclusion of calcite, gypsum, and pyrites in Oxford Clay (Parry 1972).

The other case (James 1970) with larger back-calculated mobilized shear strength was a cut slope in Upper Lias Clay, at Charwelton, UK. James (1970) assumed a porewater pressure ratio, $\bar{r}_u = 0.30$, for this slope, which failed 16 years after the cut was made. Skempton (1977) studied the time-dependent equilibration of porewater pressures in cuttings in Brown London Clay, and reported the porewater pressure ratios as a function of slope age. Skempton (1977) suggested a porewater pressure ratio of 0.3 ± 0.05 for "long term stability" in Brown London Clay. Similar investigations were made for cuttings in Upper Lias Clay by Chandler (1974), and Chandler and Skempton (1974). Although a direct relationship between the porewater pressure ratio and slope age was not presented for Upper Lias Clay, according to the available information reported by Chandler (1974), and Chandler and Skempton (1974), a porewater pressure ratio of 0.30, is probably too high for a cut slope of 16 years old. A more reasonable, smaller porewater pressure

ratio, would result in a lower back-calculated shear strength mobilized on the back-scarp in this first-time slide.

In a first examination, the back-calculated secant friction angles in two cases, were approximately 5 degrees smaller than those from the empirical correlation in the present study. The slip surface of first-time slide in Upper Lias Clay (I_p = 28 – 41%), at Wellingborough, UK (Chandler 1974, Chandler and Skempton 1974), included a long basal segment at residual shear strength condition (Fig.8.11). According to Mesri and Shahien (2003), for Upper Lias Clay which is laminated, the reported values of Atterberg limit underestimated the plasticity index of Upper Lias Clay. The residual shear strength of Upper Lias Clay on the horizontal and sub-horizontal basal part of slip surface, is more likely controlled by layers with higher plasticity index, while the mobilized shear strength on the back-scarp, cutting through various layers, is controlled by the entire slope material, which can be best characterized by an average plasticity index. In the present study, by applying a residual shear strength corresponding to I_p = 50 – 60%, suggested by Mesri and Shahien (2003), to the sub-horizontal basal segment of slip surface in Wellingborough, the back-calculated secant friction angles on the back-scarp, turned out to be comparable to those from the empirical correlation in the present study, at reported values of I_p = 28% - 41%. The other case in Weald Clay at Hildenborough, UK (James 1970), was a shallow first-time slope failure with maximum depth of sliding mass less than 4m (Fig.8.12). In this case, the back-analysis was carried out assuming similar shear strength condition on the entire slip surface, because there was no distinct horizontal or sub-horizontal basal segment. Weald Clay often exhibits inclined bedding (James 1970), and it is possible that a major portion of the slip surface was on the inclined bedding plane which was at residual shear strength condition. In summary, it is possible to provide an explanation for back-calculated friction angles of 5 case histories that are within ± 5° of the proposed empirical correlation for fully softened shear strength.

8.4.2. First-time slope failures with mobilized shear strength close to fully softened shear strength on the entire slip surface

For first-time slope failures in unstratified deposits where the shear strength on the entire slip surface is assumed to be greater than the residual shear strength condition, the back-calculated secant friction angles on the entire slip surface, are in general, equal to those from the empirical

correlation in the present study, with an average difference of ± 1.5°. These rotational first-time slope failures in unstratified deposits justify the assumption of mobilized shear strength greater than the residual on the entire slip surface.

For the cut slope failure in boulder clay at Selset, UK (Skempton and Brown 1961), the back-calculated shear strength is significantly greater than that from the empirical correlation in the present study (Fig.8.13). The back-calculated mobilized shear strength of boulder clay on the entire slip surface, is close to the upper bound of the intact shear strength of boulder clay (solid circles) measured in drained triaxial compression tests (Skempton and Brown 1961). Therefore, the back-calculated secant friction angles of boulder clay are not included in Figures 8.9 and 8.10.

For 3 first-time slides in clayey marls at Athens-Thessaloniki motorway (slide 1 shown as example in Fig.8.14), Alexandris et al (2011) assumed a porewater pressure ratio, $\bar{r}_u$, in the range of 0.20 – 0.35, with the consideration of rainfall infiltration. For $\bar{r}_u = 0.20$, the back-calculated mobilized shear strength, is close to the upper bound of empirical fully softened shear strength developed in the present research, defined by Ip in the range of 25 - 40%. For $\bar{r}_u = 0.35$, the back-calculated shear strength is higher than that from the empirical correlation in the present study. The back-calculated shear strength is in the range of the shear strength (solid triangles) determined from drained direct shear tests on intact samples retrieved from the slides (Alexandris et al 2011). It's possible that the 20% to 40% calcium carbonate, which is mainly responsible for the cementation of the marls (Alexandris et al 2011), contributes to the high mobilized shear strength. It should also be noticed that, before the rainfall, the water table was 8 to 10 m below the ground surface following the slope relief (Alexandris et al 2011). It is likely that, the porewater pressure ratio was close to 0.20 by the time of failure, because the rainfall infiltration would not have an immediate significant influence in the ground water condition. For this reason, only the back-calculated secant friction angles corresponding to $\bar{r}_u = 0.20$, are included in Figures 8.9 and 8.10.

In conclusion, the mobilized shear strength on the entire slip surface of first-time slope failures in unstratified geologic materials including 1) soft to firm clays of low to medium plasticity excluding soft clays of Eastern Canada, 2) stiff clays or clay shales with significant amount of calcium carbonate or quartz content or 3) clayey silts including loess, is near the fully softened shear

strength according to the empirical correlation developed in the present study. The mobilized shear strength of (glacial) boulder clays, is greater than that from the empirical correlation for fully softened shear strength developed in the present study, and close to the intact shear strength.

8.4.3. Field application of fully softened shear strength

For the 45 first-time slides in stiff fissured clays, clay shales and mudstones, examined in this study, fully softened shear strength was mobilized on the back-scarp segment of slip surfaces, which was 28% to 85%, with an average of 58%, of the global slip surface (Table 8.1). For first-time slides in stiff fissured clays and clay shales examined here, a basal segment of slip surface at residual condition was included, either as a pre-existing stratigraphic or structural discontinuity before a cut was made, or as a result of progressive deformation along horizontal or sub-horizontal portion of the slip surface. For the 18 first-time slope failures in unstratified deposits including 1) glacial clays, 2) stiff clays or clay shales with significant amount of calcium carbonate or quartz content, 3) soft to firm clays of low to medium plasticity excluding soft clays of Eastern Canada, or 4) clayey silts or loess, a shear strength equal or greater than the fully softened shear strength was mobilized on the entire slip surface.

The empirical correlation of secant fully softened friction angles developed in the present study, based on triaxial compression tests on remolded, normally consolidated specimens prepared from stiff clays and clay shale compositions, can be applied to the stability evaluation of natural and cut slopes in stiff fissured clays and clay shales using the following procedure. First, the location of critical slip surface should be determined based on a knowledge of geology with special structural and lithological features, together with an stability analysis, using intact shear strength (Abdel-Ghaffar 1990, Mesri and Abdel-Ghaffar 1993), with the consideration of observed pre-existing discontinuities. Then to calculate the factor of safety, residual shear strength from Mesri and Shahein (2003) is applied to the horizontal or sub-horizontal basal part; and the fully softened shear strength from the empirical correlation developed in the present study, is assigned to the back-scarp of the translational critical slip surface.

The mobilized shear strength over the entire slip surface in 1) soft to firm clays of low to medium plasticity excluding soft clays of Eastern Canada, or 2) clayey silts including loess, is near the fully

softened shear strength of a stiff clay or clay shale compositions with similar I_p. Empirical correlation for secant fully softened friction angle developed in the present study, can be applied to the entire critical slip surface, the location of which is determined using the intact strength, to calculate the factor of safety. For boulder clays and stiff clays or clay shales with significant amount of carbonate or quartz content, fully softened shear strength is a conservative lower bound for the mobilized shear strength.

8.5. Ratio of length of slip surface segment assumed at fully softened condition to total slip surface length

As reviewed in Chapters 3 and 4, Skempton (1977) studied the slope failures in London Clay in terms of the constant friction angle of 20 degree, independent of effective normal stress. The constant fully softened friction angle of 20 degree for London Clay at all normal stress levels, was based on drained direct shear tests by Gibson (1953) on remolded specimens, undrained triaxial compression tests with porewater pressure measurement by Bishop et al (1965) on specimens consolidated from slurry, and drained direct shear tests by Petley (1966) using specimens consolidated from slurry (Fig.8.15) and direct shear tests on fissures and joints. A similar approach, i.e., back-calculation of constant strength parameters, on the entire slip surface, was adopted by James (1970) for first time slides in English stiff clays including London Clay, and by Chandler (1974), Chandler and Skempton (1974), and Chandler (1984a, 1984b) for first time slope failures in London Clay and Upper Lias Clay. The back-calculated strength by Chandler and Skempton (1974) are also shown in Fig.8.15.

Because of the assumption of constant shear strength parameters on the entire slip surface, it is expected that, in general, the constant friction angles back-calculated for first-time slope failures in stiff clays in UK, are smaller than those from the empirical correlation in the present study. Figure 8.16 compares the constant friction angles, ϕ', on the entire slip surfaces of 30 first-time slides in stiff clays of UK (Table 8.1), back-calculated by James (1970), Chandler (1974), Chandler and Skempton (1974), and Skempton (1977), with the secant fully softened friction angles, $[\phi'_{fs}]_s^{\sigma'_n}$, from the empirical correlation in the present study. These slopes were in stiff clays of I_p in the range of 21% - 60%, and failed at effective normal stresses equal or smaller than 200 kPa.

The secant fully softened friction angles, $[\phi'_{fs}]_s^{\sigma'_n}$, according to the plasticity indices of the stiff clays, for the effective normal stress ranges on the slip surfaces, were interpolated using Eq.5.5, together with $[\phi'_{fs}]_s^{100}$ and m_{fs} values reported in section 6.4. Therefore, in Fig.8.16, the range of friction angles based on proposed empirical correlation in each slide, is presented by a horizontal line. It can be seen from Fig.8.16 that, in general, the back-calculated constant friction angles are equal or smaller than those from the empirical correlation in the present study. Back-calculated friction angles which are close to $[\phi'_{fs}]_s^{\sigma'_n}$, correspond to slope failures with short horizontal, or sub-horizontal basal parts of slip surfaces; or in other words, large ratios of length of slip surface segment at fully softened condition to the total slip surface length. In these cases, values of $[\phi'_{fs}]_s^{\sigma'_n}$ interpolated for the maximum effective normal stresses on the slip surfaces, are sometimes, even slightly smaller than the back-calculated constant friction angles. If the residual shear strength condition is assumed on the horizontal or sub-horizontal basal part of slip surface, the back-calculated mobilized secant friction angles on the back-scarp of the slip surfaces of the 30 first-time slope failures in stiff clays of UK, as indicated in Fig.8.17, are comparable to those from the empirical correlation developed in the present study.

Figure 8.18 shows the influence of the assumed length of slip surface segment at fully softened shear strength condition, on the constant friction angle along the slip surface of first-time slides in stiff clays of UK, back-calculated by James (1970), Chandler (1974), Chandler and Skempton (1974), and Skempton (1977). The $\tan[\phi']/\tan[\phi'_{fs}]_s^{\sigma'_n}$, is reported in Fig.8.18 as a function of L_{fs}/L, a measure of length of slip surface segment at fully softened condition, to total slip surface length, where $[\phi'_{fs}]_s^{\sigma'_n}$ is from the empirical correlation in the present study, at the effective normal stress range on the slip surface of each failure, according to the plasticity index of the stiff clay. The mean relationship between $\tan[\phi']/\tan[\phi'_{fs}]_s^{\sigma'_n}$ and L_{fs}/L, with $\tan[\phi']/\tan[\phi'_{fs}]_s^{\sigma'_n}$ equal to 1.0, at L_{fs}/L of unity, for average effective normal stress on the slip surface equal or smaller than 100 kPa, is presented by a dash line at L_{fs}/L in the range of 36% to 85%. An extension of the relationship (dot line) to L_{fs}/L of 0, which implies residual shear strength mobilized on the entire slip surface, or in other words, leads to $\tan[\phi']/\tan[\phi'_{fs}]_s^{\sigma'_n} = 0.53$. For stiff clays and clay

shales with I_p in the range of 21% to 60%, and at effective normal stress in the range of 10 kPa to 100 kPa, $\tan[\phi'_r]_s^{\sigma'_n}/\tan[\phi'_{fs}]_s^{\sigma'_n}$ ranges from 0.39 to 0.67, based on empirical residual shear strength data from Mesri and Shahien (2003), and the empirical fully softened shear strength developed in the present study. According to the dash line in Fig.8.18, $\tan[\phi']$ is only 60% of $\tan[\phi'_{fs}]_s^{\sigma'_n}$, for a slip surface with 36% of total length at fully softened condition, whereas $\tan[\phi']$ is as high as 95% of $\tan[\phi'_{fs}]_s^{\sigma'_n}$, for a slip surface with 90% length at fully softened condition,

8.6. First-time slope failures in soft clays of Eastern Canada

The mobilized shear strength in first-time slope failures in structured soft to firm clays in Eastern Canada, typically with a shallow slip surface, is close to the large-strain strength from triaxial compression tests, following the structural breakdown starting at peak strength (Lefebvre and La Rochelle 1974, Lefebvre 1981, Mesri and Abdel-Ghaffar 1993), and is always higher than those from the empirical correlation of fully softened shear strength by Mesri and Shahien (2003). In the present study, 6 first-time slope failures in soft clay of Eastern Canada (Fig.8.19) were examined, by means of the same back-analysis procedure used for first-time slope failures without distinct horizontal or sub-horizontal basal segment of slip surface. The 6 slides in soft clays of Eastern Canada, with I_p in the range of 8% - 40%, are summarized in Table 8.4. Two slides are described in sub-section 8.6.1 as examples, and the other 4 are elaborated in Appendix C.

8.6.1. Example of slope failures in soft clays of Eastern Canada

Saint-Vallier Slide

The Saint-Vallier site was chosen as one of the sites to study the bonded structure of Champlain Sea Clay reported by Lefebvre and LaRochelle (1974) after the failure in May 1968. This site is 30km east of Quebec City on the South Shore of the Saint Lawrence River. An area 1.6 km south east of the village of Saint-Vallier was identified by Chagnon (1968) as one of the "unstable" areas where 17 scars of slides were observed. The initial slide scar that occurred in Saint-Vallier, in 1968, was about 15m wide and 28m long. The elevation difference between the intact surface at the rear edge of the crater and the river bed was about 12m. Although nobody witnessed the slide, it was

assumed to have taken place all at once in a retrogressive progression temporarily jamming the river with debris. Two other failures increased the length of the crater in 1969 during the investigation. The back-analysis in this research was made of the initial slide, and the cross-section of this slope together with the reported slip surface and ground water condition is given in Fig.8.20.

The field study and instrumentation of this site started in the summer of 1968. The slip surface was located using a small hand vane with rods extending up to 3m. In the early fall of 1968, nine piezometers of an "open tube" type were installed in Saint-Vallier to evaluate the groundwater pressure in this site in a 1-year observation period. An artesian pressure was observed at the toe of the slope, and the most critical recorded flow condition was used in the analysis in Fig.8.20. The soil in the slope is a fairly homogeneous gray clay with occasional stones or sand strata, and a 2m thick brownish fissured clay at the surface. The average liquid limit and plasticity index of the gray clay are 60% and 37% respectively.

The slip surface was quite shallow with an average $\bar{r}_u = 0.33$, which resulted in low effective normal stresses on the slip surface only up to 40 kPa. As can be seen from the back-analysis results in Fig.8.20, the mobilized shear strength on the slip surface is higher than that from the fully softened shear strength at I_p = 37%, from the empirical correlation in the present study.

Saint Louis Slide

The Saint Louis site was the second site studied by Lefebvre and LaRochelle (1974), where the slope failure took place in May 1968. It is located 160 km west of Quebec City on the south side of the Saint Lawrence River along the Yamaska River. The initial slide, with an 18m elevation difference between the intact surface at the rear edge of the crater and the river bed, lead to a 40m breach in the river bank and retrogressed to 70 m away from the shore. In 1969, the rear end of the crater was extended by 9-15m by a second failure.

Field investigations were carried out in Saint Louis from the summer of 1968. Eighteen open-tube piezometers were placed in the fall of 1968 to measure the ground water conditions. The artesian condition again was observed at the toe. The soil in Saint-Louis is not as homogenous as the one in Saint-Vallier. At the surface, there was a 1-2 m sandy layer, overlying the gray clay down to 17

m depth with light tone bands alternating with dark tone bands of 5 to 10 mm thickness. The average liquid limit and plasticity index of the gray clay are 50% and 25%, respectively. In the initial slide, a major portion of the slip mass was cutting through the surficial sandy layers, which minimizes the influence of the shear strength of the clay. Therefore, only the second slide was examined in the present study (Fig.8.21)

The highest effective normal stresses on the slip surface is only slightly larger than 40 kPa, resulting from the shallow depth and relatively high average $\bar{r}_u = 0.41$. The back-calculated shear strength is appreciably higher than that from the empirical correlation in the present study corresponding to I_p of 25%.

8.6.2. Mobilized shear strength in first-time slope failures in soft clays of Eastern Canada

The back-calculated mobilized secant friction angles on the entire slip surface are compared in Fig.8.22, with those from the empirical correlation in the present study. Figure 8.22 also includes the friction angle values reported in section 6.5, from triaxial compression tests on undisturbed soft clays of Eastern Canada, both drained, and undrained with porewater pressure measurement, defined at 8% axial strain as suggested for the large strain strength by Lefebrve (1981). According to Fig.8.22, a) all the slopes failure experiences in soft clays were subjected to effective normal stresses smaller than 100 kPa, b) the mobilized shear strength in first-time slope failures in soft clays of Eastern Canada, is greater than that from the empirical correlation in the present study, and c) the back-calculated friction angles mobilized on the global slip surface, are comparable to those defined at 8% axial strain in triaxial compression tests on undisturbed specimens, and at effective normal stress greater than 10 kPa. In effective normal stress range of 30 to 50 kPa, the $\phi'_s(\text{mob}) = \left[\phi'_{fs}\right]_s^{\sigma'_n} + 10°$.

TABLES

Table 8.1. First-time slope failures with a segment of slip surface at residual shear strength condition

No	Slope Failure	Slope material	Ip(%)	CF(%)	$\bar{r}_u$	Discontinuity	Slope height (m)	Slope age (yr)	L_{fs}/L (%)	Reference
1	New Cross Cutting, UK	Brown London Clay	50-60	55	-0.46	Layer Contact	17	3	54	Chandler and Skempton (1974); Skempton (1977)
2	Sudbury Hill Cutting 2, UK	Brown London Clay	50-60	55	0.3	-	7	46	64	Chandler and Skempton (1974); Skempton (1977)
3	Northolt, 1, 3, 6, 9, 11, UK	Brown London Clay	50-60	64-69	0.14, 0.20, 0.25, 0.25,	Layer Contact	6.0-6.7	35	43-67	James (1970)
4	Fareham, UK	Brown London Clay	50-60	64-69	0.29	-	10	58	48	James (1970)
5	West Acton 8 and 9, UK	Brown London Clay	50-60	64-69	0.3	-	4.9	46	56	James (1970)
6	Tulse Hill UK	Brown London Clay	50-60	64-69	0.3	-	8	101	28-44	James (1970)
7	Grove Park, UK	Brown London Clay	50-60	64-69	0.1	Bedding Plane	3.3	98	39	James (1970)
8	Kingsbury 1, UK	Brown London Clay	50-60	64-69	0.3	-	6	16	76	James (1970)
9	St. Helier, UK	Brown London Clay	50-60	64-69	0.25	-	7	22	64	James (1970)
10	Crews Hill, UK	Brown London Clay	50-60	64-69	0.3	Layer Contact	6.2	47	53	James (1970)
11	Cuffley, UK	Brown London Clay	50-60	64-69	0.3	-	7.2	38	63	James (1970)
12	Whitstable, UK	Brown London Clay	50-60	64-69	0.3	Layer Contact	8.8	99	58	James (1970)
13	Grange Hill, UK	Brown London Clay	50-60	64-69	0.3	-	12.2	50	42	James (1970)
14	Hadley Wood, UK	Brown London Clay	50-60	64-69	0.3	-	10.4	65	47	James (1970)
15	Dauntsey, UK	Oxford Clay	43-51	45	0.28	-	8.8	121	35	James (1970)
16	Hullavington, UK	Oxford Clay	33	-	0.3	-	9.4	57	72	Cassel (1948); James (1970)

Table 8.1 (Cont'd)

17	Ampthill, UK	Oxford Clay	33	-	0.3	-	11.8	90	64	James (1970)
18	Bincombe, UK	Oxford Clay	34	54	0.3	-	18.6	41	74	James (1970)
19	Albedosa, Italy	Lugagnano Clay	26	20-40	0.44	-	19	?	60	Cancelli (1981)
20	Santa Barbara, Italy	Santa Barbara Clay	35	30	0.22	Layer Contact	131	?	40	Esu et al. (1984)
21	Wettern, Brussels	Loam/ Blue Clay	12-25 / 60-100	18/46	0.22	Layer Contact	13.6	37	42	Marivoet (1948)
22	Selborne, UK	Gault Clay	40-50	38-48	0.17	-	8		71	Cooper et al. (1998)
23	Akistu, Japan	Mudstone	60	46	0.24	Layer Contact	17.5	?	20	Nakamori et al. (1996)
24	Hunsburry Hill, UK	Upper Lias Clay	32	31	0.19	-	14.5	44	81	Chandler (1974); Chandler and Skempton (1974)
25	Barrowden, UK	Upper Lias Clay	31	52	0.36	-	5.5	83	45	Chandler (1974); Chandler and Skempton (1974)
26	Stowehill A, UK	Upper Lias Clay	31	36	0.23	-	14.6	66	85	Chandler (1974); Chandler and Skempton (1974)
27	Wellingborough, UK	Upper Lias Clay	31	62	0.2	-	10.3	105	45	Chandler (1974); Chandler and Skempton (1974)
28	Ardley Tunnel, UK	Upper Lias Clay	31	33	0.3	-	6	52	60	James (1970); Chandler (1974); Chandler and
29	Charwelton, UK	Upper Lias Clay	34	30	0.3	-	9.6	16	65	James (1970)
30	Standish JCT, UK	Lower Lias Clay	31	-	0.3	-	7.4	129	82	James (1970)
31	Wothorpe, UK	Upper Lias Clay	41	48	0.37	-	6.3	6	81	James (1970); Chandler (1974); Chandler and Skempton (1974)

Table 8.1 (Cont'd)

32	Heyford, UK	Upper Lias Clay	28	-	0.22	-	10	126	77	James (1970); Chandler (1974); Chandler and Skempton (1974)
33	Seaton, UK	Upper Lias Clay	29	42	0.38	-	8.9	68	82	Chandler (1974); Chandler and Skempton (1974)
34	Haslemere A and B, UK	Atherfield Clay	21	-	0.3	-	4.7-6.1	104	51-60	James (1970)
35	Hildenborough, UK	Weald Clay	22-39	60	0.3	-	8.4	68	91	James (1970)
36	Earlswood, UK	Weald Clay	39	-	0.3	-	11.9	68	67	James (1970)
37	Capo Spulico, Italy	Argille Varicolori Clayshale	32-42	38-66	0.47-0.51	-	65.3	?	57	D'Elia et al. (1991)
38	Isle of Sheppey, England	Brown London Clay	50-60	55	-0.02	Bedding Plane	41.1	?	52	Dixon and Bromhead (1991)
39	Grava, Greece	Blue Marly Clay	38-48	-	0	-	9.1	1	39	Sotiropoulos and Cavounidis (1980)
40	Devon, Canada	Till/ Edmonton Bedrock/ Bentonitic Clay	24/60	32/47	0.21	Weak Seam/ Pre-existing Shear Plane	11.7	1	41	Eigenbrod and Morgenster (1971)
41	North to Central National Highway, Greece	Dark Brown Stiff Silty Clay	54	-	0.54	Layer Contact	24.6	?	66	Anagnostopoulos and Georgiadis (2004)
42	Pendakomo, Cyprus	Moni Melange (Firm to Stiff Clay)	60-100	50-90	0	-	9.9-11.4	1	57	Gostelow and Loucaides (1988)
43	Salvador, Brazil	Residual Granulite	36-50	38-53	0	-	19.8	?	69	Magalhaes et al (1992)
44	Risalaimi, Italy	Stiff Tectonized Marly Clay	18-37	17-37	0.27	-	30	0	47	Valore (1995)
45	Grassano, Italy	Blue Clay	21-33	40	0.39	Pre-existing Shear Plane	18.5	?	52	Di Maio and Vassallo (2011)

Table 8.2. First-time slope failures with mobilized shear strength close to fully softened shear strength on the entire slip surface

No	Slope Failure	Slope material	Ip(%)	CF(%)	$\bar{r}_u$	Slope height (m)	Slope age (yr)	Reference	Remarks
1	Voltaggio, Italy	Colluvial Soil/ Clay Shales	12/10	-	0.4	24.8	?	Cancelli and Olcese (1984)	Including frequent lenses of quartz
2	People's Republic of China	Stiff fissured Clay	20	41	0.03	28.8	11	Li and Zhao (1984)	-
3	River Fossate, Italy	Variegated Clay Shales	14-37	33-58	0.31	25.5	?	D'Elia et al. (1980)	Including marly limestones and limestone layers
4	Allori Coal Field, Italy	Argille Scagliose Clay Shales	8-20	19-42	0.44	210.2	8	D'Elia et al. (1988)	15% marly and siliceous limestones
5	Roccella Valemone, M2, Italy	Stiff Tectonised Clay	18-34	16-21	0.24	38.5	?	Valore et al (2007)	Including random small blocks of calcilutite and limestone
6	Aghios Konstantinos 1, 2, 3, Greece	Clayey Marls	25-40	20-40	0.20-0.35	15.2-19.2	1	Alexandris et al (2011)	20% to 40% calcium carbonate
7	Selset, UK	Boulder Clay	12	25	0.4	13.8	1	Skempton and Brown (1961)	Uniform without fissures or joints
8	Kimola Floating Canal, Finland	Slightly Overconsolidated Glacial Clay	25-40	-	0.39	11.4	1	Kankare (1969a, b)	-
9	Selnes, Norway	Quick Clay	5-8	40	0.56	10.2	?	Kenney (1967)	-
10	Trondheim, Norway	Homogenous Overconsolidated Clay	3-7	15-25	0.55	31	?	Janbu et al. (1977)	-
11	Lodalen, Norway	Firm, Homogenous Marine Clay with Thin Silt Layers	8-20	30-50	0.38	19.8	?	Sevaldson (1956)	-
12	Ullensaker, Norway	Weathered/Quick Clay	9-24/6	40	0.52	7.5	?	Kenney and Drury (1973)	-
13	Ukuwela 1 and 2, Sri Lanka	Sandy Clay	19-29	15-25	0	8.1-20.9	0	Balasubramaniam et al. (1977)	-
14	Gjerdrum, Norway	Soft Clay/Sensitive Clay	5-20	-	0.25	20.5	3	Heyerdahl et al. (2015)	-

Table 8.2 (Cont'd)

15	Fu Yung Shan Tsuen, Hong Kong	Colluvium/Decomposed Granodiorite (clayey silt)	11-37	-	0.13	12.6	?	Ho et al. (2013)	-
16	No 312 National Road, P.R. China	Loess	8-9	-	0	46.6	?	Feng (1992)	-
17	Snowdon, Himalayan Region	Clayey Silt with Phyllitic Slates	15	-	0	33.2	?	Bhandari (1977)	-
18	Lachute, Sation 8+85 and 10+50, Canada	Overconsolidated fissured Clay	22	-	0.38-0.41	7.1	1.5	Silvestri (1980)	-

Table 8.3. First-time slope failures in soft clays of Eastern Canada

No	Slope Failure	Slope material	Ip(%)	CF(%)	$\bar{r}_u$	Slope height (m)	Slope age (yr)	Reference
1	Rosemere, Canada	Silty Clay	33	-	0.47	11.9	2	Lefebvre (1981)
2	Saint-Vallier 1, Canada	Brownish Fissured Clay / Homogenous Gray Clay with Occasional Stones or Sand Strata	37	65	0.33	10.0	?	Lefebvre and LaRochelle (1974); Lefebvre (1981)
3	Saint-Louis 2, Canada	Sandy Layer / Gray Clay with Light Stone Bands Alternating with Dark Bands	25	80	0.41	6.8	?	Lefebvre and LaRochelle (1974); Lefebvre (1981)
4	Orleans, Canada	Leda Clay	20-40	-	0.40	9.7	5	Eden and Jarrett (1971)
5	Rockcliffe, Canada	Leda Clay	8-28	57-65	0.62	13.9	?	Crawford (1963); Eden and Mitchell (1970)
6	Breckenridge, Canada	Leda Clay	38	-	0.62	14.7	?	Eden and Mitchell (1970)

FIGURES

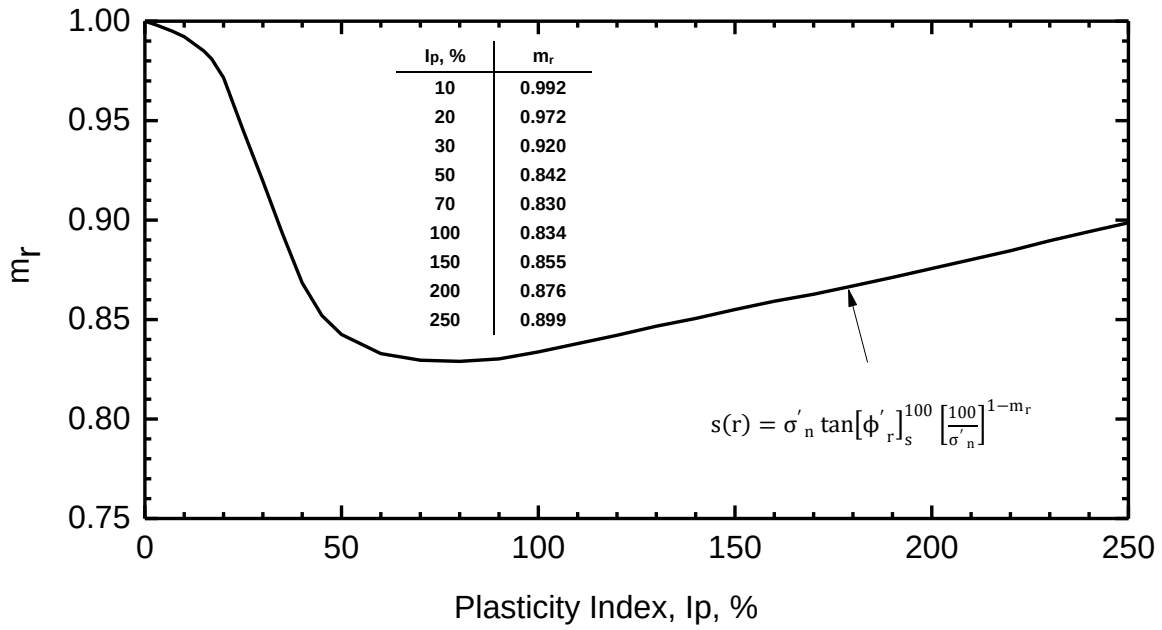

Figure 8.1. m_r as a function of plasticity index, determined from empirical data of residual shear strength from Mesri and Shahien (2003)

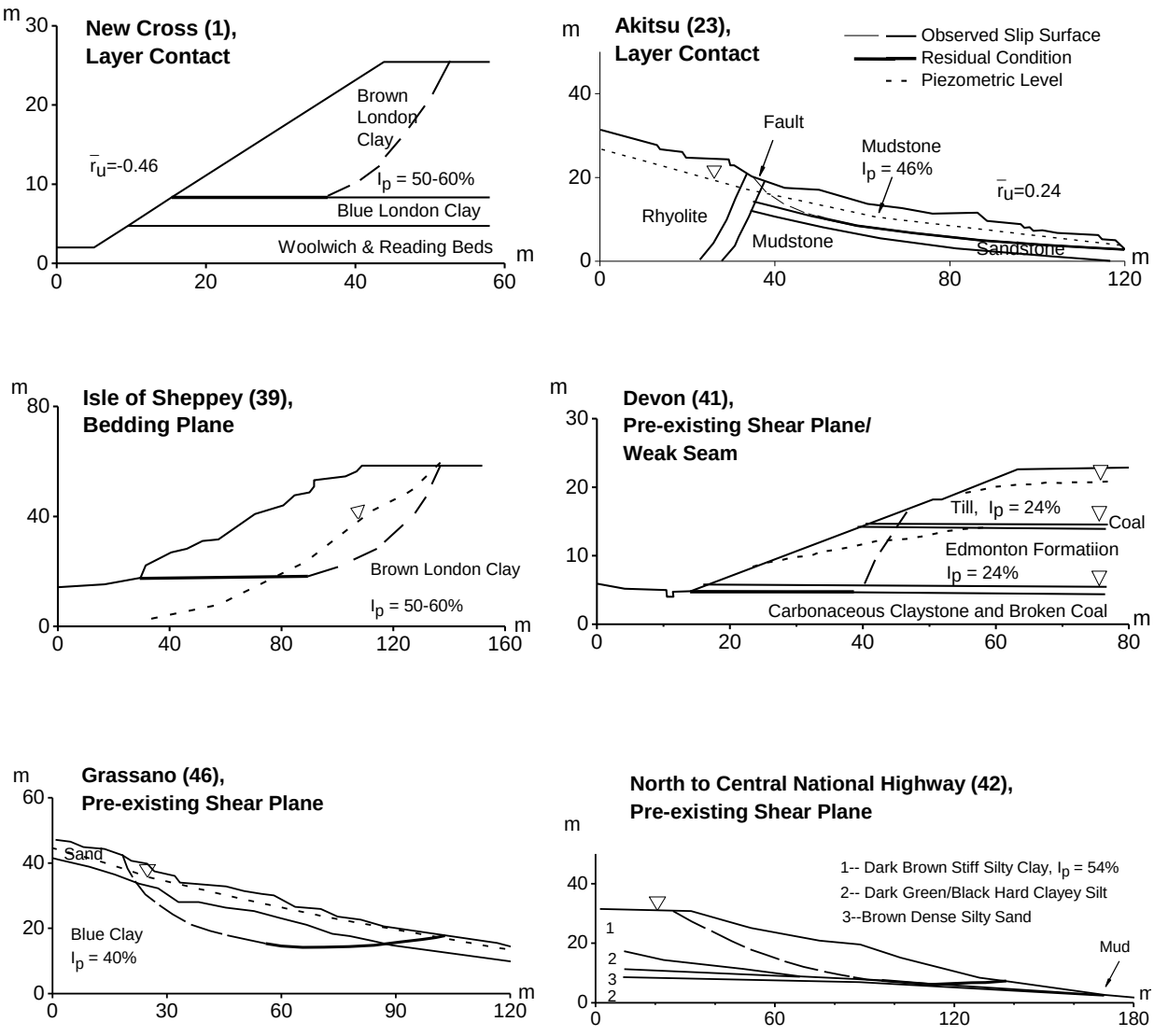

Note: Number in the parenthesis refers to the slope failure No. in Table 7.1.

Figure 8.2. Examples of first-time slope failures with segment of slip surface at residual shear strength condition, along pre-existing discontinuities

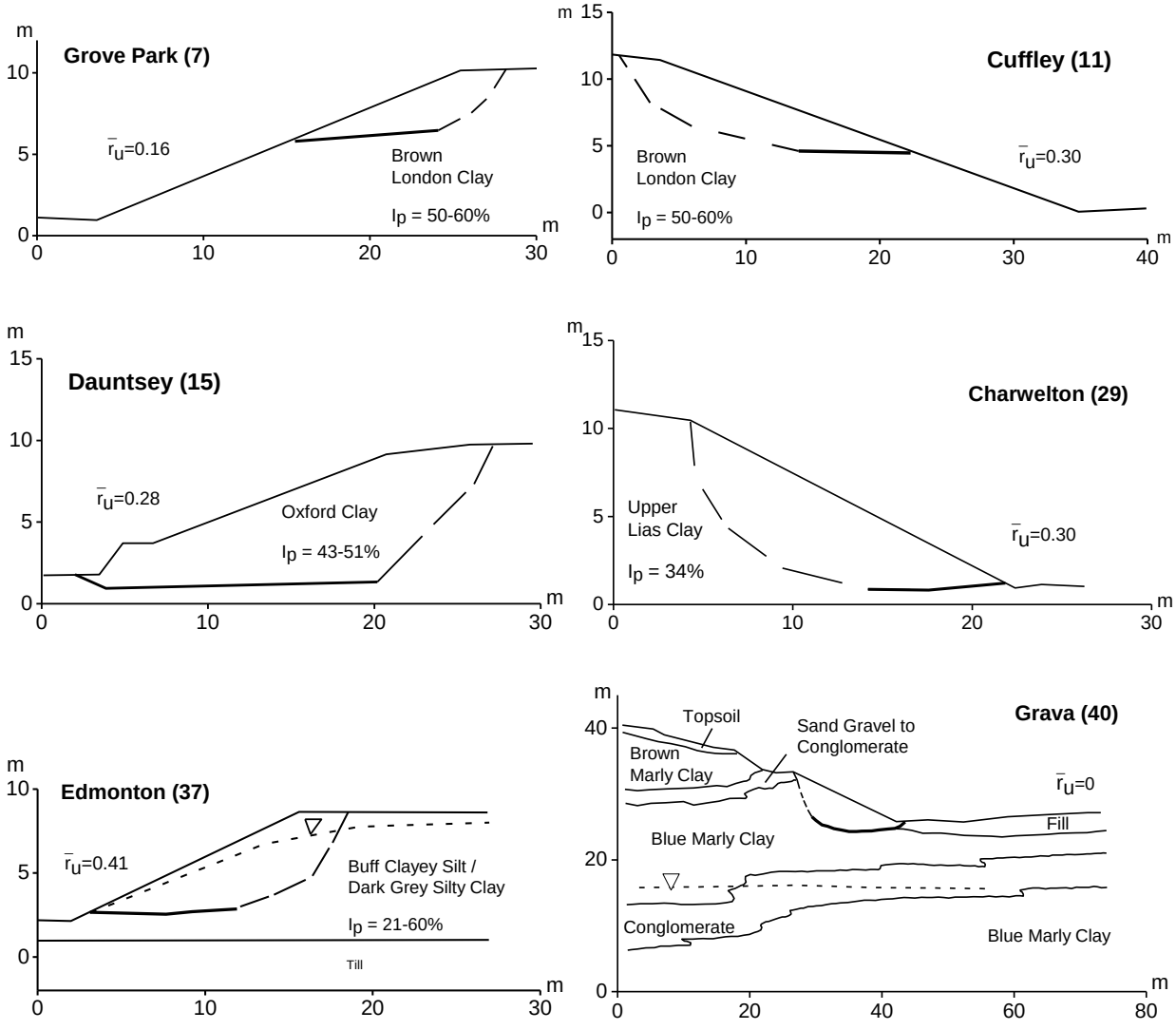

Note: Number in the parenthesis refers to the slope failure No. in Table 7.1.

Figure 8.3. Examples of first-time slope failures with segment of slip surface at residual shear strength condition, as a result of progressive deformation

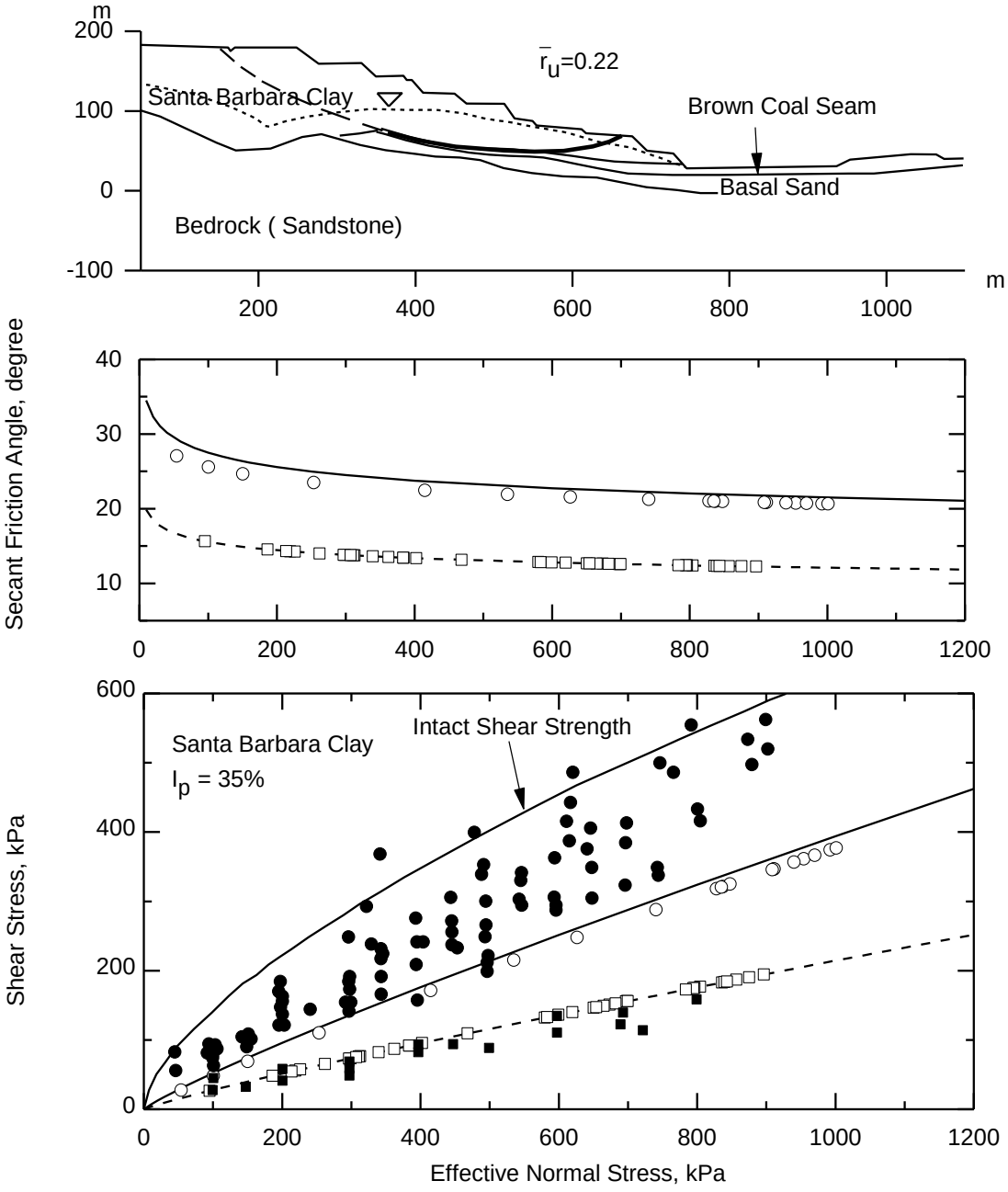

Figure 8.4. First-time slope failure at Santa Barbara, Italy 1983 (Esu et al 1984), with intact shear strength envelope from Mesri and Shahien (2003)

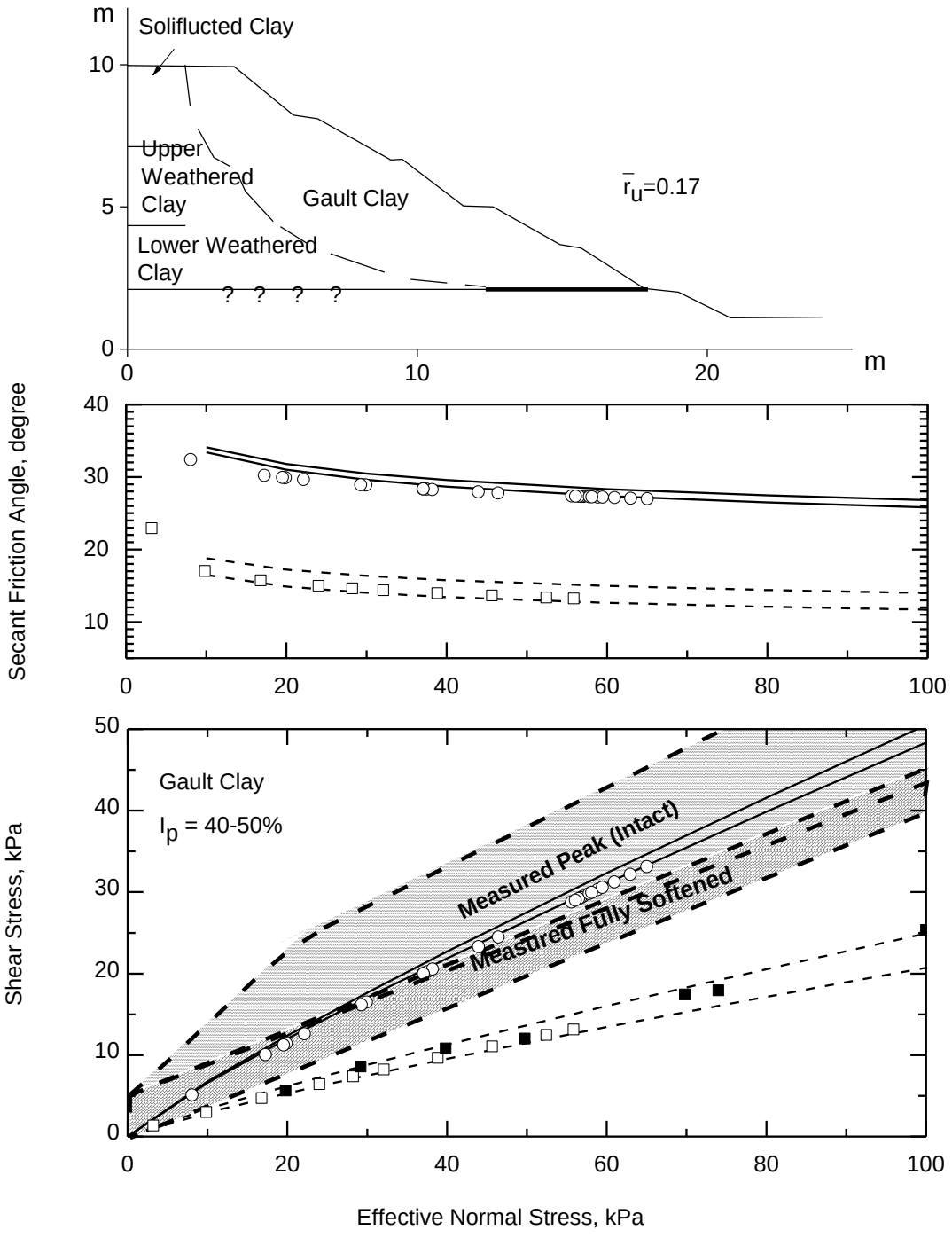

Figure 8.5. First-time slope failure at Selborne, UK, 1989 (Cooper et al. 1998, Mesri and Shahien 2003)

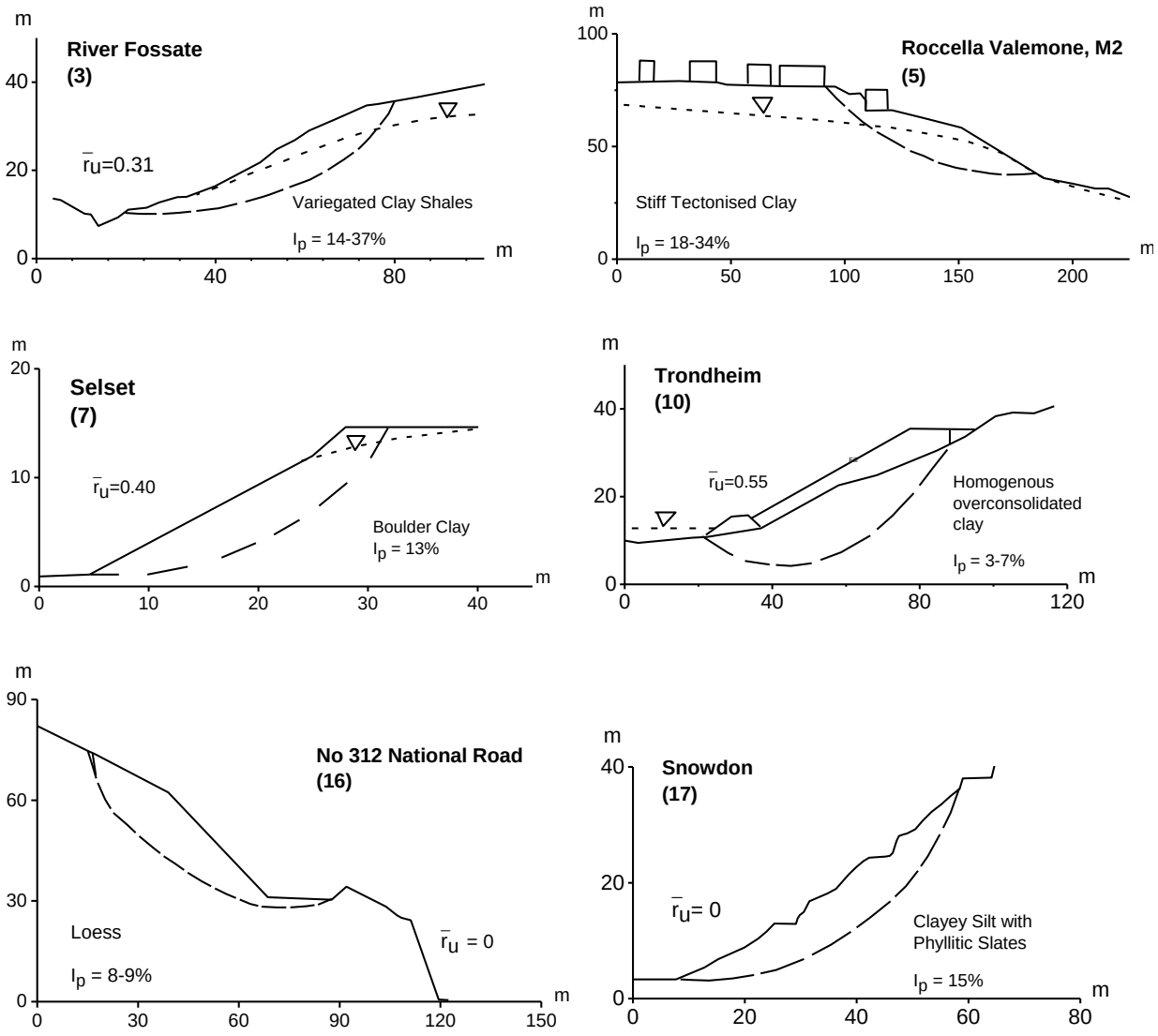

Note: Number in the parenthesis refers to the slope failure No. in Table 7.2.

Figure 8.6. Examples of first-time slope failures with mobilized shear strength equal or greater than fully softened shear strength on the entire slip surface

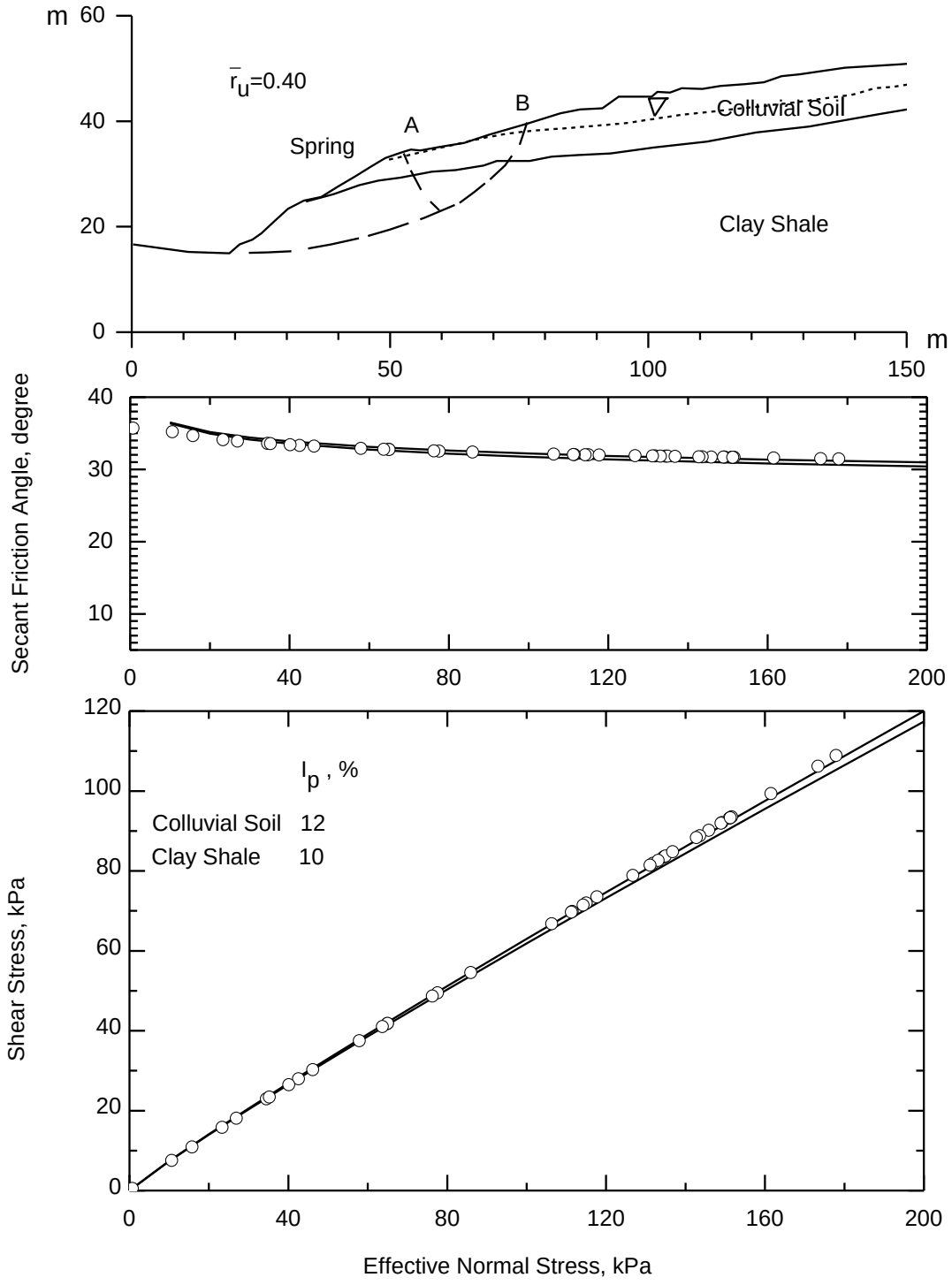

Figure 8.7. First-time slope failure at Voltaggio, Italy, 1980 (Cancelli and Olcese, 1984)

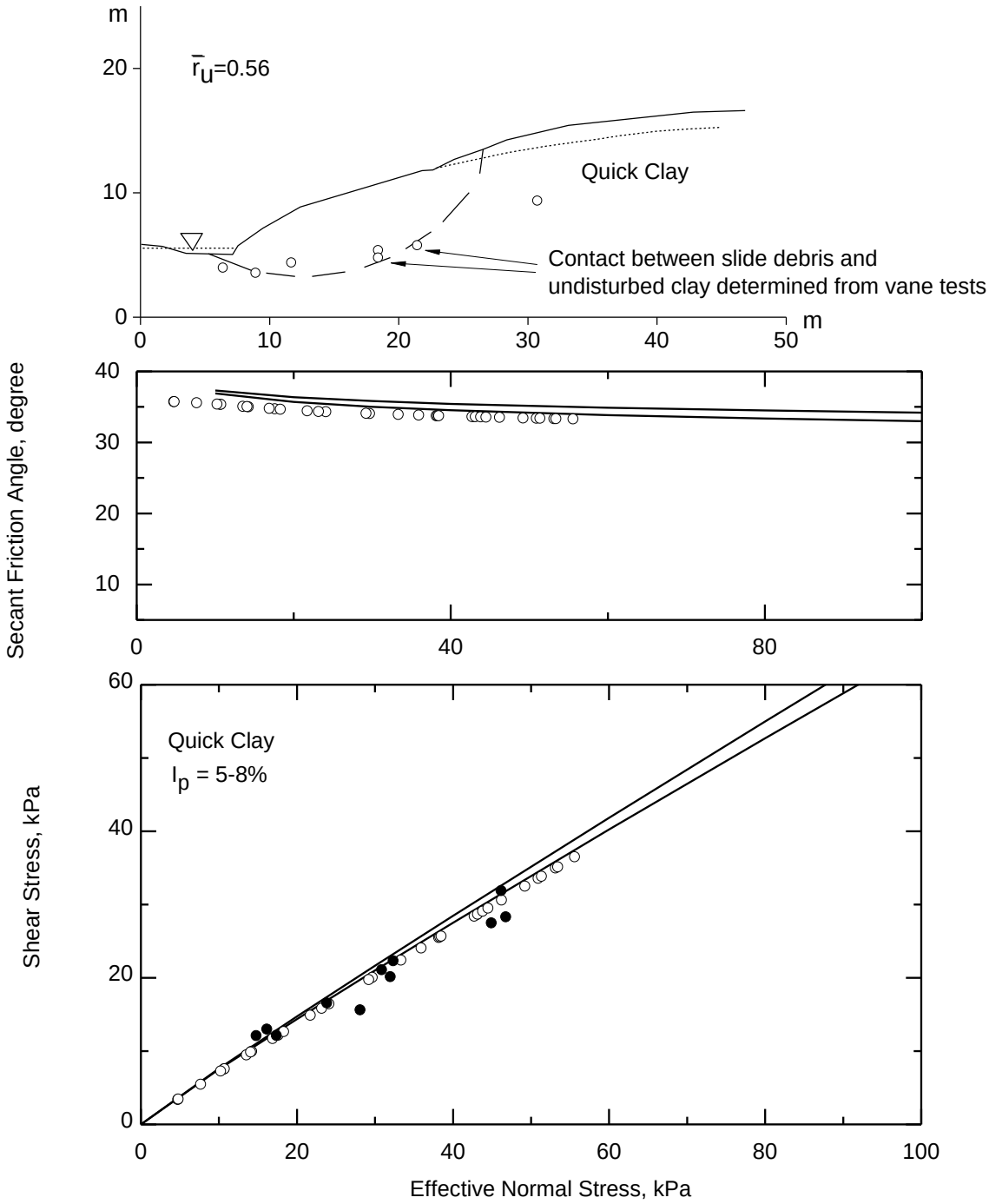

Fig x. First-time slope failure at Selnes, 1965 (Kenney 1967)

Figure 8.8. First-time slope failure at Selnes, Norway, 1965 (Kenney 1967)

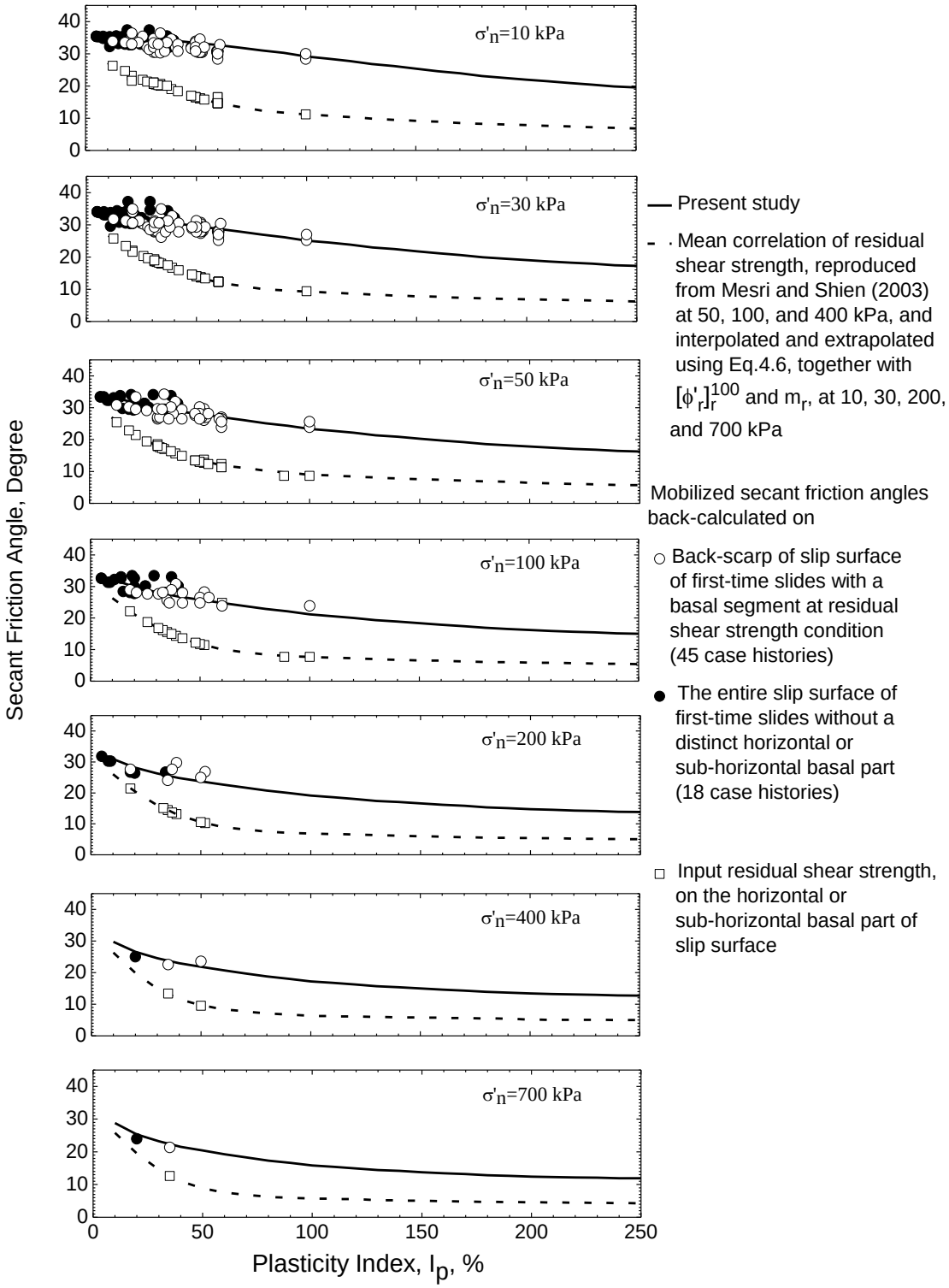

Figure 8.9. Secant fully softened friction angles back-calculated from 63 first-time slope failures in 38 geologic materials, including stiff clays, clay shales, mudstone, soft to firm clays excluding soft clays of Eastern Canada, clayey slits, and loess

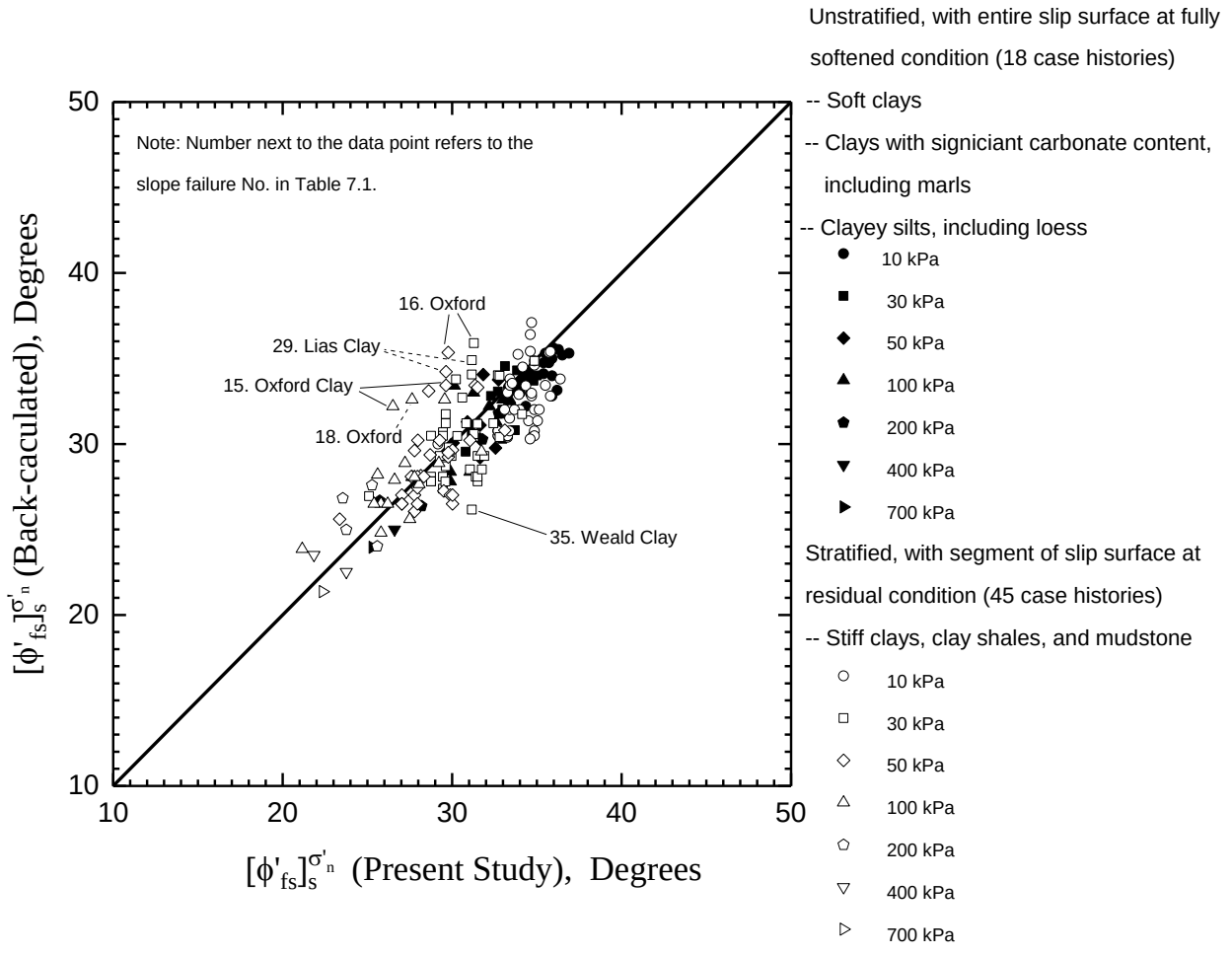

Figure 8.10. Mobilized secant fully softened friction angle back-calculated in the present study, of 63 first-time slope failures, compared with secant friction angles from the empirical correlation of fully softened shear strength, developed in the present study

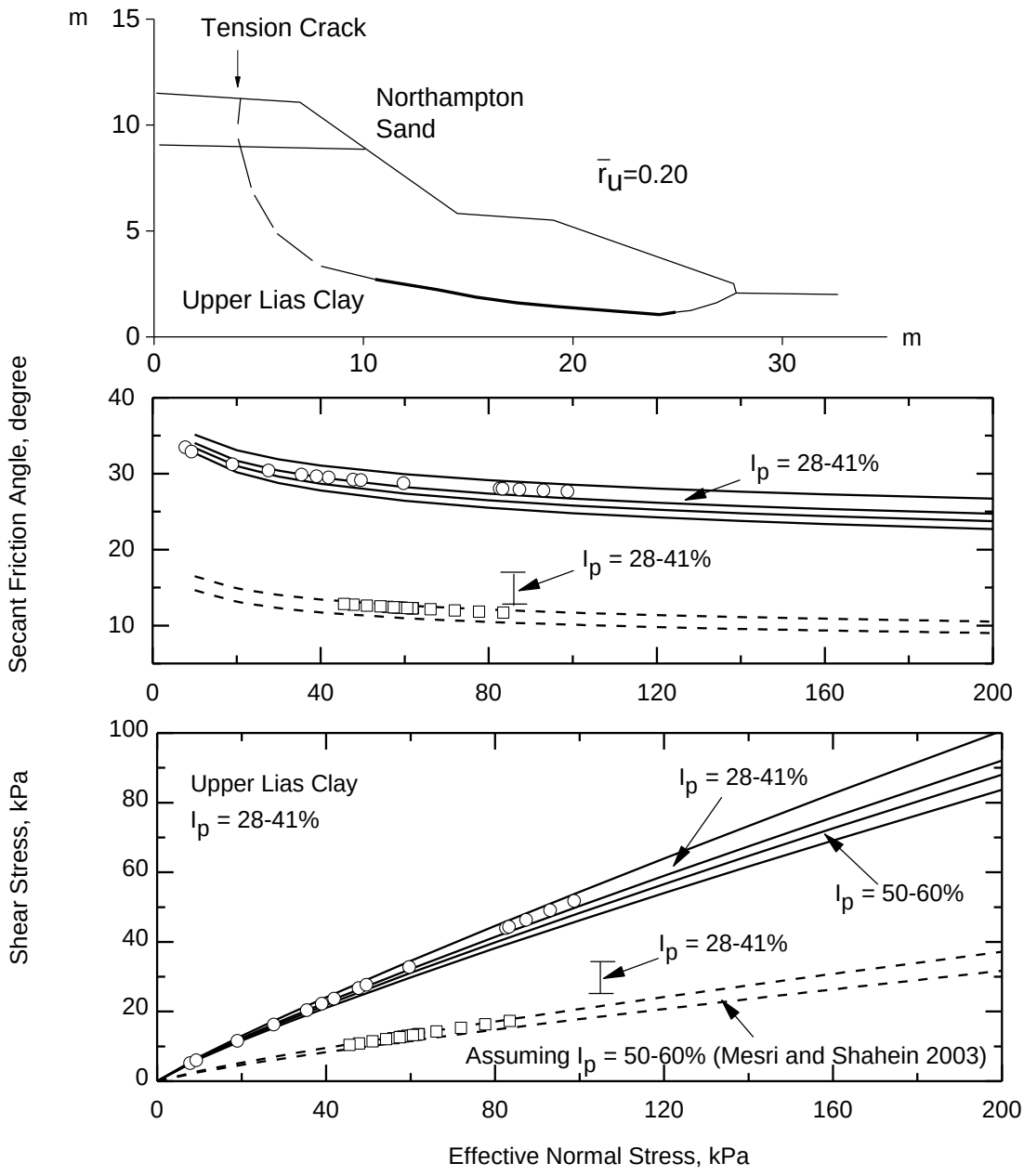

Figure 8.11. First-time slope failure at Wellingborough, UK, 1961 (Chandler 1974, Chandler and Skempton 1974)

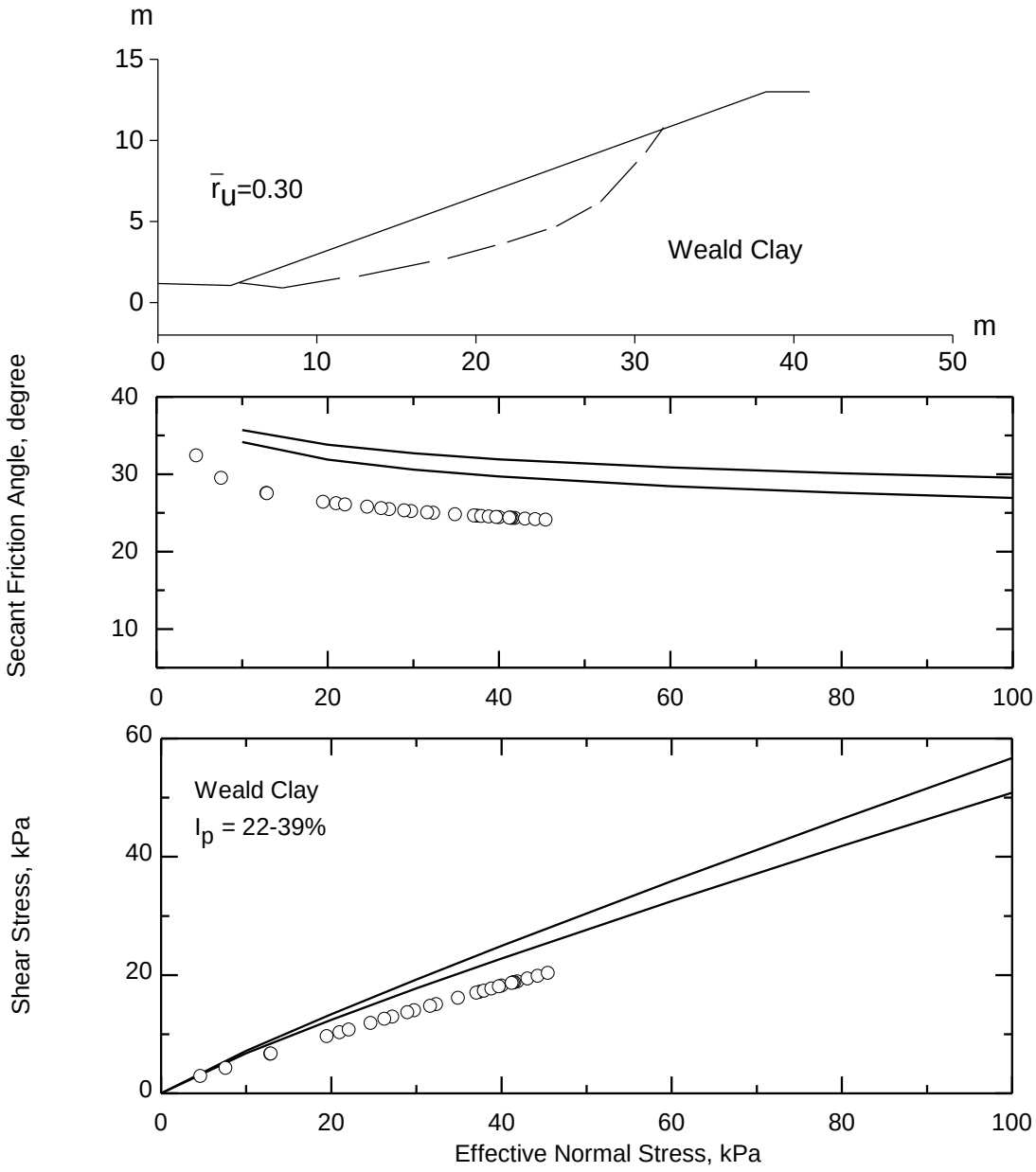

Figure 8.12. First-time slope failure at Hildenborough, UK, 1936 (James 1970)

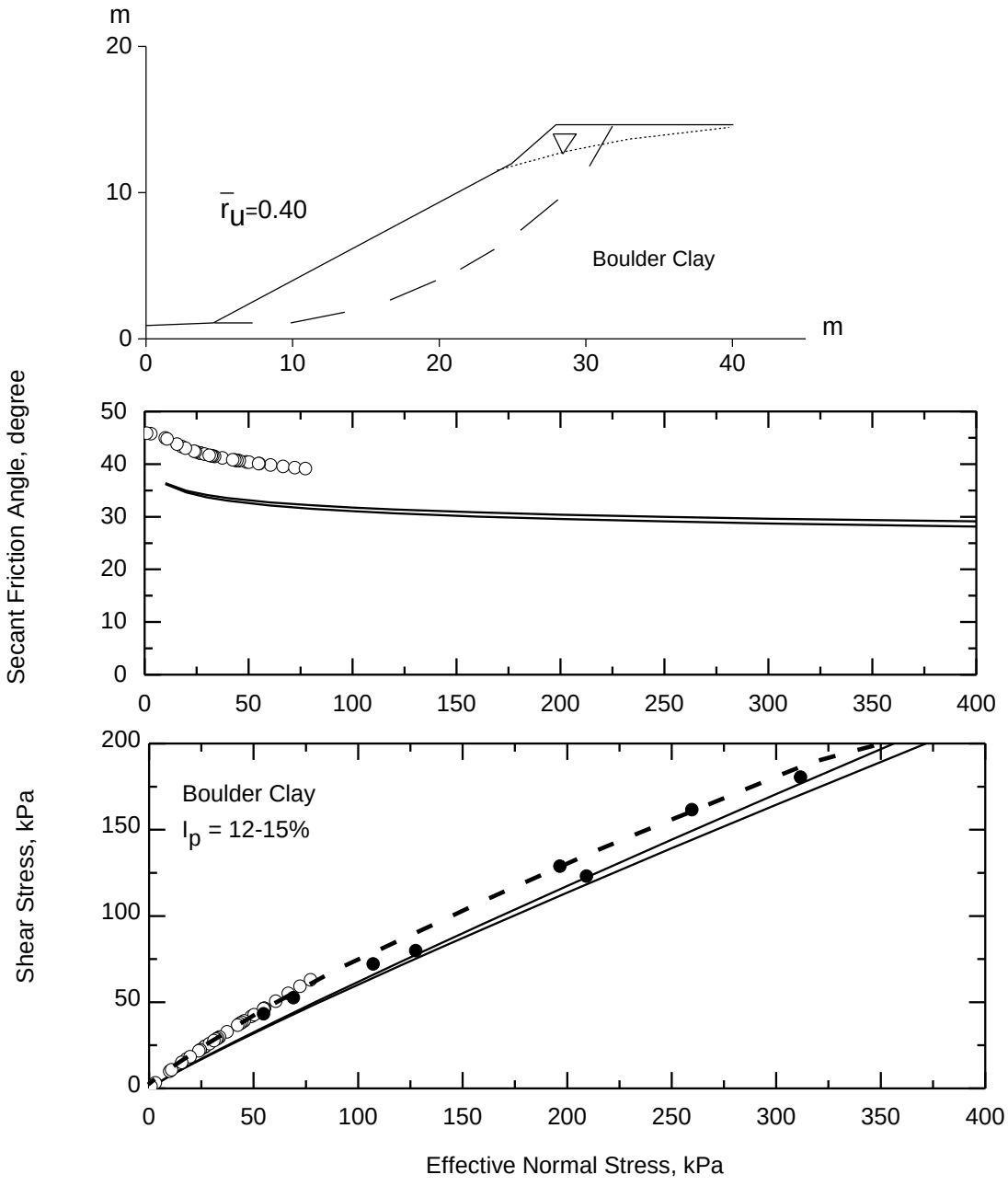

Figure 8.13. First-time slope failure at Selset, UK, 1954 (Skempton and Brown 1961)

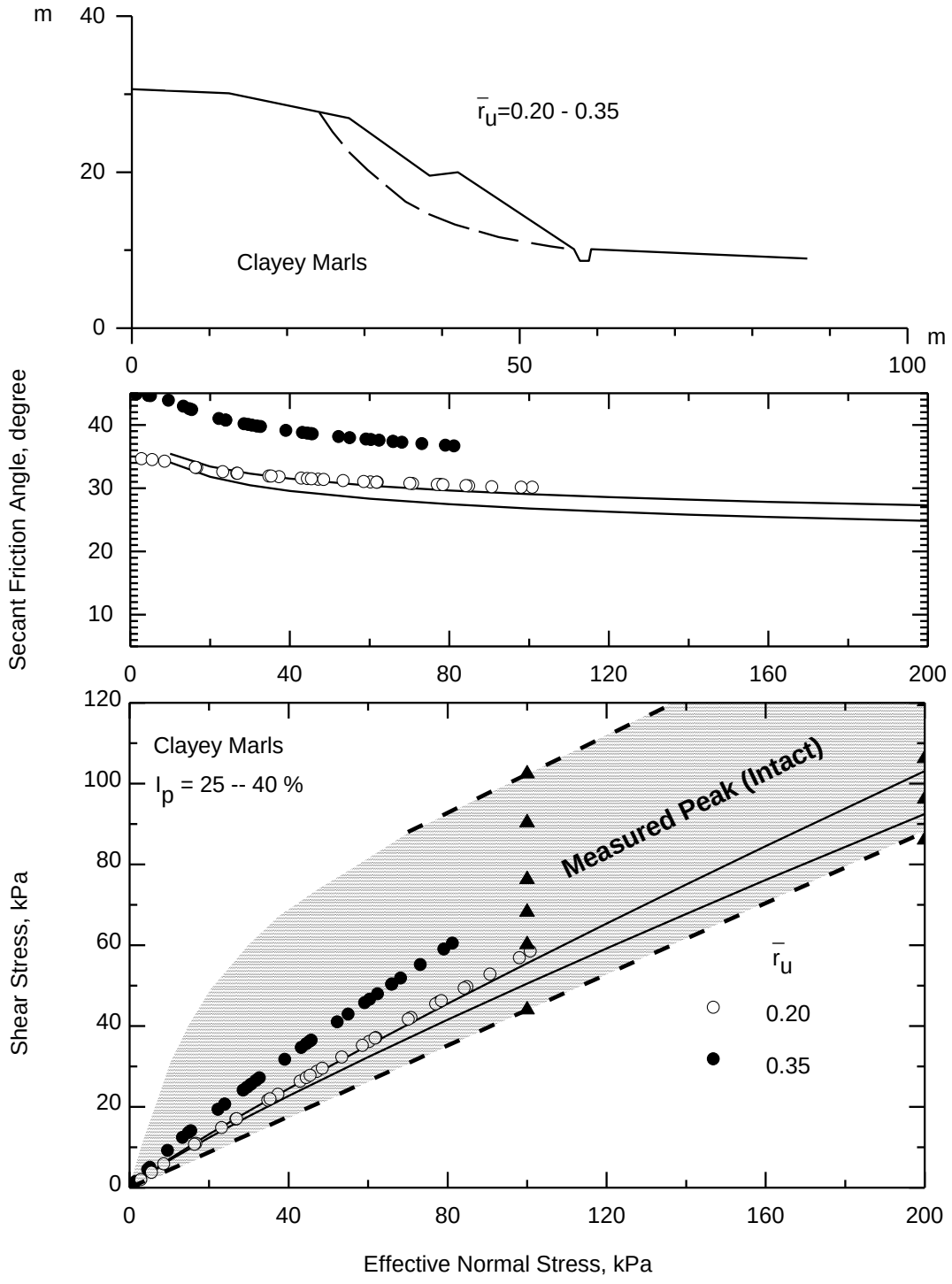

Figure 8.14. First-time slope failure (slide 1) at Aghios Konstantinos Greece, 2006 (Alexandris et al 2011)

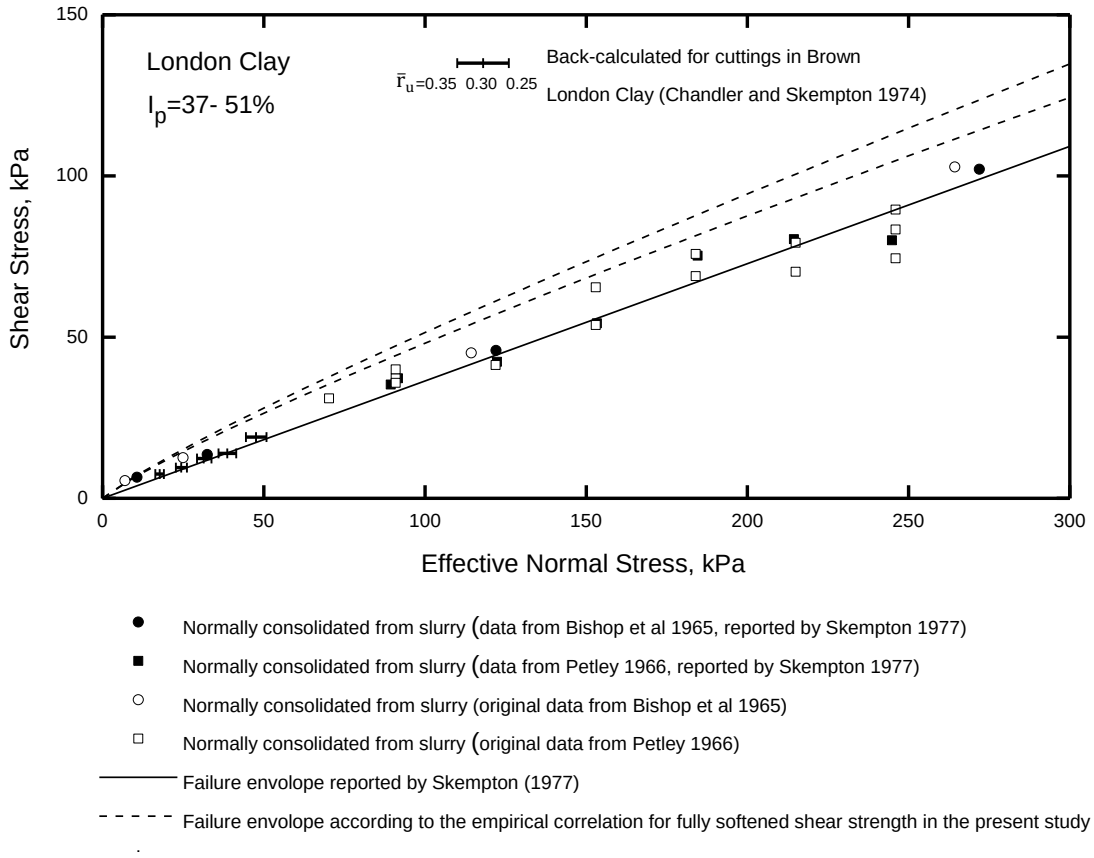

Figure 8.15. Fully softened shear strength of London Clay determined from laboratory tests, together with back-calculated shear strength for cuttings in Brown London Clay

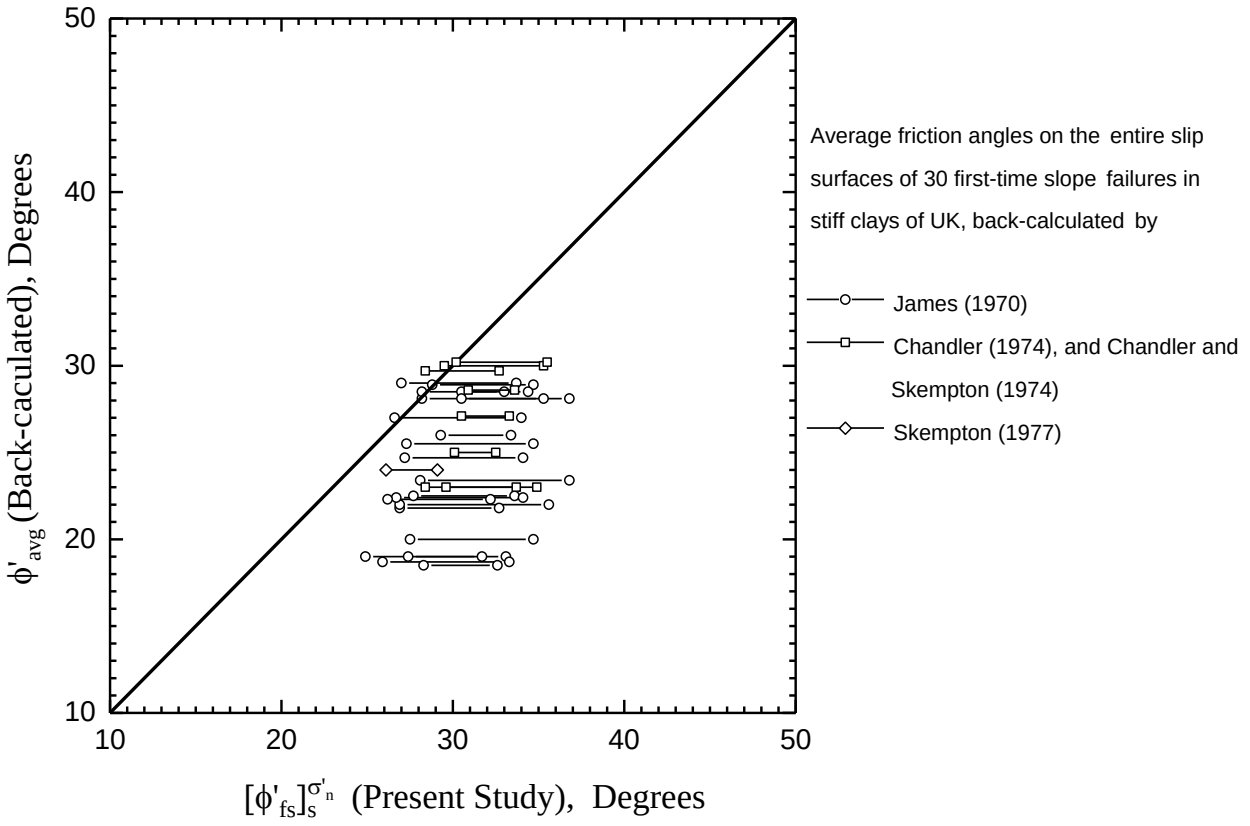

Figure 8.16. Average friction angle on the entire slip surfaces of first-time slope failures in stiff clays of UK, back-calculated by James (1970), Chandler (1974), Chandler and Skempton (1974), and Skempton (1977), compared with secant friction angles corresponding to Ip and σ'n, from the empirical correlation of fully softened shear strength, developed in the present study

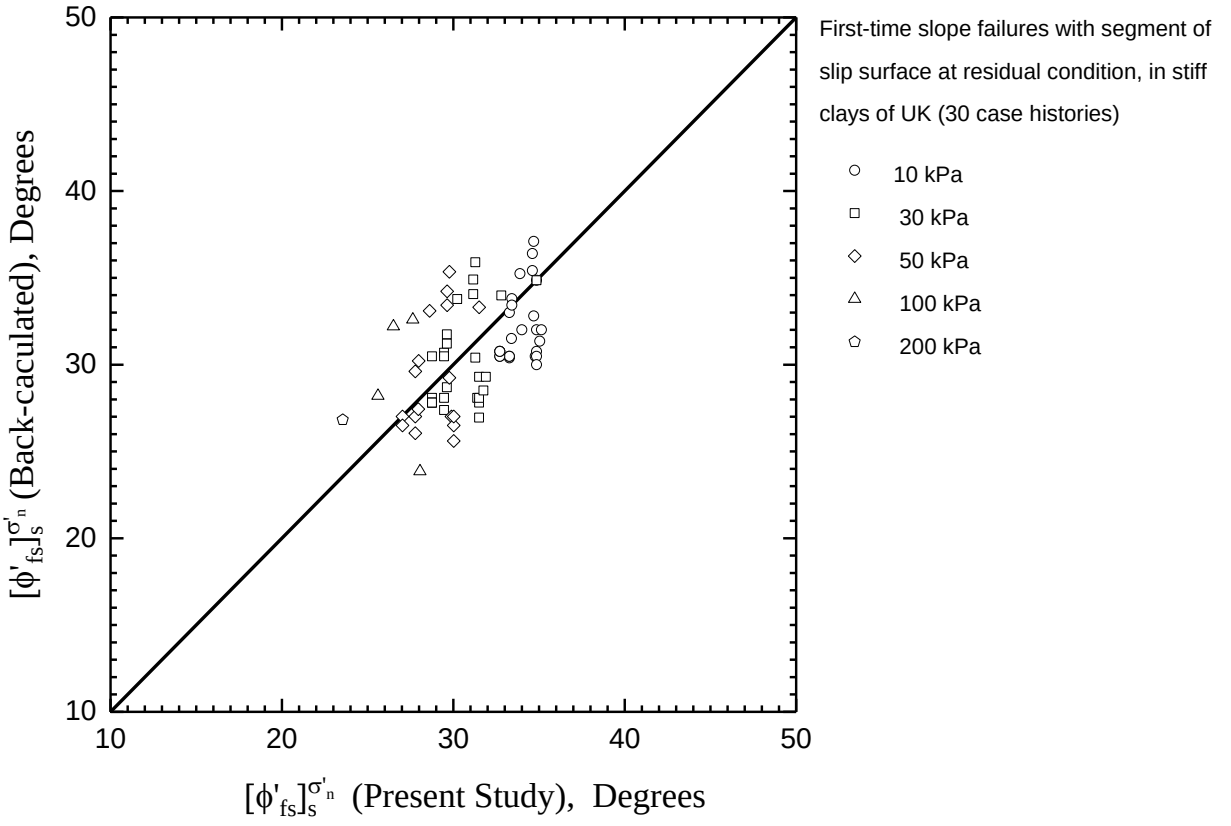

Figure 8.17. Mobilized secant fully softened friction angles back-calculated in the present study, on the back-scarps of 30 first-time slope failures in stiff clays of UK, compared with secant friction angles from the empirical correlation of fully softened shear strength, developed in the present study

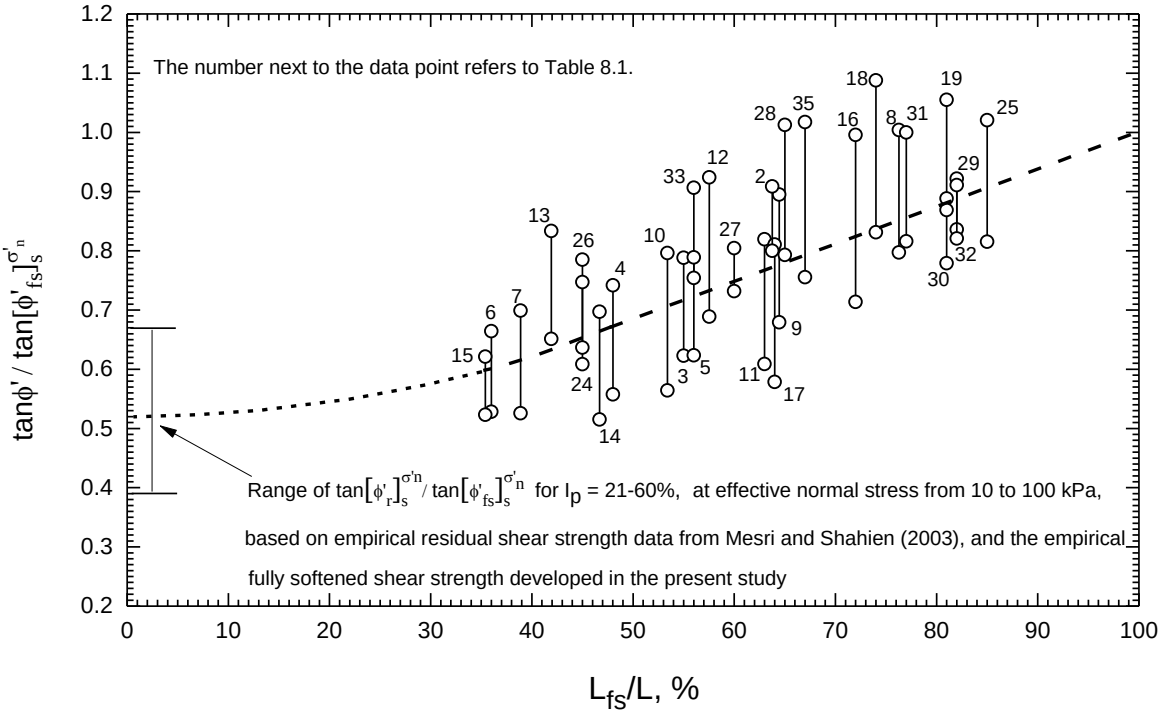

Figure 8.18. $\tan\phi' / \tan\left[\phi'_{fs}\right]_s^{\sigma'_n}$, against length of slip surface segment at fully softened condition / total slip surface length, for stiff clays with I_p in the range of 21 to 60% (The values of ϕ' from James 1970, Chandler 1974, Chandler and Skempton 1974, Skempton 1977)

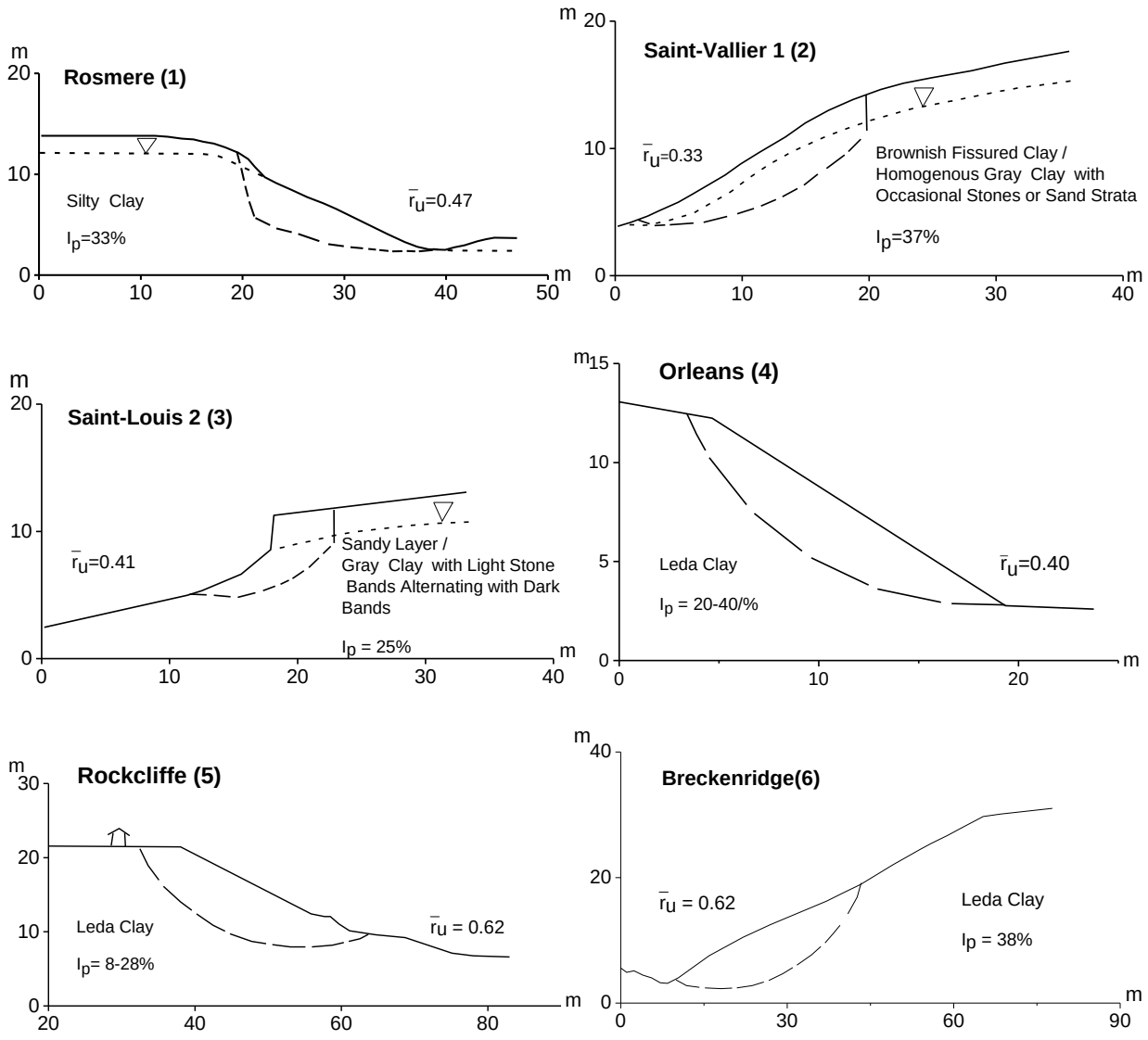

Note: Number in the parenthesis refers to the slope failure No. in Table 7.4.

Figure 8.19. First-time slope failures in soft clays of Eastern Canada with reported slip surface and ground water condition at failure

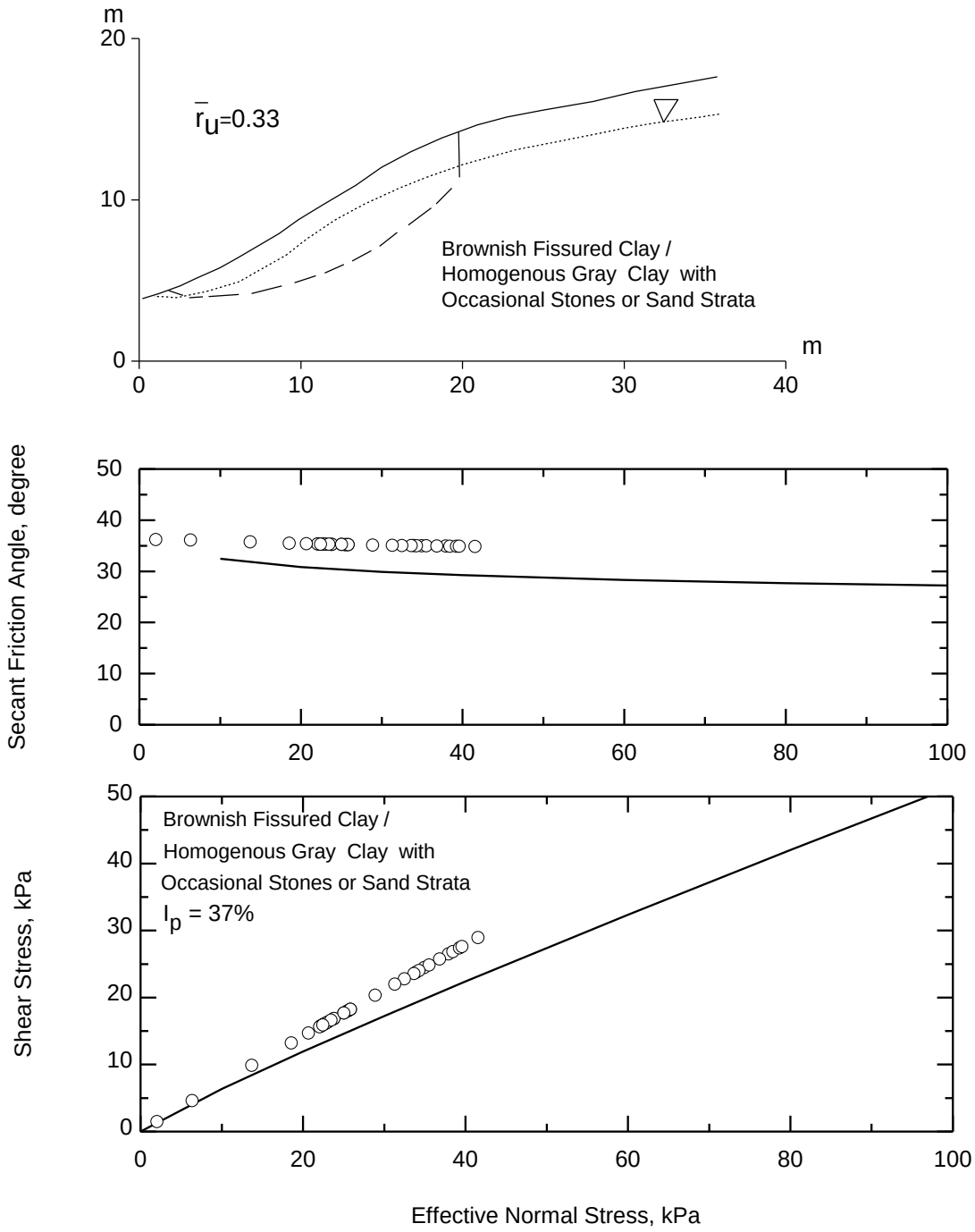

Figure 8.20. First-time slope failure at Saint-Vallier, Canada, 1968 (Lefebvre and LaRochelle 1974, Lefebvre 1981)

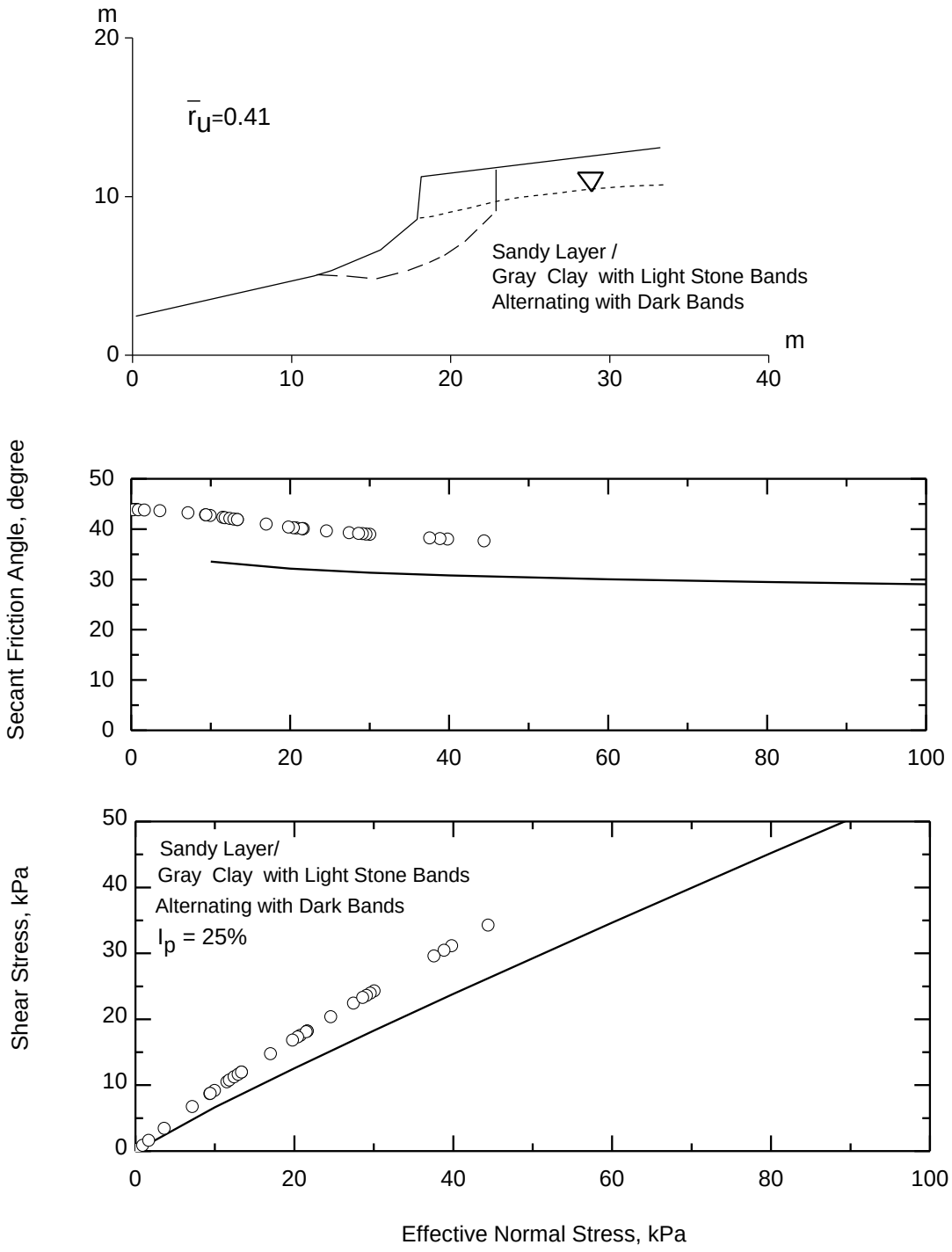

Figure 8.21. First-time slope failure at Saint-Louis, Canada, 1968 (Lefebvre and LaRochelle 1974, Lefebvre 1981)

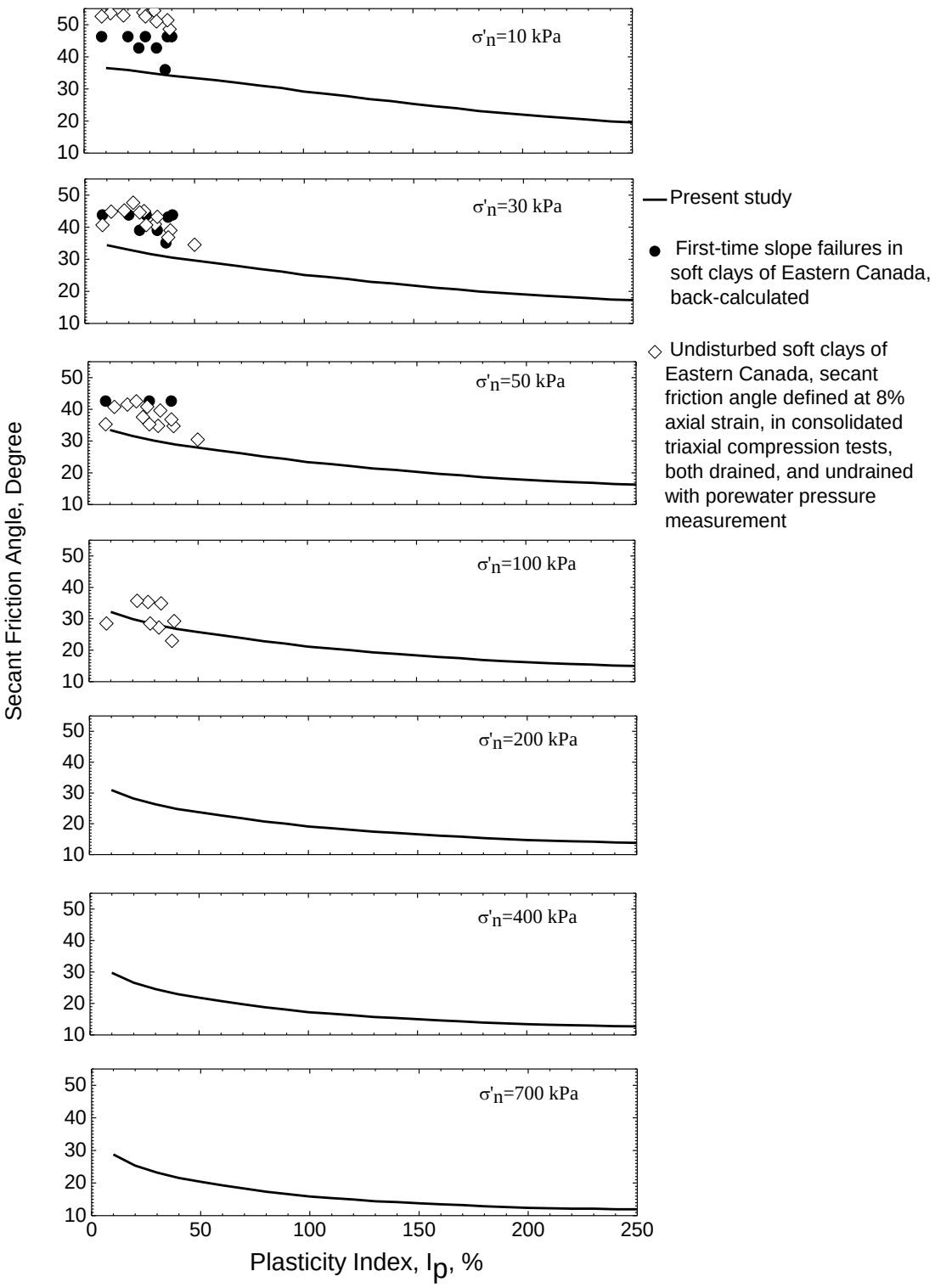

Figure 8.22. Back-calculated mobilized secant friction angles in first-time slope failures in soft clays of Eastern Canada

CHAPTER 9: SUMMARY AND CONCLUSIONS

The study has been conducted to clarify the meaning of fully softened shear strength, to examine the best procedure for its measurement in laboratory tests, and to generalize its field application.

An empirical correlation of secant fully softened friction angle has been developed at effective normal stress in the range of 10 kPa to 700 kPa, for a wide range of clay compositions, characterized in terms of plasticity index, from 10% to 250%, based on consolidated triaxial compression tests on saturated remolded specimens of 15 stiff clay and clay shale compositions. These specimens of stiff clay and clay shale compositions, with plasticity index in the range of 13% - 217%, were remolded at liquidity index in the range of 0.5 to 1.0, with an average of 0.8, normally consolidated under equal all-around pressure, and subjected to undrained shear with porewater pressure measurement. For comparison, a limited number of drained tests were performed. The empirical correlation as a function of plasticity index, presented by smooth curves at 7 effective normal stresses, 10, 30, 50, 100, 200, 400, and 700 kPa, was developed using the secant fully softened friction angles at 100 kPa determined from the triaxial compression tests, together with Eq.5.5, $s(fs) = \sigma'_n \tan\left[\phi'_{fs}\right]_s^{100} \left[\frac{100}{\sigma'_n}\right]^{1-m_{fs}}$, and m_{fs}, which was determined based on entire data at all effective normal stresses.

The secant fully softened friction angle data interpreted from laboratory tests reported in the literature on reconstituted, normally consolidated specimens, likely with a random fabric, were compared to the empirical correlation for fully softened shear strength developed in the present study. These data are on reconstituted specimens prepared for 55 materials, including soft to stiff clays, clay shales, mudstones, and clay minerals, with plasticity index in the range of 9% - 170%. An examination was made to the potential dependence of laboratory measurements for fully softened shear strength on (1) specimen preparation procedure (specimens prepared by mechanical remolding and specimens consolidated from slurry, or sedimented from suspension), and (2) different drainage condition during shear. The friction angles were also interpreted for data from

triaxial compression tests, both drained, and undrained with porewater pressure measurement, on undisturbed specimens.

Fully softened shear strength mobilized in a full-scale situation was estimated by means of back-analyses of first-time slope failures using the observed slip surface or possible slip surface determined based on adequate field observations, together with the reported or assumed groundwater conditions in the original references. Sixty-three first-time slope failures in 38 geologic materials were studied, including soft clays to stiff clays, clay shales, mudstones, marls, clayey silts, and glacial clays. Forty-five case histories are first-time failures with a segment of slip surface at residual condition, and the remaining 18 cases are first-time failures without distinct horizontal or sub-horizontal basal part pf slip surface. An examination was also included, in relation to the mobilized shear strength of first-time slides in soft clays of Eastern Canada.

The following conclusions are in relation to the meaning, measurement, and field application of fully softened shear strength of stiff clays and clay shales.

1. Fully softened shear strength is defined at a random, predominantly edge to face arrangement and interaction of clay particles in a destructured stiff clay or clay shale composition. In the field, though geological weakening may bring stiff clays and clay shales to the fully softened condition, it is not a prerequisite as fully softened condition results from progressive deformation and destructuration along a global slip surface.
2. Fully softened shear strength can be measured either by laboratory tests, or by back-analyses of first-time slope failures in a full-scale situation.
3. In triaxial compression, the random arrangement and interaction of clay particles, is mobilized at failure in reconstituted, normally consolidated specimens, prepared by mechanical remolding at water content close to liquid limit, or by consolidation from a slurry/suspension water content. Because fully softened shear strength data interpreted from specimens subjected to undrained shear with porewater pressure measurement, at all effective normal stresses, are comparable to those from specimens subjected to drained shear, the consolidated undrained triaxial compression tests, which requires less duration for porewater pressure equalization in undrained tests, than porewater pressure dissipation in drained tests, are preferred for the measurement of fully softened shear strength.

4. The fully softened friction angle may be underestimated using a post-peak axial strain level, determined from triaxial compression tests on undisturbed stiff clay and clay shale specimens, resulting from some face to face interaction of clay particles on the shear plane which is likely to develop at early stages of shearing.
5. The m_{fs} value in equation $s(fs) = \sigma'_n \tan\left[\phi'_{fs}\right]_s^{100} \left[\frac{100}{\sigma'_n}\right]^{1-m_{fs}}$, decreases from 1.00 at Ip = 0%, to 0.840 at Ip range between 100 and 130%, and slightly increases afterward, to 0.878 at Ip = 250%. The relationship between fully softened shear strength and effective normal stress is linear at Ip = 0%, because at low plasticity index, edge-to face interaction of clay particles is predominate even at high effective normal stresses. The relationship is most curved at Ip = 100 to 130%, as the fabric of stiff clay and clay shale compositions is most significantly influenced by the increase of effective normal stresses at an "intermediate" plasticity index, which promotes face to face interaction of clay particles. For stiff clay and clay shale compositions with very high plasticity index (Ip greater than 130%), some face to face interaction is already present at low effective normal stresses; therefore, the influence of effective normal stress increase is not as significant as that for stiff clay and clay shale compositions which display Ip = 100 to 130%.
6. The empirical correlation for fully softened shear strength developed in the present study, agrees with other fully softened shear strength data reported in the literature, in each investigation, obtained from a wide range of clay compositions, characterized in terms of plasticity index. These data include a) fully softened friction angles at 200 kPa, of 24 stiff clay and shale compositions, and 4 pure minerals determined from drained triaxial compression tests by Mesri and Cepeda-Diaz (1986); b) fully softened shear strength data reported by Mesri and Shahien (2003) at effective normal stresses of 50, 100, and 400 kPa; and c) mean curves at all effective normal stresses developed based on corrected fully softened friction angle data from modified Bromhead ring shear device reported by Eid and Rabie (2017).
7. For the 45 first-time slides in stratified deposits including stiff fissured clays, clay shales and mudstones, fully softened shear strength was mobilized on the back-scarp segment of slip surfaces, which was 28% to 85%, with an average of 58%, of the global slip surface. A basal segment of slip surface at residual condition was included, either as a pre-existing

stratigraphic or structural discontinuity before a cut was made, or as a result of progressive deformation along horizontal or sub-horizontal portion of the slip surface.

8. Fully softened shear strength from the proposed empirical correlation, represents the mobilized shear strength on the back-scarp of full-scale slip surfaces of first-time slope failures in stratified deposits including stiff clay and clay shales, and can be applied to the stability evaluation of natural and cut slopes in stiff fissured clays and clay shales using intact shear strength to locate the critical slip surface, or observed slip surface.
9. The mobilized shear strength over the entire slip surface in unstratified deposits including 1) soft to firm clays of low to medium plasticity excluding soft clays of Eastern Canada, or 2) clayey silts including loess, is near the fully softened shear strength of a stiff clay or clay shale compositions with similar I_p. Empirical correlation for secant fully softened friction angle developed in the present study, can be applied to the entire slope material, to calculate the factor of safety. For boulder clays and stiff clays, clay shales, or marls with significant amount of carbonate or quartz content, fully softened shear strength is a conservative lower bound for the mobilized shear strength.

The following conclusions are reached in relation to the triaxial compression tests in the present study, on remolded, normally consolidated specimens prepared from 15 stiff clay and clay shale compositions, including 51 undrained tests with porewater pressure measurement, and 28 drained tests,

1. For normally consolidated clays, the effective normal stress on the failure plane continues to increase in drained tests, so the specimen is still in a normally consolidated state. However, the effective normal stress on the failure plane in an undrained test, decreases with increase of shear induced porewater pressure, and the specimen behaves like an overconsolidated clays, in which a shear plane is more likely to develop.
2. The water content distribution along the specimen height, determined at the end of the tests, is quite uniform, with an average difference smaller than 1% among the 5 pieces, which indicates that the redistribution of porewater pressure, due to the positive shear induced porewater pressure near the shear plane, is not significant.
3. The responses of the 15 remolded normally consolidated clay and clay shale compositions are contractive -- positive shear induced porewater pressure was observed in all the

undrained tests with A-coefficient at the point of stress path tangency generally less than 1.2, and positive volumetric strain smaller than 10% was measured in all the drained tests. The ductile stress-strain behaviors are similar for the 15 compositions, except slight differences observed in remolded specimens of Mud Gully Clay (shear planes formed in all the undrained and drained tests), and the three clays with plasticity index no greater than 26%. After maximum stress difference is reached, either a minor decrease in stress difference takes place, or the axial stress levels off.

4. The stress paths for undrained tests are related to the plasticity index, and are divided into three groups -- a) stress paths of stiff clay and clay shale compositions with high plasticity index (I_p > 30%), start first with a vertical segment, bend to the left, reaching a maximum $(\sigma'_1 - \sigma'_3)$, and then drop off to the left; b) stress paths of Glen Forest Clay (I_p = 15%) and Kuykendahl Clay (I_p = 14%) are initially similar to a) and then display a distinct phase transformation point; c) South Richey Clay with medium plasticity of 25%, exhibits an intermediate behavior without distinct bending to the left or right.
5. Although the stress paths of undrained tests are different depending on the plasticity index, limiting condition defined by the maximum stress difference, $(\sigma'_1 - \sigma'_3)$, yields similar drained shear strength parameters as those determined from the maximum effective principle stress ratio, σ'_1/σ'_3 or by the stress path tangency.
6. A single failure envelope for a stiff clay or clay shale composition, could be determined from the stress paths of drained, and undrained triaxial compression tests with porewater pressure measurement. A detailed comparison at 7 effective normal stresses, shows a good agreement between the secant fully softened friction angle determined from drained triaxial compression tests and the friction angle determined from undrained tests with porewater pressure measurement.
7. The axial strain at failure in drained tests, $[\varepsilon_f]_{DTC}$, has an average value of 16%, independent of consolidation pressure. For undrained tests with porewater pressure measurement, though with some scatter, average $[\varepsilon_f]_{UTC}$ increases with the consolidation pressure, from 5% at 30 kPa, to 10% at 600 kPa, with an average equal to 8%.

The following conclusions are based on back-analyses of 6 first-time slope failures in soft clays of Eastern Canada, and triaxial compression tests, both drained, and undrained with porewater pressure measurement in literature, on undisturbed soft clays of Eastern Canada.

1. All the slopes failure experience in soft clays of Eastern Canada with shallow slip surface were subjected to effective normal stresses smaller than 100 kPa.
2. The mobilized shear strength in first-time slope failures in soft clays of Eastern Canada at a given plasticity index, is greater than that from the empirical correlation for fully softened shear strength developed in the present study. In effective normal stress range of 30 to 50 kPa, the $\phi'_s(\text{mob}) = \left[\phi'_{fs}\right]_s^{\sigma'_n} + 10°$.
3. For soft clays of Eastern Canada, the back-calculated friction angles mobilized on the global slip surface, are comparable to those defined at 8% axial strain in triaxial compression tests on undisturbed specimens, and at effective normal stress greater than 10 kPa.
4. At effective normal stresses equal or smaller than 50 kPa, large-strain friction angles of soft clays of Eastern Canada, are higher than fully softened friction angles from the empirical correlation. At effective normal stress of 100 kPa, large-strain friction angles of soft clays of Eastern Canada, become similar to fully softened friction angles from the empirical correlation. High consolidation pressures, in addition to shear strain, contribute to the breakdown of bonding between clay particles.

REFERENCES

Abdel-Ghaffar, M. E. (1990). *The meaning and practical significance of the cohesion intercept in soil mechanics.* Ph.D. Thesis: Univ. of Illinois at Urbana-Champaign.

Adachi, K. (1974). *Influence of pore water pressure on the engineering properties of intact rock.* Ph.D. Thesis: Univ. of Illinois at Urbana-Champaign.

Alexandris, A., Paschalidou, A., Griva, E., and Kavvadas, M. (2011). End of construction failures of cuttings in stiff clayey marls - a case from Central Greece. *Proc., of the 15th European Conference on Soil Mechanics and Foundation Engineering, 2*, pp. 1219-1224. Athens.

Alias, R., Kasa, A., and Taha, M.R. (2014). Effective shear strength parameters for remolded granite residual soil in direct shear and triaxial tests. *Electronic Journal of Geotechnical Engineering, 19*, 4559-4569.

Al-Layla, M. (1970). *Study of Certain Geotechnical Properties of Beaumont Clay.* Ph.D. Thesis: Texas A&M University.

Anagnostopoulos, C. and Georgiadis, K. (2004). Stabilization of a highway with piles in a landslide area. *Proc., 9th Int. Symposium on Landslides, 2*, pp. 1697-1700. Rio de Janeiro.

Arndt, B. M. (1977). *Stratigraphy of offshore sediment Lake Agassiz – North Dakota.* Report of Investigation No. 60: North Dakota Geological Survey, 58 pp.

ASTM D4318. (2017). *Standard Test Methods for Liquid Limit, and Plasticity Index of Soils.* ASTM International: West Conshohocken, PA.

Balasubramaniam, A. S., Munasinghe, N. T. K., Tennekoon, B. L., and Karunaratne, G. P. (1977). Stability of cut slopes for installation of penstocks. *Proc., Int. Symp. on the Geotechnics of Structurally Complex Formations, 1*, pp. 29-39. Capri.

Banks, D. (1978). *A reanalysis of the east Culebra Slide.* Ph.D. Thesis: Univ. of Illinois at Urbana-Champaign.

Bareither, C. A., Edil, T. B., and Benson, C. H. (2012). Investigation of White Bluffs Landslides in Washington State. *Proceedings of GeoCongress 2012*, (pp. 546-555). Oakland.

Bhandari, R. K. (1977). Some typical landslides in the Himalaya. *Proc., 2nd Int. Symp. on Landslides,* (pp. 1-24). Tokyo.

Bishop, A. (1954). Correspondence. *Geotechnique, 4*(1), 43-45.

Bishop, A. W. and Henkel, D. J. (1957). *The measurement of soil properties in the triaxial test.* London: E. Arnold.

Bishop, A. W., Green, G. E., Garga, V. K., Andresen, A., and Brown, J. D. (1971). A new ring shear apparatus and its application to the measurement of residual strength. *Geotechnique, 21*(4), 273–328.

Bishop, A.W., Webb, D.L. and Lewin, P.I. (1965). Undisturbed samples of London Clay from the Ashford Common Shaft: strength-effective stress relationships. *Geotechnique, 15*, 1-31.

Bjerrum, L. (1967). Progressive failure in slopes of overconsolidated plastic clay and clay shales. *J. Soil Mech. Found. Div., Am. Soc. Civ. Eng., 93*(5), 3–49.

Bjerrum, L., and Simons, N. E. (1960). Comparison of shear strength characteristics of normally consolidated clays. *Proc., Conf. on Shear Strength of Cohesive Clays, ASCE*, (pp. 711-726). New York.

Blight, G. E. (1963). The effect of nonuniform pore pressures on laboratory measurement of the shear strength of soils. In *Laboratory Shear Testing of Soils* (pp. 173-184). ASTM Special Technical Publication No. 361.

Bohac, J., Feda, J., Herle, I., and Klablena, P. (1995). Properties of fissured Brno Clay. *Proc., of the 11th European Conference on Soil Mechanics and Foundation Engineering, 3*, pp. 3.19-3.24. Copenhague.

Bouazza, A., W. F. Van Impe, and W. Haegeman. (1996). Some mechanical properties of reconstituted Boom Clay. *Geotechnical & Geological Engineering, 14*(4), 341–352.

Bromhead, E. N. (1979). A simple ring shear apparatus. *Ground Engrg., 12*(5), 40-44.

Bromhead, E. N. and Curtis. R. D. (1983). A comparison of alternative methods of measuring the residual strength of London Clay. *Ground Engineering, 16*, 39-41.

Bromhead, E. N. and Dixon. N. (1986). The field residual strength of London Clay and its correlation with laboratory measurements, especially ring shear tests. *Geotechnique, 36*(4), 449-452.

Brooker, E. W., and Peck, R. B. (1993). Rational design treatment of slides in overconsolidated clays and clay shales. *Can. Geotech. J., 30*, 526–544.

Burnett, A.D. and Fookes, P.G. (1974). A regional engineering geology study of the London Clay in the London and Hampshire basins. *Q.J. Eng. Geol., 7*, 257-295.

Butcher, A. P. (1991). The observation and analysis of a failure in a cliff of glacial clay till at Cowden, Holderness. *Proc. of the International Conference on Slope Stability*, (pp. 271-276). Isle of Wight.

Calabresi, G. and Rampello, S. (1987). Swelling of overconsolidated clays in excavations. *Proc., of the 9th European Conference on Soil Mechanics and Foundation Engineering, 1*, pp. 11-15. Dublin.

Cancelli, A. (1981). Evolution of slopes in overconsolidated clays. *Proc., 10th Int. Conf. on Soil Mechanics and Foundation Engineering, 3*, pp. 377–380. Stockholm.

Cancelli, A., and Olcese, A. (1984). Stabilization of landslide in sheared clay shale. *Proc., 4th Int. Symposium on Landslides, 2*, pp. 1-6. Toronto.

Carvalho, T. M. O., de Campos, T. M. P., Antunes, F. S. (2011). Effects of structure changes in the stress-strain-strength behavior of a sienitic residual soil. *Proc., of the 15th European Conference on Soil Mechanics and Foundation Engineering, 1*, pp. 143-148. Athens.

Casagrande, A. and Wilson, S. D. (1953). Prestress induced in consolidated-quick triaxial tests. *Proc., 3rd Int. Conf. on Soil Mechanics and Geotechnical Engineering, 1*, pp. 106-110. Zurich.

Casagrande, A., and Fadum, R. F. (1940). *Notes on soil testing for engineering purposes.* Harvard Soil Mechanics Series No. 8.

Casagrande, A., and Poulos, S. J. (1964). *Fourth report on investigation of stress-deformation and strength characteristics of compacted clays.* Harvard Soil Mechanics Series No. 74.

Cassel, F. L. (1948). Slips in fissured clays. *Proc., 2nd Int. Conf. on Soil Mechanics and Foundation Engineering, 2*, pp. 46-50. Rotterdam.

Castellanos, B. A. (2014). *Use and measurement of fully softened shear strength.* Ph.D. Thesis: Virginia Polytechnic Institue and State University.

Castellanos, B. A., and Brandon, T. L. (2013). A comparison between the shear strength measured with direct shear and triaxial devices on undisturbed and remolded soils. *Proc., 18th Int. Conf. on Soil Mechanics and Geotechnical Engineering*, (pp. 317-320). Paris.

Chandler, R. J. (1969). The effect of weathering on the shear strength properties of Keuper Marl. *Geotechnique, 19*, 321–334.

Chandler, R. J. (1974). Lias clay: the long-term stability of cutting. *Geotechnique, 24*(1), 21–38.

Chandler, R. J. (1982). Lias clay slope sections and their implications for the prediction of limiting or threshold slope angles. *Earth Surf. Processes Landforms, 17*, 427–438.

Chandler, R. J. (1984b). Delayed failure and observed strengths of firs-ttime slides in stiff clays. *Proc., 4th Int. Symposium on Landslides, 2*, pp. 19–25. Toronto.

Chandler, R. J. and Skempton, A. W. (1974). The design of permanent cutting slopes in stiff fissured clays. *Geotechnique, 24*(4), 457-466.

Chanlder, R. J. (1984a). Recent European experience of landslides in overconsolidated clays and soft rocks. *Proc., 4th Int. Symposium on Landslides, 1*, pp. 61–81. Toronto.

Choi, Y. K. (1982). *Consolidation behavior of natural clays.* Ph.D. Thesis: Univ. of Illinois at Urbana-Champaign.

Christiansen, E. (1982). The Denholm landslide, Saskatchewan. Part I: Geology. *Canadian Geotechnical Journal, 20*(2), 197-207.

Clarke, C. L., James, P. M., and Morgenstern, H. (1970). Foundation conditions at Munda Dam. *Proc., 2nd Int. Conf. Rock Mechanics, 13*, pp. 6-15. Belgrade.

Cooper, M. R., Bromhead, E. N., Petley, D. J., and Grant, D. I. (1998). The Selborne cutting stability experiment. *Geotechnique, 48*(1), 83–101.

Crabb, G. I., and Atkinson, J. H. (1991). Determination of soil strength parameters for the analysis of highway slope failures. *Proc., of the International Conference on Slope Stability*, (pp. 13-18). Isle of Wight.

Crawford, C. B. (1963). Cohesion in an undisturbed sensitive clay. *Géotechnique, 13*(2), 132-146.

D4318-10e1, A. (2010). *Standard Test Methods for Liquid Limit, and Plasticity Index of Soils.* West Conshohocken, PA,: ASTM International.

D'Elia, B., Distefano, D., Esu, F. and Federico, G. (1988). Deformations and stability of high cuts in a structurally complex formation: Analysis and prediction. *Proc., 5th Int. Symposium on Landslides, 1*, pp. 599-604. Lausanne.

D'Elia, B., Esu, F., Grisolia, M., and Tancredi, G. (1980). Stability of slopes in a clay shale formation. *Proc., 3rd Int. Symp. on Landslides, 1*, pp. 157-164. New Delhi.

D'Elia, B., Lanzo, G. and Rossi-Doria, M. (1991). Landsliding in the coastal slopes of Capo Spulico area in the Gulf of Taranto. *Proc. of the International Conference on Slope Stability*, (pp. 297-302). Isle of Wight.

Dev, K.L., Pillai, R. J., and Robinson, R. G. (2013). Estimation of critical state parameters from one-dimensional consolidation and triaxial compression tests. *Indian Geotech J, 43*(3), 229–237.

Di Maio, C., and Vassallo, R. (2011). Geotechnical characterization of a landslide in a Blue Clay slope. *Landslides, 8*(1), 17-32.

Dixon, N., and Bromhead, E. N. (1991). The mechanics of first-time slides in the London clay cliff at the Isle of Sheppey, England. *Proc., of the International Conference on Slope Stability*, (pp. 277–282). Isle of Wight.

Eden, W. J., and Jarrett, P. M. (1971). Landslide at Orleans, Ontario. *Technical paper no. 321, Div. of Build. Res., Nat. Res. Council of Canada, Ottawa, Canada*.

Eden, W. J., and Mitchell, R. J. (1970). The mechanics of landslides in Leda Clay. *Can. Geotech. J., 12*(3), 285-296.

Eid, H. T. (1996). *Drained shear strength of stiff clays for slope stability analyses.* Univ. of Illinois at Urbana-Champaign: PhD thesis.

Eid, H. T. (1996). *Drained shear strength of stiff clays for slope stability analyses.* PhD thesis: Univ. of Illinois at Urbana-Champaign.

Eid. H.T., and Rabie. K. H. (2017). Fully softened shear strength for soil slope stability analyses. *International Journal of Geomechanics, 17*(1), 1-10.

Eigenbrod, K.D. and Morgenstern, N.R. (1971). A slide in Cretaceous bedrock at Devon, Alberta. *Proc., Geotechnical Practice for Stability in Open Pit Mining*, (pp. 223-238).

Esu, F., Di Stefano, D. M., Grisolia, M., and Tancredi, G. (1984). Stability of a high cut in overconsolidated lacustrine deposits. *Proc., 4th Int. Symposium on Landslides, 2*, pp. 63-68. Toronto.

Feda, J., Bohác, J., and Herle, I. (1995). Shear resistance of fissured Neogene clays. *Engineering Geology, 39*(3-4), 171-184.

Feng, L. C. (1992). Modification and selection of strength parameters in calculating stabilities of loessal landslide. *Proc., 6th Int. Symposium on Landslides, 1*, pp. 403-408. Christchurch.

Focht, J. A. and Sullivan, R. A. (1969). Two slides in overconsolidated Pleistocene clays. *Proc. 7th Int. Conf. Soil Mech. and Found. Engng,, 2*, pp. 571-576. Mexico.

Gamez, J. A. and Stark, T. D. (2014). 2014. *Fully Softened Shear Strength at Low Stresses for Levee and Embankment Design, 140*(9), 1-6.

GEO-SLOPE. (2007). *Stability Modeling with SLOPE/W.* GEO-SLOPE International Ltd: Calgary, Alberta, Canada.

Ghahremannejad, B. (2003). *Thermo-mechanical behaviour of two reconstituted clays.* Ph.D. Thesis: University of Sydney.

Gibo, S. (1994). Ring shear apparatus for measuring residual strengths and it's measurement accuracy. *Journal of Japan Landslide Society, 31*(3), 24-30.

Gibson, R. (1953). Experimental determination of the true cohesion and true angle of internal friction in clays. *Proc., 3rd Int. Conf. in Soil Mechanics and Foundation Engineering, 1*, pp. 126-130. Zurich.

Gibson, R. E. and Henkel, D. J. (1954). Influence of duration of tests at constant rate of strain on measured "drained" strength. *Geotechnique, 4*(1), 6-15.

Glaser, J. D. (1971). *Geology and mineral resources of southern Maryland.* Maryland Geological Survey, 56 pp.

Gostelow, T.P. and Loucaides, G. (1988). Slope instability in allochthonous sediments: An example from the Moni Melange, Cyprus. *Proc., 5th Int. Symposium on Landslides, 1*, pp. 161-168. Lausanne.

Green, M. G., and Wallace, W. A. (1993). Large diameter tunneling in a soft clay shale - a case history of the San Antonio Flood Control Tunnels. *bit. J. Rock Mech. Min. Sci., 30*(7), 1461-1467.

Green, R. and Wright, S. G. (1986). *Factors affecting the long term strength of compacted Beaumont Clay.* Research Report 436-1, Center for Transportation Research, The University of Texas at Austin.

Gulla, G., Mandaglio, M. C., and Moraci, N. (2006). Effect of weathering on the compressibility and shear strength of a natural clay. *Canadian Geotechnical Journal, 43*(6), 618-625.

Henkel, D. J. (1956). The effect of overconsolidation on the behavior of clays during shear. *Geotechnique, 6*, 139-150.

Henkel, D. J., and Sowa, V. A. (1964). The influence of stress history on stress paths in undrained triaxial tests on clay. In *ASTM Special Technical Publication No. 361 (Laboratory shear testing on soils)* (pp. 280-291). West Conshohoken, PA: ASTM.

Heyerdahl, H., Jostad, H. P., Vernang, T. and Kalsnes, B. G. (2015). Case history: Failure of a clay sope involving tme effects. *Engineering Geology for Society and Territory, 2*, 1823–1827.

Hirschfeld, R. C. (1959). The relation between shear strength and effective stress. *Proc., Panamerican Conference on Soil Mechanics and Foundation Engineering.* Mexico.

Ho, K. K. S., Chao, P. A., Lau, T. M. F. and De Silva, S. (2012). Investigation of the 20 August 2005 fatal landslide at Fu Yung Shan Tsuen, Hong Kong. *Landslides, 10*(3), 285–297.

Hong. Z. S, Bian. X, Cui. Y. J, Gao. Y. F, Zeng. L. L. (2013). Effect of initial water content on undrained shear behaviour of reconstituted clays. *Géotechnique, 63*(6), 441–450.

Huang, M.S., Liu, Y.H., and Sheng, D.C. (2011). Simulation of yielding and stress–stain behavior of shanghai soft clay. *Computers and Geotechnics, 38*, 341-353.

Hutchinson, J. N. (1969). A reconsideration of the coastal landslides at Folkestone Warren, Kent. *Geotechnique, 19*, 6–38.

Huvaj-Sarihan, N. (2009). *Movement of reactivated landslides.* Ph.D. Thesis: University of Illinois at Urbana-Champaign.

Hvorslev, M. J. (1936). A ring shearing apparatus for the determination of the shearing resistance and plastic flow of soils. *Proc., 1st Int. Conf. on Soil Mechanics and Foundation Engineering*, *2*, pp. 125-129.

Hvorslev, M. J. (1939). Torsion ring shear tests and their place in the determination of the shearing resistance of soils. In ASTM, *Proc., Symp. of Shear Testing of Soils* (Vol. 39, pp. 999-1022).

Imrie, A. S. (1991). Stress-induced response from both natural and construction-related processes in the deepening of the Peace River Valley, B.C. *Can. Geotech. J., 28*(5), 718–728.

Insley, A.E., Chatterji, P.K., and Smith, L.B. . (1977). Use of residual strength for stability analyses of embankment foundations containing preexisting failure surfaces. *Canadian Geotechnical Journal, 14*(3), 408–428.

James, P. M. (1970). *Time effects and progressive failure in clay slopes.* PhD thesis: Univ. of London, London.

Janbu, N. (1977). Slopes and excavations in normally consolidated and lightly overconsolidated clays. *Proc., 9th Int. Conf. in Soil Mechanics and Foundation Engineering, 2*, pp. 549–566. Tokyo.

Johns, E. A., Burnett, R. G., and Craig, C. L. (1963). Oahe Dam: influence of shale on Oahe Power structure design. *Journal of the Soil Mechanics and Foundations Division, 89*(2), 95-113.

Kamal, R. H., Coop, M. R., Jardine, R. J., and Brosse, A. (2014). The post-yield behaviour of four Eocene-to-Jurassic UK stiff clays. *Geotechnique, 64*(8), 620–634.

Kankare, E. (1969a). *Geotechnical properties of the clays at the Kimola canal area with special reference to the slope stability.* PhD thesis: State Institute for Technical Research at Helsinki, Helsinki, Finland.

Kankare, E. (1969b). Failures at Kimola floating canal in southern Finland. *Proc., 7th Int. Conf., on Soil Mechanics and Foundation Engineering, 2*, pp. 609–616. Mexico.

Kawaguchi, T., Mitachi, T., and Shibuya, S. (2005). Drained and undrained elastic moduli of reconstituted clay. *Proc., 16th Int. Conf. on Soil Mechanics and Geotechnical Engineering, 2*, pp. 397-400. Osaka.

Kayyal, M.K. and Wright, S. G. (1991). *Investigation of long-term strength properties of Paris and Beaumont Clays in earth embankments.* Research Report 1195-2F, Center for Transportation Research, The University of Texas at Austin.

Kenney, T. C. (1967). Slide behavior and shear resistance of a quick clay determined from a study of the landslide at Selnes, Norway. *Proc. of the Geotech. Conf., 1*, pp. 57-64. Oslo.

Kenney, T. C. (1969). Stability of natural slopes and embankment foundations. *Proc., 7th Int. Conf. in Soil Mechanics and Foundation Engineering, 3*, pp. 381–385. Mexico.

Kenney, T. C., and Drury, P. (1973). Case record of the slope failure that initiated the retrogressive quick-clay landslide at Ullensaker, Norway. *Geotechnique, 23*(1), 33-47.

Kim, T.H., and Lee, K. (2006). Stress-strain behavior of remolded clay from intermediate principal stress controlled tests. *International journal of offshore and polar engineering, 16*(4), 313-319.

Kimura, S., Nakamura, S., and Vithana, S. B. (2015). Influence of effective normal stress in the measurement of fully softened strength in different origin landslide soils. *Soil & Tillage Research, 145*, 47-54.

Kjaernsli, B., and Simons, N. (1962). Stability investigations of the north bank of the Drammen river. *Geotechnique, 12*(2), 147–167.

Knight, D. K. (1963). Oahe Dam: geology, embankment, and cut slopes. *Journal of the Soil Mechanics and Foundations Division, 89*(2), 99-128.

Kong, L. W., Zang, M., Guo, A. G., and Tuo, Y. F. (2015). Effect of stress path on strength properties of Zhanjiang strong structured clay. *Rock and Soil Mechanics, 36*(1), 19-24.

LaGatta, D. P. (1970). Residual strength of clays and clay-shale by rotation shear tests. In *Rep. Harvard Soil Mechan. Ser. No. 86* (p. 204). Cambridge, Mass: Harvard Univ.

Lambe, T. W. (1985). Amuay Landslides. *Proc., 11th Int. Conf. on Soil Mechanics and Foundation Engineering, Golden Jubilee Volume,* pp. 137–158. San Francisco.

Larsen, A. (2011). *Laboratory investigation of the sealing properties of the Lea Park Shale with respect to carbon dioxide*. MS thesis: University of Saskatchewan.

Lau, W. H. (1988). *The behaviour of clay in simple shear and triaxial tests.* Ph.D. Thesis: City University of London.

Lefebvre, G. (1981). Fourth Canadian geotechnical colloquium: strength and slope stability in Canadian soft clay deposits. *Can. Geotech. J., 18*(3), 420–442.

Lefebvre, G., and LaRochelle, P. (1974). The analysis of two slope failures in Champlain sea clays. *Can. Geotech. J., 11*(1), 89–108.

Li, P. Q., and Baudet, B. A. (2016). Strain rate dependence of the critical state line of reconstituted clays. *Géotechnique Letters, 6,* 66-71.

Li, Q., Wu, H. W., and Liu, G. B. (2012). Low secondary compressibility and shear strength of Shanghai Clay. *J. Cent. South Univ., 19,* 2323-2332.

Li, T. D., and Zhao, Z. S. (1984). A method of back analysis of the shear strength parameters for the first-time slide of the slope of fissured clay. *Proc., 4th Int. Symposium on Landslides, 2*, pp. 127–129. Toronto.

Liu, X. L., Loo, H., Min, H., Deng, J. H., Tham, L. G., and Lee, C. F. (2006). Shear strength of slip soils containing coarse particles of Xietan Landslides. *Proc., sessions of GeoShanghai,* (pp. 142-149). Shanghai.

Maccarini, M. (1993). A comparison of direct shear box tests with triaxial compression tests for a residual soil. *Geotechnical and Geological Engineering, 11*(2), 69–80.

Magalhaes, J. A. C., Dias, R. D., Presa, E. P. and Campos, L. E. P. (1992). Deep-seated landslide of a granulite residual soil. *Proc., 6th Int. Symposium on Landslides, 2,* pp. 1375-1378. Christchurch.

Mandaglio, M. C., Moraci, N., Rosone, M., and Farulla, C. A. (2016). Experimental study of a naturally weathered stiff clay. *Canadian Geotechnical Journal, 53*(12), 2047–2057.

Marivoet, L. (1948). Control of stability of a sliding slope in a railway cut near Wetteren. *Proc., 2nd Int. Conf. on Soil Mechanics and Foundation Engineering, 2,* pp. 38-42. Rotterdam.

Marsland, A. (1972). The shear strength of fissured clay. *Stress-Strain Behavior of Soils, Rosco Memorial Symposium, Foulis*, (pp. 59–68). Henley-on-Thames, U.K.

Marsland, A. and Butler, M. E. (1967). Strength measurement on stif fissured Barton Clay from Fawley (Hampshire). *Proc. of the Geotech. Conf., 1*, pp. 139-145. Oslo.

Meijer Drees, N.C. and Myhr, D.W. (1981). The Upper Cretaceous Milk River and Lea Park Formations in Southeastern Alberta. *Bulletin of Canadian Petroleum Geology, 29*(1), 42-74.

Mesri and Shahien. (2003). Residual shear strength mobilized in first-time slope failures. *J. Geotech. Geoenviron. Eng, 129*(1), 12-31.

Mesri, G. (1969). *Engineering Properties of Montmorillonite.* Ph.D. Thesis: University of Illinois at Urbana-Champaign.

Mesri, G. and Ali, S. (1987). *Laboratory tests for soil mechanics and soil behavior.* University of Illinois at Urbana-Champaign, 93 p.p.

Mesri, G. and Cepeda-Diaz, A. F. (1986). Residual shear strength of clays and shales. *Geotechnique, 36*(2), 269–274.

Mesri, G. and Huvaj, N. (2004). Residual shear strength moblized in Red River slope failures. *Proc., 9th Int. Symposium on Landslides, 2*, pp. 925-931. Rio de Janeiro.

Mesri, G. and Huvaj-Sarihan, N. (2012). Residual shear strength measured by laboratory tests and mobilized in landslides. *Journal of Geotechnical and Geoenvironmental Engineering, 138*(5), 585-593.

Mesri, G. and Olson, R. E. (1970). Shear Strength of Montmorilonite. *Geotechnique, 20*(3), 261-270.

Mesri, G. and Shahien, M. (2003). Residual shear strength mobilized in first-time slope failures. *J. Geotech. Geoenviron. Eng, 129*(1), 12-31.

Mesri, G., and Abdel-Ghaffar, M.E.M. (1995). Cohesion intercept in effective stress-stability analysis. *Journal of Geotechnical Engineering, 119*(8), 1229-1249.

Mesri, G., and Ali, S. (1987). *Laboratory tests for soil mechanics and soil behavior.* University of Illinois at Urbana-Champaign, 93 p.p.

Mesri, G., and Ali, S. (1987). *Laboratory tests for soil mechanics and soil behavior.* University of Illinois at Urbana-Champaign, 93 p.p.

Mesri, G., and Cepeda-Diaz, A. F. (1986). Residual shear strength of clays and shales. *Geotechnique, 36*(2), 269–274.

Mesri, G., and Cepeda-Diaz, A. F. (1986). Residual shear strength of clays and shales. *Geotechnique, 36*(2), 269–274.

Mesri, G., and Huvaj-Sarihan, N. (2004). Residual shear strength moblized in Red River slope failures. *Proc., 9th Int. Symposium on Landslides, 2*, pp. 925-931. Rio de Janeiro.

Mesri, G., and Huvaj-Sarihan, N. (2012). Residual Shear Strength Measured by Laboratory Tests and Mobilized in Landslides. *J. Geotech. Geoenviron. Eng., 138*(5), 585–593.

Mesri, G., and Olson, R. E. (1970). Shear Strength of Montmorilonite. *Geotechnique, 20*(3), 261-270.

Mesri, G., and Olson, R. E. (1970). Shear Strength of Montmorilonite. *Geotechnique, 20*(3), 261-270.

Mesri, G., and Shahien, M. (2003). Residual shear strength mobilized in first-time slope failures. *J. Geotech. Geoenviron. Eng, 129*(1), 12-31.

Mesri, G., Pakbaz, M. C., and Cepeda-Diaz, A. F. (1994). Meaning, measurement and field application of swelling pressure of clay shales. *Geotechnique, 44*(1), 129-145.

Mesri, G., Ullrich, C. R., and Choi, Y. K. (1978). The Rate of Swelling of Overconsolidated Clays Subjected to Unloading. *Geotechnique, 28*(3), 281-307.

Mesri,G., Pakbaz, M. C., and Cepeda-Diaz, A. F. (1994). Meaning, measurement and field application of swelling pressure of clay shales. *Geotechnique, 44*(1), 129-145.

Mitchell, R. A., Hatch, S. E., and Siegel, R. A. (1992). Stability and closure design for a landfill on soft clay and peat. *Stability and performance of slopes and embankments, 2*, pp. 685-704. Berkeley.

Moon, A. T. (1984). Effective shear strength parameters for stiff fissured clays. *4th Australia-New Zealand Conference on Geomechanics*, (pp. 107-111). Perth.

Morgenstern, N. R. (1977). Slopes and excavations. *Proc., 9th Int. Conf. on Soil Mechanics and Foundation Engineering, 2*, pp. 567–581. Tokyo.

Morgenstern, N. R. (1990). Instability mechanisms in stiff soils and weak rocks. *Proc., 10th Southeast Asian Geotechnical Conf.*, (pp. 27–36). Taipei.

Morgenstern, N. R. and Price, V. E. (1965). The analysis of the stability of general slip surfaces. *Geotechnique, 15*(1), 79-93.

Nagaraj, T. S., and Somashekar, B. V. (1979). Stress deformation and strength of soils in plane strain. *Proceedings of the 6th Asian Regional Conference on Soil Mechanics and Foundation Engineering, 1*, pp. 43-46. Singapore.

Nakamori, K., Yang, P., and Sokobiki, H. (1996). Strength characteristics characteristics of undisturbed landslide clays in tertiary mudstone. *Soils Found., J. Jpn. Geotech. Soc., 36*(3), 75–83.

Nakano, R. (2002). On the validity of Japanese conventional method of taking cohesion as a function of depth in back analysesof landslides. *Proceedings of the first European conference on Landslides*, (pp. 661-666). Prague.

Nash, K. L. (1953). The shearing resistance of a fine closely graded sand. *Proc., 3rd Int. Conf. on Soil Mechanics and Foundation Engineering, 1*, pp. 160-164. Zurich.

Nichol, C. F., Froese, K., Sharma, J. S., and Barbour, S. L. (2016). Effects of oxidation on residual shear strength of shales within Lea Park Formation. *Canadian Geotechnical Journal, 53*(12), 1952-1964.

Ohtsuka, S., and Isobe, K. (2009). Deformation characteristics of clay at slip lines in repetitive type landslides. *Proc., 17th Int. Conf. on Soil Mechanics and Foundation Engineering, 3,* pp. 1682-1685. Alexandria.

Olson, R. E. (1962). Shear strength properties of Calcium Illite. *Geotechnique, 12*(1), 23-43.

Olson, R. E. (1963). Shear Strength Propertis of sodium illite. *Journal of Soil Mechanics & Foundations Div, 89*(SM1), 183-208.

Olson, R. E., and Campell, L. M. (1967). Bushing friction in triaxial shear testing. *Materials Research & Standards, 7*(2), 45-52.

Olson, R. E., McDonald, V. J., and Sterner, J. N. (1971). Control of Deformation Rates in Soil Testing. *Journal of the Soil Mechanics and Foundations Division, 97*(1), 283-286.

Parry, R. H. (1972). Some properties of heavily overconsolidated Oxford clay at a site near Bedford. *Geotechnique, 22,* 485–507.

Petley, D. (1966). *The Shear Strength of Soils at Large Strains.* Ph.D. Thesis: University of London.

Potts, D. M., Kovacevic, N., and Vaughan, P. R. (1997). Delayed collapse of cut slopes in stiff clay. *Geotechnique, 47*(5), 953–982.

Quigley, R. M. (1980). Geology, mineralogy, and geochemistry of Canadian soft soils: a geotechnical perspective. *Canadian Geotechnical Journal, 17*(2), 261-285.

Saihi, F., Leroueil, S., Rochelle, P. L., and French, I. (2002). Behaviour of the stiff and sensitive Saint-Jean-Vianney clay in intact, destructured, and remoulded conditions. *Canadian Geotechnical Journal, 39*(5), 1075-1087.

Schluger, P.R., and Roberson, H.E. (1975). Mineralogy and chemistry of the Patapsco Formation, Maryland, related to the ground-water geochemistry and flow system: A contribution to the origin of Red Beds. *Bulletin of the Geological Society of America, 86*(2), 153-158.

Schultze, E., and Horn, A. (1965). The shear strength of silts. *Proc., 6th Int. Conf. on Soil Mechanics and Foundation Engineering, 1*, pp. 350-353. Toronto.

Selvadurai A., and Ghiabi H. (2007). Consolidation behavior of a soft clay composite. *Proceedings of the 4th International Conference on Soft Soil Engineering - Soft Soil Engineering*, (pp. 437-446).

Sevaldson, R. A. (1956). The slide in Lodalen, October 6th, 1954. *Geotechnique, 6*(4), 167–182.

Silvestri, V. (1980). The long-term stability of a cutting slope in an overconsolidated sensitive clay. *Canadian Geotechnical Journal, 17*(3), pp. 337-351.

Sivakumar, V., Doran, I.G., and Graham, J. (2002). Particle orientation and its influence on the mechanical behaviour of isotropically consolidated reconstituted clay. *Engineering Geology, 66*(3/4), 197-209.

Skempton, A. W. (1948). The rate of softening in stiff fissured clays, with special reference to London clay. *Proc., 2nd Int. Conf. on Soil Mechanics and Foundation Engineering, 2*, pp. 50–53.

Skempton, A. W. (1964). Long-term stability of clay slopes. *Geotechnique, 14*(2), 77–101.

Skempton, A. W. (1970). First time slides in overconsolidated clays. *Geotechnique, 20*(3), 320–324.

Skempton, A. W. (1977). Slope stability of cuttings in Brown London clay. *Proc., 9th Int. Conf. on Soil Mechanics and Foundation Engineering, 3*, pp. 261–270.

Skempton, A. W. (1985). Residual strength of clays in landslides, folded strata and the laboratory. *Geotechnique, 35*(1), 3-18.

Skempton, A. W., and Brown, J. D. (1961). A landslide in boulder clay at Selset, Yorkshire. *Geotechnique, 11*(4), 280–293.

Skempton, A. W., and Petley, D. J. (1967). The strength along structural. *Proc., Geotechnical Conf., 2*, pp. 29-47. Oslo.

Skempton, A.W., Schuster, R.L. and Petley D.J. (1969). Joints and fissures in the London Clay at Wraysbury and Edgware. *Geotechnique, 19*(2), 205-217.

Sotiropoulos E., and Cavounidis, S. (1980). A case of minor slope failure in Marly clay, in Epirus, Greece. *J. Civ. Engrg. Des., 2*(2), 209-219.

Stallebrass, S. E., and Seward, L. J. (2011). The effect of mechanical remoulding on the compression and strength characteristics of a Mercia Mudstone. *Proc., of the 15th European Conference on Soil Mechanics and Foundation Engineering, 1*, pp. 281-286. Athens.

Stark, T. D. and Hussain, M. (2013). Empirical Correlations: Drained Shear Strength for Slope Stability Analyses. *J. Geotech. Geoenviron. Eng., 139*(6), 853–862.

Stark, T. D. and Vettel, J. J. (1992). Bromhead ring shear test procedure. *ASTM Geotechnical Teslillg Journal, 15*(1), 24-32.

Stark, T. D., and Eid, H. T. (1992). Comparison of field and laboratory residual strengths. *Proc., ASCE Spec. Conf. on Stability and Performance of Slopes and Embankments-II, A 25-Year Perspective. 1*, pp. 876–889. Geotechnique, Special Publication No. 31.

Stark, T. D., and Eid, H. T. (1993). Modified Bromhead ring shear apparatus. *ASTM Geotechnical Teslillg Journal, 16*(1), 100-107.

Stark, T. D., and Eid, H. T. (1994). Drained residual strength of cohesive soils. *J. Geotech. Eng, 120*(5), 856–871.

Stark, T. D., and Eid, H. T. (1997). Slope stability analyses in stiff fissured clays. *J. Geotech. Geoenviron. Eng, 123*(4), 335–343.

Stark, T. D., Choi, H., and McCone, S. (2005). Drained Shear Strength Parameters for Analysis of Landslides. *J. Geotech. Geoenviron. Eng., 131*(5), 575–588.

Sun, D., Chen, B., and Wei, C. (2014). Effect of fabric on mechanical behavior of marine clays. *Marine Georesources qnd Geotechnology, 32*(1), 1-17.

Suzuki, Y., and Dyvik, R. (2017). Comparisons of Two Reconstitution Methods for Clay Specimens. *ASTM Geotechnical Special Publication, GSP 280*, 347-357.

Taha, M. R., Hossain, M. K., Chik, Z., and Nayan, K. A. M. (1998). Geotechnical behaviour of a Malaysian residual granite soil. *Pertanika J. Sci. & Technol, 7*(2), 151-169.

Tavenas, F., Blanchet, R., Garneau, R., and Leroueil, S. (1978). The stability of stage-constructed embankments on soft clays. *Can. Geotech. J., 15*(2), 283-305.

Taylor, D. W. (1939). A comparison of results of direct shear and cylindrical compression test. *Proc., of Am. Soc. for Testing and Mat., ASTM,* (p. 1058). Conshohocken, Pa.

Terzaghi, K. (1936). Stability of slopes of natural clay. *Proc., 1st Int. Conf. on Soil Mechanics and Foundation Engineering, 1*, pp. 161–165.

Terzaghi, K., Peck, R. B., and Mesri, G. (1996). *oil mechanics in engineering practice, 3rd Ed.* New York: Wiley.

Thomson, S. (1971a). The Lesuer landslide, a failure in Upper Cretaceous clay shale. *Proc. 9th Annual Engineering Geology and Soils Engineering Symposium*, (pp. 257–287). Boise, Idaho.

Thomson, S. (1971b). Analysis of a failed slope. *Can. Geotech. J., 8*(4), 596–599.

Thomson, S., and Kjartanson, B. H. (1985). Study of delayed failure in a cut slope in stiff clay. *Canadian Geotechnical Journal, 22*(2), 286–297.

Toyota, H., Sugimoto, M., Nakamura, K., and Sakai, N. (2009). Ring shear tests to evaluate strength parameters in various remoulded soils. *Geotechnique, 59*(8), 649-659.

Valore, C. (1995). Structure and mechanical behaviour of tectonized clays. *Proc., of the 11th European Conference on Soil Mechanics and Foundation Engineering, 7*, pp. 7.149-7.156. Copenhague.

Valore, C., Ziccarelli, M., and Tedesco, A. M. (2007). An interpretation of the landsliding process affecting the town of Roccella Valdemone. *Proc., of the 14th European Conference on Soil Mechanics and Foundation Engineering, 2*, pp. 869-874. Madrid.

Wang, J. F., Li, Y. L., Gao, Y. B., and Yang, Y. X. (2011). Experimental Study on Structural Properties Influencing on Shear Strength of Soft Clay. *Advanced Materials Research, 243-249*, 2487–2490.

William, E. (2004). Understanding the effects of structure and bonding in the bringelly shale. *Geotechnical Practice Publication, Geo Jordan*, *1*, pp. 277-286.

William, E. (2005). *Engineering performance of Bringelly shale.* Ph.D. Thesis: University of Sydney.

Wilson, S. D. (1970). Observational data on ground movements related to slope instability. *J. Soil. Mech. Found Div., Am. Soc. Civ. Eng., 96*(SM5), 1521–1544.

Wong, S. and Ong, D. (2015). Characterization of reconstituted Malaysian kaolinite silts with varying clay contents. *Japanese Geotechnical Society Special Publication, 2*(11), 478-483.

Yagi, N., Enoki, M., and Yatabe, R. (1988). Consideration on mechanical characteristics of landslide clay. *Proc., 5th Int. Symposium on Landslides*, *1*, pp. 361-364. Lausanne.

Yan, W.M., and Ma, Y. (2010). Geotechnical characterization of Macau marine deposits. *Engineering Geology*, *113*(1-4), 62–69.

Yatabe, R., Yagi, N., Enoki, M., and Nakamori, K. (1991). Strength characteristics of landslide clay. *Journal of Japan Landslide Society*, *28*(1), 9-16.

Yong, R., and Vey, E. (1963). Dependency of stress locus on method of loading and pore pressure measurement. *Proceedings of the 2nd Asian Regional Conference on Soil Mechanics and Foundation Engineering*, *1*, pp. 126-129. Tokyo.

APPENDIX A: BACK-ANALYSES OF FIRST-TIME SLOPE FAILURES WITH A SEGMENT OF SLIP SURFACE AT RESIDUAL CONDITION

First-time slope failures in Brown London Clay

London Clay, which is one of the intensively studied stiff clays in UK, is a marine deposit of Eocene age, which crops out in the southeast of England (Skempton et al 1969, Skempton 1977). It was overconsolidated by the erosion of at least 150m of sediments. The upper 5 to 15 m of Lonon Clay is oxidized to a brown color, which overlies the massive blue-gray clay (Skempton et al 1969, Skempton 1977). The first-time slope failures were either in Brown London Clay, or included a basal part of slip surface along the contact between Brown and Blue London Clay. The main mineralogy of the clay fraction is illite and montmorillonite (Burnett and Fookes 1974). London clay is described as a stiff, fissured clay (Bishop et al 1965, Skempton and Petley 1967, Skempton et al 1969, Skempton and Chandler 1974, Skempton 1977). The plasticity index of Brown London Clay is in the range of 50% to 60%, with a typical value of 52%, and the liquidity index is close to 0 (Skempton 1977).

Skempton (1977) studied the time-dependent equilibration of porewater pressures, as a function of slope age, in cuttings in Brown London Clay, and suggested a porewater pressure ratio of 0.3±0.05 for "long term stability". In the present study, the porewater pressure ratio, reported or assumed in each first-time slide in the original references, was used for the reanalyses.

New Cross Cutting (Skempton 1977)

New Cross cutting, excavated in 1838 on the London & Croydon Railway, was one of the earliest deep cuttings in London Clay. The cut slope (Fig.A.1) with an inclination of 1 ½ :1, H: V, failed on 2 November 1841, 3 years after the excavation. The slip was 17m deep, and the back-scarp of slip surface cut through the Brown London Clay. It was reported by Gregory (1844) that, the base of the slip surface was on the contact between Brown and Blue London Clay, which is related to the greater shear strength of Blue London Clay. Porewater pressure equilibrium was not reached in New Cross cutting at the time of failure, and the porewater pressure ratio, $\bar{r}_u$, was reported to be -0.46.

In the present study, residual shear strength interpolated from Mesri and Shahien (2003), defined by I_p = 52%, was assigned to the basal part of the slip surface, which was on the contact between Brown and Blue London Clay. The back-calculated shear strength on the back-scarp of the slip surface, is slightly higher than that at I_p in the range of 50% to 60%, from the empirical correlation of fully softened shear strength developed in the present study.

Sudbury Hill (Skempton 1977)

The cutting at Sudbury Hill is on the Neasden-Northolt line of the Great Central Railway. The excavation began in 1903, and the slope failure took place on the south side in 1949. According to the piezometric reading, the porewater pressure equilibrium was reached by the time of failure, with a porewater pressure ratio, $\bar{r}_u$= 0.30. The entire 7m deep slip in the 3:1 (H:V) cut, was in Brown London Clay. The reanalysis in the present study, using the reported porewater pressure ratio, assumed a sub-horizontal basal part of the observed slip surface at residual shear strength condition near the toe (Fig.A.2), as a result of progressive deformation. The back-calculated mobilized shear strength on the rest of the slip surface, is close to the fully softened shear strength corresponding to I_p = 60%, from the proposed empirical correlation.

Northolt (James 1970)

Northolt cuttings are located to the east of Northolt Station, Metropolitan Line. The cuttings were made before the opening of the line in 1948, and it was assumed the slope age was 35 years by the time of failure. The slips which took place in 1955 along a considerable length of the line, were well documented by means of boreholes, piezometers, and trenches which were made to determine the slip surface. Five sections (Figures A. 3 to A. 7) were reported by James (1970), and studied in the present study. The slips in the 5 sections were 6.0 to 6.7m deep, and the porewater pressure ratio was in the range of 0.14 to 0.30.

All the slip surfaces in the 5 sections exhibited a curved back-scarp and a horizontal or sub-horizontal basal part on the contact between Brown and Blue London Clay. Residual shear strength interpolated from Mesri and Shahien (2003) was assigned to the basal portion of slip surface, which

yields the mobilized shear strength on the rest of the slip surface, similar to that defined by I_p = 50% - 60%, from the empirical correlation for fully softened shear strength in the present study.

Fareham (James 1970)

Fareham cut, located one mile north of Fareham Station, was excavated starting from 1898, but was completed after 9 years, because of the "treacherous ground". During the construction, several slips were reported. The slope failure in Fig.A.8 took place in 1961, with a maximum depth of sliding mass of 8m, and a width of 28m. The slip surface was determined by flexible plastic (Alkathene) tubes in the site investigation in 1962, and the porewater pressure ratio, $\bar{r}_u$ = 0.29, was assumed by James (1970). Assuming residual shear strength corresponding to I_p = 60% (Mesri and Shahien 2003) on the sub-horizontal basal part of the observed slip surface, the back-calculated moblized shear strength on the rest of the slip surface, is comparable to that at I_p = 60%, from the empirical correlation in the present study,

West Acton (James 1970)

The cutting on the westbound side above the westbound platform of the Central Line, West Acton, began in 1916, and the line was opened in 1920. The cut was shallow, with a depth generally less than 6m and slope inclination of 3:1 (H: V). The slips occurred in 1966 at the eastern end of the station, and two sections (8 and 9) are shown in Fig.A.9 and Fig.A.10. Back-analyses in the present study utilized the reported slip surfaces, and $\bar{r}_u$ = 0.30, assumed by James (1970), assigning residual shear strength defined by I_p = 60%, from Mesri and Shahien (2003), on the sub-horizontal base segment of the slip surface near the toe. The back-calculated mobilized shear strength on the back-scarp is slightly smaller than that at I_p = 60%, from the proposed empirical correlation for fully softened shear strength.

Tulse Hill (James 1970)

Tulse Hill cutting is located at the southern portal of the Knight's Hill Tunnel, on the upside line. The excavation started in 1867, and the line was opened the next year. Major slope failures

occurred in 1964, before which signs of movement were observed for a number of years. Investigations were carried out in the spring of 1964, which found that slipping was at two locations near the toe, indicating a wedge shaped failure (Fig.A.11). James (1970) suggested that the movements may be part of a retrogressive failure involving the entire slope. The four slips shown in Fig.A.11 were determined from slope indicators and surface features including large tension cracks. The largest slip was approximately 22m wide, and 5m deep. Water level measured by open tubes was considered not reliable, and porewater pressure ratio, $\bar{r}_u$= 0.30, was assumed by James (1970) and used in the back-analyses in the present study. Residual shear strength from Mesri and Shaien (2003), corresponding to I_p in the range of 50 – 60%, was applied to the horizontal basal portion of reported slip surface. A good agreement is obtained between the back-calculated shear strength on the rest of the slip surface and that defined by I_p = 50%-60%, from the empirical correlation in the present study,

Grove Park (James 1970)

The cutting on the north of Grove Park was excavated in 1984, and the line was opened the next year. The cut was 10 to 11m deep, with a 2:1 (H:V) slope. The slip shown in Fig.A.12, confined to the upper half of the slope, took place in 1962, and was determined by boreholes and alkanthene tube indicators. The investigation revealed that part of the failures was along the bedding plane, inclined around 5° to the horizontal. James (1970) assumed two porewater pressure condition for the slope, i.e. $\bar{r}_u$= 0.30 and 0.10, and suggested that the latter may be the more realistic case. The back-analysis in the present study, using $\bar{r}_u = 0.10$, and assigning residual shear strength at I_p = 60% (Mesri and Shahien 2003) on the basal segment of the slip surface along the bedding plane (Fig.A.12), gives the back-calculated mobilized shear strength on the back-scarp slightly lower than the empirical fully softened shear strength developed in the present study.

Kingsbury (James 1970)

Kingsbury cutting was excavated in 1931, located 120 m south of Kingsbury Station on the Bakerloo Line. The line was open in 1932, and the cut slope failed in 1947, 16 years after the excavation. Remedial measures were undertaken, but were not fully successful. The cut was 6m

high, with a 2 ¼: 1 (H: V) slope (Fig.A.13). The back-analysis in the present study, using the reported slip surface, and porewater pressure ratio of 0.30 assumed by James (1970), and applying residual shear strength defined by I_p = 50% (Mesri and Shahien 2003) on the sub-horizontal basal part of slip surface, gives the back-calculated mobilized shear strength on the back-scarp slightly greater than the empirical fully softened shear strength developed in the present study, corresponding to I_p in the range of 50-60%.

St. Helier (James 1970)

The cutting located between St. Heiler and Morden South Stations was excavated in 1930, and the line was opened the same year. The 2:1 (H: V) slope was 7 m deep (Fig.A.14), with a thin layer of sand at the top. Movements had been observed at this location during rainy seasons for years, with slipped materials at a water content close to the liquid limit. The failure, confined between two 18m-apart counterforts, took place in 1952, and extended 3m back into the top of the slope. The back-analysis in the present study, utilized the reported slip surface, and porewater pressure ratio of 0.25 assumed by James (1970). Residual shear strength interpolated from Mesri and Shahien (2003) at I_p = 50%, was assigned to the sub-horizontal basal portion of slip surface. The back-calculated shear strength on the back-scarp is slightly larger than that for I_p = 50% - 60%, from the proposed empirical correlation.

Crews Hill (James 1970)

The cutting made in 1908 and 1909 with a maximum depth of 6.2m is located on the Cuffley Line, south of Crews Hill. Several failures took place before 1956, and the slip in 1956, which was studied in the present study, was the best documented case. Sand and Gravel layers were observed at the top of the slope, but not involved in the slip shown in Fig.A.15. The basal portion of the slip surface was on the contact between Brown London Clay and Blue London Clay, and was assumed to be at residual shear strength condition [empirical residual shear strength from Mesri and Shahien (2003) at I_p = 60%]. Using the porewater pressure ratio, $\bar{r}_u = 0.30$ (James 1970), the back-calculated mobilized shear strength on the rest of the slip surface, is close to that defined by I_p = 60%, from the empirical correlation for fully softened shear strength developed in the present study,

Cuffley (James 1970)

This 7.2m high cutting is located between Enfield and Hertford, on the Endfield-Stevenage Line, south of the Cuffley Tunnel. The 3:1 (H: V) cutting was made sometime between 1910 and 1917, and slips were observed from the late winter of 1951. The failure studied here occurred sometime between 1953 and 1957, and is shown in Fig.A.16. The movements included two sections, the upper translational slip, and the subsequent lower slip which involved the whole slip. In the present study, only the first slip was studied (Fig.A.16). The back-analysis using porewater pressure ratio of 0.30 (James 1970), and applying residual shear strength defined by I_p = 60% (Mesri and Shahien 2003) on the sub-horizontal basal part of slip surface, gives the back-calculated mobilized shear strength on the back-scarp similar to the empirical fully softened shear strength developed in the present study, corresponding to I_p = 60%.

Whitstable (James 1970)

Whitstable cutting is approximately 10m deep, with an average slope of 3:1 (H: V). The excavation was made in 1860, and the line was opened the same year. The slip in 1959 in Fig.A.17, included a basal portion on Brown/Blue London Clay interface. A porewater pressure ratio of 0.30 (James 1970) was used in the back-analysis in the present study, together with residual shear strength defined by I_p = 50-60 % (Mesri and Shahien 2003) on the contact between Brown and Blue London Clay. A good agreement is obtained between the back-calculated shear strength on the rest of the slip surface and that corresponding to I_p in the range of 50% - 60%, from the proposed empirical correlation for fully softened shear strength.

Grange Hill (James 1970)

Grange Hill cutting is located on the Woodford-Chigwell Line Line, west of the Grange Hill Tunnel. The line was opened in 1947, but the excavation was made at the end of last century. The 12.2m high cut has an inclination of 3 ¼: 1 (H: V). The failure took place in 1950 (Fig.A.18) was 33m wide, with a maximum depth of sliding mass of 4.5m. The back-analysis in the present study, using $\bar{r}_u = 0.30$ (James 1970), and assigning residual shear strength at I_p = 60% (Mesri and Shahien 2003) on the basal segment of the slip surface, gives the back-calculated mobilized shear

strength on the back-scarp slightly lower than the empirical fully softened shear strength developed in the present study.

Hadley Wood (James 1970)

The 10m high cutting at Hadley Wood was excavated in 1850 and widened in 1882. The slip (Fig.A.19) studied here took place in 1947, and was 34m wide, with maximum depth of sliding mass of 5m. Residual shear strength from Mesri and Shaien (2003), corresponding to I_p = 60%, was applied to the horizontal basal portion of reported slip surface. Using the porewater pressure ratio, $\bar{r}_u = 0.30$, assumed by James (1970), the back-calculated mobilized shear strength on the rest of the slip surface is similar to the proposed empirical fully softened shear strength defined by I_p = 60%.

First-time slope failures in Oxford Clay

Oxford Clay is a marine deposition of Upper Jurassic Age, defined as a stiff clay or clay shale (James 1970). Oxford Clay is strongly laminated, and often contains sand and calcium carbonate (Parry 1972), which possibly contributed to the large mobilized shear strength on the back-scarp of the slip surface of first-time slides studied in the present study. The dominant mineralogy of Oxford Clay is illite (80%), with some Kaolinite and Montmorillonite (James 1970, Parry 1972). The liquid limit of Oxford Clay is in the range of 50% to 65%, and plastic limit is between 20% and 30%. Oxford Clay in the case histories studied in the present research, has a plasticity index in the range of 33% to 51% (James 1970).

Dauntsey (James 1970)

The cutting at Swindon to Bath Line, between Dauntsey and Whooten-Basset, was made in 1840. The slope failure occurred in the winter of 1960 in this 8m high cut. The slip surface was determined by alkathene tubes, with a long horizontal basal portion below the toe (Fig.A.20), which possibly followed the laminations of Oxford Clay. Piezometers and standpipes were used to locate the water table, and a corresponding porewater pressure ratio, $\bar{r}_u = 0.28$, was reported

by James (1970). Oxford Clay at this site has a plasticity index in the range of 33% - 51%. Residual shear strength interpolated from Mesri and Shahien (2003), defined at I_p = 43%, was applied to the horizontal basal part of the slip surface. The back-calculated mobilized shear strength on the back-scarp is larger than that from the empirical correlation in the present study for the corresponding I_p range.

Hullavington (James 1970)

The cut excavated in 1902 is located 2 miles east of Hullavington, on the Swindon Line. Instabilities were observed over some thirty years prior to the major slope failure in 1959. Various remedial measures were attempted before 1959, which were not successful. The slip in Fig.A.21, determined by post-failure investigation, including a tension crack at the top, was involved in 12m of the cut slope. Assuming residual shear strength at I_p = 33% (Mesri and Shahien 2003) on the sub-horizontal basal part of the slip surface near the toe, the back-analysis was carried out using a porewater pressure ratio of 0.30, assumed by James (1970). The back-calculated mobilized shear strength on the rest of the slip surface, is again greater than that from the proposed empirical fully softened shear strength.

Ampthill (James 1970)

Ampthill cutting locates at the London to Bedford Line, adjacent to Ampthill Tunnel. The 12m high cut was made in 1865, and failed in 1955. A second slip took place three years later in a nearby section. In the present study, only the first slip was examined, which was involved in the entire height of the cut slope (Fig.A.22). The back-analysis in the present study, using $\bar{r}_u = 0.30$ (James 1970), and assigning residual shear strength at I_p = 33% (Mesri and Shahien 2003) on the basal segment of the slip surface near the toe, gives the back-calculated mobilized shear strength on the back-scarp equal to that for I_p = 33%, from the empirical correlation for fully softened shear strength developed in the present study.

Bincombe (James 1970)

The cutting was made in 1849 to a 2:1 (H: V) slope, between Dorchester and Weymouth, on the south end of the Bincombe Tunnel. The first slip took place in 1890, and was analyzed in the present study. The slip involving the entire cut slope (Fig.A.23) has a maximum depth of sliding mass of 10m. A porewater pressure ratio, $\bar{r}_u = 0.30$ was assumed by James (1970). Applying residual shear strength interpolated from Mesri and Shahien (2003), defined by I_p = 34%, on the basal portion of the slip surface near the toe, the back-calculated shear strength on the rest of the slip surface, is greater than that from the proposed empirical correlation for fully softened shear strength.

First-time slope failures in Lias Clay

Lias Clay is a fissured, heavily consolidated, illitic Jurassic clay shale, having been subjected in the past to a maximum overburden in excess of 1000m (James 1970, Chandler 1972, Chandler 1974). According to ammonite evidence, Lias Clay is divided into three zones, Lower, Middle, and Upper. Middle Lias Clay contains significant amount of hard rock, and slope failures were only reported in Upper and Lower Lias Clay (James 1970).

Upper Lias Clay outcrops extensively in the Midland of England, which has a liquid limit range of 61% - 68%, plastic limit range of 27% - 31%, plasticity index range of 28% - 41%, and a natural water content below its plastic limit (Chandler 1972, Chandler 1974). Lower Lias Clay contains limestones or marls, and was reported to have a plasticity index in the range of 23% - 40% (James 1970, Chandler 1974). According to Mesri and Shahien (2003), for Upper Lias Clay which is laminated, the reported values of Atterberg limit underestimated the plasticity index of Upper Lias Clay. The residual shear strength of Upper Lias Clay on the horizontal and sub-horizontal basal part of slip surface, is more likely controlled by layers with higher plasticity index, while the mobilized shear strength on the back-scarp, cutting through various layers, is controlled by the entire slope material, which can be best characterized by an average plasticity index. In the present study, the slip surface of most of the first-time slope failures in Upper Lias Clay only include a short horizontal or sub-horizontal basal segment. Indeed, out of the 9 first-time slope failures in Upper Lias Clay, for 7 cases, the ratio of length of slip surface segment assumed at fully softened condition to total slip surface length, L_{fs}/L, ranges from 60% to 82%. Therefore, only for slips with

long segment at residual condition (Wellingborough with $L_{fs}/L = 45\%$), the residual shear strength on the basal portion of the slip surface was interpolated from Mesri and Shahien (2003) assuming $I_p = 50 – 60\%$, because the input residual shear strength in this case, would have a significant influence on the back-calculated mobilized shear strength on the back-scarp.

Chandler (1974), and Chandler and Skempton (1974) studied the ground water conditions for long term stability of cuttings in Upper Lias Clay, and established piezometric conditions, in terms of porewater pressure ratio, $\bar{r}_u$, in all the first-time slope failures, based on available piezometric data from 4 sites. The porewater pressure ratio, $\bar{r}_u$, ranges from 0.19 to 0.38 (Chandler 1974).

Slip surfaces in Lias Clay were determined by one of the three methods, 1) flexible plastic (Alkathene) tubes, 2) locating the "soft" shear zone in borings, and 3) observing the generally sharply dipping bedding within the slip and the horizontal bedding below the slipped mass, and noting the position of polished, slickensided shear surfaces. It should be noted that, Upper Lias Clay was capped by Northampton Sandstone in some cases. The back-analyses in the present study assumed tension crack filled with water at the time of failure, as suggested by Chandler (1974).

Hunsburry Hill (Chandler 1974, Chandler and Skempton 1974)

The approach cutting to the south portal of the tunnel at Hunsburry Hill, on the London-Northampton railway, was excavated about 1877, to a depth of 21m. The slip in Fig.A.24 took place in 1921 in the 2 ¼: a (H: V) cut slope. The Upper Lias Clay in this site was capped by Northampton Sand, and tension crack was observed in the sand, with back-analysis assuming tension crack filled with water at the time of failure (Chandler 1974). It was suggested by Chandler and Skempton (1974) that, for the cut at Hunsburry Hill, where the porewater pressure had not yet reached the long term values, the porewater pressure ratio, $\bar{r}_u$, was 0.19. Applying residual shear strength at $I_p = 32\%$ (Mesri and Shahien 2003) on the basal segment of the slip surface near the toe, a good agreement is obtained between the back-calculated shear strength on the rest of the slip surface and that from the empirical correlation of fully softened shear strength developed in the present study.

Barrowden (Chandler 1974, Chandler and Skempton 1974)

In 1961, about 83 years after the excavation, a slip occurred in a 5m high cut slope of the now disused Stamford to Seaton line about 2 km south of Barrowden. The slip was involved in the entire slope, which consists of a sandstone head and underlying Upper Lias Clay (Fig.A.25). The slip surface was determined in the tube samples recovered from hand auger holes in which piezometers were subsequently installed to establish the ground water condition. It was suggested by Chandler (1974) that, the failure was triggered by unusually high season porewater pressures, because no movement was observed in the post-failure investigation. The ground water table corresponding to this high porewater pressure at the time of failure, is shown in Fig.A.25. Although the basal portion of the reported slip surface is more or less curved, residual shear strength interpolated from Mesri and Shahien (2003), at I_p = 31%, was applied to the segment at elevation below the toe. The back-calculated mobilized shear strength on the back-scarp, is lower than that defined by I_p = 28% - 41%, from the empirical fully softened shear strength developed in the present study,

Stowehill (Chandler 1974, Chandler and Skempton 1974)

The cutting at the approach to the south portal of the Stowehill tunnel, on the London-Rugby main line, south of Weedon, Northamptonshire, was constructed in about 1835. A slope failure took place in this 10m deep cut in 1901 and stabilized by the installation of counterfort drains. A porewater pressure ratio of 0.23, was assumed by Chandler (1974), and Chandler and Skempton (1974). In the present study, a short sub-horizontal segment near the toe was assumed to be at residual condition (Fig.A.26), by applying residual shear strength from Mesri and Shahien (2003), defined by I_p = 31%. The back-calculated mobilized shear strength on the rest of the observed slip surface is slightly lower than that from the empirical correlation in the present study.

Wellingborough (Chandler 1974, Chandler and Skempton 1974)

The 10m cutting north of Wellingborough station was made in about 1855. A slip occurred in 1960 (no details available) and a second slip adjacent to it took place in May 1961. Although the cut slope was regraded and a retaining wall was constructed after the 1961 failure, a reactivation of

the second slip took place in March 1964. By superimposition of the 1964 slip surface, which was determined by Alkathene tube indicators, on the 1961 cutting slope profile, the slip surface of 1961 slip was obtained and is shown in Fig.A.27. A thick Northampton Sand was on the top of Upper Lias Clay, where a tension crack was observed. A porewater pressure ratio of 0.20, suggested by Chandler and Skempton (1974), was used in the back-analysis in the present study. By applying a residual shear strength corresponding to Ip = 50 – 60%, suggested by Mesri and Shahien (2003), to the long sub-horizontal basal segment of slip surface in Wellingborough, the back-calculated secant friction angles on the back-scarp, turned out to be comparable to those at reported Ip = 28% - 41%, from the empirical correlation for fully softened shear strength in the present study,

Ardley Tunnel (James 1970, Chandler 1974, Chandler and Skempton 1974)

The cutting was excavated in 1908, at the Bunbury end of the Ardley Tunnel, on Bicester to Bunbury Line. In 1960 a slip occurred in this cut slope, partially rupturing the retaining wall near the tunnel portal. The slip located by Alkathene tube indicators, was 6m deep, including a tension crack in the thick Northampton Sandstone capping the Upper Lias Clay (Fig.A.28). It was suggested by James (1970) that the presence of Northampton Sandstone possibly resulted in the measured high ground water table. A short basal segment near the toe was assumed to be at residual condition (Fig.A.28), by applying residual shear strength from Mesri and Shahien (2003), defined by I_p = 31%. The back-calculated mobilized shear strength on the rest of the observed slip surface is similar to that from the empirical correlation in the present study for fully softened shear strength, at the lower bond of reported plasticity index.

Charwelton (James 1970)

The 10m high cutting located 15 miles south of Rugby, near Charwelton Station, was widened in 1939. No failures were recorded before the widening. On 19th April, 1955, a slip developed over some 50m length, with instability observed two days before. The slip was active for a week or more. Post-failure investigation by means of six boreholes and a trench, located the slip surface in Fig.A.29. James (1970) reported that the slip surface was dry except for the toe area, and suggested that the failure might have been triggered by a plane of weakness. Residual shear strength at Ip =

34%, interpolated from Mesri and Shahien (2003), was applied to the sub-horizontal basal portion of the slip surface, and a porewater pressure ratio of 0.30, assumed by James (1970), was used for the back-analysis in the present study. The back-calculated mobilized shear strength on the back-scarp is higher than the empirical fully softened shear strength developed in the present study. It should be noticed that, according to the available information on porewater pressure ratio and slope age, reported by Chandler (1974), and Chandler and Skempton (1974), a porewater pressure ratio of 0.30, is probably too high for a cut slope 16 years old. A more reasonable, smaller porewater pressure ratio, would result in a lower back-calculated shear strength mobilized on the back-scarp.

Standish JCT (James 1970)

The Standish Junction cutting was made in 1835, between Haresfield and Stonehouse Stroud, in Lower Lias Clay covered by clayey head and mudflows. Slips along the cutting were observed for many years, in sections varying from 3 to 8m in height. The failure in 1964, located by 12 boreholes, was below depressions in the base of the Head (Fig.A.30). James (1970) suggested that the slip was in the upper soft clay. The back-analysis in the present study, using $\bar{r}_u = 0.30$ (James 1970), and assigning residual shear strength at I_p = 31% (Mesri and Shahien 2003) on the short sub-horizontal basal segment of the slip surface near the toe, gives the back-calculated mobilized shear strength on the back-scarp comparable to the proposed empirical fully softened shear strength, at the lower bond of reported plasticity index.

Wothorpe (James 1970, Chandlsdder 1974, Chandler and Skempton 1974)

The road cutting forming an underpass to the Stamford by-pass, approximately, 6m deep, was excavated in 1959, and slips occurred during construction. During the winter of 1964 and 1965, a shallow slip (Fig.A.31), with maximum depth of sliding mass less than 2m, developed at the eastern end of the cutting with a top solifluxion layer. The slip surface of the 1964-1965 failure was determined based on the points of deflection of piezometer tubes, which were installed in 1967, with their tips just below the slip surface. The ground water condition obtained using piezometers, corresponded to a porewater pressure ratio of 0.37 (Chandler 1974, Chandler and Skempton 1974). In the present study, a short sub-horizontal segment near the toe was assumed to be at residual condition (Fig.A.31), by applying residual shear strength from Mesri and Shahien

(2003), defined by I_p = 41%. The back-calculated mobilized shear strength on the rest of the observed slip surface is slightly lower than that at I_p = 41%, from the empirical correlation for fully softened shear strength in the present study.

Heyford (James 1970, Chandler 1974, Chandler and Skempton 1974)

The London-Rugby railway, constructed in 1835, cut through the toe of a slope near Heyford, resulting a 10m high cutting on the west side of the line. The shallow slip (maximum depth of sliding mass of 3m) occurred in Jan. 1961 (Fig.A.32), was located by Alkathene tube indicators. Chandler (1974), and Chandler and Skempton (1974), suggested porewater pressure ratio, $\bar{r}_u = 0.22$, for this cut slope. The back-analysis in the present study, assigning residual shear strength at I_p = 28%, interpolated from Mesri and Shahien (2003), to the short sub-horizontal basal portion of the slip surface, yields back-calculated mobilized shear strength on the back-scarp comparable to that defined by the reported plasticity index range, from the empirical correlation in the present study for fully softened shear strength,

Seaton (Chandler 1974, Chandler and Skempton 1974)

In 1963, about 68 years after the excavation, a slip occurred in a 9m high cut slope of the now disused Stamford to Seaton-Uppingham line 4 km northeast of Seaton. The slip was involved in the entire slope, consisting of a sandstone head and underlying Upper Lias Clay (Fig.A.33). The slip surface was determined in 1969, in the tube samples recovered from hand auger holes in which piezometers were subsequently installed to establish the ground water condition. The maximum ground water level corresponded to a porewater pressure ratio of 0.38 (Chandler 1974, Chandler and Skempton 1974). In the present study, a short sub-horizontal basal segment of observed slip surface was assumed to be at residual condition (Fig.A.33), by applying residual shear strength from Mesri and Shahien (2003), defined by I_p = 29%. The back-calculated mobilized shear strength on the rest of the slip surface is slightly lower than that at I_p = 28% - 41%, from the proposed empirical fully softened shear strength.

First-time slope failure in Atherfield Clay, at Haslemere (James 1970)

The cutting a quarter mile north east of Haslemere Station, UK, was excavated in 1859. A failure occurred in 1960 at the south east side of the 5m high cutting in Atherfield Clay, underlain by the Hythe Beds. The slip extended along some 60m of the line. Atherfield Clay is of Cretaceous Age, at the upper part of the Lower Greensand series. It consists of blue and black stiff clay/clay shales and mudstone, with ironstone concretions, and is sometimes turns into sands or glauconitic towards the top. Atherfield Clay is subjected to natural landslips, which affect the overlying Hythe and Sandgate Beds. The liquid limit, plastic limit, and plasticity index of Atherfield Clay at Haslemere, is 40%, 19%, and 21%, respectively. A porewater pressure ratio of 0.30, suggested by James (1970), was used in the back-analysis in the present study. By applying a residual shear strength corresponding to Ip = 21%, interpolated from Mesri and Shahein (2003), to the sub-horizontal basal segment of the observed slip surface (Fig.A.34), the back-calculated shear strength on the back-scarp, is slightly higher than that from the empirical correlation for fully softened shear strength developed in the present study.

First-time slope failure in Weald Clay

Weald Clay is a stiff clay in UK, of lacustrine or deltaic origin, derived from Paleozoic and Mesozoic rocks, and deposited in a subsiding basin. Weald Clay, consisting of shales, mudstones, silts, soft sandstones and limestones, was deposited during a quiet period, often exhibiting inclined beddings (James 1970). It is dark, and weathered to brown or grey. The dominant mineralogy of Weald Clay is Illite, with a smaller amount of Kaolinite. The liquid limit, and plasticity index, of Weald Clay, according to James (1970), ranges from 41% to 65%, and 22% to 39%, respectively.

Hildenborough (James 1970)

Hildenborough cutting is located on Sevenoaks to Hildenborough Line. The 12m high cut was constructed in 1868, and failed in 1936. The slip in Weald Clay has a maximum depth of sliding mass less than 4m (Fig.A.35). The porewater pressure ratio of 0.30, assumed by James (197), was used in the back-analysis. In this case, the back-analysis was carried out assuming similar shear strength condition on the entire slip surface, because there was no distinct horizontal or sub-

horizontal basal segment. The back-calculated shear strength is lower than that at the reported plasticity index range, from the empirical correlation for fully softened shear strength in the present study. It is possible that a major portion of the slip surface was on the inclined bedding plane which was at residual shear strength condition.

Earlswood (James 1970)

The cutting excavated in 1899 near Redhill, north of Earlswood Station, failed on the east side in May 1966. Alkathene tubes were used to determine the slip surface. A 5m tall retaining wall was involved in the slip, which forced the basal segment of the slip surface to develop below the base of the wall (Fig.A.36). The porewater pressure ratio of 0.30, assumed by James (197), was used in the back-analysis. The basal segment of the slip surface, which was forced to develop below the base of the wall was assumed to be at residual condition, by applying residual shear strength at I_p = 39%, from Mesri and Shahien (2003). The back-calculated mobilized shear strength on the back-scarp of the slip surface, is close to that defined by I_p = 22%, from the empirical correlation for fully softened shear strength developed in the present study.

First-time slope failures in other stiff clays and clay shales

Albedosa, Italy (Cancelli 1981)

The first-time slide (Fig.A.37) in 1978 at the source of a small stream tributary of River Albedosa, near S. Cristoforo, Italy, was induced by the slope angle increase as a result of continuous erosion at the head of the valley by the stream source. The sliding mass was approximately 70m long and 45m wide, with a maximum height of 14m. The slope material, from top to bottom, are, 3m colluvial cover, 5m weathered Lugagnano Clay, and unweathered Lugagnano Clay, respectively. The index properties for the slope material are fairly consistent, with natural water content around 30%, plasticity index between 22% and 34%, and clay size fraction between 20% and 40%, respectively. Lugagnano Clay was defined as “weakly marly clay” (Cancelli 1981) according to the calcium carbonate content, which is a fissured, overconsolidated clay.

The slip surface and the piezometric level at failure reconstructed by geomorphological survey, drainage trench, and 3 borings are shown in Fig.A.37. Because 1) the slip surface is more of a

translational type, 2) Lugagnano Clay is highly fissured, and 3) part of the slip surface (basal portion) may be at the bedding contact according to the sloping ground topography, a residual segment was determined assuming inclined stratigraphy. The residual shear strength at Ip = 26% interpolated from Mersri and Shahien (2003), results to the back-calculated mobilized shear strength on the rest of the slip surface close to that defined by I_p = 34%, from the empirical correlation for fully softened shear strength developed in the present study, and in the range of the measured fully softened shear strength (Cancelli 1980) on remolded Lugagnano Clay in triaxial compression tests.

Wettern, Brussels (Marivoet 1948)

The 10m high railway cutting near Wettern, Brussels, was excavated in the early years of the nineteenth century, and protections such as retaining walls at the toe were constructed. In spite of all the protections, a slip took place in 1943. Post-failure investigation by means of deepsounding tests and 7 borings, revealed that the cut slope consists of Yellow Loam, Blue Clay, and fine sand, in a downward session. The sliding mass was only in the loam and clay. The loam has a plasticity index range of 12% - 25%, and Blue Clay has a plasticity index between 60% and 100%. Based on the observed displacements and the boundary between "weak" material and undisturbed materials, two possible slip surfaces were determined by Marivoet (1948), assuming a circular slip surface. The slip surface (Fig.A.38) which cuts through the loam, and follows the contact between the upper loam and lower clay, is considered to be more realistic, because the basal portion of slip surface, is more likely to be controlled by the weaker Blue Clay of very high plasticity index. The most unfavorable ground water condition determined by piezometers is shown in Fig.A.38.

Residual shear strength interpolated from Mesri and Shahien (2003), at I_p = 100%, was applied to the basal portion of the slip surface, namely, on the contact between the loam and clay. The back-calculated mobilized shear strength on the rest of the slip surface, is close to that corresponding to I_p = 25%, from the proposed empirical correlation for fully softened shear strength.

Akitsu, Japan (Nakamori et al 1996)

Akitsu landslide was triggered by heavy rainfall at the end of the rainy season in 1991, which was one of the typical landslides in Tertiary mudstone along the Inland Sea coast of Japan. This landslide was considered to be a first-time failure (Nakamori et al 1996) because there was no record of a large-scale landslide in this region. The landslide in a slope of an average inclination of 12 degrees, was approximately 100m wide and 80m long (Fig.A.39). The highest and lowest ground water level were determined during December 1992 and January 1995 by three automatic water-level gauges. The slip surface determined by inclinometers cutting through the mudstone merged to the boundary between mudstone and sandstone. The heavily overconsolidated Tertiary mudstone with few fissures, has a natural water content of 29%, liquid limit of 76%, plasticity index of 60%, and clay size fraction of 46%.

Because part of the slip surface was at the contact between the mudstone and sandstone, residual shear strength at Ip = 60%, interpolated from Mesri and Shahien (2003) was applied to this basal portion. The back-analysis using lowest water level (Fig.A.39), yields the back-calculated mobilized shear strength on the rest of the slip surface comparable to that defined by Ip = 60%, from the empirical correlation for fully softened shear strength, developed in the present study. The back-calculated shear strength on the back-scarp is lower than the shear strength measured on undisturbed specimens (solid circles) in direct shear tests by Nakamori et al (1996).

Capo Spulico, Italy (D'Elia et al 1991)

To study the instability of coastal slopes in Capo Spulico, Italy, 10 years of investigation was carried out in 3 zones in this area. The climax of first-time landslide occurrence in Zone 1, in the winter of 1972 and 1973, coincided with the peak of cumulative rainfall in 4 to 6 months. It is therefore, suggested by D'Elia et al. (1991) that the first-time slope failures were triggered by the excessive rainfall which significantly increased the porewater pressure in the slopes in this semi-arid area. The cross-section of one of the first-time landslides is shown in Fig.A.40, and the slip surface was determined from ground morphological evidence and borehole logs. The slip was shallow with maximum depth less than 30m, compared to its length of approximately 300m.

The coastal slope in Capo Spulico mainly consists of "Argille Varicolori", which is a structurally complex clayshale formation. In some areas the clayshale is formed of minute scales with slickensided surfaces where tectonic stress has been significant. The weathered clayshales in the surface to 10 m depth in the slope are loosened and weathered. According to the investigation, the landslide material has a plastic limit ranging from 21% to 36%, liquid limit ranging from 53% to 61%, and plasticity index ranging from 32% to 42%. D'Elia et al. (1991) obtained a factor of safety of 1 for the slope stability analysis when the ground water level was 0 to 1m below the ground surface, and concluded that this shallow ground water level is reasonable for the recorded climax of cumulative rainfall. Therefore, this assumption of water level 0 to 1m below the ground surface was used in this research, which gives an average $\bar{r}_u$ of 0.47 to 0.51.

It was assumed that the sub-horizontal basal part of the slip surface (Fig.A.40) was at residual condition. The back-calculated shear strength on the back-scarp is comparable to that from the empirical correlation for fully softened shear strength, developed in the present study, when the water level is at ground surface ($\bar{r}_u$=0.51), and slightly lower than that from the empirical correlation, when the water level is 1m below the ground surface ($\bar{r}_u$=0.47). Similar results are obtained by using the reported residual friction angle of 13 degree (straight line in Fig.A.40) from ring shear tests on remolded landslide material (D'Elia et al 1991). The present assumption and its results are consistent with the conclusion made by D'Elia et al. (1991) in terms of the magnitude of shear strength. By using average effective normal stress and average shear strength for the slip, D'Elia et al. (1991) obtained an average friction angle of 20 to 22 degrees for the water level range, and suggested that the mobilized shear strength corresponds to the fully softened condition. The average friction angle of 20 to 22 for the effective normal stress range in the slip is in between the secant fully softened friction angle and residual friction angle. The shear strengths of undisturbed partially weathered clayshale in Fig.A.40, determined from direct shear tests (D'Elia et al. 1991), are not significantly higher than the shear strengths mobilized on the back-scarp of the slip surface.

Isle of Sheppey, England (Dixon and Bromhead 1991)

A number of first-time slides in the north coast of the Isle of Sheppey, England, where the slopes have been steepened by erosion, was investigated by researchers. Particular attention was paid to an area around Warden Point because the rate of cliff retreat there was such that a number of first-

time slides were recorded in 1970s and 1980s (Dixon and Bromhead 1991). These slope failures occurred in London Clay which was extensively investigated; therefore, the index properties used in the back-analysis here are selected based on earlier research by James (1970), Chandler and Skempton (1974), Skempton (1977).

Porewater pressure measurement was carried out from September 1983 to 1985 in the slopes which had been actively eroded. The response of simple standpipe type piezometer indicated a depressed porewater pressure. Suction existed in the slopes in the long term, which is expected due to the stress relief caused by rapid erosion. Four slope failure areas with certain length in Warren Point from east to west were investigated. Inclinometers were installed to determine the slip surfaces in each area, and the general mode of failure was classified as rotational sliding (Dixon and Bromhead 1991). It was suggested that the variation of position and shape of slip surface is probably controlled by the planes of weakness (Dixon and Bromhead 1991). Field evidence also indicated that the base of slip was sub-horizontal, paralleling to the dip of bedding.

Because sufficient data was not available for back-analysis for single first-time slope failure, a typical "idealized" cross-section (Fig.A.41) was developed. The slope file was based on the 1984 survey at the studied area K38 as it provides a representative slope angle for the cliffs in Warren Point. The slip surface with a curved back scarp and a horizontal base was determined from field evidence. The ground water condition used in the present study (Fig.A.41) was measured at K38. Positive porewater pressure existed in the back-scarp while negative porewater pressure was recorded in the planar base.

Residual strength based on the empirical correlation at I_p = 50% - 60%, from Mesri and Shahien (2003), was applied to the horizontal basal portion of the slip surface, which gives the mobilized shear strength on the back-scarp slightly higher than that defined by this plasticity index range, from the empirical correlation for fully softened shear strength developed in the present study. Dixon and Bromhead (1991) first assumed uniform shear strength distribution and obtained a constant friction angle of 16° from back-analysis for the entire slip surface. This assumption was regarded as unrealistic according to Dixon and Bromhead (1991), indeed, a non-uniform distribution of shear strength was then assumed by Dixon and Bromhead (1991) to examine the slope failure. Dixon and Bromhead (1991) assigned a constant friction angle of 20° on the back scarp, which is equal to the fully softened friction angle of London Clay suggested by Skempton

(1977), and obtained a back-calculated mobilized friction angle of 14° on the horizontal basal segment. This assumption of non-uniform shear strength distribution was based on field evidence at the slip base, such as a fault with 1meter throw, and a scree like material at K38.

Dixon and Bromhead (1991) concluded that the first-time slope failures in Warden Point are controlled by the depressed porewater pressure caused by erosion type of stress relief, and the position and shape of slip surface are controlled by the beddings in London Clay. The shear strength on the horizontal base had reduced to residual condition.

Grava, Greece (Sotiropoulos and Cavounidis 1980)

A minor landslide, Grava, took place in early spring 1975, about 9 months after its excavation for a new highway in western Epirus, Greece, where several slides occurred during or after the rainy season when the excessive precipitation significantly increased the ground water level. The Ionian area where the slides occurred is hilly to almost mountainous, and is a geosyncline zone which has not yet equilibrated. The slides were all on the western side of the hills, about 1 km inland from the coastline of Inion Sea. The slide has a maximum depth of 6 m and a width of 16m (Fig.A.42)

The area has 2 major formations, namely, Pliocene upper formation and Triassic limestone (bedrock). The Pliocene upper formation consists of successive layers of marly clays, sand-gravels or conglomerates (Fig.A.42). The Grava slide occurred in the blue marly clay, which is a stiff to very hard, overconsolidated and fissured clay with occasionally polished surfaces. Surface sampling reveals the presentative plasticity index in the range from 38% to 48% for the blue marly clay, with plastic limit from 17% to 23%, and liquid limit from 33% to 70%. The possible slip surface (Fig.A.42) was established by Sotiropoulos and Cavounidis (1980) based on the position and orientation of the back-scarp, and the bulge of the ground at the toe. It should be noticed that unlike the other slides in this area which occurred under very high ground water level, Grava slide took place in a condition that the ground water level was much blow the toe of the slope as shown in Fig.A.42 ($\bar{r}_u = 0$ according to Sotiropoulos and Cavounidis 1980).

It was assumed that the residual condition had been reached on the sub-horizontal basal portion of the slip surface. Back-analysis using the empirical residual strength from Mesri and Shahien (2003) corresponding to I_p = 48%, together with the established slip surface and $\bar{r}_u = 0$, results to the

back-calculated mobilized shear strength on the back-sharp close to that at the reported I_p range, from the proposed empirical correlation for fully softened shear strength.

Devon, Canada (Eigenbrod and Morgenstern 1971)

In the summer of 1965, highway improvements required a cut at the North wall of the valley of the North Saskatchewan River near the townsite of Devon about 12 miles upstream of Edmonton, Alberta. A landslide occurred during fall, 2 month after highway reconstruction. As shown in Fig.A.43, the 20m high slope has an angle of approximately 20°, and landslide mass has a maximum depth of 13m. This first-time landslide formed within a significantly larger slide block that had moved presumably at the formation of the valley (Eigenbrod and Morgenstern 1971).

The field investigation includes 5 pits at the toe of the slide, 7 boreholes around it and piezometers installed at various depth. The slide occurred in the bedrock, Upper Cretaceous Edmonton Formation, which consists of interbedded mudstone, claystone, siltstone, and sandstone. Bentonite layers and coal seams are also present in the deposit. According to the field investigation at the landslide site, the back-scarp of the slip surface cuts through the upper 5 to 6m till overlying a thin coal seam underlain by the bedrock consisting of carbonaceous claystone, bentonite, fissured siltstone and clay stone, and bentonitic sandstone. The horizontal segment of the slip surface is at the boundary of the bentonitic clay and the coal. With additional information including the measured back-scarp inclination between 55° to 60° to the horizontal and the top point of the slide on the slope, a most critical slip surface was interpolated using Mogenstern and Price's method. As suggested by Eigenbrod and Morgenstern (1971), this critical surface was used in the back-analysis. Three piezometric levels were discovered in the slope as shown in Fig.A.43., which is related to the stratification of impermeable bedrock and very permeable coal layers acting as drains. Based on the observed piezometric levels, zero water pressure was used on the horizontal part of the slip surface for the back-analysis, and the water pressure on the back-scarp was based on the piezometric level (b), which was utilized as the ground water condition by Eigenbrod and Morgenstern (1971). Based on ground water condition (b), the average $\bar{r}_u$ is about 0.13.

Eigenbrod and Morgenstern (1971) reported a liquid limit of only 100% for the bentonitic clay, which results to a plasticity index of 60%, which is lower than the one usually found in bentonite

of marine origin. The plasticity index of the weathered bedrock is about 24%. The empirical residual strength from Mesri and Shahien (2003) corresponding to the plasticity index of bentonite was applied to the horizontal segments, and this gives the back-calculated shear strength on the rest of slip surface similar to that from the empirical correlation for fully softened shear strength developed in the present study. The strengths on the slip surface are consistent with those from the assumptions and conclusions by Eigenbrod and Morgenstern (1971). First, Eigenbrod and Morgenstern (1971) suggested that most of the back-slope material appeared softened and the slip surface was unlikely to cut through the intact bedrock. As a result, the measured shear strength from consolidated drained triaxial compression tests on what they call softened material was used in the back-analysis. Second, the back-calculated friction angle of 8° on the horizontal part is in the measured residual friction angle range from 5° to 10° determined from 3 drained triaxial compression tests under confining pressure of 30 psi (210 kPa) on samples obtained by pushing thin-walled tubes obliquely in the same pit, across the horizontal segment of the slip surface. The lowest friction angle was obtained from the test on the sample with the smallest angle of failure plane to horizontal (8 degree) while the highest one from the test on the sample with the largest angle of failure plane to horizontal (20.5 degree).

North to Central National Highway, Greece (Anagnostopoulos and Georgiadis 2004)

A landslide cutting through the highway pavement took placed at a section of the national highway connecting north to central Greece after a prolonged rainy season. The landslide mass was approximately 90m wide, with maximum depth of 12m (Fig.A.44) in a slope with an average inclination of 10 degree. The back-analysis by Anagnostopoulos and Georgiadis (2004) suggests that residual strength, of this highly plastic material in the slope, is not able to maintain its marginal stability. As a result, this case is regarded as a first-time slope failure.

Six boreholes were drilled to investigate the soil profile, and Casagrande piezometers were installed to determine the ground water level. The top 13 to 17m of the slope consists of stiff dark brown silty clay with a plasticity index of 54% (w_l = 94% and w_p = 40%). The stiff silty clay layer is underlain by a hard dark green to black clayey silt, embedded with a layer of dense fine silty to clayed sand. The landslide mass appeared to end at an area of mud, and remained in the stiff dark brown silty clay. Although the ground water table, according to the filed investigation, several

months after the failure, was almost at the top of sand layer, Anagnostopoulos and Georgiadis (2004) assumed that the ground water table had reached the ground surface at the time of failure considering the prolonged rainy period. A slip surface which remained in the top clay layer was determined from back-analysis by Anagnostopoulos and Georgiadis (2004) on the basis of the filed observation including the main scarp at the highway pavement, a disturbed zone 6m below one of the boreholes, and the toe at the mud zone. This slip surface, together with the assumed ground water condition was used in the back-analysis in the present study.

Because the sub-horizontal basal segment was on the interface between the stiff dark brown clay and silty sand layer, residual shear strength at I_p = 54%, from Mersi and Shahien (2003), was applied to this segment. The back-calculated mobilized shear strength on the rest of the slip surface from back-analysis is similar to that defined by I_p = 54%, from the empirical correlation for fully softened shear strength developed in the present study. Anagnostopoulos and Georgiadis (2004) obtained an average friction angle of 21° for the entire slip surface from their back-analysis. This friction angle is in between a fully softened and residual value at the corresponding effective normal stress range.

Pendakomo, Cyprus (Gostelow and Loucaides 1988)

Several cuttings commenced in 1980 during the construction of the Nicosia to Limassol dual carriage way road in Cyprus. A failure occurred in a cutting at Pendakomo in April 1981, approximately 1 year after the main excavation. The triggering factor of the failure in the 9.6 m deep cutting, according to Gostelow and Loucaides (1988), was a 1 to 1.5m deep re-excavation at the toe of the slope (Fig.A.45). The design value of the slope was 2:1 (H:V), which gives a slope angle of 26.6°, slightly higher than the slope angle at failure (24°). The slip has an apparent depth of 6 to 8m. It is regarded as a first-time slope failure because the shear surface did not follow any obvious planes of weakness (Gostelow and Loucaides 1988).

Casagrande type piezometers were installed in three holes on the opposite side of the failed cutting before the failure and the piezometric readings were taken for about 1 year. Six 12 to 15m deep boreholes were drilled on both sides of the cutting, so the soil profile was obtained from the ground surface to the depth below the slip. The failure was in the Moni Melange, which is a partly

allochthonous marine sediments consisting of olistoliths of limestone, calcareous or quarzitic sandstones, cherts, lavas, and serpentinite blocks in a firm to stiff clay matrix. This mixture was thought to result from an active late Crataceous subduction zone originally located to the south of Cyprus, which brought sediments from a Jurassic continental margin into the marine clays. The Moni Melange, with a montmorillonitic clay matrix, has weathered in many natural slopes with gentle inclinations. At the Pendakomo cutting, the weathered mélange extends to approximately 10m below ground surface (Fig.A.45), and the upper 4 to 5 meter of the mélange was completely weathered. The unweathered melange is a blue-grey stiff clay. The softer weathered clay with slickensided shears, is greenish brown occasionally containing contorted reddish brown and dark blue bands. The highly plastic mélange in Pendakomo has a plasticity index in the range from 60% to 100%. The two possible slip surfaces, in the weathered Moni Melange, shown in Fig.A.45, were determined by Gostelow and Loucaides (1988) based on the shape of the slide, the initial vertical deformation, the heave at the toe, and the apparent depth of slip. Positive porewater pressures were not recorded during the investigation period even with comparatively high rainfall 2 months before the slope failure, and zero or negative porewater pressures were suggested by borehole evidence. Gostelow and Loucaides (1988) assumed an average porewater pressure ratio of zero at the time of failure for the stability analysis, which was used in this research together with the two possible slip surfaces in Fig.A.45.

Because the weathered Moni Melange has slickensides, and visual evidence was available for the rapid weakening of the clay at the slope toe which was thought to be the result of swelling, residual strength was assumed for the sub-horizontal bases of the slip surfaces. It should be noted that as the slip surfaces are circular, the determination of the “sub-horizontal” base was somewhat arbitrary. With residual strength on the sub-horizontal segments, corresponding to the lower bond of the plasticity index range, from Mesri and Shahien (2003), the back-calculated shear strength on the rest of the slip surfaces is comparable to that defined by I_p = 60% - 100%, from the empirical correlation for fully softened shear strength in the present study. The assumption and results are consistent with the conclusion of Gostelow and Loucaides (1988) in terms of the magnitude of the mobilized shear strength. Gostelow and Loucaides (1988) suggested that the peak shear strength from laboratory tests is too high and the residual strength measured in ring shear tests is too low to obtain a factor of safety of 1.

It should be noted that the possible slip surfaces with rotational geometries with part of the surfaces below the toe level, assumed by Gostelow and Loucaides (1988), may not be realistic for a cut in stiff fissured clay, with the consideration of greater stress concentration near the toe. It is highly possible that the actual slip surface has a horizontal basal part near the toe and a curved back-scarp. An attempt was made to study the influence of the slip surface geometry through another back-analysis assuming a horizontal segment starting from the toe which terminates in between slip 2 and slip 3, and a curved back-scarp in the middle of slip 2 and slip 3 (Fig.A.46). In this case, the back-calculated mobilized shear strength on the back-scarp, is in the range of that from the proposed empirical correlation for fully softened shear strength.

Salvador, Brazil (Magalhaes et al. 1992)

A deep-seated first-time landslide occurred in a 25m high cut (Fig.A.47) on a hill mainly consisting of granulite residual soil, in Salvador, Brazil. The top soil underneath the fill is an evolved soil derived from Barreiras formation, overlying the granulite mature residual soil underlain by the young residual soil. The field investigation reveals that a large portion of the slip surface cuts through the young residual soil, and the sub-horizontal part is entirely in the young residual granulite. The mature residual soil has a plasticity index of 36% while the young residual granulite has a higher plasticity index (50%). Slickensides were overserved in the residual soil, which is believed to be the controlling factor for the mobilized shear strength in the slide (Magalhaes et al. 1992). The water table shown in Fig.A.47, located below the slip surface even after prolonged rainy season was utilized in the back-analysis by Magalhaes et al. (1992), and also adopted in this researcC.

With the consideration of existence of planes of weakness in the residual soil and the geometry of the slip surface, i.e., a slip surface with a sub-horizontal segment, though somewhat arbitrary, the residual strength based on Mesri and Shahien (2003) corresponding to the plasticity index of the young residual soil was applied to the sub-horizontal base. This assumption results to the back-calculated shear strength on the back-scarp close to that at I_p = 50%, from the empirical correlation for fully softened shear strength developed in the present study.

Risalaimi, Italy (Valore 1995)

In 1962, a landslide took place in Risalaimi, Italy, 6 months after the construction of an 11.5m cutting on the slope. The slip with maximum depth of 30m, displays a translational shape (Fig.A.48), including a back-scarp and a sub-horizontal basal segment. The sliding mass consists of intensely tectonized overconsolidated marly clay and very stiff clays. The tectonized marly clay in Risalaimi has a natural water content between 7% and 20%, liquid limit between 37% and 63%, plasticity index between 18% and 37%, and clay size fraction between 17 and 37%. Valore (1995) suggested that the slope failure occurred in drained condition and reported the ground water table in 1963 (Fig.A.48).

The back-analysis in the present study, using the observed slip surface and the reported ground water condition, assumed residual shear strength on sub-horizontal basal segment. The residual shear strength was interpolated from Mesri and Shahien (2003) at an intermediate I_p of the reported range. The back-calculated mobilized shear strength on the rest of the slip surface is in the range of the proposed empirical fully softened shear strength defined by I_p = 18% - 37%.

Grassano, Italy (Di Maio and Vassallo 2011)

The Fosso Spineto landslide system was reactivated in a clay slope in 1998, in the town of Grassano, Southern Italy. This large landslide which is approximately 300m long in the studied cross section, with maximum depth of 40m, caused the toppling of a sheet pile wall and significant distortions of buildings. Geotechnical investigations were carried out to evaluate whether the landsliding process could propagate uphill toward the newly built area. In the study by Di Maio and Vassallo (2011), the small landslide (slip d) at the toe of the reactivated landslide system, as a result of toe erosion, was found out to be a first-time slope failure. In this research, only slip d is re-evaluated, which is shown in Fig.A.49.

The geological formations of the Grassano hill are Irisina Conglomerate, Monte Marano Sands, and Southern Apennine Blue Clays in a downward section. For the landslide studied in this research, only Blue Clay and the surficial sands were involved. Blue Clay has an in-situ water content around 20%, liquid limit ranging from 43% to 54%, plasticity index from 21% to 33%, and clay size fraction of 40%. According to the natural water content and the unit weight of Blue

Clay, it could be described as a stiff clay. The slip surfaces of the landslide system was determined based on the inclinometer measurement. The small slide in this research, displays a back-scarp cutting through the surficial sand and Blue clay, and merges to the pre-existing subhorizontal slip surface of the ancient landslide. The groundwater condition (Fig.A.49), constructed by Di Maio and Vassallo (2011) according to measurements by means of the Casagrande piezometer, was used for the back-analysis in the researcC.

The back-analysis assuming residual shear strength at I_p = 33% (Mesri and Shahien 2003) on the sub-horizontal basal segment of the slip surface, gives the back-calculated mobilized shear strength on the rest of the slip surface close to that defined by I_p = 33%, from the empirical correlation for fully softened shear strength developed in the present study. The shear strengths (solid circles) measured from the consolidated triaxial undrained tests with porewater pressure measurement on the specimens retrieved from the landslide site are in between the fully softened shear strength and residual shear strength. Di Maio and Vassallo (2011) by back-analysis, obtained a friction angle of 21° for the entire slip surface, which is smaller than the empirical secant fully softened friction angle and greater than the empirical secant residual friction angle.

FIGURES

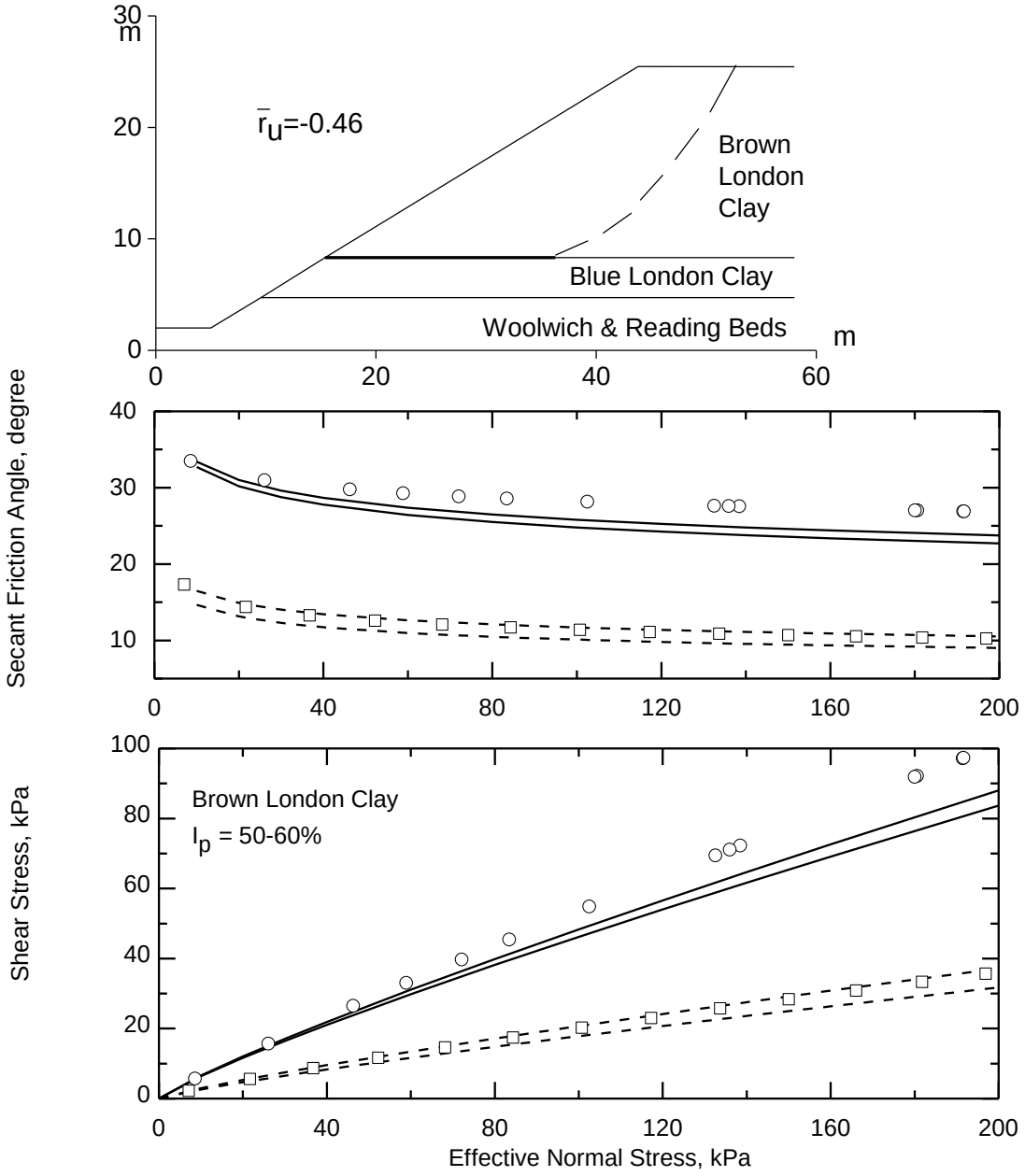

Figure A.1. First-time slope failure at New Cross cutting, UK, 1841 (Skempton 1977)

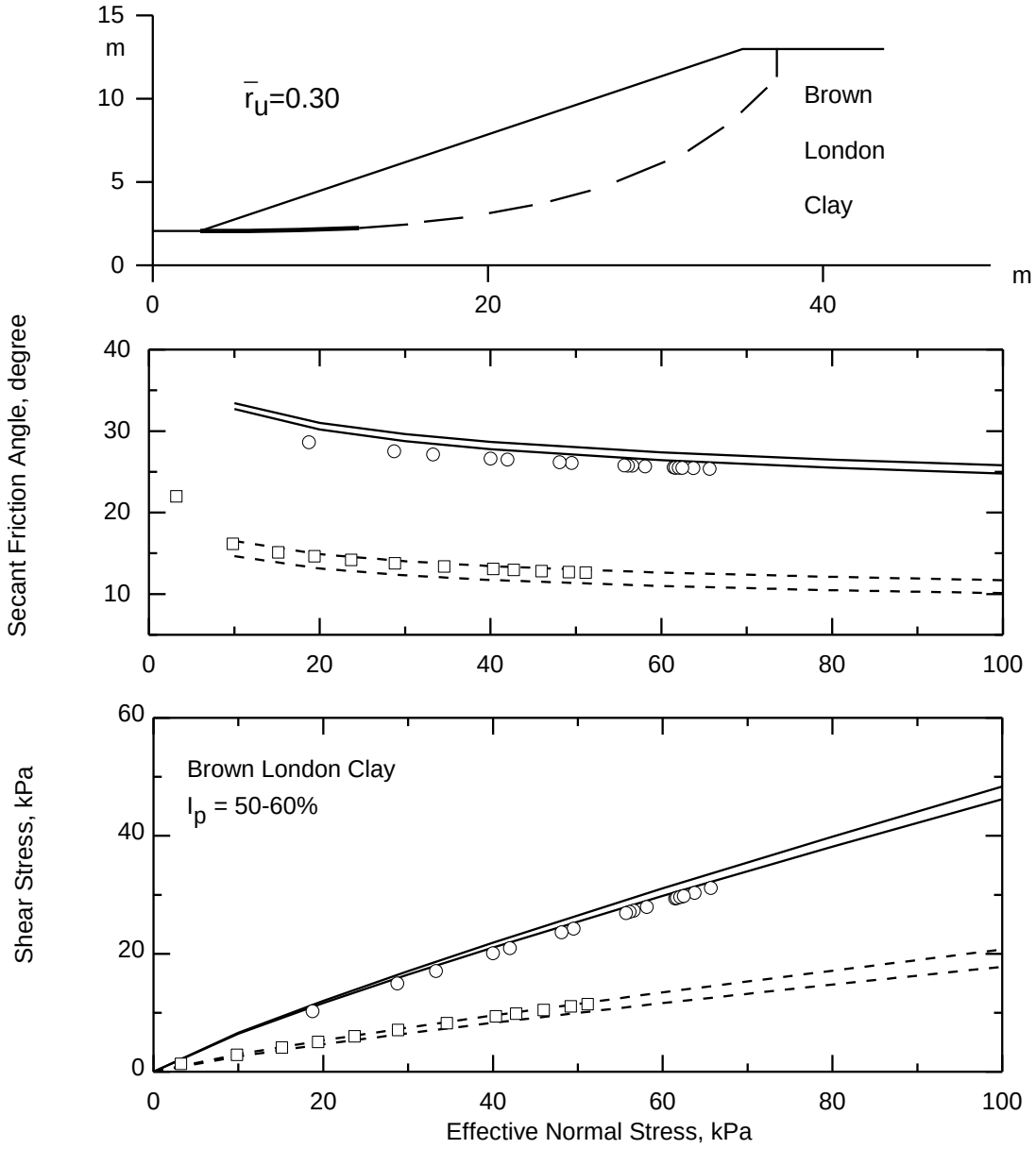

Figure A.2. First-time slope failure at Sudbury, UK, 1949 (Skempton 1977)

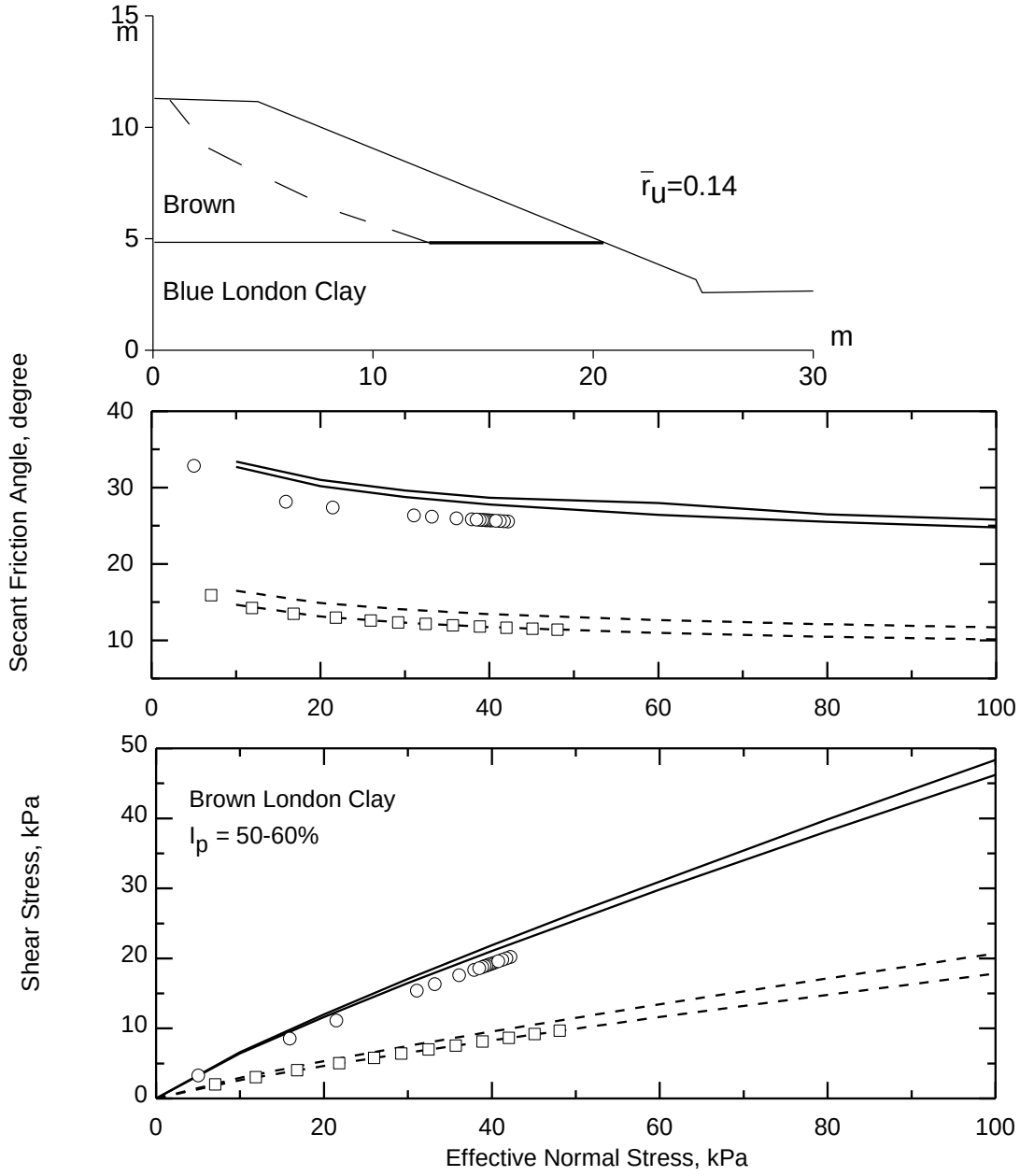

Figure A.3. First-time slope failure at Northolt 1, UK, 1955 (James 1970)

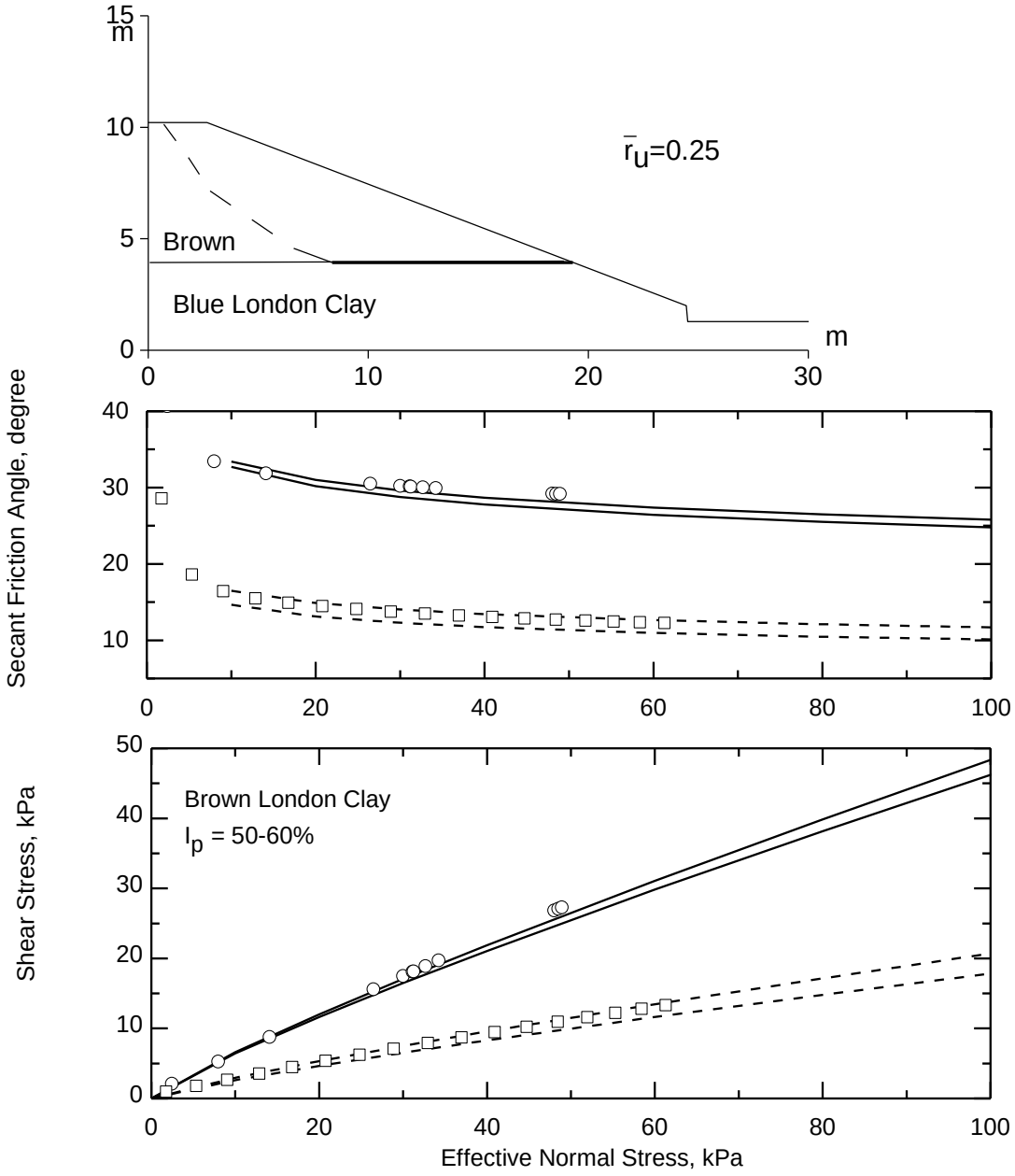

Figure A.4. First-time slope failure at Northolt 3, UK, 1955 (James 1970)

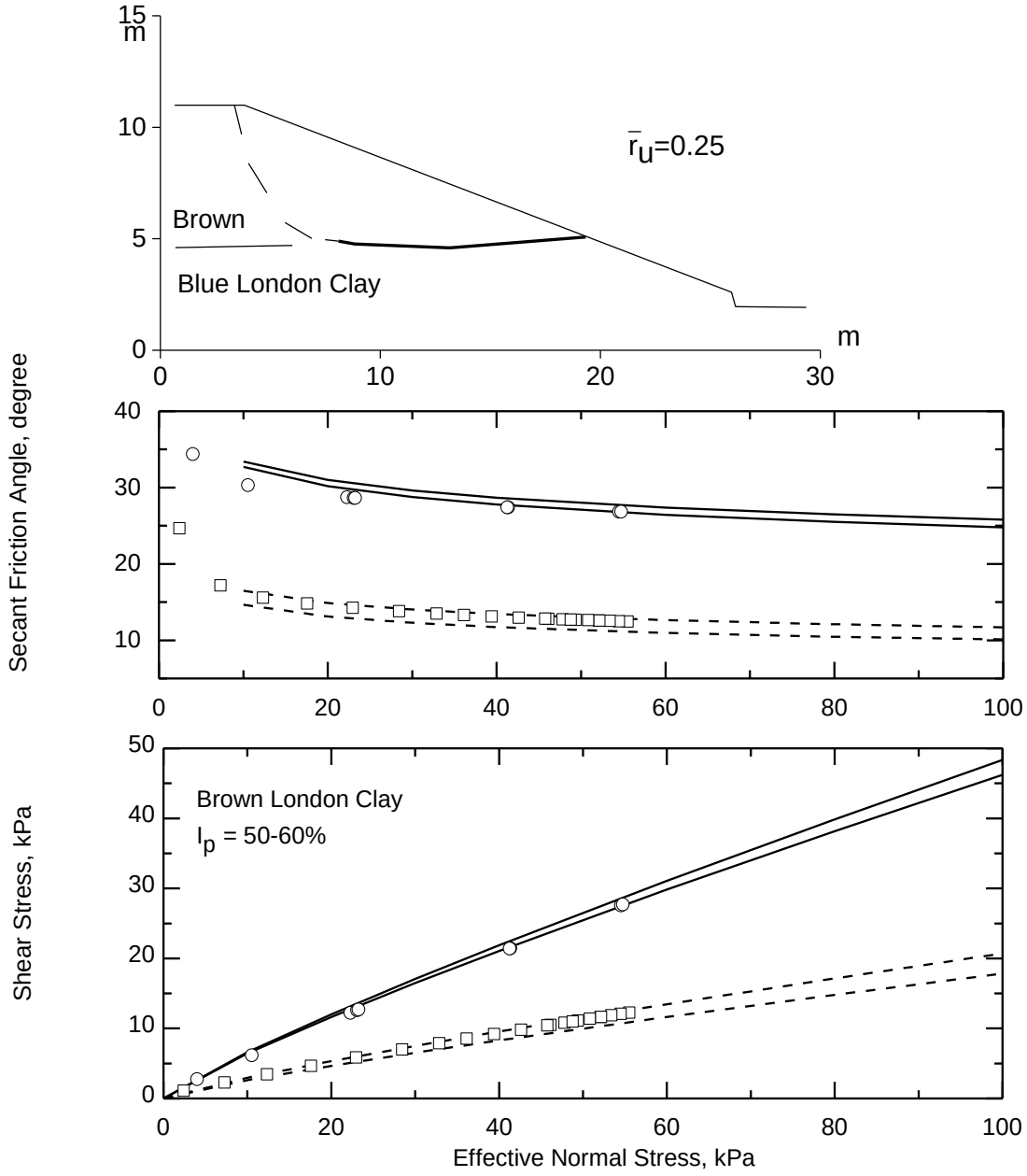

Figure A.5. First-time slope failure at Northolt 6, UK, 1955 (James 1970)

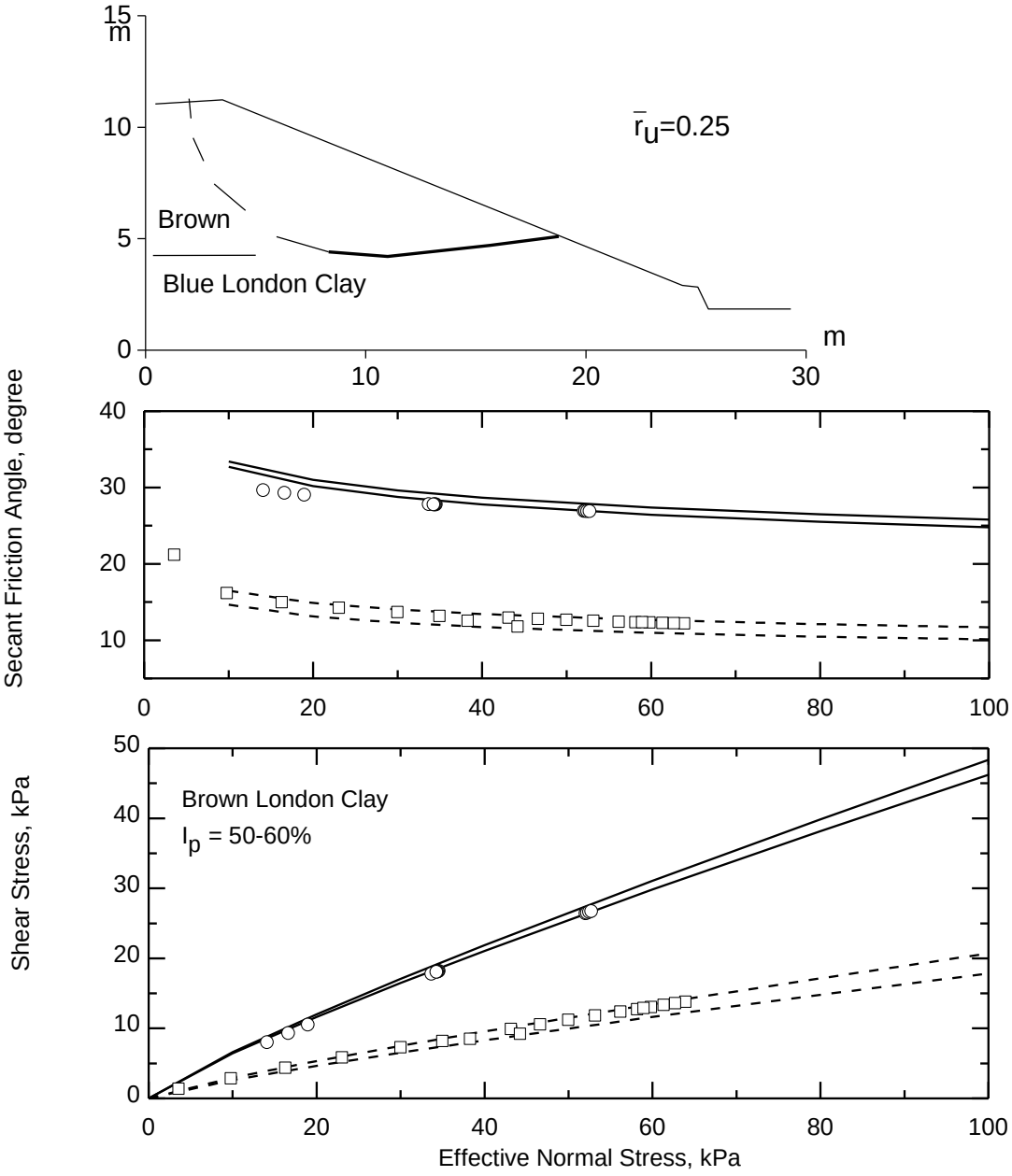

Figure A.6. First-time slope failure at Northolt 9, UK, 1955 (James 1970)

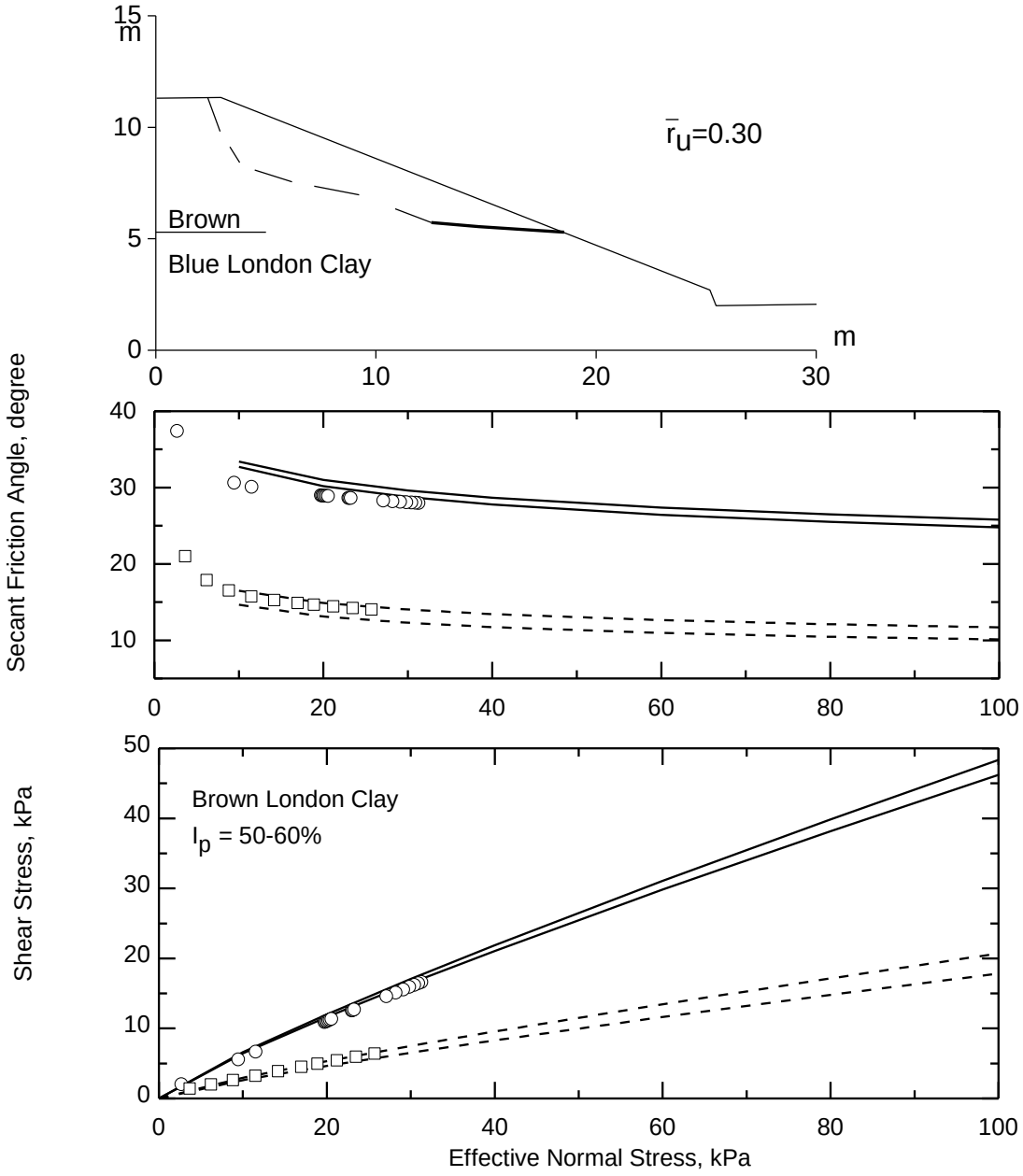

Figure A.7. First-time slope failure at Northolt 11, UK, 1955 (James 1970)

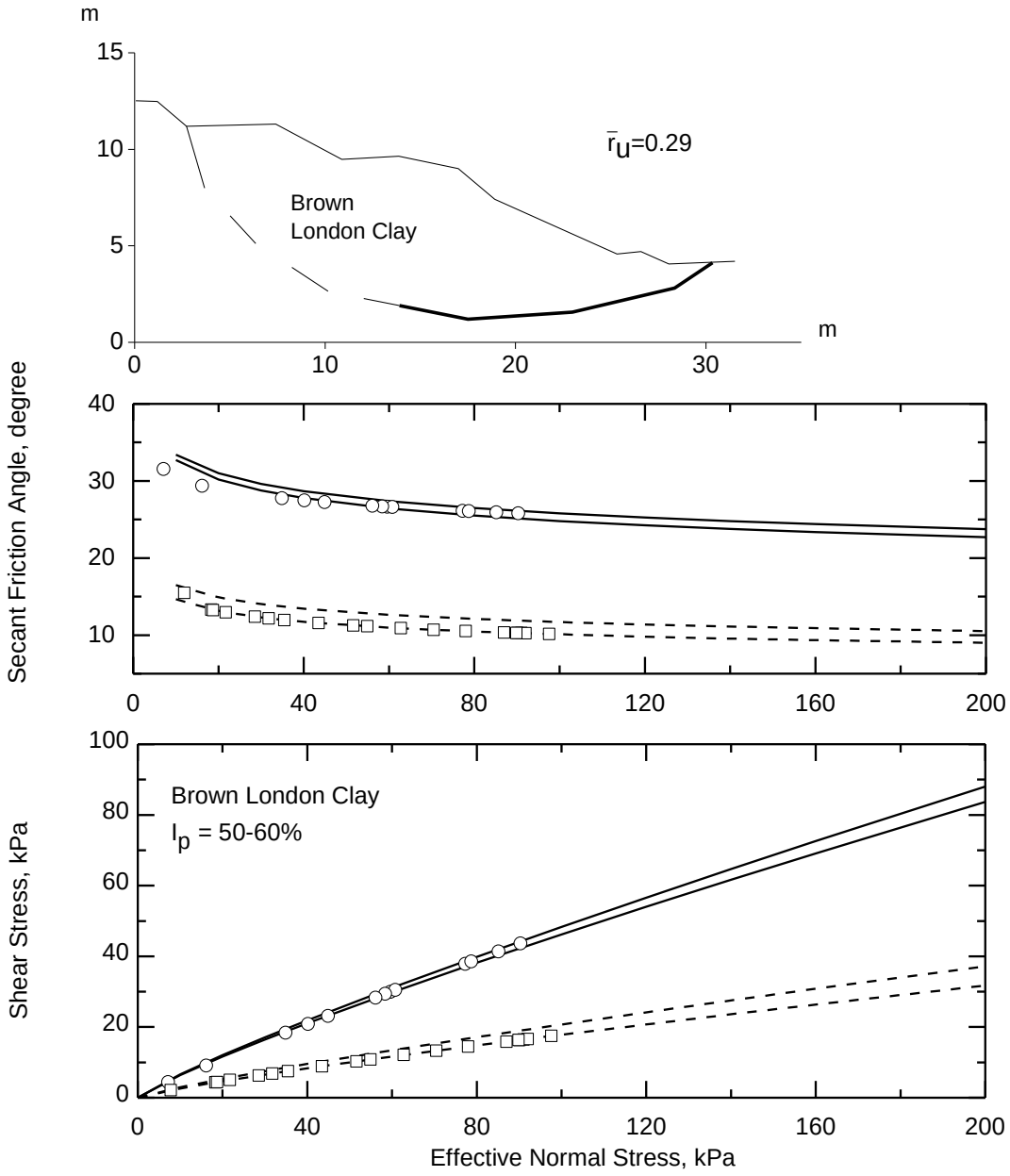

Figure A.8. First-time slope failure at Fareham, UK, 1961 (James 1970)

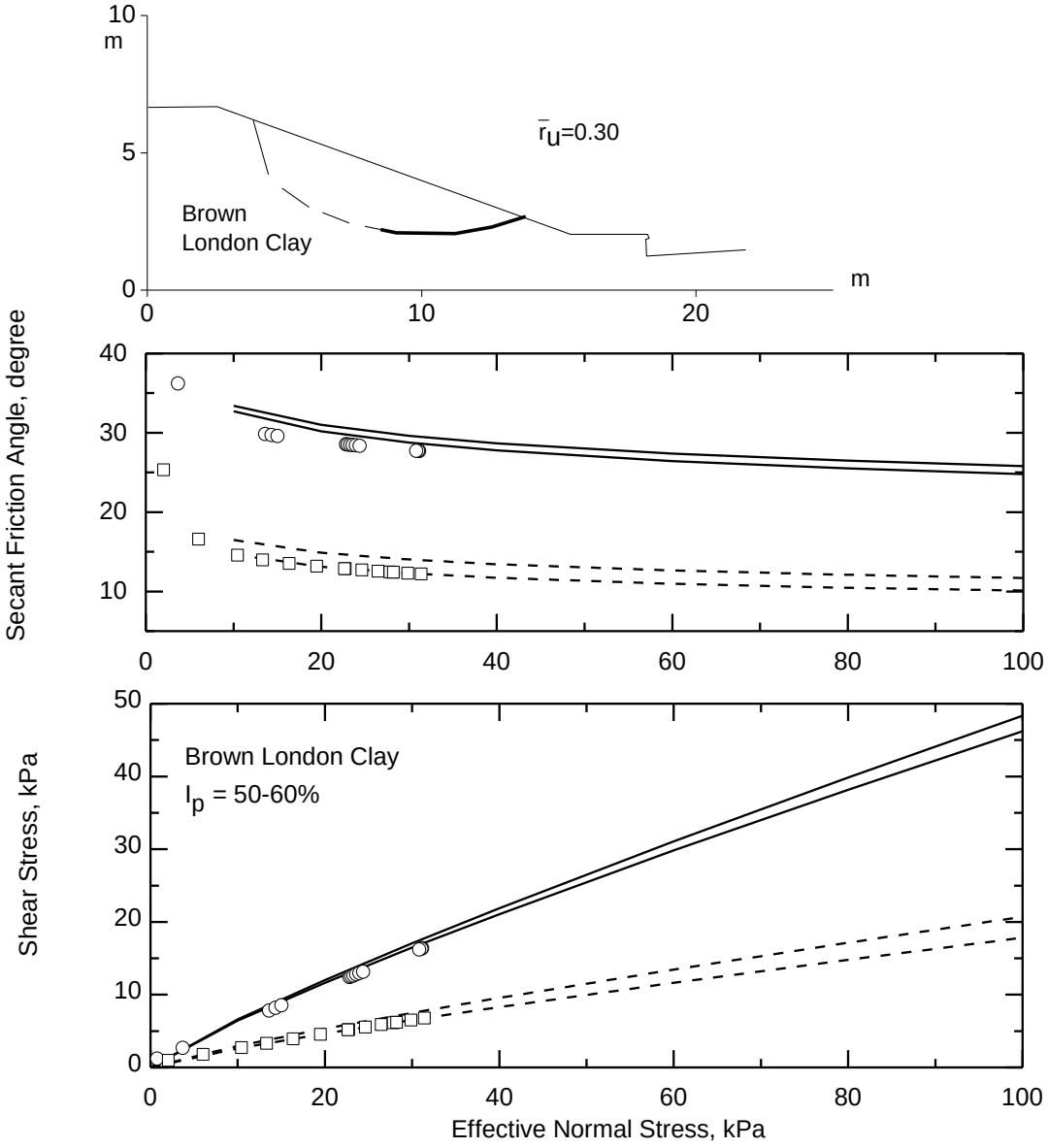

Figure A.9. First-time slope failure at West Acton 8, UK, 1966 (James 1970)

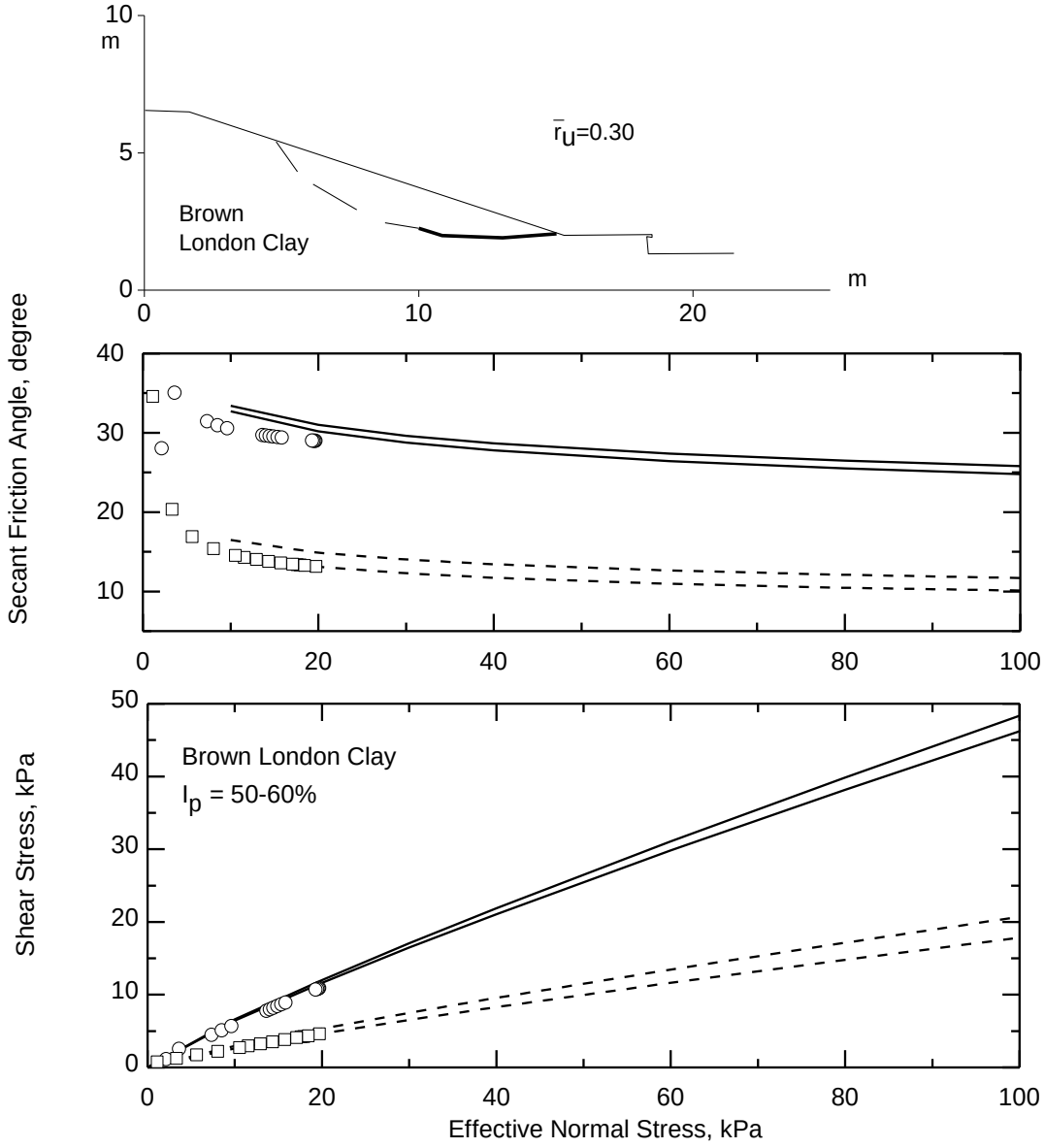

Figure A.10. First-time slope failure at West Acton 9, UK, 1966 (James 1970)

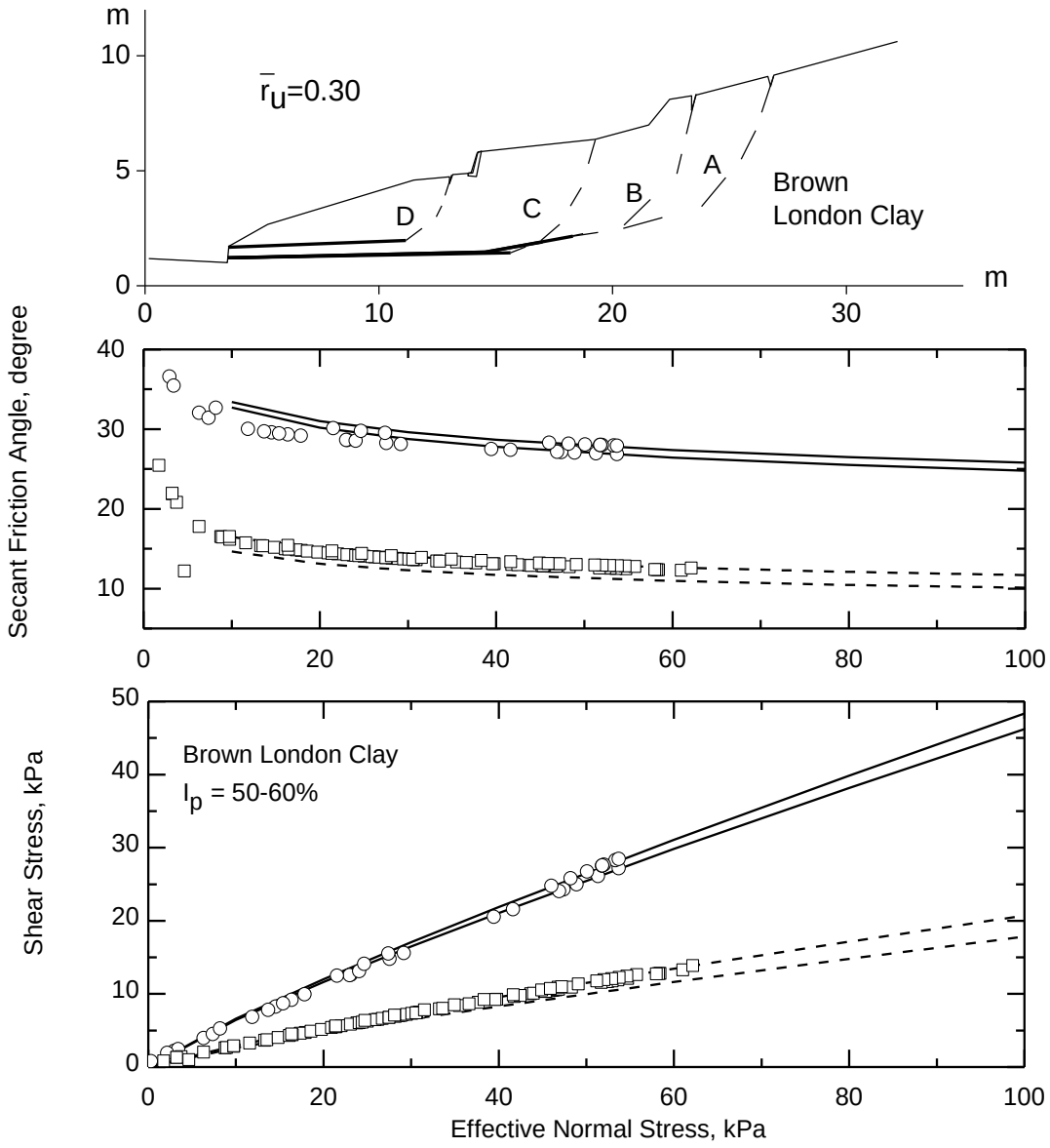

Figure A.11. First-time slope failure at Tulse Hill, UK, 1968 (James 1970)

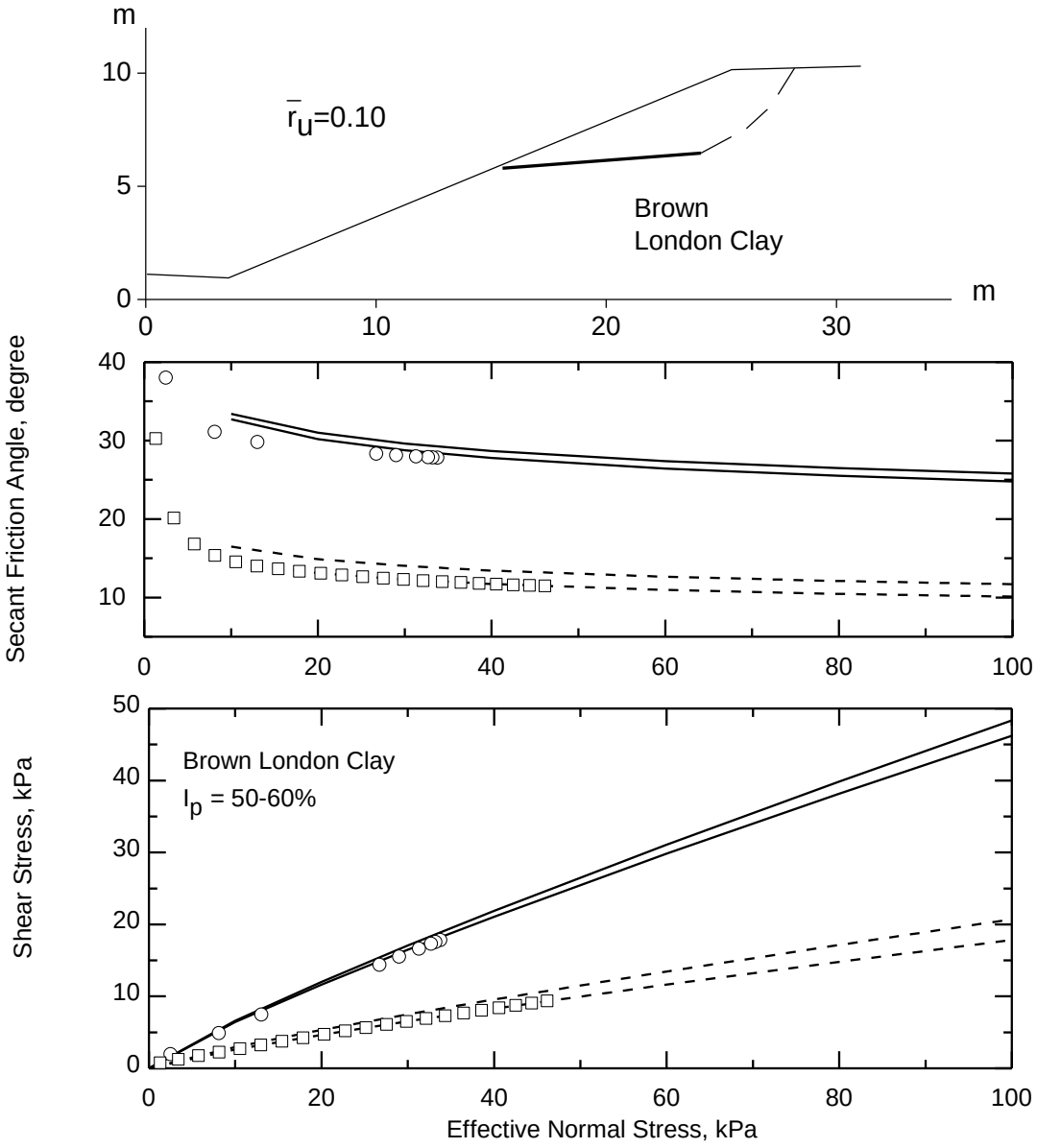

Figure A.12. First-time slope failure at Grove Park, UK, 1962 (James 1970)

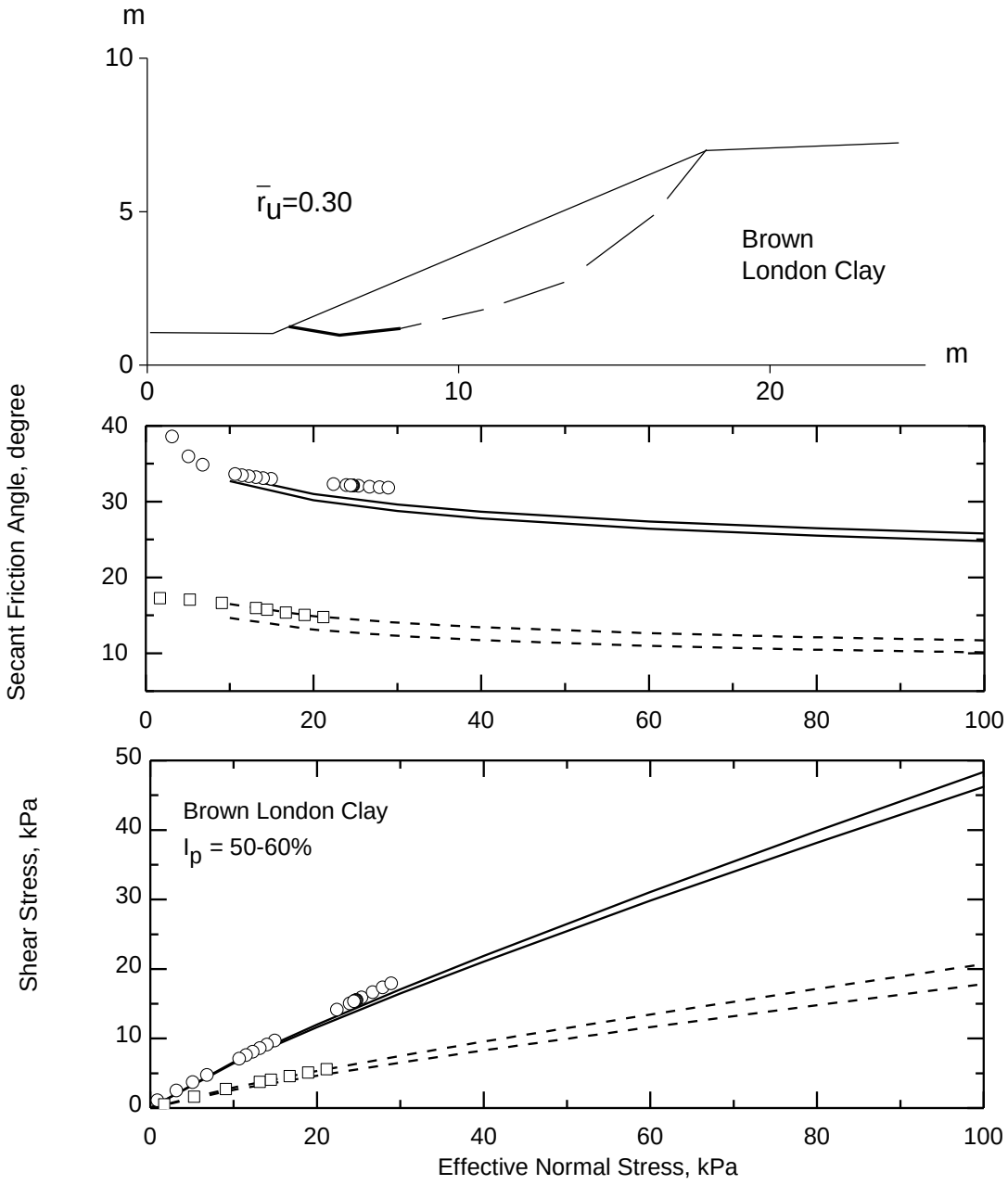

Figure A.13. First-time slope failure at Kingsbury, UK, 1947 (James 1970)

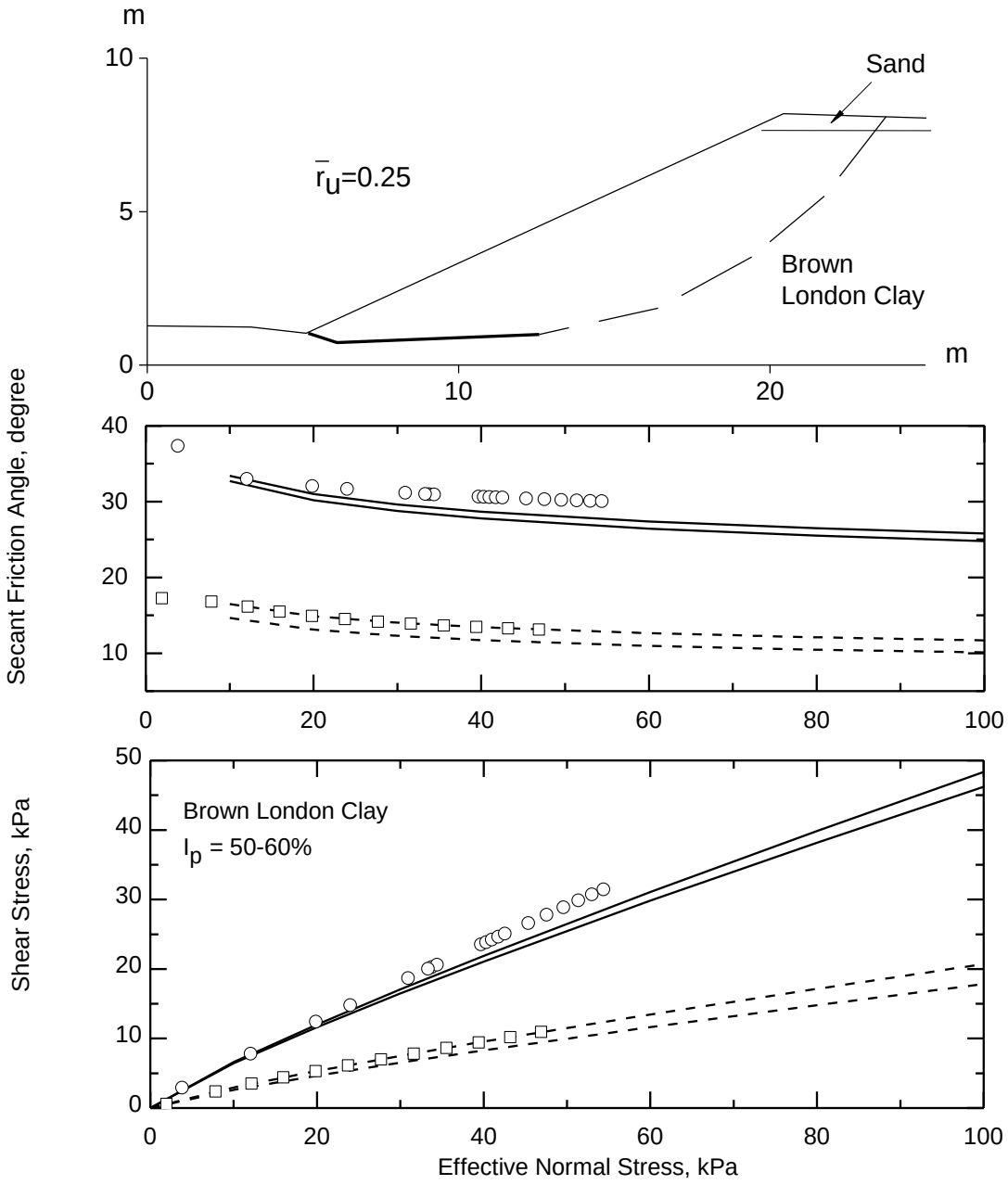

Figure A.14. First-time slope failure at St. Helier, UK, 1952 (James 1970)

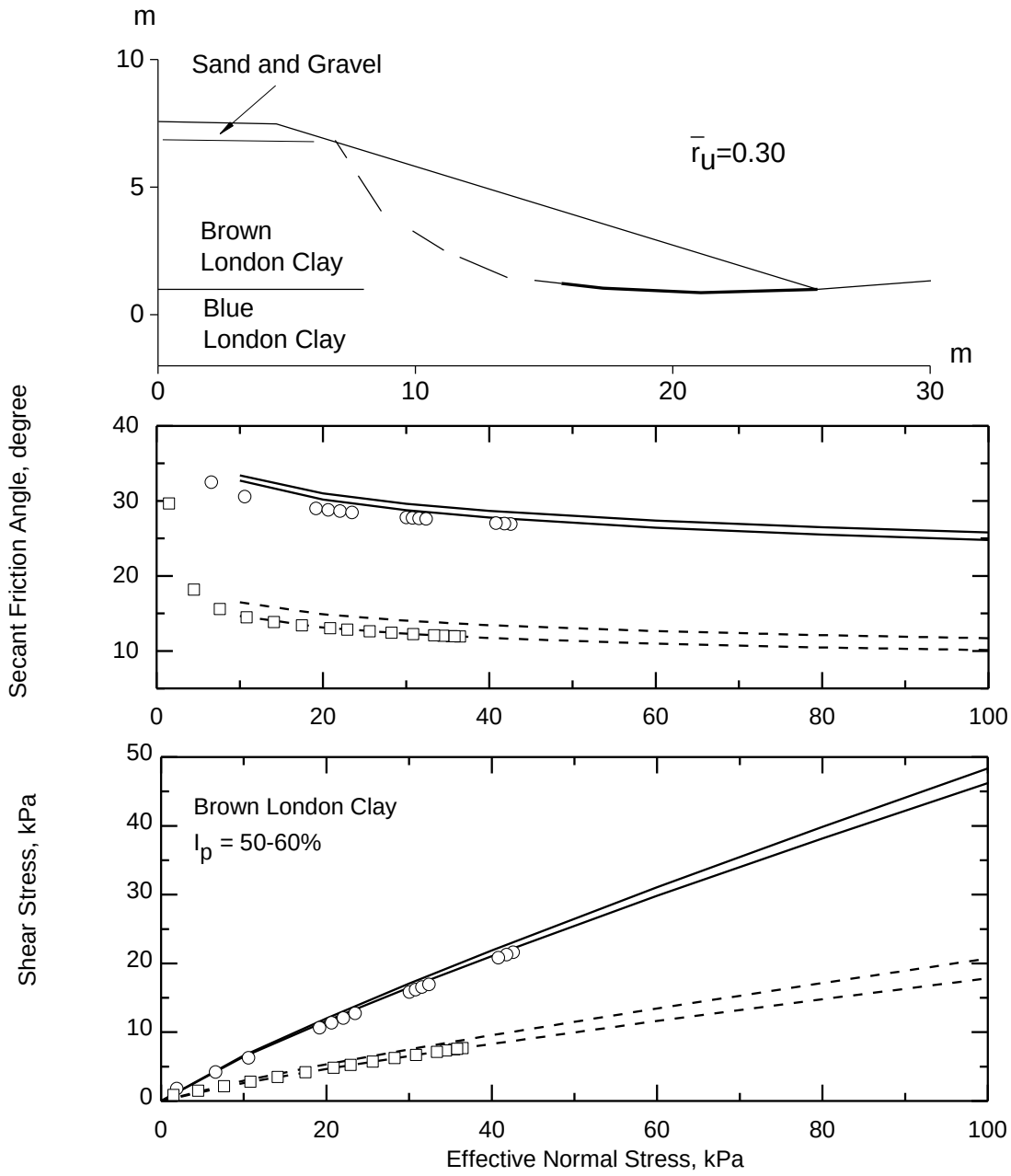

Figure A.15. First-time slope failure at Crews Hill, UK, 1956 (James 1970)

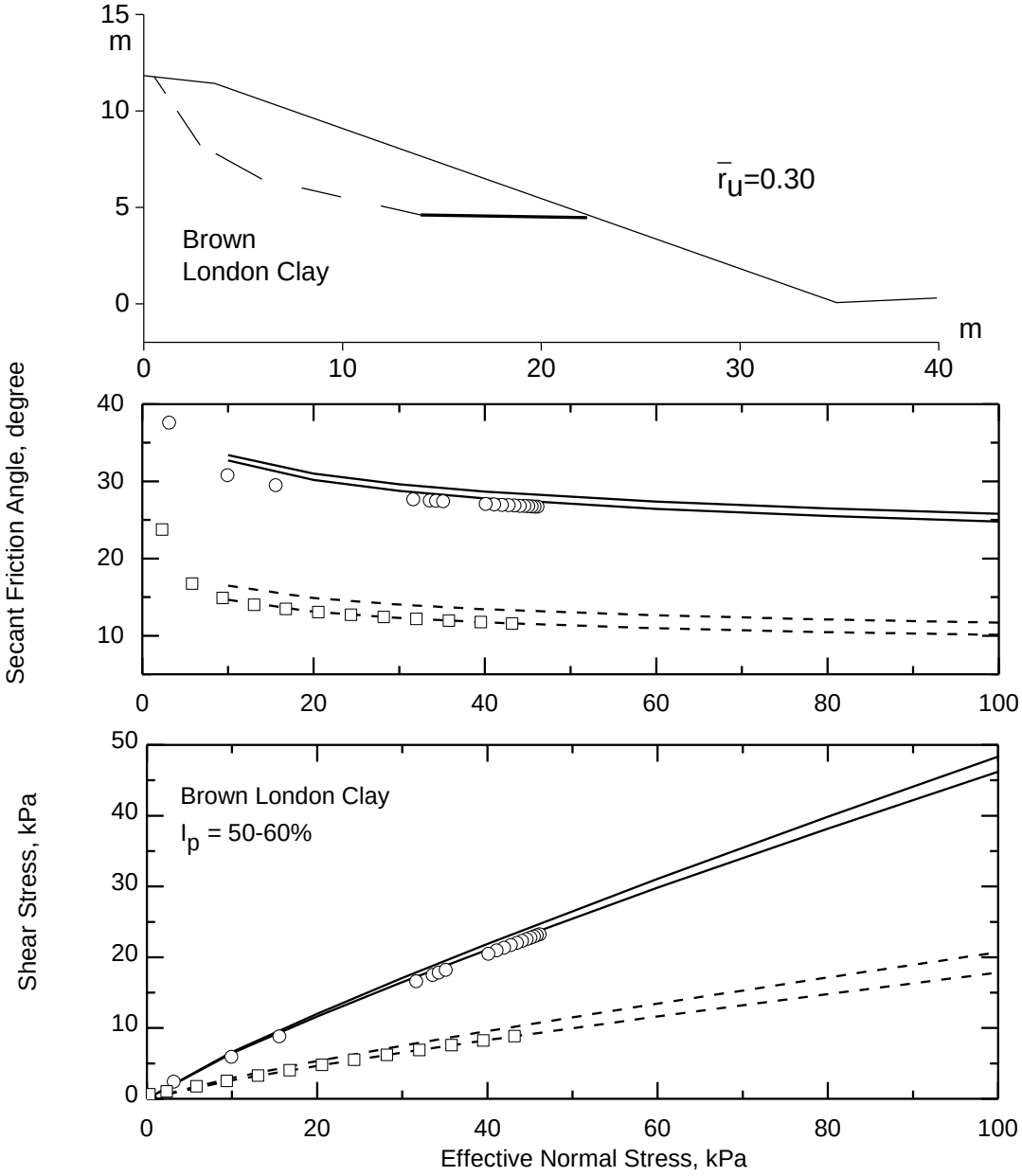

Figure A.16. First-time slope failure at Cuffley, UK, 1951(James 1970)

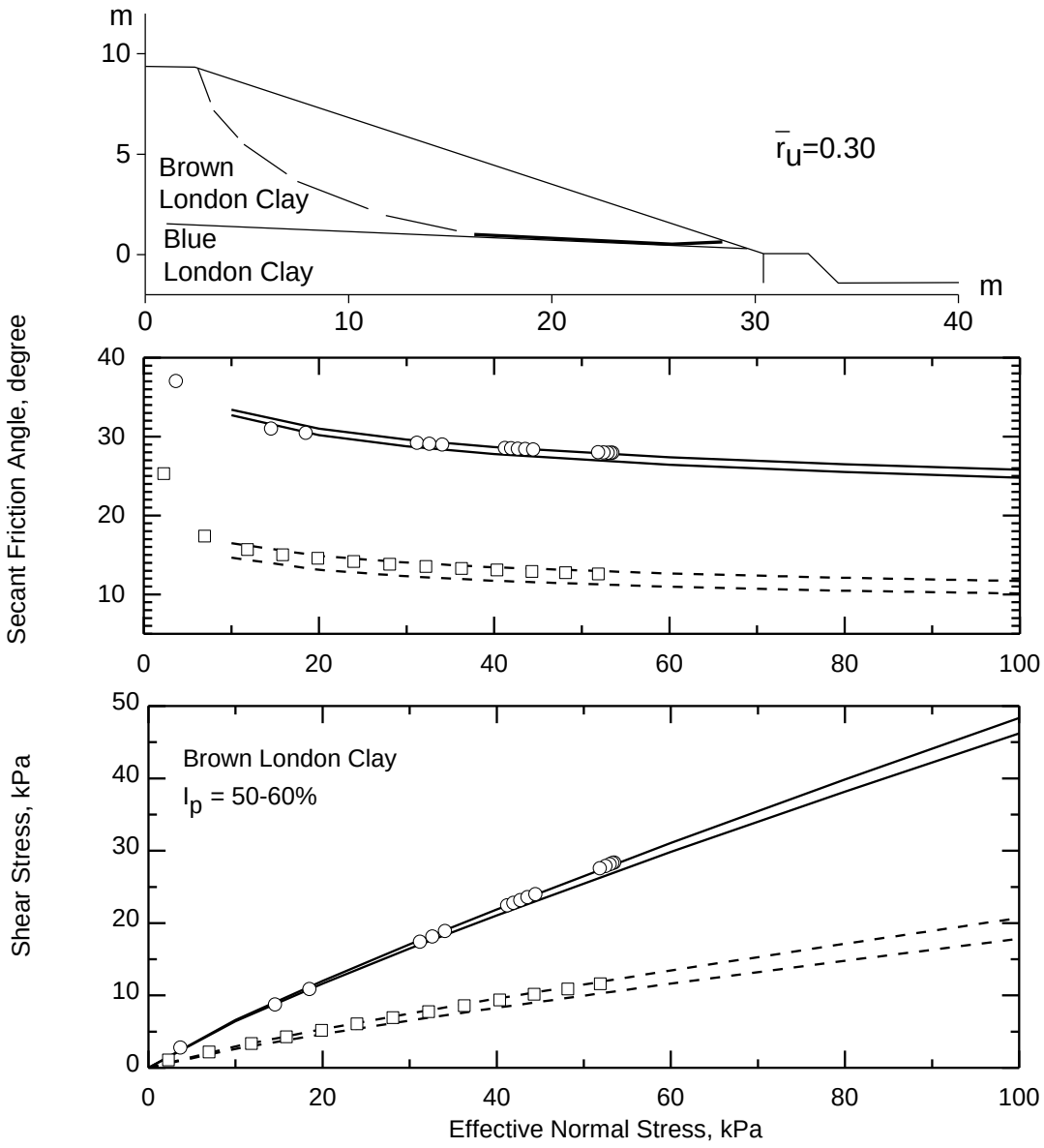

Figure A.17. First-time slope failure at Whitstable, UK, 1959(James 1970)

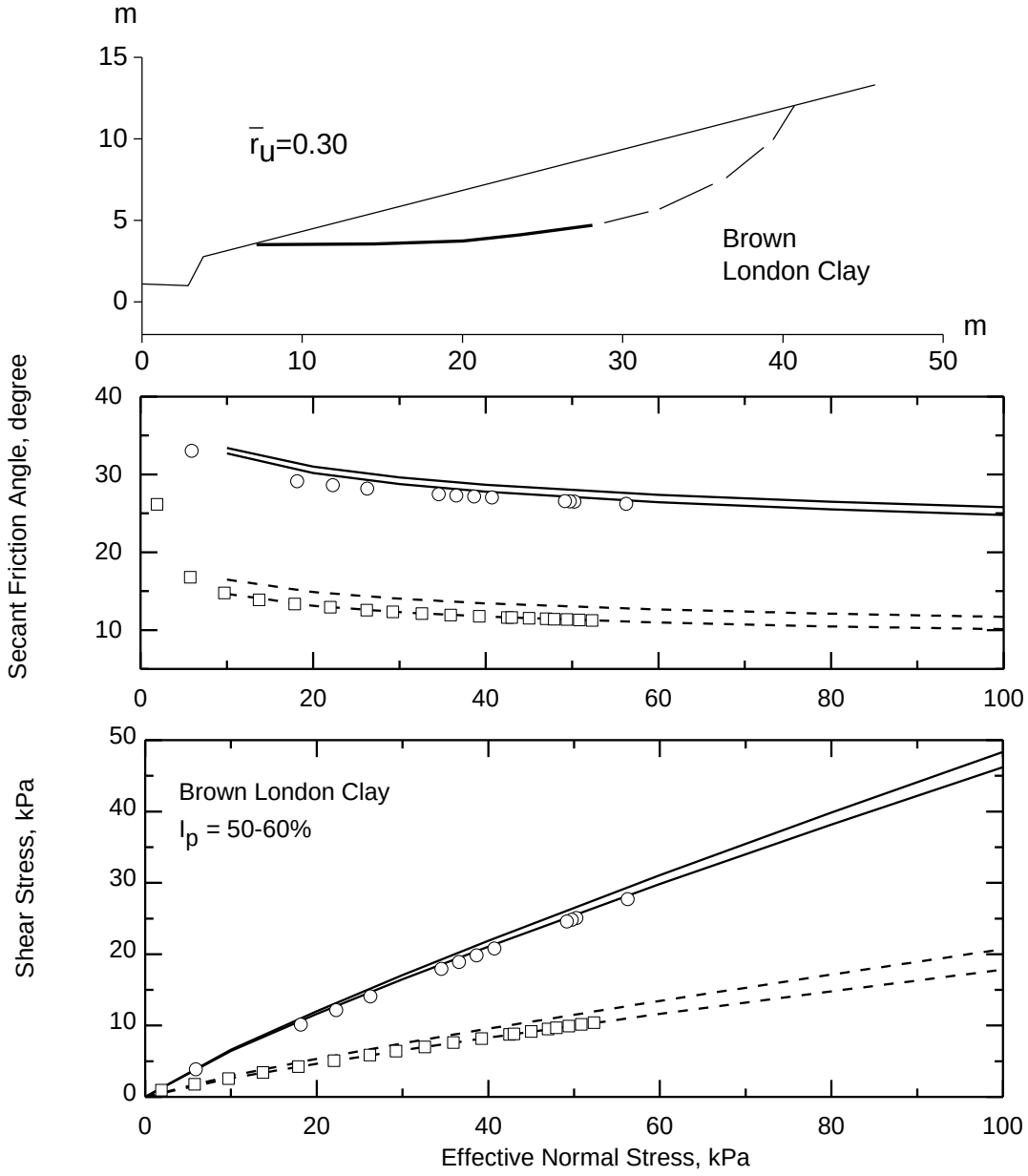

Figure A.18. First-time slope failure at Grange Hill, UK, 1950(James 1970)

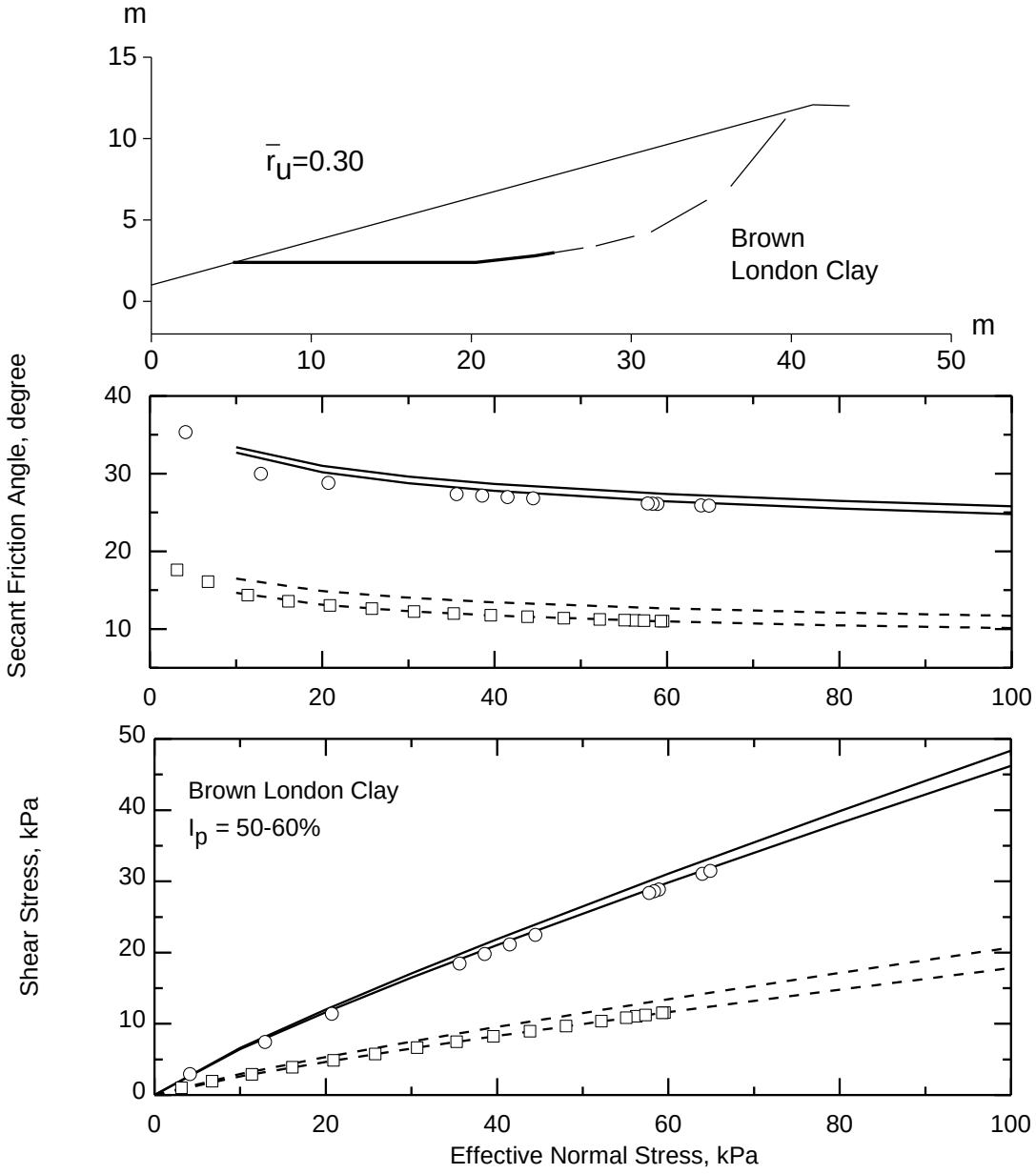

Figure A.19. First-time slope failure at Hadley Wood, UK, 1947 (James 1970)

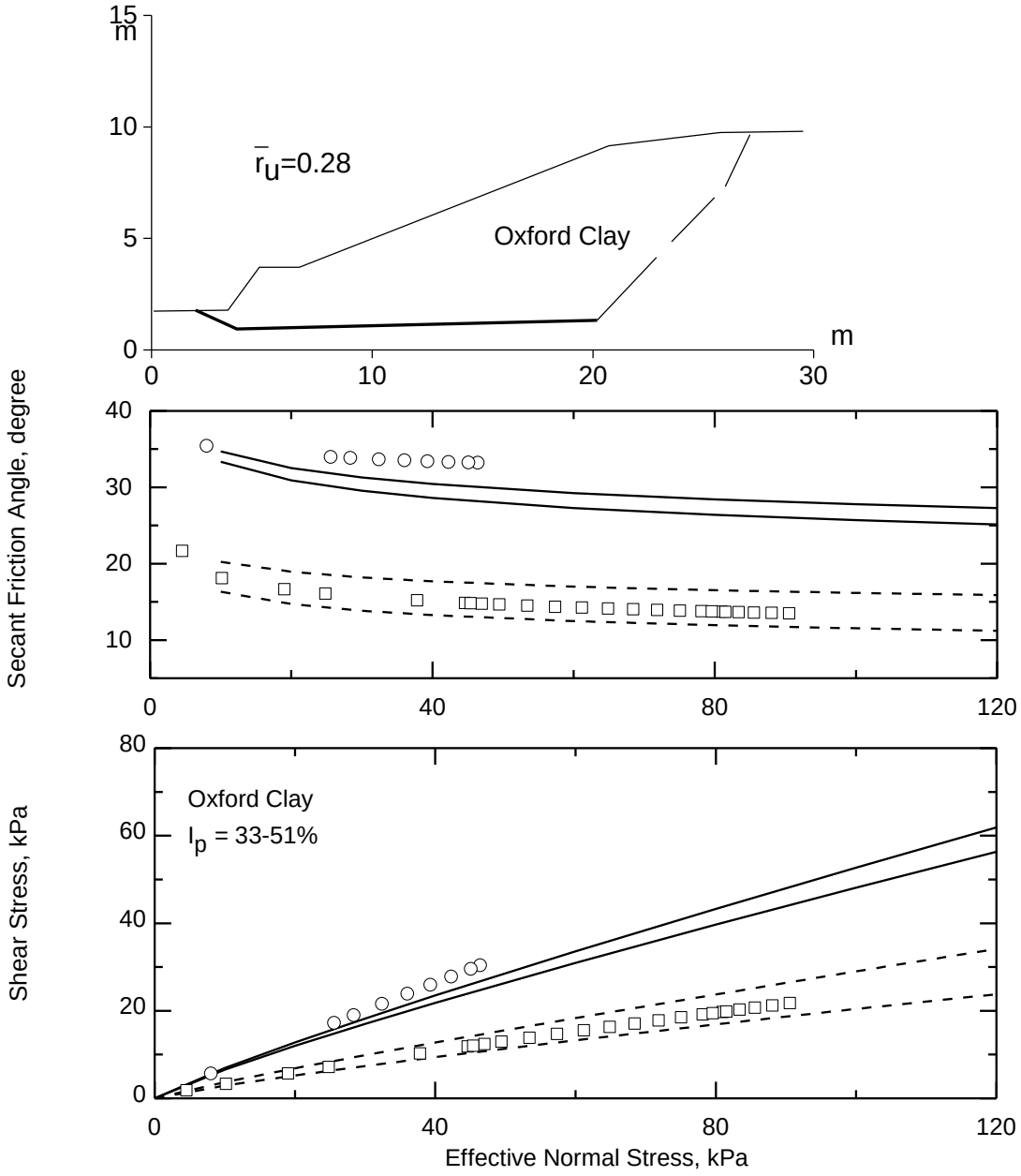

Figure A.20. First-time slope failure at Dauntsey, UK, 1960 (James 1970)

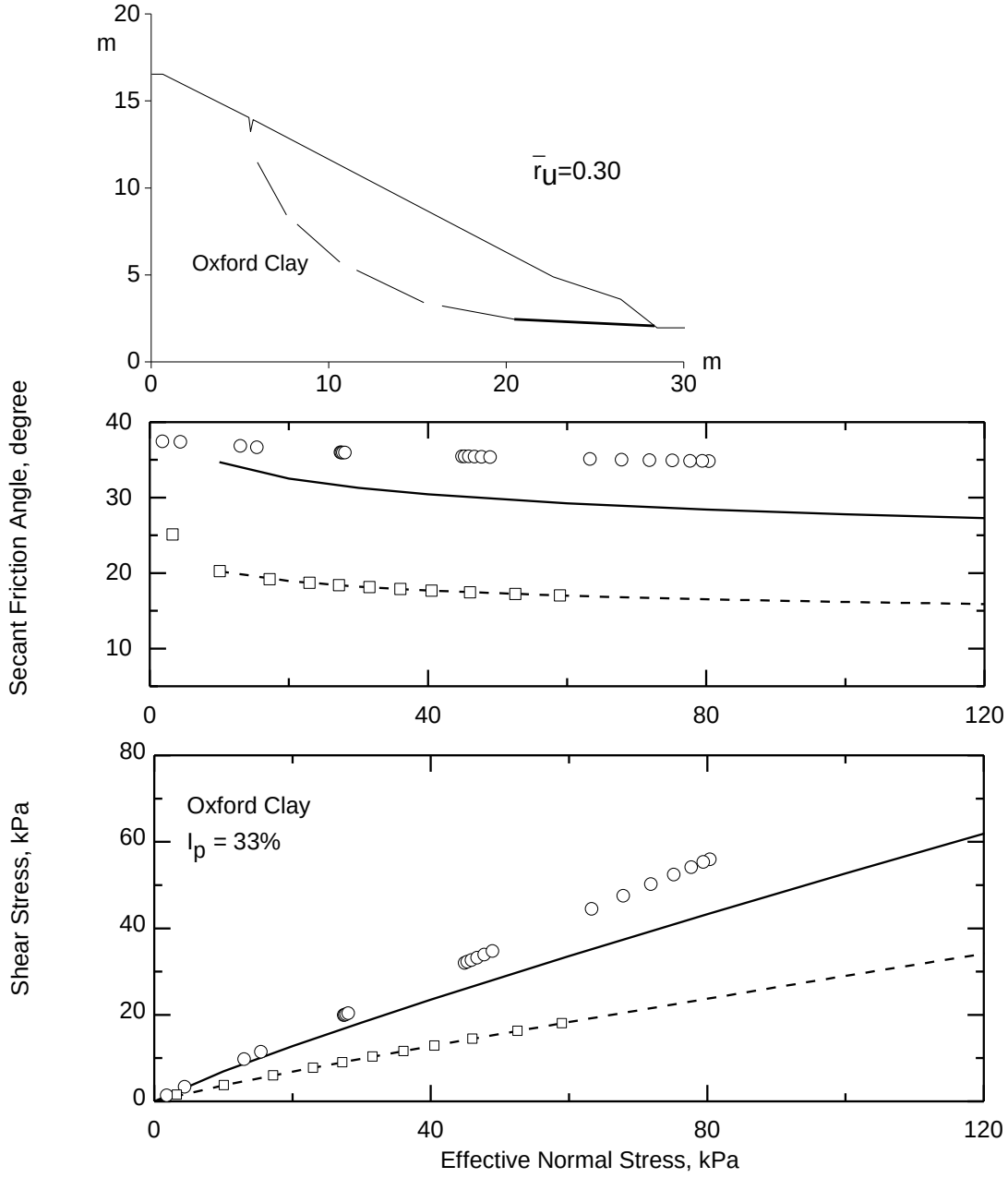

Figure A.21. First-time slope failure at Hullavington, UK, 1959 (James 1970)

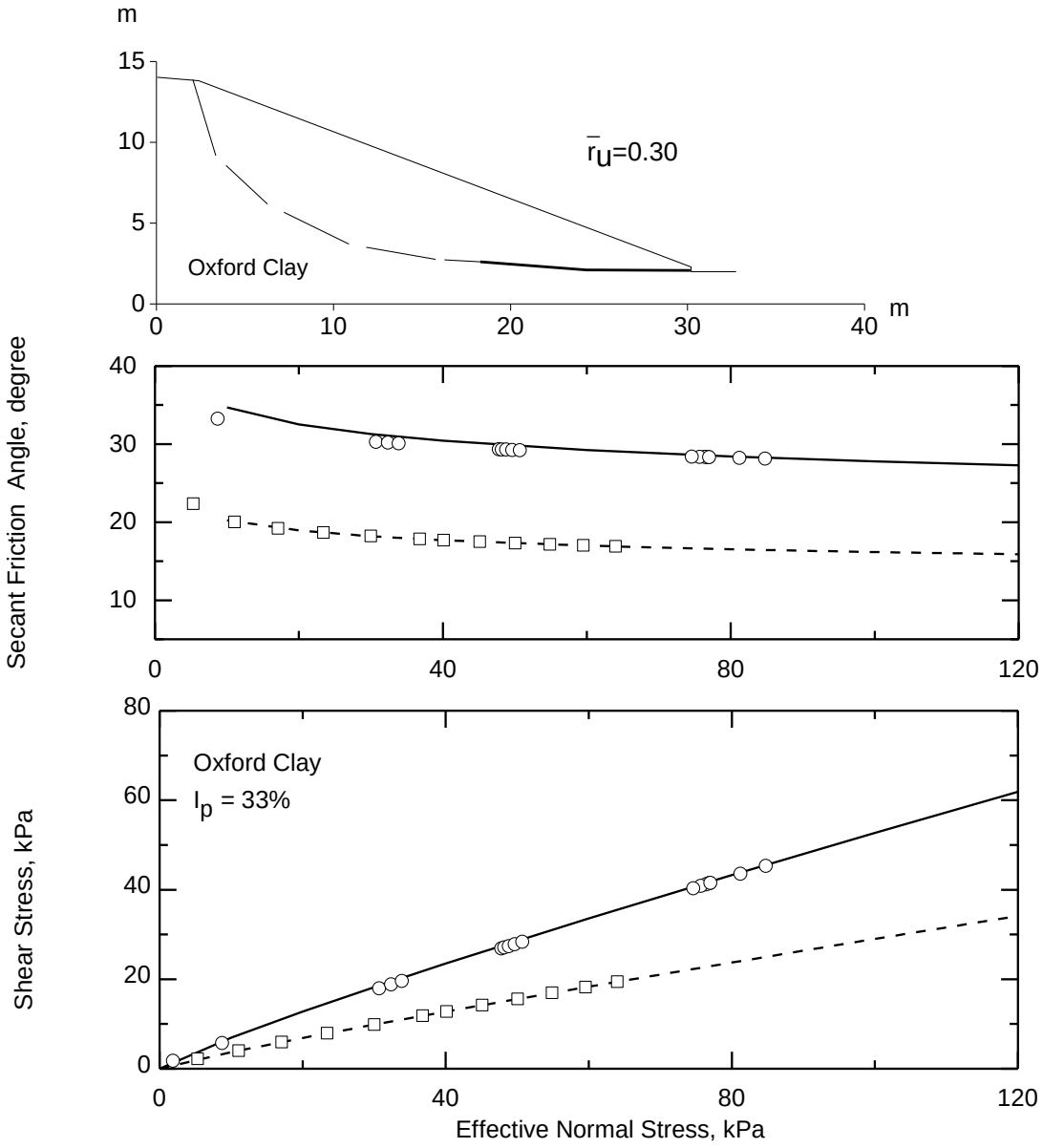

Figure A.22. First-time slope failure at Ampthill, UK, 1955 (James 1970)

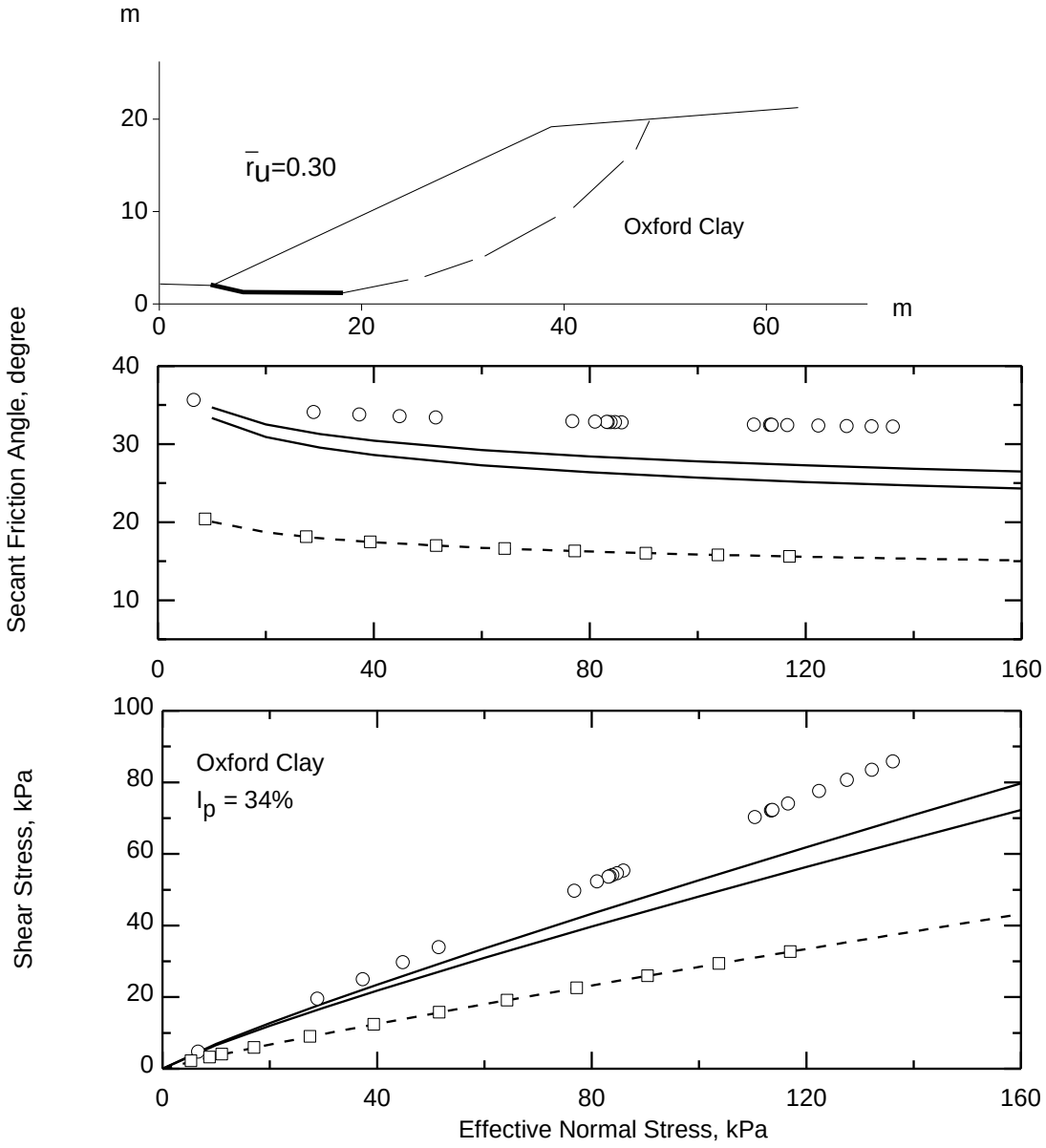

Figure A.23. First-time slope failure at Bincombe, UK, 1890 (James 1970)

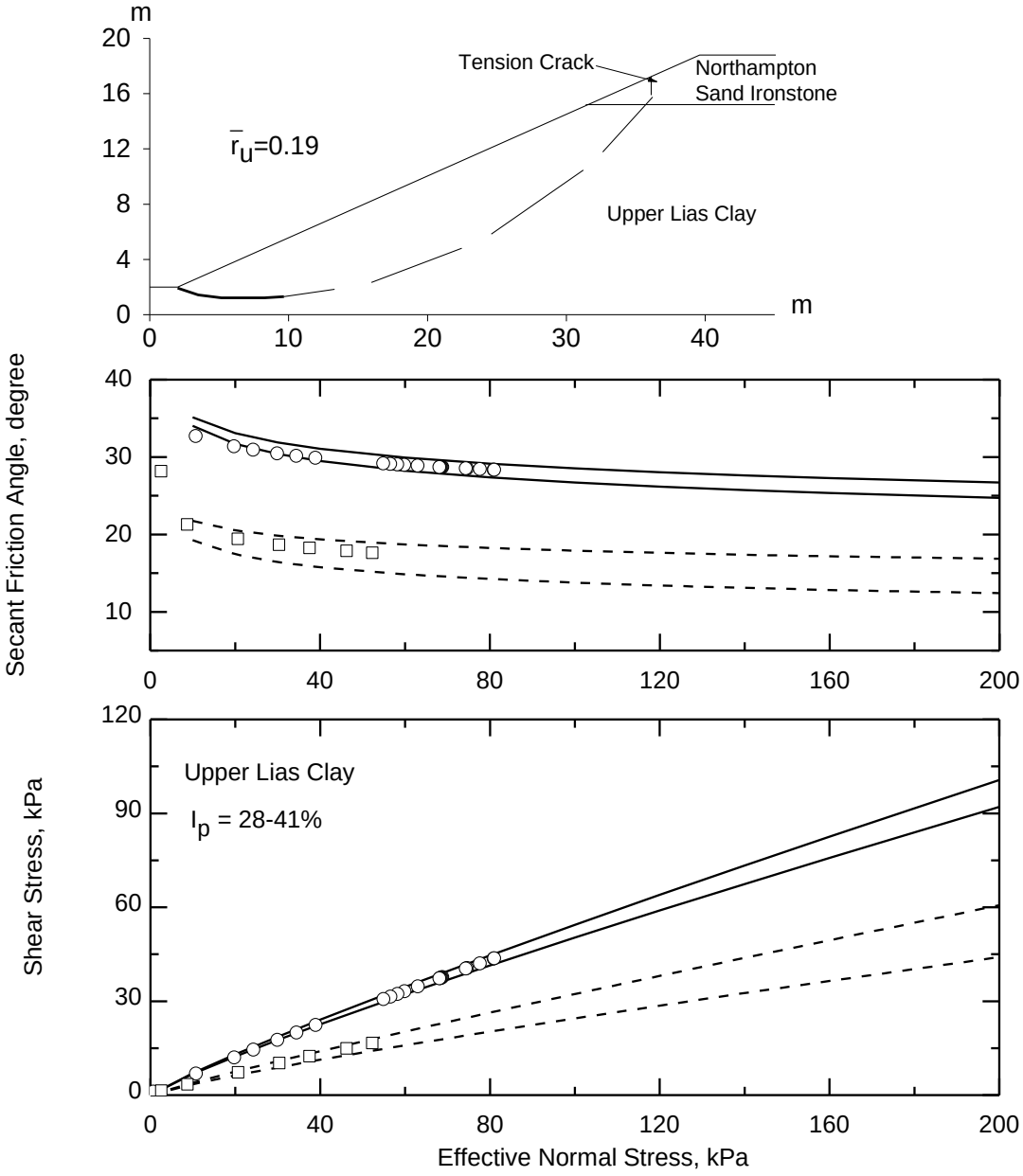

Figure A.24. First-time slope failure at Hunsburry Hill, UK, 1921 (Chandler 1974, Chandler and Skempton 1974)

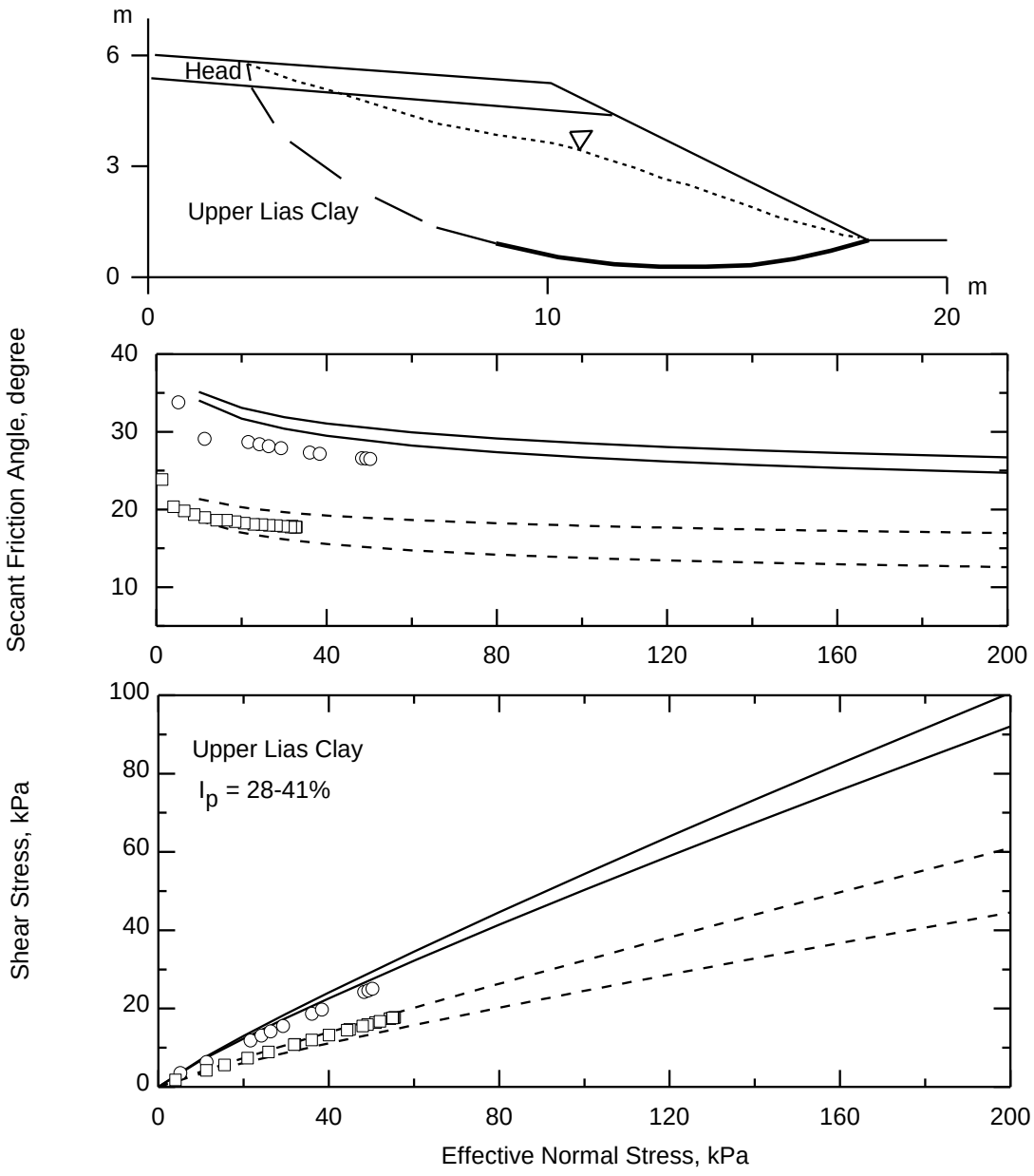

Figure A.25. First-time slope failure at Barrowden, UK, 1961 (Chandler 1974, Chandler and Skempton 1974)

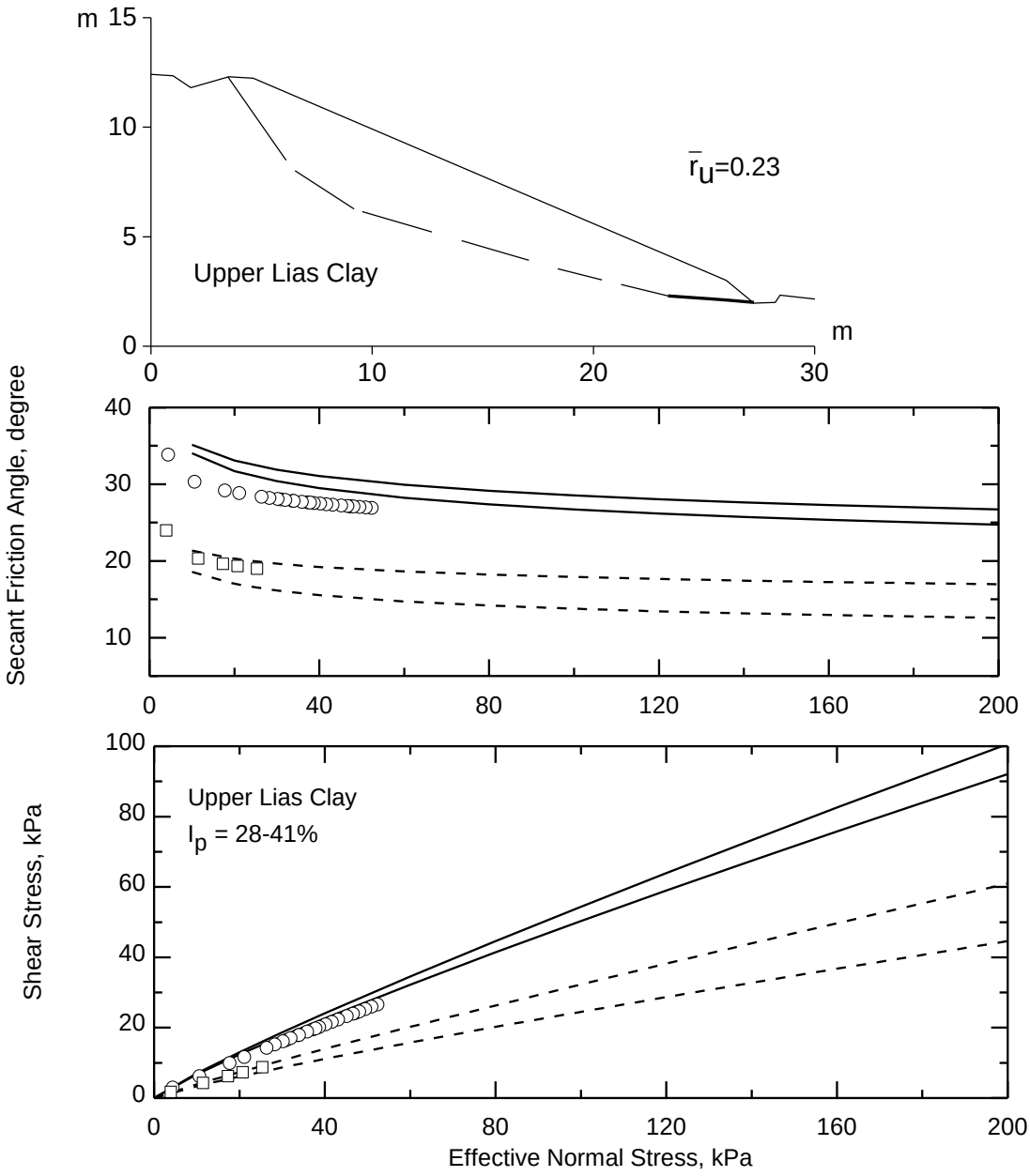

Figure A.26. First-time slope failure at Stowehill, UK, 1901 (Chandler 1974, Chandler and Skempton 1974)

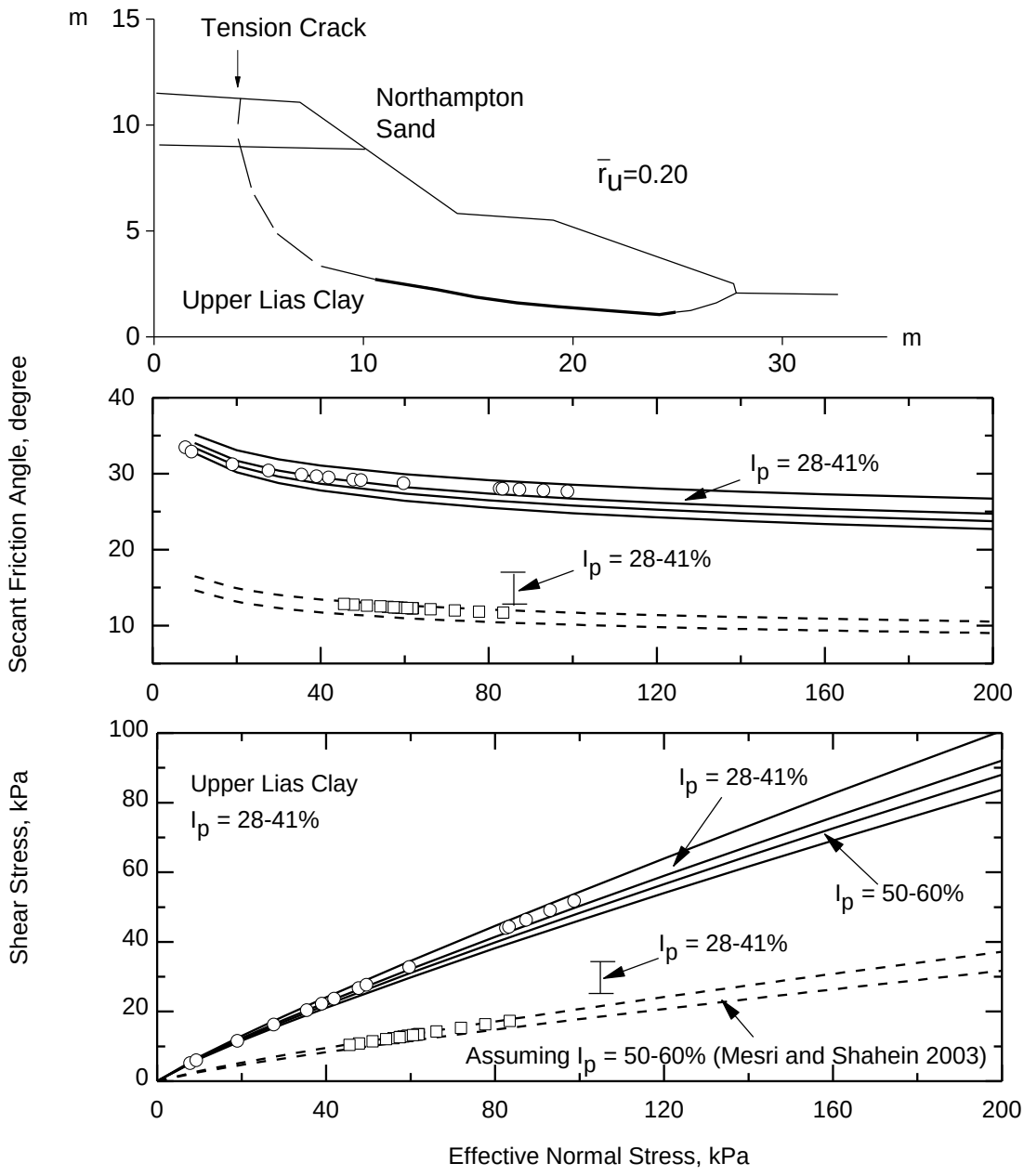

Figure A.27. First-time slope failure at Wellingborough, UK, 1961 (Chandler 1974, Chandler and Skempton 1974)

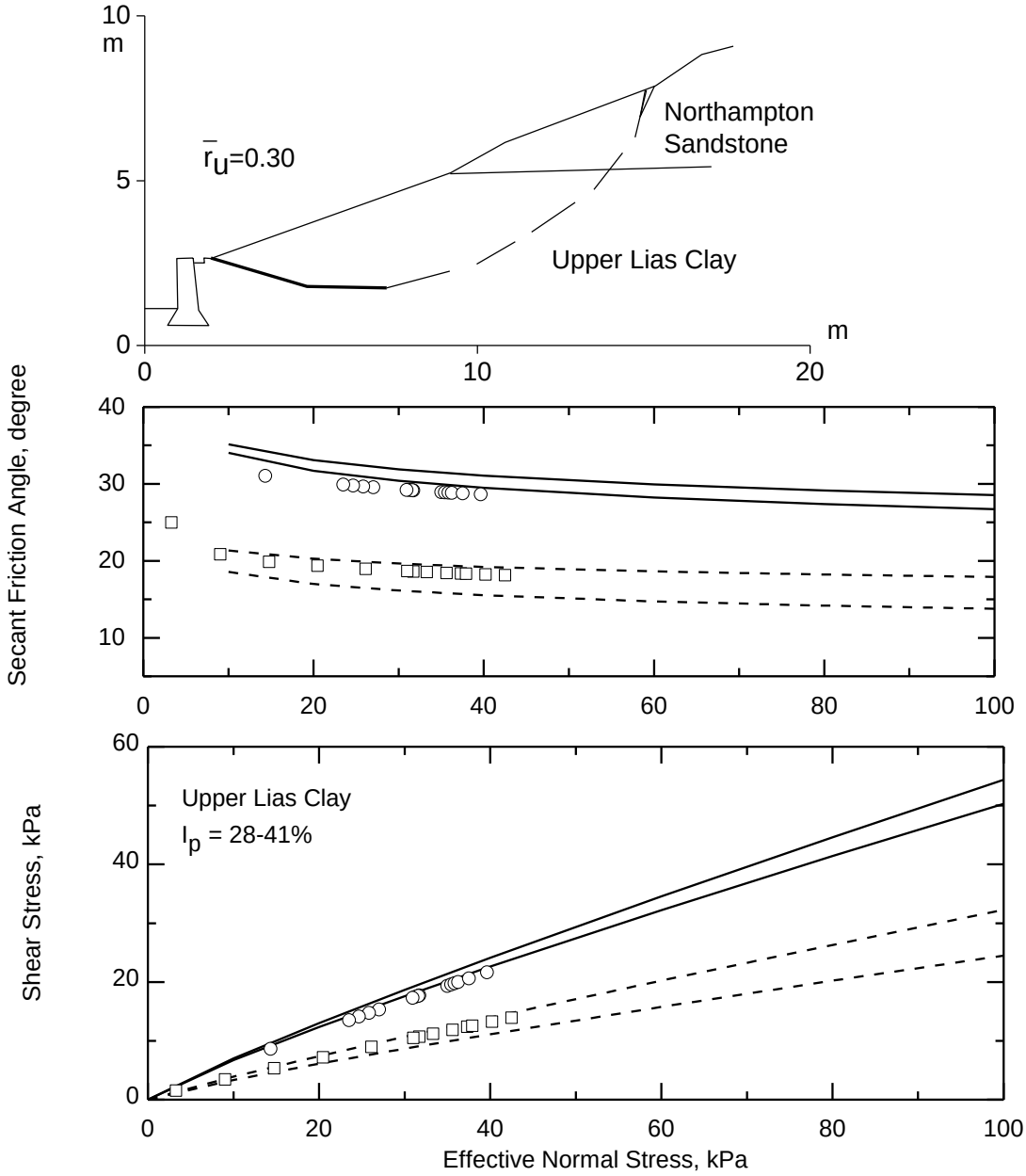

Figure A.28. First-time slope failure at Ardley Tunnel, UK, 1960 (James 1970, Chandler 1974, Chandler and Skempton 1974)

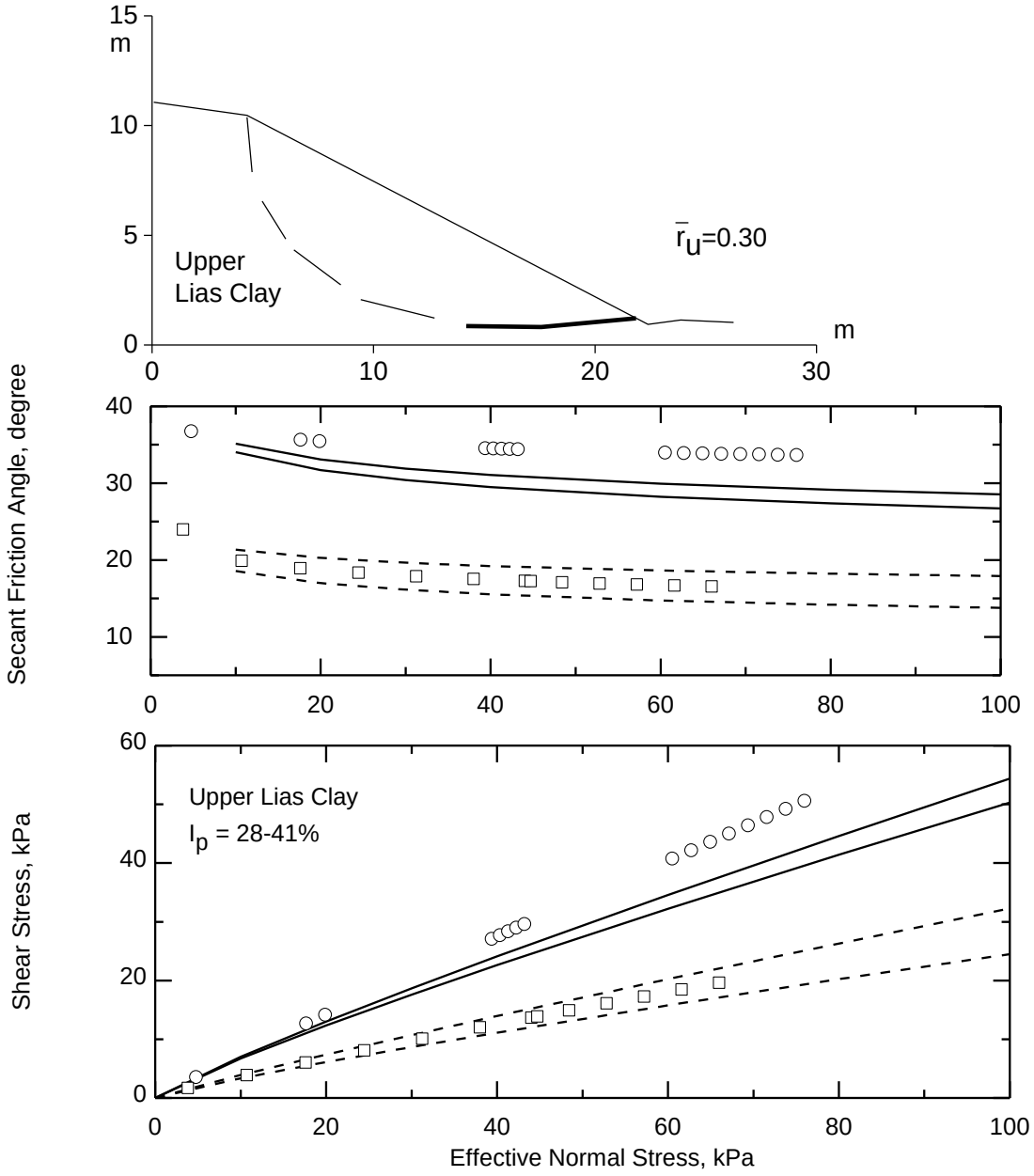

Figure A.29. First-time slope failure at Charwelton, UK, 1955 (James 1970)

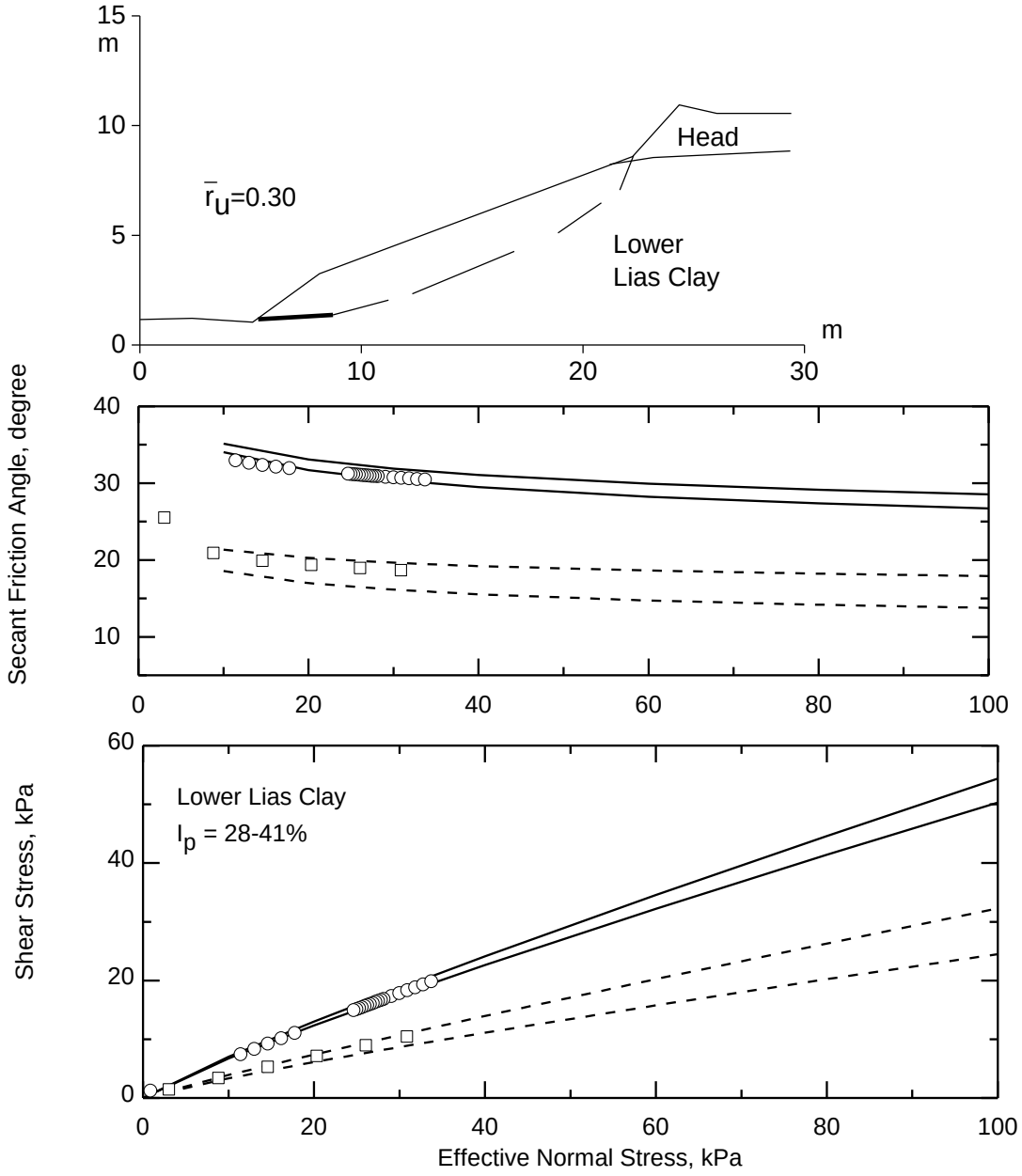

Figure A.30. First-time slope failure at Standish JCT, UK, 1964 (James 1970)

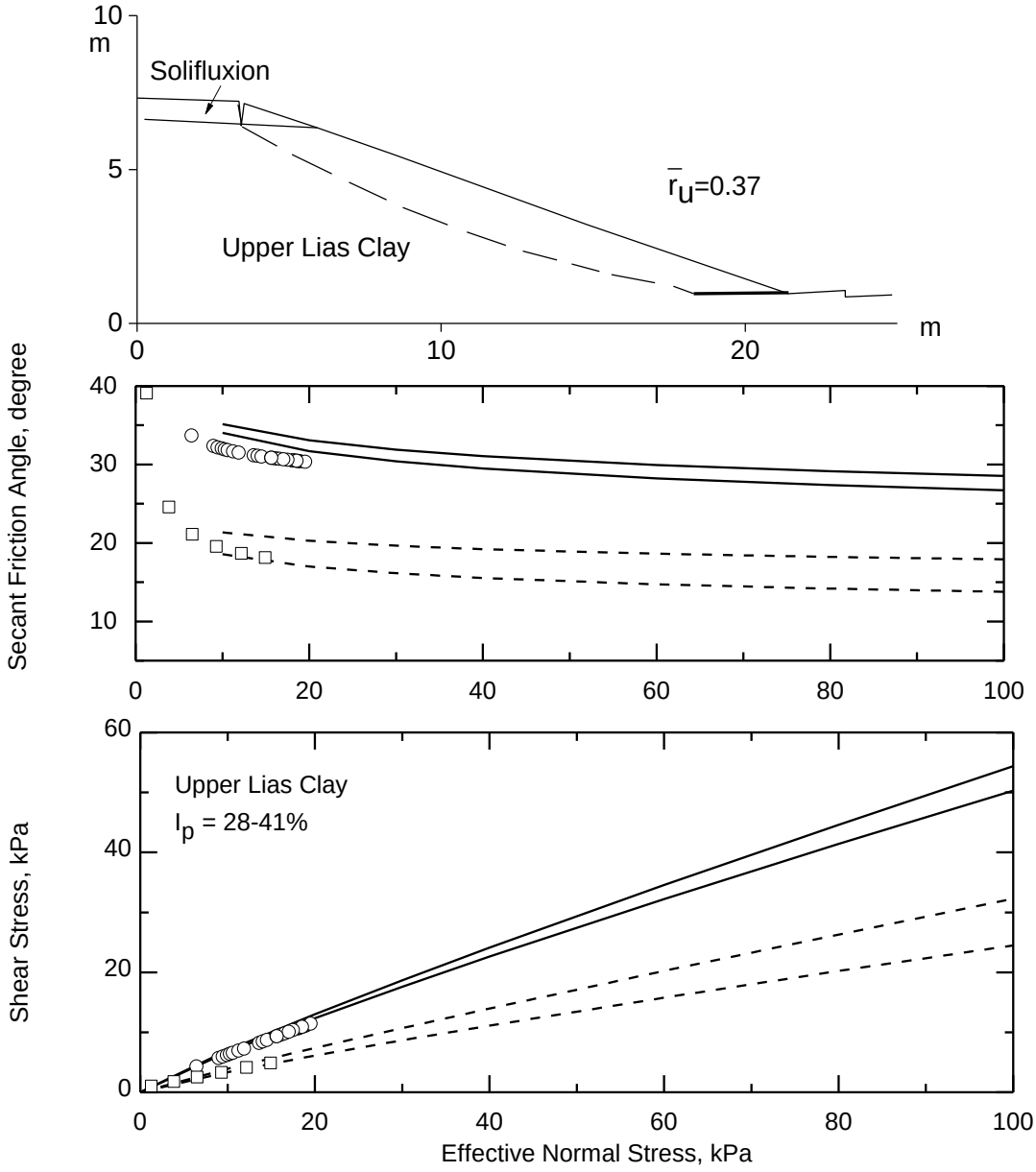

Figure A.31. First-time slope failure at Wothorpe, UK, 1964-1965 (James 1970, Chandler 1974, Chandler and Skempton 1974)

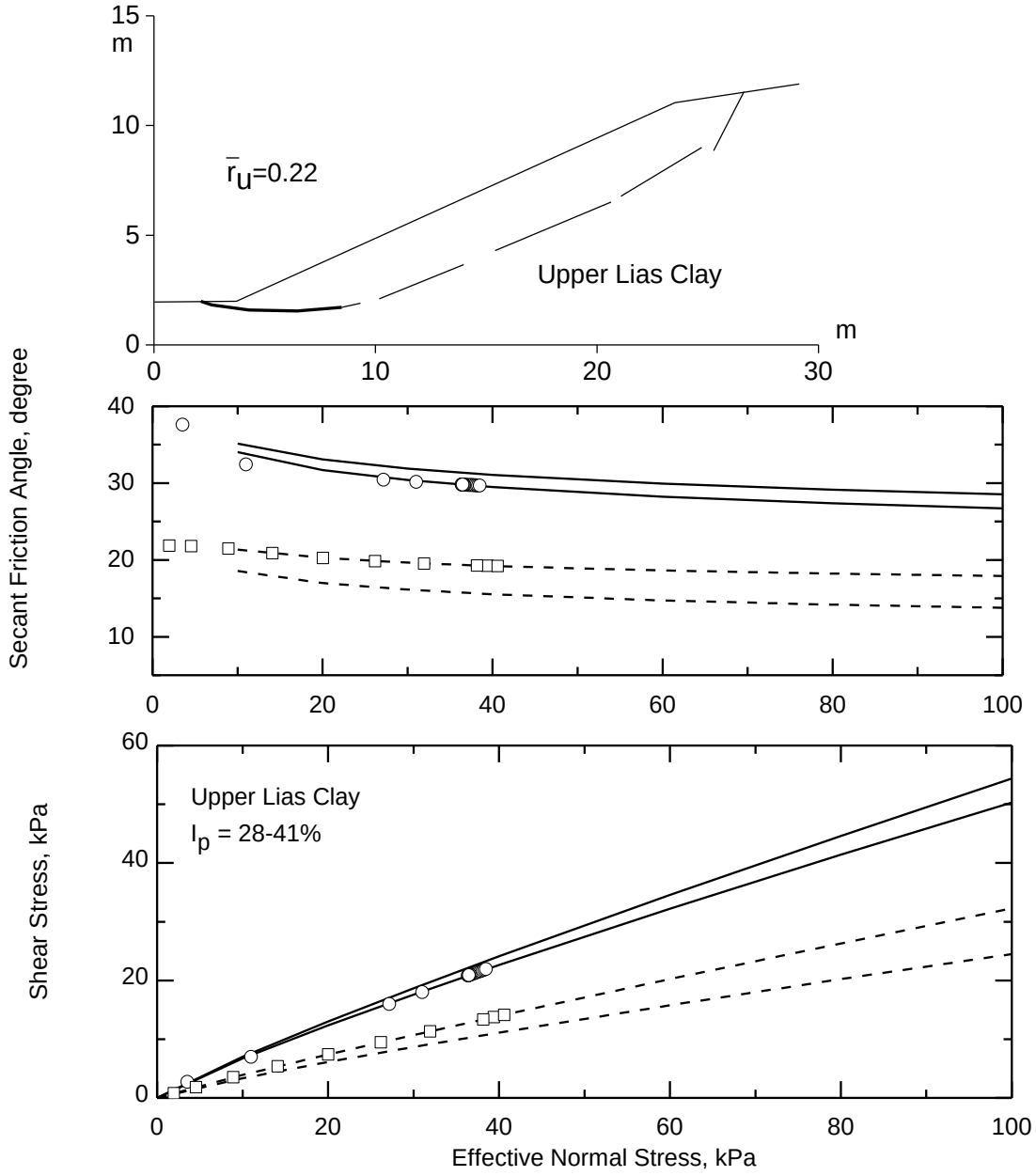

Figure A.32. First-time slope failure at Heyford, UK, 1961 (James 1970, Chandler 1974, Chandler and Skempton 1974)

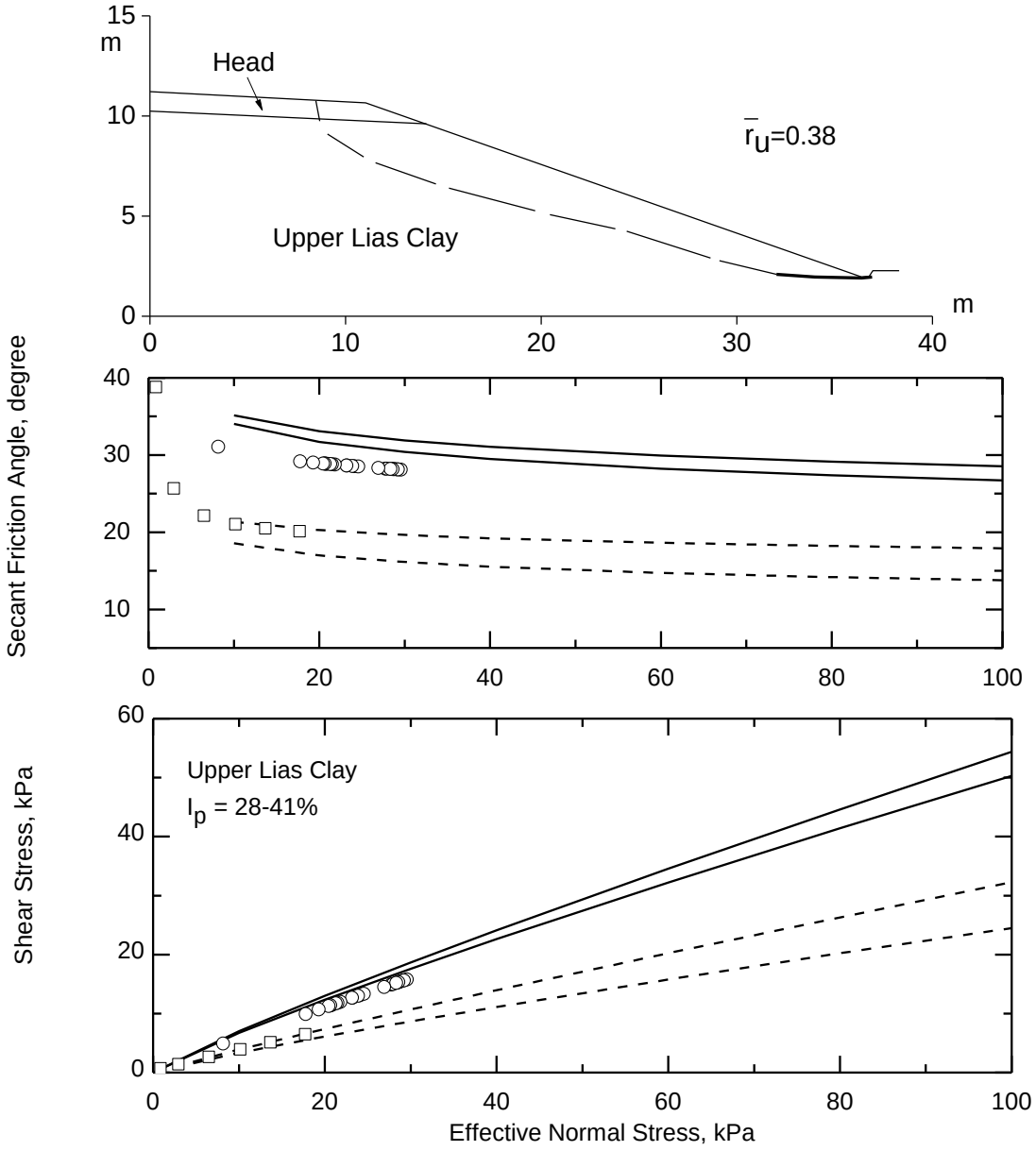

Figure A.33. First-time slope failure at Seaton, UK, 1963 (Chandler 1974, Chandler and Skempton 1974)

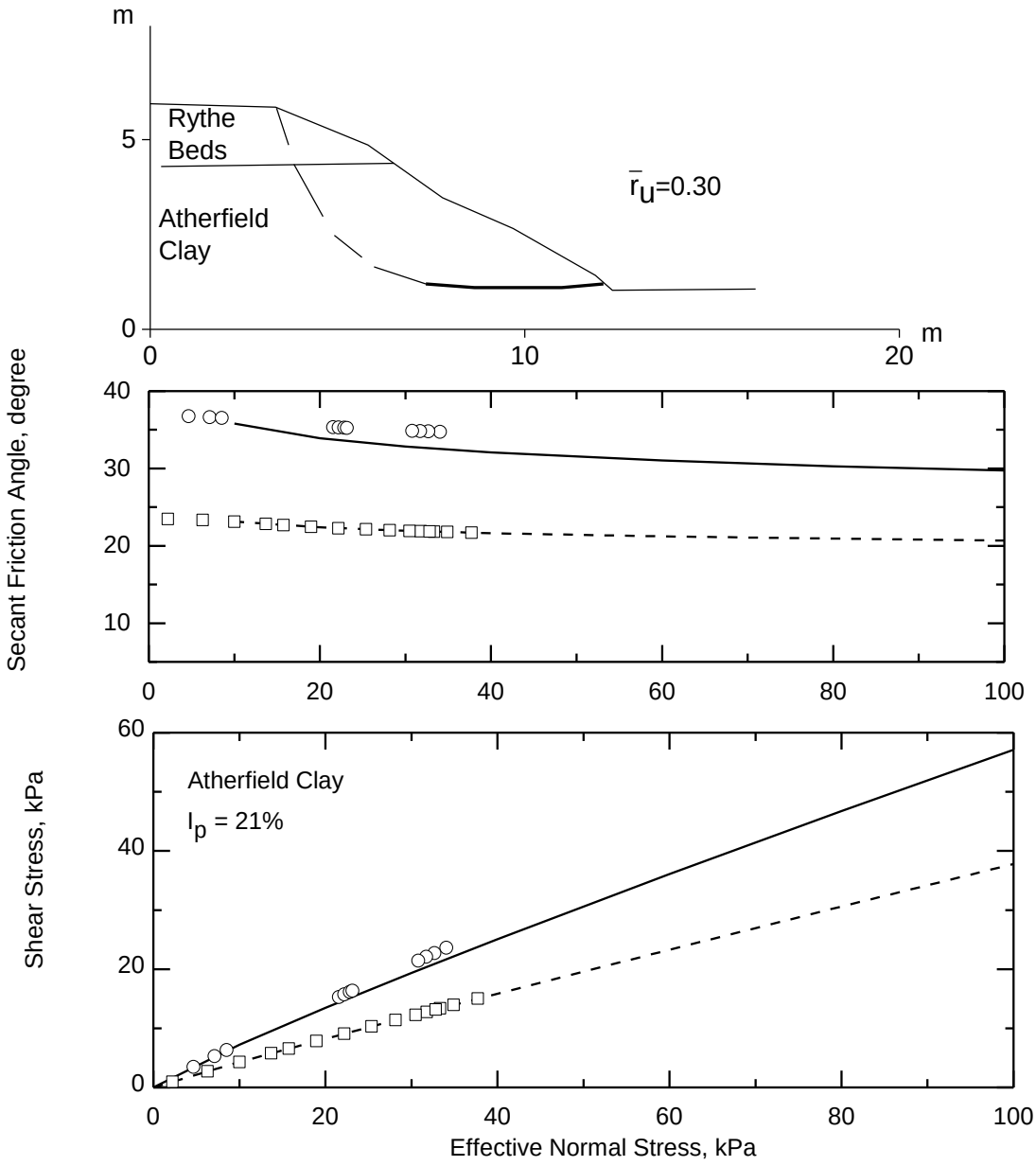

Figure A.34. First-time slope failure at Haslemere, UK, 1960 (James 1970)

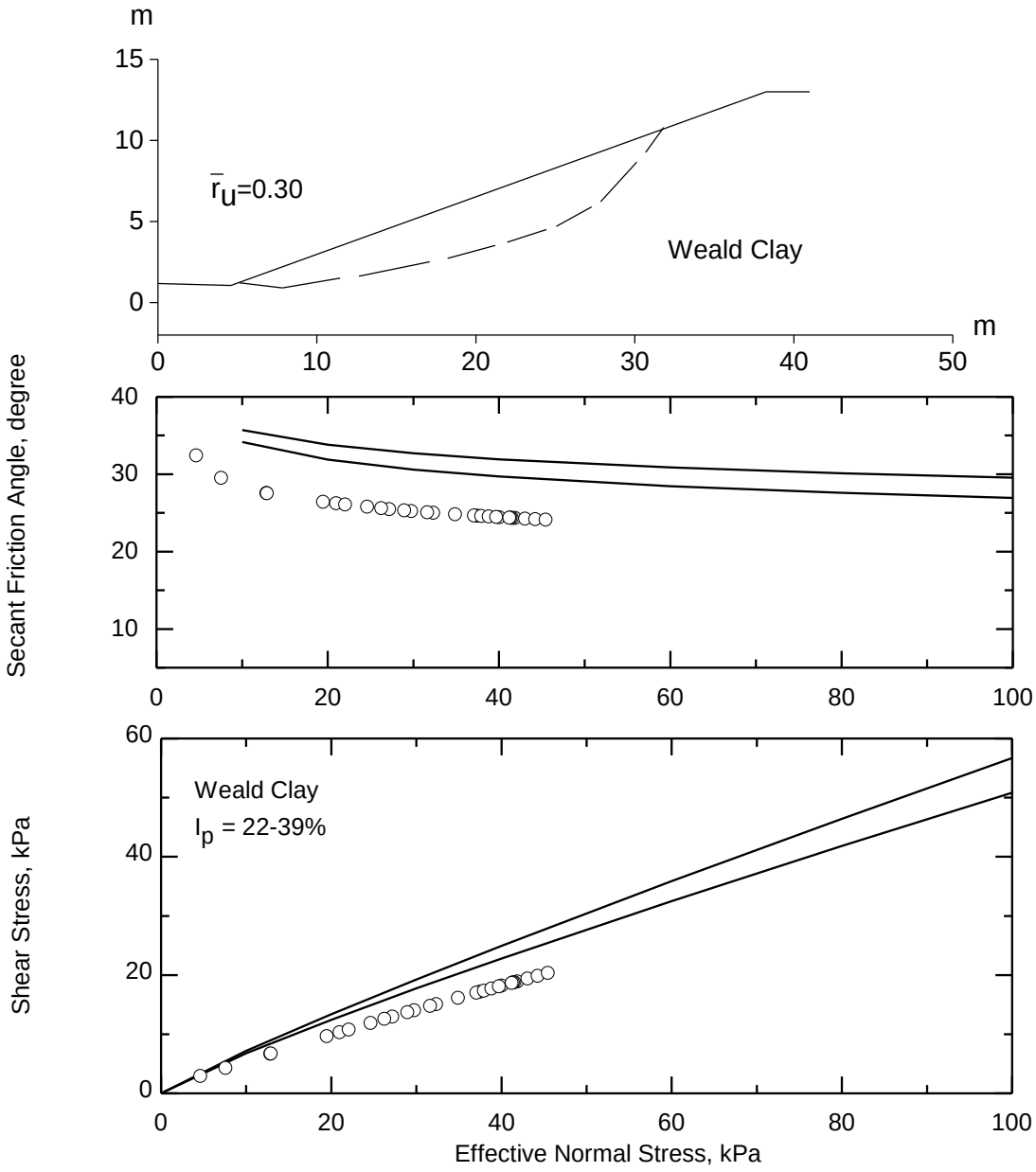

Figure A.35. First-time slope failure at Hildenborough, UK, 1936 (James 1970)

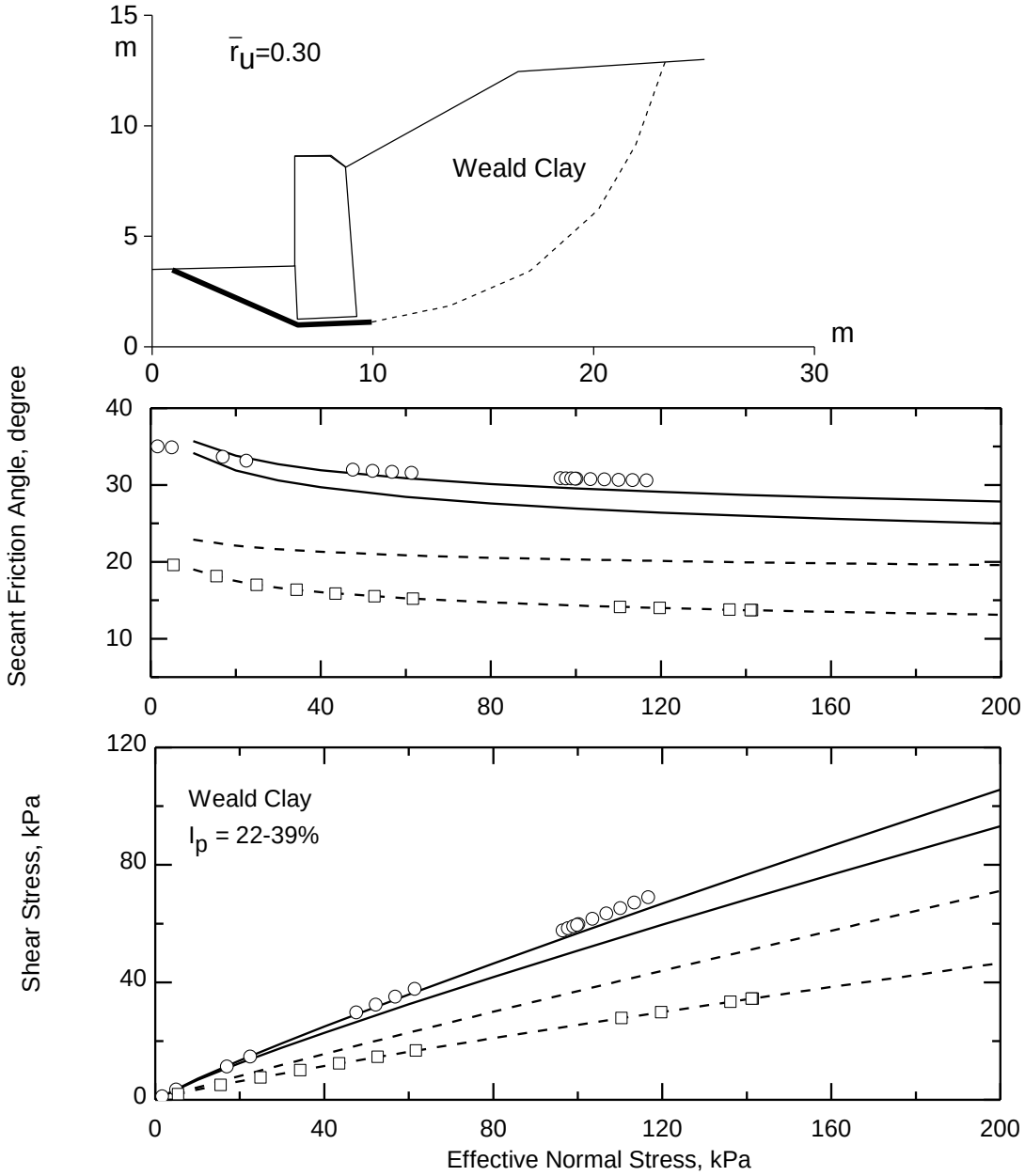

Figure A.36. First-time slope failure at Earlswood, UK, 1966 (James 1970)

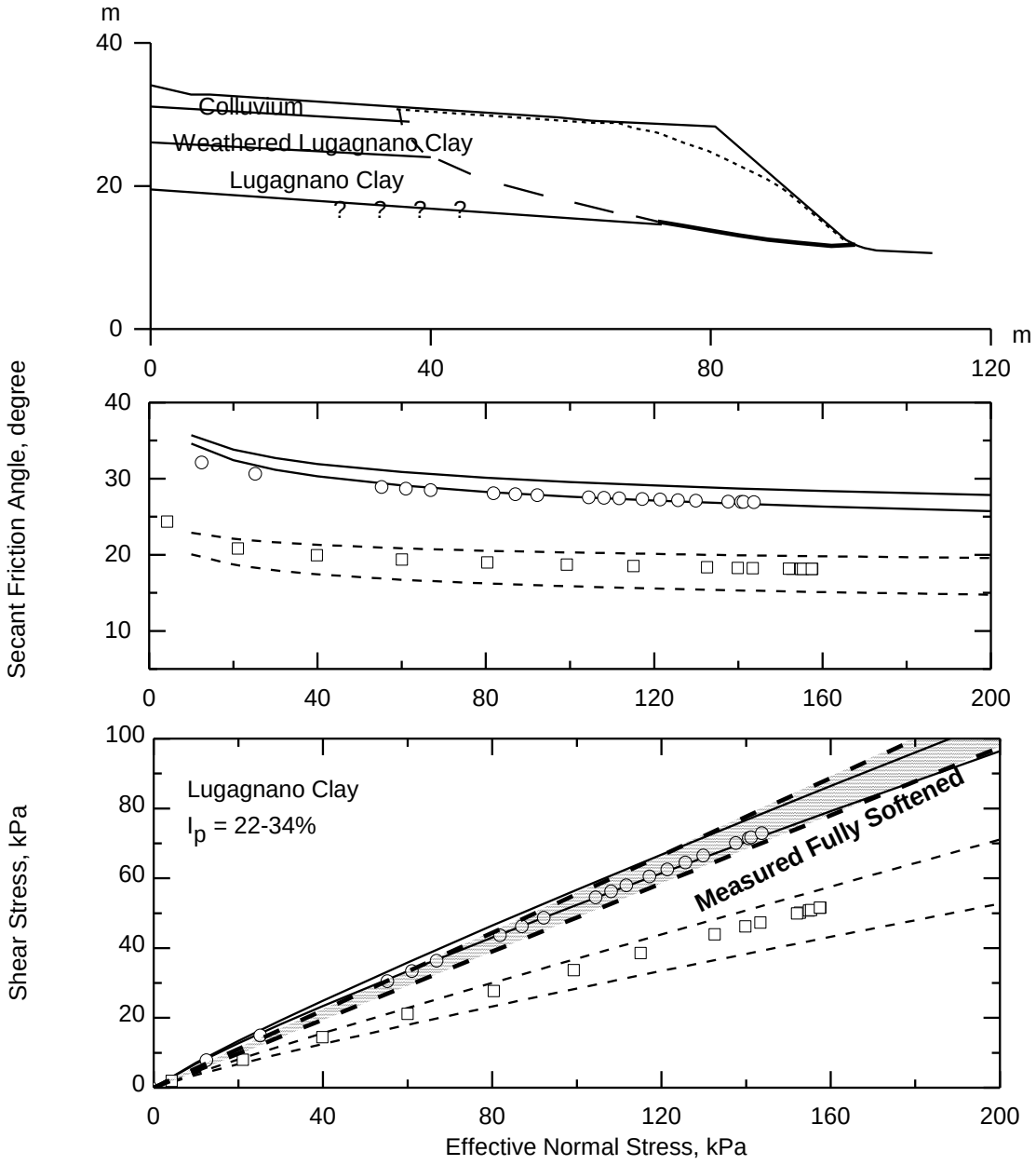

Figure A.37. First-time slope failure at Albedosa, Italy, 1978 (Cancelli 1981)

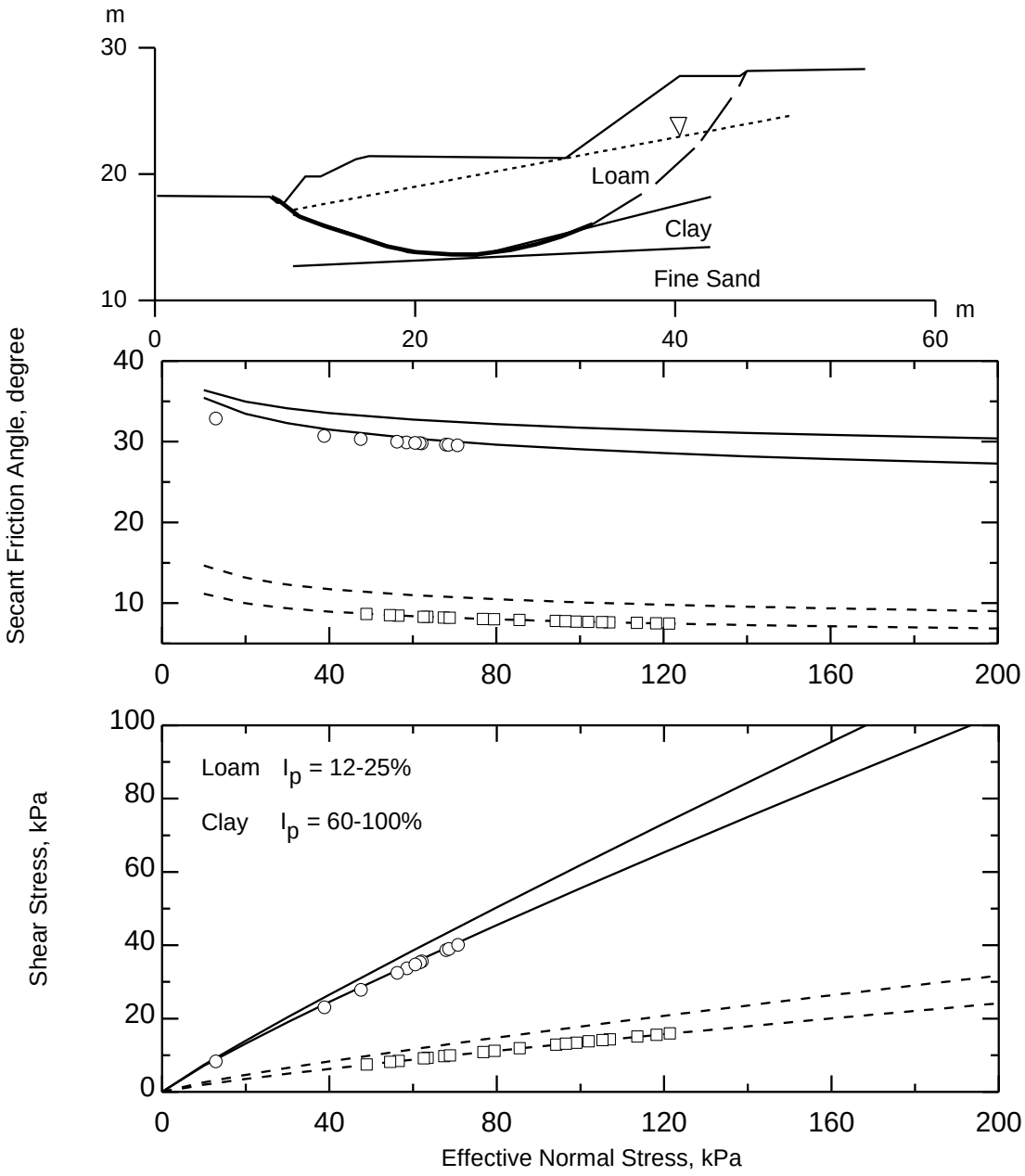

Figure A.38. First-time slope failure at Wettern, Brussels, 1943 (Marivoet 1948)

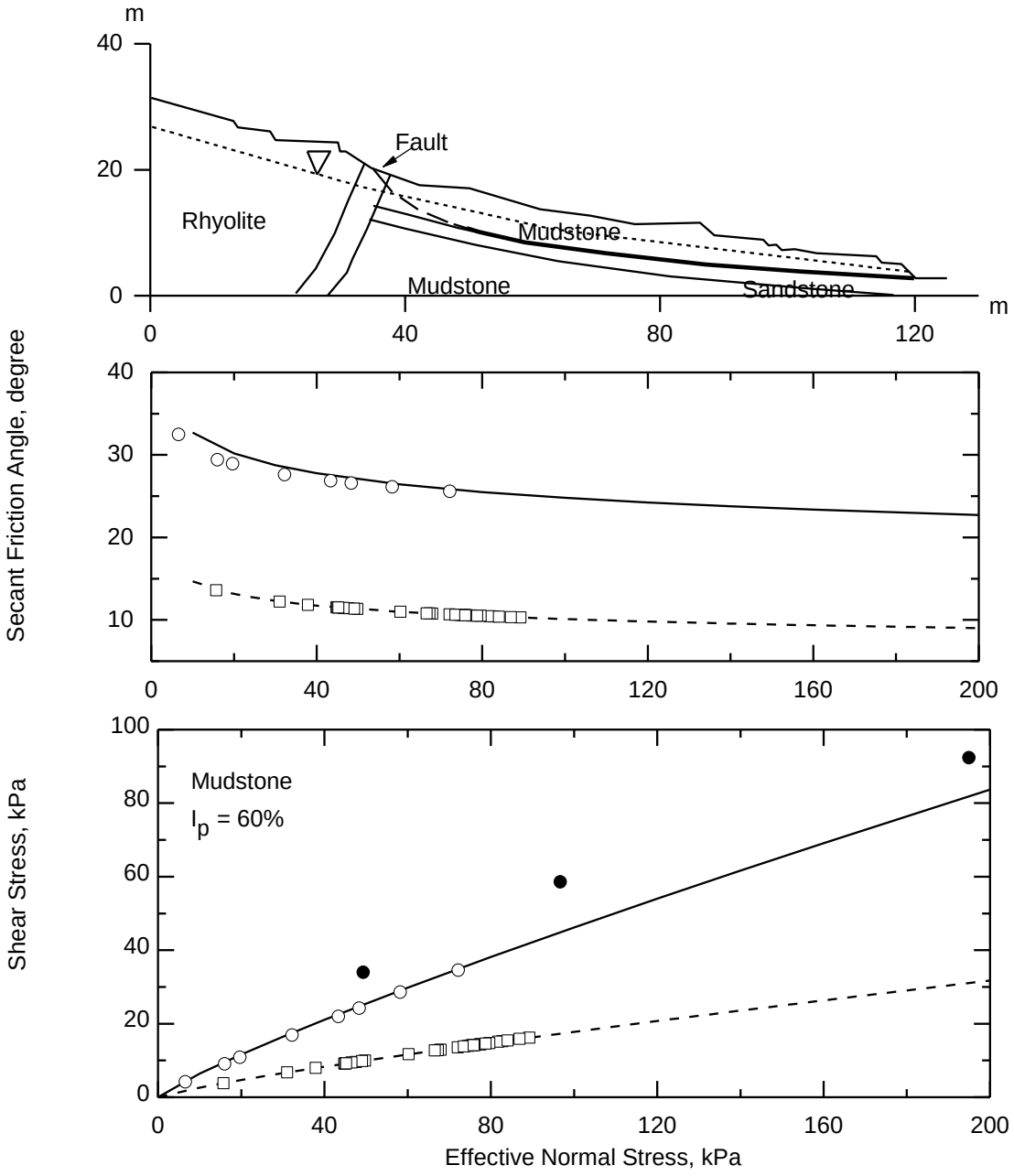

Figure A.39. First-time slope failure at Akitsu, Japan, 1991 (Nakamori et al 1996)

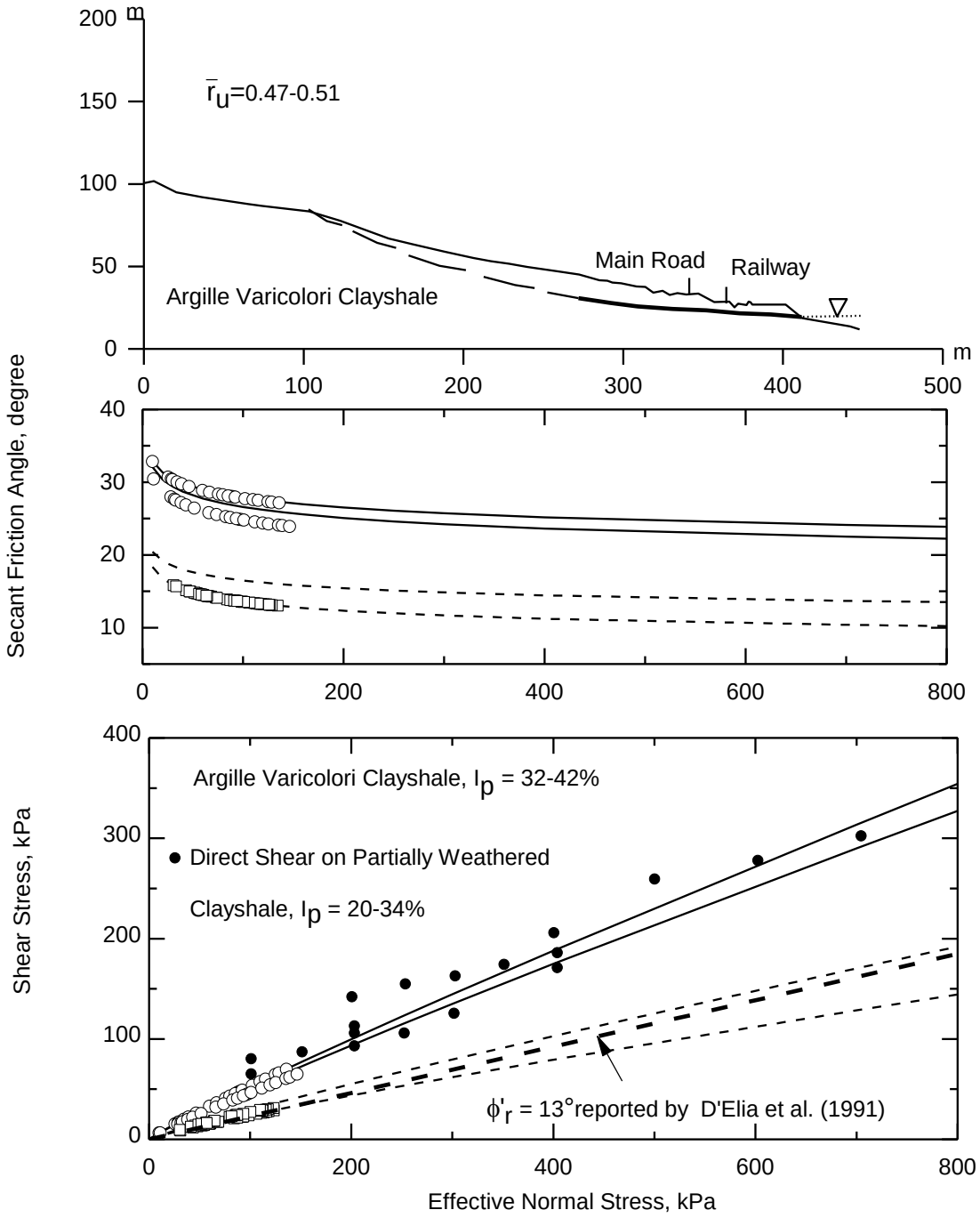

Figure A.40. First-time slope failure at Capo Spulico, Italy, 1973 (D'Elia et al 1991)

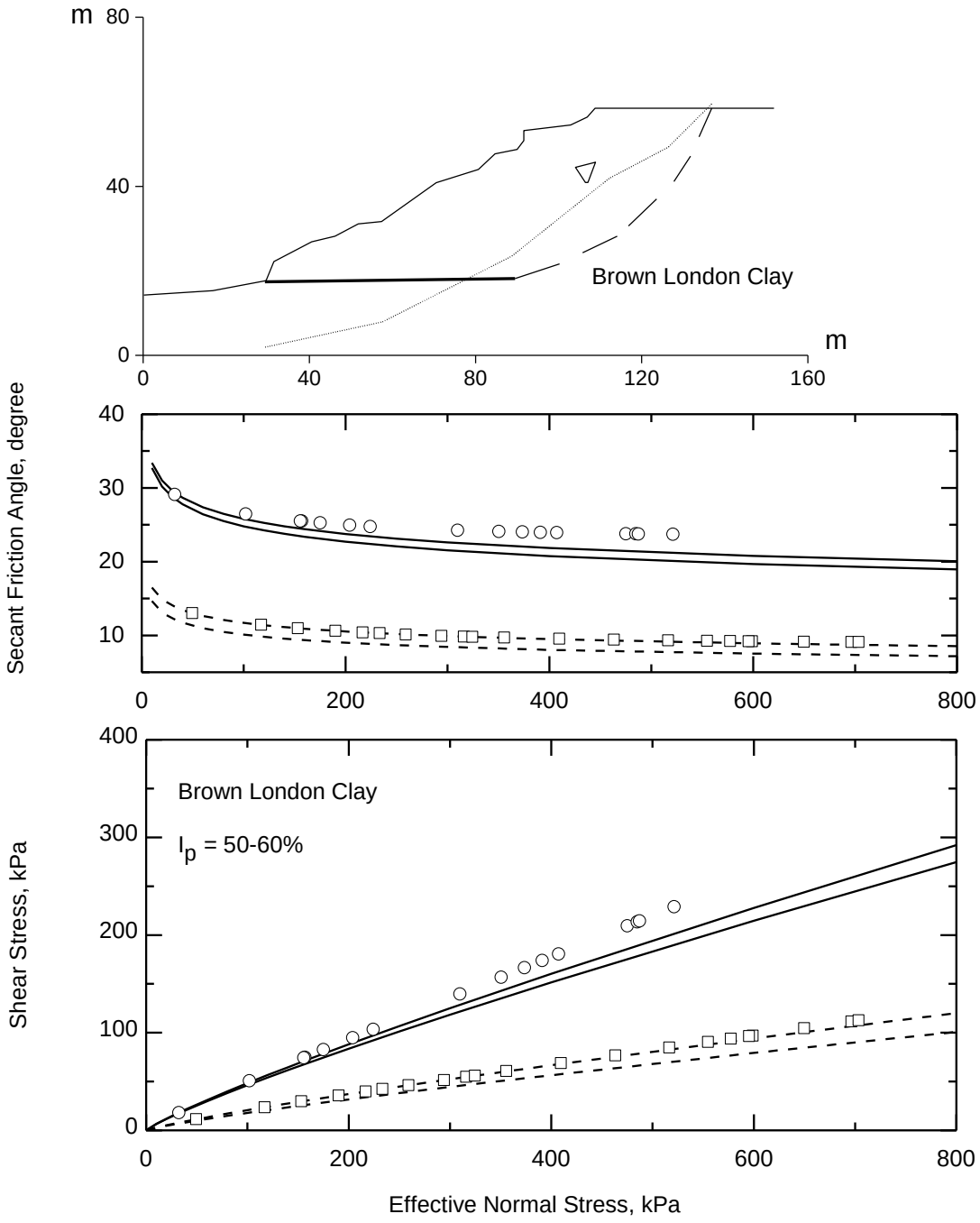

Figure A.41. First-time slope failure at Isle of Sheppey, England (Dixon and Bromhead 1991)

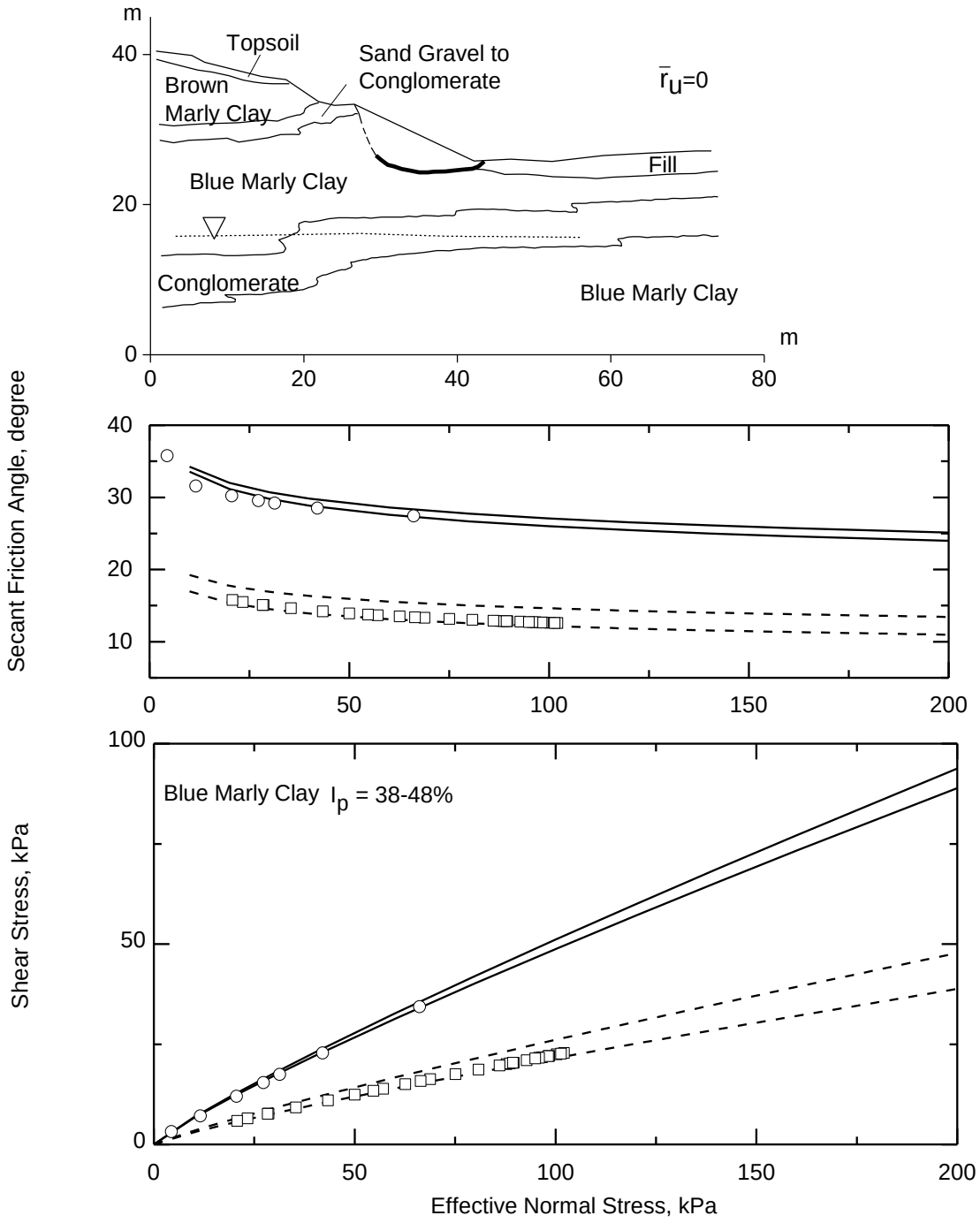

Figure A.42. First-time slope failure at Grava, Greece, 1975 (Sotiropoulos and Cavounidis 1980)

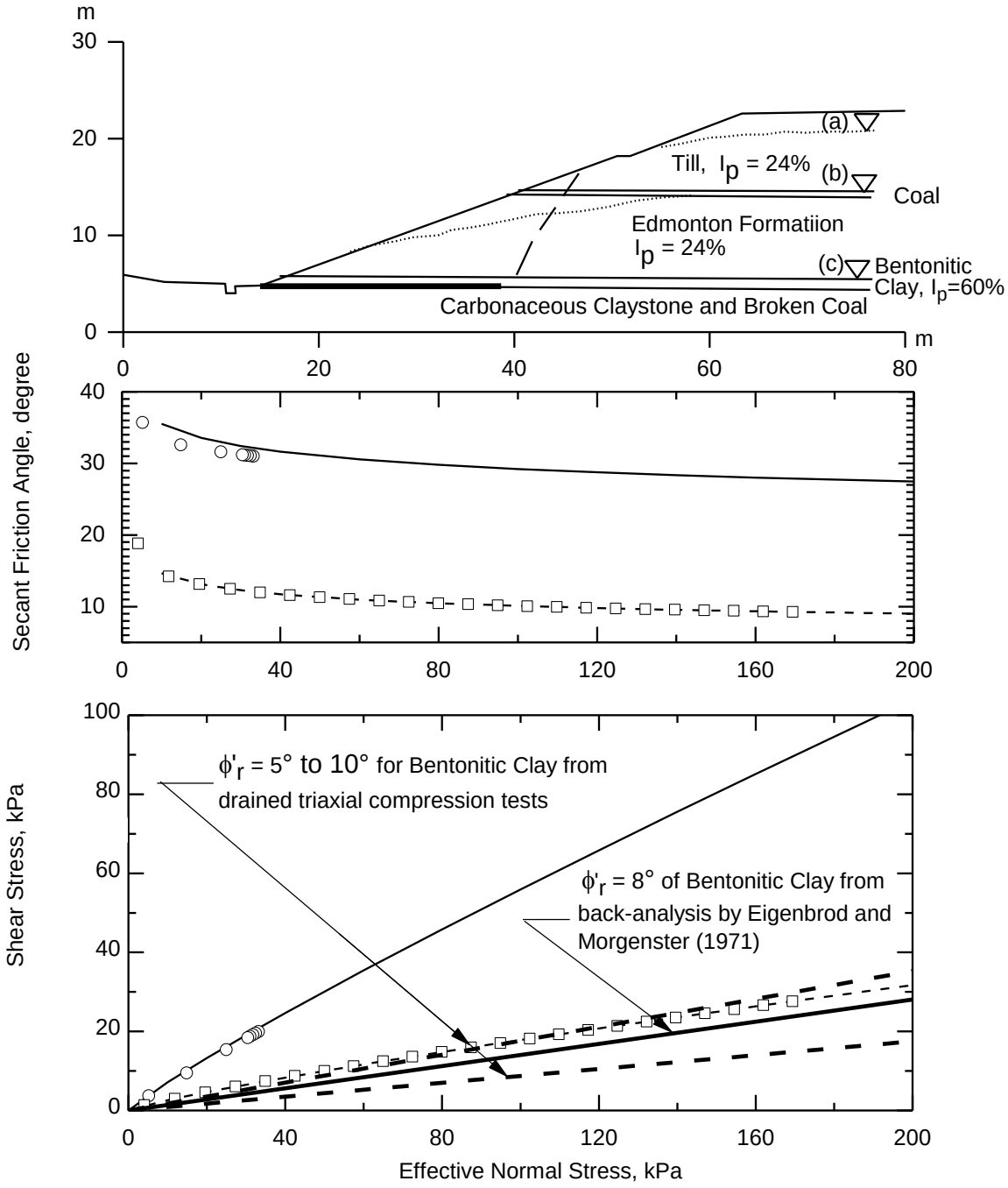

Figure A.43. First-time slope failure at Devon, Canada, 1965 (Eigenbrod and Morgenstern 1971)

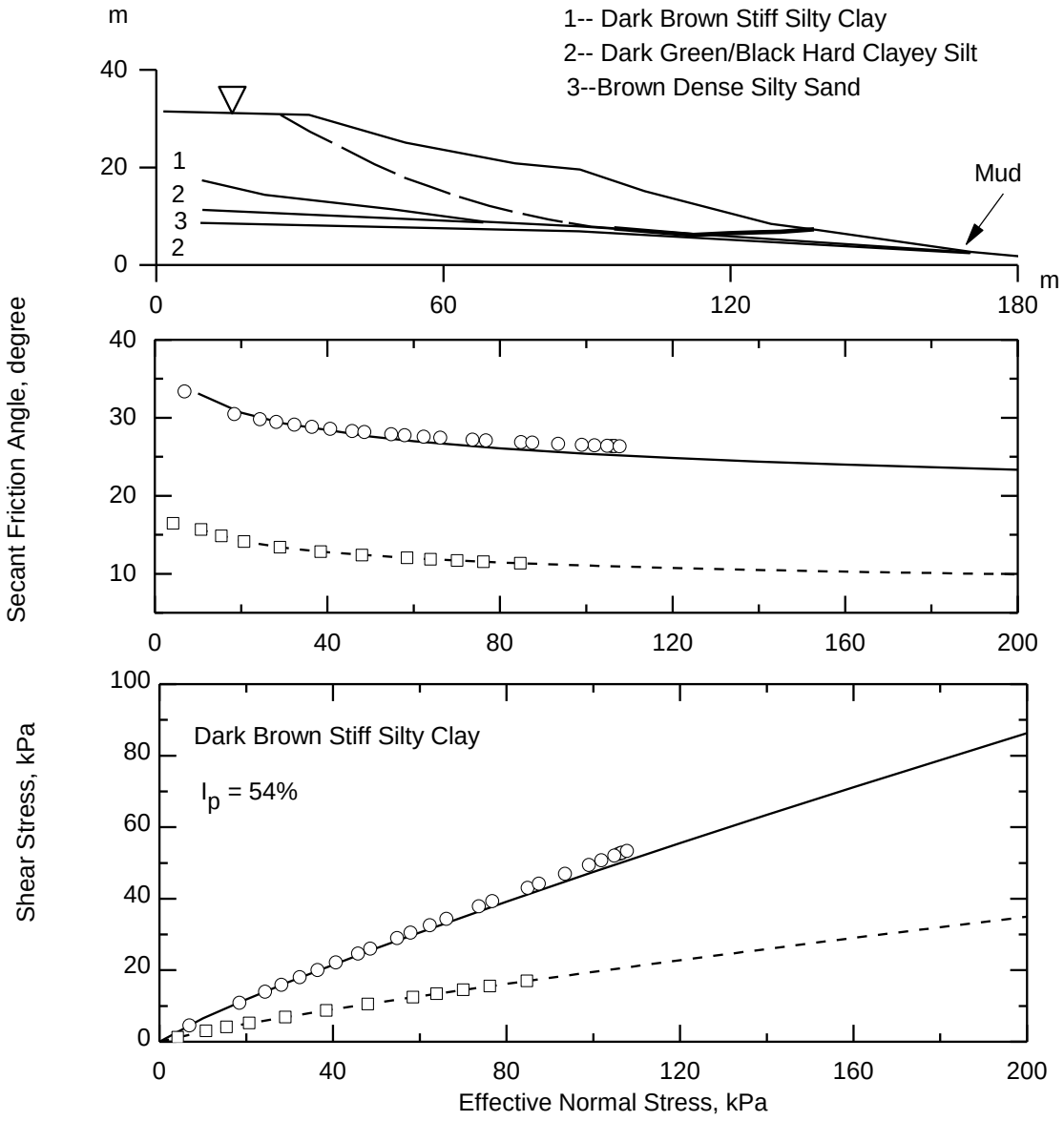

Figure A.44. First-time slope failure at North to Central National Highway, Greece (Anagnostopoulos and Georgiadis 2004)

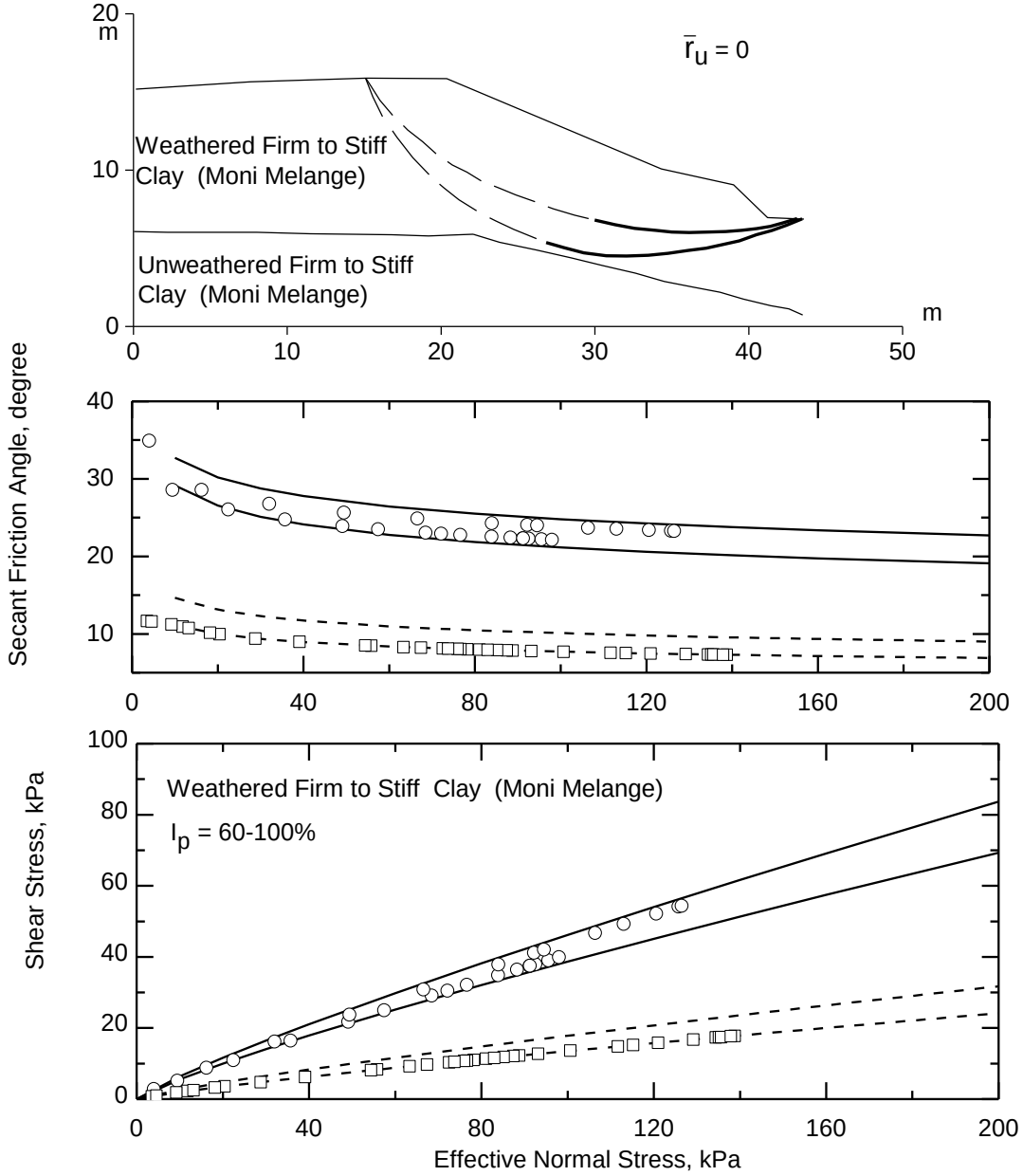

Figure A.45. First-time slope failure at Pendakomo, Cyprus, 1981, using reported slip surfaces (Gostelow and Loucaides 1988)

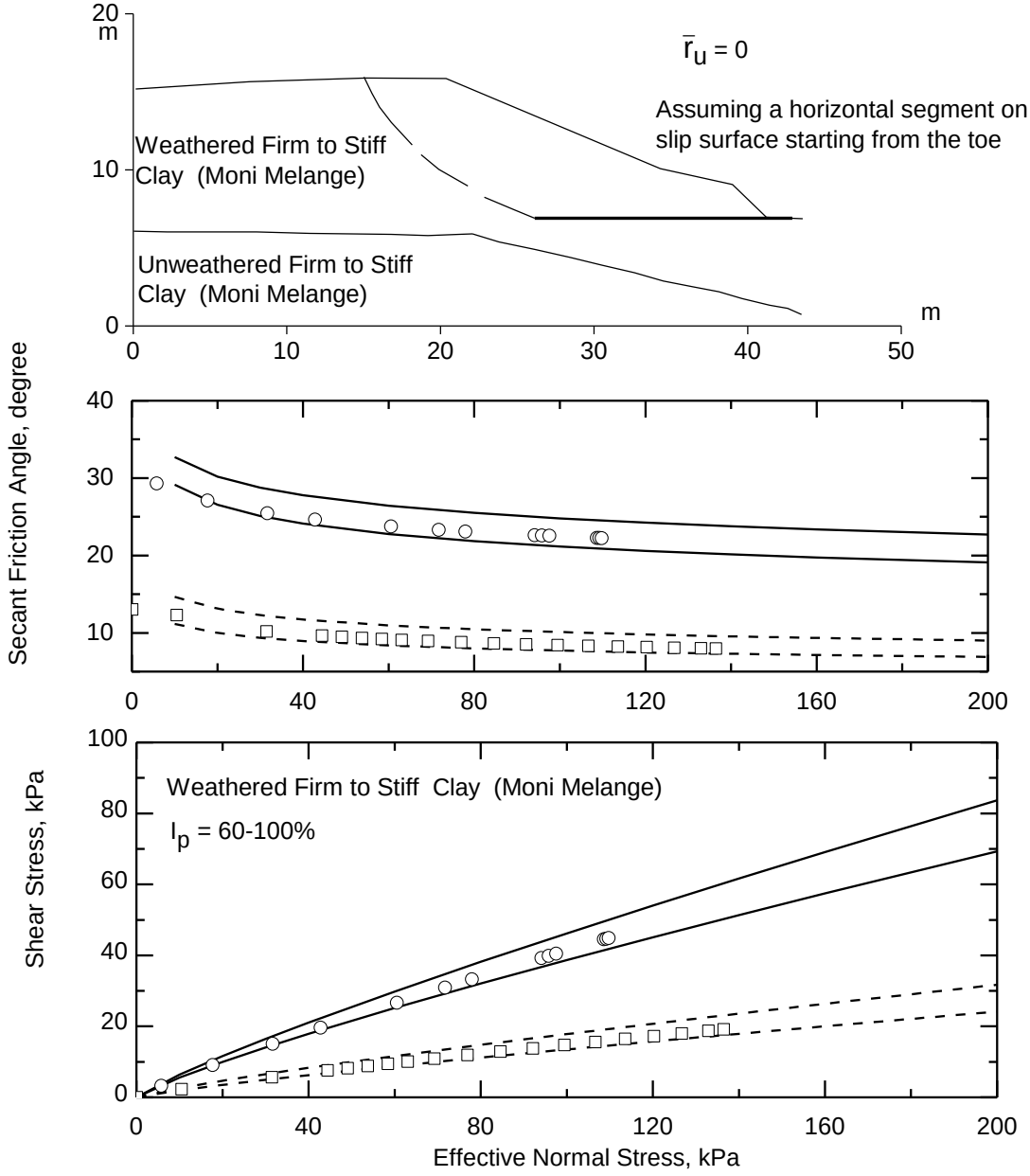

Figure A.46. First-time slope failure at Pendakomo, Cyprus, 1981, assuming a sub-horizontal basal segment of slip surface (Gostelow and Loucaides 1988)

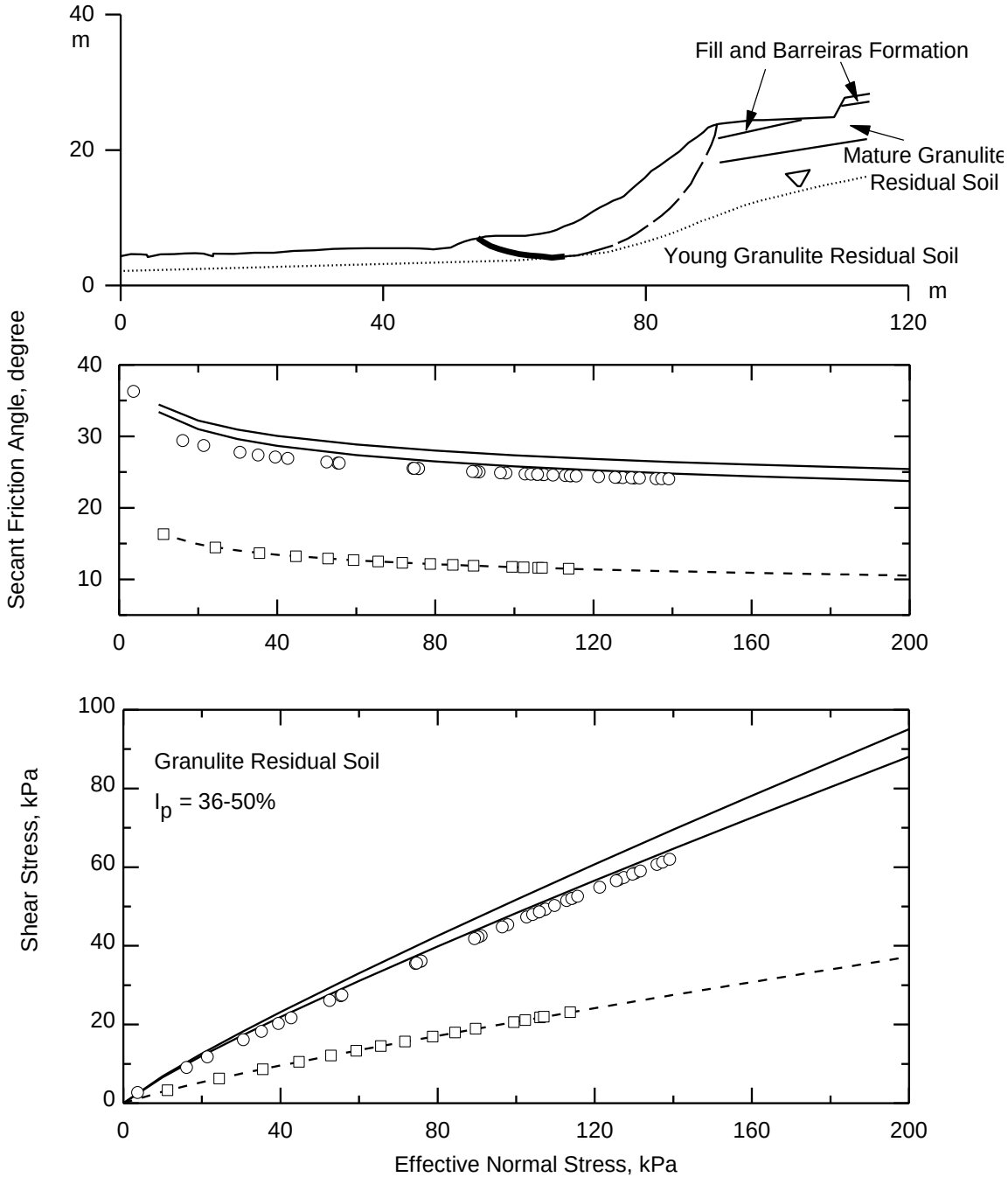

Figure A.47. First-time slope failure at Salvador, Brazil (Magalhaes et al. 1992)

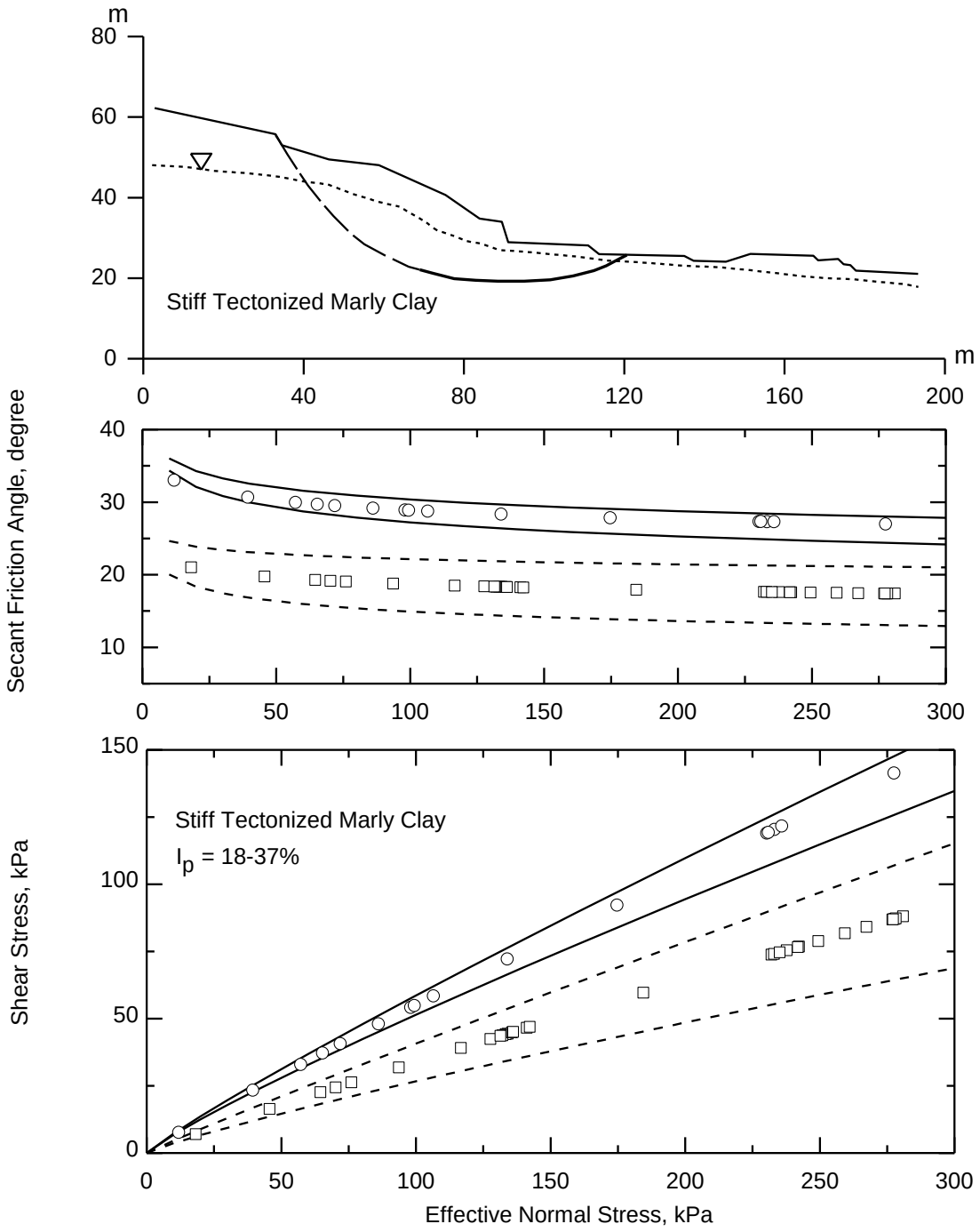

Figure A.48. First-time slope failure at Risalaimi, Italy, 1962 (Valore 1995)

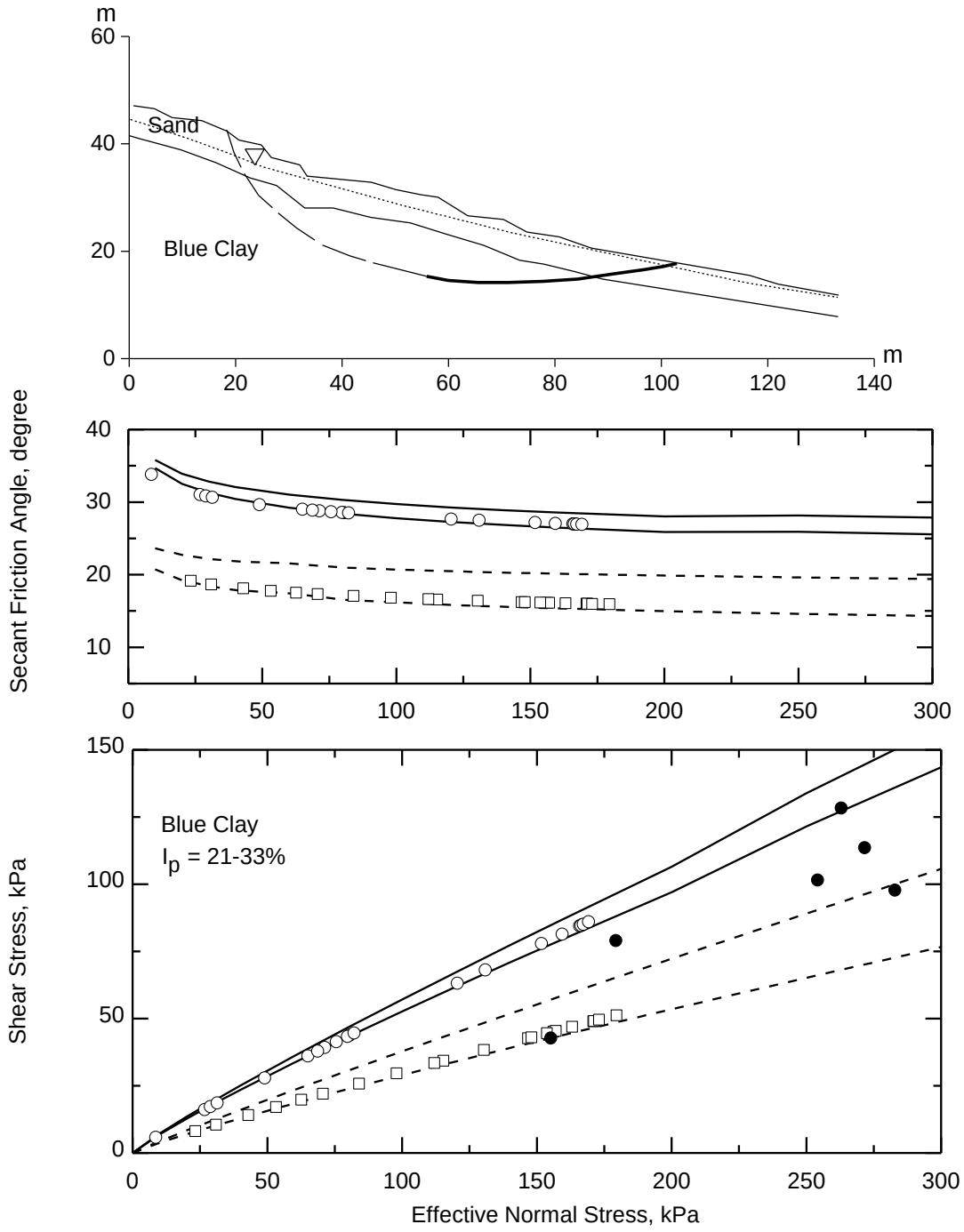

Figure A.49. First-time slope failure at Grassano, Italy, 1998 (Di Maio and Vassallo 2011)

APPENDIX B: BACK-ANALYSES OF FIRST-TIME SLOPE FAILURES WITH MOBILIZED SHEAR STRENGTH CLOSE TO FULLY SOFTENED SHEAR STRENGTH ON THE ENTIRE SLIP SURFACE

People's Republic of China (Li and Zhao 1984)

Li and Zhao (1984) reported a first-time failure in a cut slope in fissured clay in China. The excavation began in 1970, and was completed in one year. The cut slope (Fig.B.1) with two banquettes, which has a height of 23m and inclination of 1:1.25 (H: V), failed after the rainy season in 1981. The slip surface based on test pits, turned out to be an arc of a circle. The brown fissured clay has a natural water content of 22%, liquid limit of 40%, plasticity index of 20%, and clay size fraction of 20%. The ground water condition was not reported, however, according to the back-analyses of the slide by Li and Zhao (1984), an equivalent $\bar{r}_u = 0.03$ was used in the present study. Because a horizontal or sub-horizontal segment of slip surface was not reported, the back-calculation was made to the entire rotational slip surface, with the assumption of mobilized shear strength greater than the residual condition. The back-calculated shear strength on the entire slip surface is equal to that defined by $I_p = 20\%$, from the empirical correlation for fully softened shear strength developed in the present study.

River Fossate, Italy (D'Elia et al 1980)

This slope failure in upper basin of River Fossate, Italy, is located in an unstable area formed by a complex formation "variegated clay shales" which is highly tectonized. The valley slopes in this area studied by D'Elia et al (1980) were involved in two types of landslides. The first one was the mudflow type, in which the residual strength was mobilized along a pre-existing failure surface. Slumps and complex landslides (Skempton and Hutchinson, 1969) were also active in this area, and they are regarded as first-time slides. In this research, only the slump and complex landslide is examined, which was referred as slide 2 in D'Elia et al (1980). The slope has in average inclination of 23° and the depth of the sliding mass is about 30 m (Fig.B.2).

The "variegated clay shales" consists mostly of clay shales with sheared structures including blocks or thin marly limestones and limestone layers. Shiny and polished surfaces are sometimes

observed in the clay shales. The site investigation reveals that the top layer is a loosened and weathered clay shale of 1-2m thickness in the sloping areas and 4-5m thickness in the level area. The lower unloosened formation consisting of dense mass of clay shales, has a liquid limit in the range of 45% - 79%, and plastic limit in the range of 25% to 42%. As a result, the plasticity index is in a relatively wide range, from 14% to 37%. The piezometric surface shown in Fig.B.2 is at 5 to 10 m below ground surface according to the Cassagrande and pneumatic piezometer readings. Slip surface in Fig.B.2 was determined by D'Elia et al (1980) based on the surface observations.

The shallow rotational slip with an equivalent $\bar{r}_u$ of 0.31, results in effective normal stresses on a large portion of the slip surface no greater than 100 kPa. The back-calculated mobilized shear strength on the entire slip surface is similar to that defined by I_p = 14%, from the proposed empirical correlation for fully softened shear strength. The back-calculated secant friction angles are greater than those determined from the consolidated drained triaxial compression tests (solid circles) and direct shear tests (solid diamonds) on undisturbed specimens reported by D'Elia et al (1980). The shear strength of the clay shales determined from the drained triaxial compression tests is lower than that at Ip = 14% - 37% from the empirical correlation for fully softened shear strength developed in the present study; and the shear strength determined from the drained direct shear tests is in the range of the proposed shear strength. It is possible that the inclusion of polished surfaces in the clay shale specimens, results in the shear strength determined on the undisturbed specimens lower than the intact shear strength.

Allori Coal Field, Italy (D'Elia et al 1988)

The monitoring of mine high cuts in the southern part of Allori coal field, Italy, during the excavations, was carried out for more than 10 years. A large rotational slope failure took place in 1986 when the cut slope height reached 205m. These investigated cut slopes in Santa Barbara locate along the western shore of the old Valdarno Lake. The slope angle was about 32° (Fig.B.3) by the time of failure and the maximum depth of the slide was up to 70 to 80m.

The field investigation, laboratory tests and monitoring were commenced from 1978. The monitoring included 1) ground surface displacements, displacements in depth by means of inclinometric probes, fixed in-place inclinometer, or slip indicators, and 2) pore-water pressure

measurements using open tube, Casagrande piezometers and electropeumatic cells. As shown in Fig.B.3, the bottom of the lake consists of Macigno Formation while Argille Scagliose is the main component material of the shore. Argille Scagliose is an allochthones which can be partly suggested by the occurrence of the underlying lacustrine deposits and the brown coal seams which are distorted. The mostly involved slide material Argille Scagliose is composed of 85% clay shales and 15% marly and siliceous limestones. Laboratory tests reveals that the clay shale has a plasticity index in the range of 8% - 20% according to Atterberg limit tests on the weakest fraction of the sample. The slip surface in Fig.B.3 determined based on morphological evidence and slip indicator, was used in the back-analysis in the present study, together with the reported ground water condition shown in Fig.B.3.

The back-calculated mobilized shear strength on the entire rotational slip surface, is close to that at I_p = 20%, from the empirical correlation for fully softened shear strength developed in the present study. The mobilized shear strength on the entire slip surface being similar to the fully softened strength, is possibly related to the significant amount of calcium carbonate content, which contributes to the mobilized shear strength of the clay matrix, on entire slip surface, higher than the residual shear strength of a stiff clay and clay shale composition with similar I_p. D'Elia et al (1988) suggested that there was no immediate and noticeable decrease of shear strength because the rate of movement of the slide at the time of failure and in the following months was relatively small. It is also worth mentioning that the monitored deformation in the slope, increasing with excavation height, which is close to rigid rotation, was in much greater depth compared to the depth of slip. D'Elia et al. (1988) suggested that the slope failure had been induced by the high stress levels and in part independent of the deformation process.

Roccella Valemone, Italy (Valore et al 2007)

The western slope of Nebroli Moutains in Sicily, Italy, where the small town of Roccella Valdemone is located, was affected by landsliding process, starting around 1880 in the lower part of the slope. The landslide progressed uphill until 1996. Reliable documentation of the landslide evolution was available only after 1950, including aerial photos of the slope and direct surveys. The main scarp and the crown were closely observed and monitored during 1990 and 1996, when

remedial measures were studied and partially implemented. During this period, three slope failures (M1, M2, and M3, in sequence) took place in discrete steps in the winter-spring season, and were reported as first-time sliding (Valore et al 2007). However, the specific dates of failures are not reported. Slope failure M2 (Fig.B.4) is studied here. M1 was not analyzed because it is possible that the failure occurred under undrained condition. Slide M3 was not analyzed because significant slope profile changes would have occurred after slide M1 and M2, which was however, not available.

The slope consists of stiff tectonised clays, overlain by a 2m to 9m heterogeneous debris cover which is formed by silt and argillaceous material. The stiff tectonised clays are rarely interbedded with sandstone, and include random small blocks of calcilutite and limestone. The clay size fraction, liquid limit, plastic limit, and plasticity index of the clays, determined from the undisturbed samples are, respectively, 16% to 21%, 40% to 44 %, 10% to 22%, and 18% to 34%. The natural water content of the stiff clays is between 8% and 15%. The groundwater table based on the piezometric measurement in Fig.B.4 is at very shallow depth and even near the slope surface, which is suggested to be the key cause for the upward landslide propagation (Valore et al 2007).

Although the porewater condition at failure is not available, Valore et al (2007) suggested that drained condition prevailed for the slope failures which occurred successively with long time interval, considering rather high permeability of the clays, together with low effective stresses. As a result, the groundwater table in Fig.B.4 was used in the present study. The back-analysis was performed on the entire reported slip surface assuming mobilized shear strength greater than the residual condition, because a horizontal or sub-horizontal segment of the slip surface was not observed. The back-calculated mobilized shear strength, is similar to that at the reported I_p range, from the proposed empirical correlation for fully softened shear strength, and close to the lower bound of the peak shear strength (solid circles) determined from drained direct shear tests on undisturbed specimens (Valore et al 2007).

Aghios Konstantinos 1, 2, 3, Greece (Alexandris et al 2011)

Three major slides and more than 10 minor slides were observed during or shortly after the construction of a new section of the Athens-Thessaloniki motorway, which bypasses the town of

Aghios Konstantinous, in Central Greece. In the construction, 5 major cuttings with a 3:2 (H: V) inclination, which were planned to be 15 to 30m deep, were excavated between 2003 and 2007, and all the slides occurred following rainfall events.

The cuttings were in the Neogene deposits, consisting of the upper weakly cemented conglomerate, and the lower stratum of stiff to hard clayey marls. The slides were only involved in the clayey marls, which contain sandy and gravelly horizons, and interbeds of more plastic hard clays with distinct scaly fabric. According to the field investigation including boreholes executed before the construction and after the slope failures, the clayey marls have a natural water content of 15 to 25%, a liquid limit between 40 and 70%, liquidity index close to 0, plasticity index between 25 and 40%, and clay size fraction between 20 and 40%. The calcium carbonate content of these clayey mars is between 20% and 40%. The first major slide (Fig.B.5) exhibiting a rotational slip surface, occurred during a very intense storm in Nov. 2006, two months after slope grading. The second (Fig.B.6) and third slides (Fig.B.7) which took place in March 2007 and February 2009, respectively, were similar in size (shallow to medium deep) and shape of slip surface (rotational), similar to the first slide. Prior to the excavation, the water table was at 8 to 10 m below the ground, following the ground surface relief. The porewater pressure ratio, $\bar{r}_u$, was assumed by Alexandris et al (2011), to be between 0.20 and 0.35 at the time of slope failure with the consideration of rainfall infiltration.

Because the observed slip surface reported by Alexandris et al (2011), does not include a horizontal or subhorizontal segment (Mesri and Shahien 2003), the back-analysis in this research was performed on the entire slip surface, assuming a mobilized shear strength higher than the residual condition. For $\bar{r}_u = 0.20$, the back-calculated mobilized shear strength, is close to the upper bound of empirical fully softened shear strength developed in the present research, defined by Ip in the range of 25 - 40%. For $\bar{r}_u = 0.35$, the back-calculated shear strength is higher than that from the empirical correlation in the present study. The back-calculated shear strength is in the range of the shear strength (solid triangles) determined from drained direct shear tests on intact samples retrieved from the slides (Alexandris et al 2011). It's possible that the 20% to 40% calcium carbonate, which is mainly responsible for the cementation of the marls (Alexandris et al 2011), contributes to the high mobilized shear strength. It should also be noticed that, before the rainfall, the water table was 8 to 10 m below the ground following the slope relief (Alexandris et al 2011).

It is more likely that, the porewater pressure ratio was close to 0.20 by the time of failure, because the rainfall infiltration would not have an immediate significant influence in the ground water condition. For this reason, only the back-calculated secant friction angles corresponding to $\bar{r}_u = 0.20$, are included in Fig.8.10 and Fig.8.11.

Selset, UK (Skempton and Brown 1961)

In 1954, a slip occurred in the south slope of the River Lune valley, 180m upstream of Selset Weir at the head of Grassholme Reservior, which was constructed in 1910. The slope (Fig.B.8) is 13m high with an inclination of 1.9: 1 (H: V). Field investigations were carried out during 1955-57 and 1958-60, including drilling of boreholes and installation of shallow and deep piezometers. The bedrock, at depth 10m beneath the valley floor, consists of sandstone, shale, and limestone strata of the Lower Carboniferous. The bedrock is overlain by heavily consolidated intact boulder clay, which was formed during an early stage of the Last Glaciation. The natural water content, liquid limit, plasticity index, and clay size fraction of boulder clay, is respectively, 12%, 26%, 12%-15%, and 17%-25%. The critical slip surface suggested by Skempton and Brown (1961) is shown in Fig.B.8, together with the groundwater condition, reported by Skempton and Brwon (1961) according to the piezometric readings, and artesian condition at the toe.

The back-analysis in the present study was made on the entire slip surface, because there is no distinct horizontal or sub-horizontal basal segment. The back-calculated shear strength is significantly greater than that from the empirical correlation in the present study. The back-calculated mobilized shear strength of boulder clay on the entire slip surface, is close to the upper bound of the intact shear strength of boulder clay (solid circles) measured in drained triaxial compression tests (Skempton and Brown 1961). Therefore, the back-calculated secant friction angles of boulder clay are not included in Chapter 8.

Kimola Floating Canal, Finland (Kankare 1969a, b)

A large landslide took place on November 3rd 1965 at the Kimola floating canal in Finland, which was designed for the floating timber in the southern part of Paijanne lake system. The Kimola floating canal, consisting of the upper canal and lower canal with a timber lift in between, locates

at the southern border of the Mid-Finnish lake district about 120 km northeast from Helsinki. The excavation of the canal commenced in the winter of 1962, and many minor slips were observed immediately at the end of the stage when the excavation reached the level of 67m in the winter of 1963. Investigations were carried out after the minor slips in some control sections until the large slope failure occurred on November 3rd 1965, nine months after the excavation to the final deptC.

The failure was in slightly overconsolidated glacial clay (OCR of 1.5 to 2.0 in the failure area), which has an average liquid limit and plasticity index, respectively, of 53% and 27%. The plasticity index ranges from 25% to 40%. It was suggested by Kankare (1969a) that the clay is structurally homogeneous. The slide occurred in only few seconds, and was concluded to be a rapid retrogressive failure instead of a single movement according to Kankare (1969a,b). One of the most important control sections happened to be near the center of the failure area and is shown in Fig.B.9. While obvious seasonal pore pressure variations were recorded, the ground water condition used in the back-analysis in the present study (Fig.B.9) was produced by Kankare (1969a,b) based on the measurements 1 week before the failure. The initial slip surface in Fig.B.9 was the most critical surface using Bishop's simplified method according to Kankare (1969a,b). This initial failure, is much smaller than the final slide; however, it is of the same magnitude as the failures in the vicinity.

A good agreement is obtained between the back-calculated mobilized shear strength on the entire slip surface and that defined by the reported I_p range from the proposed empirical correlation for fully softened shear strength. Consolidated drained triaxial compression tests (solid circles) and undrained triaxial compression tests with porewater pressure measurements (solid diamonds) were carried out on specimens trimmed from the undisturbed samples taken from the control section, at maximum effective normal stress in the laboratory tests exceeding the effective normal stress on the slip surface. It can be seen that in the effective normal stress range encountered in the slip surface, the measured shear strength is equal or larger than that from the back-analysis.

Trondheim, Norway (Janbu et al 1977)

On August 15, 1972, a slide, which was 160m along the highway, occurred beneath a road embankment on a slope 4km south of downtown Trondheim, Norway, during the construction of

the fill, which started 2 month before. The embankment was about 30m high at the time of failure (Fig.B.10). According to the witness, the movement of the slide was fully completed in 10 minutes, after a crack was noticed on the top. Extensive site investigations were carried out, including borehole sampling, static soundings, vane testing, porewater pressure measurement, and settlement observations. It was revealed by site investigations that the slope is in homogenous overconsolidated clay with a number of thin seams of sand, silt and isolated pockets of quick clay. The overconsolidated clay has a natural water content of 22%-25%, plasticity index of 3%-7%, and clay size fraction of 15%-25%. The slip surface determined from 4 boreholes is shown in Fig.B.10. A reported porewater pressure ratio of 0.55, which corresponds to the high water table (Janbu 1977) was used in the back-analysis in the present study.

The back-calculated mobilized shear strength on the entire slip surface, which does not include a distinct horizontal or sub-horizontal basal segment, is similar to that defined by I_p = 7%, from the empirical correlation for fully softened shear strength developed in the present study. The back-calculated mobilized shear strength is lower than the intact shear strength of the overconsolidated clay, determined in undrained triaxial compression tests (Janbu 1977) at low effective normal stresses, and close to the intact shear strength at effective normal stresses larger than 200 kPa.

Lodalen, Norway (Sevaldson 1956)

On October 6th, 1954, a slide occurred in the area of Lodalen marshalling yard, about 2 kilometers east of Oslo East railway station, Norway, close to the main northern line. It was described by Sevaldson (1956) that, a whole chunk of the slope had slide out as a monolithic body in a rotary motion. The slide damaged three railway carriages at the side rail line, and pushed two carriages off the neighboring line. The slope was excavated in several stages before the failure, and remained with an inclination of 2:1 (H: V), as shown in Fig.B.11. According to the site investigation, the slope was in late-glacial and post-glacial marine clays, which have a natural water content of 19%-30%, liquid limit of 29%-39%, and plasticity index of 8%-20%. Vane borings were performed to locate the slip surface, which was approximately 19m deep (Fig.B.11). The ground water condition in Fig.B.11 was determined from porewater pressure measurement in 4 borings at different depths.

The back-analysis in the present study was performed on the entire slip surface because a distinct horizontal or sub-horizontal basal segment was not included. A good agreement is obtained between the back-calculated mobilized shear strength and that at I_p = 8%, from the empirical correlation for fully softened shear strength developed in the present study. The back-calculated shear strength is slightly lower than the peak shear strength (solid circles) determined from drained triaxial compression tests on normally consolidated undisturbed specimens (Sevaldson 1956).

Ullensaker, Norway (Kenney and Drury 1973)

The site of Ullensaker landslide is 35 km northeast of Oslo in the district of Romerike. The slope failure occurred on 23 December 1953, and initiated a retrogressive landslide, which was 150m across at its widest section. The retrogressive landsliding was observed by a farmer. Post-failure field investigations were carried out to obtain information on soil condition, to determine the ground water condition, and to locate the slip surface. The slope consists of surface weathered clay (to depth about 5m at the head of the slope and about 3m below the stream bed), and underlying quick clay. The natural water contents of weathered clay and quick clay are both 30%. For weathered clay, liquid limit, plasticity index, and clay size fraction, are respectively, 32%-48%, 9%-24%, and 40%; and for quick clay, are respectively, 28%, 6%, and 40%. The possible slip surfaces of the initial failure were determined by Kenney and Drury (1973) based on the boundary of undisturbed and weak soil according to the vane tests, together with the location of tension crack at the top. In the present study, the slip surface shown in Fig.B.12 is in the middle of the possible slip surfaces suggested by Kenney and Drury (1973). The ground water condition used in the analysis in Fig.B.12, was developed by Kenney and Drury(1973), based on piezometric measurement on the opposite side of the failed slope, which included hydrostatic pressures near the head of the slope and overpressure at the toe of the slope, together with a ground water surface 1m below the head of the slope. A 1m deep tension crack was assumed at the top of the slope.

The back-analysis in the present study, using the estimated slip surface and ground water condition, yields back-calculated mobilized shear strength on this rotational slip surface, at effective normal stresses less than 40 kPa, similar to that defined by I_p = 6%, from the proposed empirical correlation for fully softened shear strength. The back-calculated mobilized shear strength is also

comparable to the intact shear strength (solid circles) determined from drained triaxial compression tests (Kenney and Drury 1973).

Ukuwela 1 and 2, Sri Lanka (Balasubramaniam et al 1977)

Several slides occurred in 1972 at the Ukuwela Power House site as part of the Mahaweli River Diversion Scheme, Sri Lanka, during the construction of a 1:1 (H:V) excavation for the installation of the penstocks. The hilly regions of Sri Lanka is recognized as an area where the landslides are a common geological phenomenon. The slope (Figures B.13 and B.14) studied here was about 30 m deep, partly in a talus material and partly in in-situ weathered residual soil.

The construction started from 1971, and slide 1 (Fig.B.13) occurred almost along the penstock trace in October, 1972. The small soil mass slipped in December in the same year, and is labeled as slide 2 in Fig.B.14. The slip surfaces were determined by penetrometer tests. The material involved in the failure was found to be mainly sandy clay, while the weathered rock existed below the two slips. The disturbed samples taken from the exposed slope at three locations have a plastic limit of about 22% to 23%, and liquid limit in the range of 41% to 52%, which gives a plasticity index range between 19% and 29%. Balasubramaniam et al (1977) first assumed no seepage and a water table below the slips for the stability analysis, and later carried out the analysis assuming that seepage would take place. The more realistic case without seepage as suggested by Balasubramaniam et al (1977) is reasonable, considering the installation of horizontal perforated pipes in the slope and peripheral drains made to release the build-up of high pore water pressures inside the slope and improve the surface drainage. As a result, an average $\bar{r}_u$ of 0 was used in the back-analysis in the present study. For both failures, the back-calculated mobilized shear strength on the entire slip surface is higher than that from the empirical correlation for fully softened shear strength, developed in the present study.

Gjerdrum, Norway (Heyerdahl et al 2015)

Three years after its excavation, a 20 m high clay slope failed on 20 May 2012 in Gjerdrum, Eastern Norway. In this area, the terrain was reshaped by humans to expand the arable land in Norway

from 1960s, which resulted in numerous landslides in poorly drained fills. This 20m high cut was made in 2008 to expand a warehouse.

The water level in the slope (Fig.B.15) is about 8 to 9 m below the ground surface, indicating a top soil of dry crust. Below the crust, there is a clay layer with low sensitivity, intersected by a sensitive clay layer. The plasticity index decreases from 20% to 10% and even to 5% in one borehole, from the top soil to the depth of sensitive clay (personal communication with Heyerdahl). The observed slip surface is more or less rotational, cutting through the crust and clay including the sensitive clay. Heyerdahl (2015) suggested that the primary swelling due to the removal of the slope material in the excavation had come to the end by the time of the failure at the corresponding depth of the failure surface. Therefore, the original water level could be directly used in the back-analysis as the porewater pressure equilibration had been reached. Using the observed slip surface and the reported ground water condition, the back-calculated mobilized shear strength on the entire rotational slip surface, is slightly lower than that at I_p = 20%, from the proposed empirical correlation for fully softened shear strength.

Fu Yung Shan Tsuen, Hong Kong (Ho et al 2013)

A fatal landside took place on 20 August 2005 at Fu Yung Shan Tsuen, Hong Kong, during a prolonged and intense rainfall which has a return period of about 100 years. The slope failure was on a densely vegetated hillside in the squatter village, Fu Yung Shan Tsuen, located at the southern part of Tsuen Wan. The landslide is regarded as a first-time slope failure because no landslides were reported previously in the immediate vicinity of this landslide (Ho et al 2013). According to the witness and post-failure observations, the slope failure took place in 2 phases between 5:25 pm and 6:30 pm. Figure B.16 shows the initial slip surface in the hillside with a slope angle of 28° to 34°. The initial landslide mass is approximately 18m, with maximum depth of 4m. Ho et al (2013) suggested that the failure was induced by positive porewater pressure buildup and loss of suction during prolonged rainfall.

The investigation commenced at about 7:30pm on the same night of the slope failure, including installation of standpipe piezometer, trial pits, and trial trenches, etc. The investigation reveals that the superficial deposits of the hill consists of a thin fill mantle and 3m of colluvium. The fill is a

reddish brown, sandy silty clay with cobble and gravel-sized rock fragments, and the colluvium consists of sandy clay or sandy silt with occasional cobbles and boulders. The slope material underlying the colluvium is decomposed granodiorite with maximum depth up to 20m, underlain by slightly to moderately decomposed granodiorite. The decomposed granodiorite comprises yellowish brown, spotted white and black, sandy clayey silt. The slip surface (Fig.B.16) cuts through the fill and colluvium, and is predominantly within the upper zone of the decomposed granodiorite, slightly below the interface between the colluvium and the decomposed granodiorite. Atterberg limits of the colluvium and decomposed granodiorite have a wide range, with the plasticity index from 11% to 37% for the landslide debris. A monitored water level 1.9m below the ground was used in the back-analysis in the present study, which corresponds to a porewater pressure ratio, $\bar{r}_u$ of 0.13.

Because the colluvium and decomposed granodiorite have similar plasticity index, and the slip surface did not coincide with the interface between the two layers, the slope materials can be regarded as homogeneous. As a result, the mobilized shear strength is back-calculated for the entire slip surface. Due to the small depth of the slip, the effective normal stress on the slip slices is only up to approximately 45 kPa. The back-calculated mobilized shear strength is close to that defined by Ip = 37%, from the empirical correlation for fully softened shear strength developed in the present study, and lower than the intact shear strength (solid circles) determined from consolidated undrained triaxial compression tests and drained direct shear tests on undisturbed specimens (Ho et al 2013).

No 312 National Road, P.R. China (Feng 1992)

Landslides in loess are common in China, one of which was studied by Feng (1992). This first-time failure took place in a cut slope on the No.312 National Road of China. The cut (Fig.B.17) was 32m high, with an inclination of 1: 0.75 (V:H). In this area, the formation overlying the lateritic bedrock, consists of upper loess, lower lossal, and mixed earthes. The geotechinical properties of loess and mixed earthes, are very similar, with plasticity index of 8% to 9%.

The possible slip surface determined from field evidence by Feng (1992), including an open crack on the back of the sliping mass, and shown in Fig.B.17. A porewater pressure ratio, $\bar{r}_u$=0 was

suggested by Feng (1992), because there was no groundwater in the loess layer. The back-analysis using the reported slip surface and porewater pressure ratio, results in the mobilized shear strength on the entire slip surface, similar to that defined by I_p = 8% - 9%, from the empirical correlation for fully softened shear strength developed in the present study.

Snowdon, Himalayan Region (Bhandari 1977)

Bhandari (1977) studied a first-time slide in detritus material in the Himalayan region to determine which in-situ shear strength, i.e., the one of the overall detritus material, or of the matrix soil alone, controls the slope stability. The landside was in Snowdon, where a 37° slope (Fig.B.18) had acted as a satisfactory support for a dispensary and a hospital building at its top. A six story Medical College building (Phase 1) was constructed 14m away from the slope toe during December 1966 and May 1970. The landslide took place in February 1971 following the monsoon in the previous year, in the process of excavation for Phase 2 construction, which was intended for an extension of Phase 1 building toward the toe.

The 2-month geotechnical investigation commenced in March, including boring, sampling, testing, and installation of surface markers, deflection tubings, and Casagrande open type piezometers. The slope material involved in the landslide, consists of phyllitic slates in a clayey silt matrix with a low plasticity index of 15%, overlaying the disintegrated phyllite and quartzite formation. The sliding surface is close to the interface between the clayey silt with phyllitic slates and the disintegrated phyllite and quartzite, indicated by the deflection tubes. The observed slip surface (Fig.B.18) is rotational, with a maximum depth of 9m. Because the piezometers were found to be dry and the slide mass only had a 25% saturation, a $\bar{r}_u$ of 0 was adopted by Bhandari (1977), and used in this research.

The back-calculated shear strength on the entire slip surface is slightly smaller than that from the proposed empirical fully softened shear strength defined by I_p = 15%. Bhandari (1977), based on analysis of the slope failure, concluded that the peak shear strength of the remolded matrix soil measured in direct shear had governed the slope stability. The factor of safety was overestimated using the peak shear strength of the overall detritus material, and was underestimated using the residual strength of both the matrix soil and the overall detritus material. It should be noticed that

1) the laboratory peak strength of the matrix soil (solid circles) corresponds to the fully softened condition, according to the testing procedure, and 2) though the specimens were tested under very low effective normal stresses (lower than 30kpa) the measured strength is closer to the back-calculated value in this research in this stress range (Fig.B.18). One possible explanation for the measured fully softened strength and the back-calculated shear strength being lower than the proposed empirical value for Ip = 15%, is the measurement of the plasticity index. To be more specific, as the index properties were determined for the overall detritus material, the plasticity index may be underestimated. However, the stability is controlled by the weaker clayey silt, which has a higher plasticity index.

Lachute, Sation 8+85 and 10+50, Canada (Silvestri 1980)

For the excavations on the two roads, Rang Est and Rang Quest, crossing Highway 50 on both sides of the Riviere du Nord, near the town of Lachute (Quebec), Cananda, slopes of 2.5:1 (H: V) were suggested based on the preconstruction stability analysis of long-term stability. The construction of cuttings started in January 1974 and was completed in May 1974, when fissures and shallow slope failures were observed. Three major slides occurred, in sequence, in the early summer of 1974, beginning of October 1975, and end of October 1975, on the southern slope of Rang Est road, with no occurrence of failures on Rang Quest road. The failures in two stations, station 8+85 (end of October 1975), and station 10+50 (beginning of October 1975) are studied here.

Geotechnical investigations were carried out prior to the design of road cuttings. The slope material, with 3.5 to 4m weathered crust of brownish clay, consists of 37 m fairly homogenous silty clay and clayey silt overlying dense till. The silty clay has a liquid limit of 50%, plastic limit of 28%, and plasticity index of 20%. The natural water content increases from 40% near the surface to 69% at deptC. The clay was decided as overconsolidated and fissured by Silvestri (1980). The ground water conditions shown in Figures.B.19 and B.20 were determined by open-tube piezometers installed before the occurrence of the last major slide at station 8+85, which presents the most critical condition. The observed slip surfaces in the 7m road cuttings at two stations shown in Figures.B.19 and B.20, display a rotational shape.

Because a distinct horizontal or sub-horizontal basal segment of the slip surface was not observed, back-analyses in the present study were performed on the entire slip surface with the assumption of mobilized shear strength greater than the residual condition. The back-calculated mobilized shear strength, for both stations, is close to that at I_p = 22%, from the proposed empirical correlation for fully softened shear strength. Consolidated undrained triaxial compression tests with porewater pressure measurements on remolded specimens were performed (Silvestri 1980) at effective normal stresses greater than those on the slip surfaces in the road cuttings (data presented by solid circles in Figures.B.19 and B.20). Silvestri (1980) determined a linear failure envelope (bold dash lines in Figures.B.19 and B.20) with $\phi' = 34\ °$, for the remolded specimens. These measurements, according to the definition, give the fully softened shear strength. The back-calculated shear strength agrees with the fully softened shear strength from the laboratory measurements at low effective normal stresses which were encountered on the slip surface.

FIGURES

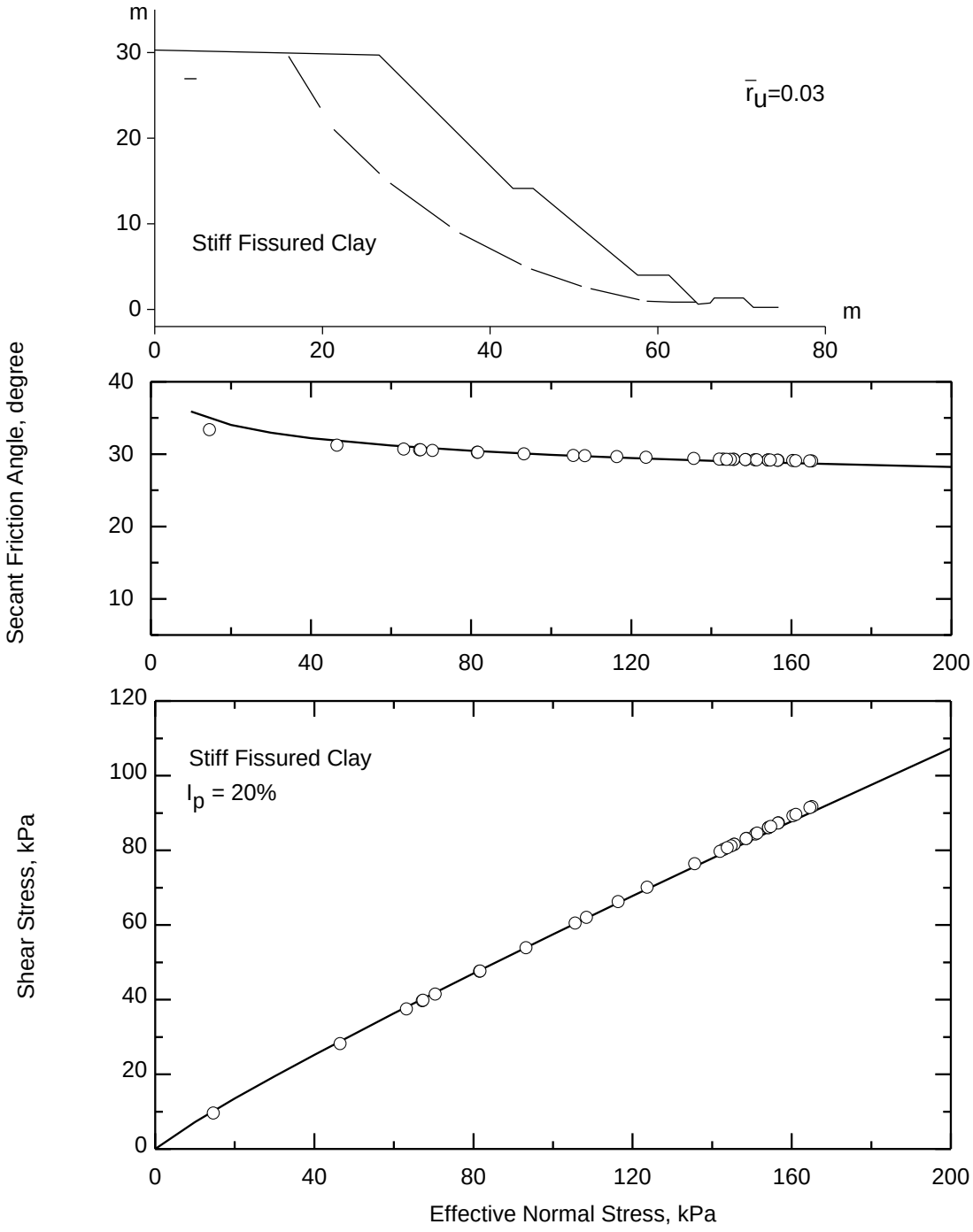

Figure B.1. First-time slope failure at People's Republic of China, 1981 (Li and Zhao 1984)

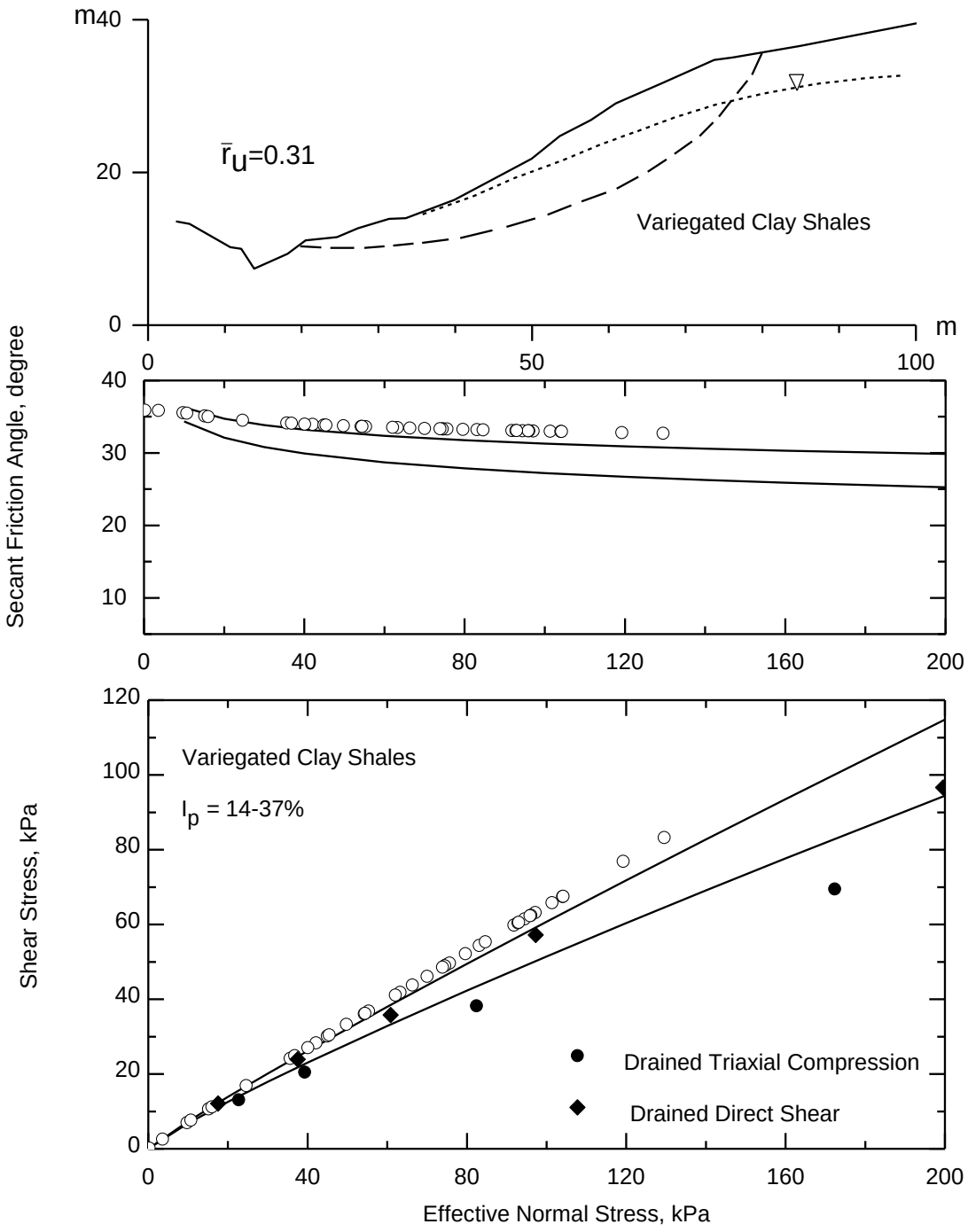

Figure B.2. First-time slope failure at River Fossate, Italy (D'Elia et al 1980)

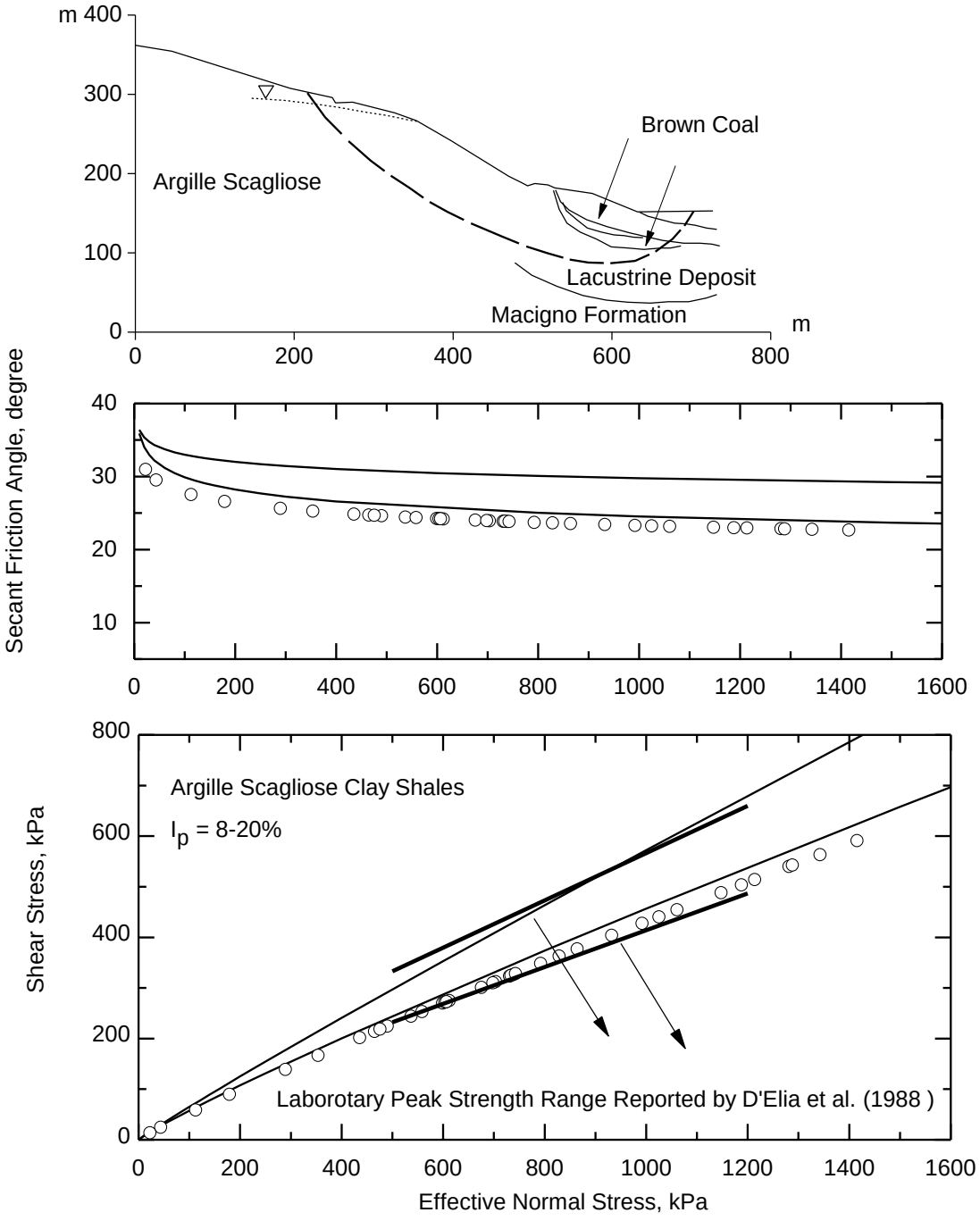

Figure B.3. First-time slope failure at Allori Coal Field, Italy, 1986 (D'Elia et al 1988)

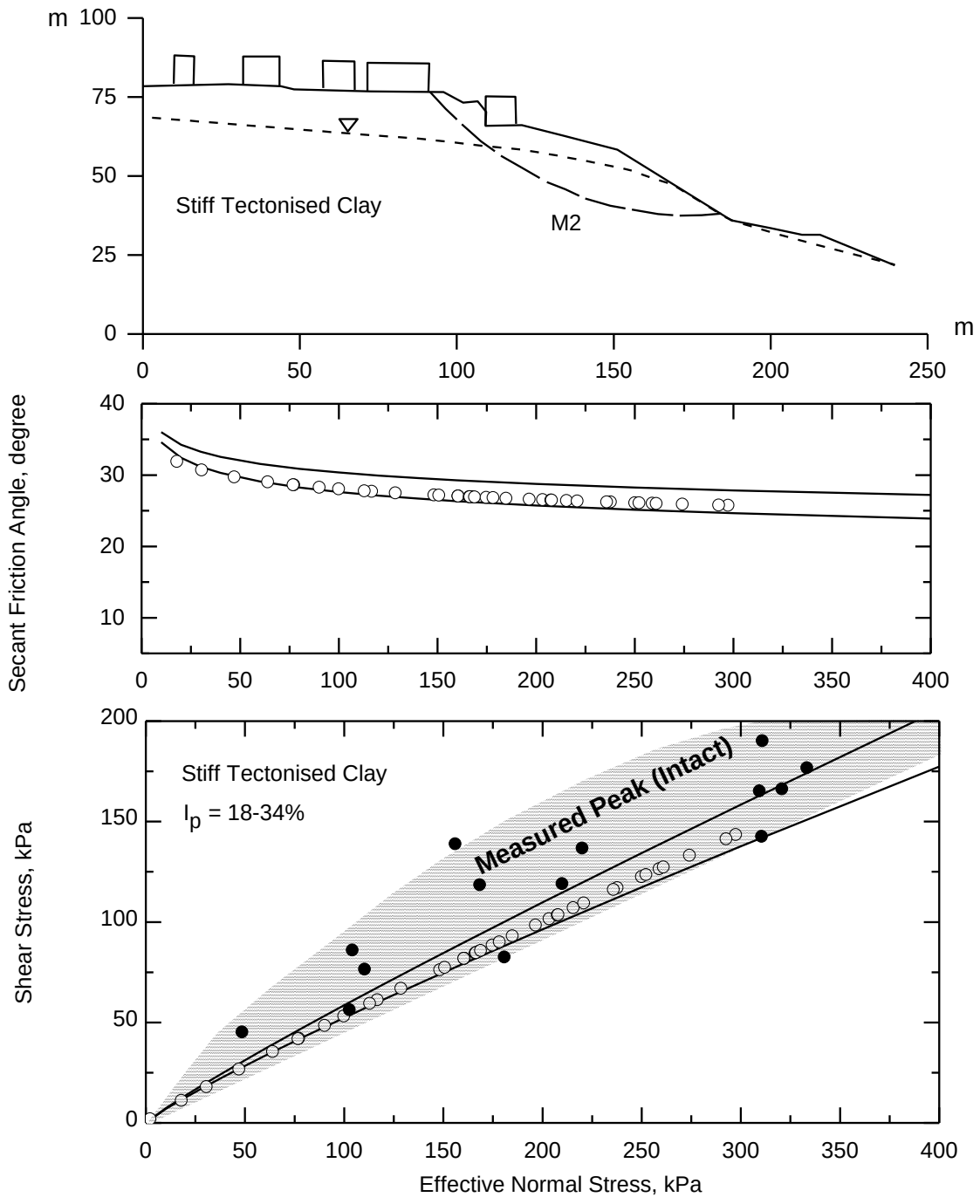

Figure B.4. First-time slope failure at Roccella Valemone, Italy (Valore et al 2007)

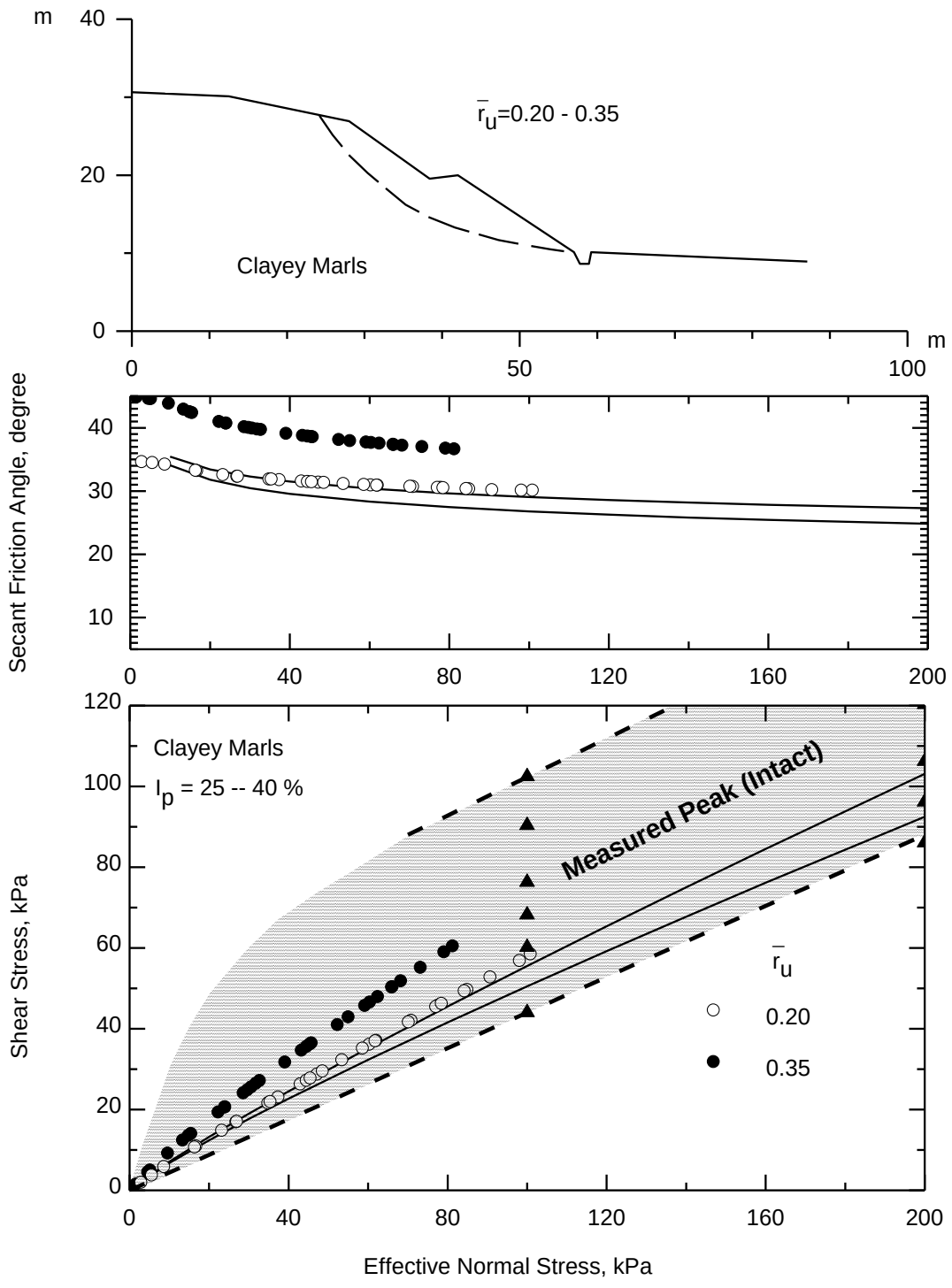

Figure B.5. First-time slope failure at Aghios Konstantinos 1, Greece, 2006 (Alexandris et al 2011)

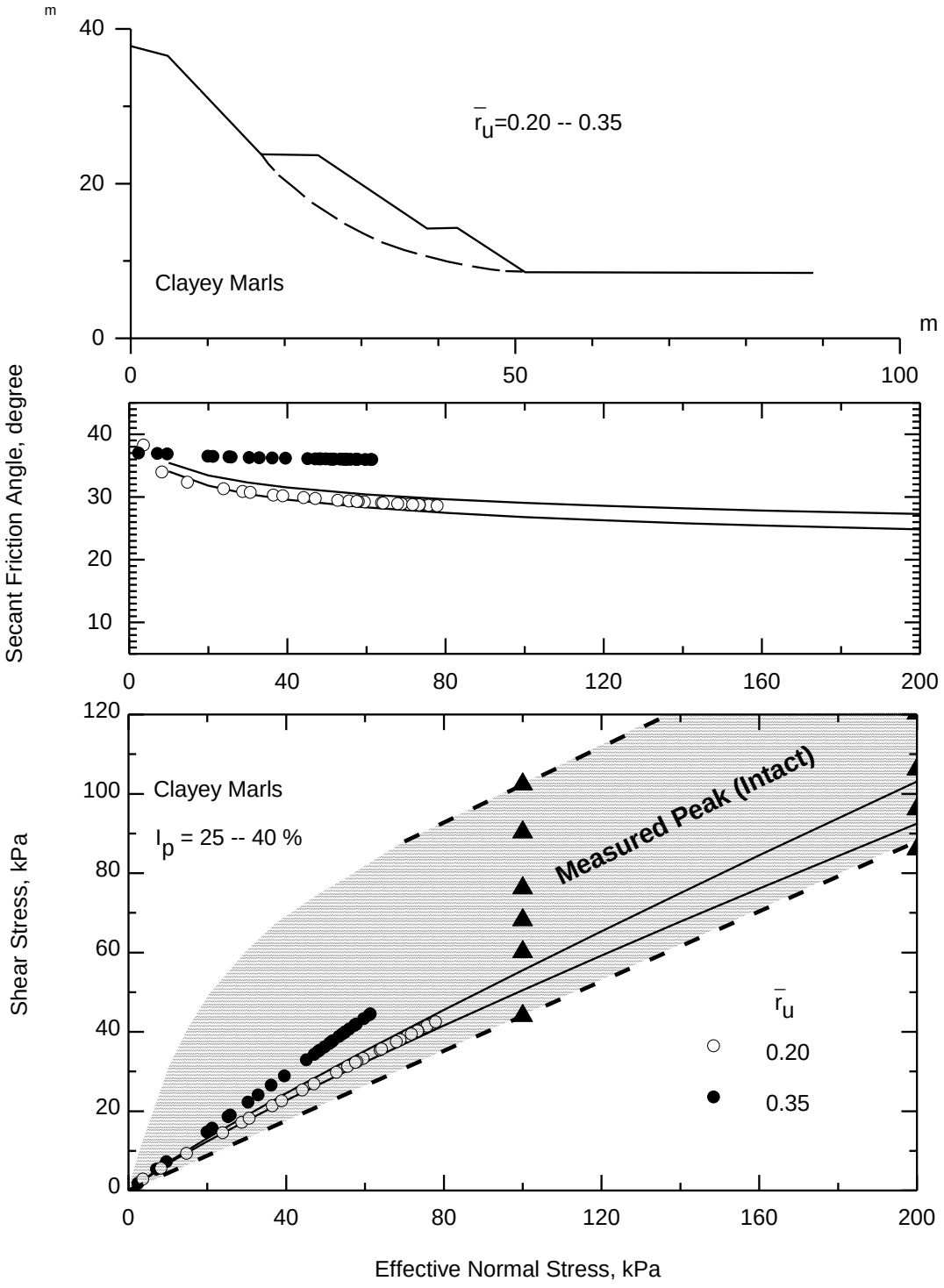

Figure B.6. First-time slope failure at Aghios Konstantinos 2, Greece, 2007 (Alexandris et al 2011)

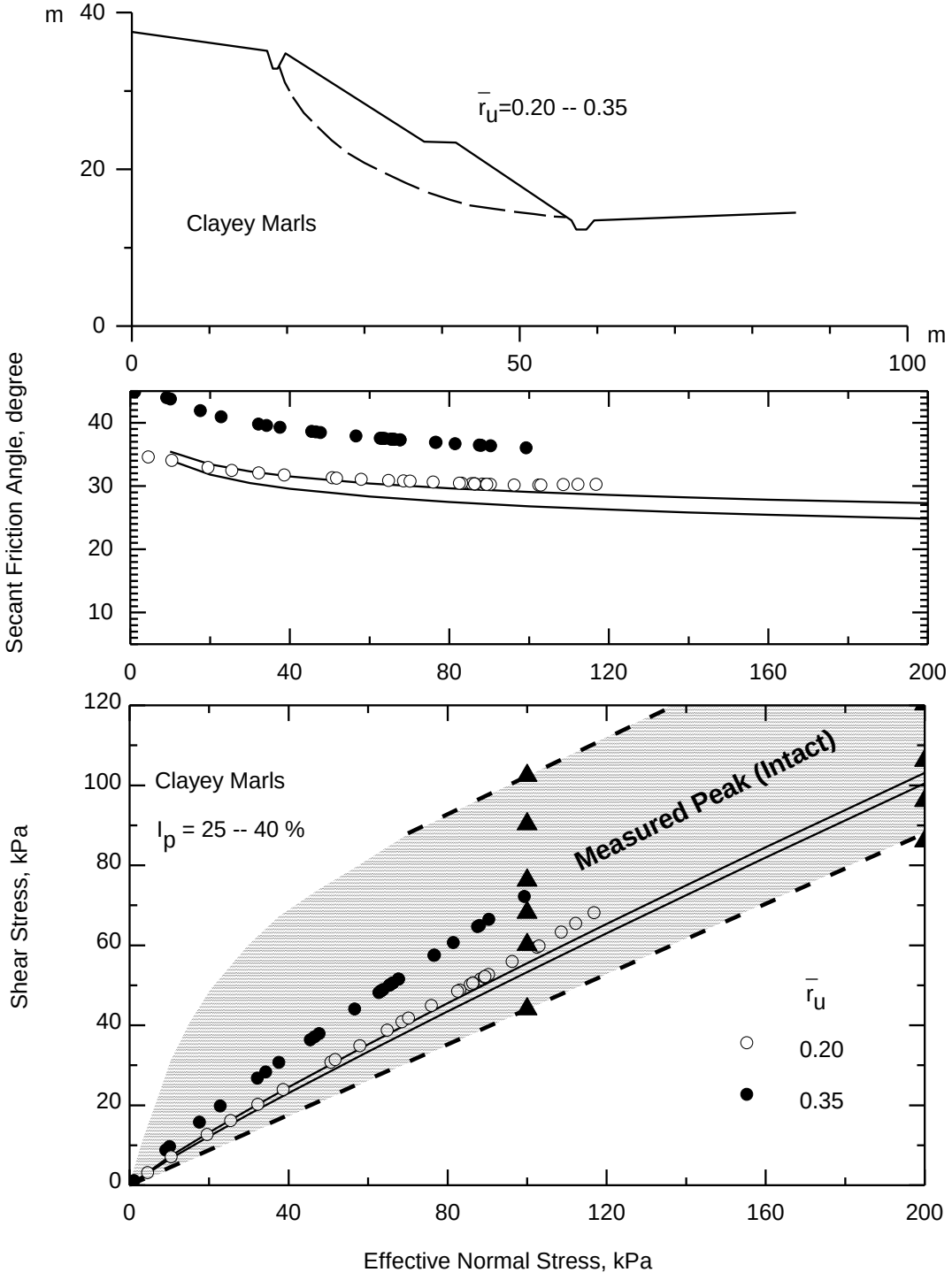

Figure B.7. First-time slope failure at Aghios Konstantinos 3, Greece, 2009 (Alexandris et al 2011)

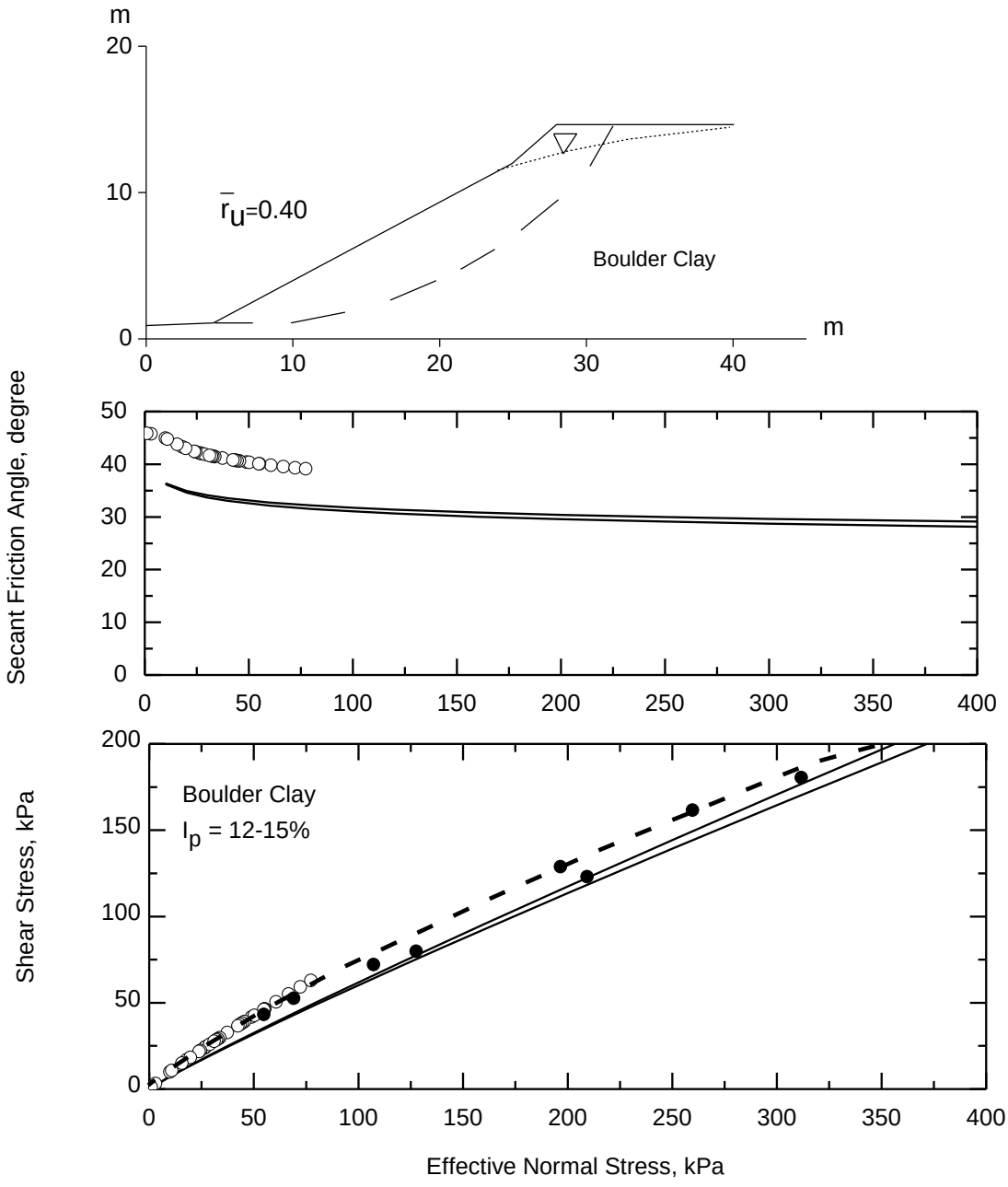

Figure B.8. First-time slope failure at Selset, UK, 1954 (Skempton and Brown 1961)

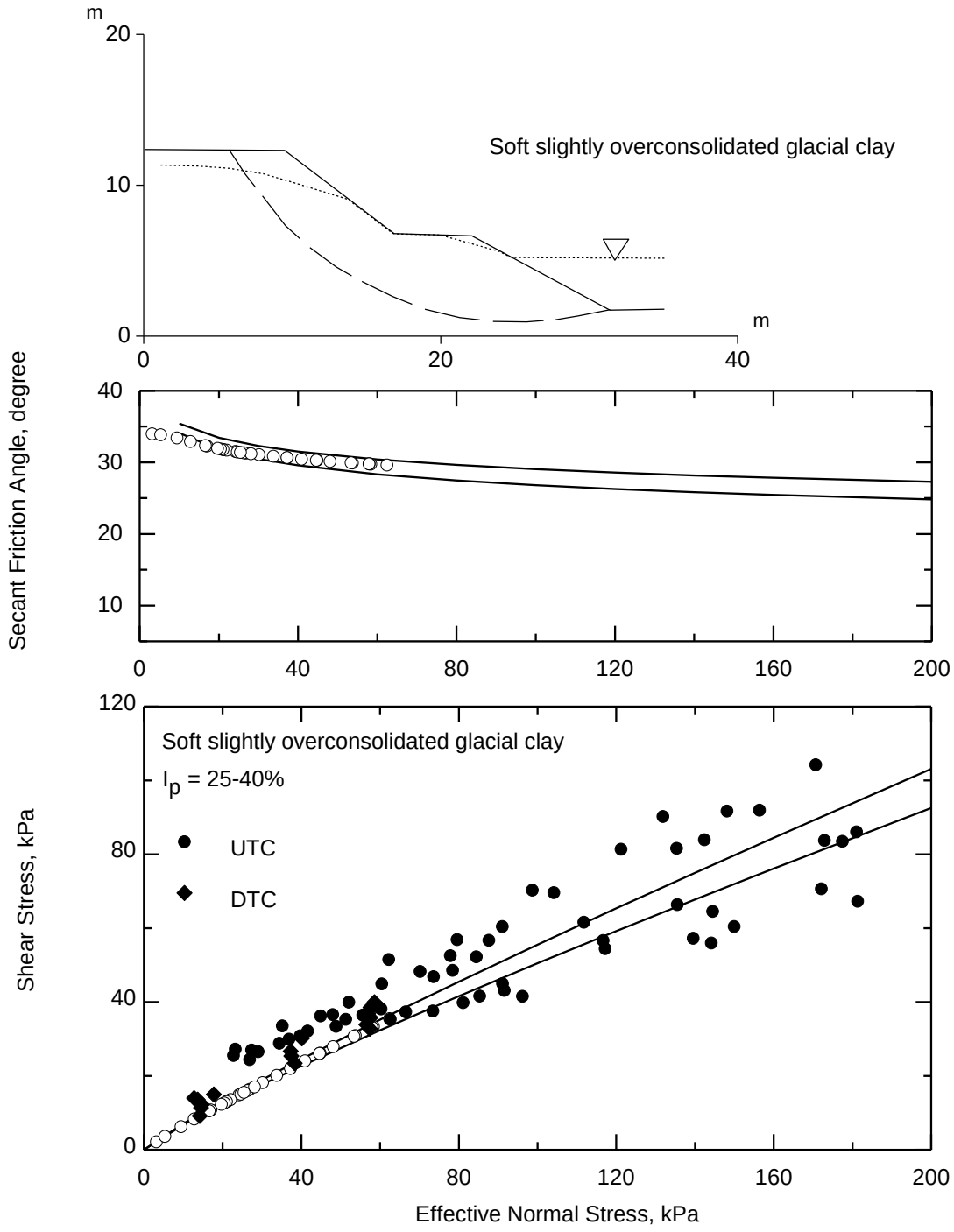

Figure B.9. First-time slope failure at Kimola Floating Canal, Finland, 1965 (Kankare 1969a, b)

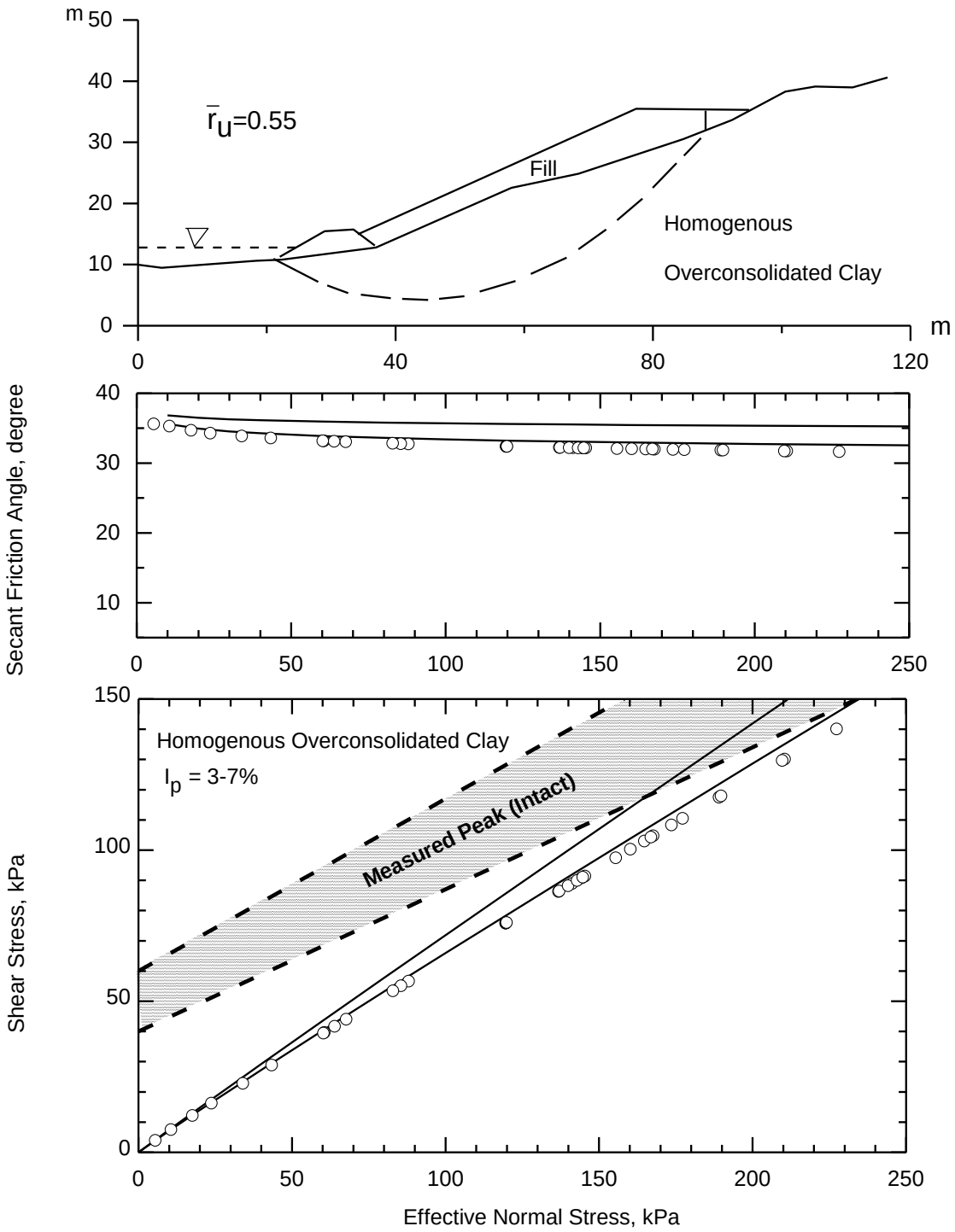

Figure B.10. First-time slope failure at Trondheim, Norway, 1972 (Janbu et al 1977)

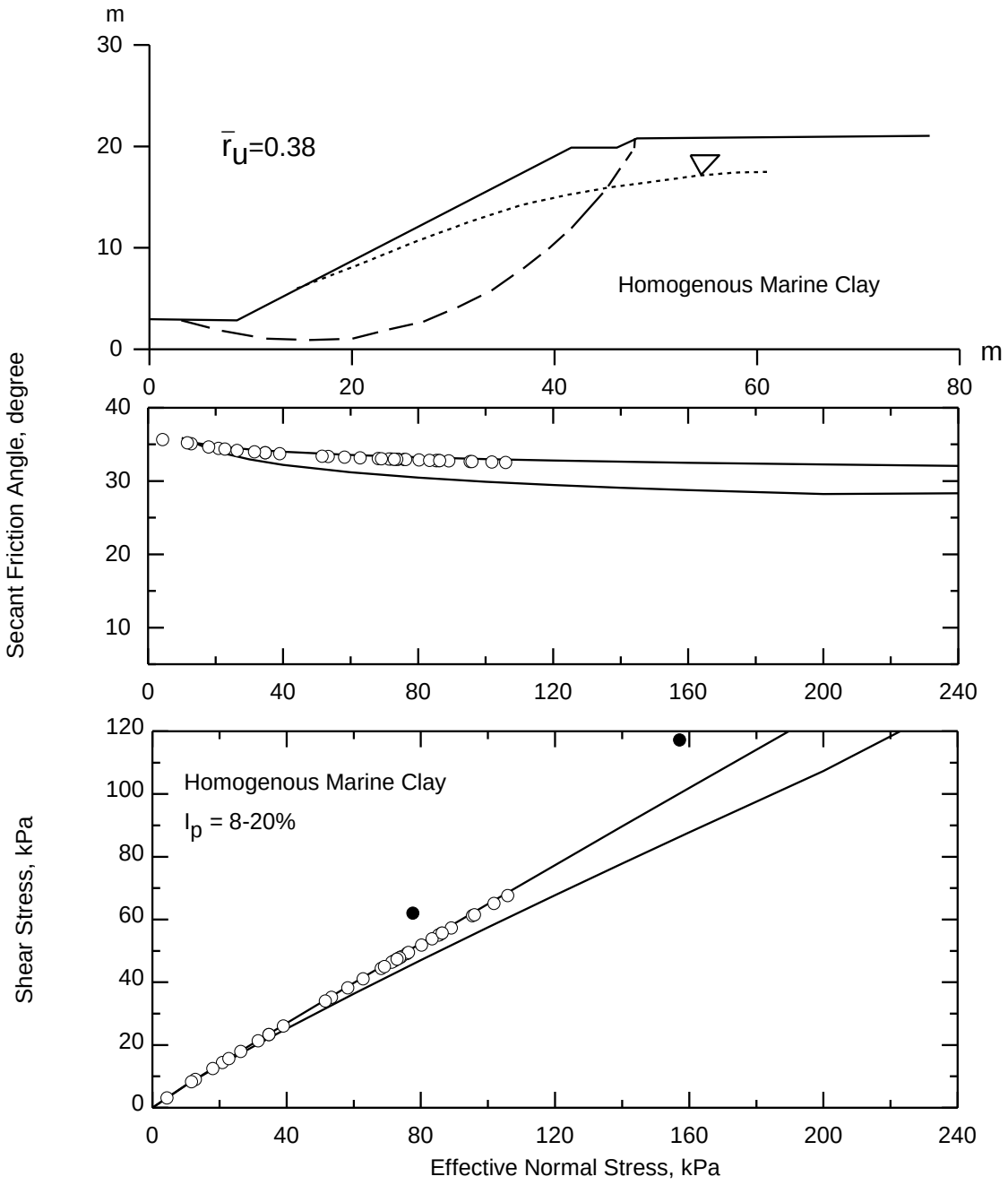

Figure B.11. First-time slope failure at Lodalen, Norway, 1954 (Sevaldson 1956)

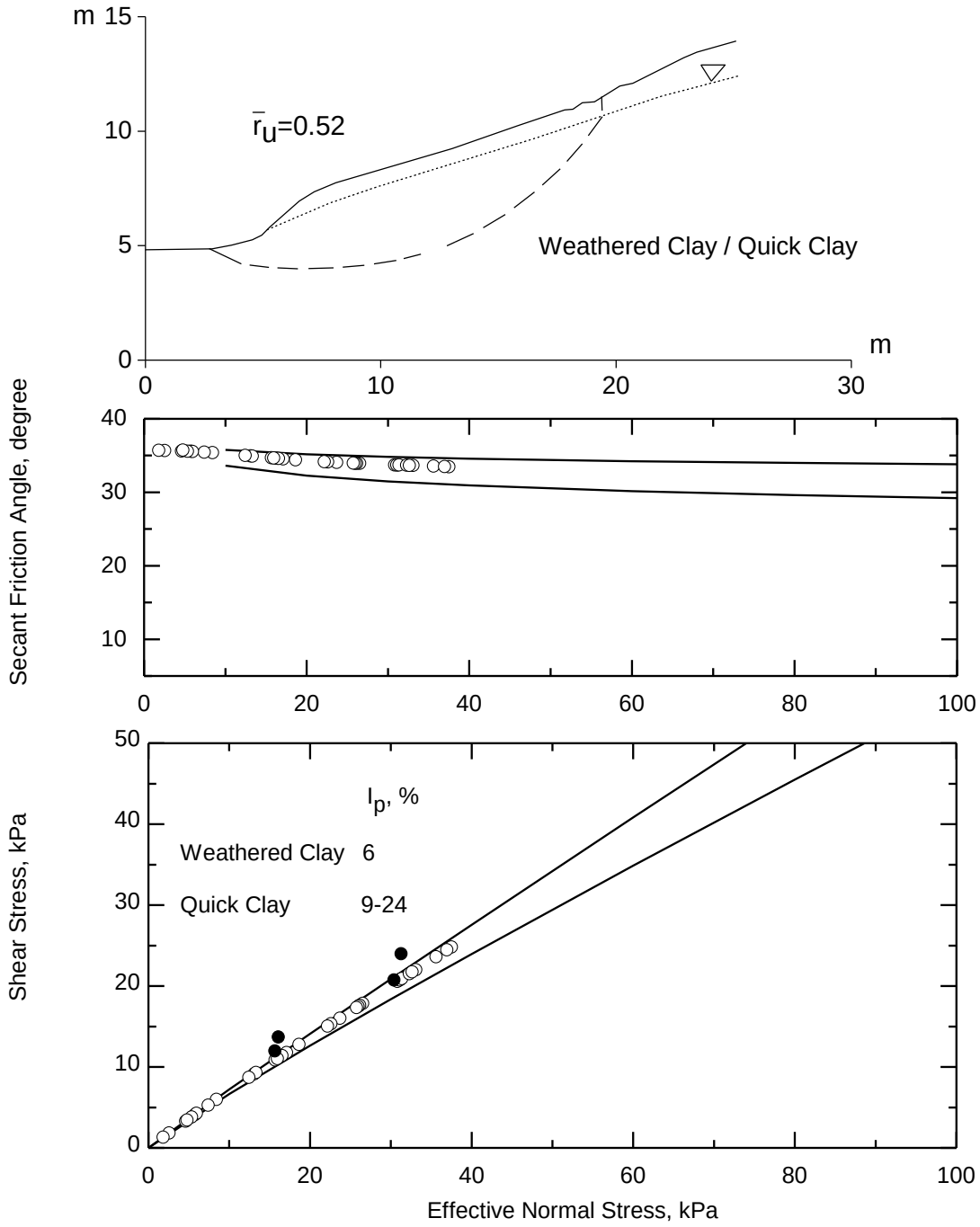

Figure B.12. First-time slope failure at Ullensaker, Norway, 1953 (Kenney and Drury 1973)

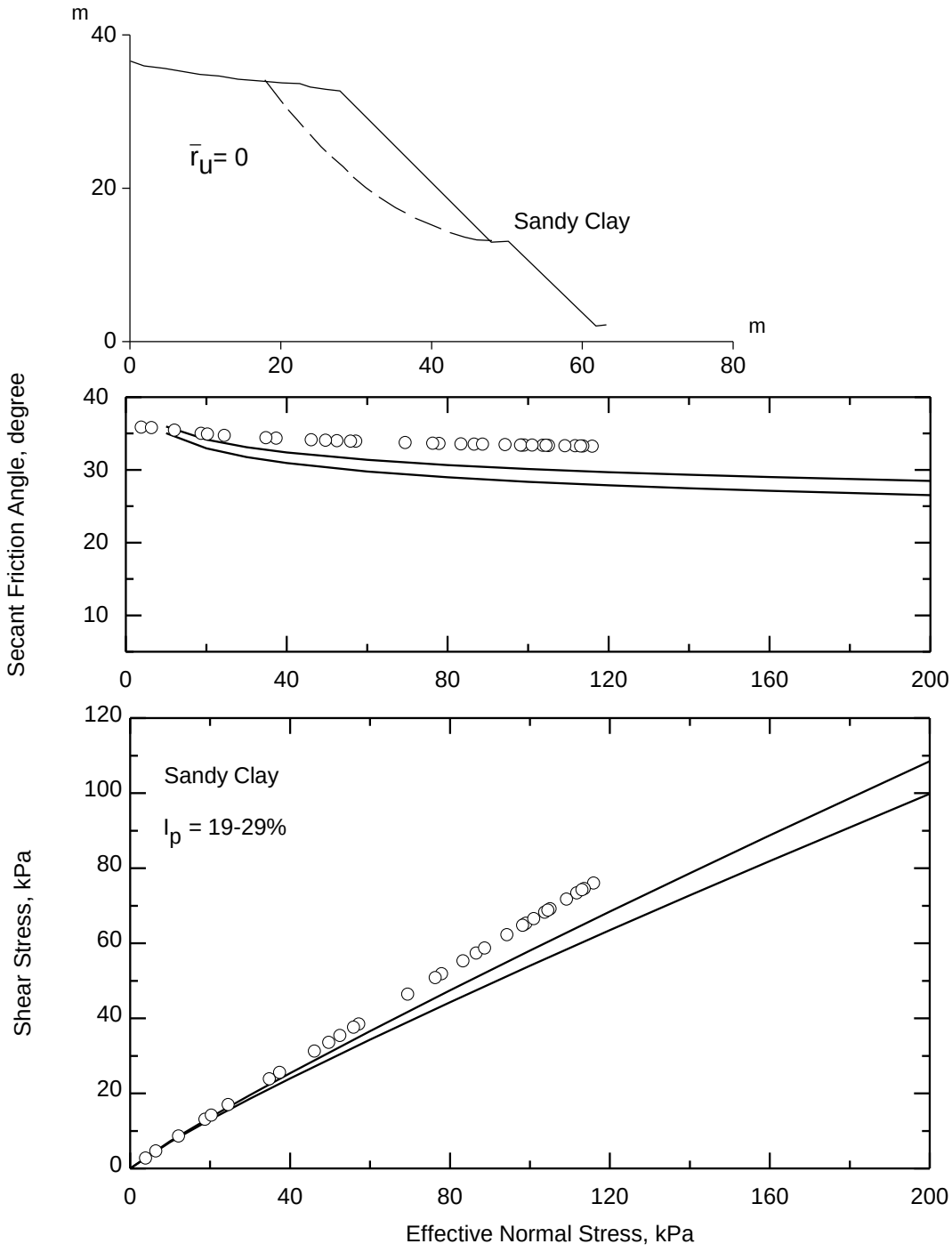

Figure B.13. First-time slope failure at Ukuwela 1, Sri Lanka, 1972 (Balasubramaniam et al 1977)

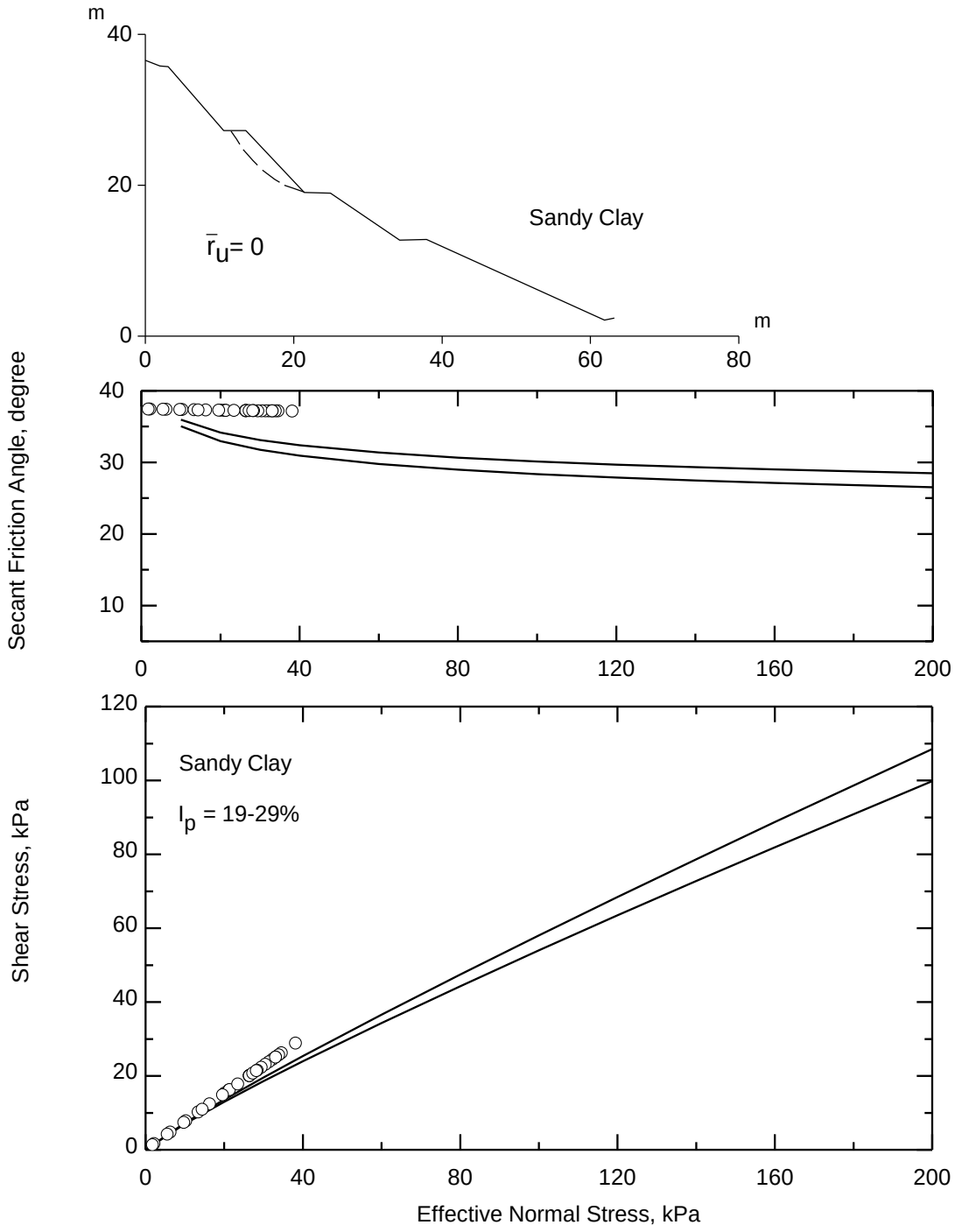

Figure B.14. First-time slope failure at Ukuwela 2, Sri Lanka, 1972 (Balasubramaniam et al 1977)

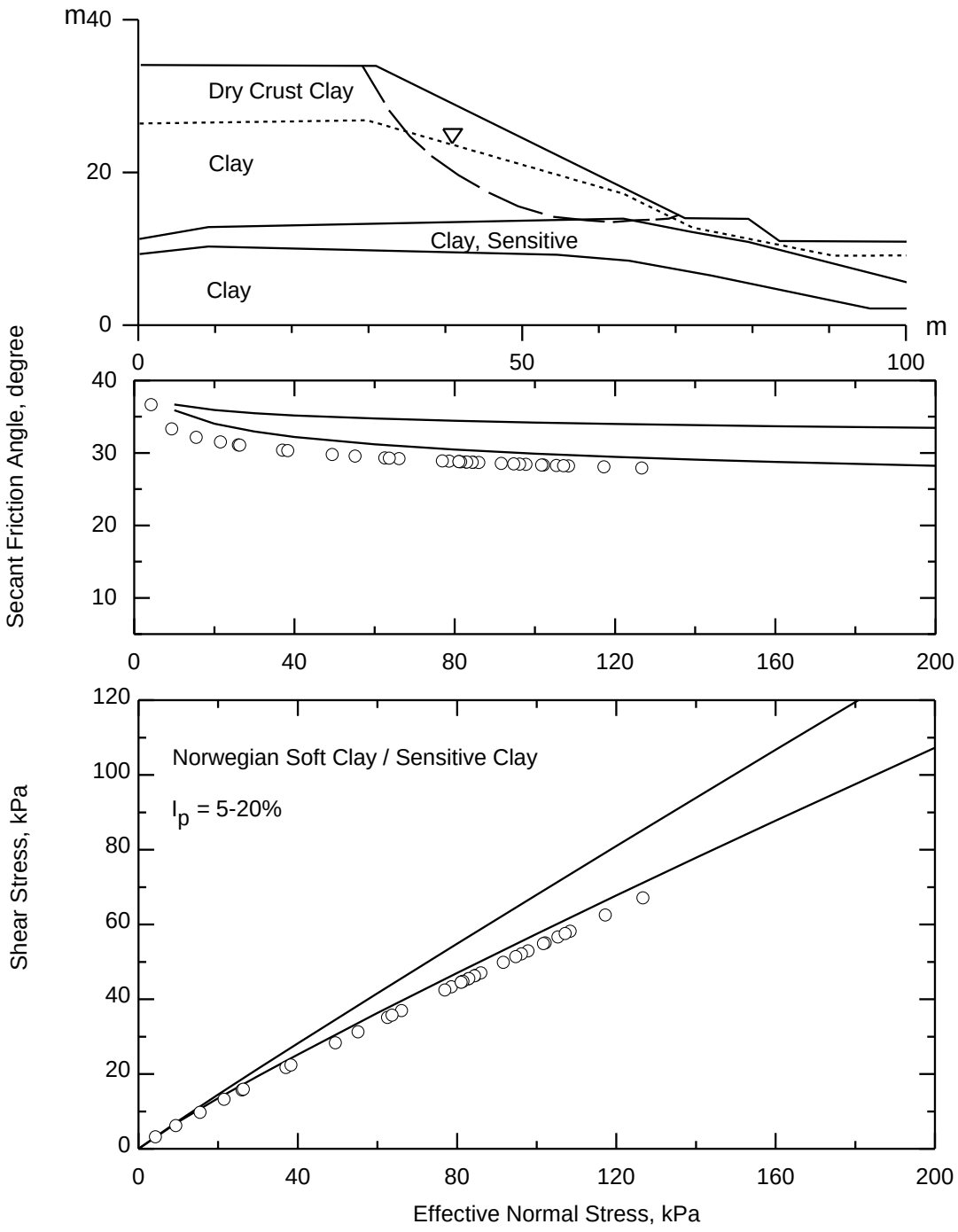

Figure B.15. First-time slope failure at Gjerdrum, Norway, 2012 (Heyerdahl et al 2015)

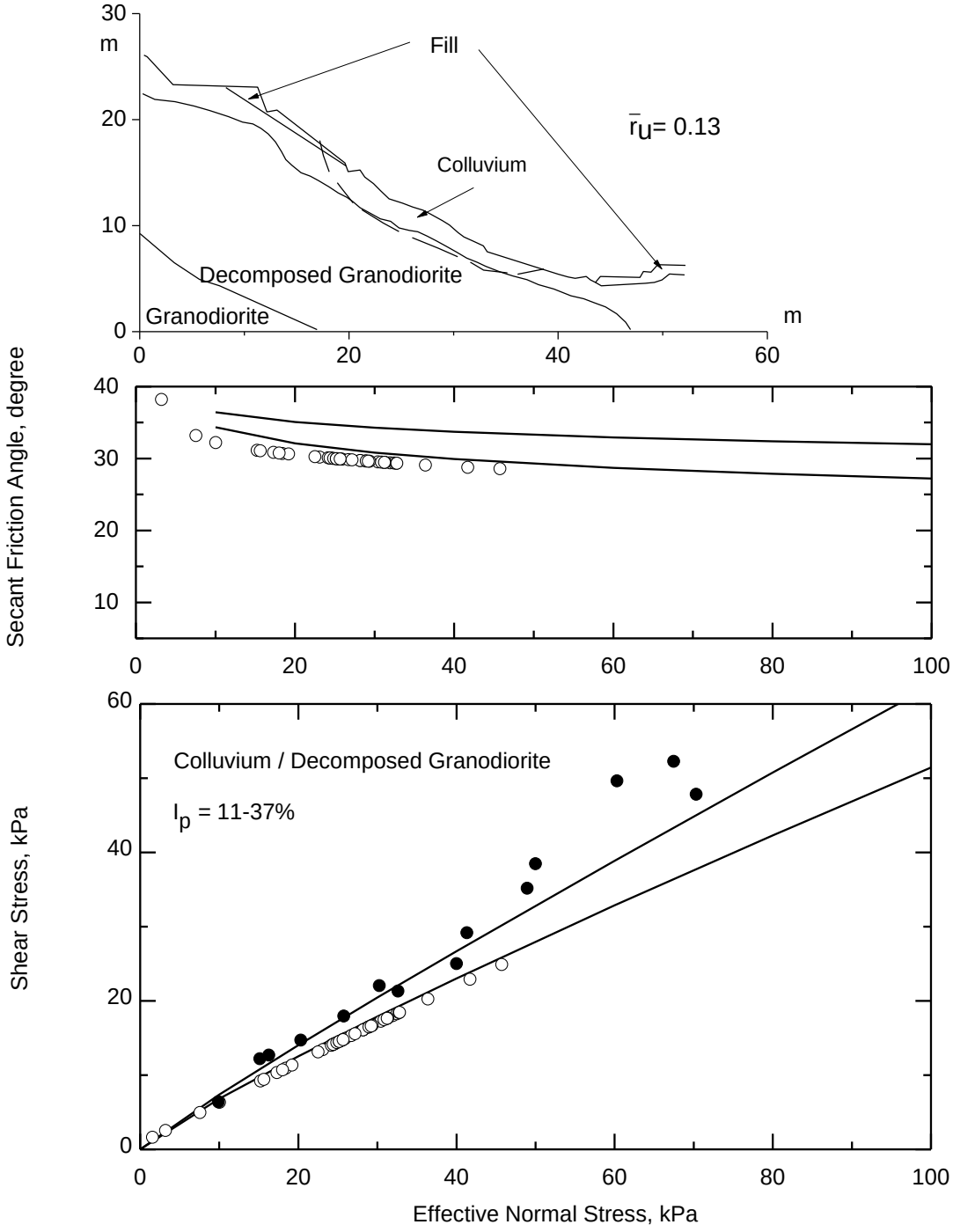

Figure B.16. First-time slope failure at Fu Yung Shan Tsuen, Hong Kong, 2005 (Ho et al 2013)

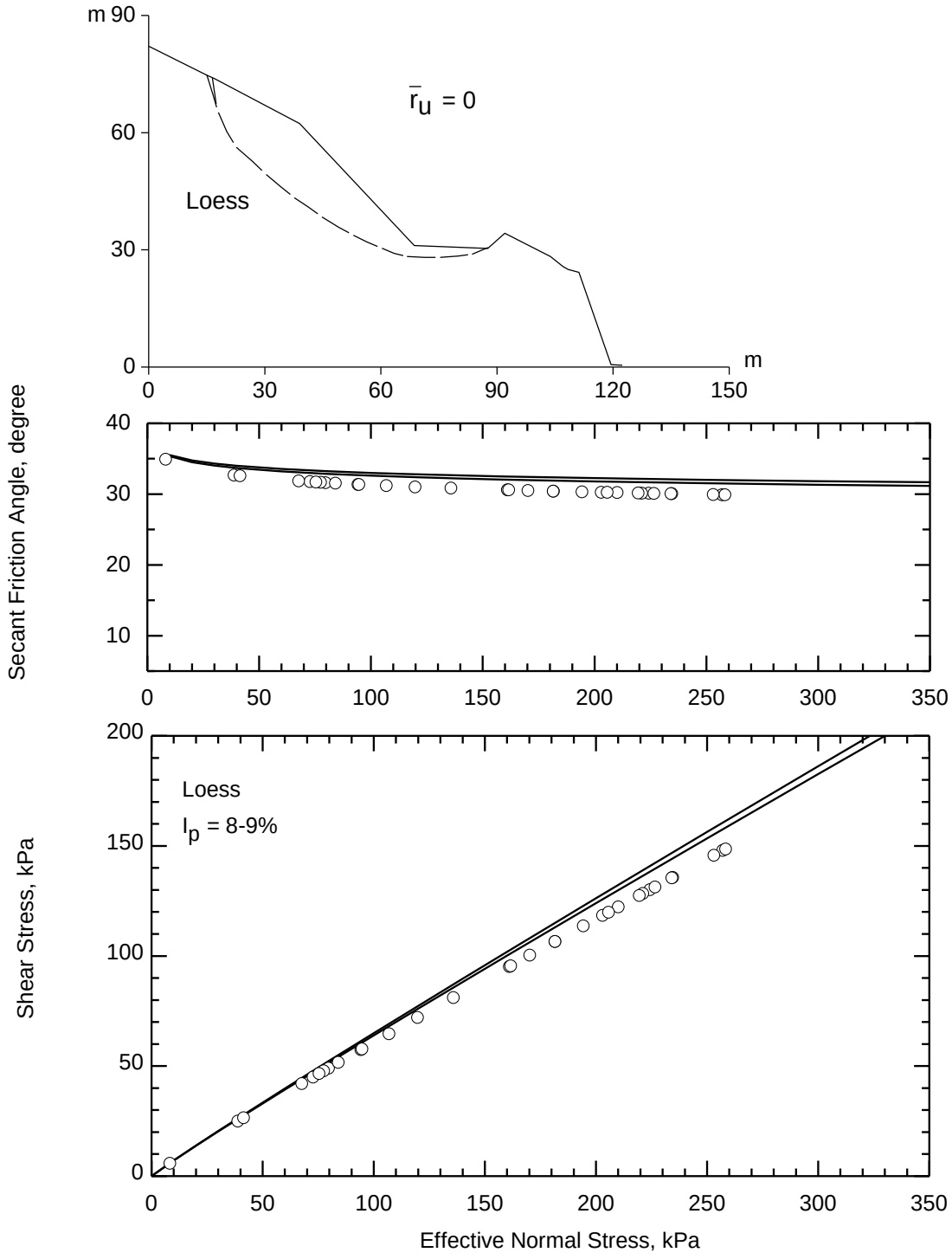

Figure B.17. First-time slope failure at No 312 National Road, P.R. China (Feng 1992)

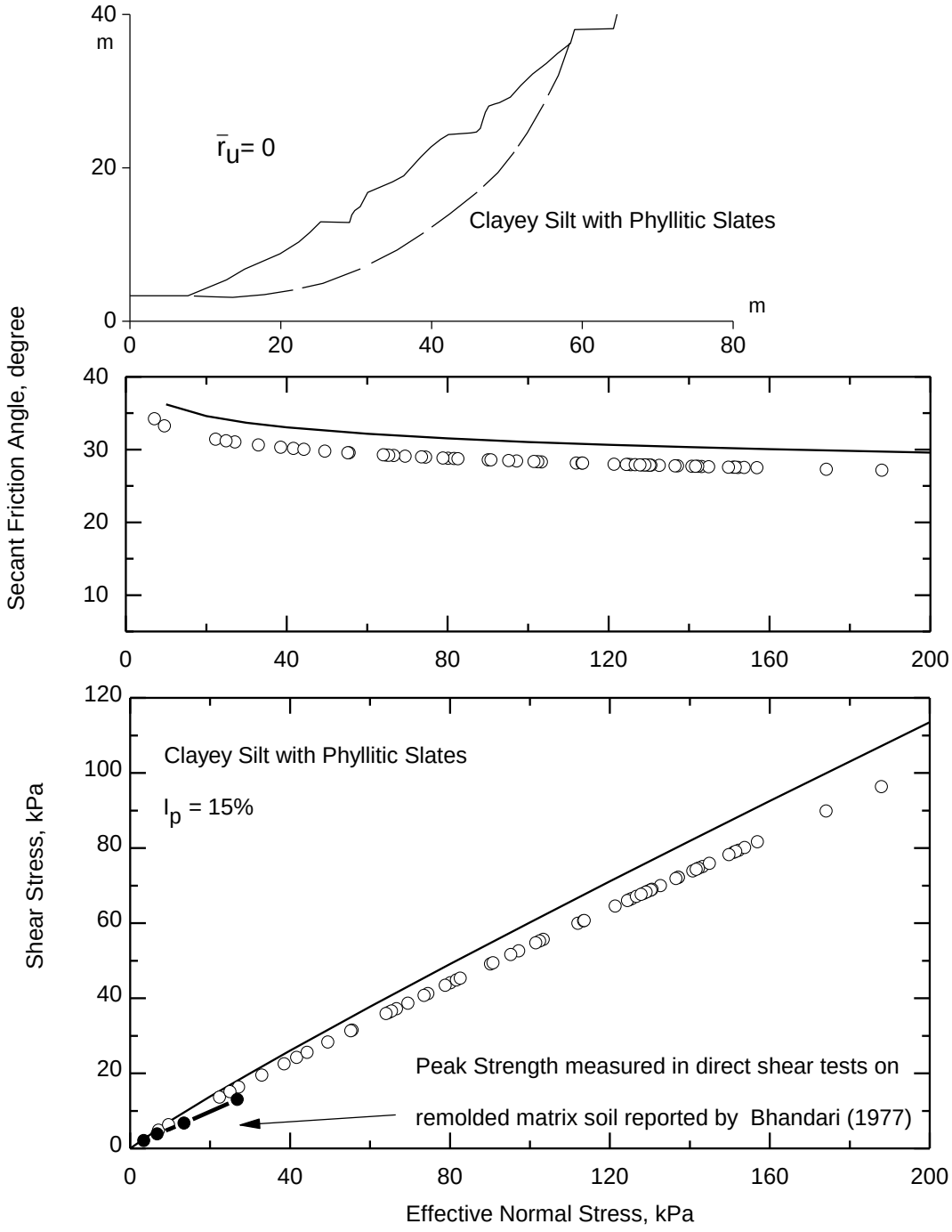

Figure B.18. First-time slope failure at Snowdon, Himalayan Region, 1971 (Bhandari 1977)

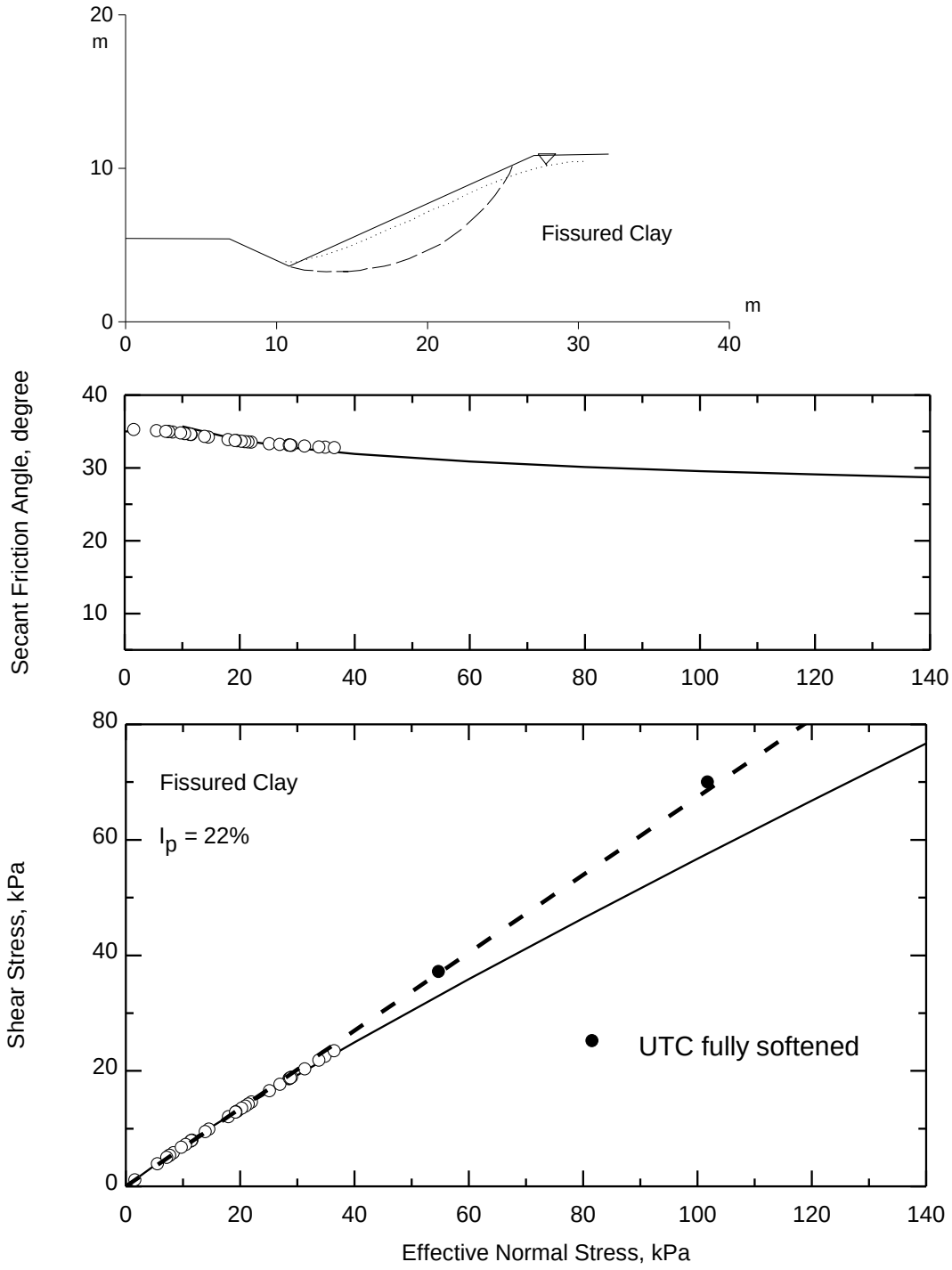

Figure B.19. First-time slope failure at Lachute Sation 8+85, Canada, 1975 (Silvestri 1980)

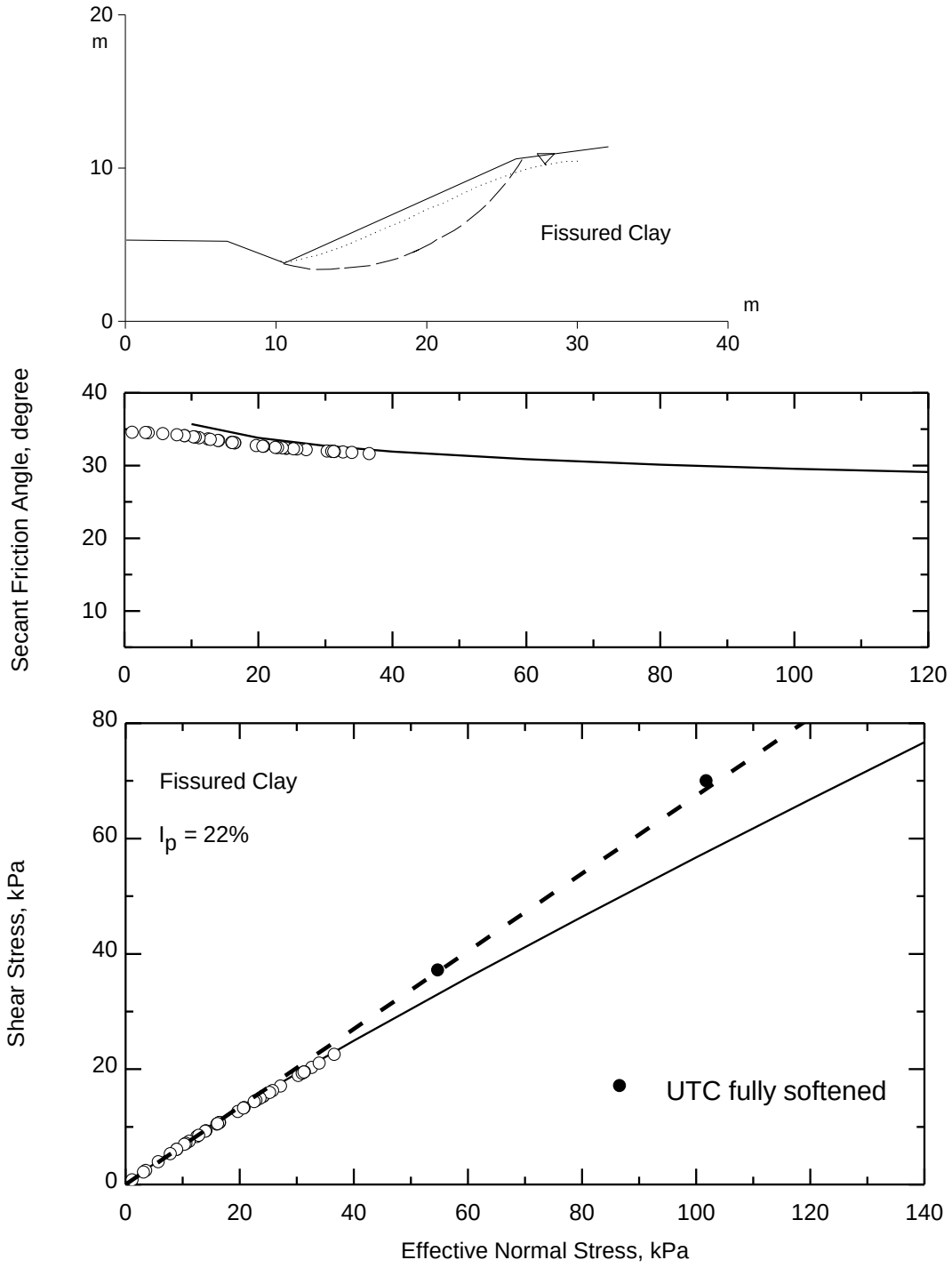

Figure B.20. First-time slope failure at Lachute Sation 10+50, Canada, 1975 (Silvestri 1980)

APPENDIX C: BACK-ANALYSES OF FIRST-TIME SLOPE FAILURES IN SOFT CLAYS OF EASTERN CANADA

Rosemere (Lefebvre 1981)

Rosemere is 25km north of Montreal, Canada. In July 1974, more than 2 years after the excavation, the failure occurred in the 11.9m high cut slope, of an angle of 24 degree with the horizontal (Fig.C.1). The slope is in silty clay, with plasticity index of 33%. The observed slip surface (Lefebvre 1981) is shown in Fig.C.1, together with the reported ground water condition. The back-analysis in the present study, gives back-calculated mobilized shear strength on the entire slip surface, larger than that defined by I_p = 33%, from the empirical correlation for fully softened shear strength developed in the present study.

Orleans (Eden and Jarrett 1971)

On October 1965, a small cut slope for a roadway failed 5 years after its construction at Orleans, Canada. The initial slip involved the total height of the slope, 35ft, after a period of heavy rain. The second and third slides occurred in 1965 and 1966, respectively.

Field investigations were carried out immediately after the first slide. A hand auger was used to establish the failure surface (Fig.C.2). The slip surface was believed to have passed through the toe of slope as a culvert passing under the road beyond the toe was intact. The slope is formed mostly of firm clay with some layers of silt or fine sand (Leda Clay), with plasticity index ranging from 20% to 40%. The soil is found to be fissured, which is consistent with the foundings from previous studies of landslides in the Ottawa area that the clay in the slopes was not intact. Four piezometers were installed, and piezometer readings were taken frequently in exceptionally wet periods. An average $\bar{r}_u$ of 0.40 was determined on the slip surface. It is likely that fully hydrostatic pressure could exist for this shallow slip after a long period of heavy rain, due to the downward gradient and low permeability of the clay.

The shallow slip surface and exceptionally high porewater pressure results to relatively low effective normal stresses on the failure plane, only up to 40 kPa. The shear strength from the proposed empirical correlation for fully softened shear strength at I_p = 20% - 40% is significantly

smaller than that back-calculated for the entire slip surface. This observation is not surprising with the consideration that Leda Clay is strongly cemented (Crawford 1963, Eden and Mitchell 1970).

Rockcliffe (Crawford 1963, Eden and Mitchell 1970)

The 1967 retrogressive landslide at Rockcliffe was the largest of several that occurred along the south bank of the Ottawa River in the unusually wet season. It was found by post-failure field investigations that the ground water table was near the ground surface at the time of failure. The failure was in the natural slope of 24 degree inclination (Fig.C.3), in fairly uniform gray Leda Clay, which is considered to be strongly bonded (Crawford 1963). Leda Clay at Rockcliffe site has a plasticity index of 8% - 28%. The initial slip surface which initiated the retrogressive landsliding, examined in the present study (Fig.C.3), was selected from the possible slip surfaces suggested by Eden and Mitchell (1970), with the consideration that the initial failure surface would intersect the upper terrace close to the hut (Fig.C.3). A porewater pressure ratio of 0.62, was used in the analysis, to present the full saturation of the slope under hydrostatic ground water condition (Eden and Mitchell 1970). The back-calculated mobilized shear strength on the entire slip surface, is higher than that defined by the plasticity index range of Leda Clay, from the empirical correlation for fully softened shear strength developed in the present study. The back-calculated mobilized shear strength is comparable to the large-strain strength (solid circles) of Leda Clay defined at 8% axial strain (Lefebrve (1981), determined from drained triaxial compression tests (Eden and Mitchell 1970).

Breckenridge (Eden and Mitchell 1970)

In April 1963, a retrogressive slide occurred in a natural slope at Breckenridge Creek, Quebec, Canada. The slope, which had a 25 degree inclination with the horizontal, was also in uniform Leda Clay, with plasticity index of 38%. The initial slip surface which initiated the retrogressive failure, suggested by Eden and Mitchell (1970), is shown in Fig.C.4. A porewater pressure ratio of 0.62, was used in the back-analysis in the present study, as suggested by Eden and Mitchell (1970) for full saturation of the slope under hydrostatic ground water condition. The back-calculated mobilized shear strength on the entire slip surface, is significantly higher than that at I_p

= 38%, from the empirical correlation for fully softened shear strength developed in the present study.

FIGURES

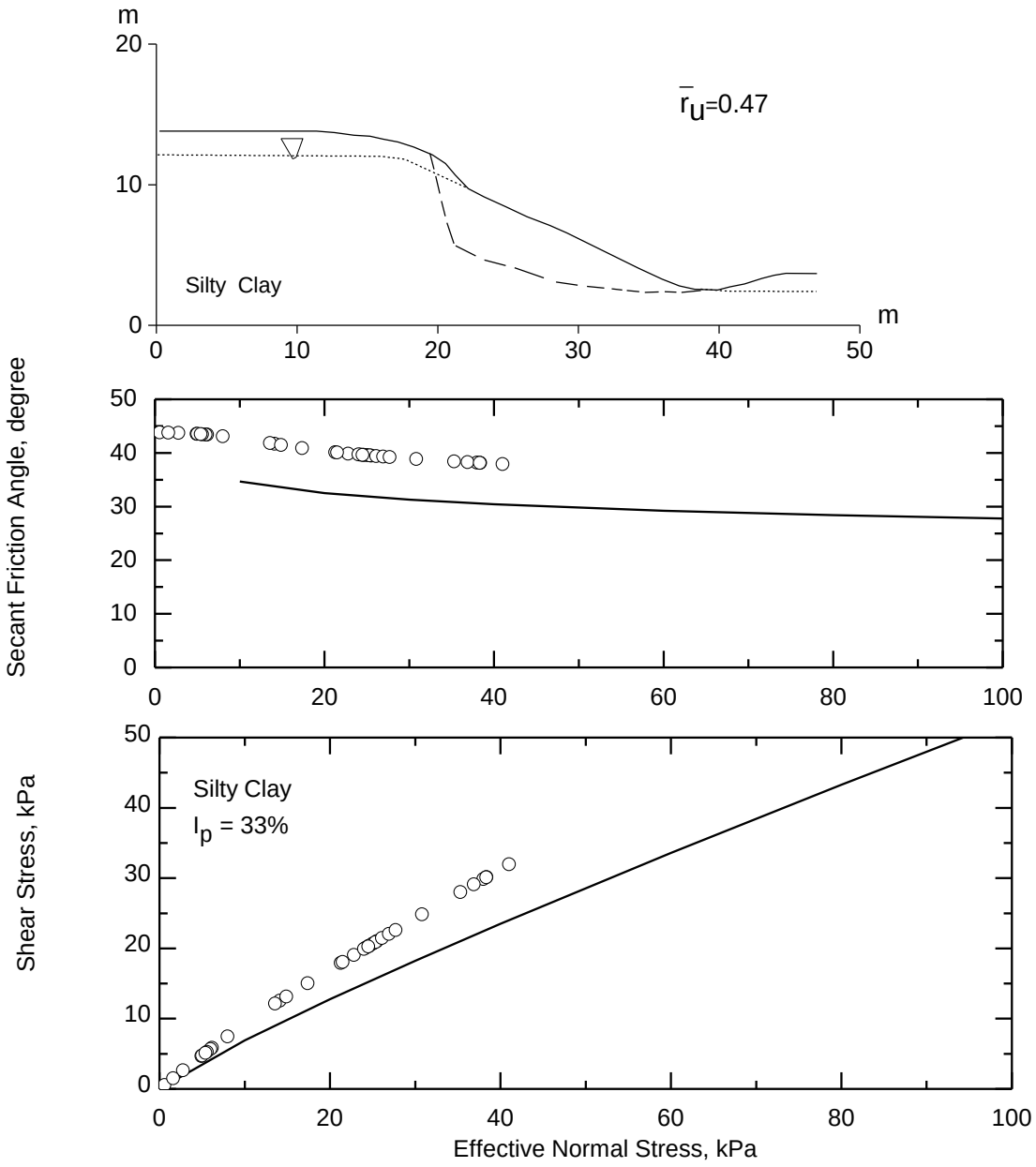

Figure C.1. First-time slope failure at Rosemere, Canada, 1974 (Lefebvre 1981)

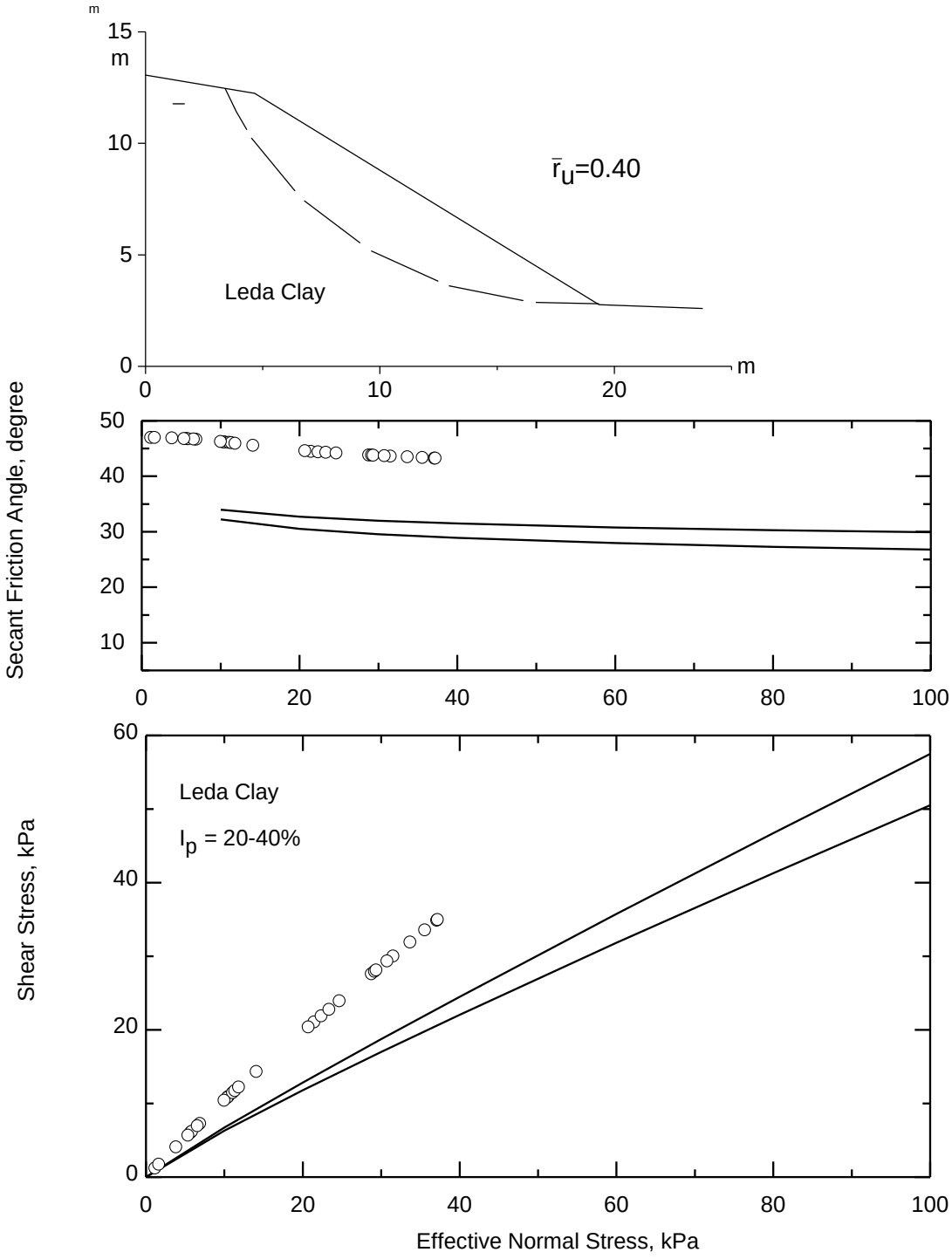

Figure C.2. First-time slope failure at Orleans, Canada, 1965 (Eden and Jarrett 1971)

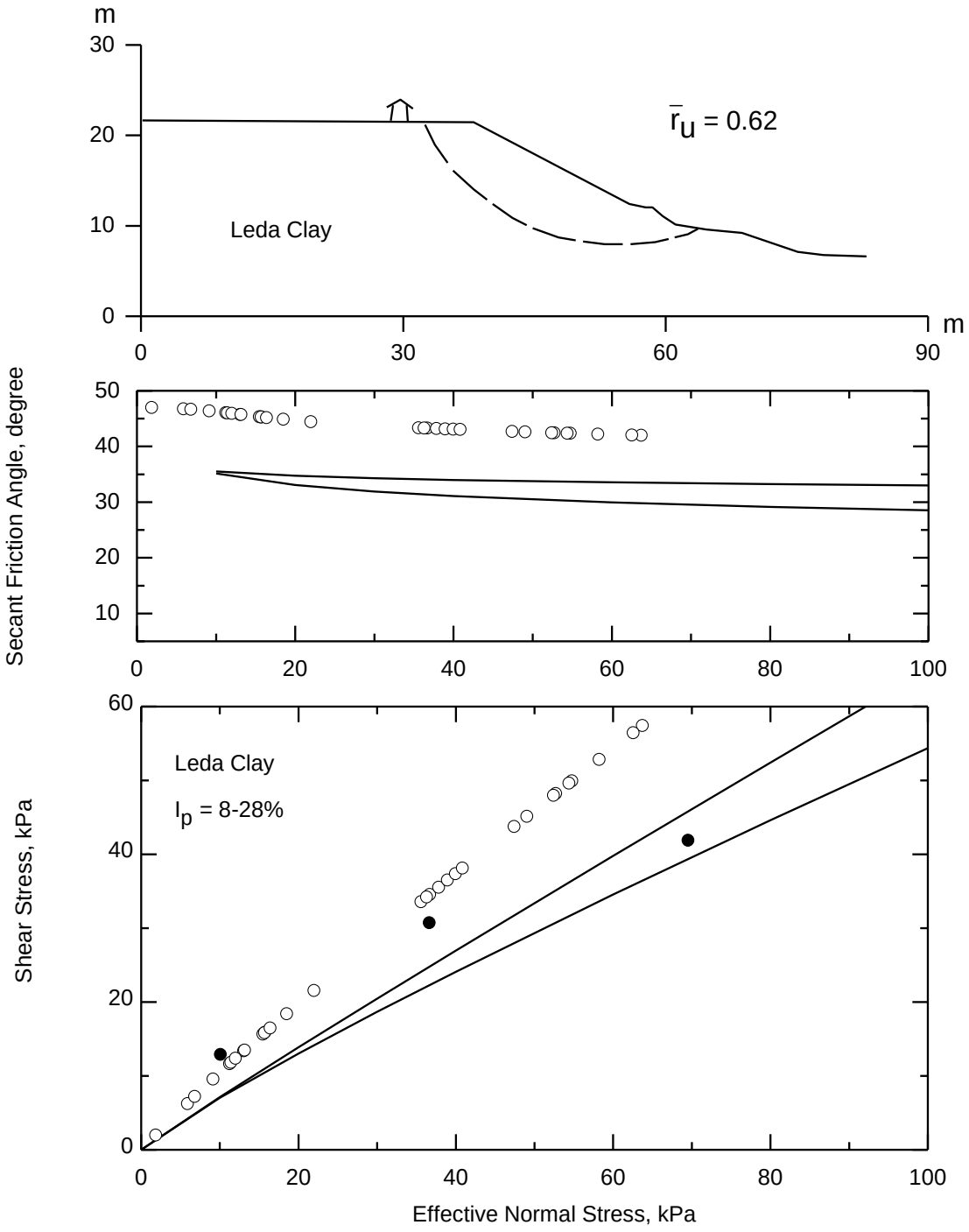

Figure C.3. First-time slope failure at Rockcliffe, Canada, 1967 (Crawford 1963, Eden and Mitchell 1970)

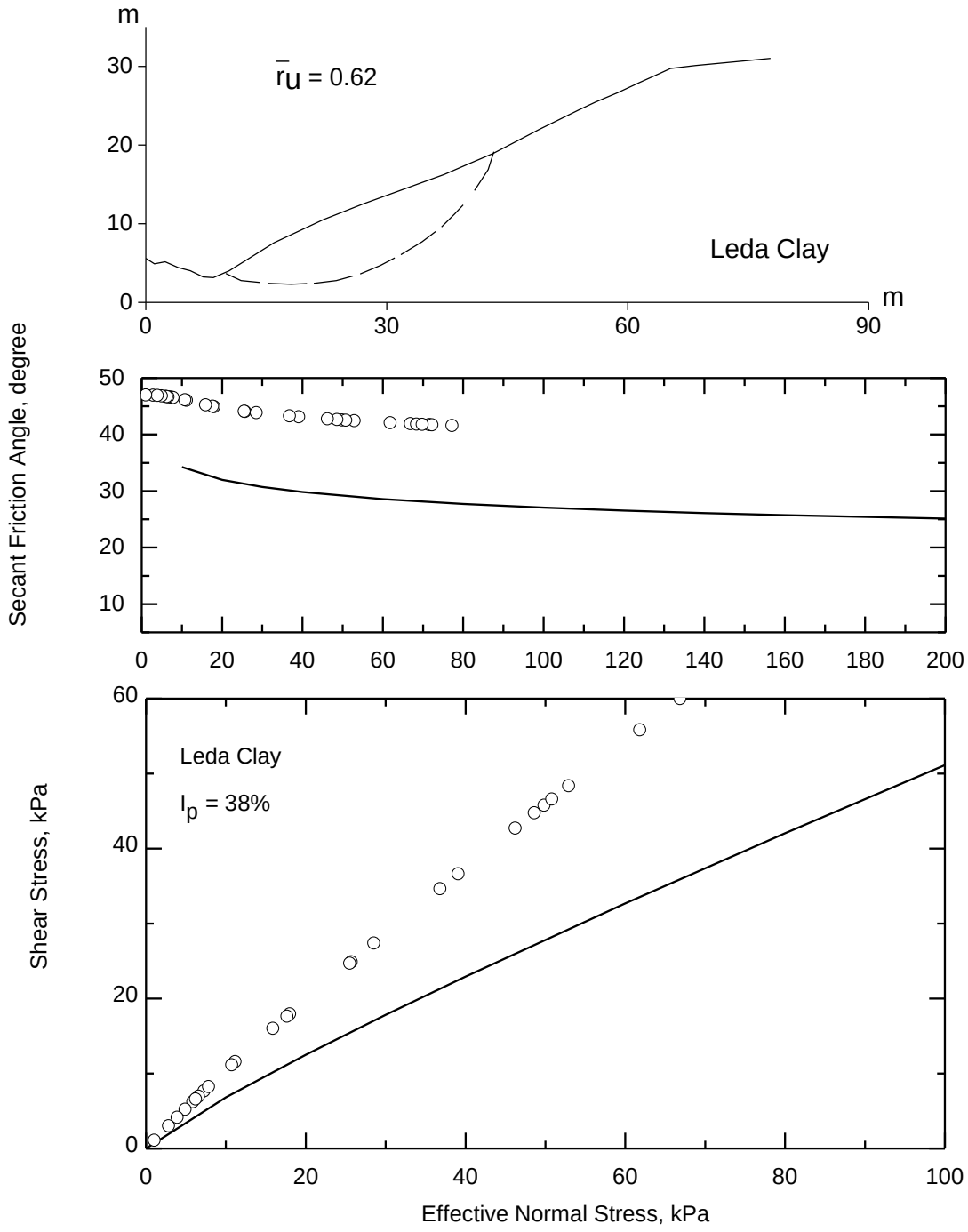

Figure C.4. First-time slope failure at Breckenridge, Canada, 1963 (Eden and Mitchell 1970)